Investigating the isoform-specific role of phosphoinositide 3-kinase p110delta

GEMMA NOCK

2008

Ludwig Institute for Cancer Research

University College London Branch, 91 Riding House Street,

London

AND

University College London

Department of Biochemistry and Molecular Biology,

Gower Street, London

AND

Barts & The London School of Medicine

Queen Mary, University of London

Charterhouse Square, London

ABSTRACT

Phosphoinositide 3-kinases (PI3Ks) are a family of enzymes that regulate a diverse array of biological functions in every cell type by generating lipid second messengers. The PI3K family is comprised of multiple isoforms that are divided into three main classes; class I, II and III. All class I PI3Ks are heterodimers consisting of a ~110 kDa catalytic subunit associated with a regulatory subunit. Class I PI3Ks are further subdivided into class IA and class IB, which are activated downstream of tyrosine kinases or G protein-coupled receptors, respectively. The mammalian catalytic subunits of class IA PI3Ks are p110α, p110β and p110δ. PI3Ks are involved in multiple cellular processes, and deregulation of PI3K signalling pathways have been linked to a number of diseases such as cancer, inflammation and immunity and diabetes. Targeting PI3K itself or downstream effectors of PI3K is an approach that has the potential to be of huge therapeutic benefit, however, PI3K signalling is also important in normal cell homeostasis and inhibition of all the PI3K isoforms with non-selective PI3K inhibitors is toxic to the cell. To enable individual PI3K isoforms to be targeted therapeutically, it is first important to understand the specific signalling mediated by each individual PI3K isoforms.

This work focuses on addressing the isoform-specific role of p110δ. Unlike p110α and p110β, p110δ has a more restricted tissue distribution and is most abundantly expressed in leukocytes. However, there are instances where cells of non-haematopoietic origin have high levels of p110δ expression, such as breast cells, melanocytes and microglia.

Using cell-based models to explore p110δ signalling, our work has revealed that coupling of the tyrosine kinase receptor, c-kit, to p110δ appears to remain largely unaltered in primary leukocytes that stably express the transforming polyoma middle T antigen. Stable overexpression of p110δ in a non-leukocyte cell line, NIH 3T3, has revealed that p110δ overexpression results in the downregulation of p110α and p110β expression and has a striking impact on cell morphology. Finally, we have identified a potential p110δ gene promoter region that mediates leukocyte-specific p110δ gene expression.

STATEMENT

This thesis is the result of work conducted at the Ludwig Institute for Cancer Research, UCL Branch, London, between September 2004 and June 2007 followed by work at Barts & The London School of Medicine, Queen Mary, University of London between July 2007 and June 2008. Except where references are given, this thesis contains my own original work in agreement with the regulations of University College London.

Some of the work in this thesis has been published elsewhere:

Geering, B., Cutillas P.R., Nock, G., Gharbi, S., Vanhaesebroeck, B. (2007). Class IA phosphoinositide 3-kinases are obligate p85-p110 heterodimers. *Proc Natl Acad Sci U S A*, **104**(19), 7809-14.

Kok, K., Verrall, E.G., Nock, G.E., Mitchell, M.P., Hommes, D.W., Peppelenbosch, M.P., Vanhaesebroeck, B. (2008). Analysis of p110delta phosphoinositide 3-kinase gene expression. (In preparation).

ACKNOWLEDGEMENTS

First and foremost, I would like to thank Bart Vanhaesebroeck for all of his support, advice and stimulating discussions he has offered throughout the course of my PhD. He has encouraged me to think independently and to develop in all aspects of science, which will stand me in good stead for future projects I wish to take on.

I would also like to thank members of the Cell Signalling group for keeping me motivated during my PhD, for their useful suggestions and scientific discussions and for sharing and teaching me a wide range of scientific techniques, in particular Maria Whitehead, Julie Guillermet-Guibert, Inma Martin-Berenjeno, Mariona Graupera, Khaled Ali and Lazaros Foukas. I am also thankful to Pedro Cutillas who made it possible for me to incorporate mass spectrometry analysis into my PhD and to Kristina Mahnken, who helped me with the transient p110δ transfection studies. I would also like to mention Bel Kok and Lizzie Verrall, who have greatly developed our understanding of p110δ gene regulation, without this knowledge, I would not have been able to develop further our understanding in this area. Sadly, Lizzie passed away this year and I hope this thesis and a paper in the pipeline will recognise her contributions as a scientist.

I am extremely grateful to my family who have always supported me in my choices and at each stage leading up to, and throughout, my PhD and also to my friends who have helped me keep perspective during this time. I would also like to thank Doogal for all of his love and support.

Finally I am grateful for the financial support from MRC.

CONTENTS

RESULTS

3   **DOES CELL TRANSFORMATION ALTER P110 COUPLING TO TYROSINE KINASE RECEPTORS?**

4   **OVEREXPRESSION OF P110δ IN A MAMMALIAN CELL LINE THROUGH TRANSFECTION OF MAMMALIAN EXPRESSION VECTORS**

LIST OF FIGURES

1. INTRODUCTION

2. MATERIALS AND METHODS

3. DOES CELL TRANSFORMATION ALTER P110 COUPLING TO TYROSINE KINASE RECEPTORS?

4. OVEREXPRESSION OF p110δ IN A MAMMALIAN CELL LINE THROUGH TRANSFECTION OF MAMMALIAN EXPRESSION VECTORS

5 LEUKOCYTE-SPECIFIC PROMOTER ANALYSIS OF MOUSE EXON -2A

6 OVEREXPRESSION OF p110δ IN NIH 3T3 CELL LINE THROUGH RETROVIRAL INFECTION

7 CHARACTERISATION OF 5'MYC-ᴘ110δ OVEREXPRESSING NIH 3T3 CELLS

LIST OF TABLES

ABBREVIATIONS

Ab	Antibody
APS	Adapter protein with Pleckstrin homology and Src homology 2 domains
BMMC	Bone marrow derived mast cell
BH	Bcr-homology domain
BSA	Bovine serum albumin
cDNA	complementary DNA
DAG	Diacylglycerol
DAPI	4',6-diamidino-2-phenylindole
DMSO	Dimethylsulfoxide
DNA	Deoxyribonucleic acid
DNase	Deoxyribonuclease
DTT	Dithiothreitol
EC_{50}	Half maximal effective concentration
ECL	Enhanced chemiluminescence
EDTA	Ethylenediamine tetra-acetic acid
EGTA	Ethylene glycol tetraacetic acid
ERK	Extracellular signal related kinase
ETSF	ETS/Elk family [named after E26 (E twenty six) leukemogenic chicken virus]
FACS	Fluorescence activated cell sorting
FKHD	Forkhead
FBS	Foetal bovine serum
fMLP	formyl-Met-Leu-Phe
Gab	Grb2-associated binder protein
GAP	GTPase-activating protein
GDP	Guanosine diphosphate
GEF	Guanine nucleotide exchange factor
GPCR	G protein-coupled receptor
GTP	Guanosine triphosphate
GRB2	Growth factor receptor-bound protein
GST	Glutathione S-transferase
GST-PBD	Glutathione S-transferase – PAK-binding domain

GST-RBD	Glutathione S-transferase – rhotekin-binding domain
IC_{50}	Concentration giving 50% maximal inhibition
Ig	Immunoglobulin
IGF-1	Insulin growth factor-1
IL-	Interleukin
$InsP_3$	Inositol 1,3,5-trisphosphate
IP	Immunoprecipitation
IRF	Interferon regulatory factor
IRS-1	Insulin receptor substrate-1
JNK	Jun N-terminal kinase
KI	Knock-in
KO	Knock-out
LEF	Lymphoid enhancer factor-1
LLnL	N-Ac-Leu-Leu-norLeucinal
LPS	Lipopolysaccharide
MAPK	Mitogen-activated protein kinase
MCS	Multiple cloning site
mRNA	Messenger RNA
NeoR	Expression vector containing gene conferring neomycin-resistance
NFAT	Nuclear factor of activated T-cells
p110δ-2a	p110δ cDNA containing 5' untranslated exon -2a
p110δ-2b	p110δ cDNA containing 5' untranslated exon -2b
PA	Phosphatidic acid
PAGE	Polyacrylamide gel electrophoresis
PBS	Phosphate buffered saline
PCR	Polymerase chain reaction
PDGF	Platelet-derived growth factor
PFA	Paraformaldehyde
PH	Pleckstrin homology domain
PI3K	Phosphoinositide 3-kinase
PIP_2	Phosphatidylinostol-(4,5)-bisphosphate
PIP_3	Phosphatidylinositol-(3,4,5)-triphosphate
PKA	Protein kinase A

PKB/Akt	Protein kinase B
PKC	Protein kinase C
PLC	Phospholipase C
PMSF	Phenylmethylsulfonyl fluoride
PtdIns	Phosphatidylinositol
PTEN	Phosphatase and tensin homolog deleted on chromosome ten
PVDF	Polyvinylidene fluoride
pY	Phosphotyrosine
RNA	Ribonucleic acid
RT PCR	Real time polymerase chain reaction
SDS	Sodium dodecyl sulphate
SCF	Stem cell factor
SHC	Src homology 2-domain-containing transforming protein C
SHIP	SH2 domain-containing inositol phosphatise
SH2	Src homology 2 domain
TCL	Total cell lysate
TEMED	Tetramethylethylenediamine
TF	Transcription factor
TFB	Transcription factor-binding
TNF	Tumour necrosis factor
TRIS	Trishydroxymethylaminomethane
WT	Wild type

1. INTRODUCTION

1.1 PHOSPHOINOSITIDE 3-KINASE AND THEIR LIPID PRODUCTS

Phosphoinositide 3-kinases (PI3Ks) are a family of enzymes that regulate a diverse array of biological functions in every cell type by generating lipid second messengers. They catalyse the phosphorylation of the 3-OH position of the inositol head groups of phosphatidylinositol (PtdIns) and phosphoinositide (PI) lipids producing 3'PI lipid derivatives (Sotsios & Ward, 2000; Vanhaesebroeck & Waterfield, 1999). In mammalian cells these lipid derivatives are PtdIns(3)P, PtdIns(3,4)P_2, and PtdIns(3,4,5)P_3 (the latter also referred to as PIP$_3$) (Figure1.1).
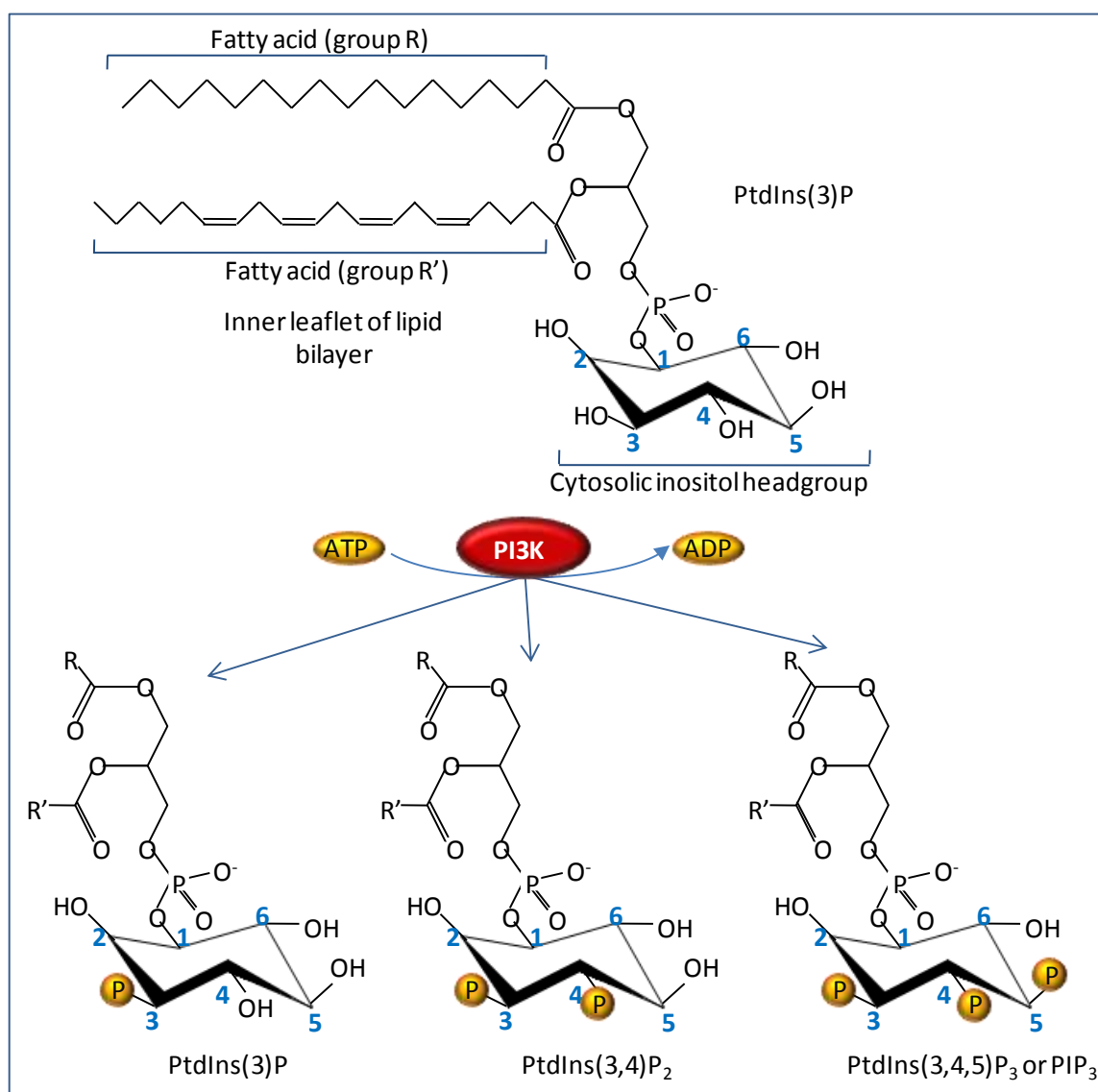
Figure 1.1: Simplified chemical structures of phosphatidylinositol (PtdIns) and the lipid products generated by PI3K. PtdIns consists of a cytoplasmic inositol headgroup and a hydrophobic tail consisting of two fatty acid chains that are incorporated into the inner leaflet of the membrane lipid bilayer. PI3Ks transfer a phosphate from ATP to phosphorylate the 3-position on the inositol ring generating PtdIns(3)P, PtdIns(3,4)P_2, and PtdIns(3,4,5)P_3.

PI3K can also indirectly generate the lipid product PtdIns(3,5)P_2 through the action of the Fab1 5-kinase on the PI3K lipid product PtdIns(3)P (Cabezas, *et al.*, 2006; Gary, *et al.*, 1998; Sbrissa, *et al.*, 1999). The basal levels of PtdIns(3)P, PtdIns(3,5)P_2, and PIP$_3$ are very low but can rise sharply upon cellular stimulation, allowing tight control of signalling pathways downstream of these lipid products (Maffucci, *et al.*, 2003; Vanhaesebroeck & Waterfield, 1999).

The 3'PI lipid derivatives generated by PI3Ks can activate sets of proteins with specific lipid binding domains. PIP$_3$ interacts with a subset of proteins that contain PH (pleckstrin homology) domains (Lemmon & Ferguson, 2000). The PH domain is the most widespread binding module in higher eukaryotes (Lindmo & Stenmark, 2006), but although most PH domains bind PIs, only some do with high affinity (Vanhaesebroeck & Waterfield, 1999). The first PtdIns(3)P-specific binding domain to be identified was the FYVE (for conserved in Fab1, YOTB, Vac1, and EEA1) zinc finger domain. This domain is evolutionary more conserved than the PH domain, but is less abundant and has a narrower substrate preference (Lindmo & Stenmark, 2006). The other known PtdIns(3)P-binding domain is the conserved Phox-homology (PX) domain, which is slightly more abundant than the FYVE domain. A few PX domains can also bind other PtdIns such as PtdIns(3,4)P_2 (Lindmo & Stenmark, 2006). PIP$_3$ activation of PH domain-containing proteins is discussed further in section 1.2.

The level of PI3K lipid products is also regulated by three main phosphatases; PTEN and SHIP2, which are broadly expressed, and SHIP1, which is expressed primarily in haematopoietic cells (Muraille, *et al.*, 1999; Stephens, *et al.*, 2005). PTEN (phosphatase and tensin homolog deleted on chromosome ten) is a well-known tumour suppressor gene and is frequently inactivated by mutation, gene deletion, or epigenetic silencing (Cully, *et al.*, 2006; Harris, *et al.*, 2008). PTEN has 3-phosphatase activity and regulates PI3K-dependent signalling events through dephosphorylation of PIP$_3$ to PtdIns(4,5)P_2, thereby preventing membrane-localization of PH domain-containing effectors. SHIP1 (SH2 domain-containing inositol 5-phosphatase) and SHIP2 are both 5'phosphatases which dephosphorylate PIP$_3$ to PtdIns(3,4)P_2 (Freeburn, *et al.*, 2002; Rohrschneider, *et al.*, 2000). As mentioned above, PH-domain containing proteins can interact with PIP$_3$, however certain PH domains exhibit dual specificity for PIP$_3$ and PtdIns(3,4)P_2, such as DAPP1 (dual adaptor of phosphotyrosine and 3-phosphoinositides 1), whereas as others exhibit selectivity toward PtdIns(3,4)P_2, such as TAPP (tandem PH domain-containing protein).

The phosphatase activity of SHIP can therefore regulate PI3K-dependent signalling events by redirecting the signalling pathway through another set of 3'PI lipid-binding effectors (Harris, *et al.*, 2008). In comparison to PTEN, SHIP genes are not widely thought of as tumour suppressors although there have been a few reported instances of *SHIP* mutations in a proportion of acute, myeloid and lymphoblastic leukaemias (Luo, *et al.*, 2004b; Zhang, *et al.*, 2006).

1.2 CLASSIFICATION OF PHOSPHOINOSITIDE 3-KINASES

The PI3K family is comprised of multiple isoforms that are divided into three main classes; class I, II and III. All three classes share a homologous region in their catalytic subunit consisting of a catalytic core domain linked to a helical or PIK (PI kinase homology) domain (Figure 1.2) (Vanhaesebroeck & Waterfield, 1999). The classification of the PI3K isoforms is based on their *in vitro* lipid substrate specificity, structure and possible mode of regulation. A group of PI3K-related kinases sometimes called class IV, also exist, which have a kinase domain that has significant homology to the kinase core domain of PI3Ks but which do not phosphorylate lipids (Vanhaesebroeck & Waterfield, 1999).

1.2.1 Class I PI3K

All class I PI3Ks are heterodimers consisting of a ~110 kDa catalytic subunit associated with a regulatory subunit. The *in vitro* substrates for class I PI3Ks are PtdIns, PtdIns(4)P or PtdIns(4,5)P_2, however their preferred *in vivo* substrate appears to be Ptd(4,5)P_2, which results in PIP$_3$ production. Class I PI3Ks have been further categorized into class IA and class IB, on the basis of whether they are activated downstream of tyrosine kinases or G-protein coupled receptors (GPCRs), respectively. However, recent evidence (discussed below) presents good reasoning for this classification to be reconsidered.

Class IA PI3Ks: The mammalian catalytic subunits of class IA PI3Ks are p110α, p110β and p110δ, as shown in Figure 1.2, which are encoded by three separate genes. There are at least five different class IA regulatory subunits: p85α, p55α and p50α, encoded by the *PIK3R1* gene, and p85β and p55γ, encoded by *PIK3R2* and *PIK3R3*, respectively. The regulatory subunits contain two Src homology 2 (SH2) domains and the region between these two domain, the inter-SH2 domain, mediates the interaction of the regulatory subunit with the p110 catalytic subunit (Vanhaesebroeck & Waterfield, 1999). All of the p110 catalytic subunits are able to bind all the regulatory subunits, with no known specificity for a particular p110 to bind a particular p85, at least in cell culture-based experiments.
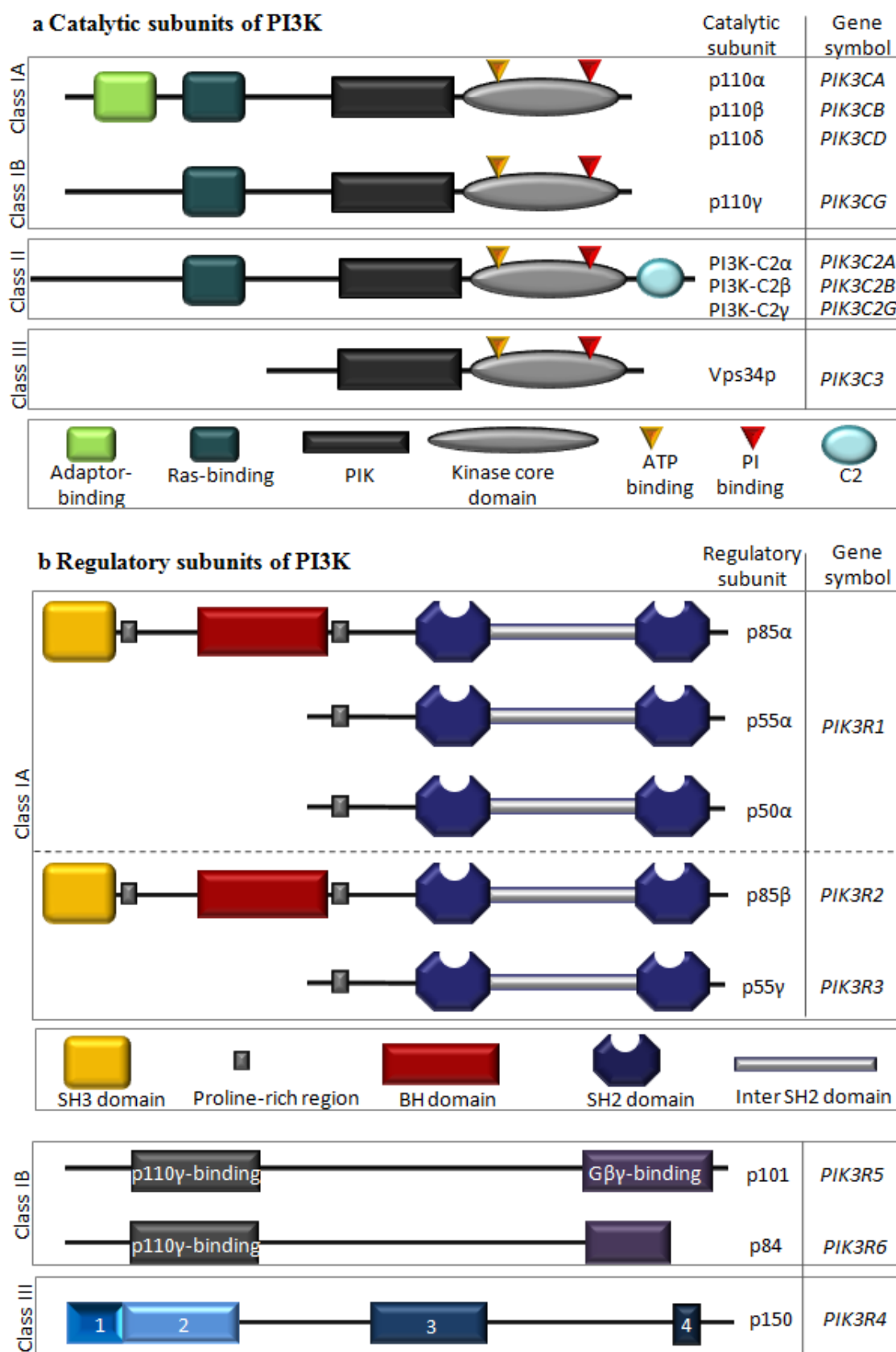
Figure 1.2: Modular structures of the PI3K catalytic and regulatory subunits. **(a)** PI3K catalytic subunits are divided into three main groups: Class I, II and III. They all share a PIK domain and a kinase core domain, which contains both the ATP and PI binding sites. Class IA catalytic subunits include p110α, p110β and p110δ, which all have a p85 adaptor binding domain. The sole class IB catalytic subunit, p110γ does not contain

the p85 adaptor binding domain. All class I and II catalytic subunits contain a Ras binding domain. Class II catalytic subunits further have a C-terminal C2 domain that binds phospholipids *in vitro* in a Ca^{2+}-independent manner. The single class III PI3K catalytic subunit is the homologue of the yeast Vps34 protein. **(b)** At least five class IA regulatory subunits exist. p85α, p55α and p50α, are encoded by the *PIK3R1* gene, and p85β and p55γ, encoded by *PIK3R2* and *PIK3R3*, respectively. All class IA regulatory subunits have two SH2 domains and an inter SH2 domain that is essential for binding the p110 catalytic subunits. p85α and p85β also have an additional Bcr homology (BH) domain. There are two class IB regulatory subunits, p101 and p84. The domains illustrated for p101 and p84 are not yet well defined. A region at the N-terminus of p101 has been identified to be essential for binding to p110γ and a separate C-terminal region mediates p101 binding to GPCRs (Voigt, *et al.*, 2005). One class III regulator subunit has been identified, p150, which has high homology to yeast Vps15p protein kinase. The domains labelled 1-4 on p150 are as follows: 1) represents an N-terminal myristoylation consensus site; (2) Ser/Thr protein kinase domain; (3) region with homology to the 65-kDa regulatory subunit of protein phosphatase 2A; (4) region containing WD repeat motifs (Panaretou, *et al.*, 1997).

The association of the regulatory subunit with p110 stabilises the catalytic subunit but inhibits its catalytic activity (Yu, *et al.*, 1998b). The interaction of p85 with p110 is extremely strong, withstanding high concentrations of salt, urea or detergent, which indicates that under physiological conditions, it is unlikely that there is dissociation of the p110-p85 heterodimer (Fry, *et al.*, 1992; Geering, *et al.*, 2007a; Geering, *et al.*, 2007b) .

Upon activation of protein tyrosine kinases, p110 catalytic inhibition is relieved through engagement of the regulatory subunit SH2 domains with phosphotyrosine residues in a specific Y(P)xxM motif, where x is any amino acid (Yu, et al., 1998b). The protein tyrosine kinases involved can be integral to the receptor itself, as is the case for many growth factor receptors or can be activated by direct or indirect association to the receptor, such as Src family of protein tyrosine kinases associated with receptors for antigen or antibodies (Figure 1.3) (Hawkins, *et al.*, 2006). Likewise, the critical tyrosine residues that are phosphorylated to mediate p50/p55/p85 binding, may be located on the receptor itself, such as PDGF receptor, or on receptor-associated proteins (or adaptors), such as IRS (insulin receptor substrate) (Hawkins, *et al.*, 2006). Through binding Y(P)xxM motifs, the regulatory subunit serves to transport the p110 subunit to the cell membrane where it is brought into close proximity with its lipid substrate $Ptd(4,5)P_2$ to generate PIP_3.

Class IA p110 isoforms are differentially distributed within tissue; p110α and p110β isoforms are widely distributed in mammalian tissue, whereas p110δ shows a more restricted distribution, and is mainly found in leukocytes (Chantry, *et al.*, 1997; Vanhaesebroeck, *et al.*, 1997).
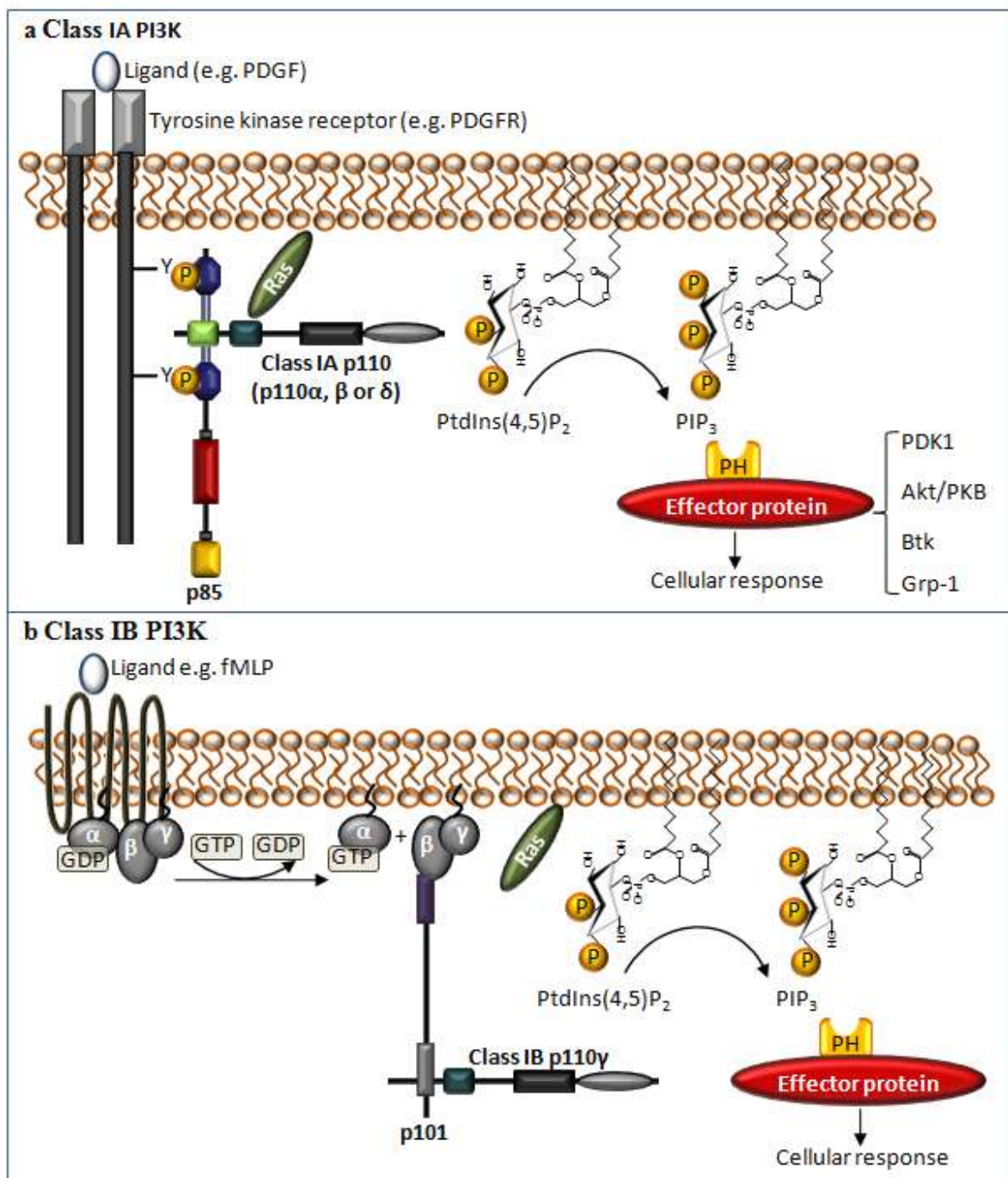
Figure 1.3: Activation of class I PI3K. (a) Activation of Class IA PI3Ks by receptors activating protein tyrosine kinases. The schematic represents the activation of Class IA heterodimers by a growth factor receptor with intrinsic protein tyrosine kinase activity. Ligand-induced dimerisation of the receptor results in phosphorylation of multiple key tyrosine residues in the cytoplasmic tails, some of which are within YxxM motifs that act as docking sites for the SH2 domains of the class IA regulatory subunits. This leads to recruitment of the p110 catalytic subunit to the plasma membrane where it can phosphorylate PtdIns(4,5)P_2 to PIP_3. GTP-bound Ras is also known to bind the catalytic subunits of class I PI3Ks. **(b)** Activation of class IB PI3Ks is downstream of heterotrimeric G-protein activation. The schematic represents the activation of p110γ-p101/p84 dimer by a G_i-coupled receptor. Ligand binding of these receptors induces a conformational change which results in an exchange of GDP for GTP on the α subunit, inducing dissociation from both the receptor and Gβγ subunits. The free Gβγ subunit binds directly to the p101/p84 subunit of p110γ, thus bringing p110γ to the plasma membrane.

Class IB PI3K: This class of PI3K only has one catalytic subunit and two regulatory subunits. The catalytic subunit p110γ binds both p101 and the relatively recently characterised p84 regulatory subunit (Stephens, *et al.*, 1997; Suire, *et al.*, 2005). p110γ/p101/p84 heterodimers are activated by the Gβγ subunits of heterotrimeric GPCRs (Figure 1.3). The role of p101/p84 in recruitment of p110γ to the cell membrane is less clear, with evidence that a substantial portion of p110γ is constitutively present at the cell membrane (Krugmann, *et al.*, 2002). p110γ, like p110δ, is predominantly, although not exclusively expressed in cells of the immune system and is involved in both innate and adaptive immune responses (Hirsch, *et al.*, 2006; Laffargue, *et al.*, 2002; Lemmon & Ferguson, 2000; Rommel, *et al.*, 2007; Sasaki, *et al.*, 2000).

Although originally classified as a class IA PI3K, p110β is also activated downstream of GPCRs. Over ten years ago, p110β (and not p110α or p110δ) was found to be activated by Gβγ subunits *in vitro* (Kurosu, *et al.*, 1997; Maier, *et al.*, 1999). In addition, dominant-negative p110β but not p110γ, has been found to inhibit mitogen-activated protein kinase (MAPK) in response to lysophosphatidic acid (LPA), a GPCR ligand (Yart, *et al.*, 2002). However, it is only recently that p110β has been found to be activated predominantly downstream of GPCRs, rather than tyrosine kinase receptors, in cell-based studies (Guillermet-Guibert, *et al.*, 2008). The classification of p110β as a class IA PI3K therefore perhaps needs to be redefined.

1.2.2 Class II PI3K

Class II PI3Ks are larger than class I PI3Ks (170 – 210 kDa). There are three class II PI3K catalytic subunits; PI3K-C2α, PI3K-C2β and PI3K-C2γ with no adaptor protein identified to date. Class II PI3K catalytic subunits share 45-50% similarity with class I PI3K, containing both a PIK and kinase core domain and also a Ras binding domain (Figure1.2). They differ at the C-terminus, containing a C2 domain that binds phospholipids *in vitro* in a Ca^{2+}-independent manner. Class II catalytic subunits also differ in a large N-terminal region, which shows no homology to any known protein.

A number of ligands can activate class II PI3K, such as insulin, EGF, integrins, chemokine, MCP-1 and more recently LPA (Maffucci, *et al.*, 2005; Vanhaesebroeck & Waterfield, 1999). However, in respect to class I PI3K, relatively few studies have been made to elucidate the isoform-specific roles of class II PI3Ks and their mechanism of

activation, partly due to the lack of class II PI3K-specific inhibitors and mutant (class II PI3K gene knock-out) mice. Nevertheless, employing other strategies such as RNAi to knock-down specific class II PI3K isoform expression, progress is being made to shed some light on the involvement of class II PI3K in various cellular processes.

In vitro, class II PI3Ks have a preference for the lipid substrate PtdIns, but can also phosphorylate PtdIns(4)P and PtdIns(4,5)P_2. Phosphorylation of PtdIns by class II PI3K generates PtdIns(3)P, which has now been recognized as dynamic intracellular messenger alongside PIP_3. PtdIns(3)P is generated upon insulin stimulation and plays a critical role in the insulin signalling pathway (Chaussade, *et al.*, 2003; Maffucci, et al., 2003). LPA also induces PtdIns(3)P production (and not PtdIns(3,4,5)P_3) at the plasma membrane in a number of cell lines (Maffucci, et al., 2005). LPA was found to induce cell migration through activation of PIK3C2β, and not PIK3C2α, identifying class II PI3K and PtdIns(3)P production as important players in cell migration (Maffucci, et al., 2005). Recently, PI3K-C2α, but not PI3KC2β has been found to be important in controlling cell survival (Elis, *et al.*, 2008). In the latter study, lowering the levels of PI3KC2α protein in a number of cancer cell lines led to reduction in proliferation and cell viability, arguing that PI3K inhibitors targeting not only the class I PI3K isoforms but also class II PI3K isoforms, in this case PIK3C2α, may contribute to an effective anticancer strategy.

Class II PI3Ks are predominantly associated with the membrane fraction of cells, as opposed to class I PI3Ks, which are mainly cytosolic. PI3KC2α and PI3KC2β are fairly ubiquitously expressed in mammalian tissue, whereas PI3KC2γ is mainly found in the liver (Vanhaesebroeck & Waterfield, 1999).

1.2.3 Class III PI3K

Class III PI3Ks are homologues of the *Saccharomyces cerivisiae* vascular protein-sorting protein, Vps34p. Vps34p can only phosphorylate PtdIns to generate PtdIns(3)P. In all eukaryotes investigated, a single Vps34 homologue has been identified, which has both the PIK and kinase core domain (Figure 1.2). In both yeast and mammals, class III PI3K catalytic subunits exist in complex with a Ser/Thr protein kinase, named Vps15p in yeast and p150 in mammals (Vanhaesebroeck & Waterfield, 1999). Originally isolated as a mutant of vesicle-mediated vacuolar protein sorting in yeast, class III PI3Ks are implicated in endosome fusion during intracellular trafficking events and are located mainly on intracellular membranes (Foster, *et al.*, 2003).

A number of studies in 2001-2002 have further implicated the involvement of class III PI3K in diverse intracellular trafficking events, such as autophagy in yeast (Kihara, *et al.*, 2001), the fusion of formed phagosomes with late endosomes/lysosomes in a mouse macrophage cell line (Vieira, *et al.*, 2001), internal vesicular formation within multivescicular endosomes in a human cancer cell line (Futter, *et al.*, 2001) and efficient endosome-to-Golgi retrograde transport in yeast (Burda, *et al.*, 2002). Recently, it has been shown that mammalian hVps34 plays an important role in the ability of cells to respond to changes in nutrient conditions, through the activation of mTOR (mammalian target of rapamycin)/S6K1 (S6 kinase 1) pathway, which regulates protein synthesis in response to nutrient availability (Backer, 2008).

1.3 SIGNALLING DOWNSTREAM OF CLASS I PI3K

As mentioned in the introduction, class I PI3K preferentially produce PIP_3 at the inner leaflet of the plasma membrane. A wide variety of cell-surface receptors stimulate class I PI3Ks, such as growth factors, inflammatory stimuli, hormones, neurotransmitters and antigens (Hawkins, et al., 2006). PIP_3 acts as a docking site for a wide variety of proteins containing the lipid-binding PH domain, including proteins include serine/threonine kinases, tyrosine kinases, nucleotide exchange factors, GTPase-activating factors, phospholipases and adaptor proteins, which mediate a diverse array of cellular functions (Hawkins, et al., 2006; Vanhaesebroeck & Waterfield, 1999) (Figure 1.4). PI3K activation, therefore, represents one of the most prevalent and varied signal transduction events associated with mammalian cell-surface receptor activation.

The precise mechanism of activation of PI3K effector proteins through engagement of PH domains with PIP_3 is, in most cases, not clear. However, in several cases the interaction is of sufficient affinity to target the effector protein from the cytoplasm to the plasma membrane (plasma-membrane translocation). This translocation brings the effector protein into proximity with substrates or binding partners. PIP_3 binding to PH domains can also relieve PH domain-mediated intramolecular inhibition in the effector protein, thereby activating the effector downstream pathways (Hawkins, et al., 2006).
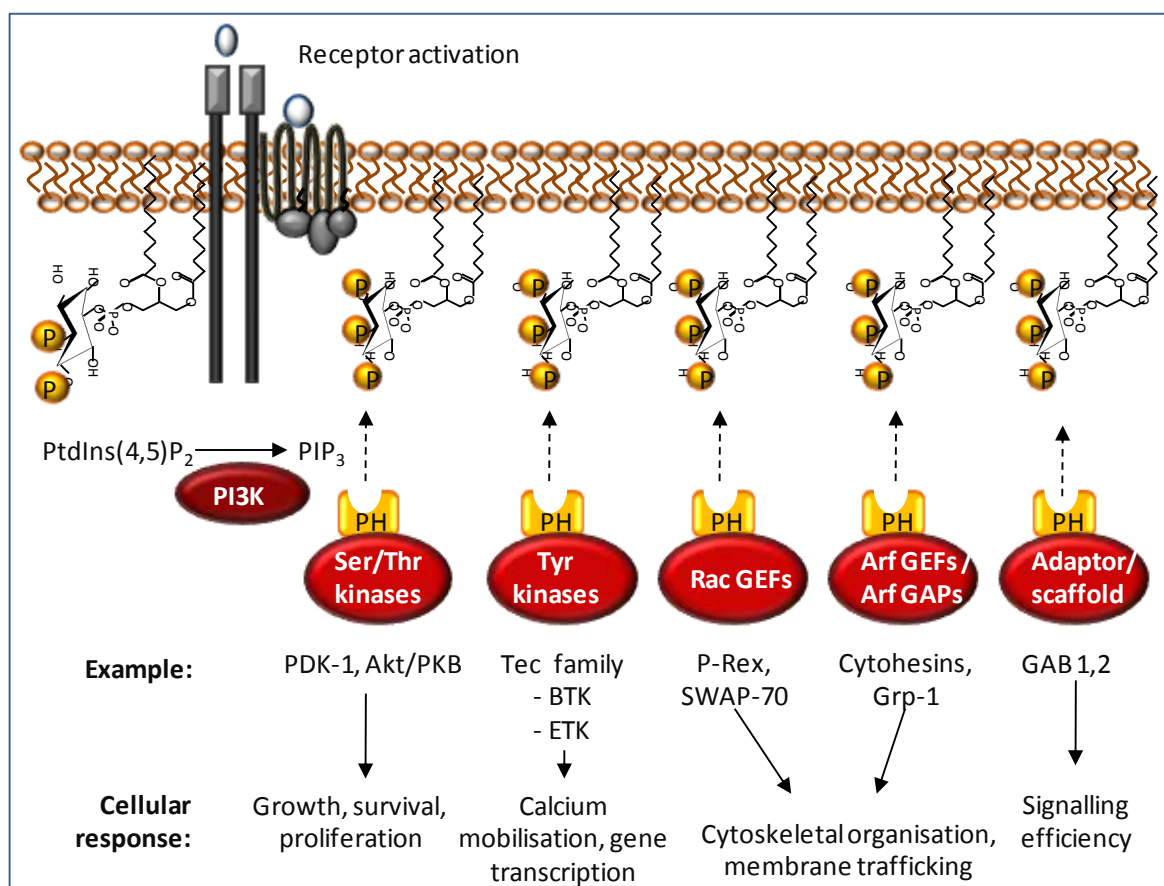
Figure 1.4: Downstream effectors of class I PI3K. There are a number of PH domain-containing proteins that act as downstream effectors of class I PI3K activation. These include Ser/Thr kinases, tyrosine kinases, regulators of small GTPases such as GAPs and GEFs and adaptor or scaffold proteins. These effector proteins regulate diverse cellular responses such as cell growth, cell survival, gene transcription and cytoskeletal organization.

1.3.1 PI3K activation of serine/threonine protein kinases

The serine/threonine protein kinase Akt (also known as PKB), is considered the major effector of the class I PI3K signalling pathway. Indeed, activation of class I PI3K is often assessed by the activation of Akt (since measuring the changes in PI products is relatively technically demanding). Full activation of Akt requires another PH-domain containing protein serine/threonine kinase, PDK1, which will be discussed in the next section.

In addition to translocating Akt to the plasma membrane, the interaction of the PH domain of Akt with PIP_3 is thought to relieve PH domain-mediated intramolecular inhibition, thus provoking a conformational change in Akt, resulting in the exposure of two main phosphorylation sites, Thr308 in the T-loop of its kinase domain and Ser473 located in a C-terminal non-catalytic region. Phosphorylation at both of these sites, Thr308 and Ser473, is necessary for full activation of Akt. In contrast, PDK1 appears to be

'constitutively active' and its activity is independent of PIP_3/PH domain binding. However, the ability of PDK1 to phosphorylate Akt on Thr308 in its kinase domain is highly dependent on the conformational change of Akt induced by class I PI3Ks, hence its name 3'-phosphoinositide-dependent kinase-1. PDK1 does not, however, phosphorylate Ser473 on Akt which is required for full activation of Akt. The kinase responsible for Akt Ser473 phosphorylation has remained elusive for many years and was initially termed 'PDK-2'. Recently, a rapamycin-insensitive form of mTOR protein kinase in complex with Rictor and GβL, termed the mTORC2 complex, has been proposed to phosphorylate Akt Ser473 (Sarbassov, *et al.*, 2005).

Akt plays a central role in multiple signalling pathways involved in cell survival, cell metabolism and proliferation pathways as shown in Figure 1.5. The involvement of Akt in certain aspects of these pathways is briefly discussed below.

Cell survival: One of the mechanisms by which Akt promotes cell survival is by phosphorylating and inhibiting the pro-apoptotic protein BAD (Bcl-2/Bcl-X_L antagonist, causing cell death). BAD binds and inhibits the anti-apoptotic proteins Bcl-2 and Bcl-X_L, therefore Akt inhibition of BAD allows Bcl-2 and Bcl-X_L to exert their anti-apoptotic effects. Another pro-apoptotic protein, Caspase-9, is also phosphorylated and inhibited by Akt (Hawkins, et al., 2006; Vanhaesebroeck & Waterfield, 1999).

Akt is also a major regulator of the forkhead box (FOXO) family of transcription factors. All mammalian FOXO proteins have highly conserved sites for phosphorylation by Akt, which include FOXO1 (FKHR), FOXO3a (FKHRL1), FOXO4 (AFX) and FOXO6 in humans (Huang & Tindall, 2007). Akt-phosphorylated FOXO proteins bind to 14-3-3 chaperone proteins and become sequestered in the cytoplasm, where they are unable to regulate gene expression. Gene expression regulated by FOXO proteins include the pro-apoptotic gene, Fas Ligand (*FasL*), which encodes a protein that activates the death receptor Fas/CD95/APO-1 and promotes mitochondria-independent apoptosis (Huang & Tindall, 2007). In addition to the death receptor ligands, FOXO proteins have also been shown to be involved in the transactivation of *BIM*, a gene that encodes a member of the pro-apoptotic BH3-only subgroup of BCL-2 family proteins, which functions in a mitochondrial-dependent apoptotic pathway. Akt-induced sequestering of FOXO proteins in the cytoplasm therefore results in increased cell survival.
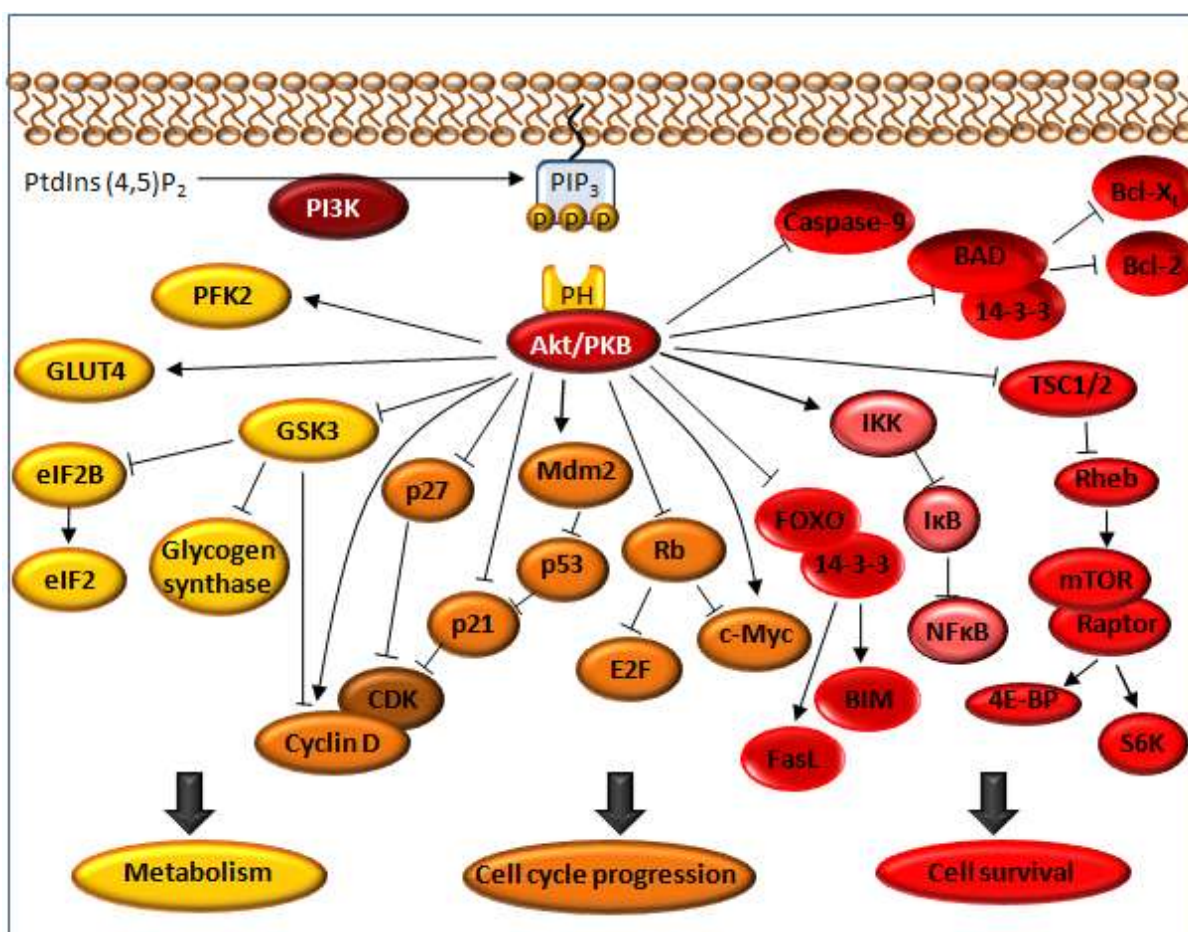
Figure 1.5: Signalling downstream of Akt activation. *Cell metabolism:* Akt activation regulates cell metabolism through phosphorylation and inhibition of GSK3 resulting in increased activation of glycogen synthase and the transcription factor eIF2B. PFK2 and GLUT4 are also activated downstream of Akt, which promote glycolysis and glucose uptake, respectively. *Cell cycle progression:* Akt activation promotes cell cycle progression through inhibiting p27 and p21, which would otherwise inhibit CDKs. Mdm2 is a phosphorylated and activated by Akt, which inhibits the tumour-suppressor activity of p53. Akt-induced inactivation of the tumour-suppressor retinoblastoma (Rb) and activation of c-Myc also promotes cell cycle progression. *Cell survival:* Akt promotes cell survival through inhibition of the FOXO family of transcription factors, which if active would induce transcription of pro-apoptotic proteins FasL and BIM. The pro-apoptotic proteins Caspase-9 and BAD are also inhibited by Akt. Akt activates NFκB-induced transcription by activating IKK which in turn phosphorylates and causes the degradation of inhibitor of NFκB, IκB. Akt phosphorylates and suppresses the TSC1/2 complex, resulting in increased activation of the Rheb GTPase and enhanced mTOR activity. The main downstream targets of mTOR are 4E-BP and S6K. It should be noted that there is overlap between the pathways involved in cell metabolism, cell cycle progression and cell survival.

NFκB is another factor involved in cell survival that has been identified as a functional target of Akt (Ozes, *et al.*, 1999). The NFκB family of transcription factors induce the expression of a wide variety of genes involved in cell survival, including the Bcl-2 family member Bfl-1, and the caspase inhibitors c-IAP1 and c-IAP2. Binding of NFκB to IκB sequesters it to the cytoplasm. Akt-induced phosphorylation of IκB kinase (IKK), result in

IκB degradation allowing NFκB to enter the nucleus and induce gene transcription (Khwaja, 1999). Akt-induced phosphorylation of IKK appears to be indirect and the exact mechanism of NFκB activation by Akt requires further investigation.

Cell metabolism: The first function that was attributed to Akt was glycogen metabolism. Upon stimulation of cells by insulin, Akt has been shown to phosphorylate a number of important components of the insulin signal transduction pathway: 1) Akt phosphorylates and inhibits glycogen synthase kinase 3 (GSK3) whose downstream targets include of glycogen synthase and translation initiation factor eIF2B; 2) Akt phosphorylates and activates 6-phosphofructo-2-kinase (PFK2), one of the enzymes that is involved in the glycolysis pathway; 3) Akt activates phospshodiesterase-3B (PDE-3B), an enzyme important in the regulation of the cellular concentration of the second messenger, cAMP; 4) activation of Akt by insulin may enhance glucose uptake by increasing the expression levels of the glucose transporters, GLUT1 and GLUT3 (Barthel, *et al.*, 1999); and 5) Insulin stimulates Akt activation of mTOR, an enzyme that regulates protein translation (Patel, *et al.*, 2002). mTOR is activated by the GTPase Rheb, which is negatively regulated by the TSC1/2GTPase-activating complex. Activation of Akt phosphorylates TSC1/2 suppressing the GTPase-activating effects of TSC1/2 on Rheb and enhances mTOR activity. The mTOR complex with Raptor mediates the phosphorylation of 4E-BP1 and S6K1, which stimulate translational initiation and contribute to cell growth. Akt can also activate mTOR through phosphorylation and relieving the inhibitory effect of PRAS40 (proline-rich Akt substrate of 40 kDa, which represses mTOR activity), a protein in complex with mTOR and Raptor (Wullschleger, *et al.*, 2006).

Cell cycle progression/proliferation: As described above, Akt activation of mTOR is involved in cell metabolism and also increased cell growth and proliferation. Numerous regulators of cell cycle progression are also activated Akt. Akt activity increases the transcription of c-Myc, which when overexpressed or hyperactivated is a strong promoter of cell cycle progression. Akt can also phosphorylate and deactivate the tumour suppressor retinoblastoma (Rb), which leads to activation of E2F, a transcription factor that drives cell cycle progression (Brennan, *et al.*, 1997). Furthermore, Akt activation leads to enhanced cyclin D1 expression, a protein that is involved in cell progression through the G_0 and G_1 stage of the cell cycle (see section 1.4.1.2 for a more detailed description of the cell cycle).

Akt activation is also associated with the regulation of the CDK (cyclin-dependent kinase) inhibitors p27 and p21. Both p27 and p21 function to block the activation of CDK-cyclin dimers, which inhibits cell cycle progression. Akt activation diminishes p27 expression levels and sequesters p21 to the cytosol, consequently promoting cells to advance through the cell cycle (Chakravarthy, *et al.*, 2000; Graff, *et al.*, 2000; Zhou, *et al.*, 2001)

Finally, the oncogene Mdm2 is a direct target of Akt in cell cycle regulation (Mayo & Donner, 2001). Mdm2 is a regulator of p53, a tumour suppressor that halts the cell-cycle in the G1 phase or triggers apoptosis in response to DNA damage or other cellular stresses. Mdm2 binds to and inhibits the tumour suppressor function of p53 by promoting its ubiquitin-dependent degradation. Akt phosphorylates and activates Mdm2, resulting in decreased p53 activity and therefore promoting cell cycle progression and cell survival (Mayo & Donner, 2001).

1.3.2 PI3K activation of protein tyrosine kinases

Tec/Btk tyrosine kinases are members of a subgroup of the Src tyrosine kinase family, which all share a homologous SH3/SH2/kinase core structure. Unlike Src family kinases Tec kinases do not contain an N-terminal membrane-targeting motif, they do however have an N-terminal PH domain. Similarly to membrane-targeting motif, the PH domain serves to target Tec family tyrosine kinases to the plasma membrane, where further activating phosphorylations occur.

Tec family members include Btk (Bruton's tyrosine kinase) and Itk (inducible T-cell kinase). The PH domain of Btk binds PIP_3 with high affinity. Btk is critical for B cell development and function and several germline mutations that map to the PH domain have been shown to cause immunodeficiency (Vanhaesebroeck & Waterfield, 1999).

1.3.3 PI3K activation of regulators of small GTPases

Small GTPases cycle between an active GTP-bound conformation and an inactive GDP-bound conformation. This cycle is regulated by guanine nucleotide exchange factors (GEFs) and GTPase activating proteins (GAPs). The regulation of small GTPases is discussed in more depth in section 1.4, but briefly, GEFs catalyse the exchange of GDP on small GTPases for GTP, activating the small GTPase. GAPs on the other hand stimulate the intrinsic GTPase activity of the small GTPases, resulting in hydrolysis of GTP to GDP and subsequent inactivation.

All GEFs for the Rho family of small GTPases (Rho, Rac and Cdc42) contain PH domains, along with GEFs for ARF family small GTPases. The binding of GEFs to PIP_3 is thought to relieve PH domain-mediated inhibition of the GEF Dbl catalytic domain, and also bring the GEF into proximity with its lipid-tethered GTPase (Hawkins, et al., 2006; Welch, *et al.*, 2003). A number of GAPs are also able to bind PIP_3, including the centaurins, GAP1[m], and GAP[IP4BP] proteins. The centaurins have homology to yeast GAPs for ARF-GTPases, whereas GAP1[m], and GAP[IP4BP] are Ras GAPs. Since the key regulators of small GTPases, namely GEFs and GAPs, are activated by PIP_3 production, it is not surprising that PI3K activation regulates the downstream cellular response of small GTPases. The Rho GTPases are involved in organisation of the cell cytoskeleton, which has implications in cell migration, cell cycle progression and cell adhesion (see section 1.4), whereas ARF GTPases play a role in vesicular membrane trafficking in several intracellular compartments (Vanhaesebroeck & Waterfield, 1999).

1.4 CONVERGING SIGNALLING PATHWAYS OF PI3K AND RHO GTPASES

1.4.1 Introduction to Rho GTPases

Rho GTPases are members of the Ras superfamily of monomeric 20 - 30 kDa GTP-binding proteins. Since the discovery of the Ras proto-oncogene more than 20 years ago (Barbacid, 1987) and the recognition that oncogenic mutations in the Ras genes occur frequently in human carcinomas, there has been a widespread effort in identifying other Ras-like small GTPases. Over 100 Ras-like GTPases are known to date. These can be classified into five main groups: Ras, Rab, Arf, Ran and Rho GTPases (Aspenstrom, *et al.*, 2004). The latter will be discussed in more detail here.

To date, twenty-two mammalian genes encoding different mammalian Rho GTPases family members have been described. These Rho GTPases can be divided into nine groups, most of which include multiple isoforms: Rho (A, B and C); Rac (1, 2 and 3); Cdc42, (Cdc42, TCL10, TCL, Chp, Wrch-1); RhoD (RhoD and Rif); Rnd (Rnd1, Rnd2, RhoE/Rnd3); RhoH/TTF; RhoBTB (RhoBTB1 and RhoBTB 2); RhoG; and Miro (Miro-1 and Miro-2) (Aspenstrom, et al., 2004; Hall, 2005). From these, RhoA, Rac1 and Cdc42 have been the most extensively studied and have been found to regulate specific aspects of actin-dependent cellular processes (Etienne-Manneville & Hall, 2002; Takai, *et al.*, 2001).

1.4.2 Regulation of Rho GTPases

Similar to other GTPases, Rho GTPases act as molecular switches, cycling between an active GTP-bound conformation and an inactive GDP-bound conformation (Figure 1.6).
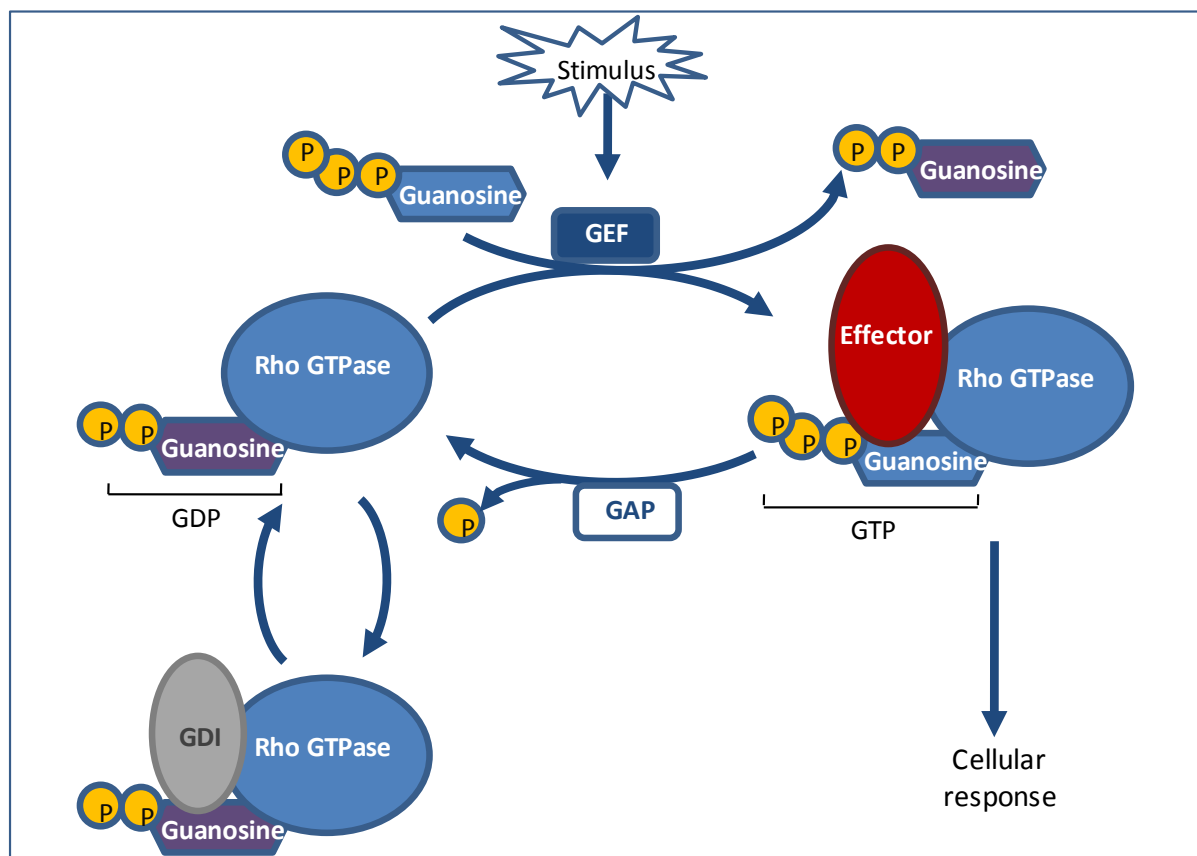
Figure 1.6: The Rho GTPase cycle. Rho GTPases cycle between an active GTP-bound conformation and an inactive GDP-bound conformation. GEFs replace GDP with GTP thereby activating Rho GTPase signalling pathways. GTP hydrolysis and therefore inactivation of Rho GTPases is facilitated by GAPs. GDIs also participate in inhibiting Rho GTPase signalling through binding GDP-bound Rho GTPases and preventing GDP-GTP exchange.

GEFs catalyse the exchange of GDP for GTP thereby activating the molecular switch. Conversely, GAPs increase the intrinsic enzymatic activity of the Rho GTPase resulting in the hydrolysis of GTP to GDP, thereby inactivating the switch (Takai, et al., 2001). Rho GTPases are further regulated by another class of regulators guanine dissociation inhibitors (GDIs) (Fukumoto, *et al.*, 1990; Hiraoka, *et al.*, 1992). GDIs appear to inhibit Rho GTPase activity by forming a soluble complex with GDP-bound Rho GTPase thus sequestering the complex in the cytoplasm and inhibiting their spontaneous GDP-GTP exchange activity. It is thought that in a resting cell, Rho GTPases reside in this inactive

GDI complex, which dissociates upon cell stimulation thereby allowing GDP-GTP exchange.

Over thirty GEFs have been identified although they still remain largely uncharacterised (Kjoller & Hall, 1999; Van Aelst & D'Souza-Schorey, 1997). All Rho-GEFs contain a Dbl-homology (DH) domain which encodes the catalytic activity and an adjacent PH domain (Bishop & Hall, 2000; Cherfils & Chardin, 1999). About twenty Rho-GAPs have been identified to date (Lamarche & Hall, 1994), eight of which are encoded on chromosome 22 (Dunham, *et al.*, 1999). Table 1.1 lists the main regulators of the best characterised Rho GTPases Rho, Rac and Cdc42.

Regulator	Substrate
GEFs	
Dbl	Rho, Rac, Cdc42
Vav1	Rho, Rac, Cdc42
Dbs	Rho, Cdc42
Lbc	Rho
Lfc	Rho
Vav2	Rho
p115	Rho
PDZ-Rho-GEF	Rho
Tiam-1	Rac
Sos	Rac, (Ras)
p-Rex1	Rac
SWAP-70	Rac
FGD1	Cdc42
Frabin	Cdc42
GAPs	
p50 RhoGAP	Rho, Rac, Cdc42
p190 RhoGAP	Rho, Rac, Cdc42
Graf	Rho
myr5	Rho, Cdc42
Bcr	Rac, Cdc42
n-Chimaerin	Rac, Cdc42
3BP-1	Rac
Abr	Rac
GDIs	
Rho GDI	Rho
D4/Ly-GDI	Rho
Rho GDI-3	RhoB (not RhoA or C)

Table 1.1: Regulators of the Rho GTPase proteins Rho, Rac and Cdc42. The GEFs, GAPs and GDIs listed have various degrees of specificity for each Rho GTPase. Adapted from Takai *et al*, 2001.

1.4.3 Effector proteins of Rho GTPases

The nucleotide-dependent alteration of protein conformation of Rho GTPases enables the enzyme to relay intracellular signals (Aspenstrom, et al., 2004). In the active GTP-bound conformation, Rho GTPases bind a specific set of downstream effector proteins. To date, around thirty potential effectors for Rho GTPases have been identified, which are listed in Table 1.2 (Bishop & Hall, 2000). The most common mechanism of effector activation by Rho GTPases appears to be the disruption of autoinhibitory interactions, to expose functional domains within the effector protein (Bishop & Hall, 2000).

Effector Protein	Type of protein	Functions	Rho GTPase selectivity
ROCKα, ROCKβ	Ser/Thr kinase	Actin/myosin	Rho
PKN/PRK1, PRK2	Ser/Thr kinase	Unknown	Rho
Citron kinase	Ser/Thr kinase	Cytokinesis	Rho
p70 S6 kinase	Ser/Thr kinase	Translation	Rac, Cdc42
Mlk2, 3	Ser/Thr kinase	JNK	Rac, Cdc42
MEKK1, 4	Ser/Thr kinase	JNK	Rac, Cdc42
PAK1, 2, 3	Ser/Thr kinase	JNK/actin	Rac, Cdc42
PAK 4	Ser/Thr kinase	Actin	Cdc42
MRCKα, MRCKβ	Ser/Thr kinase	Actin	Cdc42
Ack1,2	Tyr Kinase	Unknown	Cdc42
MBS	Phosphatase subunit	MLC inactivation	Rho
PI-4-P5K	Lipid kinase	PIP$_2$ levels/actin	Rho, Rac
PI3K	**Lipid kinase**	**PIP$_3$**	**Rac, Cdc42**
DAG kinase	Lipid kinase	PA levels	Rho, Rac
PLD	Lipid kinase	PA levels	Rho, Rac, Cdc42
PLC-β2	Lipid kinase	DAG/IP$_3$ levels	Rac, Cdc42
Rhophilin	Scaffold	Unknown	Rho
Rhotekin	Scaffold	Unknown	Rho
Kinectin	Scaffold	Kinesin binding	Rho
Dia1, Dia2	Scaffold	Actin organisation	Rho
WASP, N-WASP	Scaffold	Actin organisation	Cdc42
WAVE/Scar	Scaffold	Actin organisation	Rac
POSH	Scaffold	Unknown	Rac
POR-1	Scaffold	Actin organisation	Rac
p140Sra-1	Scaffold	Actin organisation	Rac
p67^{phox}	Scaffold	NAPDH oxidase	Rac
MSE55, BORGs	Scaffold	Unknown	Cdc42
IQGAP1, 2	Scaffold	Actin/cell-cell contacts	Rac, Cdc42
CIP-4	Scaffold	Unknown	Cdc42

Table 1.2: Potential effector proteins for Rho, Rac and Cdc42. Where a function for the Rho GTPase effector protein has been reported it is noted, but in many cells this is far from clear. Table adapted from Bishop *et al*, 2000.

1.4.4 PI3K: A downstream effector or upstream regulator of Rho GTPases?

The p85 regulatory subunit of PI3K contains a region of homology to the Rac GAP domain in Bcr (BH domain) (Fry, 1992). Although highly homologous, the BH domain in p85 differs from the Bcr Rac GAP domain at residues critical for GAP activity, suggesting p85 BH domain does not activate the intrinsic GTPase activity of Rho GTPases but retains the ability to bind small GTP binding proteins (Beeton*, et al.*, 1999). However, relatively recently, GAP activity of the p85α BH domain has been reported towards Rab5, Rab4, Cdc42, Rac1 and to a lesser extent Rab6, with little GAP activity toward Rab11 (Chamberlain*, et al.*, 2004). In a follow up study, disruption of the Rab GAP function of p85α, due to a single point mutation, was found to be sufficient to cause cellular transformation, although PI3K signalling appeared unaltered (Chamberlain*, et al.*, 2008).

In addition to the presence of a p85 BH domain, Rho GTPases and PI3Ks have several overlapping cellular functions. These observations have lead to a number of studies investigating the potential partnership between PI3K and Rho GTPases in regulating their converging signalling pathways.

Both Rac1 and Cdc42 have been found to bind PI3K *in vitro* (Zheng*, et al.*, 1994). Using an immobilised glutathione S-transferase (GST)-Rho GTPase fusion protein in either a GDP or GTP-bound state, GTP-bound Cdc42 and Rac-1 (but not RhoA) were found to bind the regulatory subunit of PI3K, p85. GTP-bound Cdc42 was further found to activate PI3K activity, albeit weakly (Zheng, et al., 1994). In another later study, PI3K activity has also been found to be associated with GTP-bound Cdc42 and also GTP-bound Rac1 *in vitro* (Tolias*, et al.*, 1995). Consistent with the earlier study by Zheng *et al*, PI3K activity was not associated with RhoA and the GTP-bound forms of Cdc42 and Rac1 were associated with increased PI3K activity compared to their GDP-bound forms. To further corroborate these findings, highly purified bovine brain p85 was found to immunoprecipitate with Rac1 and Rac2 (but not with RhoA) and p85 binding was increased when Rac was in a GTP-bound active conformation (Bokoch*, et al.*, 1996). The Bcr homology domain of p85 was indicated to be involved in the interaction between p85 and Rac1 as the isolated p85 Bcr domain showed similar levels of Rac-1 binding when compared to full-length p85 (Bokoch, et al., 1996). To corroborate these findings, a mutation in the BH domain and not SH3 domain of p85α has been found to inhibit GTP-loaded Rac-induced lipid kinase activity in p85α/p110 heterodimers (Beeton, et al., 1999).

Various cell lines have been used to investigate the potential *in vivo* capacity of Rho GTPases to interact with PI3K. Cdc42 has been found to be constitutively associated with high PI3K activity in Cdc42 immunoprecipitates from COS7 cells, whereas only a small amount of PI3K activity was detected in Cdc42 immunoprecipitates from PDGF-stimulated Swiss 3T3 cells (Tolias, et al., 1995). On the contrary to Cdc42, the *in vivo* association of Rac1 with PI3K has been found to be clearly regulated by PDGF stimulation in Swiss 3T3 cells (Tolias, et al., 1995). These results highlight the cell type and stimulus-dependency of Rho GTPase regulation.

Collectively, these investigations suggest that the interaction of PI3K with Rac is dependent on Rac/Cdc42 activation, thus placing PI3K downstream of Rac. However, there is a growing body of evidence that suggests the contrary, that PI3K may be upstream of Rac activation. Dominant-negative PI3K constructs or the PI3K inhibitor wortmannin inhibit the Rac-dependent pathways of PDGF and insulin-stimulated membrane ruffling (Hawkins*, et al.*, 1995; Kotani*, et al.*, 1995). More conclusively proof lies in that in Rac-overexpressing endothelial cells, PDGF-stimulated Rac GTP-loading is sensitive to wortmannin (Hawkins, et al., 1995).

It has been suggested that PI3K regulates Rac activation via inhibition of Rac GTPase activity and secondly, by activating a PIP_3-sensitive Rac-GEF and increasing nucleotide exchange (Hawkins, et al., 1995). Among the Rac-GEFs identified, members of the Vav, Sos, Tiam, PIX, SWAP-70 and P-Rex families have been suggested to be regulated by PI3K *in vivo*. PIP_3 directly binds and strongly activates the Rac-GEF activities of P-Rex1 and SWAP-70 *in vitro* (Shinohara*, et al.*, 2002; Welch*, et al.*, 2002), and weakly activates those of Vav1, Sos1 and possibly Tiam1 (Han*, et al.*, 1998; Innocenti*, et al.*, 2003). The ability of PI3K/PIP_3 to activate the other Rac-GEFs has not yet been studied (Welch, et al., 2003). Indeed, PIP_3 can also directly bind Rac *in vitro* and at high concentrations PIP_3 facilitates the dissociation of GDP from Rac. However PIP_3 preferentially binds the nucleotide-free form of Rac and does not promote GTP loading, therefore the significance of this interaction *in vivo* is unclear (Missy*, et al.*, 1998).

Recently, PI3K, specifically p110δ, has been shown to negatively regulate RhoA activity in macrophages (Papakonstanti*, et al.*, 2007). Under basal and CSF-1 stimulated conditions, macrophages homozygous for p110δ inactivation (p110δ$^{D910A/D910A}$) display increased levels of RhoA-GTP compared to wild-type macrophages. In contrast, upon CSF-1 stimulation, Rac-GTP levels are reduced in p110δ$^{D910A/D910A}$ macrophages. In

p110$\delta^{D910A/D910A}$ macrophages, p190RhoGAP activity is also decreased, which is accompanied by an increase in the phosphatase activity of PTEN. Furthermore, p110$\delta^{D910A/D910A}$ macrophages were found to have decreased cytosolic p27 upon CSF-1 stimulation. Cytosolic p27 has been reported to bind and inhibit RhoA, and in accordance with this in wild-type macrophages a greater proportion of RhoA was found to bind p27 than in p110$\delta^{D910A/D910A}$ macrophages. A signalling pathway was proposed to explain these findings, in which p110δ activation negatively regulates RhoA activity by increasing the activity of p190RhoGAP and increasing the cytoplasmic proportion of p27. If p110δ activity is inhibited, either genetically or pharmacologically, the negative regulators of RhoA are suppressed resulting in activation of RhoA and its downstream effector ROCK, which in turn activates PTEN and its phosphatase activity for PIP$_3$. This proposed pathway introduces an interesting concept of p110δ, and possibly other p110 isoforms, regulating its own activity via a feedback loop involving RhoA and PTEN (Papakonstanti, et al., 2007).

Cumulatively, these findings paint a somewhat confusing picture of the regulation of Rho GTPases by PI3K. On the one hand, PI3K interaction with Rac appears to be downstream of Rac activation and on the other hand the activation of Rac appears to be a target of PI3K, placing PI3K upstream of Rac. A positive feedback loop has been suggested, in which Rac once activated by PI3K, can in turn further activate PI3K. This feedback loop may play an essential role is establishing cell polarity in neutrophils (Weiner, *et al.*, 2002). In the case of RhoA, PI3K, specifically p110δ, appears to be an upstream negative regulator of RhoA activity (Papakonstanti, et al., 2007).

It is apparent however, that PI3K is not solely activated by Rac (Welch, et al., 2003). Inversely and just as clear, is that Rac activation is not exclusively PI3K-dependent, an example being PI3K-dependent but Rac-independent insulin-stimulated glucose transport (Marcusohn*, et al.*, 1995; Welch, et al., 2003). The relative importance of PI3K-dependent versus PI3K-independent pathways of Rac activation for a given downstream response is still unclear in most circumstances and requires further investigation (Welch, et al., 2003).

1.4.5 Biological functions of Rho GTPases

The first described biological function of Rho GTPases was regulating the assembly and organisation of the actin cytoskeleton. A plethora of cellular processes are regulated by changes in the actin cytoskeleton such as cell migration, cell cycle progression, cell-cell

interactions, cell adhesion, phagocytosis, pinocytosis, axon guidance and morphogenesis thereby indicating Rho GTPases as multifaceted cellular regulators. Furthermore, it is now known that Rho GTPases are involved in several other cellular processes such as transcriptional activation and cell growth. An outline of the role Rho GTPases play in these biological functions is discussed below.

1.4.5.1 Regulation of the actin cytoskeleton*:* The actin cytoskeleton of mammalian cells is composed of actin filaments and actin-binding proteins. Filamentous actin is generally organised into three discrete structures: 1) Filopodia - thin, dynamic finger-like protrusions comprising tight bundles of long actin filaments in the direction of the protrusion. They can change their length rapidly, span many cell diameters, and interact with other cells; 2) Lamellipodia – flat protrusive actin sheets that form at the leading edge of fibroblasts and many motile cells. Membrane ruffles observed at the leading edge of cells results from lamellipodia that lift up off the substrate and fold backward; 3) Actin stress fibres – bundles of actin filaments that traverse the cell and are linked to the extra cellular matrix (ECM) through focal adhesions (Van Aelst & D'Souza-Schorey, 1997).

Rho, Rac and Cdc42 have each been linked to each of the distinct types of actin assembly. Studies carried out using quiescent Swiss 3T3 fibroblasts, a cell line that has a low background of organised F-actin structures under serum-starvation conditions, have lead to the designation of Rho as a regulator of actin-myosin stress fibre assembly, Rac as a regulator of lamellipodia assembly, and Cdc42 as a regulator of filopodia assembly (Figure 1.7) (Kozma*, et al.*, 1995; Ridley & Hall, 1992; Ridley*, et al.*, 1992). In a brief summary of the findings leading to these conclusions; LPA induces stress fibres and associated focal adhesions, which is blocked by C3 transferase, a Rho inhibitor (Ridley & Hall, 1992). Growth factors, such as PDGF, insulin or EGF induce the formation of lamellipodia and membrane ruffles associated with focal contacts, a response that is blocked by the dominant-negative [Asn^{17}]Rac (Ridley, et al., 1992). Finally, bradykinin induces the formation of peripheral filopodia, which are also associated with focal contacts, and this is inhibited by dominant-negative [Asn^{17}]Cdc42 (Kozma, et al., 1995). It should be noted however, that although these findings define specific roles for Rho GTPases in Swiss 3T3 cells, the specific roles for Rho, Rac and Cdc42 in regulating the actin cytoskeleton are variable and cell type-dependent.
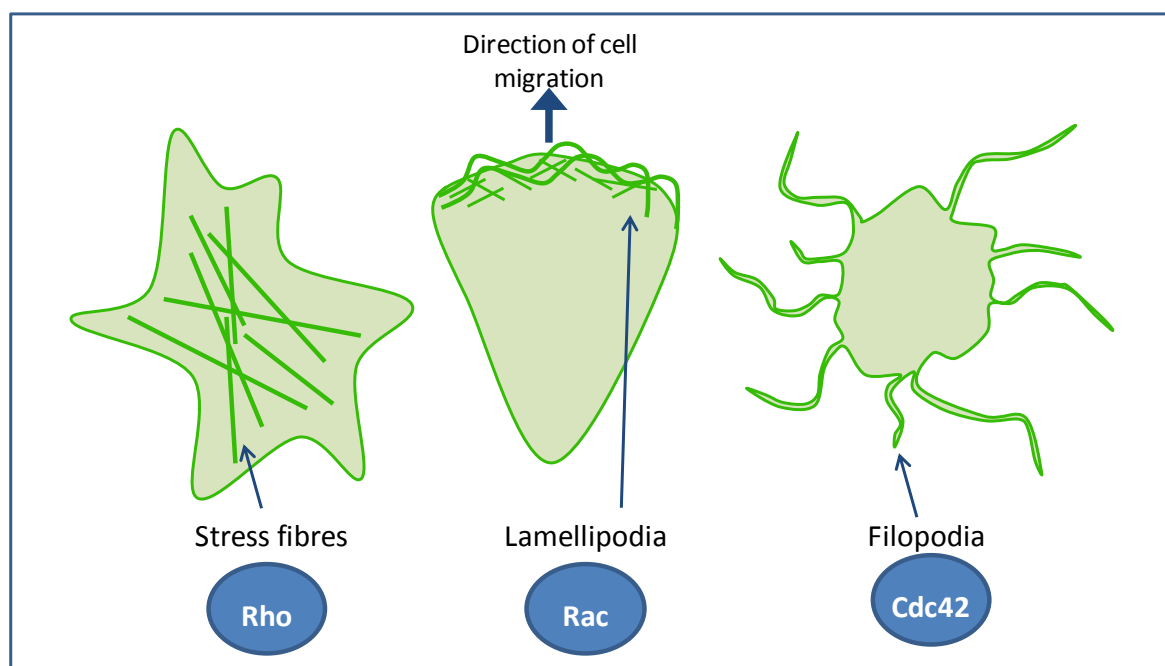
Figure 1.7: Schematic to show the types of actin filament organisation specifically induced by Rho, Rac or Cdc42 activation in Swiss 3T3 cells.

Actin filaments are polar, with a fast-growing barbed end (+ end) and a slow-growing pointed end (- end). Actin filament polymerisation occurs mostly at the barbed end and depolymerisation at the pointed end and is tightly controlled by regulatory proteins. Two major polymerisation factors are Arp2/3 and Formin. Rac and Cdc42 activate Arp2/3 via WAVE [a WASP (Wiskott-Aldrich syndrome protein) family protein] and WASP, respectively to initiate a branched filament network (Jaffe & Hall, 2005). Rho stimulates actin polymerisation in mammalian cells through diaphanous-related formin, mDia1. Rho directly activates mDia to expose a FH2 domain that binds to the barbed end of actin filaments. mDia1 also has a FH1 domain which mediates the delivery of a profilin/actin complex to the filament end (Jaffe & Hall, 2005).

1.4.5.2 Cell cycle progression: The eukaryotic cell cycle consists of four main phases, a DNA replication or synthesis phase (S) and a nuclear/cell division or mitotic phase (M) separated by two gap phases (G1 and G2) (Figure 1.8). Rho GTPases are required for progression through the G1 and M phase. Inhibition of Rho, Rac or Cdc42 blocks G_1 progression in a variety of cell types but the precise mechanism of Rho GTPase involvement is unclear and appears to be cell-type dependent (Olson*, et al.*, 1995; Yamamoto*, et al.*, 1993).
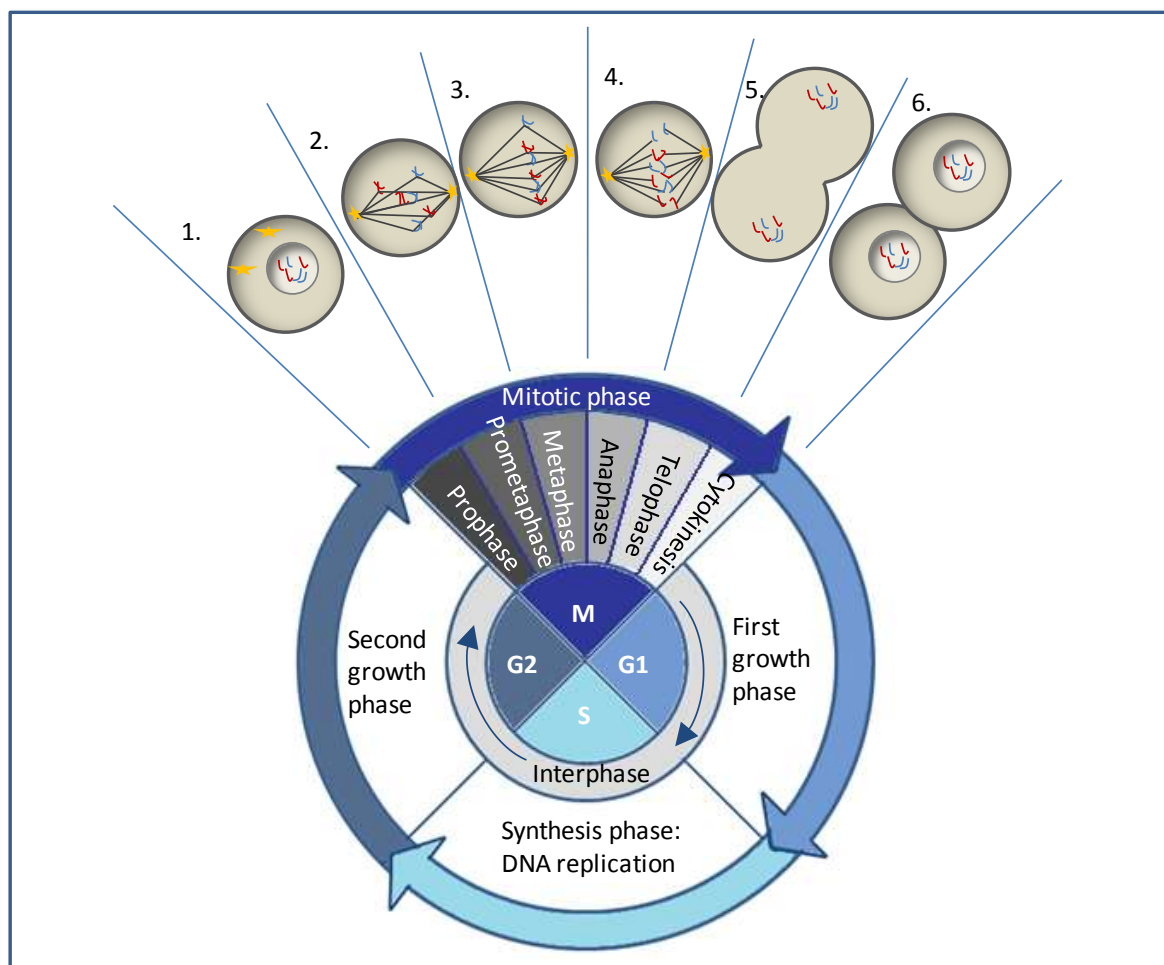
Figure 1.8: The cell cycle. The cell cycle is divided into the first growth phase (G_1), the DNA replication or synthesis phase (S), the second growth phase (G_2) and the mitotic phase (M). The M phase is further subdivided into 6 phases: 1) Prophase – each chromosome has duplicated and now consists of two sister chromatids. At the end of prophase, the nuclear envelope breaks down; 2) Prometaphase – mitotic spindles (formed from bundles of microtubules) from centrosomes attach to the kinetochore of chromosomes; 3) Metaphase – chromosomes line up along the *metaphase plate*; 4) Anaphase – sister chromatids are cleaved and pulled apart by shortening kinetochore microtubules towards their respective centrosome at opposite ends of the cells; 5) Telophase – microtubules that are not attached to kinetochores continue to length to elongate the cell. New nuclear envelopes form around the set of separated sister chromatids; 6) Cytokinesis – this is not technically a part of mitosis but is an essential process to complete cell division. A cleavage furrow and associated contractile ring forms where the metaphase plate used to be and pinches the cell into two daughter cells.

G_1 progression is controlled by two types of cyclin-dependent kinases, CDK4/CDK6 and CDK2, which are activated by binding to cyclin D and cyclin E, respectively. Rho GTPases are involved in the temporal control of cyclin D expression, although the specific role of Rho, Rac and Cdc42 and how they work together in this temporal control remains ambiguous (Joyce, *et al.*, 1999; Welsh, *et al.*, 2001). Rho GTPases also regulate the levels of the CDK2 inhibitors, p21[Cip1] and p27[Kip1] (Weber, *et al.*, 1997). The critical role of Rho

GTPases for G_1 progression is also thought to reflect the dependency on the cell for anchorage and adhesion signals for proliferation.

The M phase of the cell cycle is when nuclear division and cytokinesis (cyoplasmic division) occurs. The M phase is divided into the prophase, prometaphase, metaphase, anaphase and telophase. Microtubules make up the spindle fibres, which emanate from the two centrosomes, and play a major role during cell cycle progression through the M phase, driving the alignment and separation of chromosomes during prophase and metaphase. Microtubules are polarised polymers of α- and β-tubulin dimers and are a key component of the cytoskeleton. The minus end is usually anchored at the centrosome and the dynamic plus end usually at the cell periphery. It has been shown that ROCK, the main downstream effector of Rho, controls the actin-myosin filaments at the cell cortex required for the positioning of the centrosomes (Rosenblatt, *et al.*, 2004).

At the end of mitosis, two identical daughter cells form through cytokinesis. Cytokinesis results through the assembly of a cleavage furrow and an associated contractile ring consisting of actin and myosin filaments. When the fibre ring around the centre of the cell contracts, it pinches the cell into two daughter cells. Rho plays a crucial role in contractile ring function and localizes to the cleavage furrow along with at least three known effectors, ROCK, Citron kinase and mDia (Glotzer, 2001; Jaffe & Hall, 2005).

1.4.5.3 Cell migration: Apart from leukocytes, most cells in the human body are immotile, aside from during development and wound healing. Cell migration in the latter two processes is considerably slower than leukocyte chemotaxis and non-leukocytes do not move as single cells, but attached to one another (Barber & Welch, 2006). During cancer progression, subsets of tumour cells change from an immotile to motile state, which may lead to metastasis.

For directed leukocyte cell migration, cells first establish a polarised morphology. This involves cells responding to extracellular cues, such as chemokine gradients, growth factors or ECM molecules, resulting in relocation of signalling molecules. Subsequent actin polymerisation and filament elongation at the front of the cell, coupled to actin-myosin filament contraction in the rear of the cell results in the transformation of the cell from a spherical shape to an asymmetric polarised state with a leading edge and a trailing uropod (Figure 1.9) (Barber & Welch, 2006; Ridley, *et al.*, 2003).
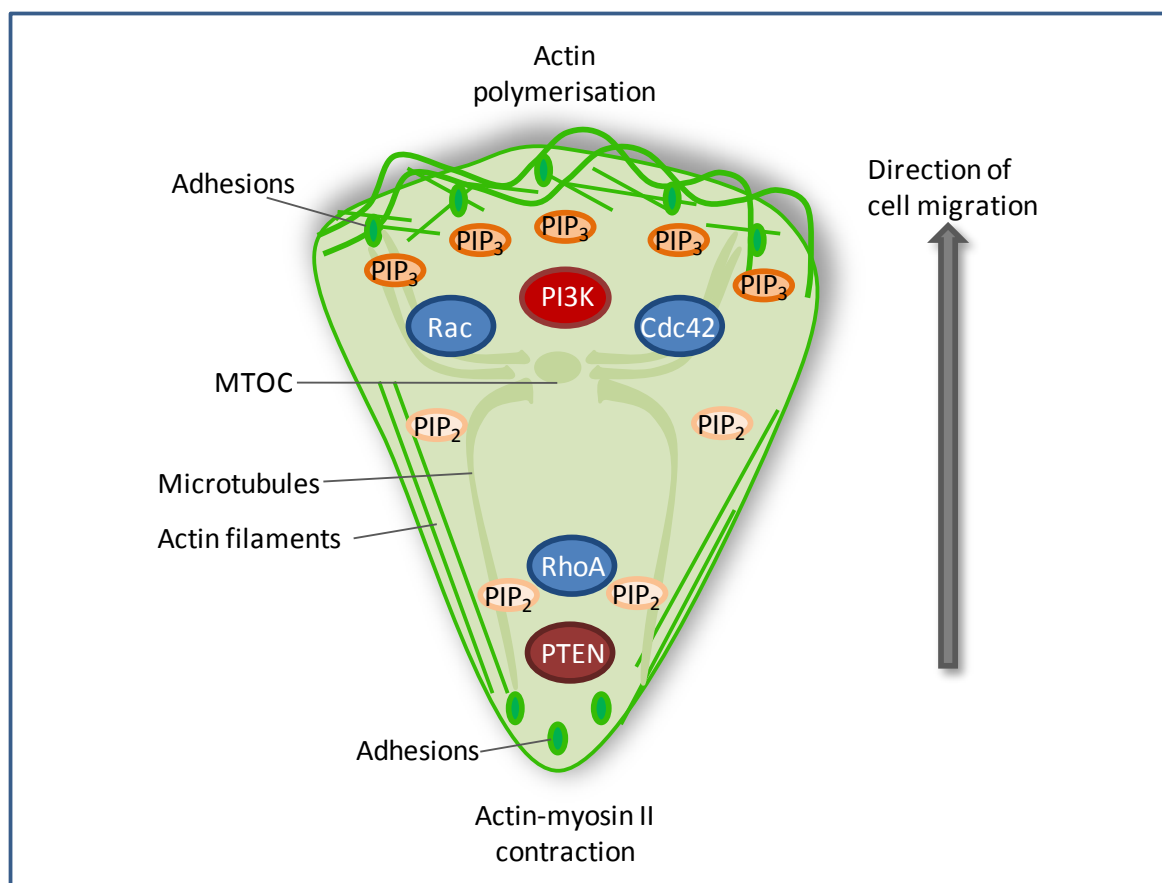
Figure 1.9: PI3K and Rho GTPases in cell polarisation and migration. In the presence of a chemoattractant gradient PIP_3 is produced at the leading edge of the cell through activation of PI3K. The polar distribution of PIP_3 in the cell is enhanced through localized phosphatase activity of PTEN at the rear and sides of the cell, which dephosphorylates PIP_3 to PIP_2. Cdc42 is essential for cell polarisation and is localized at the leading edge along with Rac. Activation of Cdc42 and Rac results in activation of WASP/WAVE proteins that regulate the formation of actin branches and cell protrusions and the cells leading edge. Protrusions are stabilised by the formation of adhesions, requiring integrin activation and clustering. Rho is located at the rear of the cell and is involved in disassembling cell adhesions and rear cell contraction to drive the cell forward. Figure adapted from Ridley *et al*, 2003.

PI3K and Rho GTPases are key signalling molecules regulating cell polarisation and migration. PIP_3 is localized at the leading edge of the cell and seems to be maintained through spatially and temporally positive feedback and negative regulation. PIP_3 stimulates PI3K to synthesis more PIP_3, a positive feedback loop which is likely to involve localized Rac and Cdc42 activity. In addition, Cdc42 has been found to be essential for maintaining cell polarity (Allen*, et al.*, 1998; Nobes & Hall, 1999). The phosphoinositide phosphatase, PTEN, is localized in the rear of the cell and catalyses the conversion of PIP_3 to PIP_2 thereby maintaining an accumulation of PIP_3 at the leading edge (Funamoto*, et al.*, 2002; Iijima & Devreotes, 2002). RhoA, localized in the rear of the cell, activates PTEN

indirectly through its downstream effector ROCK (Li*, et al.*, 2005). PIP$_3$ at the leading edge binds a large group of proteins that contain PH domains, which are subsequently translocated and/or activated in the process and mediate the PI3K signal. Indeed, as mentioned in section 1.4.4, a number of Rac-GEFs are activated by PIP$_3$, which accounts for localized Rac activity at the cells leading edge.

Actin polymerisation at the leading edge of the cell result in broad lamellipodia or spike-like filopodia protrusions, mediated by Rac and Cdc42 activity, respectively. Protrusions are stabilised by adhesions to the ECM mediated by integrin receptor activation, which serve as traction sites for migration as the cell moves forward over them. Adhesions are disassembled at the cell rear to allow cell detachment, a process promoted by Rho (Ridley, et al., 2003).

The force directing cell migration is generated from the interaction of myosin II with actin filaments attached to sites of adhesion. Myosin II activity is positively regulated by myosin light-chain (MLC) phosphorylation by MLC kinase (MLCK) or ROCK and negatively regulated by MLC dephosphorylation by MLC phosphatase. MLC phosphatase is itself phosphorylated and inhibited by ROCK. Active Rho, being directly upstream of ROCK, therefore plays a major role in cell contractility and transmission of tension to sites of adhesion (Ridley, et al., 2003; Riento & Ridley, 2003).

As for most cellular processes, the model of cell migration described above does not apply in all cell types. Recent migration studies have revealed striking differences between tumour cell migration on two-dimensional tissue culture plates and migration in three-dimensional matrices. In a three dimensional matrix, neither Rho nor ROCK activity was required in some tumour cells (Sahai & Marshall, 2003). It is likely that more *in vivo* studies will further our understanding the roles of Rho GTPases and PI3K in cell migration.

1.4.5.4 Cell-cell interactions: The morphogenesis of many cell types is driven by the assembly of distinct cell-cell adhesion complexes (Jaffe & Hall, 2005). For example, in epithelial cells, Rho GTPases regulate the formation of specialised junctional adhesion complexes, namely tight junctions and adherens junctions (AJs), which are required for the barrier function of epithelial layers and to establish apical-basolateral polarity (Malliri & Collard, 2003). In fibroblasts, AJs are the major junctional apparatus.

AJs enhance cell-cell contacts through linking transmembrane cadherin receptors, and recently identified nectin molecules, in neighbouring cells to the cytoskeleton. Cadherins are calcium-dependent cell-cell adhesion molecules, which have a single extracellular cytoplasmic domain, a transmembrane region, and a cytoplasmic domain. The extracellular domain mediates homophilic recognition and interaction with cadherin dimers on neighbouring cells (Figure 1.10). The cytoplasmic region is linked to the actin cytoskeleton through many peripheral proteins, including p120-catenin, β-catenin, α-catenin, α-actinin, and vinculin (Fukuyama, *et al.*, 2006). Rho, Rac, and Cdc42 have been implicated in AJ assembly, stability and dissolution, through regulation of cadherin function, which is dependent on cell-type.
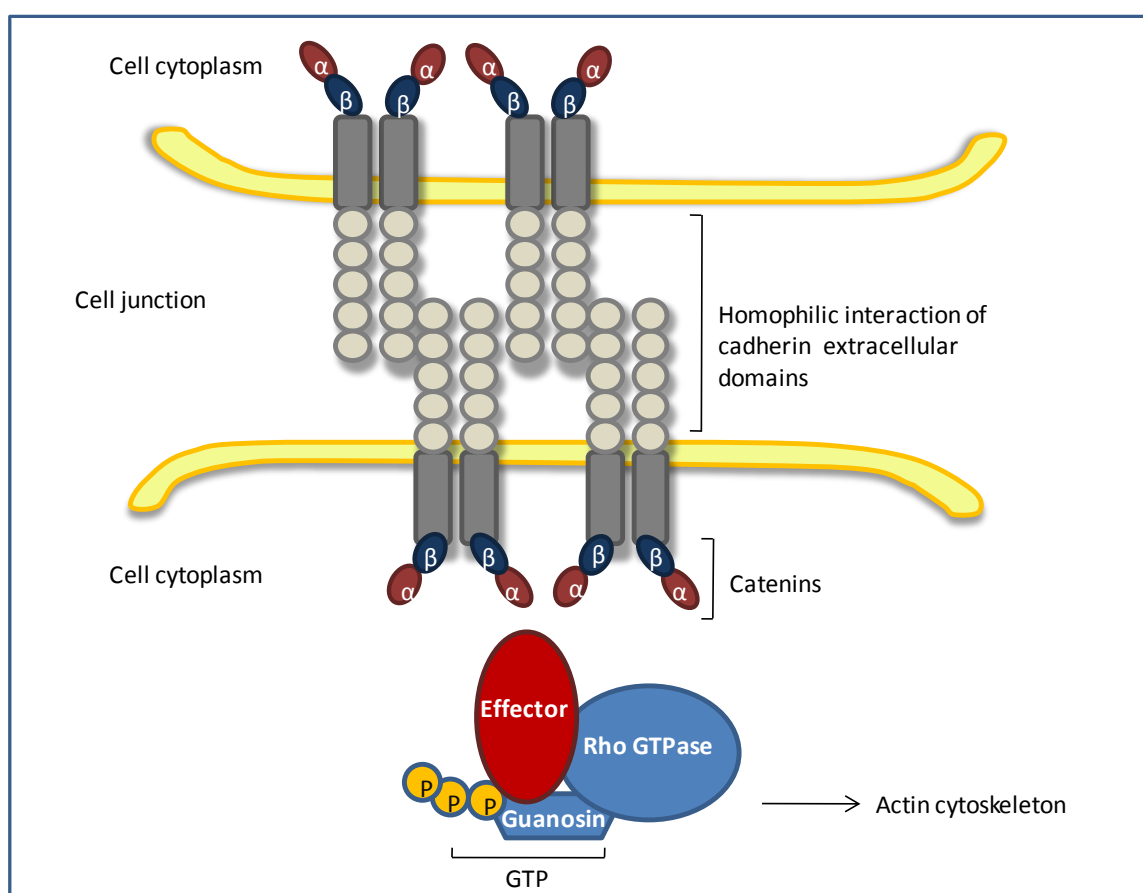
Figure 1.10: Cell-cell interactions mediated by cadherin. Cadherin receptors form dimers at the cell membrane that can interact with the same molecular dimers on neighbouring cells (homophilic binding) through its extracellular domain. This results in lateral clustering of cadherin complexes at sites of cell-cell contact. Calcium ions are required for stabilisation of the homophilic interaction and for association of the receptors to the actin cytoskeleton, mediated through Rho GTPases. The intracellular domain of cadherin receptors are constitutively associated with cytoplasmic catenin proteins such as α-catenin and β-catenin.

E-cadherin, expressed mainly on epithelial cells, activates Rac which stabilises AJs though inhibition of E-cadherin endocytosis mediated by IQGAP (Kuroda, *et al.*, 1998). It has

also been suggested that AJs stabilisation/formation is through localized induction of filopodia and/or lamellipodia (through Cdc42 and Rac activation, respectively) which drive intimate contacts between adjacent cells. Activation of Rac by E-cadherin has been found to be dependent on PI3K in L-cells stably expressing E-cadherin (Fukuyama, et al., 2006). As Rac is seemingly involved in two opposing processes, namely cell migration and AJ formation, it is fitting that Rac function is largely cell-type and environment-dependent.

Signalling through Rho has been found to both regulate the formation and dissolution of cell junctions. Constitutively active RhoA can induce an increase in the tightness of TJs in MDCK cells, which is mediated by Rho-associated kinase and a yet-to-be identified Rho effector (Fujita, *et al.*, 2000). Similarly, Rho signalling through the downstream effector Dia1 is crucial for localization of AJ components to the cell periphery mediated by changes in the actin network (Sahai & Marshall, 2002). On the other hand, activation of the effector kinase ROCK and acto-myosin contraction disrupts AJs downstream of Rho in epithelial cells (Sahai & Marshall, 2002). In direct contrast to this finding, ROCK has been suggested to regulate the recruitment of myosin II to cadherin contacts, to mediate the regional distribution of cadherins at the cell surface, positively regulating cell-cell adhesions (Shewan, *et al.*, 2005).

1.4.1.5 Gene transcription: Rho GTPase regulation of the cytoskeleton also has an impact on gene transcription. The serum response element is found in many promoters, including those of genes encoding components of the cytoskeleton (Cramer, *et al.*). Two transcription factors act at the SRE: 1) the ternary complex factor (TCF) regulated by Ras/MAP kinase pathway and 2) the serum response factor (SRF) regulated by Rho (Jaffe & Hall, 2005). Rho mediates change in the actin cytoskeleton to promote translocation of the SRF co-activator, MAL, to the nucleus (Miralles, *et al.*, 2003). It has been proposed that under serum-starvation conditions, MAL is bound to nuclear actin, which promotes nuclear export of MAL, resulting in mainly cytoplasmic MAL. Nuclear actin bound to MAL, under serum-starvation, prevents the proportion of MAL localized in the nucleus from activating SRF, possibly through recruitment of transcription repressors or inhibition of transcriptional coactivator recruitment. Upon serum-stimulation, the cellular G-actin pool is depleted through actin polymerisation, which is suggested to result in an accumulation of nuclear-actin-free MAL in the nucleus and subsequent SRF activation (Vartiainen, *et al.*, 2007). However, the precise mechanism by which Rho induces MAL

translocation remains obscure, as although Rac and Cdc42 are also strong inducers of actin polymerisation, they are poor activators of SRF in comparison to Rho.

Rho GTPases also regulate gene transcription through actin-independent pathways. Rho, Rac and Cdc42 are all capable of activating the JNK and p38 MAP kinase pathways in a cell-context dependent manner (Minden, *et al.*, 1995; Puls, *et al.*, 1999). MLK2, MLK3, and MEKK4 interact with Rac/Cdc42, whereas MEKK1 interacts with all three Rho GTPases, Rho, Rac and Cdc42, although through different sites (Burbelo, *et al.*, 1995).

Rho, Rac and Cdc42 have also been reported to activate NFκB in response to inflammatory stimuli (Perona, *et al.*, 1997). Since Rac and Cdc42 also stimulate the production of reactive oxygen species (ROS) and inflammatory cytokines, which are both potent activators of NFκB, it is difficult to elucidate the mechanism of GTPase activation of NFκB (Jaffe & Hall, 2005).

1.5 THERAPEUTIC POTENTIAL OF TARGETING PI3K

PI3Ks are involved in multiple cellular processes, therefore it is not surprising that deregulation of PI3K signalling has been linked to a number of disease contexts. To highlight the therapeutic potential of targeting PI3Ks, the involvement of PI3Ks in cancer, inflammation, immunity and diabetes is described below.

1.5.1 PI3K and cancer

Tumour formation and progression is as a result of a shift in the balance between cell proliferation and cell death. Proteins and signalling pathways regulating cell growth, cell survival and differentiation are widely implicated in oncogenesis. The PI3K pathway is no exception to this and deregulation of the PI3K pathway has been implicated in several human cancers (Berrie, 2001; Stephens, et al., 2005). To give an outline of PI3K signalling in cancer, the involvement of PI3K with oncogenes, in the context of genetic alterations, and in tumour metastasis is discussed below.

Oncogenes: Oncogenes have been found to use PI3Ks as intracellular relay or effector molecules. Such oncogenes include growth factor receptors such as the ErbB/EGFR family. This family consists of four distinct, but structurally similar, transmembrane tyrosine kinase receptors: EGFR (ErbB1, HER1), ErbB2 (HER2, neu), ErbB3 (HER3) and ErbB4 (HER4) (Bianco, *et al.*, 2006). Aberrant expression and signalling of the HER family of proto-oncogenes and the receptor tyrosine kinases encoded by these genes have

been associated with bladder, brain, breast, colon, head and neck, lung, ovarian, and pancreatic cancers (Lafky*, et al.*, 2008; Salomon*, et al.*, 1995). Several factors affect the activation status of EGFR, including receptor mutations, receptor heterodimerization, increased expression of ligands, and activation of alternative pathways (Bianco, et al., 2006). The two main signalling pathways activated downstream of EGFRs are the Ras/Raf/Mek/erk1/2 pathway together with the PI3K/Akt/mTOR pathway (Johnston, 2006). In fact, in some instances increased activation of the PI3K pathway induced by growth factors is associated with resistance to EGFR-targeted therapies, which highlights the therapeutic potential of additionally targeting PI3Ks (Jones*, et al.*, 2004; Lu*, et al.*, 2001; Pao & Miller, 2005).

Ras oncogenes are thought to play a role at multiple stages of tumorigenesis. Mutations in codon 12, 13, or 61 of one of the three ras genes, H-*ras*, K-*ras*, and N-*ras* convert these genes into active oncogenes. Ras gene mutations are found in a variety of human tumours including adenocarcinoma of the pancreas, colon and the lung; in thyroid tumours and in myeloid leukaemia (Bos, 1989). Although the role and mechanisms by which Ras oncogenes maintain the transformed state of human cancer cells are not clearly understood, it has been found that Ras-dependent PI3K activation is essential for several cell processes necessary for cell transformation (Gupta*, et al.*, 2007; Warne*, et al.*, 1993).

Genetic alterations and PI3K: One of the main discoveries that indicated a role for PI3K in cancer was the discovery that the tumour suppressor PTEN is a PIP_3 3-phosphatase. The mutation and/or loss of PTEN occurs in a variety of human cancers (Simpson & Parsons, 2001), subsequently leading to increased PIP_3 levels and a constitutively active PI3K pathway.

PIK3CA, the gene encoding the p110α catalytic subunit, has been found to have somatic (tumor-specific) mutations occurring in 32% of colorectal cancer and has also been found in glioblastomas, gastric cancers, breast cancers and lung cancers (Broderick*, et al.*, 2004; Ikenoue*, et al.*, 2005; Karakas*, et al.*, 2006; Samuels*, et al.*, 2005; Samuels & Velculescu, 2004; Samuels*, et al.*, 2004). Greater than 75% of *PIK3CA* mutations occur in the helical and kinase domain of *PIK3CA* and are thought to confer increased kinase activity (Miled*, et al.*, 2007; Samuels, et al., 2005; Samuels & Velculescu, 2004; Samuels, et al., 2004; Zhao & Vogt, 2008).

Furthermore, increased *PIK3CA* DNA copy numbers have frequently been found in human ovarian cancer cell lines and in several other human cancers, which was associated with increased *PIK3CA* transcription and p110α protein expression (Shayesteh*, et al.*, 1999). The overexpression of *PIK3CA* in ovarian cancer has been found to positively correlate with VEGF at both the mRNA and protein level implicating p110α in the process of angiogenesis, a key mark of cancer progression (Zhang*, et al.*, 2003) To date there have been no somatic mutations reported for p110β or p110δ (Cornillet-Lefebvre*, et al.*, 2006; Knobbe & Reifenberger, 2003; Phillips*, et al.*, 2006). However, p110δ has been found to be expressed at high levels in nonhaematopoietic cell types of breast or melanocytic origin, which is discussed further in section 1.8 (Sawyer*, et al.*, 2003).

There are now also several examples of somatic and oncogenic mutations in the gene for p85 that usually focus into small 'hot spot' regions resulting in mutant proteins that retain their ability to bind p110, but lose their c-terminal SH2 domains, resulting in a constitutively active heterodimer (Jimenez*, et al.*, 1998; Philp*, et al.*, 2001).

Tumor Metastasis: Tumor invasion and metastasis are multifaceted processes involving adhesion, proteolytic degradation of tissue barriers and cell migration, which leads to secondary tumor formation. Cell migration can occur in response to an extracellular chemoattractant gradient. This requires cell polarization, involving cytoskeletal reorganisation and asymmetrical distribution of multiple proteins and lipids resulting in distinct cell edges; the 'front' or leading edge protruding at the anterior of the cell and the 'back-end' or rear edge (Ward, 2004). Evidence has emerged implicating PI3K phosphoinositide lipids in determining cell polarity. As discussed in section 1.4.5.2, studies have revealed that PIP_3 accumulation occurs at the leading edge of chemoattractant-stimulated cells with relocation of PTEN from the leading edge to the rear edge (Funamoto, et al., 2002). Overexpression or deficiency of PTEN has been shown to reduce or enhance leukocyte motility, respectively, and similarly, mice deficient in SHIP suffer from lethal infiltration of the lungs by macrophages and neutrophils (Funamoto et al., 2002; Helgason et al.*,* 1998). The production and degradation of 3'-phosphoinositide lipids is crucial in maintaining a chemotactic gradient and for the selective recruitment of PH domain-containing proteins to the leading edge of chemotaxing cells. PI3K regulation of Rho family GTPases, including Cdc42, Rac1 and RhoA, further implicates PI3K signalling in cell migration and a possibly tumor metastasis.

1.5.2 PI3K and diabetes

As discussed in section 1.3, PI3K is activated by insulin stimulation and the subsequent phosphorylation and activation of Akt, the main downstream target of PI3K, results in the phosphorylation of a number of components of the insulin signalling pathway. A number of studies have investigated the involvement of PI3K in insulin signalling, largely focusing on insulin-stimulation of glucose transport and GLUT4 translocation. Expression of dominant negative forms of p85 greatly reduces the effect of insulin both *in vitro* (Katagiri*, et al.*, 1997; Quon*, et al.*, 1995)) and *in vivo* (Miyake*, et al.*, 2002)) and reversely, overexpression of constitutively active class IA PI3K is also sufficient to, at least in part, mimic the effects of insulin (Katagiri*, et al.*, 1996; Tanti*, et al.*, 1996).

Using both a pharmacological and a genetic approach p110α has been identified as the key PI3K isoform in insulin signalling (Foukas*, et al.*, 2006; Knight*, et al.*, 2006). Using pharmacological tools, p110α has been found to be the primary insulin-responsive PI3K in cultured cells, whereas p110β is dispensable for IRS signalling (Knight, et al., 2006). In corroboration with this, mice heterozygous for a p110α-inactivating mutation, have severe impairments in signalling via insulin-receptor substrate (IRS) proteins, insulin-like growth factor-1 and leptin action leading to hyperinsulinaemia, glucose intolerance, hyperphagia and increased adiposity (Foukas, et al., 2006). However, these mice do not become diabetic, even at old age (Foukas, et al., 2006).

Recent evidence also indicates that PI3K-C2α may also play a role in insulin signalling (Falasca*, et al.*, 2007; Falasca & Maffucci, 2007; Shepherd, 2005). Insulin stimulation causes a very rapid activation of PI3KC2α and it has been suggested that PIK3C2α may play a role in insulin-mediated increases in PI(3)P and in stimulation of glucose transport (Shepherd, 2005).

1.5.3 PI3K and autoimmune and inflammatory disease

PI3Ks, specifically p110δ and p110γ, represent attractive targets in autoimmune and inflammatory conditions. As will be discussed in section 1.6, through gene-targeting strategies both p110δ and p110γ have been found to play critical roles in immune function. Inhibiting p110δ and/or p110γ activity is likely to influence immune function at multiple levels, which strengthens the therapeutic value of PI3K inhibition. Furthermore, the inflammatory response is associated with multiple diseases, implicating PI3K inhibition as a common point in a therapeutic strategy. To underscore the potential of targeting PI3K in

autoimmune and inflammatory disease, the involvement of PI3K in the widespread inflammatory diseases, respiratory lung disease and rheumatoid arthritis is discussed briefly.

Lung disease: Chronic respiratory diseases are defined by inflammatory cell recruitment, inflammatory mediator expression, tissue remodelling, and altered airway smooth muscle contraction (Medina-Tato*, et al.*, 2007). Within chronic respiratory diseases, asthma and chronic obstructive pulmonary disease (COPD) are the most common clinical entities. PI3K, specifically p110δ and p110γ, have been shown to play a role in the pathology of these diseases, along with other respiratory diseases such as acute lung injury (ALI) and adult respiratory distress syndrome (ARDS). Indeed, the p110δ-selective inhibitor, IC87114, has been shown to have a therapeutic effect in a murine model of asthma (Lee*, et al.*, 2006). In general, PI3Ks have been implicated in pulmonary infiltration of lymphocytes and eosinophils, antigen-induced airway inflammation and hyperresponsiveness and Th2 cytokine production (IL-5 and IL-4) in bronchoalveolar lavage fluid (Medina-Tato, et al., 2007).

Rheumatoid arthritis: Rheumatoid arthritis (RA) is a chronic inflammatory disease, generally considered to be an immune-mediated disease. Rheumatoid joints are characterised by inflammatory infiltrates in the synovium and synovial fluid, pannus formation, and eventually by joint erosion. There are multiple steps in the pathogenesis of the disease with interplay between the adaptive and innate immune response. The activities of T cells, B cells (including the production of auto-antibodies and immune complexes and cytokine secretion), dendritic cells, mast cells, macrophages and neutrophils have all been shown to have important roles and to affect at least one or several aspects of the disease (Rommel, et al., 2007). p110δ and p110γ are both targets in the treatment of rheumatoid arthritis due to their signalling roles in cells of the immune system.

There is increasing interest in the pharmaceutical industry to generate PI3K isoform-specific inhibitors. Indeed, companies such as ICOS, PIramed, Novartis, Bayer, Pfizer, Serono, Targegen and Calbiochem are involved in the development of inhibitors that target p110δ and/or p110γ (Medina-Tato, et al., 2007). The therapeutic potential of p110δ in allergy has recently been publicly recognised, featuring in a BBC news article (http://news.bbc.co.uk/1/hi/health/7247600.stm, 2008).

1.6 ELUCIDATING THE ISOFORM-SPECIFIC ROLE OF PI3K

Targeting PI3K itself or downstream effectors of PI3K is an approach that has the potential to be of huge therapeutic benefit, since deregulation of the PI3K signalling pathway occurs in a number of disease settings, as described above. However, PI3K signalling is also important in normal cell homeostasis and inhibition of all the PI3K isoforms with non-selective PI3K inhibitors may be toxic upon chronic administration. To enable individual PI3K isoforms to be targeted therapeutically, it is first important to understand the specific signalling mediated by each PI3K isoform. This has been carried out using PI3K isoform-specific inhibitors, PI3K gene-targeted mice and cell-based overexpression studies, which are described below.

1.6.1 PI3K gene-targeted mice

There have been two main genetic approaches of targeting the catalytic PI3K genes. The first is a knockout approach, where targeting of the p110 gene results in failure of gene product expression. The second approach is a more subtle, and is where a mutation is introduced in the ATP binding site of the catalytic domain, which results in protein expression but with a resulting amino acid substitution (for example by replacing aspartic acid 910 by alanine – D910A for p110δ) in the ATP-binding region, rendering the p110 catalytically inactive. The second approach has been termed 'knock-in', and is considered to be more sophisticated than a straight forward knockout, as it is more likely to mimic pharmacological inhibition of PI3K. Furthermore, it has been observed that when a gene is completely knocked-out, there is room for compensation in the cell by other related proteins, whereas, expression of a protein, albeit a catalytically inactive one, leaves little room for compensation by other proteins.

Mouse gene targeting of PI3K class I catalytic isoforms: All class I catalytic isoforms have been inactivated by gene targeting in the mouse. Mice homozygous for knockout or D933A knockin alleles of the widely expressed p110α isoform die at embryonic stage 10.5 (Bi*, et al.*, 1999; Foukas, et al., 2006), displaying severe defects in angiogenic sprouting and vascular remodelling (Graupera*, et al.*, 2008).

Mice with a heterozygous knockout of p110α are viable and were reported to lack metabolic or growth phenotypes (Brachmann*, et al.*, 2005). In contrast, mice heterozygous for the D910A knockin mutation (p110α$^{D933A/WT}$) are viable and fertile, but display a strong metabolic phenotype (Foukas, et al., 2006). p110α$^{D933A/WT}$ mice display

hyperinsulinaemia, impaired glucose and insulin tolerance, increased food intake, increased adiposity and hyperleptinaemia compared to WT mice (Foukas, et al., 2006). As already mentioned earlier, this has identified p110α as a key intermediate in IGF-1, insulin and leptin signalling at the organismal level.

The difference between the phenotypes observed in heterozygous p110α knockout mice *versus* heterozygous p110α knockin mice has been assigned to the stoichiometry of p85-p110α complexes. In heterozygous p110α knockout mice, the capacity of any given receptor to signal through p110α will only be reduced if p110α-p85 expression is reduced to a level where it is limiting relative to the receptor. In contrast, in heterozygous p110α knockin mice, the capacity of any given receptor to signal through p110α is not dependent on the stoichiometry of p110α-p85 heterodimers. It can be assumed that 50% of receptor p110α complexes will be lacking p110α catalytic activity, which results in clear phenotypes (Foukas, et al., 2006; Graupera, et al., 2008).

Endothelial-specific homozygous genetic inactivation of p110α also caused embryonic lethality due to impaired angiogenesis. To study the role p110α is playing in vascular development, investigations have been carried out on the viable p110α$^{D933A/WT}$ mice. p110α$^{D933A/WT}$ mice also display delayed angiogenesis during development and impaired angiogenic responses to VEGF-A (Graupera, et al., 2008). This study has revealed that p110α is the key PI3K isoform in endothelial cells, promoting angiogenesis through regulating endothelial cell migration through the small GTPase RhoA (Graupera, et al., 2008).

Homozygous knockout of p110β is also embryonic lethal at the blastocyst stage of embryonic development (E 3.5) (Bi, *et al.*, 2002). Such early embryonic lethality has made it extremely difficult to study the homozygous loss of p110β, even at the cellular level as it also turned out to be impossible to culture cells from the embryo at this stage. The early embryonic lethality in p110β KO mice suggests an essential role for p110β during development. However, mice heterozygous for p110β knockout alleles are viable, and do not display any obvious phenotype. Moreover, mice heterozygous for *both* p110α and p110β deletions also show no obvious phenotype (Brachmann, et al., 2005). This result may not be a true reflection of importance of p110α and p110β, since as mentioned before, the heterozygous knockout approach relies on p110-p85 expression levels being limiting relative to the receptor.

Germ-line inactivation of p110β has also been carried out through deletion of exons 21 and 22 (p110β$^{Δ21+22}$). Preliminary results reveal that unlike the homozygous p110β knockout, homozygous p110β inactivation is only partially lethal (Guillermet-Guibert & Vanhaesebroeck, unpublished results). It is unclear at present, what causes their partial lethality and this is currently being investigated. However, this finding demonstrates that by using a protein inactivation approach as opposed to a complete knockout approach, it is feasible to investigate the homozygous loss of p110β gene-function.

Mice have recently been generated in which p110β activity has been conditionally abolished in endothelial cells, to investigate the possible role that p110β may be playing in angiogenesis. In this conditional inactivation of p110β, exons 21 and 22, which lie in the catalytic region of p110β and contain the ATP binding site, are deleted resulting the expression of a truncated, inactive p110β protein. Mice lacking catalytically active p110β in endothelial cells are viable and do not display any developmental angiogenic phenotypes, indicating that p110α is the major p110 isoform involved in angiogenesis (Graupera, et al., 2008).

Mice with a homozygous deletion of the p110δ or p110γ gene (p110δ knockout or p110γ knockout) are viable (Clayton*, et al.*, 2002; Jou*, et al.*, 2002; Sasaki*, et al.*, 2000). The viability of these mice, compared to the lethality of p110α or p110β homozygous knockout, can be attributed to the restricted tissue distribution of p110δ and p110γ in cells of the immune system, compared to the ubiquitous expression of p110α and p110β. From these knockout studies, it has been found that p110δ is critical to the adaptive immune response with p110δ$^{-/-}$ mice displaying impaired B cell development, B cell activation and antibody response (Clayton, et al., 2002; Jou, et al., 2002; Puri*, et al.*, 2004). Mice expressing a kinase-dead p110δ are also viable and display similar phenotypes to the p110δ knockout mice, with impaired B-cell development. In addition, studies on p110δ knockin mice have revealed a role for p110δ downstream of the T cell antigen receptor and in mediating the allergic response (Ali*, et al.*, 2004; Okkenhaug*, et al.*, 2002). These p110δ knockin studies have indicated that p110δ is the main provider of PI3K activity downstream of the TcR (T cell receptor) and BcR (B cell receptor) and in addition p110δ is also the main PI3K isoform involved in mast cell signalling in an inflammatory context, a component of the allergic response (Ali, et al., 2004; Okkenhaug, et al., 2002).

p110γ is activated downstream of GPCRs, and like p110δ, p110γ expression is mainly restricted to leukocytes. In accordance to the distribution of p110γ, neutrophils, macrophages and certain populations of mast cells from p110γ homozygous knockout mice, exhibit defects in migration in response to GPCR agonists and chemotactic agents (Hirsch, *et al.*, 2000a; Li, *et al.*, 2000; Sasaki, et al., 2000). In addition, p110γ has been shown to control thymocyte survival and activation of mature T cells but, unlike p110δ, does not have a role in the development and function of B cells (Sasaki, et al., 2000)

Studies with mice homozygous for p110γ deletion, have suggested a role for p110γ in the IgE/Ag-triggered allergic response. However, groups differ in their findings of the relative importance of p110γ and p110δ in allergic responses *in vivo* (Ali, *et al.*, 2008; Laffargue, et al., 2002). The reason for this discrepancy between groups is unclear at the moment.

Mouse gene targeting of class IA PI3K regulatory subunits: The regulatory subunits p85α, p55α and p50α are expressed from the same gene (*PIK3R1*) through the use of alternative promoters, p85β is the only gene product of the p85β gene (*PIK3R2*). Four mouse lines have been created targeting the different class IA regulatory subunits. The 'pan-p85α knockout' line targets all *PIK3R1* gene products (p85α, p55α and p50α) (Fruman, *et al.*, 1999), 'p85α-only knockout' has gene deletion of p85α but retains p55α and p50α expression (Suzuki, *et al.*, 1999), the 'p55α/p50α knockout' has gene deletion of p55α and p50α but retains p85α expression (Chen, *et al.*, 2004), and finally the fourth line 'p85β knockout' has p85β gene (*PIK3R2*) deletion (Ueki, *et al.*, 2002b).

Gene disruption targeting all p85α isoforms results in perinatal lethality, whereas mice with gene disruption of p85α only are viable. In both cases however, mice display defects in B-cell development and function, with no defects in T-cell function reported. In other tissues, PI3K signalling downstream of insulin was enhanced in p85α knockout mice compared to cells from wild-type mice (Fruman, *et al.*, 2000; Terauchi, *et al.*, 1999). Mice homozygous for gene deletion of p85β are viable, although they tend to be smaller than their wild-type littermates. Similar to p85α knockout mice, p85β knockout mice display hypoinsulinaemia, hypoglycaemia, and improved insulin sensitivity. These results indicating PI3K as a negative regulator of insulin signalling, appear to be in direct contrast to the study by Foukas *et al.*, 2006, where p110α was found to positively regulate insulin signalling. However, further analysis of p85α knockout cells reveals increased p85β expression (and 55α and p50α in the 'p85α-only knockout') and reduced expression of each

of the class IA catalytic isoforms. The disruption of PI3K isoform expression in the p85 knockouts makes interpretation of the phenotypes observed extremely difficult, as the phenotype may be as a result of the disruption of PI3K isoform expression rather than loss of the targeted p85.

1.6.2 Cell-based approaches

A number of different cell-based approaches have been used to investigate isoform-specific PI3K signalling at the cellular level. These include the overexpression of p110 isoforms in different cell lines, the derivation of cell lines from p110 knockout/knockin mice, the use of RNAi to knock-down p110 expression, and the use of p110 isoform-specific inhibitors, which are all further discussed below.

Overexpression of p110 isoforms in different cell lines: Transient overexpression of the p110 isoforms has given some insight into PI3K signalling. Transient expression of a constitutively active mutant p110 (called p110*), in which the inter-SH2 domain of p85 is covalently linked to the N-terminal-binding site of p110 binding site, has been found to be sufficient to activate pathways involved in the regulation of cell proliferation, independent of growth factor stimulation (Hu, *et al.*, 1995).

The effect of membrane localization of p110 has been investigated through transient expression of N-terminal myristylated (using the myristylation sequence of $pp60^{c-Src}$) or C-terminal farnesylated (using farnesylation signal from H-Ras) p110 and p110* in COS-7 cells (Klippel, *et al.*, 1996). Membrane targeting of p110 subunits also results in a constitutively activate p110. The use of activated forms of PI3Ks enables the direct study of cellular processes regulated by PI3K without prior activation by growth factor. Furthermore, the use of activated PI3K molecules allows determination of whether PI3K activation alone is sufficient for the induction of a signalling event (Klippel, et al., 1996).

It was found that when p110 was directed to the membrane, even low amounts of PI3K activity were sufficient to trigger the induction of a subset of intracellular kinases, which include p70 S6 kinase, Akt and Jnk. The activation of these kinases as a result of p110 membrane-targeting was more effective than their activation as a result of the highly active but cytoplasmic p110*. The combination of high PI3K activity of p110* with membrane-targeting signals resulted in maximal activation of downstream responses (Klippel, et al., 1996). A constitutive active form of the small G protein Ras (RasV12), but not Rac or

Cdc42, was found to increase activation of Akt and this activation was wortmannin-sensitive, suggesting Ras lies upstream of PI3K activation (Klippel, et al., 1996). However, expression of the dominant negative forms of Ras, Rac or Cdc42 with active p110 did not interfere with PI3K-dependent activation of Akt, indicating that Ras mediates activation of Akt by an independent pathway. A proposed mechanism for the observation that RasV12-induced Akt activation is wortmannin-sensitive, involves Ras-induced production of autocrine factors that subsequently activate growth factor receptors, which in turn lead to the induction of signalling pathways, including the activation of PI3K. Indeed, RasV12 was found to secrete autocrine factors in cell culture media which resulted in MAPK activation. Unfortunately, due to the lack of a suitable anti-Akt antibody at the time of publication, the authors were unable to test whether these autocrine factors could also stimulate Akt (Klippel, et al., 1996).

Further investigation into the effect of constitutive active PI3K has been carried out by generating inducible PI3K molecules, in which p110 or p110* have been fused to the hormone binding domain (HBD) of a mutated mouse estrogen receptor (mER) (Klippel, *et al.*, 1998). Proteins fused to this mutant ER domain are inactive until the addition of 4-hydroxytamoxifen (4-OHT). It was found that activation of PI3K induced immediate early responses such as activation of Akt and p70 S6 kinase and a late response of Jnk activation and entry into the S-phase of cell cycle although not complete progression through the cell cycle (Klippel, *et al.*, 1998). These studies have strengthened the idea that recruitment of p110 subunits to the plasma membrane by the regulatory subunit is a key activator of PI3K. They have also given us some indication of the time frame in which individual components downstream of the PI3K signalling pathway are activated.

The C-terminal farnesylation signal from H-Ras is often referred to as CAAX motif as it consists of a <u>C</u>ysteine residue, an <u>A</u>liphatic amino acid, a second <u>A</u>liphatic amino acid followed by any amino acid (<u>X</u>). The introduction of p110α-CAAX into bone marrow-derived mast cells has been found to increase the binding affinity of β_1 integrin very late Ag-5 (VLA-5) for fibronectin, indicating PI3K as an important modulator of β_1 integrin affinity (Kinashi, *et al.*, 1999). Employing this plasma membrane-targeting approach to investigate constitutively activate p110, p110δ-CAAX has also been transfected in mast cells. p110δ was found to be a critical effector molecule of Ras in activating integrins in mast cells (Kinashi et al, 2000).

Relatively recently, the oncogenic transformation potential of each p110 catalytic subunit has been investigated through overexpression of each isoform in chicken embryo fibroblasts (Kang, *et al.*, 2006). p110δ, β and γ were found to induce the formation of transformed cell foci within 10 days, with p110δ and p110γ inducing more distinct foci compared to p110β. The fusion of a myristylation signal to the N-terminus of the p110 isoforms (Myr-p110) enhances oncogenic transforming ability, although this enhancement is less pronounced with the δ and γ isoforms, which are potent transformers even without the added myristylation signal. In contrast, p110α only had transforming ability when myristylated or possessing an oncogenic point mutation, wild-type p110α lacked any transforming potential. It should be considered however, that overexpression of wild-type p110α is toxic to the cell and that only a low level of p110α expression is achieved, consequently not resulting in cell transformation.

The transforming ability of all the p110 isoforms is dependent on the lipid kinase activity of the p110 subunit. Interestingly, only p110δ and the oncogenic p110α mutant induce constitutive activation of Akt under serum-starvation conditions, whereas in p110β or p110γ-overexpressing chicken embryo fibroblasts no increase in phosphorylated Akt is detected compared to control transfected cells (Kang, et al., 2006).

Mutation of the Ras binding domain in each of the p110 subunits has revealed that myr-p110α or oncogenic p110α and p110δ are not dependent on Ras binding to induce cell transformation. In contrast, in p110β and p110γ-overexpressing cells, abolishing p110-Ras binding significantly compromises the transforming potential of these p110 isoforms (Denley, *et al.*, 2008; Kang, et al., 2006). The upstream requirements for cell transformation by p110β and p110γ therefore, appear to be distinct from the upstream requirements for cell transformation by p110α and p110δ, which corresponds to the finding that p110β and p110γ are activated downstream of GPCRs, whereas p110α and p110δ are activated downstream of tyrosine kinases (Guillermet-Guibert, et al., 2008; Kang, et al., 2006). p110β, p110δ, p110γ and oncogenic p110α are all however dependent on mTOR to mediate their oncogenic signal (Kang, et al., 2006).

One interesting observation from the overexpression study by Kang *et al*, 2006, is that overexpression of myr-p110α, p110β and p110δ was possible without cotransfection of a regulatory subunit. Since p110 expression is thought to depend on the availability of p85, which may stabilise the catalytic subunit, this study suggests that exogenously expressed

p110 subunits bind endogenous p85. In addition, expression of one particular p110 isoform was found to affect the expression levels of other isoforms that share the same regulatory subunit (Kang, et al., 2006). For example, the endogenous levels of p110α are downregulated in cells overexpressing the β or δ isoform and overexpression of p110δ also leads to reduced endogenous levels of p110β. It has been proposed that overexpression of a particular p110 isoform may titrate the corresponding regulatory subunit, limiting the availability to other isoforms and thus cause downregulation (Kang, et al., 2006).

Since the Ras binding domain does not appear to be necessary to target p110δ to the plasma membrane, a similar study in chicken embryo fibroblasts has looked at requirement of three basic residues within the C2 domain that have been shown to be involved in lipid–protein interactions (Denley, et al., 2008). Mutation of all three basic residues to alanine was found to almost completely inhibit foci formation in chicken embryo fibroblasts induced by p110δ overexpression.

Although these studies have provided valuable insights into PI3K signalling, transient overexpression does not allow for full functional analysis of the changes in cell signalling as a consequence of the overexpression. In addition, this work only focused on a single p110 isoform (mostly p110α); and no comparison was made between different p110 isoforms. A potentially better way to achieve this is by stable overexpression of p110 isoforms. This has proved to be more difficult and there are only a relatively small number of studies which document the effect of stable PI3K overexpression.

Stable NIH 3T3 cell lines have been created which express a myr-p110α (Auger, *et al.*, 2000). As was previously suggested by Kang *et al,* 2006, the exogenously expressed myr-p110α was formally found, by pull-down experiments, to associate with endogenous p85 regulatory subunits (Auger, et al., 2000). Myr-p110α-expressing cells were found to have altered cell morphology, displaying a more elongated morphology at confluence, and did not display strict contact inhibition of growth. Consistent with their altered morphology, myr-p110α-expressing cells possessed disorganized actin stress fibres compared to the organised bundles of actin fibres in control transfected cells (Auger, et al., 2000). In contrast to data obtained from transient assays, Akt and p70 S6 kinase were not constitutively active in cells stably expressing myr-p110α (Auger, et al., 2000). Consistent with this finding, in a separate study, NIH 3T3 cells stably expressing Myc-

p110α do not show increased basal Akt phosphorylation or p70 S6 kinase phosphorylation compared to cells transfected with control (empty) vectors (Ikenoue, *et al.*, 2005).

Myristylated p110α, p110β, p110γ, and p110δ isoforms have all been stably co-expressed with the c-Myc oncogene in Rat1 fibroblasts (Link, *et al.*, 2005). All four p110 isoforms protect c-Myc overexpressing cells from apoptosis caused by serum deprivation. Expression of each p110 isoform reduces caspase-3 like activity in this apoptosis model, which correlated with increased Akt phosphorylation. Interestingly, clones expressing myristylated p110δ were found to trigger Akt phosphorylation much more efficiently than myristylated p110α, p110β, or p110γ (Link, et al., 2005), which corroborates the findings from *transient* expression of myr-p110s previously discussed (Kang, et al., 2006).

Stable expression of GFP-tagged p85α in CHO-K1 cells has shown that in response to insulin-like growth factor (IGF), GFP-p85α translocates to distinct, foci-like complexes that contain p85 bound to tyrosine-phosphorylated insulin receptor substrate-1 (IRS-1) (Luo, *et al.*, 2005). These complexes were found to contain primarily monomeric p85 and suggests a novel mechanism to explain how monomeric p85 inhibits PI3K signalling downstream of IRS-1 (Luo, et al., 2005). It is important to mention that the p85-overexpressing clone in this study may not be representative. Indeed, one had to screen over 1000 colonies to be able to find a clone that could withstand stable overexpression of p85 (L. Cantley, personal communication to Bart Vanhaesebroeck).

All previous attempts in the Cell Signalling in Cancer laboratory (The Ludwig Institute for Cancer Research and Queen Mary's Institute for Cancer Research) to stably overexpress p110 isoforms in mammalian cell lines using cDNA expression vectors have failed. However it should be noted that 3'-Myc tagged p110 cDNAs have often been used in these transfections, which have since been shown to produce a kinase-dead p110 that can no longer phosphorylate its *in vivo* substrate PIP_2. Furthermore, the p110 cDNAs used in the transfections did not contain a membrane-targeting signal, which have since proved to be favourable in allowing stable p110 expression. Last but not least, it has now become apparent that p110 cDNAs used for transfection were not full length and did not contain 5'UTR regions found in the mRNA of the wild-type p110 genes; this issue is discussed further in section 1.9.

Creation of cell lines from p110 knockout mice: As mentioned above, p110α knockout mice die between days 9.5 and 10.5 of embryonic development (Bi, *et al.*, 1999). This

lethality has prevented investigation of the effect of the homozygous loss p110α in the adult mouse, however haematopoietic cells extracted from the p110α$^{D933A/D933A}$ embryo are currently being used to investigate homozygous loss p110α in cell-based signalling (Foukas & Vanhaesebroeck, unpublished results). p110δ knockout mice are viable and cell lines have also been established from these mice (Foukas *et al.,* 2006). The p110β knockout is embryonic lethal, mice die around the time of embryo implantation, and it has not been possible to establish stable cell lines from these mice (Bi*, et al.*, 2002). However, it has been possible to establish mouse embryonic fibroblasts from mice homozygous for the p110β$^{Δ21+22}$ alleles. These cells have proved to be a valuable tool in delineating a role for p110β downstream of GPCRs (Guillermet-Guibert, et al., 2008).

Knock-down p110 expression using RNAi: It is possible to knock-down p110 expression using small interfering RNAs (Czauderna*, et al.*, 2003a; Czauderna*, et al.*, 2003b) (Brachmann*, et al.*, 2005). Stable and transient siRNA-mediated knockdown of p110β was found to inhibit invasive cell growth *in vitro* as well as in a tumour model system (Czauderna, et al., 2003a). Downregulation of p110α in cell lines using RNAi has been found to reduce p85 expression, which is consistent with the finding that double p110α / p110β heterozygous knockout mice show approximately 50% decrease in p85 expression (Brachmann, et al., 2005).

Use of isoform-specific inhibitors: Isoform-specific inhibitors are currently in development by a number of pharmaceutical companies and have been a valuable tool in investigating the isoform-specific roles of PI3K. The main problem that accompanies the use of these inhibitors in investigative studies is the question of their selectivity. The p110δ-selective inhibitor developed by ICOS corporation (IC87114) has been employed in a number of studies at a concentration where there is confidence that it is targeting p110δ alone (Sadhu*, et al.*, 2003). Kinacia (Australia) and Serono (Geneva) have developed p110β and p110γ inhibitors which have high selectivity toward their targeted isoform (Jackson*, et al.*, 2005; Condliffe*, et al.*, 2005). Progress has been made towards developing p110α-selective inhibitors, although several of these compounds are not highly selective for p110α and target numerous other kinases (Fan*, et al.*, 2006). Although the use of p110 isoform-specific inhibitors are a useful tool in investigating the isoform-specific roles of PI3Ks, complementary experiments should be performed to ascertain that the effect observed is due to specific PI3K inhibition rather other unintended proteins being targeted.

1.7 P110δ SIGNALLING IN MAST CELLS

1.7.1 Introduction to the mast cell

Mast cells are derived from multipotential haematopoietic stem cells of the bone marrow, expressing the cell surface markers CD13, CD34 and CD117/c-kit (Metcalfe, *et al.*, 1997). They migrate from the bone marrow to the circulation into the peripheral tissues where they terminally differentiate under the influence of environmental factors (Figure 1.11).
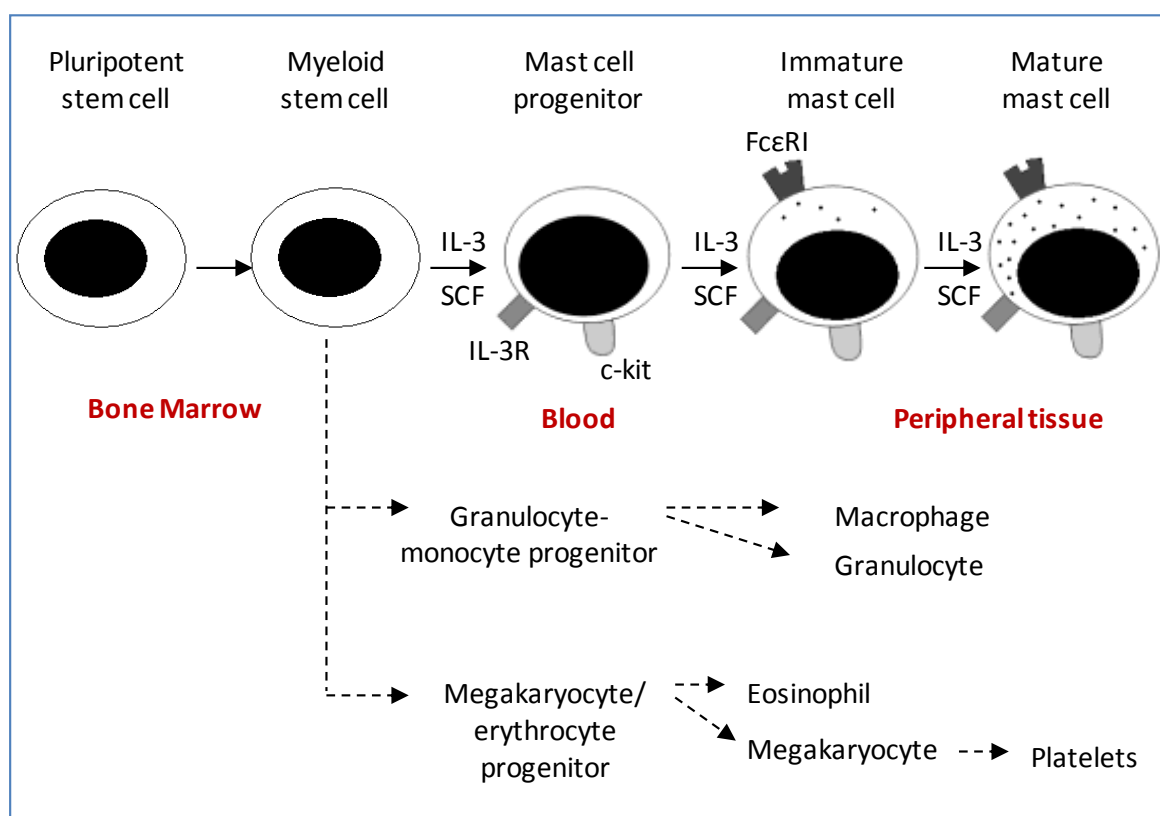
Figure 1.11: Simplified model of mouse mast cell development. Mast cells arise from multipotential haematopoietic progenitor cells but complete major parts of their differentiation in peripheral tissue. Fully mature mast cells express the cell surface receptors FcεRI, IL-3 receptor and c-kit receptor.

Mast cells are highly granulated mononuclear cells with a diameter of 4-20 μm. They are widely distributed throughout the body in connective tissues and on mucosal surfaces (Puxeddu, *et al.*, 2003). They participate in the regulation of adaptive immune responses and have a central role in allergic inflammatory responses (Metcalfe, et al., 1997). Antigen cross-linking of IgE bound to its high affinity receptor, FcεRI, at the mast cell surface, induces mast cell degranulation and the release of pro-inflammatory mediators (Metcalfe, et al., 1997; Puxeddu, et al., 2003).

In addition to FcεRI, mast cells also express the c-kit receptor, which is activated by its cytokine ligand SCF (stem cell factor, also known as c-kit ligand). The c-kit receptor and

SCF are encoded at the murine *white spotting (W)* and *steel (Sl)* loci, respectively (Chabot*, et al.*, 1988; Serve*, et al.*, 1995). Mice expressing a mutated c-kit receptor (W/W^v) or mice lacking functional membrane SCF (Sl/Sl^d) express a virtual absence of mast cells, demonstrating that SCF is an essential factor for mast cell development (Kitamura*, et al.*, 1978). The cytokine, interleukin-3 (IL-3) has also been shown to have an important role in mast development. The presence of IL-3 in cell culture media is critical for the generation of populations of immature mast cells from mouse haematopoietic cells *in vitro* (Tertian*, et al.*, 1981). In addition, IL-3 induces mouse mast cell growth and enhances their development in response to SCF *in vitro* (Puxeddu, et al., 2003).

1.7.2 PI3K signalling via the c-kit receptor

Mast cells are commonly used to study signalling downstream of the c-kit receptor, which is a single-chain receptor that has inherent protein tyrosine kinase activity. Binding of SCF to c-kit results in receptor dimerization followed by activation of its intrinsic tyrosine kinase activity (Blume-Jensen*, et al.*, 1991). Once activated, the receptor becomes autophosphorylated on multiple tyrosine residues in the cytoplasmic tail, which act as docking sites for SH2 domain-containing proteins or phosphotyrosine binding (PTB) domains (Ronnstrand, 2004). Such proteins include SHC (Src homology 2-domain-containing transforming protein C), GRB2 (growth factor receptor-bound protein), Src family kinases, phospholipase Cγ and PI3K (Figure 1.12).

Although SCF stimulation alone cannot induce mast cell degranulation, a combination of SCF and antigen leads to a synergistic PLCγ activation, leading to an increase in calcium mobilisation and degranulation (Hundley*, et al.*, 2004).

A number of studies have implicated PI3K activation in transformation through mutated c-kit. PI3K-dependent activation of Akt and phosphorylation of BAD (a pro-apoptotic molecule) by c-kit promotes cell survival. For human c-kit, Y721 has been found to directly interact with PI3K (Serve, et al., 1995), which corresponds to Y719 in mice.
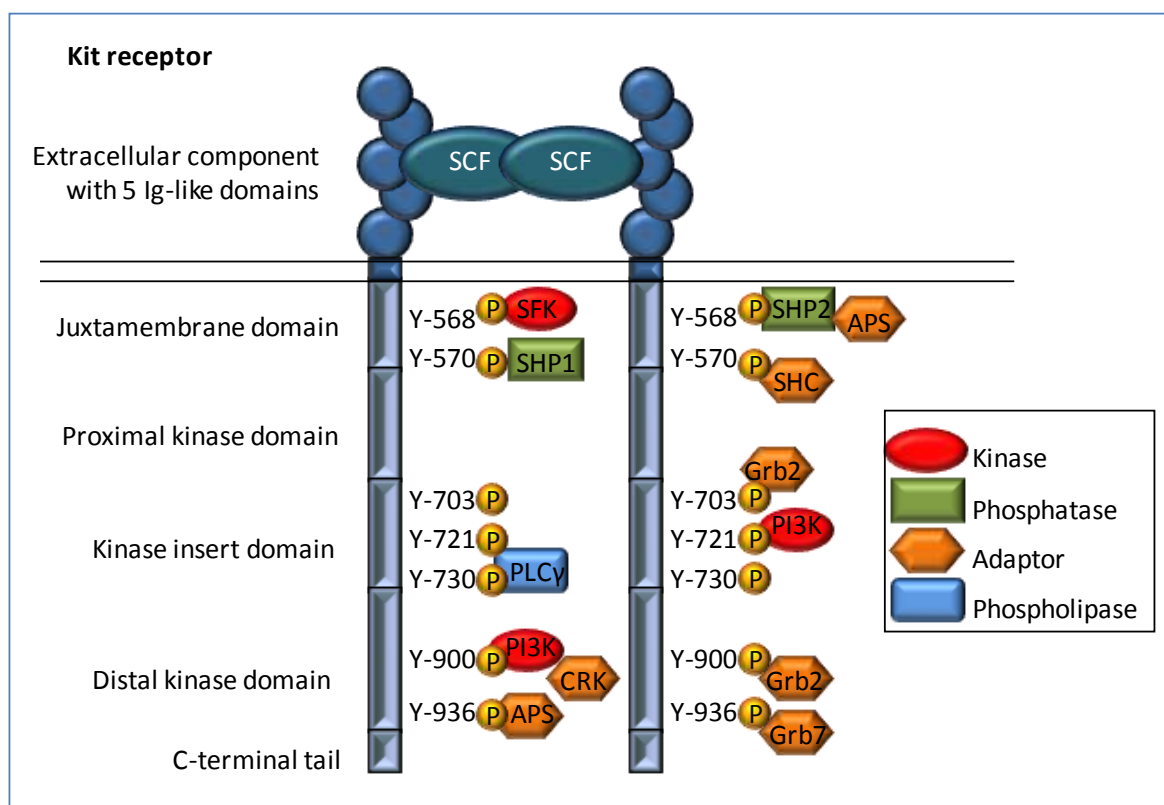
Figure 1.12: **The (human) c-kit receptor**. The adaptor APS, Src family kinases, and SHP2 tyrosyl phosphatase bind to phosphotyrosine 568. SHP1 tyrosyl phosphatase binds to phosphotyrosine 570 and the adaptor protein SHC can bind to both phosphotyrosine 568 and phosphotyrosine 570. These tyrosine residues are in the juxtamembrane domain of c-kit. Phosphorylated tyrosine resides in the kinase insert domain attract the adaptor protein Grb2 (Y-703), PI3K (Y-721) and phospholipase C-γ (Y-730). PI3K can also bind Y-900 in the distal kinase domain, which in turn binds the adaptor CRK. Phosphotyrosine 936 binds the adaptor proteins APS, Grb2 and Grb7 (Roskoski, 2005).

1.7.3 p110δ and c-kit: Implications in cancer

Gain-of-function mutations in c-kit are associated with a number of human cancers. A mutation at codon 816 of the catalytic domain of the human gene (codon 814 of the murine gene) is found in patients with mastocytosis and mast cell leukaemia, as well as some patients with acute myelogenous leukaemia and germ cell tumours (Longley, *et al.*, 1999; Nagata, *et al.*, 1995; Shivakrupa, *et al.*, 2003). These findings indicate that pharmacological inhibition of signalling components activated by this mutation could be of therapeutic benefit.

It has been shown, in a murine mast cell line, that mutant Kit^{D814Y} is constitutively phosphorylated on tyrosine 719 and that this is likely to result in constitutive association with activated PI3K (Shivakrupa, et al., 2003). STI-571 (Gleevec, imatinib) is a clinically used protein-tyrosine kinase inhibitor, which targets Abl, Bcr-Abl, c-kit and the PDGF

receptor. Its clinical efficacy was first established in the treatment of chronic myelogenous leukaemia, in which it targets the Bcr-Abl oncoprotein. However, cancers that result chiefly from mutation of c-kit at residue 816 are resistant to STI-571, which leaves PI3K inhibition as a potentially attractive targeted therapy for these disorders (Roskoski, 2005).

Mast cells, like other leukocytes, express high levels of p110δ. An investigation into the role of p110δ in mast cells has revealed that genetic or pharmacological inactivation of p110δ in murine bone marrow derived mast cells (BMMCs) leads to defective SCF-mediated *in vitro* proliferation, adhesion and migration, and to impaired allergen-IgE-induced degranulation and cytokine release (Ali, et al., 2004). In p110δ$^{D910A/D910A}$ BMMCs, the total *in vitro* class IA PI3K lipid kinase activity was found to be reduced by 90% compared to WT BMMCs, indicating that p110δ is the major isoform contributing to overall class IA PI3K activity in mast cells (Ali, et al., 2004). Furthermore, p110δ$^{D910A/D910A}$ BMMCs fail to produce PIP$_3$ upon SCF stimulation in an *in vitro* lipid kinase assay. Concurring with this result was the almost complete abrogation of SCF-induced Akt phosphorylation in p110δ$^{D910A/D910A}$ BMMCs and in WT BMMCs treated with the p110δ inhibitor, IC87114. These results indicate that p110δ is the principal p110 isoform involved downstream of the c-kit receptor in WT BMMCs.

The dependence of c-kit to signal through p110δ demonstrates p110δ inhibition as a potential targeted therapy in cancers with gain-of-function mutations in c-kit such as in mastocytomas. This has prompted investigation into the effect of p110δ inhibition on Akt phosphorylation in the human mastocytoma cell line (HMC-1). HMC-1 is a human leukaemic mast cell line, which has two point mutations in c-kit resulting in constitutive activation of the receptor and, as a consequence, constitutive Akt activation (Furitsu, *et al.*, 1993). Treatment of HMC-1 cells with the p110δ inhibitor IC87114 results in a partial abrogation of Akt phosphorylation although not complete abrogation as was observed upon IC87114 treatment of SCF-stimulated WT BMMCs (Billottet & Vanhaesebroeck, unpublished results). It is important to note, however, that although c-kit is constitutively active in HMC-1 cells, phosphorylation of Akt can be further increased upon SCF stimulation (Billottet, C. unpublished results). It has yet to be determined whether treatment of HMC-1 cells with IC87114 prior to SCF stimulation would abrogate this increase in Akt phosphorylation.

Collectively, these results indicate that p110δ is the critical PI3K isoform signalling downstream of the c-kit receptor in WT untransformed BMMCs. However the constitutive

Akt phosphorylation in the transformed mast cell line HMC-1 is less dependent on p110δ, which raises the question of whether c-kit signalling remains dependent on p110δ in other transformed cells.

1.8 P110δ AND NON-HAEMATOPOEITIC CANCER

In addition to the high level of p110δ expression in leukocytes, low levels of p110δ expression have been detected in all human and mouse non-leukocyte cell types (Verrall & Vanhaesebroeck, unpublished results). There have been no somatic mutations reported in the p110δ gene, *PIK3CD* (Cornillet-Lefebvre, et al., 2006; Knobbe & Reifenberger, 2003; Phillips, et al., 2006), although there are several cases of *PIK3CD* gene amplification in cancer (Knobbe & Reifenberger, 2003; Mizoguchi*, et al.*, 2004; Sawyer*, et al.*, 2003). Some of these cancers are of non-haematopoietic origin and it is feasible to think that overexpression of p110δ in cells that under normal conditions express very low levels, may be sufficient to induce elements of cell transformation. Some examples of *PIK3CD* gene amplification and/or high p110δ expression in non-haematopoietic cancers are described below.

1.8.1 Breast cancer and melanoma

The study by Sawyer *et al,* is the only investigation of p110δ isoform expression in cells of breast and melanocyte origin, however it brought to light some interesting results implicating a role for p110δ beyond the immune system and warrants further discussion. Through compiling information from the GenBank database on the tissue distribution of ESTs (expressed sequence tags) for p110 isoforms, it has been found that the two tissues expressing the most abundant p110δ ESTs, outside the haematopoietic system, are melanocyte/melanoma and breast tissue (Sawyer*, et al.*, 2003). This finding led to analysis of p110δ protein expression in cells of melanocyte and breast origin. In both primary normal human breast cells and in primary breast tumour cells, p110δ protein expression is high. In addition, in the primary tumour samples, there appears to be a down-regulation of p110α expression and in some cases of p110β (Sawyer, et al., 2003). This could suggest that in primary breast tumour cells, p110δ has in some cases become the principle class IA PI3K isoform, however, given that the sample size of the analysis was quite small (two primary normal breast samples and four primary tumour samples), further investigation is required to corroborate and validate this hypothesis.

In established breast tumour cell lines, including MDA-MB-361, BT20, MDA-MB-435, GI101 and MDA-MB-231, relatively high p110δ levels have been found in all cell lines with exception to MDA-MB-361 in which no p110δ expression was detected. In most cases the relative expression of p110α and p110β also remains high. Interestingly, the cell line MDA-MB-231, which has the highest level of p110δ expression (comparable to levels in a leukocyte cell line) has reduced levels of p110α and p110β expression compared to the other breast tumour cell lines. All p110 isoform expression is increased in melanoma cell lines compared to melanocytes.

Sawyer *et al*, has investigated the functional role of p110δ expression in the MDA-MB-231 breast cancer cell line in cell migration. Isoform-specific neutralisation of PI3K isoforms, by PI3K antibody microinjection or by using a p110δ-selective inhibitor, demonstrates that p110δ is the principle p110 isoform required for regulation of EGF-driven motility *in vitro*. p110δ was found to control directionality and speed of cell migration, whereas p110β was found to only control direction and not speed of cell migration. Remarkably, inhibition of p110α had no impact on cell migration in the MDA-MB-231 breast cancer cell line. A further indication that p110δ plays an important role in breast cancer cell migration is the finding that the breast cancer cell line MDA-MB-361, which has no detectable p110δ protein expression, does not migrate or chemotax when exposed to an EGF gradient.

As the authors point out, breast tissue and melanocytes share functional characteristics with regard to migration. Breast tissue is a highly dynamic tissue and migration is critical function of melanocytes during development. Furthermore, breast cancer and melanoma metastasis share a similar pattern of metastatic sites. The expression of p110δ in these cells might therefore be causally related to their shared migratory activities under normal and transformed conditions (Sawyer, et al., 2003).

1.8.2 Glioma

In addition to detecting p110δ protein expression in breast tissue and melanocytes, Sawyer *et al,* also detected high levels of p110δ expression in five other cells/tissue of non-haematopoietic origin; three mouse microglia cell lines, ovarian carcinoma cell line and primary synoviocytes. The precise origin and cell lineage of microglia, which are thought of as the 'macrophages' of the nervous system, is still a matter of some debate. Unlike macroglia (astrocytes and oligodendrocytes) and neurons, which derive from

neuroectoderm, microglia are thought to derive prenatally from mesodermal progenitors, that are distinct from monocytes (Chan*, et al.*, 2007). Microglia-like cells can be derived *in vitro* from embryonic stem cells and it is most likely that microglia are in fact of haematopoietic origin (Chan*, et al.*, 2007). This would indeed help to explain the high p110δ protein expression in these cells.

Malignant gliomas range from low grade glioma, astrocytoma, oligodendroglioma to high grade glioblastoma. The origin of cells found in malignant gliomas remains enigmatic, although it is possible that they are derived from neural progenitor cells. The invasion of tumour cells into brain tissue is a pathologic hallmark of high grade gliomas and contributes significantly to the failure of current therapeutic treatments (Louis, 2006). Activated microglial cells are abundant in brain tumours and have actually been shown to stimulate the motility of glioma cells (Markovic*, et al.*, 2005). It would be extremely interesting to investigate the role of PI3K, specifically p110δ in microglia cells and in glioma progression. In fact, genetic alterations of the gene encoding p110δ, *PIK3CD*, have been found, albeit at a low frequency of 6%, in cases of glioblastoma (Knobbe & Reifenberger, 2003; Mizoguchi*, et al.*, 2004). Both *PIK3CD* mRNA and gene copy number has been found to be increased in glioblastoma tumours.

Although p110δ is the predominant PI3K isoform in cells of the immune system, it is becoming apparent that the role it plays in other cell types should not be overlooked.

1.9 REGULATION OF PI3K GENE EXPRESSION

The restricted tissue distribution of p110δ and p110γ, compared to the more broadly expressed p110α and p110β catalytic subunits, has led to studies investigating the mechanisms by which PI3K gene expression is regulated. It has been demonstrated that for all class I PI3K isoforms, mRNA and protein levels show a reasonable level of correlation (Geering, et al., 2007b; Verrall & Vanhaesebroeck, unpublished results), indicating that significant regulation of PI3K expression occurs at the transcriptional level.

1.9.1 Transcription

Transcription is the enzymatic process of synthesising a complementary RNA strand, in the form of messenger RNAs (mRNAs), transfer RNAs or ribosomal RNAs, from DNA. RNA polymerase II is involved in the synthesis of mRNAs and is one of the first steps leading to gene expression.

In eukaryotes, DNA is found wrapped around a set of eight histone molecules making up the nucleosome, which is the fundamental repeating unit of <u>chromatin</u>. The nucleosome serves as general repressor of gene transcription, however remodelling of chromatin structure transiently exposes promoter DNA sequences allowing interaction of the promoter regions with transcription machinery (the transcription core promoter is discussed in more detail in section 1.9.3) (Boeger, *et al.*, 2003). Chromatin modifying and remodelling complexes target the nucleosome either through acetylation/deacetylation of histones or through disruption of histone-DNA interactions and in this way can affect gene expression (Vignali, *et al.*, 2000).

The promoter region contains specific DNA sequences that are recognised by DNA-binding proteins, or transcription factors (TFs), which are involved in the recruitment and binding of RNA polymerase II. The RNA polymerase II machinery comprises 6 proteins: RNA polymerase II, and five general TFs, known as TFIIB, -D, -E, F, and –H (Conaway & Conaway, 1997). Although RNA polymerase II alone is capable of unwinding DNA, synthesising RNA, and rewinding DNA, it requires the general TFs to recognise a promoter. Another protein complex, termed Mediator, which consists of more than 20 subunits, with a total mass in excess of a million Daltons, is also required for transcription regulation (Kim, *et al.*, 1994). The completed assembly of TFs and RNA polymerase II bound to the DNA promoter is called the transcription initiation complex (Figure 1.13).

The promoter surrounds the first base pair that is transcribed into RNA. From this point, RNA polymerase II moves along the template DNA strand, synthesising RNA until it reaches a terminator sequence. This forms a transcription unit, which may include more than one gene.
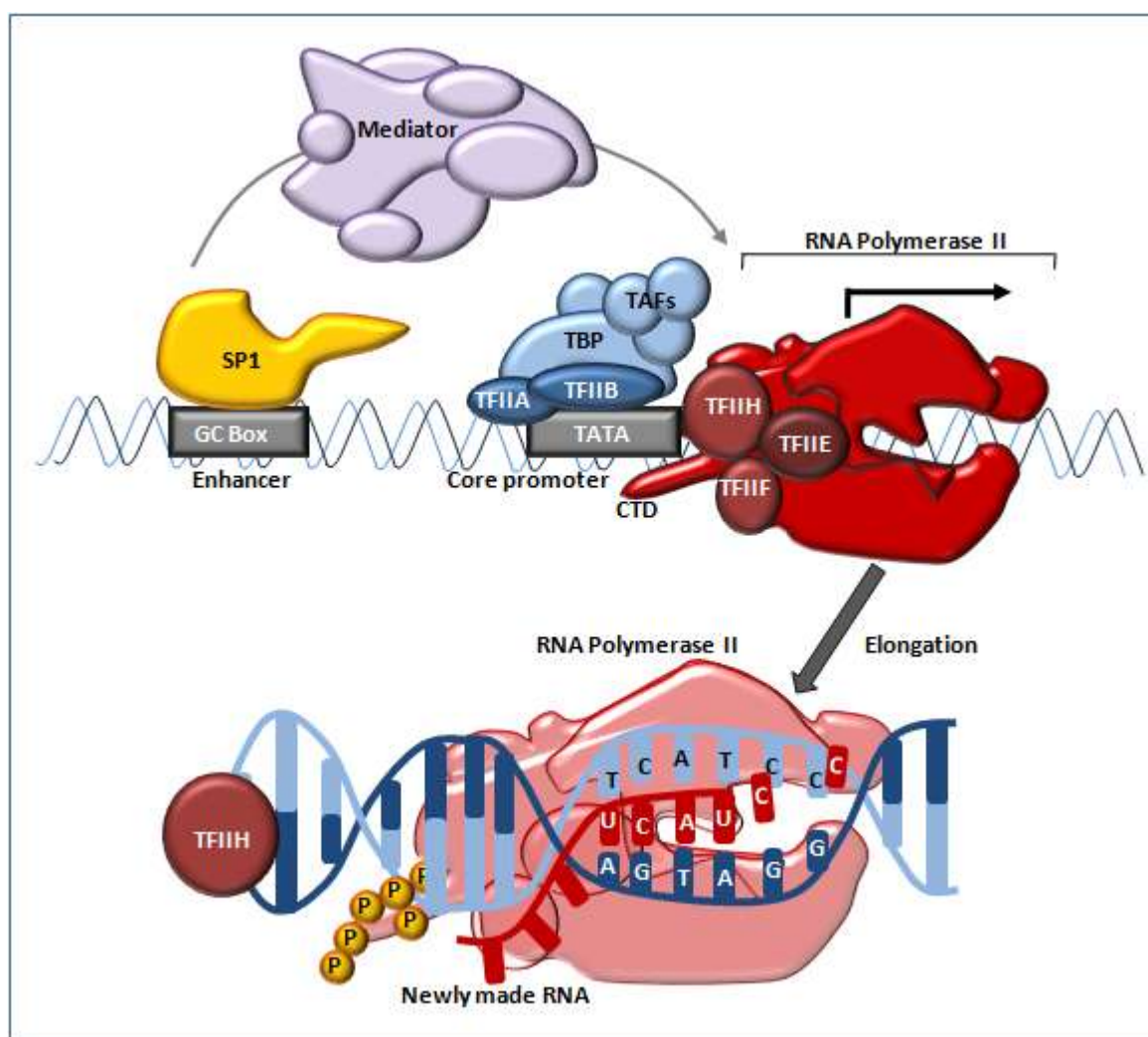
Figure 1.13: Initiation of transcription. The first step in initiating eukaryotic transcription is assembly of the preinitiation complex, which comprises of TBP (TATA Binding Protein) and an attached complex of TAFs (TBP Associated Factors), collectively known as TFIID (Transcription Factor for polymerase II D). TFIIB and TFIIA binds TFIID and DNA, stabilizing the first complex, which allows for subsequent recruitment of TFIIF associated with RNA polymerase II, followed by TFIIE and TFIIH recruitment. TFIIH is a protein complex that contains a DNA helicase, which separates the DNA strands at the transcription start site (Lennartsson*, et al.*), and protein kinase that phosphorylates the C-terminal domain (CTD) of RNA polymerase II. CTD phosphorylation of RNA polymerase II induces it to release from the DNA promoter and initiation of RNA synthesis. Multisubunit cofactors, such as Mediator, can interact with enhancers such as SP1, which may be located several kilo-bases away from the core promoter, and the transcriptional machinery to enhance gene transcription. It is should be noted that some promoters do not contain a TATA box.

1.9.2 Transcript processing

Before an RNA gene transcript is transported out of the nucleus it undergoes 3 processing events: 1) addition of a 5'cap, 2) addition of a 3' poly(A) tail (polyadenylation) and 3) removal of introns (splicing), events depicted in Figure 1.14.
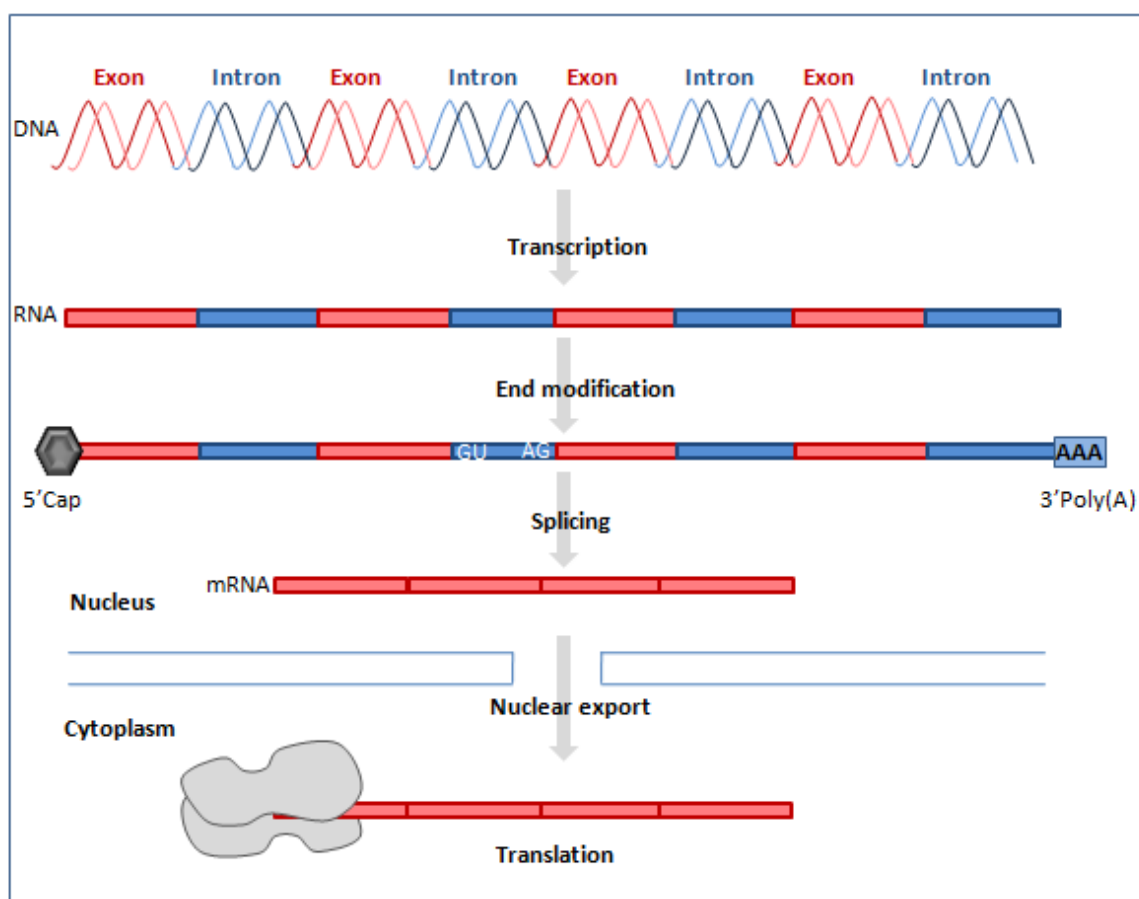
Figure 1.14: Schematic of transcript processing.   An ensemble of transcriptional complexes in the nucleus transcribes a complementary RNA strand from a DNA template strand.   The RNA transcript is subject to modification in the nucleus, which involves the addition of a 5'cap and 3' polyadenylation.   Prior to RNA nuclear export, intronic sequences are removed from the RNA transcript, in a process termed RNA splicing, resulting in mature mRNA.   Intron splicing most commonly occurs at GU-AG intron sequences. Mature cytoplasmic mRNA is subsequently translated.

5' Capping: Transcription starts with a nucleoside triphosphate, usually either purine A or G.   The first nucleotide retains its 5' triphosphate group and makes the usual phosphodiester bond from its 3' position to the 5' position of the next nucleotide, which can be represented as 5' pppA/GpNpNpNp and so on.   However, immediately after transcription initiation, all transcripts made by RNA polymerase II undergo a 5' capping process in which a guanine nucleotide is added onto the 5' terminal by the nuclear enzyme guanylyl transferase. The additional guanine nucleotide is added in reverse orientation via an unusual 5' to 5' triphosphate linkage (Bentley, 2002). The guanine residue is substrate for several methylation events, the first of which involves the addition of a methyl group to the 7' position of the terminal guanine resulting in a cap structure resembling $m^7G(5')ppp(5')A/GpNpNp$. The cap is thought to influence splicing of the first intron,

mRNA stability and mRNA transport to the cytoplasm, where it binds translation initiation factors. Any mRNA lacking a cap structure is rapidly degraded by exonucleases.

3' Polyadenylation: Many transcripts contain a 3' terminal stretch of adenosine residues, often referred to as a poly(A) tail. The poly(A) sequence is added to RNA in the nucleus after transcription and is a process requiring many nuclear proteins. Cleavage and polyadenylation specificity factor (CPSF) recognises and binds RNA at the 3' hexamer site 'AAUAAA', while cleavage and stimulatory factor interacts with U-rich or GU-rich regions enhancing CPSF affinity for the hexamer (Cramer, et al., 2001).   Poly(A) polymerase associated with these two factors initiates the polyadenylation reaction, which occurs in two stages. Poly(A) can increase mRNA stability and is important for mRNA nuclear export and translation (Wickens*, et al.*, 1997).

Splicing: The primary transcript, referred to as pre-mRNA, has the same organisation the DNA from which it was transcribed. The removal of introns from pre-mRNA, in a process called RNA splicing, results in mRNA which contains only exons. Splice sites, which occur at exon-intron boundaries have well-conserved, although short, consensus sequences. The most frequently observed splice site consensus sequence, GT-AG is found immediately within the intron, shown here in blue and underlined, AG**GT**AAGT...YYY**AG**N, with exon residues shown in red (in RNA the sequence is, of course, GU-AG). Introns can be removed by the spliceosome, a complex of specialized RNA and protein subunits, within 30 seconds of transcription of the 3′ splice site, however, post-transcriptional splicing also occurs (Bentley, 2002).

1.9.3 The transcription core promoter

The core promoter is the minimal stretch of immediate DNA sequence that is sufficient to direct accurate initiation of transcription by the RNA polymerase II machinery (Butler & Kadonaga, 2002). The core promoter typically encompasses the site of the transcription initiation and extends approximately 35 nucleotides upstream or downstream. There are several motifs that are frequently found in some but not all core promoters (Figure 1.15), which will be discussed further below.

The initiator: The Inr element contains the TSS and has been found in a variety of eukaryotes in both TATA-containing and TATA-less core promoters (Butler & Kadonaga, 2002). The consensus for the Inr in mammalian cells is Py-Py(C)-A_{+1}-N-T/A-Py-Py, where the A_{+1} represents the common nucleotide at which transcription is initiated (Javahery*, et*

al., 1994). However, more generally, transcription initiates at a single site or in a cluster of multiple sites in the vicinity of the Inr and not necessarily at the A_{+1} position (Butler & Kadonaga, 2002). A number of factors have been found to interact with Inr motifs and may participate in Inr-dependent transcription at a subset of promoters (Liston, *et al.*, 2001; Malecova, *et al.*, 2007).
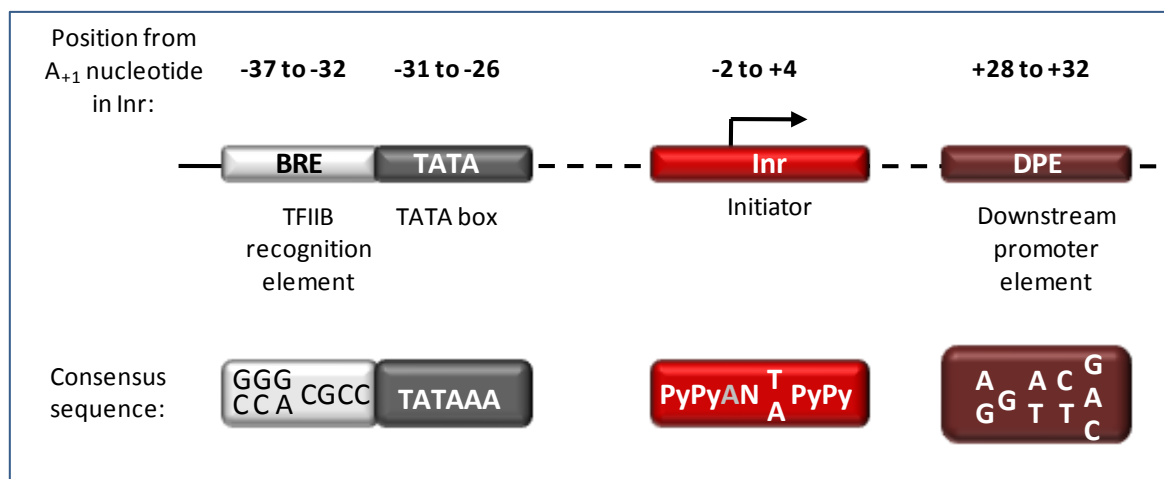
Figure 1.15: Core promoter elements. Common promoter motifs that can participate in transcription by RNA polymerase II are depicted, however, a specific promoter may contain some, all or none of these elements. The **BRE** (TFIIB recognition element) is an upstream extension of a subset of TATA boxes. The **DPE** (downstream core promoter element) requires an **Inr** (Initiator), and is located precisely at +28 to +32 relative to the A_{+1} nucleotide in the Inr. The DPE consensus was determined with *Drosophila* transcription factors and core promoters. Adapted from Butler & Kadonaga, 2002.

The downstream core promoter element (DPE): The DPE was identified in *Drosophila* and acts as cooperative binding site for TFIID in addition to the Inr, although it is also present in humans (Burke & Kadonaga, 1996; Zhou & Chiang, 2001). Mutation of either Inr or DPE results in loss of TFIID binding. DPE motifs most commonly occur with TATA-less promoters located precisely at +28 to +32 relative to the A_{+1} position in the Inr. Alteration of the spacing between these two elements by a single nucleotide results in a several fold-reduction of transcription activity (Burke & Kadonaga, 1996).

The TFIIB recognition element (BRE): The BRE is a TFIIB binding site that is located immediately upstream of some TATA boxes (Lagrange, *et al.*, 1998). The BRE consensus is G/C-G/C-G/A-C-G-C-C' where the 3' C of the BRE is followed by the 5' T of the TATA box (Butler & Kadonaga, 2002). *In vitro* studies have revealed BRE motifs to have both a positive and negative effects on transcription (Evans, *et al.*, 2001; Lagrange, et al., 1998).

***CpG Islands*:** CpG sites are regions of DNA in which a cytosine nucleotide is situated next to a guanine nucleotide, linked by a phosphate group. CpG dinucleotides are the substrates of DNA methyltransferase, which catalyses the covalent addition of a methyl group ($-CH_3$) to the 5' position of the cytosine ring. Spontaneous deamination of the 5-methylcytosine to give a TpG dinucleotide, which is not repaired by the DNA repair machinery, has subsequently led to loss of CpG sits in the human genome. Regions of DNA that have a higher concentration of CpG sites are known as CpG islands.

CpG islands are often but not always found in promoter regions with around 40% of genes containing CpG islands that are situated at the 5' region incorporating the promoter, untranslated regions and exon 1 (Jones & Baylin, 2002). The rest of the genome, such as the intergenic and the intronic regions, is considered to be CpG poor (Miranda & Jones, 2007). CpG islands typically lack TATA or DPE core promoter elements, but contain multiple GC box motifs that are bound by SP1 and related transcription factors (Butler & Kadonaga, 2002).

DNA methylation of CpG islands at a promoter region usually prevents gene expression. Genome-wide demethylation of normally methylated and silenced chromosomal regions, and hypermethylation and silencing of genes including tumour suppressors are common features of cancer cells (Barton*, et al.*, 2008; Stirzaker*, et al.*, 2004). It has been suggested that DNA methylation can directly impede the binding of transcriptional factors to their target sites, thus prohibiting transcription. Other proposed mechanisms are based on the idea that methylation of CpG sequences can alter chromatin structure by affecting histone modifications and nucleosome occupancy within the promoter regions of genes. In addition, DNA methylation has been found to recruit methyl-binding proteins that specifically bind to methylated CpG dinucleotides, which have been shown to play a role in methylation-dependent silencing of transcription (Nan*, et al.*, 1998a; Nan*, et al.*, 1998b).

All of the "housekeeping" genes that are constitutively expressed have CpG islands, which accounts for approximately half of the islands altogether. The rest of the CpG islands occur at promoters of tissue-regulated genes, although less than 40% of these genes have CpG islands (Jones & Gonzalgo, 1997; Sulewska*, et al.*, 2007). CpG islands located in promoter regions are usually unmethylated in all normal tissues, regardless of the transcriptional activity of the gene. Therefore, the presence of unmethylated CpG islands indicates genes that can be potentially active, rather than their certain transcription.

1.9.4 Spatial and temporal control of gene expression

Transcription initiation is a key regulatory step in controlling gene expression. Formation of the preinitiation complex must occur at the correct time at a specific promoter to induce appropriate mRNA synthesis, for example in tissue-specific gene expression. Metazoan organisms have evolved specialized transcription initiation complexes and promoter-selectivity modules that direct coordinated regulation of functionally related gene networks (Hochheimer & Tjian, 2003). As previously mentioned, transcription activation is governed by an ensemble of multisubunit transcription factor complexes at specific DNA sequences. Regulation of transcription may occur at the level of chromatin remodelling and nucleosome mobilisation, to expose promoter elements, or at the level of regulation of the transcription machinery itself.

Certain genes display tissue-restricted expression, an example of such a gene is *Vav*. Vav is a Rho family GTPase GTP/GDP exchange factor, which is expressed in virtually all cells of haematopoietic lineage and only expressed in embryonic stem cells outside the haematopoietic system (Katzav, *et al.*, 1989; Keller, *et al.*, 1993). The restricted tissue distribution of Vav is suggested to be due to the presence of five major DNase I hypersensitive sites found upstream of the TSS in the murine *Vav* gene in cells of haematopoietic lineage but not in fibroblasts (Ogilvy, *et al.*, 1998). DNase I hypersensitive sites are destroyed by extremely low concentrations of DNase, indicating that they are readily accessible to outside molecules. This accessibility appears to arise from the almost complete absence of nucleosomes in this region of DNA, and as a result DNase I hypersensitive sites are associated with regions of chromatin containing active promoters or enhancers, where DNA-binding proteins are found. In addition, the murine *Vav* promoter sequence contains potential binding sites for tissue-restricted TFs, such as GATA, Myb, Oct and Ets proteins, in addition to ubiquitous TF binding sites.

Temporal control of gene expression is exemplified by studies of neuronal gene expression. Neural activity-dependent gene transcription occurs over various time periods, from minutes to days. A group of genes called 'immediate early genes' are rapidly upregulated after neuronal enhancement, such as *Arc* transcription which occurs in rat brain after 5 min after the animal is moved to a novel environment (Vazdarjanova, *et al.*, 2002). Rapid activation of gene transcription occurs is directly regulated by presence of specific TFs, in addition to epigenetic processes such as DNA methylation and histone modification. An intensively studied TF involved in neuronal activity-dependent gene

regulation is the CREB (cAMP response element-binding) family of TFs (Mayr & Montminy, 2001). CREB promotes cell survival of neurons during development and in adult neurons and is involved in the formation of long-term memory (Abe, 2008). The TF CREB and family members CREM and ATF1 are activated by multiple pathways in neurons and regulate the transcription of a number of neuronal-associated genes.

Differential gene expression may be regulated by multiple promoters. For example, the lymphocyte-specific proto-oncogene *lck* is transcribed from two developmentally regulated, independently functioning promoters. It has been found that the *lck* proximal promoter is used in thymocytes, but not in peripheral T lymphocytes, whereas the distal promoter operates in all stages of T cell development, but predominates in more mature cells (Wildin*, et al.*, 1995). Another example of gene transcription arising from multiple promoters is expression of the active hormonal form of vitamin D, which has a central role in calcium and phosphate homeostasis and the maintenance of bone. Upstream untranslated exons of the human vitamin D receptor gene (a member of the nuclear receptor family) are incorporated into numerous variant transcripts, which suggested the presence of multiple promoters (Crofts*, et al.*, 1998). Indeed, transcripts containing one particular upstream untranslated exon (exon 1f) were only found in kidney tissue and one particular intestinal cell line. This tissue-specific expression of so-called exon 1f-containing transcripts was found to be mediated by a distal promoter more than 9 kb upstream of the other untranslated exons identified (Crofts, et al., 1998).

Heterogeneity in the 5' region is a common feature of other nuclear receptor genes. Tissue-specific alternative-promoter usage generates multiple transcripts of the human estrogen receptor a (ERα), the human and rat mineralocorticoid receptors, and the mouse glucocorticoid receptor, which differ in their 5' UTRs but code for identical proteins (Keaveney*, et al.*, 1991; Strahle*, et al.*, 1992; Zennaro*, et al.*, 1995). Other members of the nuclear receptor superfamily have multiple, functionally distinct isoforms arising from differential promoter usage and/or alternative splicing (Lazar, 1993; Zhu*, et al.*, 1995).

1.9.5 Transcriptional regulation of PI3K expression

Both p110δ and p110γ are highly expressed in cells of haematopoietic origin compared to other cell types, p110α and p110βs in contrast are more broadly expressed, suggesting specific PI3K isoform expression can be regulated by alternative mechanisms. It is likely that p110δ and p110γ gene expression is under the control of haematopoietic-specific

transcriptional regulators, whereas p110α and p110β gene expression is under the control of widely expressed regulators of transcription.

1.9.5.1 p110γ gene analysis

There has been little investigation into the transcription control of p110γ, however, a promoter region for murine p110γ has been identified (Hirsch, *et al.*, 2000b). Murine p110γ cDNA is 86% homologous to its pig and human orthologues at the nucleotide level. Multiple transcriptional start sites exist for p110γ, which results in transcripts with varying 5'UTRs, the longest being 874 bp upstream of the translational start site. Analysis of 1.2 Kb of 5′ flanking genomic DNA revealed that the putative promoter region does not contain a TATA box and is not GC-rich. However, consensus sites for housekeeping transcription factors such as AP1 and SP1, were identified along with consensus sequences included binding sites for transactivators involved in haematopoietic differentiation such as C/EBP β, GATA-1 and Ets-2 (Hirsch, et al., 2000b). Functional analysis of the p110γ putative promoter region revealed it has enhanced promoter activity in the myelomonocytic cell line U937, which expresses high level of endogenous p110γ, compared to the human epithelial cell line HeLa, which express undetectable levels of p110γ protein expression (Hirsch, et al., 2000b). These data suggest that the presence of haematopoietic-specific TF-binding sites contributes to the tissue-restricted gene expression of p110γ.

1.9.5.2 Transcriptional regulation of PIK3CA oncogene

PIK3CA upregulation, amplification and mutations have been identified in solid tumours in a number of studies (Bachman, *et al.*, 2004; Broderick, *et al.*, 2004; Campbell, *et al.*, 2004; Karakas, *et al.*, 2006; Samuels & Velculescu, 2004; Samuels, *et al.*, 2004). Recently, the 5' upstream regulatory region of human *PIK3CA* has been located 50 Kb upstream of the translational start codon and was found to be around 60% homologous to the murine *PIK3CA* 5' upstream regulatory region (Yang, *et al.*, 2008). Predicted TF-binding sites in the human *PIK3CA* 5' upstream regulatory region include NFκB, hypoxia-inducible factor (HIF), heat-shock protein (HSP) and activator protein 1 (AP1). Consistent with these findings, strong HIF and NFκB staining is associated with areas of high *PIK3CA* expression in solid tumours. Furthermore, the human *PIK3CA* promoter NFκB binding site can be activated by NFκB, illustrating it is indeed functional, and results in upregulation of *PIK3CA* mRNA in ovarian cancer cell lines *in vitro* (Yang, et al., 2008). Based on these findings, stress signalling pathways, namely HIF and NFκB, are implicated

in *PIK3CA* regulation in cancer. NFκB plays a critical role in inflammation-driven tumour formation, growth and progression, promoting transcription of diverse genes encoding inflammatory cytokines, growth factors and cell adhesion molecules (Lenardo & Baltimore, 1989; Luo*, et al.*, 2004a; Pikarsky*, et al.*, 2004). This recent data provides evidence that NFκB activation directly upregulates *PIK3CA* transcription. However, given that NFκB expression is highly inducible in response to inflammatory stimuli (Tak & Firestein, 2001; Xiao & Ghosh, 2005) whereas p110α expression appears to be unaltered, it is clear that the regulation of *PIK3CA* gene expression by NFκB is more complex than what is initially perceived from the study by Yang, *et al*.

1.10 AIMS OF THE STUDY

PI3Ks are attractive therapeutic targets in inflammation and cancer. Broad-spectrum PI3K inhibitors have proved to be toxic to the organism and therapeutic interference with PI3K signalling will most likely have to be targeted at single PI3K isoforms or selected groups of PI3K isoforms. It is therefore critical to elucidate the isoform-specific roles of PI3K so that individual isoforms may be targeted. Various genetic and cell-based approaches have revealed non-redundant roles for PI3K isoforms and have greatly enhanced our understanding of specific isoform-mediated functions.

This study is focused on investigating the role of p110δ. p110δ has a more restricted tissue distribution than p110α and p110β and is predominantly expressed at high levels in leukocytes and cells of the immune system. To illustrate an important role of p110δ in cells of the immune system, in mast cells, p110δ is the principle isoform mediating PI3K-dependent signalling downstream of the tyrosine kinase receptor, c-kit. The mechanism of regulation of p110δ gene (*PIK3CD)* expression leading to predominantly leukocyte-restricted p110δ expression is unknown. In addition to high expression of p110δ in leukocytes, an abundant expression of p110δ has also been found in breast cells and melanocytes and has been found to play an important role in the EGF-driven *in vitro* migration of breast cancer cell lines.

The aim of this study was to further investigate the isoform-specific signalling of p110δ using cell-based models, aimed at addressing three main questions:

1) Using p110δ coupling to c-kit in mast cells as model, does coupling of class IA PI3Ks to tyrosine kinase receptors remain the same under normal and transformed cellular states?
2) Using *in silico* promoter analysis and luciferase reporter assays, is the leukocyte-restricted p110δ gene expression mediated by a leukocyte-specific *PIK3CD* promoter?
3) Through stable overexpression of p110δ in the fibroblast cell line NIH 3T3, what is the impact of p110δ overexpression in non-leukocyte mammalian cells?

2. MATERIALS AND METHODS

Company names and catalogue numbers are provide between brackets.

2.1 BUFFERS, SOLUTIONS AND REAGENTS

2.1.1 General buffers

PBS: 137 mM NaCl, 2.7 mM KCl, 9.5 mM Na_2PO_4H, 1.4 mM $K_2PO_4H_2$ (Severn Biotech LTD).

TAE buffer: 50 mM Tris-Acetate, 1 mM EDTA, pH8

PBS-T: 0.1% (v/v) TWEEN®20 (Sigma, #P1379) in PBS

TBS: 20 mM Tris-HCl pH7.5, 137 mM NaCl in ddH_2O

TBS-T: 0.1% (v/v) TWEEN®20 in TBS

TE: 10 mM Tris-HCl pH 7.5, 1 mM EDTA

2.1.2 General reagents

Bio-Rad Protein Assay Dye Reagent (BioRad, #500-0006)

Trypsin-EDTA (GIBCO, #25300)

Gelatin (Sigma, G1393)

Fibronectin (Sigma, #F-2006)

Collagen R (Serva, #47254)

DMSO (Sigma)

Giemsa stain (Sigma, 48900)

May-Grunwald solution (Thermo Scientific 89027)

Inhibitors: (For PI3K inhibitors see section 2.1.5)

Rac inhibitor: NSC23766 (Calbiochem)

ROCK inhibitor: Y-27632 (Calbiochem, #688000)

Cytokines:

Recombinant murine PDGF-BB (Peprotech, #315, 18)

Recombinant murine IL-3 (Peprotech, #210-31)

Recombinant murine SCF (Peprotech, #250-03)

Transfection reagents:

SuperFect Transfection Reagent (Qiagen, 301305).

FuGENE® 6 Transfection Reagent (Roche, 11 814 443 001).

Antibiotics:

Geneticin® (Invitrogen, 10131-019)

Ampicillin (Invitrogen, 11593-027)

Dual luciferase reagents:

Dual-Luciferase® Reporter Assay System (Promega, E1910). Each system includes:

Passive Lysis Buffer, Luciferase Assay Reagent II and Stop & Glo® Reagent.

Matrigel preparations:

Collagen type I (Marathon, #354249)

Powdered α MEM (GIBCO, #11900-073)

Matrigel (Marathon)

Bacteria:

LB media: 12.5g LB broth (BD, #244620) in 500 ml dd H_20.

LA plates: 12.5g LB broth (BD, #244620) + 7.5 g Agar (Sigma, #L2897) in 500 ml dd$H_2$0.

Antibiotics: 100 μl ampicillin (100 mg/ml) / ml LB media and LA plates.

S.O.C. media: (Invitrogen, 15544-034)

2.1.3 Lysis buffer reagents

Standard lysis buffer :	Final concentration of inhibitors added before use :
50 mM Tris-HCl pH 7.4	50 mM NaF [phosphatase inhibitor (BDH, #102464T)]
100 mM NaCl	1 mM Na_3VO_4 [tyrosine phosphatase inhibitor (Sigma, #S6508)]
50 mM NaF	10 μM leupeptin [serine and cysteine protease inhibitor (SIGMA, #L2884]
5 mM EDTA	0.7 mM pepstatin A [acid protease inhibitor (Sigma, #P4265)]
2 mM EGTA	27 μM TLCK [serine protease inhibitor (Sigma, #T7254)]
40 mM β-glycerophosphate	1 mM PMSF [serine protease inhibitor, dissolved in isopropanol (Sigma, #F1428)]
10 mM sodium pyrophosphate	1 μM okadaic acid [phosphatase inhibitor (Calbiochem, #495604)]
1% Triton X-100	1 μg/ml aprotinin [trypsin inhibitor (Sigma, #A6103)]

Lysis buffer for Rho-pull downs:	*Final concentration of inhibitors added before use :*
50 mM Tris-HCl pH 7.5	0.5% β-mercaptoethanol (Sigma M7522)
1 mM EDTA	1 mM PMSF
500 mM NaCl	1 mM DTT
10 mM $MgCl_2$	0.2 mM Na_3VO_4
1% Triton X-100	1 μg/ml aprotinin
0.5% Na Deoxycholate	1 μg/ml leupeptin
0.1% SDS	1 μg/ml pepstatin A
10% Glycerol	

2.1.4 Buffers and reagents for SDS-PAGE and protein detection

Preparation of acrylamide separating and stacking gels:

	1 x large gel system (Hoefner)		2 x small gel system (BioRad)	
	8% Separating gel	Stacking gel	8% Separating gel	Stacking gel
1.5 M Tris-HCl pH 8.8	7.5 ml	-	3.75 ml	-
1 M Tris-HCl pH 6.8	-	1.25 ml	-	0.625 ml
H_2O	13.9 ml	6.8 ml	6.95 ml	3.4 ml
30% Acrylamide solution	8.0ml	1.7 ml	4.0 ml	0.85 ml
10% SDS	0.3 ml	0.1 ml	0.15 ml	0.05 ml
10% APS	0.3 ml	0.1 ml	0.15 ml	0.05 ml
TEMED	0.018 ml	0.01 ml	0.01 ml	0.005 ml

(TEMED = Tetramethylethylenediamine; APS = ammonium persulfate)

The separating gel was made first and left to set before making up the stacking gel to layer over the top of the separating gel.

Running buffer: 0.25 M Tris, 0.192 M glycine, 0.1% w/v SDS, pH 8.3

Transfer buffer: 48 mM Tris-HCl pH 8.5, 0.39 M glycine, .1% SDS, 20% methanol

5x SDS sample buffer:

156.25 mM Tris-HCl pH 6.8

5% w/v SDS

25% v/v glycerol

0.0025% w/v bromophenol blue

250 mM DTT (add just before use)

Home-made ECL:

Solution A: 20 mM Tris-HCL pH 8.5, 0.02% H_2O_2

Solution B: 20 mM Tris-HCL pH8.6, 13.2 mg coumaric acid (Sigma, #C9008), 0.868 mg luminal (Sigma, #A8511).

Equal volumes of solution A and solution B were mixed before use.

Stripping buffer:

191.06g guanidine hydrochloride (Sigma, #G4505) dissolved in 250 ml ddH_2O. Once dissolved, concentrated HCl was added drop wise to reach pH 3.

<u>2.1.5 PI3K inhibitors</u>

LY294002: Pan PI3K inhibitor (Calbiochem)

TGX-115: p110β-selective (Merck-Serono, Geneva)

IC87114: p110δ-selective (Merck-Serono, Geneva)

AS604850: p110γ-selective (Merck-Serono, Geneva)

	IC_{50}s (µM) of PI3K inhibitors on class I PI3K p110 isoforms			
Inhibitor	**p110α**	**p110β**	**p110δ**	**p110γ**
LY294002	9.3	2.9	6.0	>20
TGX-115	>20	0.03	0.34	>20
IC87114	>200	16	0.13	61
AS604850	3.44	>20	>20	0.19

Table 2.1: IC_{50} values of PI3K isoform-selective inhibitors. (Knight, *et al.*, 2004; Knight, et al., 2006).

2.1.6 Antibodies

Primary antibodies

Name	Specificity	Source and cat. #	Secondary	Concentration/ dilution
Akt	Akt	Cell Signalling, 9272	Rabbit, pAb	1:1000 (WB)
pS473	P-Akt (S473)	Cell Signalling, 9271	Rabbit, pAb	1:1000 (WB)
pT308	P-Akt (T308)	Cell Signalling, 4056	Rabbit, mAb	1:1000 (WB)
β-actin	β-actin	Sigma, ac-15	Mouse, mAb	1:1000 (WB)
9E10	c-Myc	Abcam, ab32	Mouse, mAb	1:1000 (WB)
9B11	Myc-tag	Cell Signalling, 2276	Mouse, mAb	1:1000 (WB) 1:1000 (IP)
p110α-15	p110α	In house	Rabbit, pAb	1:500 (WB) 1:500 (IP)
p110α	p110α	Transduction Labs P94520150	Mouse, mAb	0.25 mg / ml 1:1000 (WB)
PI 3-kinase p110β (S-19)	p110β	Santa Cruz, sc-602	Rabbit, pAb	0.2 mg /ml, 1:1000 (WB)
p110δ	p110δ-CT	In house	Rabbit, pAb	1 mg / ml 1:5000 (WB), 1:1000 (IP)
PI 3-kinase p110δ	p110δ-CT	Abcam, 1678	Rabbit, pAb	1 mg / ml 1:1000 (WB), 1:1000 (IP)
p110γ	p110γ	In house	Mouse, mAb	1:100 (WB)
PI3-Kinase, p85	Pan-p85	Upstate, 06-195	Rabbit, pAb	1:5000 (WB)
4G10	Phospho-Tyr	Upstate, 05-1050	Mouse, mAb	1:5000 (WB)
PMT	PMT	Provided by Dr. S. Dilworth (Imperial College, London)	Mouse, mAb	1:1000 (WB)
HOX11 (1D7)	HOX11	Santa Cruz, sc-12760	Mouse, mAb	1:1000 (WB)
Kit (C-14)	c-Kit receptor	Santa Cruz, sc-1493	Goat, pAb	1:500 (WB) 1:500 (IP)
FcεRI (G-14)	FcεRI	Santa Cruz, sc-33484	Goat, pAb	FACS

RhoA (26C4)	RhoA	Santa Cruz, sc-418	Mouse, mAb	1:100 (WB)
Rac1 (C-23A8)	Rac1	Upstate, 05-389	Mouse, mAb	1:500 (WB
Cdc42	Cdc42	Abcam, M152	Mouse, mAb	1:500 (WB
p190RhoGAP (CD2D6)	P190RhoGAP	Upstate, 05-378	Mouse, mAb	1:1000 (WB)
PTEN	PTEN	Cell Signalling , 9552	Rabbit, pAb	1:1000 (WB)
Cyclin D1 (C-20)	Cyclin D1	Santa Cruz, sc-717	Rabbit, pAb	1:1000 (WB)

Immunofluorescence

P-FAK (Y397)	p-FAK	Biosource, 44-624G	Rabbit, pAb	1:100 (IF)
P-paxillin	p-paxillin	Biosource, 44-722G	Rabbit, pAb	1:100 (IF)
N-cadherin (D-4)	N-cadherin	Santa Cruz, sc-8424	Mouse, mAb	1:100 (IF)
Phalloidin-fluorescein	F-actin	Sigma, P5382		1:400 (IF)
DAPI	DNA	Santa Cruz, sc-3598		1:100 (IF)

Secondary antibodies

Secondary	**Source**	**Source and cat. #**	**Dilution**
HRP-anti-rabbit IgG	Donkey	Amersham, NA934-1ML	1:5000 (WB)
HRP-anti-mouse IgG	Sheep	Amersham, NXA931	1:5000 (WB)
Anti-mouse IgG-FITC	Donkey	Jackson Immuno Research, 715-095-150	1:400 (IF)
Anti-rabbit IgG-FITC	Donkey	Jackson Immuno Research, 711-095-152	1:400 (IF)
Anti-rabbit IgG-Cy5	Donkey	Jackson Immuno Research, 711-175-152	1:400 (IF)
Anti-mouse IgG-Cy5	Donkey	Jackson Immuno Research, 715-175-151	1:400 (IF)
Anti-rabbit IgG-Cy3	Donkey	Jackson Immuno Research, 711-165-152	1:400 (IF)
Anti-mouse IgG-Cy53	Donkey	Jackson Immuno Research, 715-165-151	1:400 (IF)
Anti-mouse IgE-FITC	Rat	BD PharMingen, 553415	1:400 (FACS)
Anti-mouse c-kit-PE	Rat	BD PharMingen, 553355	1:400 (FACS)

2.1.7 Reagents for pull downs and immunoprecipitations

Beads	Used to pull down:	Source and cat. #
GST-tagged Rhotekin-RBD on agarose beads	RhoA-GTP	Cytoskeleton, RT02
GST-tagged PAK-RBD on agarose beads	Rac1-GTP/Cdc42-GTP	Cytoskeleton, PAK02
Protein A sepharose	Anti-rabbit polyclonal or monoclonal antibodies	Amersham, 17-5280-01
Protein G sepharose	Anti-mouse polyclonal or monoclonal antibodies	Amersham, 17-0618-01
Glutathione sepharose	GST-tagged proteins	Amersham, 17-5132-01

2.2 MICE

p110δ$^{D910A/D910A}$ mice have been described previously (Okkenhaug, et al., 2002) and were back-crossed on a Balb/c background. Age-matched, 6-10 week old littermate mice were used for all experiments.

2.3 CELL CULTURE

2.3.1 Cell lines and culture media

Cell line	Species	Type of cell line
A20	*Mus musculus*	Mature B cell line
CT26	*Mus musculus*	Colon carcinoma cell line
HEK293T	*Homo sapiens*	Embryonic kidney cell line
NIH 3T3	*Mus musculus*	Fibroblast cell line
RAW 264	*Mus musculus*	Macrophage cell line
Thp-1	*Homo sapiens*	Acute monocytic leukaemia cell line
WEHI-231	*Mus musculus*	Immature B-cell line
GP E86	*Mus musculus*	Fibroblast ectropic packaging cells

WEHI-231, A20 and Thp-1:

RPMI 1640 supplemented with 10% FBS, 1% penicillin/streptomycin and 50 μM β-mercaptoethanol (for β-mercaptoethanol, 500 μl of a 50 mM stock solution was added to 500 ml RPMI).

NIH 3T3, CT26, HEK 293T and GP E86:

DMEM supplemented with 10% FBS and 5 ml penicillin/streptomycin.

RAW 264:

RPMI 1640 supplemented with 10% certified FBS (GIBCO), 1% penicillin/streptomycin.

2.3.2 Primary cells and culture media

Primary murine bone marrow-derived mast cells (BMMCs):

RPMI 1640 supplemented with 10% ultra low IgG FBS, 1% penicillin/streptomycin and 1% L-glutamine. Cells were cultured in 20 ng / ml recombinant murine IL-3 and 20 ng / ml recombinant murine SCF.

2.3.3 Maintenance of mammalian cell lines

Cells were grown in the indicated cell culture media at $37^{o}C$ in a humidified incubator with 5% CO_2. In general cells were passaged every 2-3 days. For suspension cells, cells were diluted in pre-warmed media. For adherent cells, cells were washed with PBS and detached using trypsin-EDTA before being diluted in pre-warmed media.

For the adherent RAW 264 cell line, cells were grown in 10 cm^2 dishes. Cells were detached using a cell scraper. Cells were thoroughly mixed by pipetting to break up cell clumps and diluted 1:10 in pre-warmed media every 3-4 days.

2.3.4 Isolation and maintenance of BMMCs

Isolation: Bone marrow progenitors were isolated from the femurs of mice following dissection. Isolated femurs were cleaned with alcohol spray and the end the bones carefully cut off. Bone marrow progenitors were flushed out of each bone with 2 ml of RPMI using a 25 gauge needle. Cells were counted using a haemocytometer to distinguish mast cell progenitors from red blood cells, muscle cells, fibroblasts, neutrophils and other cell types. Generally isolated cell were diluted 1:10 in RPMI containing IL-3 and SCF.

Maintenance: 24 h after isolation of bone marrow progenitors, non-adherent cells were transferred to new culture flask (20 ml media in a 75 cm^2 flask). Media, containing 20 ng / ml IL-3 and 20 ng / ml SCF, was replaced every 3 days for the first 2 weeks and then every 4 days after this time, maintaining cells at a density of 0.5 X 10^6 cells / ml.

2.4 CELL STIMULATION

Cytokine stimulation of mast cells: Cells were starved overnight of IL-3 and SCF-1 in normal cell culture media containing 10% serum. Cells were stimulated with 20 ng/ml SCF-1 for 5-10 min at 37°C. Cells were then washed twice in ice-cold PBS and total cell lysates prepared.

Serum stimulation of cell lines: Cells were seeded in cell culture dishes in media containing serum and left to adhere for 6 − 8 h. After this time, media was aspirated and replaced with media containing no serum and left on the cells overnight. The following day cells were stimulated by adding the appropriate volume of serum over the whole cell culture dishes drop by drop. During the serum-stimulation, cells were incubated at 37°C. After the allocated time of stimulation, media was removed and cells washed once with PBS prior to cell lysis.

2.5 CELL LYSIS, IMMUNOPRECIPITATION AND PULL DOWN

Cell lysis: Cells were harvested by centrifugation at 1200 rpm for 5 min and subsequently washed twice with ice-cold PBS. The cell pellet was resuspended in ice-cold lysis buffer (1 ml lysis buffer/10^7 cells) containing protease and phosphatase inhibitors and incubated for 20-30 min on ice, vortexing every 10 min. The lysate was centrifuged at 10,000 x g for 10 min at 4°C. The supernatant was transferred to a fresh tube and the protein concentration determined using Bio-Rad protein assay dye reagent.

Immunoprecipitations: Primary antibody was added directly to the lysate and incubated for 2 h to overnight at 4°C. After this time, 10-100 μl of prewashed protein A/G sepharose beads in lysis buffer were added to the lysates and samples incubated for a further 2 h at 4°C. Subsequently, beads were washed three times with lysis buffer. 30-100 μl of SDS sample buffer was then added to the washed beads and boiled for 5 min at 100°C.

GTP-RhoGTPase pull downs: Cells were seeded in 10 cm^2 cell culture dishes the day before performing the pull down. On the day of the pull down, cells were 60-70% confluent. The cell culture dishes were placed on a bed of ice and the media carefully aspirated. 500 μl of pre-cooled lysis buffer was subsequently added onto each dish and cells scraped (on ice) with a pre-cooled scraper. Scraped cells and lysate were collected in pre-cooled 1.5ml Eppendorf tube. Samples were centrifuge at 13000 rpm for 5 min at 4ºC and the supernatant transferred into a fresh pre-cooled 1.5 ml Eppendorf tube. 60 μl of the

lysate was taken to which 15 µl SDS sample buffer was added and the sample boiled for 5 min at 100°C, for the quantification of total RhoGTPase. To the remaining lysate, 15 µl of GST-tagged Rhotekin-RBD agarose beads (for pull down of RhoA-GTP) or GST-tagged PAK-RBD on agarose beads (for pull down of Rac1-GTP or Cdc42-GTP) was added and sample incubated for 45 min at 4°C, rotating. After this time, beads were washed three times with lysis buffer by centrifuging samples at 10,000 rpm for 2 min at 4°C. After final wash, lysis buffer was aspirated and 20 µl of SDS-PAGE sample buffer added to the samples. Samples were boiled for 5 min at 100°C and proteins separated on 12.5% gels by SDS-PAGE.

2.6 PROTEIN ANALYSIS AND DETECTION

The immunoblots presented throughout this thesis are representative examples that have been selected to most clearly illustrate the data. In most cases, unless stated, all or parts of each experiment have been repeated to allow confidence in the immunoblot presented.

2.6.1 Determination of protein concentration

The protein concentration of lysates was measured using Bio-Rad protein assay dye reagent, which is based on the Bradford method in which a differential colour change of a dye occurs in response to varying protein concentrations. 5 µl of lysate was added to 1 ml of Bio-Rad protein assay dye reagent and the absorbance measured at 595 nm with a spectrophotometer. The spectrophotometer was first blanked by reading the absorbance of 5 µl of lysis buffer in Bio-Rad protein assay dye reagent at 595 nm. The obtained value for the cell lysate samples were then multiplied by a constant of 24.75 and the dilution factor (200) to give the protein concentration in mg/ml.

2.6.2 Sodium dodecyl sulphate-polyacrylamide gel electrophoresis (SDS-PAGE)

The separating and stacking acrylamide gels were made as described in section 2.1.4. For separation of PI3K subunits, an 8% gel was used, whereas a 12.5% gel was used for separation of Rho GTPases. Protein samples that had been boiled in lysis buffer and SDS-PAGE sample buffer were loaded into the wells of the stacking gel. For large gels, up to 100 µl of sample was loaded/well and in small gels, up to 50 µl. For the large gel systems, the gel was run at a constant voltage of 200 V for 5 h at 4°C or 50 V at room temperature overnight. For the small gel system, the gel was run at a constant voltage 100 V for 2 h at room temperature.

2.6.3 Electroblotting

After SDS-PAGE, proteins were transferred from the acrylamide gel onto a PVDF membrane (Immobilon^{TM}-P, Millipore) by electroblotting. The PVDF membrane was cut slightly larger than the size of the gel and was briefly soaked in methanol and then rinsed with ddH$_2$0 for 5 min. Both the gel and the membrane were pre-equilibrated in transfer buffer and then sandwiched between two sheets of Whatman 3MM paper and two sponges, which had also been pre-equilibrated in transfer buffer. The 'sandwich' was placed into the electroblotting apparatus cassette and placed in a blotting tank filled with transfer buffer, such that the gel was facing the cathode. For large gels using the Hoefner apparatus, proteins were transferred at 60 V for 4 h at 4°C, for small gels using the BioRad electroblotting system, proteins were transferred at 100 V for 1 h at 4°C.

2.6.4 Antibody incubation and protein detection

After proteins had been transferred to the PVDF membrane, the membrane was blocked for 1 h in 5% milk dissolved in PBS-T. The membrane was then washed two times for 5 min with PBS-T, before being incubated with the primary antibody. Primary antibodies were either diluted in 5% milk or 3% BSA in PBS-T. The membrane was incubated with the primary antibody overnight, rocking at 4°C. The following day, the membrane was washed thoroughly with PBS-T and then incubated with the secondary HRP-conjugated antibody diluted in 5% milk in PBS-T for 1 h at room temperature. The membrane was then was thoroughly washed again with PBS-T before being incubated with ECL^{TM} Western Blotting Detection Reagents (Amersham Biosciences) or home-made ECL for 1-3 min. The membrane was wrapped in cling film and exposed to super RX Fuji medical X-ray films (Fuji).

2.6.5 Stripping of blots

Membranes were washed thoroughly in ddH$_2$0. Guanidine hydrochloride stripping buffer, described in section 2.1.4, was poured onto the membrane and the left until the membrane had become transparent (after approximately 30 seconds). Membranes were then thoroughly washed again in ddH$_2$0 until they were no longer transparent. Membranes were blocked again in 5% milk in PBS-T before primary antibody incubation.

2.7 PREPARING SAMPLES FOR IMMUNOFLUORESCENCE

2.7.1 Preparation of cells

Cells were seeded on coverslips in 12-well tissue culture plates. For fixation, cells were washed with PBS and then incubated with 1 ml 4% paraformaldehyde (PFA) for 15 min at

room temperature. After this time, cells were washed with PBS and permeabilised with 1 ml 0.5% Triton X-100 in TBS for 10 min at room temperature, followed by three separate 5 minute incubations with 0.1% Triton X-100 in TBS at room temperature. Cells were washed in TBS-T and then incubated with 2% BSA in TBS-T for 10 min at room temperature. Subsequently, cells were washed with TBS-T and incubated with the primary antibody (50 μl / coverslip), diluted in 2% BSA in TBS-T, overnight at 4°C. From this point onwards cells were protected from the light. Following three 5 min washes in TBS-T, the secondary antibody, diluted in 2% BSA in TBS-T, was added to the cells (50 μl / coverslip) and left for 1-2 h at room temperature. Following three 5 min washes in TBS-T, phalloidin-fluorescein (if staining for F-actin) diluted in 2% BSA in TBS-T, was added onto cells (50 μl / coverslip) and left for 20 min at room temperature. After this time cells were washed three times with TBS-T, including DAPI during the last wash step if staining DNA. Coverslips were mounted on slides using Mowiol (Calbiochem, 475904).

2.7.2 Preparation of coverslips

Fibronectin and collagen solutions were made up at a concentration of 10 μg/ml in PBS. For gelatin, a 0.1% solution in sterile ddH$_2$0 was used. Single autoclaved coverslips were placed in individual wells of a 12-well tissue culture plate. 1 ml of the fibronectin/collagen/gelatin solution was added to each well to cover the coverslips. Fibronectin and collagen solutions were left on coverslips overnight at 4°C, whereas coverslips covered in gelatin solution were left at room temperature for 30 min – 1 h. Coverslips were washed once with PBS and incubated with 1 ml 2% BSA solution (in PBS) for 1 h at 37°C. Subsequently, coverslips were washed once with PBS and left to air dry before seeding the cells.

2.7.3 Cell adhesion assay

NIH 3T3 cells were detached using trypsin-EDTA and seeded onto fibronectin/collagen/gelatin-coated coverslips in 12-well plates at a concentration of 10,000 cell / well. Cells were left to adhere to the coverslips for time periods ranging from 30 min to 6 h. After this time, cells were fixed with 4% PFA and prepared for immunofluorescence analysis.

2.7.4 Confocal imaging

To eliminate the detection of background and non-specific fluorescence from the secondary fluorophore-conjugated antibodies, the microscope settings were set so that no fluorescence was observed from samples that had been incubated with secondary antibodies alone (i.e.

without the primary antibody). Once microscope settings had been optimized for detection of a specific primary antibody, these settings were maintained for all samples from the same experimental sample set to allow for a direct comparison of signal intensity.

2.8 QUANTITATIVE REAL TIME PCR

2.8.1 Reagents

Primer mixes were supplied by Applied Biosystems (see table below). The primer mix contained two unlabeled gene-specific PCR primers and a FAM^{TM} dye-labelled gene-specific Taqman® probe. Taqman® Universal PCR Master Mix (Applied Biosystems, 4304437) and sample cDNA were added to the primer mix, which could then be used for real time (RT)-PCR. Primers specifically for exon -2a and exon -2b upstream of mouse p110δ were ordered as part of Applied Biosystems Assays-on-demand scheme. This involved submitting the sequences for exon -2a and exon -2b to Applied Biosystems who designed primers and probes specifically for PCR amplification of these sequences. Primers for the coding region of mouse p110δ, and for p110α, p110β, p85α, p85β, p55γ and β-actin were commercially available from Applied Biosystems.

Quantitative RT PCR primers

Gene Symbol	ABI assay ID	Gene name
pik3cd -2a	Assay-on-demand	p110δ with exon -2a (mouse)
pik3cd -2b	Assay-on-demand	p110δ with exon -2b(mouse)
pik3cd	Mm00435674_m1	p110δ (mouse)
pik3ca	Mm00435669_m1	p110α (mouse)
pik3cb	Mm00659576_m1	p110β (mouse)
pik3r1	Mm00803163_g1	p85α (mouse)
pik3r2	Mm00435694_m1	p85β (mouse)
pik3r3	Mm00725051_m1	p55γ (mouse)
β-actin	Mm00607939_s	β-actin (mouse)
β-actin	Hs99999903_m1	β-actin (human)

2.8.2 Methods

The primer mix supplied by Applied Biosystems contains a forward and reverse primer for the gene of interest and a FAM^{TM} dye-labelled gene-specific Taqman® probe. FAM is a high energy green fluorescent dye which is attached to the 5' end of the probe (the reporter dye). A low energy quencher molecule attached to the 3' end of the probe. During PCR if

the target cDNA of interest is present, the Taqman® probe hybridises to a complementary sequence between the forward and reverse primers. When the probe is intact, the proximity of the reporter dye to the quencher dye results in suppression of the reporter dye fluorescence. During each PCR extension cycle, the 5'-3' exonuclease activity of Taq DNA polymerase (in the Taqman® Universal PCR Master Mix) cleaves the probe between the reporter dye and quencher molecule displacing the two probe fragments, and polymerisation of the strand continues (Figure 2.1).
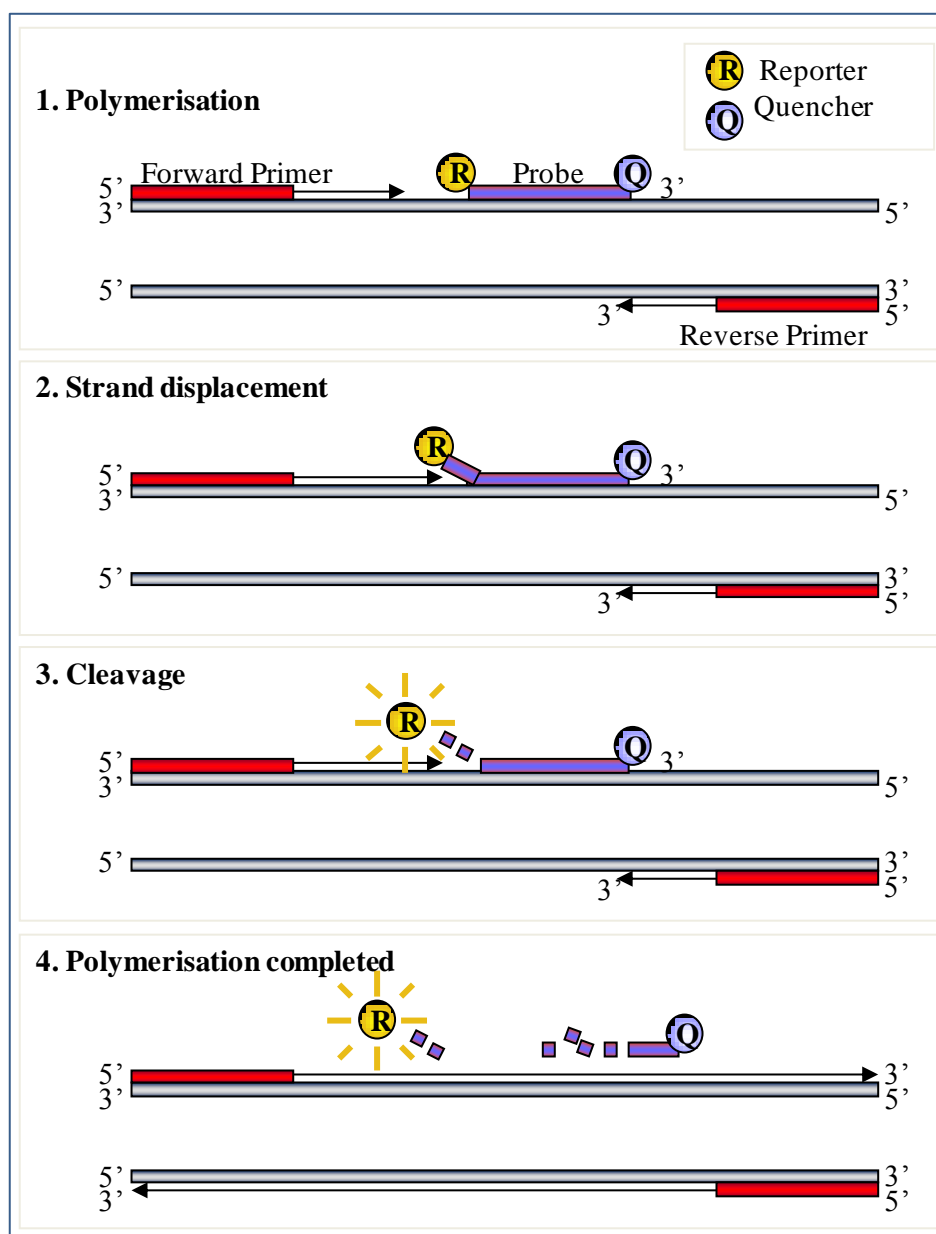
Figure 2.1: Quantitative real time PCR. Two fluorescent dyes, a reporter (R) and a quencher (Q) are attached to 5' and 3' end of a Taqman probe, which hybridises to a complementary sequence between the forward and reverse primer sites. When both dyes are attached, the reporter dye emission is quenched. *Taq* DNA polymerase drives DNA synthesis from the primer sites. During each extension cycle, the *Taq* DNA polymerase cleaves reporter dye from the probe by its 5'-exo-nuclease activity. Once separated from the quencher dye, the reporter dye fluorescence emission is detected.

The separation of the reporter dye from the quencher molecule results in fluorescence emission from the reporter dye. The fluorescence is detected by the Applied Biosystems 7500 Real Time PCR System, and is proportional to the amount of PCR product being amplified. The PCR cycle at which the fluorescence intensity is greater than the background, when target cDNA amplification is first detected is referred to as the 'cycle threshold' or C_T value. If there is a high quantity of target cDNA in the starting sample, this will yield a low C_T value. Samples were normalised to the endogenous control, β-actin.

2.8.3 Quantifying the amount of cDNA

Relative standard curve: A relative standard curve is commonly used to quantify the amount of target cDNA in samples. To construct a relative standard curve, a stock of cDNA from a cell line known to contain the gene of interest, is used to create a set of standards, such as 1 ng of total cDNA diluted in a series of 10-fold dilutions. Each of these standards is added to the Taqman® – gene-specific primer mix and the gene of interest amplified to give a series of C_T values. The Applied Biosystems 7500 Real Time PCR System constructs a standard curve by plotting the C_T value against the log [ng cDNA input]. This standard curve can be used to calculate the quantity of target cDNA in a sample by using the C_T value obtained from sample cDNA amplification.

Limitations of the relative standard curve approach

This method can only be used to compare the amount of target cDNA between samples that have been amplified by the *same* primer set i.e. it allows for the comparison of a specific gene between different samples but it does not, however, allow for the comparison of different genes in one or more samples. The reason for this is that the given starting concentration of total cDNA isolated from a certain cell line, for example 1 ng, will contain varying copy numbers of individual genes. 1 ng total cDNA may contain 10,000 copies of gene 'A' and only 100 copies of gene 'B', which will result in the detection of gene 'A' amplification earlier than gene 'B', yet they will both be given the same log [ng cDNA input] when constructing the standard curve. The effect of this is that the calculated concentration of gene B from the standard curve will be artificially high. In addition, this approach does not take into consideration different primer efficiencies.

Absolute standard curve: To permit the comparison of the levels of different cDNAs in cell types, standard curved were constructed that enabled the absolute quantification of the amounts of target cDNA. Plasmids containing the full length DNA sequences for p110α, p110ß, p110δ, p110δ-2a, p110δ-2b, p85α, p85ß, p55γ were used to create a set of standards

containing $160 - 1 \times 10^8$ gene copies / μl (160, 800, 4×10^3, 2×10^4, 1×10^5, 1×10^6, 1×10^7 and 1×10^8). This was achieved using the following procedures:

1) Plasmid DNA concentrations (ng / μl) were determined using a Nanodrop ND-1000 spectrophotometer (Nanodrop Technologies)
2) The following equation was used to calculate pMol concentration:

pMol DNA = mass of DNA (pg) ÷ [DNA length (bp) x 650pg/pmol/bp]

3) The Molar concentration was determined (pMol concentration x 10^{12})
4) The number of molecules / μl were calculated: [Molar concentration x Avogadro's constant (6×10^{23})]

2.8.4 Plasmids used to construct quantitative RT PCR standard curves

p110α: Riken Fantom Clones, Accession # AK051885

p110β: Riken Fantom Clones, Accession # AK090116

p110δ-2a: Mammalian Gene Collection, Accession # BC035203

p110δ-2b: Riken Fantom Clones, Accession # AK040867

p85α: Mammalian Gene Collection # 13952, Image #3979333, Accession # BC026146

p85β: Mammalian Gene Collection #11459, Image #2581969, Accession # BC0067961

p55γ: Mammalian Gene Collection # 62506, Image #6405534, Accession # BC053102

2.9 TRANSFECTION

2.9.1 Transfection with SuperFect Transfection Reagent

Transfection of NIH 3T3 and HEK 293T cells with full length p110δ constructs (p110δ-2a/2b) were carried using SuperFect transfection reagent (Qiagen) according to the manufacturer's protocol. Similarly, the pMX(s)-neo retroviral vector containing human p110δ cDNA sequences was transfected into the GP E86 packaging cell line also using SuperFect transfection reagent.

2.9.2 Transfection with FuGENE® 6 Transfection Reagent

Transfections of RAW 264.7, Thp1, CT26 and NIH 3T3 cells with luciferase reporter constructs were carried using FuGENE® 6 Transfection Reagent (Roche), according to manufacturer's protocol.

2.9.3 Retroviral infection

Transfection of BMMCs with PMT and HOX11: Transfection of BMMCs was enhanced using RetroNectin®-coated plates.

Preparation of retronectin plates: RetroNectin® (Takara, #T00A/B) is a ~63 kDa protein that enhances retroviral-mediated gene transfer into mammalian cells by co-localization of retrovirus particles with target cells. This is accomplished through direct binding of retroviral particles to the heparin-binding domain II of RetroNectin® and binding of target cells to a central cell-binding domain of RetroNectin®. A stock RetroNectin® solution was prepared at a concentration of 1 mg/ml in sterile ddH₂0. A working solution at 20 μg/ml was prepared by diluting the stock retronectin solution with PBS. 1 ml of the working RetroNectin® solution was added per well of a 6-well tissue culture plate and left to stand at room temperature for 2 h. After this time, the solution was removed and 1 ml of 2% BSA in PBS was added per well, and the plate left to stand at room temperature for 30 min. The BSA solution was removed and the well washed once with PBS. The plates were then ready to be used.

Cell culture media from packaging cells stably expressing PMT or HOX11 (i.e. the viral supernatant) was collected after 24 h from 80% confluent flasks. The viral supernatant was passed through a 0.45 μM filter and pre-loaded onto the RetroNectin®-coated wells. Plates were incubated for 4 h at 37°C. After this time the viral supernatant was removed and fresh, filtered viral supernatant was added into the wells and plates incubated for a further 4 h at 37°C. After this time, viral supernatant was aspirated and 1×10^{6} BMMCs added per well and plates incubated at 37°C with 5% CO_2 overnight. The following day the BMMCs were subjected to a second round of retroviral infection in the same manner as described above.

Transfection of NIH 3T3 cells with human p110δ cDNA: GP E86 packaging cells stably expressing pMX(s)-neo retroviral vectors containing p110δ constructs were used for retroviral infection of NIH 3T3 cells. Fresh cell culture media was added to GP E86 packaging cells at 70% confluency. After 24 h the GP E86 media (viral supernatant) was collected and replaced with fresh media. The viral supernatant was passed through a 0.45 μM filter and added onto NIH 3T3 cells at 60% confluency and incubated for 24 h at 37°C with 5% CO_2. After this time, NIH 3T3 cells were subjected to a second round of retroviral infection, by aspirating the viral supernatant and collecting the fresh GP E86 media, which had been on the GP E86 cells for 24 h and contained fresh viral supernatant. NIH 3T3 cells were incubated for a further 24 h with the filtered fresh viral supernatant at 37°C with 5% CO_2. After this time, the viral supernatant was replaced with fresh normal cell culture media.

2.9.4 Selection of cells stably expressing neomycin-resistance genes

Cells were selected either as single colonies or as a pool of colonies. For single colony selection and expansion, cells were diluted 1:10 48 h after transfection and seeded in 6 cm^2 cell culture dishes in media containing 500 μg/ml geneticin. When individual colonies were ready to be picked (once they had expanded to a total diameter of approximately 3-5 mm) the media was aspirated and the colonies marked on the bottom of the plate using a pen. Cloning rings were stuck down surrounding the marked colonies, using autoclaved grease. 50 μl of trypsin-EDTA was added onto the cells within the cloning ring and left until the cells had detached. The detached cells were transferred into individual wells of 12-well tissue culture plate to expand, grown in media containing 500 μg/ml geneticin for at least 15 days. For selection of pooled colonies, 48 h after transfection, cells were diluted 1:2 in 10 cm^2 cell culture dishes and grown in media containing 500 μg/ml geneticin for at least 15 days, passaging accordingly if cells reached confluency.

2.10 DUAL LUCIFERASE ASSAY

Cells were seeded in 6-well cell culture dishes. On the day of transfection cells were 60% confluent. 2 μg of luciferase reporter vector + 0.5 μg renilla vector were used for the transfections with FuGENE® 6 Transfection Reagent (Roche) and each transfection was carried out in triplicate. 48 h following transfection, cells were lysed using Passive Lysis Buffer [PLB (Promega, #E194A)]. Cells were washed once with PBS and 500 μl of 1 x PLB added per well onto adherent cells. Plates were left at room temperature, rocking for 30 min. For suspension cells, cells were washed once in PBS and centrifuged for 5 min at 1200 rpm. Cell pellets were resuspended in 500 μl PLB in 1.5 ml Eppendorf tubes. Samples were left at room temperature rotating for 30 min. Following cell lysis, 30 μl of the cell lysate was pipetted into each well of a 96-well White Cliniplate (Thermo Fisher Scientific, #9502887). Luciferase Assay Buffer II and Stop & Glo® Buffer (Promega) were prepared according to the manufacturer's protocol. *Firefly* and *Renilla* luciferase activity was measured using a luminescence plate reader (Perkin Elmer VICTOR™ *X* Light Luminescence Plate Reader, #2030-0010).

The *Firefly* luciferase activity of each reporter construct was calculated by normalising the *Firefly* luciferase activity against the *Renilla* luciferase activity (*Firefly* luciferase measurement divided by the *Renilla* luciferase measurement). Following normalisation, the average *Firefly* luciferase activity of pGL3-Basic, which represents the background luciferase activity, was subtracted from the normalised *Firefly* luciferase activity of each reporter construct. The average and standard deviation of the *Firefly* luciferase activity of each reporter construct was subsequently calculated.

2.11 NUCLEIC ACID MANIPULATION

2.11.1 Preparation of plasmid DNA

Small and large scale plasmid preparations were carried using QIAprep Spin Miniprep Kit (Qiagen, 27106) or QIAGEN Plasmid Maxi Kit (Qiagen, 12163), respectively, according to the manufacturer's protocol.

2.11.2 Purification of PCR DNA products

For purification of PCR DNA products for subsequent cloning steps, QIAquick PCR Purification Kit (Qiagen, 28104) was used according to the manufacturer's protocol.

2.11.3 Preparation of cDNA for quantitative real time PCR

Purification of total RNA from cells: Total RNA was isolated from cells using RNeasy Mini Kit (Qiagen, 74104) according to the manufacturer's protocol.

Reverse transcription of mRNA to cDNA: Using Oligo(dT), mRNA was reversed transcribed to cDNA using SuperScript™ II Reverse Transcriptase (Invitrogen, 18064-022) according to the manufacturer's protocol.

2.11.4 Agarose gel electrophoresis of DNA

Molecular biology grade agarose (Helena Biosciences) was dissolved in TAE buffer to a final concentration of 0.8-2.0% depending on the size of DNA fragments separated. The solution was heated in the microwave until the agarose powder had completely dissolved. Ethidium bromide was added to the solution to a final concentration of 10 μg/ml and the solution poured into the gel apparatus and allowed to set. DNA samples were mixed with 6x DNA Loading Dye solution (Fermentas, #R0611) and loaded into gel wells, with the chamber filled with TAE buffer. DNA samples were run at a constant voltage of 100 V for 0.5-1 h. For determination of fragment size, either MassRuler™ DNA Ladder, Low Range (Fermentas, SM0383) or MassRuler™ DNA Ladder, High Range (Fermentas, SM0393) were used depending on the size of DNA fragments expected. DNA bands were visualized under UV-light.

2.11.5 DNA cloning procedures

2.11.5.1 Restriction enzyme digest of DNA

Approximately 1 μg of DNA was diluted in 1 x restriction enzyme buffer (Fermentas or NEB) to a final volume of 20 μl. For NEB buffers, an appropriate volume of BSA was added if required. 5-10 units of the desired restriction enzyme(s) were added to reaction mix. If more DNA was required for subsequent cloning stages, this reaction was scaled up

accordingly. The reaction mix incubated for 1-2 h at the temperature recommended by the manufacturer, usually 37°C or 55°C. The reaction products were analysed by gel electrophoresis.

2.11.5.2 DNA extraction from agarose gel

To extract DNA from agarose gel fragments for subsequent cloning steps, QIAquick Gel Extraction Kit (Qiagen, 28704) was used according to the manufacturer's protocol.

2.11.5.3 Ligation of DNA fragments

DNA fragments were ligated using Quick Ligation™ Kit (NEB, #M2200S) according to the manufacturer's protocol.

2.11.5.4 Transformation of competent cells

XL2-Blue ultracompetent cells (Stratagene, 200150) were transformed with Quick Ligation products as follows: Competent cells were thawed on ice, 2 μl of the ligation mixture was added to the competent cells, mixed gently and incubated on ice for 30 min. Competent cells were heat shocked for 2 min at 37°C and then chilled on ice for 5 min. 500 μl of S.O.C. media was added to each sample and incubated shaking for 1 h at 37°C. 100 μl of the transformed competent cells was then spread on selective LA plates, which were left at 37°C overnight.

2.11.5.5 Sequencing reactions

DNA sequencing reactions were carried out by MWG-Biotech, Germany. 1 μg of air-dried DNA was supplied, along with necessary primer sequences if required.

2.11.5.6 In vitro translation

In vitro translations were carried out using the TNT$^{®}$ Quick Coupled Transcription/Translation Systems (Promega, #L1170) according to the manufacturer's protocol using [^{35}S]methionine.

2.12 DNA VECTORS

2.12.1 Vectors used for cloning and expression of p110δ-2a, p110δ-2b and p85 cDNA in mammalian cell lines

2.12.1.1: p110δ-2a

p110δ-2a cDNA was obtained from The Mammalian Gene Collection (MGC; http://mgc.nci.nih.gov/) in pCMV.Sport6 mammalian expression vector (accession number BC035203), inserted between *Not* I and *Sal* I.
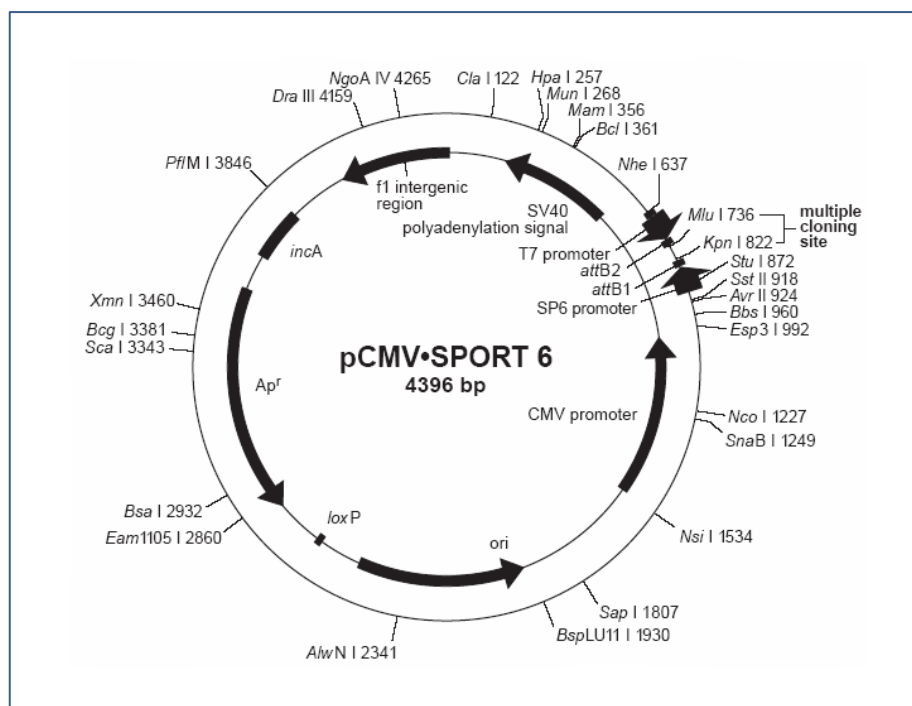
Figure 2.2: pCMV.Sport6 vector. Map taken from Invitrogen Life Technologies.

2.12.1.2: p110δ-2b

p110δ-2b cDNA was obtained from Riken Fantom Clones (http://www.cgb.ki.se/se/cgb/groups/liang/RIKEN+.htm) in pBluescript (accession number AK040867), inserted between *Sal* I and *Bam* HI.
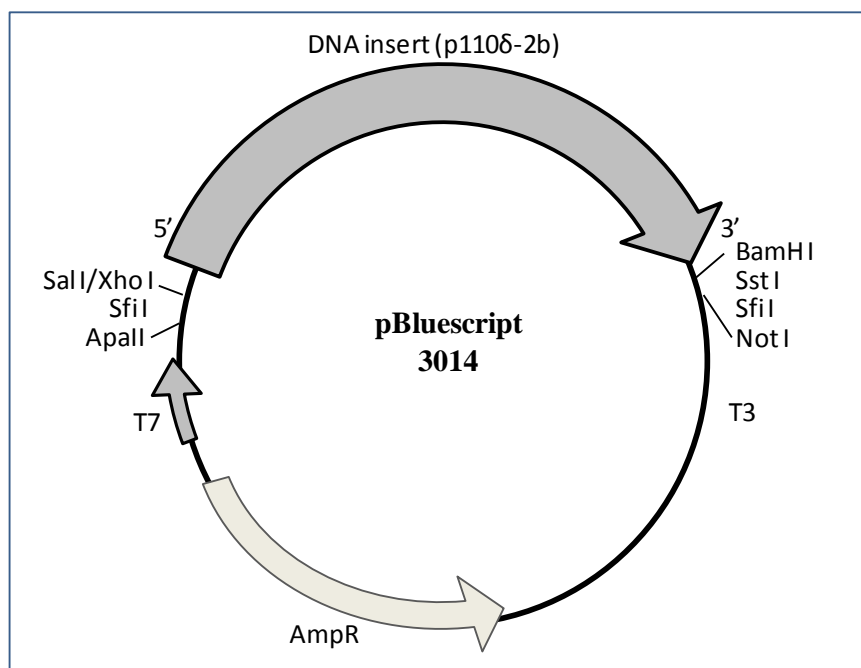
Figure 2.3: p110δ-2b cDNA in pBluescript.

p110δ-2b cDNA was cloned into the mammalian expression vector pcDNA3.1(+) (Figure 2.4) from pBluescript, inserted between *Not* I and *Apa* I.
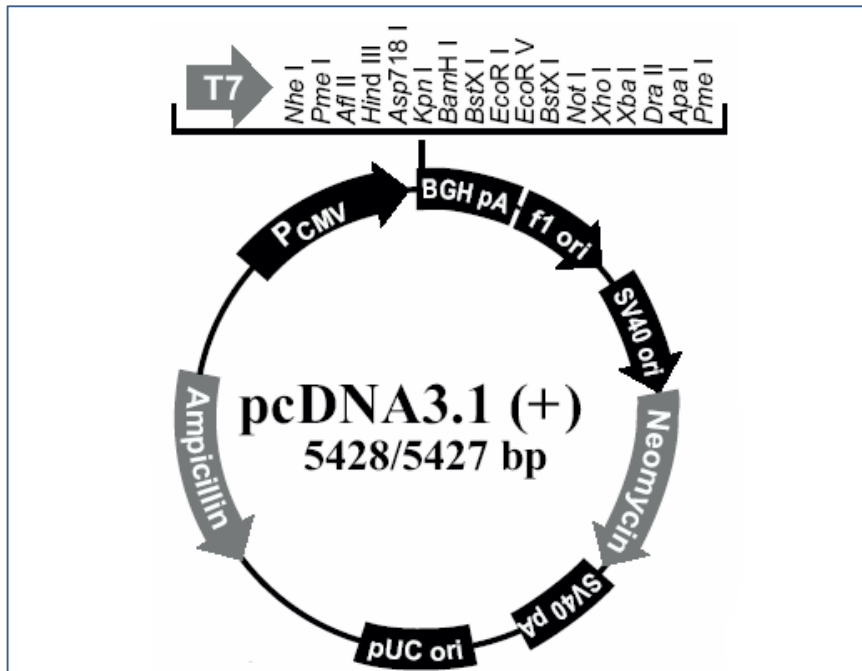
Figure 2.4: pcDNA3.1(+) vector. Map taken from Invitrogen Life Technologies.

2.12.1.3 Vectors conferring antibiotic-resistance

pIRES vector (Figure 2.5a) was used in cotransfections with p110δ-2a in pCMV.Sport6 to enable selection of neomycin-resitant stable transfectants. pBabe-Hygro (Figure 2.5b) was used in cotransfections with p85α in pCMV.Sport6 in cells stably expressing p110δ-2a cDNA (neomycin-resistant), to enable selection of hygromycin-resitant stable transfectants.
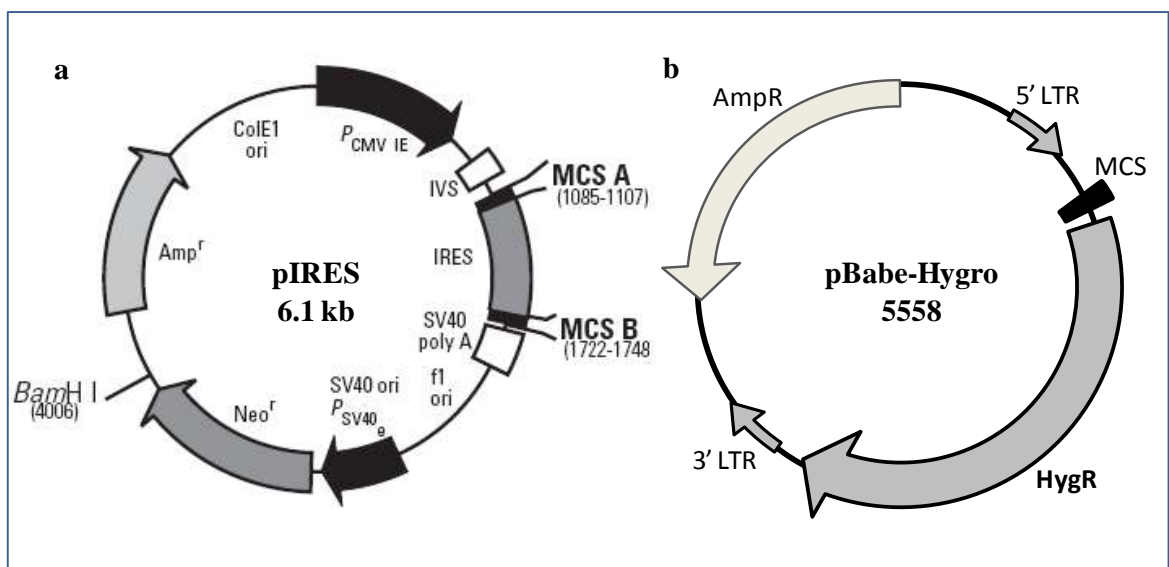
Figure 2.5: Vectors conferring antibiotic-resistance. a) pIRES vector (map taken from Clontech) and **b)** pBabe-Hygro vector.

2.12.1.4 p85 expression vectors

pCMV.Sport6 mammalian expression vectors (Figure 2.2) were obtained from the Mammalian Gene Collection containing cDNA for p85α (accession # BC026146) or p85β (accession # BC0067961).

2.12.2 Cloning and expression of human p110δ cDNAs in pMX-neo retroviral vector

2.12.2.1: 5'Myc-p110δ-3'CAAX

Human 5'Myc-p110δ-3'CAAX cDNA in the pMX-neo retroviral expression vector (Figure 2.6) was obtained from Dr. Tatsuo Kinashi (Kinashi, et al., 1999), inserted between *Bam*H I and *Eco*R I.
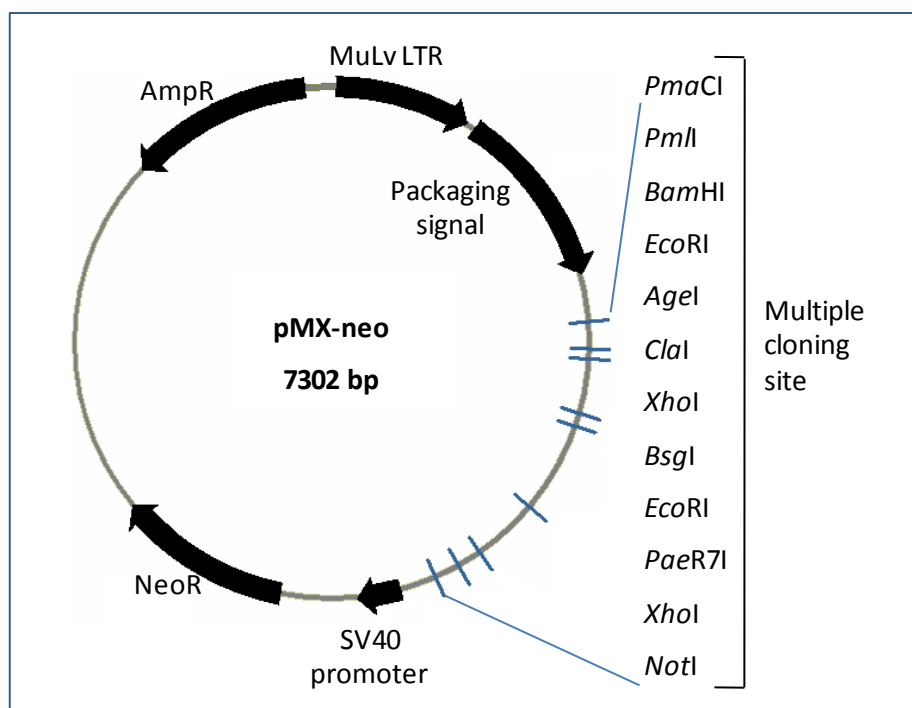
Figure 2.6: pMX-neo retroviral vector.

2.12.2.2: p110δ-3'CAAX

cDNA for human p110δ-3'CAAX was available in the pcDNA3.1(+) mammalian expression vector (Figure 2.4). The pcDNA3.1(+)-p110δ-3'CAAX vector and the pMX-neo vector (Figure 2.6) were digested with the restriction enzymes *Bam*HI and *Xho*I. The resulting digest fragments were separated on a DNA agarose gel and the fragments corresponding to linearised pMX-neo and p110δ-3'CAAX DNA excised, purified and ligated as described in section 2.11.

2.12.2.3: 5'Myc-p110δ

cDNA for human 5'Myc-p110δ-3'CAAX had previously been obtained for the laboratory in the pUAST vector (Figure 2.7). The pUAST-5'Myc-p110δ vector and pMX-neo (Figure 2.6) were digested with the restriction enzymes *Bam*HI and *Xho*I. The resulting digest fragments were separated on a DNA agarose gel and the fragments corresponding to linearised pMX-neo and 5'Myc-p110δ DNA excised, purified and ligated as described in section 2.11.
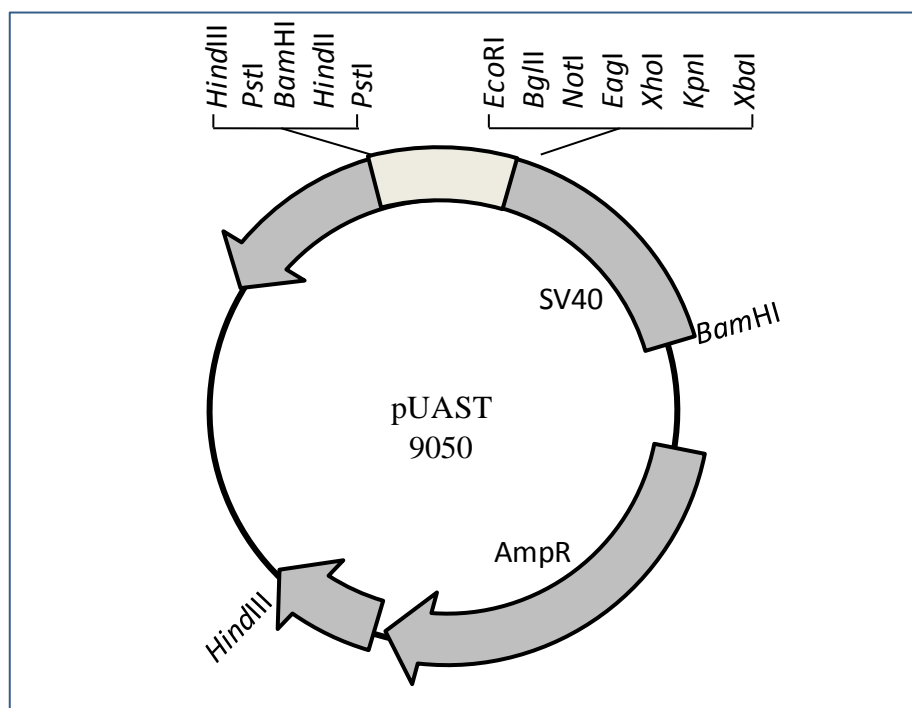
Figure 2.7: pUAST vector.

2.12.2.4: Untagged-p110δ

To obtain the pMX-neo expression vector containing untagged human p110δ cDNA, the pMX-neo expression vectors containing 5'Myc-p110δ and p110δ-3'CAAX were employed. Both vectors were digested with the restriction enzyme *Eco*RI, which cuts within p110δ cDNA to after the 5'Myc-tag and within the pMX-neo vector after the 3'CAAX motif, and the appropriate DNA fragments ligated together (Figure 2.8). Ligated DNA products were sequenced to check the correct orientation of untagged p110δ cDNA in pMX-neo.
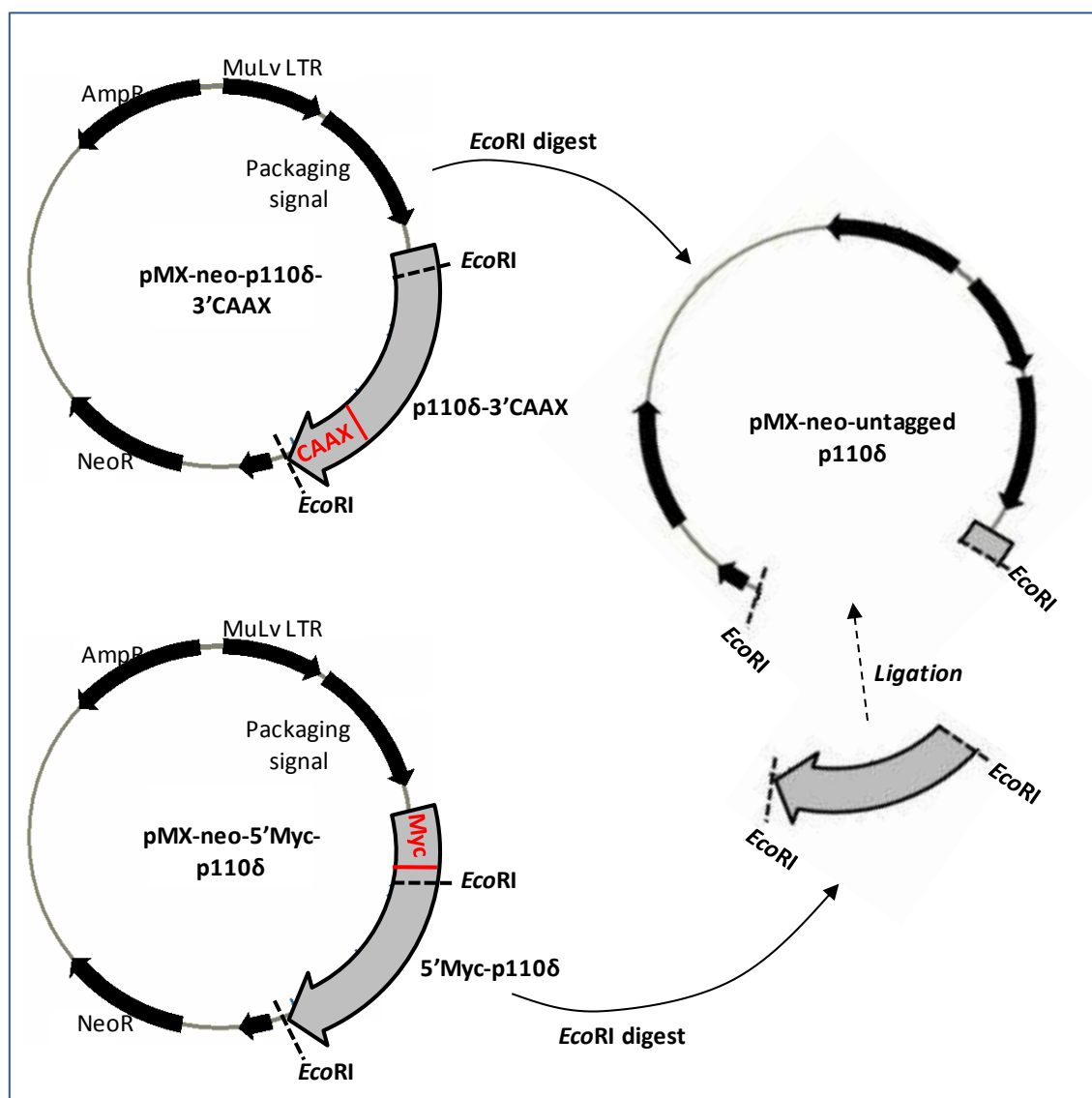
Figure 2.8: Cloning strategy used to obtain untagged p110δ cDNA in the pMX-neo retroviral vector. pMX-neo retroviral vector containing DNA inserts for either 5'Myc-p110δ or p110δ-3'CAAX were digested with the restriction enzyme *Eco*RI. The indicated DNA fragments from each digest were purified and ligated, resulting in untagged p110δ cDNA in pMX-neo.

2.12.3 Vectors used in dual luciferase assays

Murine *PIK3CD* exon -2a DNA was cloned into pGL3-Basic (Figure 2.9), which is described in the following section (section 2.12.4). DNA for HS21-Vav (Ogilvy, et al., 1998) had previously been cloned into pGL2-Basic vector (Figure 2.10) (Verrall & Vanhaesebroeck, unpublished results).

pGL3/pGL2-Basic vector: These vectors lack a eukaryotic promoter and enhancer sequence, which allows maximum flexibility in assessing the promoter activity of putative regulatory sequences (Figure 2.9 and Figure 2.10). Expression of luciferase activity in cells

transfected with this vector depends on insertion of a functional promoter upstream of luc^+ (*Firefly* luciferase gene) (Promega, Technical Manual #TM033).
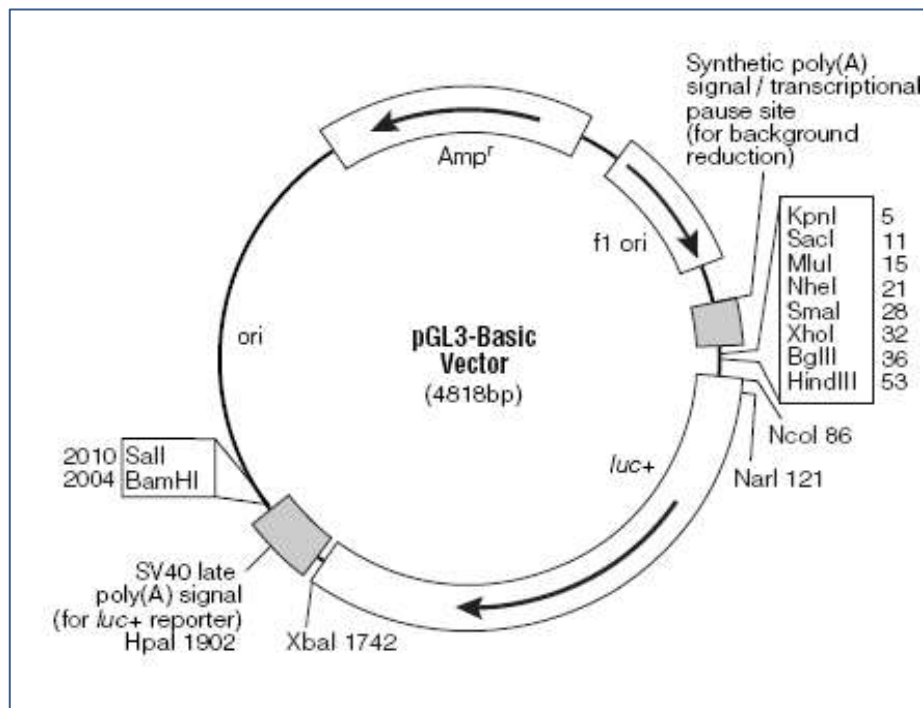
Figure 2.9: pGL3-Basic vector (Promega, #E1751).
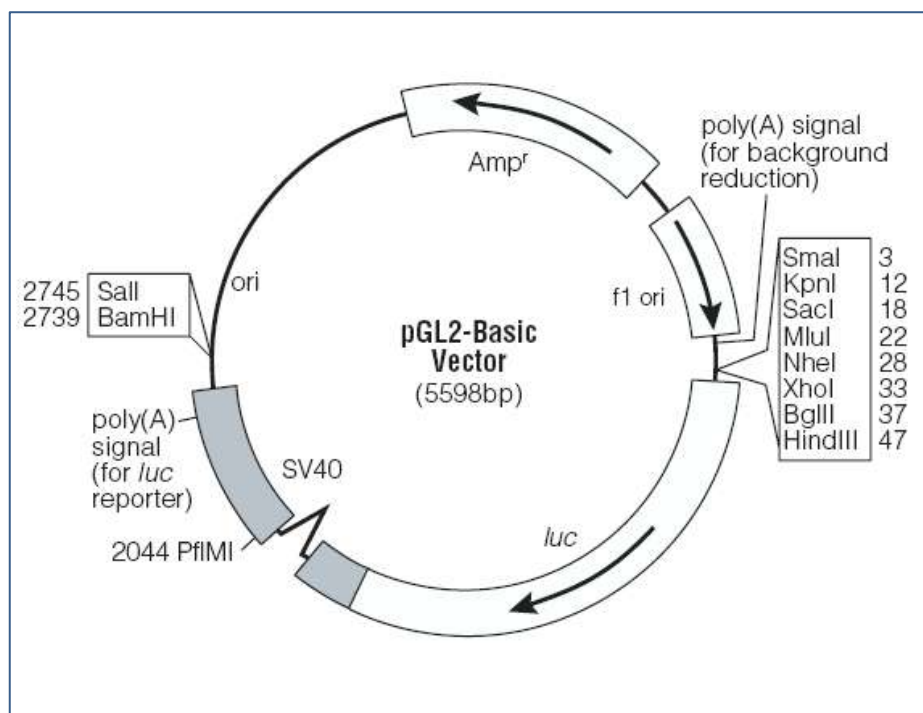
Figure 2.10: pGL2-Basic vector (Promega, #E1611).

pGL3-Promoter vector: This vector contains an SV40 promoter upstream of luc^+, and was used a positive control for luciferase activity in transfected cells (Figure 2.11).
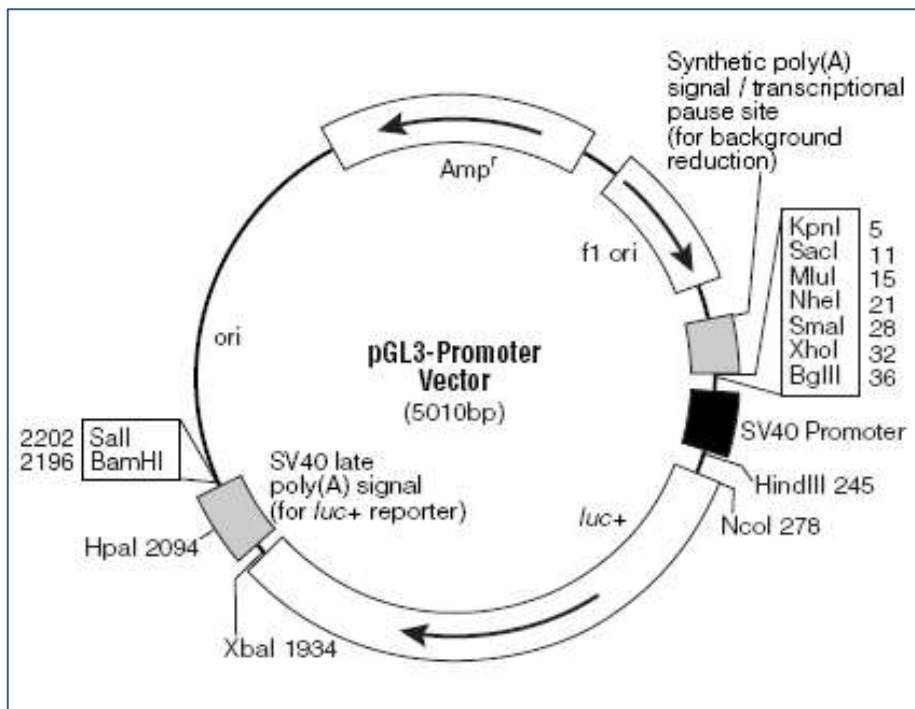
Figure 2.11: pGL3-Promoter vector (Promega, # E1761).

pGL3-Control vector: This vector contains an SV40 promoter upstream of *luc*⁺ and an SV40 enhancer sequence located downstream of *luc*⁺ and the poly(A) signal, often resulting in strong expression of *luc*⁺ in many cell types (Figure 2.12) (Promega, Technical Manual #TM033).
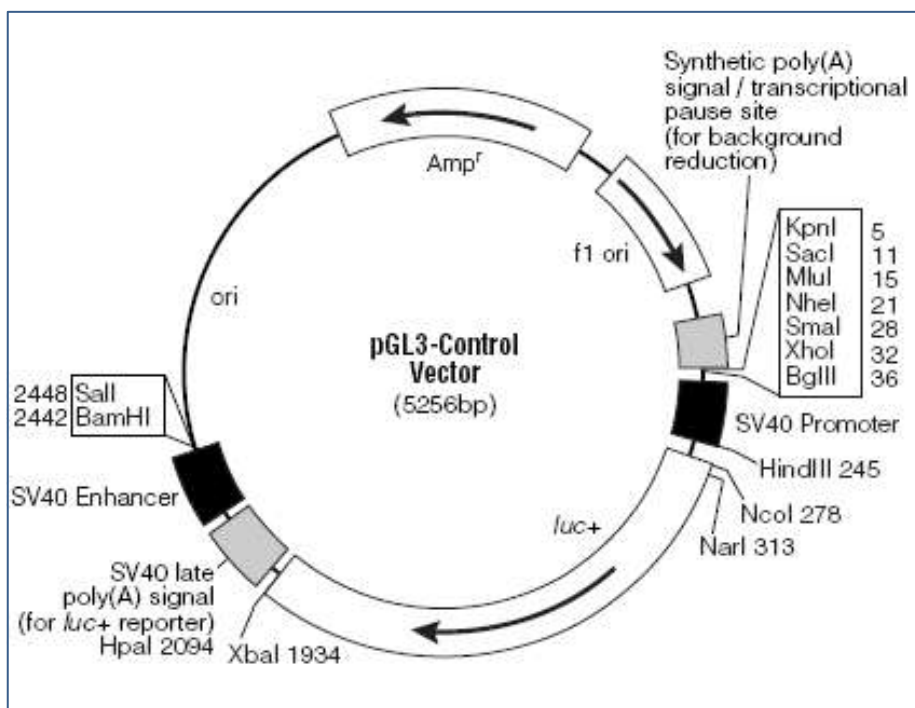
Figure 2.12: pGL3-Control vector (Promega, # E1741).

pRL-SV40 vector: This vector was used as an internal control reporter and was co-transfected with the pGL3-reporter vectors. The pRL-SV40 Vector contains the SV40 enhancer and early promoter elements to provide high-level expression of *Renilla* luciferase in co-transfected mammalian cells (Figure 2.13) (Promega, Technical Bulletin #TB239).
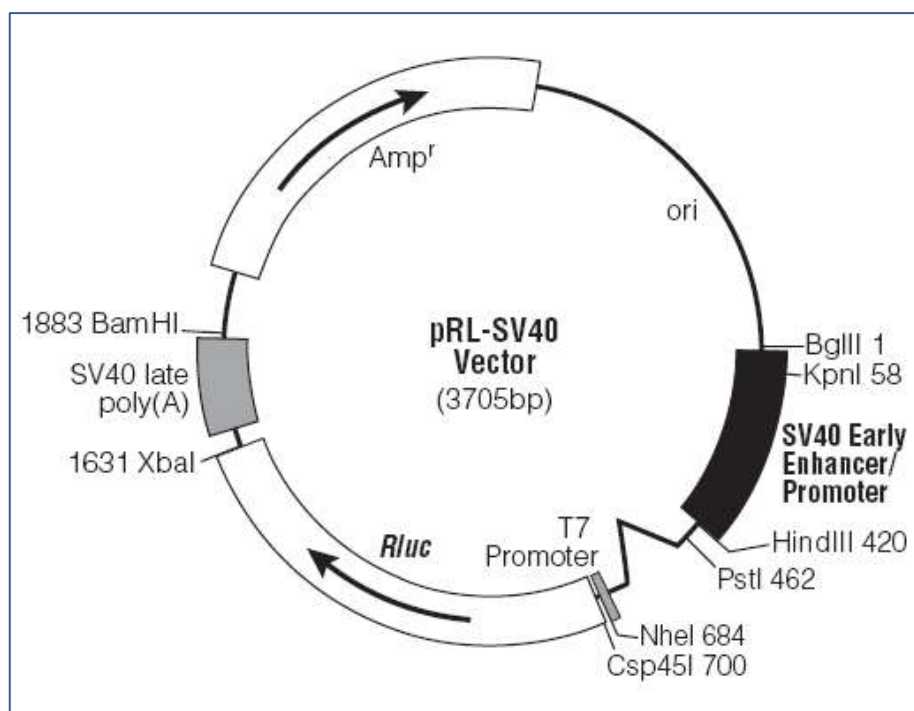
Figure 2.13: pRL-SV40 (Renilla) vector (Promega, # E2231).

2.12.4 Cloning of exon -2a into the pGL3-Basic vector

PCR was first performed to amplify exon -2a from p110δ-2a in the pCMV.Sport6 expression vector. PCR products were run on an agarose gel and the gel fragments containing the amplified exon -2a cDNA excised. DNA was purified from the agarose gel and ligated into the pGEM®-T Easy vector (Figure 2.14). Transformed competent cells were plated on LA/ampicillin/IPTG/X-Gal plates. Plates were incubated at 37°C overnight and white colonies picked the following day. Cultures were expanded and a small scale DNA preparation carried out. DNA was digested with the restriction enzymes *Xho* I and *Bgl* II to cleave exon -2a cDNA from the pGEM®-T Easy vector. The pGL3-Basic (Figure 2.9) was also digested with *Xho* I and *Bgl* II. The restriction digest products from the pGL3-Basic and the pGEM®-T Easy vector-exon -2a digest were run on an agarose gel and the required DNA fragments excised and purified for ligation of exon -2a into the pGL3-Basic vector.

2.12.4.1 Primers to amplify exon -2a

Forward primer incorporating *Xho* I restriction site

5' GACTCTCGAGCCGGAATTCCCGGGATATCGTCGACGAGCTC 3'

Reverse primer incorporating *Bgl* II restriction site:

5' GACTAGATCTGATGTCGGTCCAGCAGCTGGGTCCGCGG 3'

2.12.4.2 pGEM®-T Easy vector
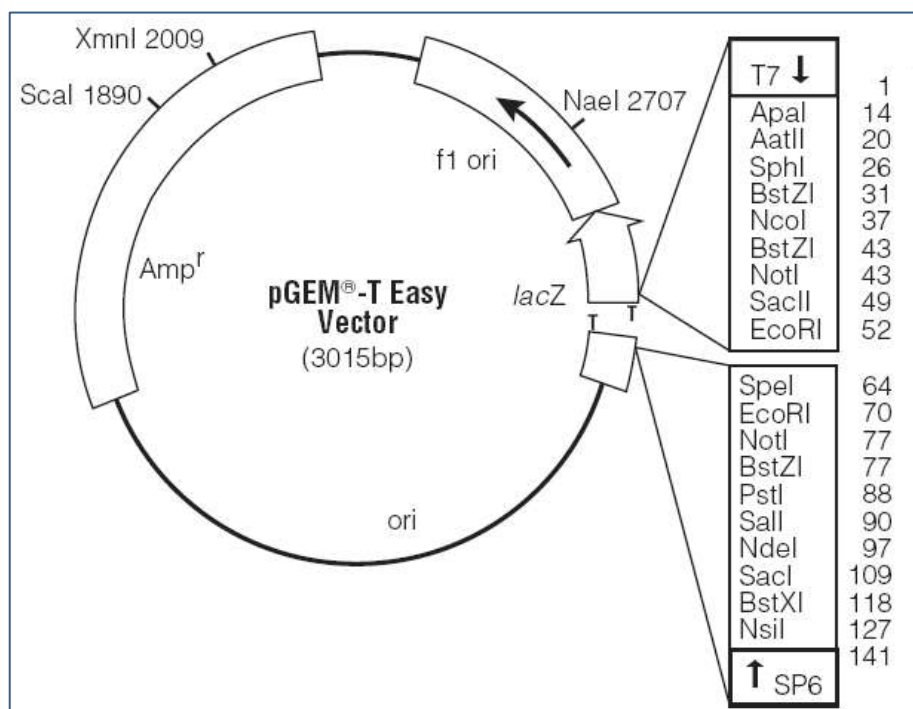
Figure 2.14: pGEM®-T Easy vector (Promega, #A1380).

2.13 CRYSTAL VIOLET STAINING

Cells were fixed by incubation with 4% PFA for 15 min at room temperature. 0.1% crystal violet solution made in 25% methanol was left on cells for 10 min at room temperature. Cells were washed three times with ddH$_2$O and plates left to dry.

2.14 MAY-GRUNWALD/GIEMSA STAINING OF BMMC CYTOSPIN SLIDES

150 μl of BMMCS at a concentration of 0.5 x 10^6 cell/ml were loaded onto cytoslides (Cytoslide, Double Circle, Coated, Thermo Scientific, #5991055) using the Shandon EZ Double Cytofunnel (Thermo Scientific). Cytoslides were spun for 5 min at 1000 rpm. BMMCs were fixed in 100% methanol for 15 min. After this time, slides were immersed in May-Grunwald stain for 5 min (undiluted), followed by immersion in 10 % Giemsa stain (diluted in ddH$_2$0, pH 6.8) for 10 min. Slides were rinsed briefly in water and excess dye

wiped off the back of the slide. Coverslips were wet-mounted onto the slides using VectorMount®.

2.15 DNA SYNTHESIS AND CELL EXPANSION ASSAYS

2.15.1 BMMCs

DNA synthesis: Following 24 h starvation in culture media without IL-3 and SCF, $1x10^5$ cells were seeded / well in a 96 well plate, in triplicate, with 20 ng/ml IL-3 and/or 20 ng/ml SCF, together with 0.5 μCi [^{3}H]-Thymidine (Amersham). Cells were harvested 24-72 h later cells were harvested and [^{3}H]-Thymidine incorporated into DNA measured by scintillation counting (Perkin-Elmer Microbeter counter).

Cell expansion: Following 24 h starvation in culture media without IL-3 and SCF, cells were seeded at a concentration of $0.5x10^6$ cells/ml in media containing 20 ng/ml IL-3 and 20 ng/ml SCF. Viable cell numbers were determined every 24 – 72 h using a Casy cell counter (Scharfe System). Cell media containing 20 ng/ml IL-3 and 20 ng/ml SCF was replaced every 3 days.

2.15.2 Cell lines

DNA synthesis: Cells were incubated at 2×10^5 cells per well in 96-well plate, in cell culture media without FBS for 24 h. After this time cell culture media was replaced with media containing 10% FBS together with 0.5 μCi [^{3}H]-Thymidine. Cells were harvested 24-72 h later cells were harvested and [^{3}H]-Thymidine incorporated into DNA measured by scintillation counting (Perkin-Elmer Microbeter counter).

2.16 FACS ANALYSIS OF c-KIT and FcεRI EXPRESSION ON BMMCs

100,000 cells were used per FACS tubes. BMMCs were washed two times in PBS, at 1400 rpm for 5 min. Cells were resuspended in FACS buffer and 100 μl distributed per FACS tube. In general, the antibody incubations were as follows: 1) anti-c-kit-PE (BD PharMingen, # 553355), 2) purified mouse IgE (BD PharMingen, #553413) + anti- mouse IgE-FITC (BD PharMingen, #553415), 3) anti-IgE-FITC alone and 4) unstained cells. For detection of FcεRI, 20 μl of purified IgE was added per FACS tube and samples left for 20 min at 4°C. Subsequently, 5 μl of anti-IgE-FITC was added per tube and samples incubated for a further 30 min at 4°C in the dark. For detection of c-kit, 2.5 μl of anti-c-kit conjugated to Phycoerythrin (anti-c-kit-PE) was added per FACS tube and samples incubated for 30 min at 4°C in the dark. To determine the background fluorescence for FITC, 5 μl of anti-

IgE-FITC (without the addition of purified IgE) was added to tubes and samples incubated for 30 min at 4°C in the dark. Cells were washed once with FACS buffer and resuspended in 400 µl FACS buffer per FACS tube.

2.17 MASS SPECTROMETRY

I carried out the colloidal Coomassie staining of acrylamide gels and preparation of peptides for mass spectrometry analysis, however the actual mass spectrometry analysis was performed by Dr. Pedro Cutillas (Barts & The London School of Medicine, Queen Mary).

2.17.1 Colloidal Coomassie staining of acrylamide gel

Colloidal Coomassie staining of acrylamide gels was performed using GelCode® Blue stain reagent according to the manufacturer's protocol (Pierce, 24592). Briefly, acrylamide gels were fixed in 40% ethanol/10% acetic acid for 1 h to overnight. Gels were subsequently washed 3-5 times with excess ddH$_2$O and 20 ml of GelCode® Blue was added for 1 h. Gels were washed in ddH$_2$O for a further 1 h to decrease background staining.

2.17.2 Preparation of peptides for mass spectrometry analysis

To minimise protein contamination, sample preparations were performed in a ventilated hood. Colloidal Coomassie-stained gel bands were excised from the acrylamide gel and cut into small pieces and placed into 0.625 ml siliconised tubes. Gel pieces were washed and dehydrated by the addition of 50% acetonitrile (ACN) three times. Gel loading tips were used to aspirate ACN between washes. The gel pieces were dried in a speed vacuum for approximately 1 h. Protein disulphide bridges were reduced by adding a sufficient volume of 10 mM DTT in 25 mM ammonium bicarbonate (AmBic) pH 8.0, to cover gel pieces, and incubating for 45 min at 50°C. For alkylation of cysteine residues, a sufficient volume of 50 mM iodoacetamide in 25 mM to cover gel pieces and the reaction incubated for 1 h at room temperature in the dark. Following this, gel pieces were washed twice in 50% ACN and fully dried in a speed vacuum for approximately 1 h.

To digest the peptides, 25 mM AmBic pH8 containing 150 ng / sample of trypsin (Promega, 608-274-4330) was added to cover the gel pieces. After 5 min, this was overlaid with 25 mM AmBic to completely cover the gel pieces and incubated at 37°C overnight. The following day, samples were centrifuged to spin down liquid from tube lid. 20 µl of 50% ACN 5% trifluoroacetic acid was added to the samples and the total supernatant removed to a fresh tube. 80 µl of 50% ACN 5% trifluoroacetic acid was then added to the

gel pieces again, the sample vortexed, centrifuged and the supernatant removed to the fresh tube. This was repeated one more time to extract as much of the digested peptides from the gel pieces as possible. The extracted peptides were concentrated by drying samples in a speed vacuum and resuspending in 5 µl 0.1% formic acid.

3. DOES CELL TRANSFORMATION ALTER p110 COUPLING TO TYROSINE KINASE RECEPTORS?

3.1 Introduction

The question addressed in this part of my thesis is whether coupling of class IA PI3Ks to tyrosine kinase receptors remains the same under normal and transformed cellular states. The reasoning behind this work is that in primary, untransformed cells, a single PI3K isoform often appears to carry most PI3K activity downstream of a given receptor. This is evidenced by the observation that blockade of a single PI3K isoform downstream of a given tyrosine kinase receptor often results in a severe impact on the biological responses controlled by this tyrosine kinase receptor. For example, in primary leukocytes, p110δ is often the 'dominant' class IA isoform, with p110δ inhibition having a major impact on, for example, the c-kit receptor and antigen receptor signalling. In transformed leukocytes, however, the relative contribution of p110δ appears to become less important, with p110δ inhibition having less of an impact compared to that in primary cells. For example, in primary macrophages, CSF-1 receptor signalling is dependent on p110δ activity, whereas in immortalized macrophage cell lines, p110α is the principle PI3K isoform downstream of the CSF-1 receptor (Papakonstanti, et al., in preparation). One possible explanation could be that coupling of class IA PI3Ks to tyrosine kinase receptors is altered in normal and transformed cellular states. I have investigated this question, focusing on the coupling of p110δ to the tyrosine kinase receptor, c-kit, in bone marrow-derived mast cells (BMMCs).

To investigate whether p110δ remains the principal p110 isoform activated downstream of c-kit in a 'transformed' mast cell, three approaches were used to experimentally transform or immortalize primary wild-type (WT) BMMCs, namely by introduction of the HOX11 homeobox gene or the polyoma middle T antigen (PMT). The third approach was to assess whether in p110δ$^{D910A/D910A}$ BMMCs, another p110 isoform than p110δ is able to signal downstream of c-kit to substitute for the kinase-dead p110δ, to restore c-kit signalling. This could perhaps be referred to as a 'spontaneous transformation' phenomenon. Previous findings (Ali & Vanhaesebroeck, unpublished results) have indicated that such a change may occur in long-term cultured p110δ$^{D910A/D910A}$ BMMCs, possibly leading to a switch in p110 recruitment to c-kit, with p110α being the most likely candidate. The main finding that led to this conclusion was that p110δ$^{D910A/D910A}$ BMMCs maintained in culture for more than 6 weeks were often found to have increased p110α protein expression associated with increased p110α kinase activity compared to WT BMMCs (Ali & Vanhaesebroeck, unpublished results).

3.2 HOX11 immortalisation of BMMCs results in a less differentiated mast cell phenotype

The HOX11 homeobox gene encodes an oncogenic transcription factor that is frequently activated in a subset of T-cell acute lymphoblastic leukaemia (Riz & Hawley, 2005). HOX11 transfection is frequently used in our laboratory to immortalise leukocyte cell lines. Using a retroviral infection method, HOX11 was introduced into primary WT BMMCs 6 weeks after isolation. Cells stably expressing HOX11 were selected using neomycin and HOX11 expression determined by western blot (Figure 3.1).
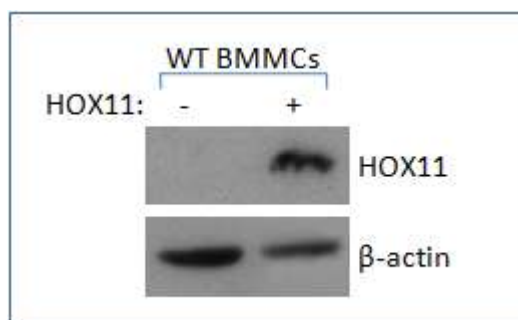
Figure 3.1: HOX11 expression in HOX11-infected BMMCs. HOX11 expression was assessed in WT BMMCs after selection with neomycin. Cell lysates were separated by SDS-PAGE and immunoblotted for HOX11.

Cells expressing HOX11 were fixed and stained using May-Grünwald and Giemsa stain to assess cell morphology (Figure 3.2). It was observed that HOX11-expressing cells had a less differentiated 'early progenitor-like' appearance, with less granular cells and a large round nucleus.
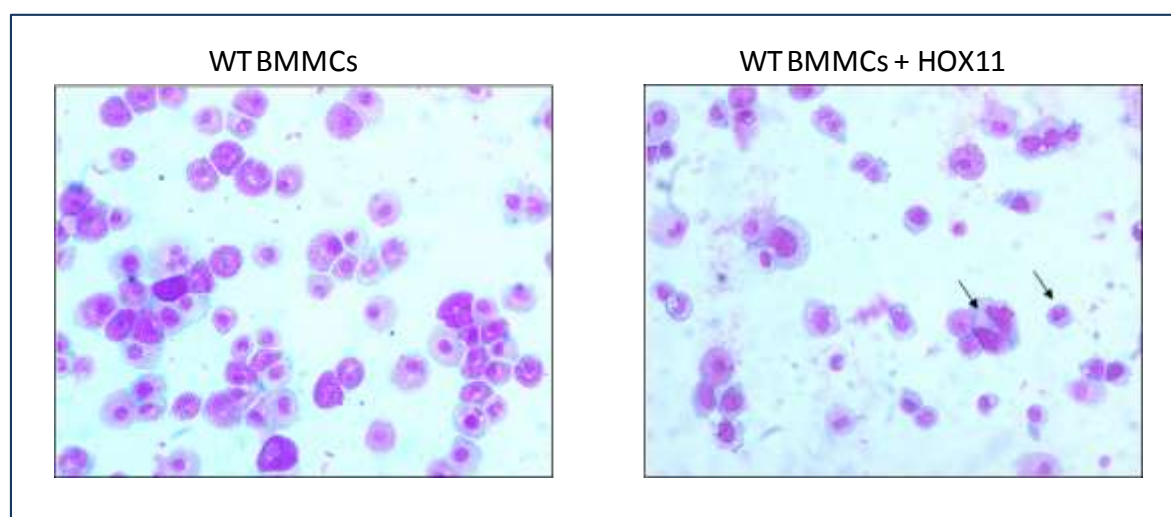
Figure 3.2: Cell morphology of WT BMMCs transfected with HOX11. Cells were fixed and stained with May Grünwald and Giemsa. HOX11-expressing cells have a less differentiated morphology compared to WT BMMCs. Arrows indicate cells with an early progenitor-like appearance with large rounded nuclei.

To establish if WT BMMCs expressing HOX11 still maintained mast cell characteristics, the levels of c-kit and FcεRI expression were determined by FACS (Figure 3.3). Only a small proportion of WT HOX11-expressing cells (15%) expressed c-kit compared to non-transfected cells, which had almost 100% expression of c-kit. Expression of FcεRI was also reduced in HOX11-positive BMMCs, with only 20% of cells expressing this receptor compared to 95% of non-transfected cells. These results indicate that expression of HOX11 in BMMCs results in cells that no longer express characteristic mast cell markers.
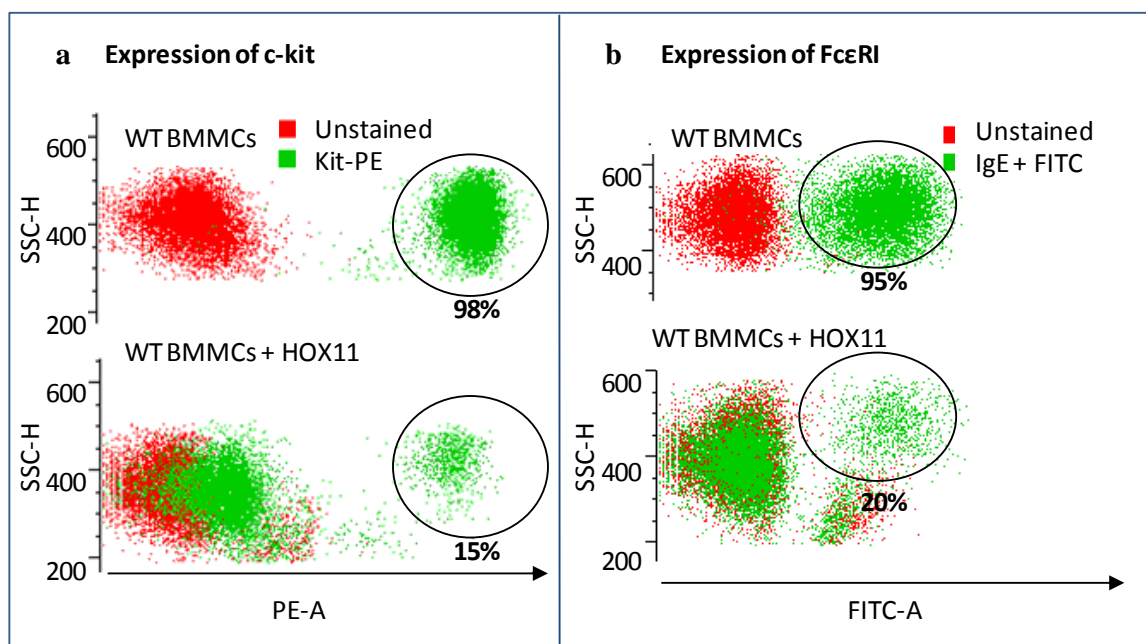
Figure 3.3: c-kit and FcεRI expression in HOX11-immortalised BMMCs. The expression of **(a)** c-kit and **(b)** FcεRI was determined by FACS analysis. Cells were incubated with a PE-conjugated anti-c-kit antibody, or with purified IgE followed by a FITC-conjugated anti-IgE antibody.

To study the effect of HOX11-immortalisation on c-kit signalling, a larger population of c-kit-positive cells was required. The 15% of HOX11-expressing WT BMMCs that expressed c-kit were separated from the c-kit-negative cell population by FACS in order to expand this cell population for further studies. However, after continued culture of the sorted cells, further FACS analysis on this theoretically '100% c-kit-positive' population revealed that only 12% of cells expressed c-kit and 15% of cells expressed FcεRI (Figure 3.4). In other words, HOX11-positive cells had a tendency to lose expression of the c-kit receptor, most likely an effect of HOX11 on cell differentiation, causing what were thought of as terminally differentiated mast cells to take on less differentiated progenitor cell characteristics. Importantly, for this study, HOX11-expressing cells no longer expressed

the c-kit receptor and could therefore not be used to study coupling of p110δ to the c-kit receptor.
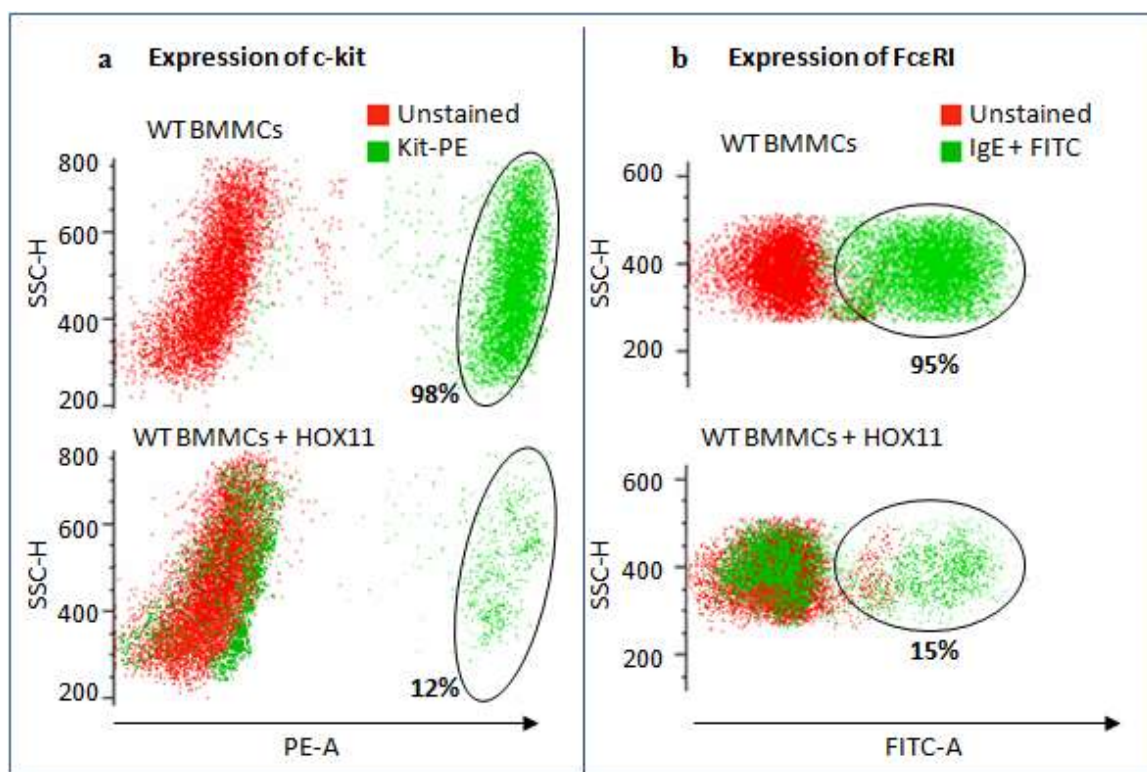
Figure 3.4: Expression of c-kit and FcεRI in HOX11-transduced BMMCs, following sorting for expression of c-kit and two weeks culture. HOX11-transfected BMMCs were sorted on the basis of c-kit expression. c-kit-positive cells were expanded for two weeks, followed by determination of **(a)** c-kit and **(b)** FcεRI expression by FACS analysis.

3.3 Transformation of BMMCs with PMT

The Polyoma middle T antigen (PMT) has been shown to be responsible for the oncogenicity of the virus in susceptible cells. PMT associates with and activates Src family tyrosine kinases. Tyrosine kinases of the Src family play an essential role in cell signalling, regulating cell growth, differentiation and morphology (Dunant & Ballmer-Hofer, 1997; Gottlieb & Villarreal, 2001). Phosphorylation of tyrosine 527 on Src kinase (by members of the Csk family kinases) permits an intramolecular interaction between this C-terminal phosphotyrosine residue and the SH2 domain causing a closed catalytically inactive conformation of Src. When this intramolecular interaction is disrupted and the protein is in an open conformation, the Src kinase is active (Dunant & Ballmer-Hofer, 1997). PMT associates more efficiently with the active conformation of Src at the catalytic domain, which has led to the proposition that PMT increases Src kinases activity through stabilisation of active Src molecules in this open conformation (Dunant & Ballmer-Hofer, 1997).

PMT activation of Src kinases gives rise to phosphorylation of specific tyrosine residues in PMT as well as in other molecules in the PMT-complex. Phosphorylated-tyrosine residues on PMT act as docking sites for intracellular signalling molecules. The phosphorylated tyrosine residue 315 associates with one of the SH2 domains of p85, most likely leading to recruitment of PI3K to the membrane (Dunant & Ballmer-Hofer, 1997; Gottlieb & Villarreal, 2001).

3.3.1 Expression of PMT does not affect mast cell differentiation

Using a retroviral infection method, WT BMMCs were infected with PMT with the aid of retronectin. Infected BMMCs were selected using neomycin and cell cultures expanded. PMT expression was assessed by western blot and found to be highly expressed in infected cells (Figure 3.5).
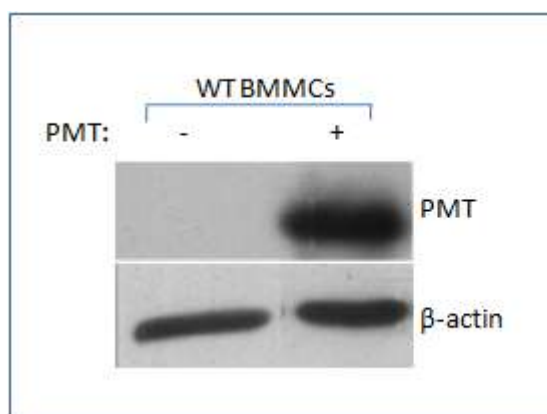
Figure 3.5: PMT expression in PMT-infected BMMCs. PMT expression was assessed in WT BMMCs cells selected with neomycin. Cell lysates were separated by SDS-PAGE and immunoblotted for PMT.

To give an insight if PMT-expressing cells maintained mast cell characteristics, cells were fixed and stained with May Grünwald and Giemsa to look at cell morphology. PMT-expressing cells appeared to have a similar morphology to uninfected cells (Figure 3.6), maintaining a granular appearance and a similar size and shape to uninfected BMMCs. Importantly, PMT-expressing cells maintained a similar level of c-kit and FcɛRI expression to uninfected BMMCs. FACS analysis showed that almost 100% of both WT and PMT-expressing BMMCs expressed both the c-kit receptor and FcɛRI (Figure 3.7).

Overall, these data suggest that unlike HOX11, PMT does not affect BMMC differentiation. Given that PMT-expressing cells retain c-kit expression, they could be used to investigate p110 coupling to c-kit.
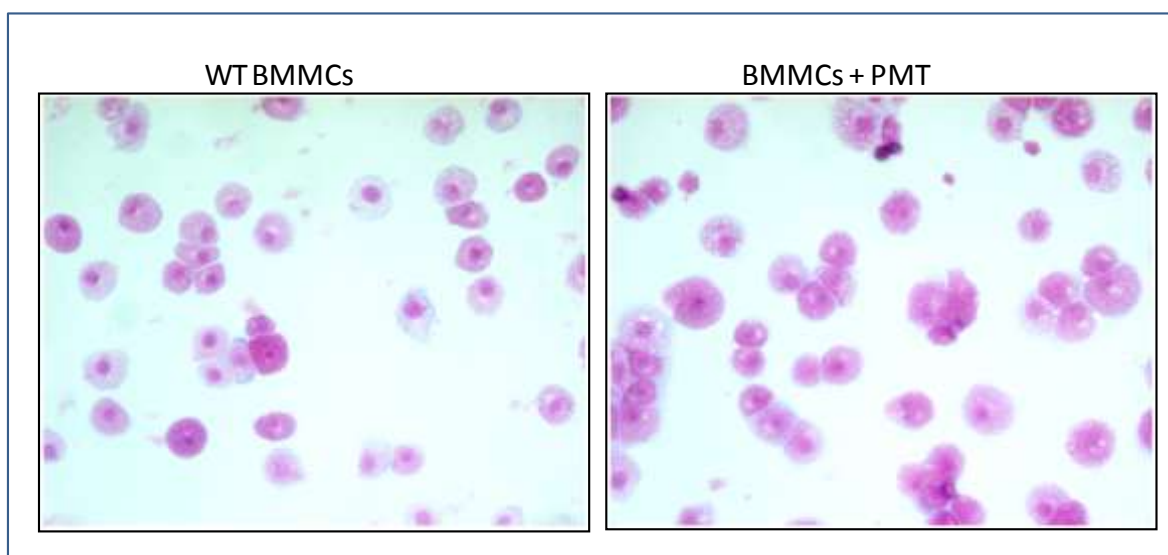
Figure 3.6: Cell morphology of WT and PMT-expressing BMMCs. Cells were fixed and stained with May Grünwald and Giemsa.
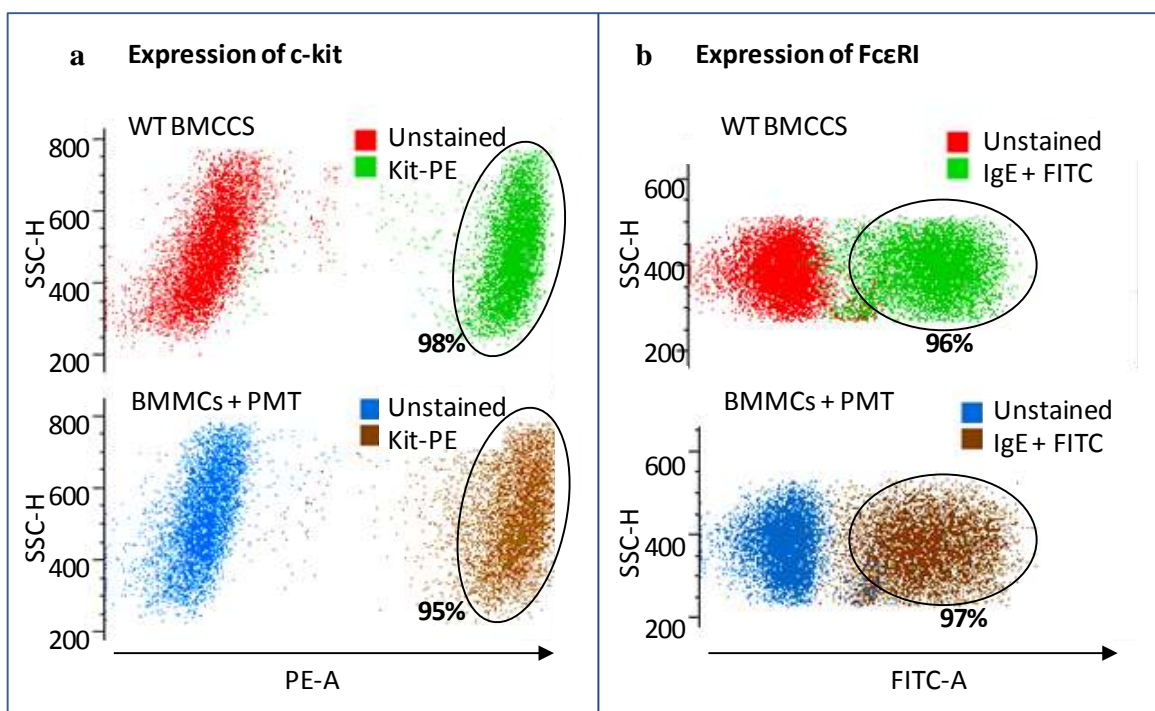
Figure 3.7: Expression of c-kit and FcεRI in PMT-expressing BMMCs. The expression of **(a)** c-kit **(b)** and FcεRI was determined by FACS analysis. Cells were incubated with a PE-conjugated anti-Kit antibody, or with purified IgE followed by a FITC-conjugated anti-IgE antibody.

3.3.2 PMT-expressing BMMCs maintain IL-3-dependence

IL-3 is an essential component of the culture media required for proliferation of BMMCs. To assess whether PMT expression in BMMCs resulted in cell transformation, which would be expected to render cells independent of IL-3, a cell expansion assay was performed on WT and PMT-expressing cells in media with or without IL-3 (Figure 3.8). In

the complete absence of IL-3, both WT and PMT-expressing BMMCs failed to expand (Figure 3.8a), indicating that PMT-expressing BMMCs were still dependent on IL-3 for cell growth. However, they showed increased cell growth in media containing 5 ng or 20 ng/ml IL-3, compared to WT BMMCs (Figures 3.8b, c). Therefore, although PMT-expressing BMMCs appeared to not be 'fully' transformed (in that they are not cytokine-independent), they had a proliferative advantage over WT cells.
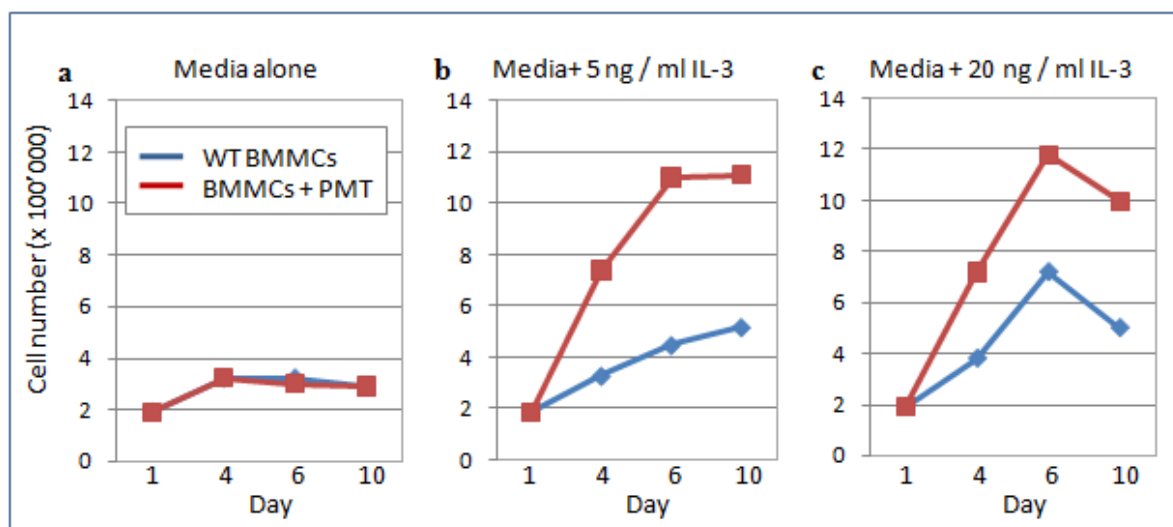
Figure 3.8: Effect of IL-3 on cell expansion of WT and PMT-expressing BMMCs. WT and PMT-expressing BMMCs were seeded at the same density in **(a)** media alone, **(b)** media containing 5 ng/ml IL-3, or **(c)** media containing 20 ng/ml IL-3. Cell counts were performed over a period of 10 days, during which media was replaced every 2 days.

3.3.3 PMT-expressing BMMCs do not have increased basal or SCF-induced Akt phosphorylation

The effect of PMT expression on PI3K signalling in BMMCs was assessed by examining basal and SCF-induced Akt phosphorylation. PMT-positive cells did not show an increase in basal phosphorylation of Akt compared to WT cells (Figure 3.9). Furthermore, SCF-induced phosphorylation of Akt appeared somewhat lower in PMT-expressing BMMCs compared to WT BMMCs. This result is surprising given that expression of PMT results in activation of Src, which in turn activates PI3K. However, this result does help explain the finding that PMT-positive BMMCs are not cytokine-independent for cell growth. In conclusion, PMT-infection of BMMCs appears to result in a 'semi-transformed' state, in which PMT-expressing cells have a proliferative advantage over uninfected cells, but remain cytokine-dependent and do not have constitutive Akt activation.
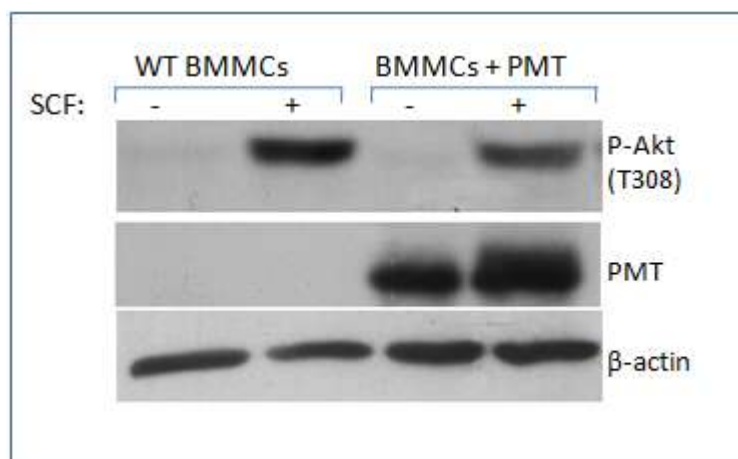
Figure 3.9: Levels of Akt phosphorylation under basal and SCF-stimulated conditions in WT and PMT-expressing BMMCs. WT and PMT-expressing BMMCs were stimulated with 20 ng/ml SCF for 5 min. Cell lysates were separated by SDS-PAGE and immunoblotted for P-Akt and PMT.

3.3.4 c-kit remains dependent on p110δ in PMT-expressing BMMCs

Given that cell numbers were a limiting factor and that a large number of cells was required for successful c-kit immunoprecipitation, to investigate whether functional c-kit coupling to p110δ is affected in cells 'semi-transformed' by PMT, isoform-specific inhibitors were used to assess the dependence of the c-kit receptor on individual p110 isoform to induce Akt phosphorylation (Figure 3.10). Cells that had been in culture for 12 weeks were used in this study, which is considered a long period for primary cells to be maintained in culture. However, due to the number of cells required for the experiment and the relatively slow proliferative rate of BMMCs, a 12 week culture time was necessary.

In WT BMMCs, the p110δ inhibitor (IC87114) reduced SCF-induced Akt phosphorylation to almost the same extent as LY294002 (Figure 3.10), supporting previous findings that p110δ is the primary p110 isoform downstream of c-kit activation (Ali, et al., 2004). In PMT-expressing BMMCs, p110δ appeared to remain the principle isoform downstream of c-kit as IC87114 treatment also inhibited SCF-induced Akt phosphorylation to the same extent as LY294002. In PMT-expressing BMMCs, inhibition of p110γ reduced SCF-induced Akt phosphorylation to around 40% of the maximal response, whereas in WT BMMCs, inhibition of p110γ (AS604850 treatment) had no effect on Akt phosphorylation. This result indicates p110γ may be playing a role downstream of c-kit in PMT-expressing cells. Treatment of both WT and PMT-expressing cells with the p110β inhibitor (TGX115) at 0.5 μM reduced SCF-induced Akt phosphorylation by around 40%. It is possible that this is an off-target effect of TGX115, as this inhibitor has also been shown to inhibit p110δ at this concentration (see Table 2.1, section 2.1.5, for IC$_{50}$ values of PI3K inhibitors).
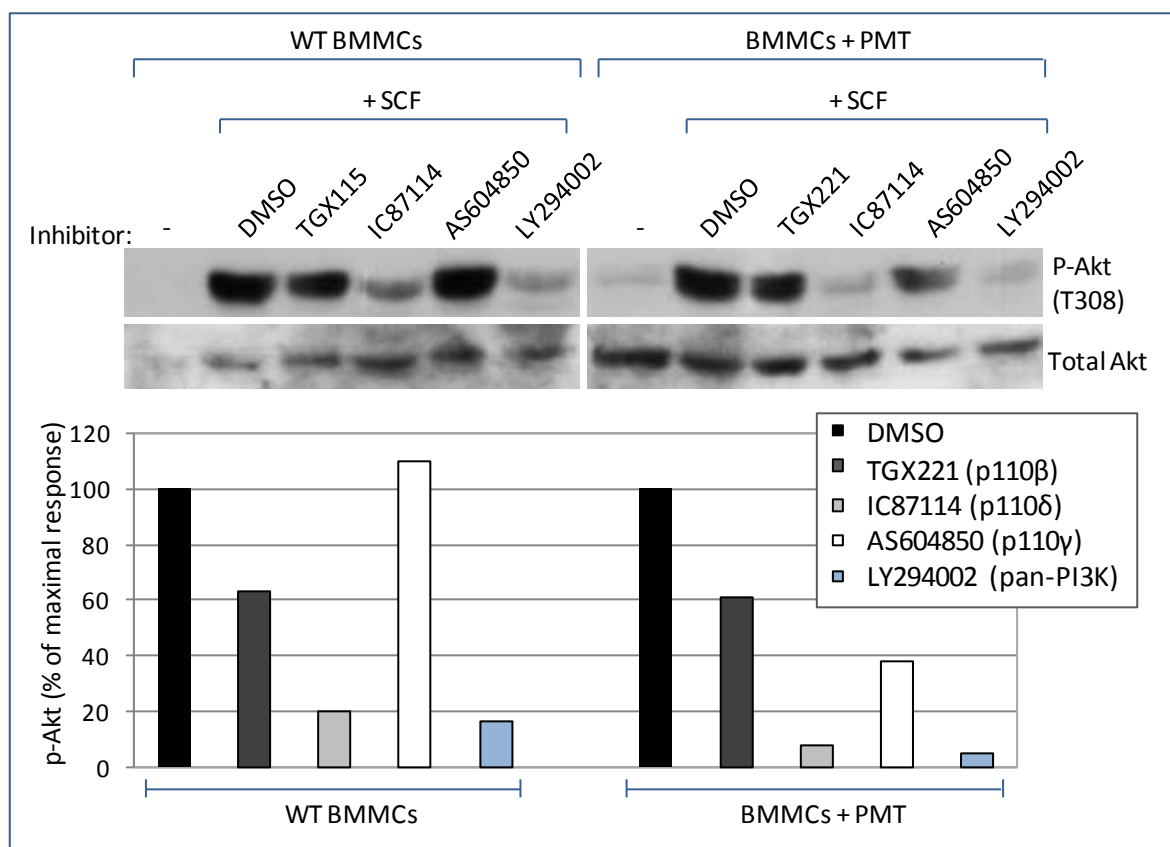
Figure 3.10: Effect of PI3K inhibition on SCF-induced Akt phosphorylation in WT and PMT-expressing BMMCs. WT and PMT-expressing BMMCs that had been cultured for 12 weeks, were incubated with a p110 inhibitor or DMSO for 1 h prior to stimulation with 20 ng/ml SCF. The p110β inhibitor, TGX115, was used at 0.5 μM, the p110δ inhibitor, IC87114, was used at 5 μM and the p110γ inhibitor, AS604850, was used at 1 μM. The pan-PI3K inhibitor, LY294002 was used at 10 μM.

Collectively, these data indicate that c-kit remains dependent on p110δ in PMT-expressing cells to induce Akt phosphorylation, suggesting that p110 isoform recruitment to the c-kit receptor is not significantly altered. Experiments need to be repeated in order to comment on a possible role of p110γ in PMT-expressing BMMCs. These data do not however provide information regarding c-kit-p110 coupling in fully transformed BMMCs.

3.4 Spontaneous transformation of p110δ$^{D910A/D910A}$ BMMCs in long-term culture

As mentioned in the introduction, it has been observed that p110δ$^{D910A/D910A}$ BMMCs maintained in culture for over 6 weeks become more responsive to SCF. Given that p110δ is kinase-dead in these cells, it is likely that another p110 isoform is signalling downstream of c-kit. It was hypothesised that an adaptation of p110δ$^{D910A/D910A}$ BMMCs may occur that enables them to become responsive to SCF, which from previous findings may involve p110α (Ali & Vanhaesebroeck, unpublished results).

3.4.1 Upregulation of p110α isoform expression in p110δ$^{D910A/D910A}$ BMMCs maintained in long-term culture

After 36 days in culture, both WT and p110δ$^{D910A/D910A}$ BMMCs had similar p110 expression profiles (Figure 3.11).
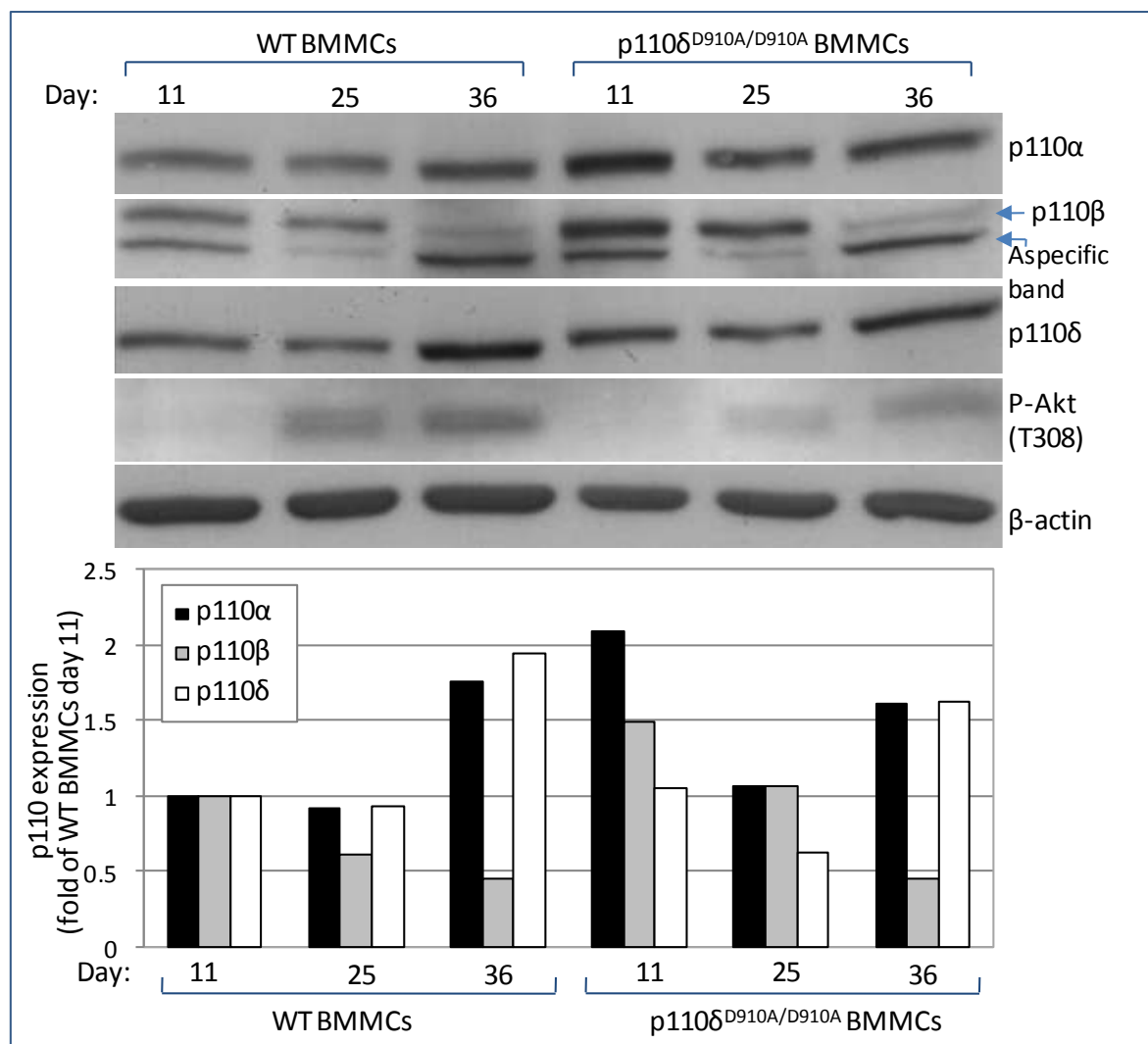
Figure 3.11: p110 isoform expression in WT and p110δ$^{D910A/D910A}$ BMMCs over a time period of 36 days after isolation. Total cell lysates were taken from WT and p110δ$^{D910A/D910A}$ BMMCs at days 11, 25 and 36 after isolation. Cell lysates were separated by SDS-PAGE and immunoblotted for p110α, p110β and p110δ.

11 days after isolation, p110δ$^{D910A/D910A}$ BMMCs appeared to have a higher level of p110α expression compared to WT BMMCs, however after 36 days, when the mast cells are fully differentiated, both WT and p110δ$^{D910A/D910A}$ BMMCs had a similar level of p110α expression (Figure 3.11). p110δ expression increased in both WT and p110δ$^{D910A/D910A}$ BMMCs at each time point after isolation, which correlates with the high levels of p110δ found in fully differentiated mast cells. When immunoblotting for p110β, two bands are detected with the p110β antibody used and it is the upper band which has been verified as

p110β (Guillermet-Guibert, et al., 2008). In contrast to p110δ, p110β expression appeared to decrease in both WT and p110δ$^{D910A/D910A}$ BMMCs after 36 days in culture. The important finding from this study is that at day 36, when the haematopoietic progenitors are fully differentiated into mast cells, p110α, p110β and p110δ are expressed at similar levels in WT and p110δ$^{D910A/D910A}$ BMMCs (Figure 3.11).

It was thought that for an adaptation to occur in p110δ$^{D910A/D910A}$ BMMCs, cells may need to be cultured for a time period exceeding 36 days. Two further independent batches of BMMCs (subsequently referred to as batch B and batch C) were isolated and maintained in culture for longer time periods, 77 and 54 days, respectively. At both of these later time points, increased p110α expression was observed in WT and p110δ$^{D910A/D910A}$ BMMCs (Figure 3.12). The increase in p110α expression was more apparent in p110δ$^{D910A/D910A}$ BMMCs and appeared to correlate with a decrease in p110δ expression. p110β expression was undetectable in all cell lysates taken from BMMCs in batch B, however a noticeable decrease in p110β expression was observed at day 54 in batch C compared to day 25 in WT and p110δ$^{D910A/D910A}$ BMMCs.

Collectively, the data suggests that long-term culture of p110δ$^{D910A/D910A}$ BMMCs results in upregulation of p110α expression and a concomitant decrease in both p110β and p110δ expression, which suggests cells may be adapting to expressing a kinase-dead p110δ isoform through upregulation of p110α. Although an increase in p110α expression was also observed in WT BMMCs after long-term culture, this was not associated with a decrease in p110δ expression, which suggests that in WT BMMCs, p110δ remains the principal p110 isoform.
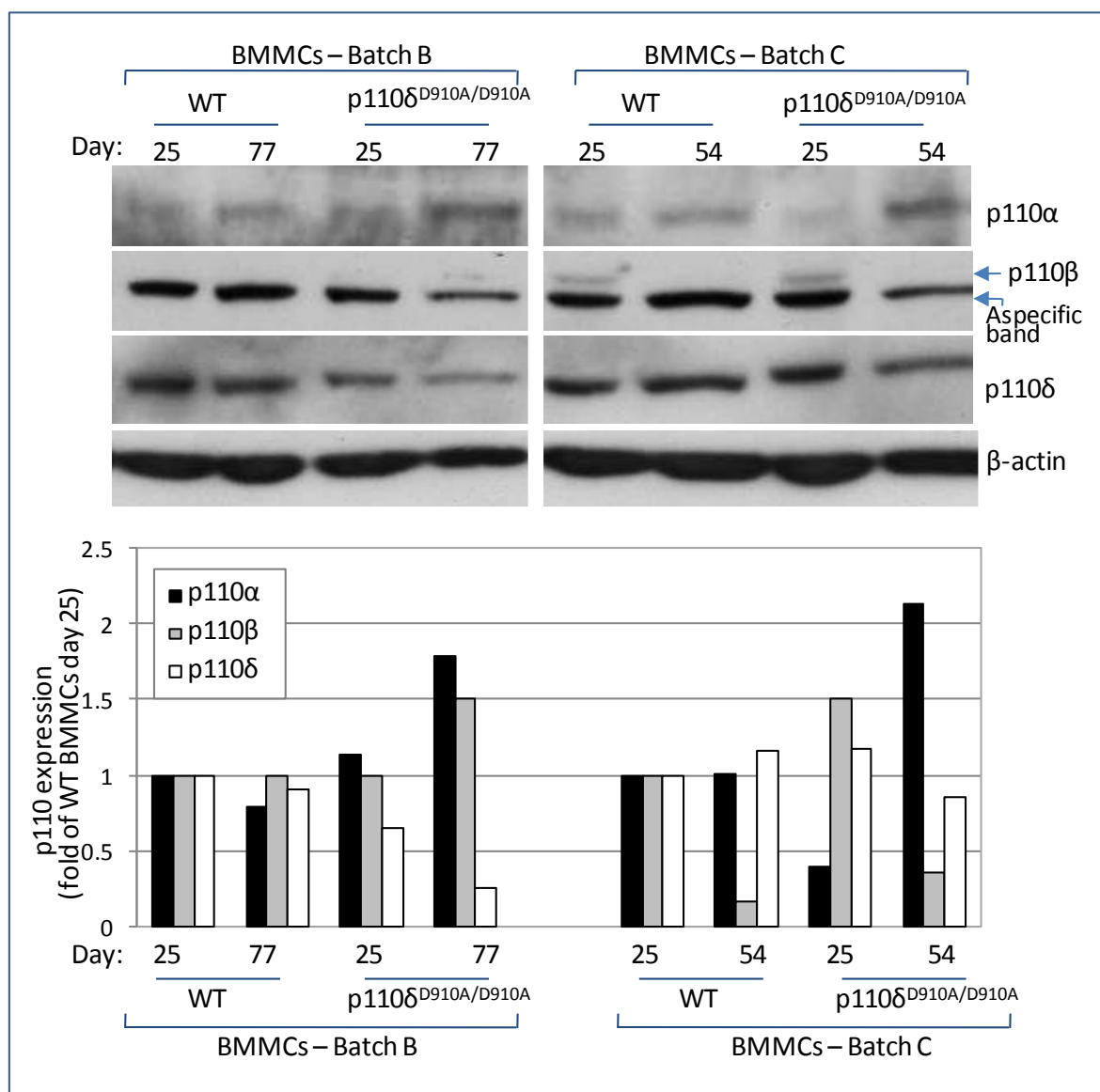
Figure 3.12: p110 isoform expression in WT and p110δ$^{D910A/D910A}$ BMMCs over a time period of 77 and 54 days after isolation. Total cell lysates were taken from WT and p110δ$^{D910A/D910A}$ BMMCs at days 25 and 77 for batch B and days 25 and 54 for batch C after isolation. Cell lysates were separated by SDS-PAGE and immunoblotted for p110α, p110β and p110δ.

3.4.2 p110α isoform upregulation in p110δ$^{D910A/D910A}$ BMMCs does not correlate with increased cell proliferation

To investigate whether long-term cell culture affects cell proliferation in p110δ$^{D910A/D910A}$ BMMCs, cell counts were performed over a period of 78 days after isolation for BMMCs from batch B (Figure 3.13). The initial drop in cell numbers of both WT and p110δ$^{D910A/D910A}$ BMMCs reflects the selection and differentiation period for mast cells progenitors from the heterogenous haematopoietic progenitor population initially isolated from the bone marrow.
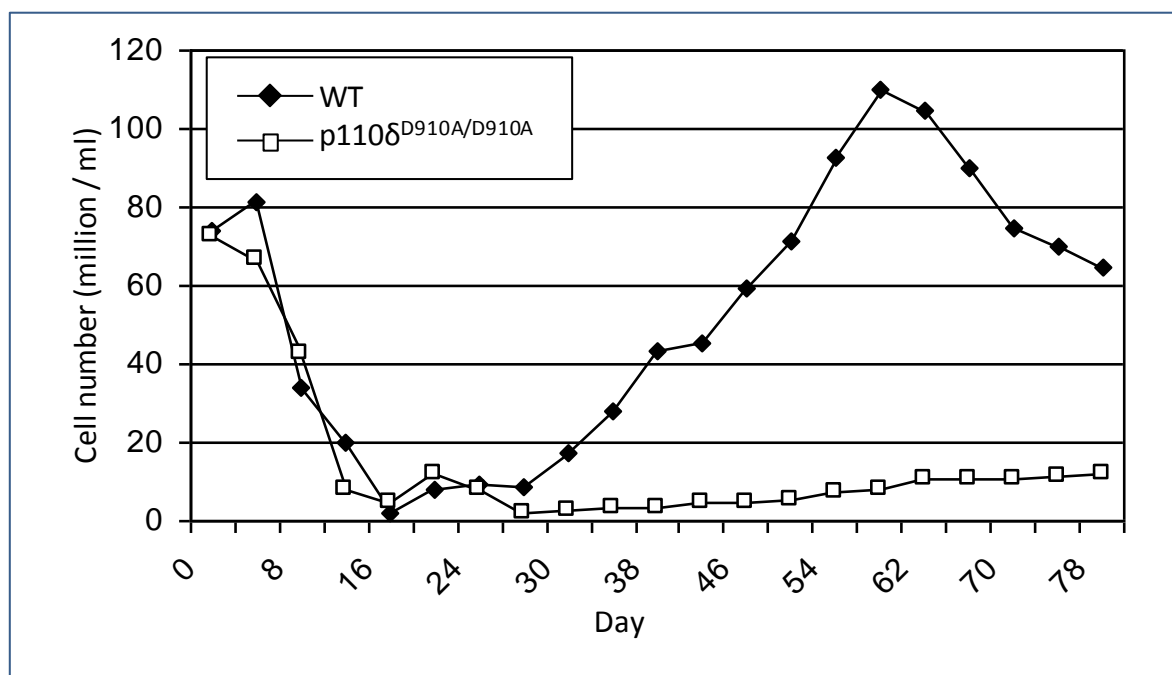
Figure 3.13: Cell counts of WT and p110δ$^{D910A/D910A}$ BMMCs up to 78 days after isolation. BMMCs were counted over a period of 78 days after isolation. Cells isolated from the bone marrow of mouse femurs were cultured in media containing 10 ng/ml SCF and 10 ng / ml IL-3 for selection and differentiation of mast cells.

Despite the apparent upregulation in p110α expression in p110δ$^{D910A/D910A}$ BMMCs, cell expansion of p110δ$^{D910A/D910A}$ BMMCs remained substantially lower than WT BMMCs throughout the 78 day course of cell counts. After 60 days in culture, WT BMMC numbers began to decrease indicating cell death. However, in p110δ$^{D910A/D910A}$ BMMCs, although cells did not appear to be readily expanding, cells did not appear to be dying either (Figure 3.13). The data suggest that if p110δ$^{D910A/D910A}$ BMMCs are adapting when maintained in long-term culture through upregulation of p110α, this does not translate into increased cell proliferation but may protect the cells from cell death.

3.4.3 Restoration of SCF-induced phosphorylation of Akt in p110δ$^{D910A/D910A}$ BMMCs upon long-term culture

An almost complete abrogation of SCF-induced Akt phosphorylation was reported in p110δ$^{D910A/D910A}$ mast cells cultured for 6 weeks (Ali et al., 2004). Remarkably in p110δ$^{D910A/D910A}$ BMMCs that had been maintained in culture for 12 weeks, SCF induced Akt phosphorylation (Figure 3.14). This result raised the possibility that a switch in c-kit-p110 receptor coupling had occurred, with p110α as the most likely candidate from the data shown in Figure 3.12.
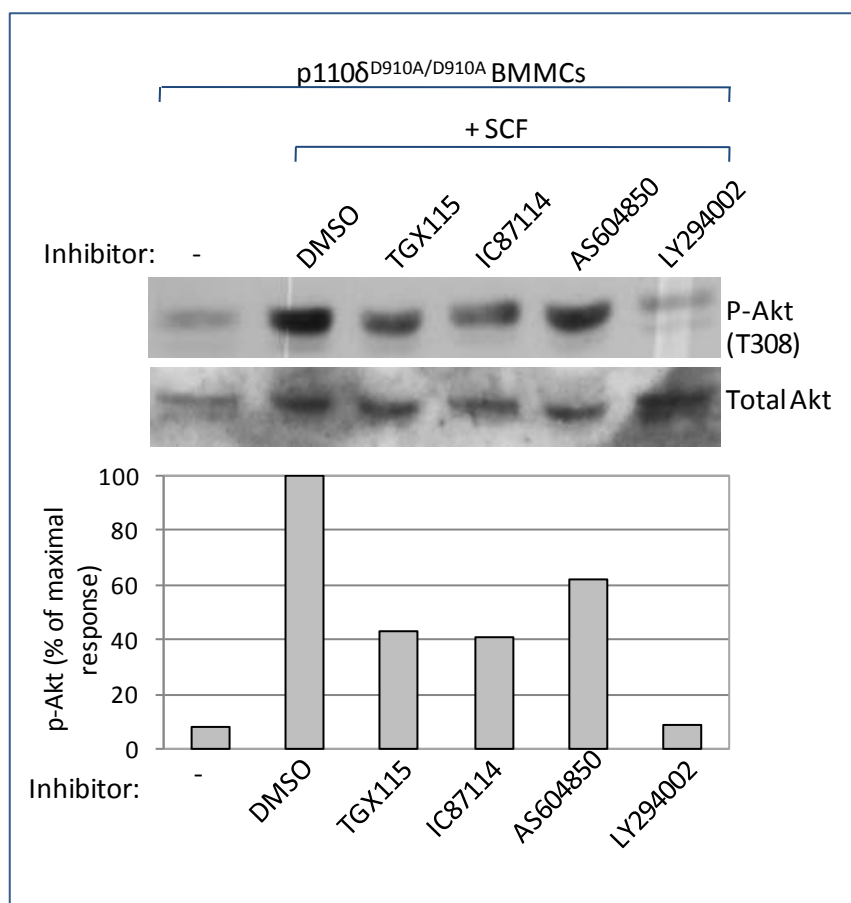
Figure 3.14: Effect of PI3K inhibition on SCF-induced Akt phosphorylation in p110δ^{D910A/D910A} BMMCs. p110δ$^{D910A/D910A}$ BMMCs were incubated with a p110 inhibitor or DMSO for 1 h prior to stimulation with 20 ng/ml SCF. The p110β inhibitor, TGX115, was used at 0.5 μM, the p110δ inhibitor, IC87114, was used at 5 μM and the p110γ inhibitor, AS604850, was used at 1 μM. The pan-PI3K inhibitor, LY294002, was used at 10 μM.

Due to the lack of p110α-specific inhibitor at the time of this study, the dependency of c-kit on p110α to induce Akt phosphorylation in response to SCF could not be tested. However c-kit dependency on p110β, p110δ and p110γ could be investigated. As shown in Figure 3.14, the p110β inhibitor and surprisingly the p110δ inhibitor had the greatest effect on reducing SCF-induced Akt phosphorylation besides the pan PI3K inhibitor LY294002. Since p110δ in p110δ$^{D910A/D910A}$ BMMCs is kinase-dead, the inhibitory effect induced by 5 μM IC87114 treatment is most likely the result of off-target p110β inhibition (see Table 2.1 for the IC$_{50}$ values of the PI3K-specific inhibitors). Evidence to support off-target p110β inhibition by IC87114 has been found in NIH 3T3, a cell line that expresses low endogenous levels of p110δ. Treatment of NIH 3T3 cells with 5μM IC87114 reduces LPA-induced Akt phosphorylation to a similar extent as that for the p110β inhibitor (Guillermet-Guibert & Vanhaesebroeck, unpublished results).

3.4.4 Association of p110α and p110δ with c-kit in WT and p110δ$^{D910A/D910A}$ BMMCs upon SCF stimulation

To investigate if there is a p110 isoform switch in recruitment to the c-kit receptor in long-term cultured BMMCs, an immunoprecipitation with an anti-Kit antibody was performed on long-term cultured (16 weeks) BMMCs and p110 recruitment to the c-kit receptor analysed (Figure 3.15).
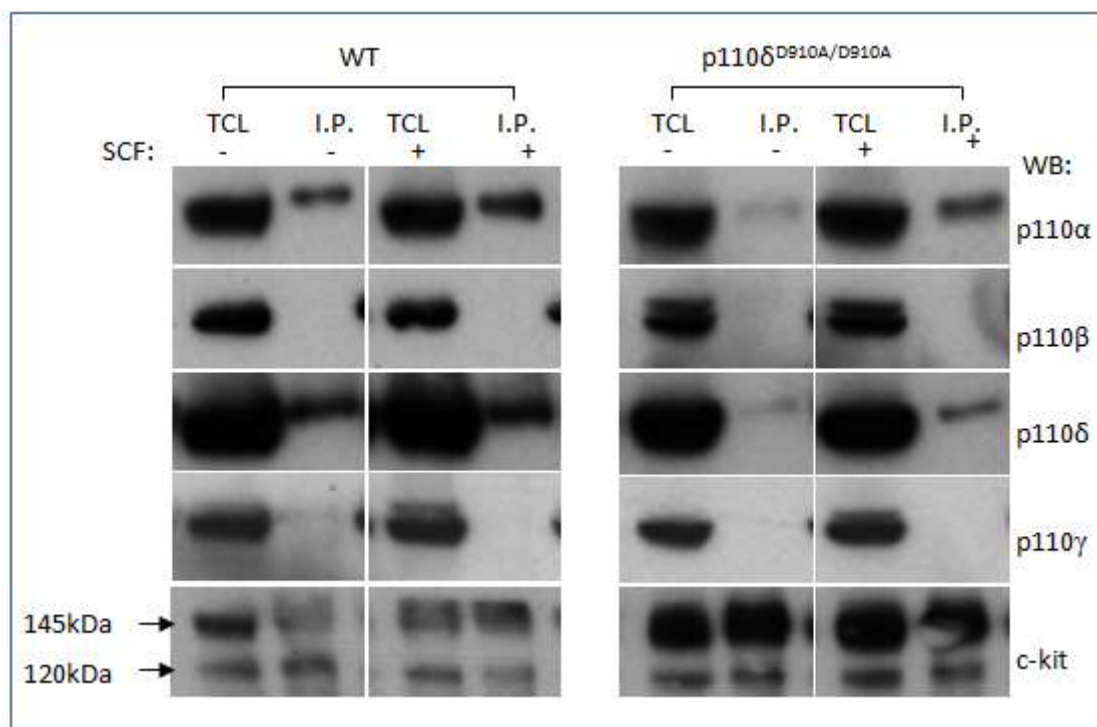
Figure 3.15: Recruitment of p110 isoforms to c-kit upon SCF-stimulation in WT and p110δ$^{D910A/D910A}$ BMMCs. Long-term cultured WT BMMCs and p110δ$^{D910A/D910A}$ BMMCs were stimulated with 20 ng / ml SCF for 10 min. An immunoprecipitation was performed on cell lysates with c-kit antibody. Cell lysates were separated by SDS-PAGE and immunoblotted with specific p110 antibodies or antibodies to c-kit.

In WT BMMCs, p110α was constitutively bound to c-kit with additional p110α recruitment upon SCF stimulation (Figure 3.15). p110β and p110γ did not constitutively bind to c-kit and were not recruited to the receptor upon SCF stimulation like p110α. p110δ was constitutively bound to c-kit with no obvious additional recruitment to the receptor upon SCF stimulation.

In p110δ$^{D910A/D910A}$ BMMCs, p110α and p110δ also constitutively bound to c-kit, but at lower levels compared to WT BMMCs. However in p110δ$^{D910A/D910A}$ BMMCs, there was considerable recruitment of p110α and p110δ to the c-kit receptor upon SCF stimulation. The level of recruitment of p110α to c-kit appeared to be greater than the level of p110δ

recruitment. As was observed in WT BMMCs, p110β or p110γ did not bind to c-kit in p110δ$^{D910A/D910A}$ BMMCs.

3.5 Discussion

3.5.1 Expression of HOX11 or PMT in WT BMMCs does not result in full cell transformation

Overall, my findings, in conjunction with the study by Ali *et al*, 2004, have shown that p110δ is the critical p110 isoform downstream of c-kit in WT BMMCs. My aim was to assess whether transformation of BMMCs resulted in a switch of p110 isoform recruitment to c-kit. Immortalising BMMCs with HOX11 resulted in the cells losing their mast cell characteristics and displaying a less differentiated phenotype. Homeobox genes encode transcription factors which appear to play managerial roles in embryonic development and also in many subsequent differentiation processes (Perkins & Cory, 1993). HOX-2.4 and HOX11 have strong immortalisation potential for bone marrow as well as embryonic stem cell-derived haematopoietic cells (Hawley*, et al.*, 1994; Perkins & Cory, 1993). Primitive hemopoietic cells are more susceptible to immortalization by HOX-2.4 compared to differentiated hemopoietic cell lineages (Perkins & Cory, 1993). It is possible that at the time of transfection of BMMCs with HOX11, a small population of undifferentiated hemopoietic progenitors were present that were preferentially transfected over differentiated mast cells. It is possible that increased expansion of this cell population over the differentiated mast cell population subsequently resulted in loss of c-kit expression. Alternatively, HOX11 expression in BMMCs may have a direct effect on BMMC differentiation, forcing cells to take on a less differentiated state. HOX11 is a potent repressor of transcription from a wide range of natural promoters in cells of human and murine origin and it has been proposed that HOX11-mediated transcriptional activation and/or repression of downstream targets may negatively regulate haematopoietic differentiation programs (Owens*, et al.*, 2003). For the purpose of this study, the mechanism by which HOX11 induces a less differentiated mast cell phenotype was not considered of critical importance. The key finding was that HOX11-transfected cells no longer expressed c-kit and therefore could not be used to study p110 coupling to the c-kit receptor.

Transfection of BMMCs with PMT resulted in a cell line that maintained mast cell characteristics and expressed the c-kit receptor to the same extent as untransfected BMMCs. However, PMT-transfection of BMMCs did not result in cytokine-independent cell growth, which indicated that PMT expression in BMMCs did not lead to full cell

transformation. An unexpected finding was that PMT expression was not associated with increased Akt phosphorylation. This was surprising given that PI3K signalling is one of the key pathways activated downstream of PMT-induced Src activation at least in fibroblasts (Meili, *et al.*, 1998; Penuel & Martin, 1999). The reason for this is unclear, it is possible that this PMT-effect is cell-type dependent. In order to gain more insight into this, it would be of interest to assess if Src is activated in BMMCs upon expression of PMT. It is also possible that PI3K is recruited to the PMT complex and activated but that this is not reflected in the phosphorylation state of Akt. Indeed, in some instances stable overexpression of a membrane-targeted PI3K does not result in constitutive activation of Akt (Auger, et al., 2000).

In PMT-expressing BMMCs, p110δ remained the principal isoform downstream of c-kit activation. However given that the cells were not fully transformed by PMT, it is likely that this is the main reason that c-kit selectivity for p110δ was retained. The aim of the study, to create a transformed mast cell line, was not met through PMT-infection and so it is not possible to ascertain whether p110δ would remain the principal isoform downstream of c-kit in transformed cells. A potentially useful finding from this line of investigation is that PMT-expressing BMMCs may be advantageous over WT BMMCS to screen p110δ inhibitors as they have an increased growth rate compared to WT BMMCs, requiring a lower concentration of IL-3, whilst remaining dependent on p110δ downstream of c-kit.

3.5.2 SCF-induced Akt phosphorylation in long-term cultured p110δ$^{D910A/D910A}$ BMMCs may be the result of p110α upregulation

It has been reported that c-kit-induced Akt phosphorylation in p110δ$^{D910A/D910A}$ BMMCs is completely abrogated (Ali, et al., 2004), highlighting the essential role of p110δ in c-kit signalling. Investigation into the possibility that 'spontaneous transformation' may occur in p110δ$^{D910A/D910A}$ BMMCs maintained in long-term culture, led to the finding that SCF could indeed induce Akt phosphorylation in p110δ$^{D910A/D910A}$ BMMCs maintained in culture for over 12 weeks. Given that p110δ in p110δ$^{D910A/D910A}$ BMMCs is kinase-dead, another p110 isoform must be acting downstream of c-kit. After 6 weeks in culture, both WT and p110δ$^{D910A/D910A}$ BMMCs displayed a similar expression profile of class IA p110 subunits, however after continued culturing of the cells a clear upregulation of p110α expression associated with a downregulation of both p110δ and p110β expression was observed in p110δ$^{D910A/D910A}$ BMMCs. This result suggests that p110α may be mediating SCF-induced c-kit signalling.

The upregulation of p110α in p110δ$^{D910A/D910A}$ BMMCs was not associated with increased cell expansion, however unlike WT BMMCs whose numbers began to drop after 9 weeks of being in culture, the numbers of p110δ$^{D910A/D910A}$ BMMCs were maintained, albeit at a much lower level compared to WT BMMCs, for up to 12 weeks. It is possible that upregulation of p110α in p110δ$^{D910A/D910A}$ BMMCs protects the cells from apoptosis or alternatively induces cells to enter senescence.

3.5.3 p110δ and p110α are constitutively bound to c-kit in WT and p110δ$^{D910A/D910A}$ BMMCs

Immunoprecipitation of cell lysates from long-term cultured WT and p110δ$^{D910A/D910A}$ BMMCs with an antibody against c-kit, revealed that both p110δ *and* p110α were constitutively bound to c-kit in WT and p110δ$^{D910A/D910A}$ BMMCs. p110β and p110γ were not found constitutively bound or recruited to the c-kit receptor upon SCF stimulation, in both WT and p110δ$^{D910A/D910A}$ BMMCs. These data indicate that in addition to p110δ, p110α could also potential signal directly downstream of c-kit in WT BMMCs. However, since inhibition of p110δ in WT BMMCs reduced SCF-induced Akt phosphorylation to that of the pan-PI3K inhibitor LY294002, it appears as though p110α does not does not play a role in c-kit signalling. This raises the question of what role p110α is playing, given that it is coupled to c-kit, if it is not involved in c-kit signalling.

The finding that in addition to p110δ, p110α was also constitutively bound to c-kit in p110δ$^{D910A/D910A}$ BMMCs and was further recruited to c-kit upon SCF-stimulation, suggests p110α is indeed the principal PI3K isoform mediating SCF-induced Akt phosphorylation in cells expressing a kinase-dead p110δ. It is possible, given that both p110δ and p110α are bound to c-kit, that a switch from p110δ to p110α isoform signalling downstream of c-kit in p110δ$^{D910A/D910A}$ BMMCs occur. It is unclear how this switch in p110 isoform signalling occurs since it does not appear to be due to a switch in p110 binding to c-kit. It would be interesting to investigate whether after maintaining p110δ$^{D910A/D910A}$ BMMCs in long-term culture, another signalling molecule is selectively recruited to the activated c-kit receptor complex. This could be investigated through immunoprecipitating SCF-stimulated c-kit receptors in short-term and long-term cultured p110δ$^{D910A/D910A}$ BMMCs, followed by mass spectrometry analysis of recruited proteins. This experiment would however require a substantial number of cells to obtain a high enough concentration of c-kit protein complexes that when separated by SDS-PAGE are visible by Coommassie colloidal staining.

To investigate whether p110α kinase activity is required in long-term cultured p110δ$^{D910A/D910A}$ BMMCs to mediate c-kit signalling, BMMCs isolated from p110δ$^{D910A/D910A}$/p110α$^{D933A/WT}$ mice could be used to assess whether c-kit signalling is compromised by reduced p110α kinase activity in these cells after long-term culture. Progress has also been made in the development of a p110α-selective inhibitor (Hayakawa, *et al.*, 2007a; Hayakawa, *et al.*, 2007b; Hayakawa, *et al.*, 2007c; Knight, et al., 2006), which could be used to assess whether in long-term cultured p110δ$^{D910A/D910A}$ BMMCs, p110α inhibition abrogates SCF-induced Akt phosphorylation.

The absence of p110γ binding to c-kit was not unexpected since p110γ is known to be activated downstream of GPCRs as opposed to tyrosine kinase receptors. Given that the p110β inhibitor reduced SCF-induced Akt phosphorylation in p110δ$^{D910A/D910A}$ BMMCs it was expected that p110β may be recruited to c-kit in these cells. p110β was neither constitutively bound nor recruited to c-kit upon SCF-stimulation, indicating that it does not play a direct role in c-kit signalling. There is a growing body of evidence that p110β is also predominantly activated downstream of GPCRs (Guillermet-Guibert, et al., 2008; Kurosu, et al., 1997), which is corroborated by the finding that the tyrosine kinase receptor, c-kit, does not bind p110β. It is possible that p110β is activated downstream of c-kit through the action of an autocrine loop by GPCR agonists. However, since p110β appeared to be downregulated in long-term cultured p110δ$^{D910A/D910A}$ BMMCs, this seems to contradict the idea that p110β, in addition to p110α, may also play a role in c-kit signalling.

Overall, the data indicate that long-term culture of p110δ$^{D910A/D910A}$ BMMCs may indeed result in a type of 'spontaneous transformation', in which cells adapt to the loss of catalytically active p110δ by a switch to p110α isoform signalling downstream of c-kit. The switch in p110-isoform signalling does not appear to be entirely regulated by differential p110 coupling to c-kit, and does not result in a highly proliferative cell population, indeed p110δ$^{D910A/D910A}$ BMMC expansion remained considerably low throughout 3 months of culturing the cells. The slow rate of cell expansion for p110δ$^{D910A/D910A}$ BMMCs made it extremely difficult to obtain large enough cell numbers for detailed biochemical studies to be carried out. The cost of maintaining cells in culture for this time period was also an issue, since BMMCs are cultured in media containing the cytokines IL-3 and SCF, which needs to be replaced frequently. Although this approach generated some potentially interesting areas for further investigation, it is not a

straightforward model to investigate p110-coupling to tyrosine kinase receptors and it was decided against pursuing this line of investigation any further.

4. OVEREXPRESSION OF p110δ IN A MAMMALIAN CELL LINE

4.1 Introduction

To investigate the isoform-specific signalling role of p110δ, we used the approach of stable overexpression in a mammalian cell line. As described in the introduction (section 1.6.2), a number of investigations into the isoform-specific roles of PI3K have been carried out through overexpression studies. However, the majority of these studies have employed transient transfection of the p110 isoforms, which can provide limited information about the full functional consequences of p110 overexpression.

Unlike p110α and p110β, p110δ has a more restricted tissue distribution and is most abundantly expressed in leukocytes. However, there are instances where cells of non-haematopoietic origin have high levels of p110δ expression, such as breast cells, melanocytes, microglia, ovarian carcinoma and primary synoviocytes (Knobbe & Reifenberger, 2003; Mizoguchi, et al., 2004; Sawyer, et al., 2003). The role that p110δ may be playing in these cells was investigated by attempting to stably overexpress p110δ in a mammalian cell line that has low endogenous levels of p110δ expression. This was done by transfection of standard mammalian expression vectors or by a retroviral expression system in which p110δ expression is under the control of a strong promoter.

At the time when I initiated these studies, our laboratory had discovered the presence of upstream untranslated exons in the p110δ gene (Verrall & Vanhaesebroeck, unpublished results). We speculated that the presence of these 5' untranslated exons could possibly be important for effective expression of p110δ.

4.2 Transfection of full length p110δ cDNA

4.2.1 Multiple p110δ transcripts exist which encode upstream untranslated exons

Rapid amplification of 5' cDNA ends (5'RACE) on both human and mouse p110δ mRNA has identified several potential transcriptional start sites (Kok, et al., in preparation; Verrall & Vanhaesebroeck, unpublished results). An in-frame stop codon, present immediately upstream of the published translational start site, rules out the possibility that the newly identified upstream exons are translated as part of the p110δ protein. To date five distinct upstream exons have been identified in the murine p110δ gene (termed exons -1, -2a, -2b, -2c and -2d) and three distinct upstream exons in the human p110δ gene (termed exons -1, -2a and -2b), shown schematically in Figure 4.1. The coding region for p110δ is around 90% homologous for the murine and human p110δ gene, however, the upstream

untranslated exons exhibit little or no homology. Exon -1 is around 60% homologous between human and mouse, exon -2a has overlapping regions of high homology (illustrated in Figure 5.2, Chapter 5), and exon -2b displays no sequence homology between the two species.
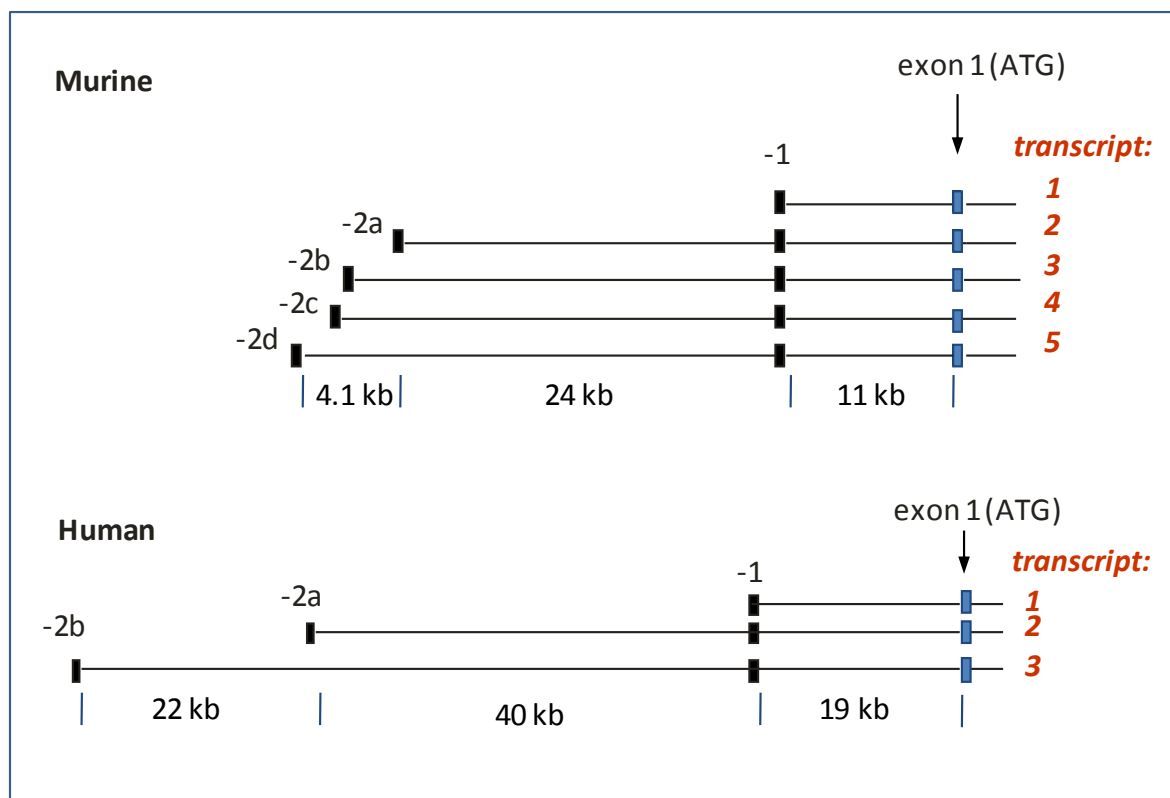
Figure 4.1: Murine and human p110δ transcripts as revealed by 5'RACE. Exon 1, which contains the ATG translational start site, is represented by the blue boxes; upstream unstranslated exons are shown as black boxes.

All the upstream exons identified have a classical splice donor (GT) and splice acceptor (AG) sequence with the exception of the -2 exons which only have a splice donor sequence, which is in line with the observation that p110δ transcripts only contain a single -2 exon spliced onto exon -1. Quantification of the amount of each p110δ mRNA transcript in murine cell lines has revealed that leukocytes express significantly higher amounts of the different p110δ transcripts compared to non-leukocytes, with the p110δ transcript containing exon -1 with exon -2a being the most abundant (Kok, et al., in preparation). A great deal of time has been invested in our laboratory to identify the role of these upstream exons and whether they are involved in the restricted leukocyte expression of p110δ. Indeed, recently exon -2a has been identified as having a condensed transcription factor binding cluster correlating with a high TSS prediction score (Kok, et al., in preparation),

which indicated this region as a putative *PIK3CD* promoter. Promoter analysis of this region is described in the following chapter.

At the start of my PhD work, the information about exon -2a as a potential p110δ promoter was not known. It was thought however that the upstream exons may provide mRNA stability or some other function that enables stable overexpression of p110δ. To investigate this, p110δ cDNAs containing the upstream exon -1 with exon -2a (referred to p110δ-2a) or exon -1 with exon -2b (referred to as p110δ-2b) were cloned into mammalian expression vectors and transfected into mammalian cell lines.

4.3 *Stable* transfection of expression vectors containing full length p110δ cDNA in NIH 3T3 cells

4.3.1 p110δ-2a mRNA makes up approximately 80% of the total p110δ mRNA found in A20 cells

To determine the absolute levels of p110δ-2a and p110δ-2b mRNA compared to the total p110δ mRNA levels in the A20 leukocyte cell line, quantitative real-time PCR (a detailed description of the method is described in section 2.8) was used. p110δ-2b only contributed to approximately 10% of the total p110δ mRNA levels, whereas p110δ-2a mRNA contributed to approximately 80% (Figure 4.2). It is likely that the other identified p110δ transcripts make up the remaining 10% of total p110 mRNA.
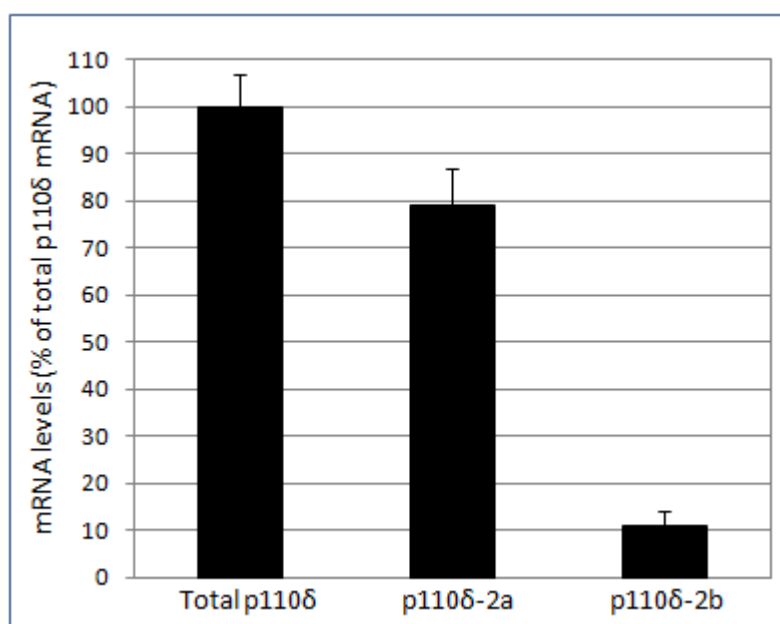
Figure 4.2: Absolute amounts of p110δ-2a and p110δ-2b mRNA in A20 cells relative to total p110δ mRNA. p110δ-2a mRNA and p110-δ-2b mRNA was compared to total p110δ mRNA levels in A20 cells assessed by quantitative real time PCR.

4.3.2 The murine fibroblast cell line, NIH 3T3, is a suitable mammalian cell line for transfection of p110δ cDNA

To investigate the biological impact of introducing p110δ into cells, a cell line that has low endogenous p110δ expression was required. It is known that p110δ is predominantly expressed in leukocytes, therefore a non-leukocyte cell line was an obvious candidate for expressing low levels of p110δ. Western blot analysis was performed on total cell lysate extracted from the murine A20 leukocyte cell line, the WEHI-231 pre-B cell line, and the murine NIH 3T3 fibroblast cell line and analysed for p110δ protein expression. The p110δ mRNA levels in these cell lines was also assessed using quantitative real time PCR. As expected, the murine fibroblast cell line NIH 3T3 expressed low levels p110δ protein and p110δ mRNA compared to the leukocyte cell lines (Figure 4.3).

In addition to expressing low levels of p110δ, NIH 3T3 cells have a reasonably high transfection capability and are easily maintained in culture. Therefore, NIH 3T3 were considered a suitable candidate cell line to examine the functional consequences of introducing and stably overexpressing p110δ.
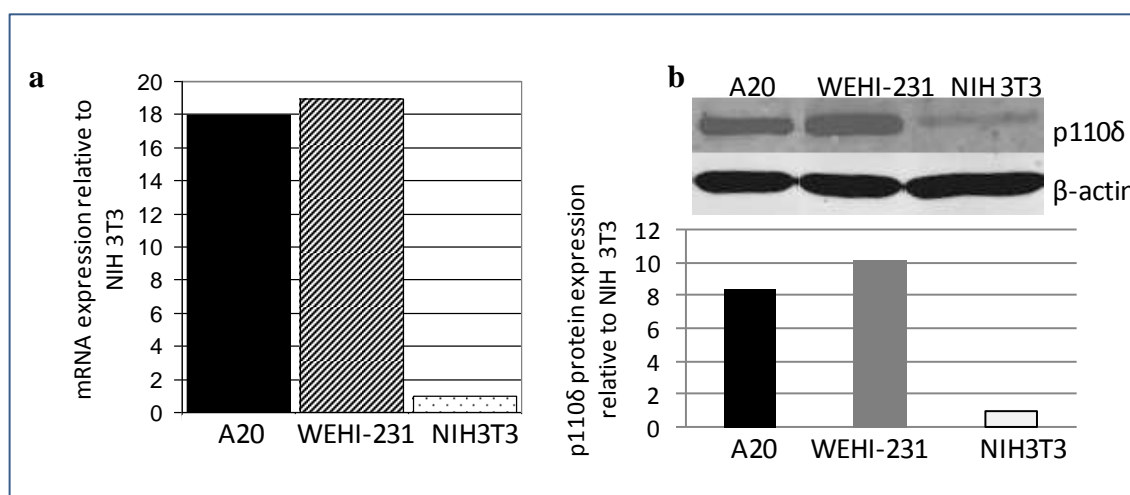
Figure 4.3: p110δ mRNA and protein expression in NIH 3T3 cell line *versus* leukocyte cell lines. Relative expression of **(a)** p110δ mRNA and **(b)** p110δ protein in NIH 3T3 cells compared to A20 and WEHI-231 cells.

4.3.3 *In vitro* translation of p110δ-2a, p110δ-2b and p85 expression vectors

To assess the functionality of PI3K-containing vectors, *in vitro* translations of the plasmids containing cDNAs for p110δ-2a, p110δ-2b, p85α and p85β (vector maps and cloning strategies can be found in section 2.12.1) were performed using SP6 and T7 TNT® Quick Coupled Translation Systems. The results indicated that p110δ could be translated from

both the p110δ-2a and p110δ-2b expression vectors, although pcDNA3.1(+) containing p110δ-2b cDNA may not be as effective as pCMV.Sport6 containing p110δ-2a cDNA (Figure 4.4). p85α was also successfully translated from pCMV.Sport6, however there appeared to be a problem with pCMV.Sport6 containing p85β as no 85 kDa band was detected from this *in vitro* translation, suggesting this expression vector is not functional.
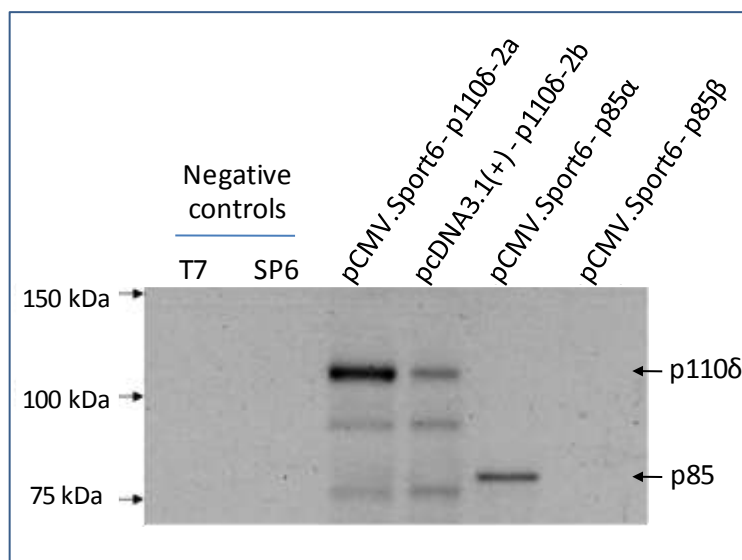
Figure 4.4: *In vitro* **translation of p110δ and p85 cDNAs from expression vectors**. *In vitro* translations were performed on the p110δ-2a, p110δ-2b, p85α and p85β plasmids to ensure the cDNAs could be translated into the expected proteins. Reaction mix where no plasmid DNA were used as negative controls.

4.3.4 No evidence for counter selection of NIH 3T3 clones expressing p110δ-2a cDNA

p110δ-2a in the vector pCMV.Sport6 was cotransfected in NIH 3T3 cells with a vector encoding neomycin resistance (NeoR) (pIRES, Figure 2.5). Control transfections included pCMV.Sport6 vector alone to ensure only cotransfection with the NeoR vector conferred neomycin-resistance and transfection of pCMV.Sport6 without the p110δ cDNA insert to assess whether transfection of p110δ altered the number of neomycin-resistant colonies obtained. After 14 days in growth media containing neomycin, neomycin-resistant cell colonies were stained using methylene blue. Approximately the same number of colonies were obtained for p110δ and control transfected NIH 3T3 cells (Figure 4.5), suggesting there was no counter-selection upon transfection of p110δ expression constructs.
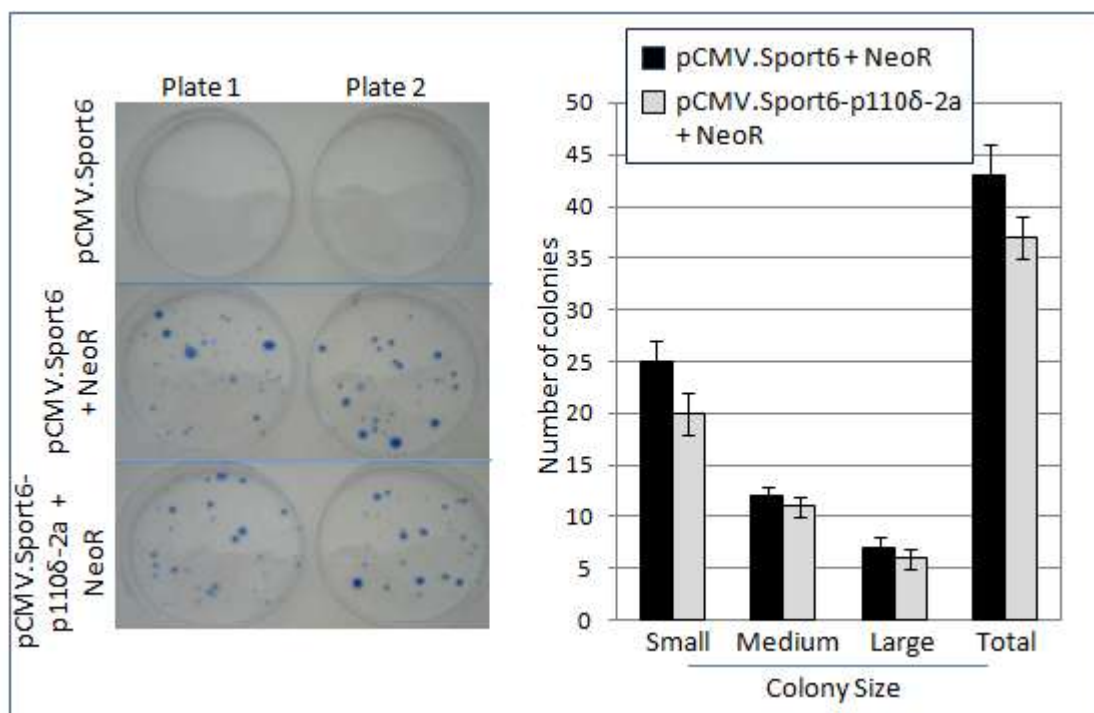
Figure 4.5: Colony formation of NIH 3T3 cells transfected with p110δ-2a. (a) NIH 3T3 cell colonies transfected with pCMV.Sport6, pCMV.Sport6 + NeoR or p110δ-2a in pCMV.Sport6 + NeoR, visualized by staining with methylene blue. Colony staining was carried out in duplicate. **(b)** Graphical representation of the number of colonies formed.

4.3.5 Increased p110δ-2a mRNA in p110δ-2a-transfected NIH 3T3 clones does not correlate with increased p110δ protein expression

Seven individual neomycin-resistant colonies transfected with p110δ-2a were expanded and the remaining colonies pooled. Total RNA was then extracted and reverse transcribed to cDNA, followed by determination of the level of p110δ cDNA by quantitative real time PCR. Primers specific for exon -2a or the p110δ coding region were used to amplify p110δ-2a cDNA or total p110δ cDNA, respectively. p110δ-2a-transfected clones expressed varying levels of p110δ mRNA compared to untransfected and vector control-transfected NIH 3T3 cells (Figure 4.6). This difference is likely to be dependent on the location in the genome in which the p110δ gene is incorporated since some loci are transcriptionally more active than others. Also, as cell resistance to neomycin was achieved through cotransfection of p110δ-2a with pIRES, it is possible that some colonies may have only integrated the gene conferring neomycin-resistance without p110δ-2a.

Clones 1, 2 and 7 displayed the largest increase in p110δ-2a mRNA, with clone 1 expressing approximately 10-fold more p110δ-2a mRNA compared to the control transfected cells (Figure 4.6a), which correlated with a 10-fold increase in *total* p110δ mRNA (Figure 4.6b). Although the level of p110δ-2a and total p110δ mRNA in this clone

was increased, it did not reach the level of that found in the A20 leukocyte cell line. The pCMV.Sport6-control transfected cells expressed the same amount of p110δ mRNA as untransfected NIH 3T3 cells, indicating that the transfection process itself did not have any effect on p110δ mRNA levels.
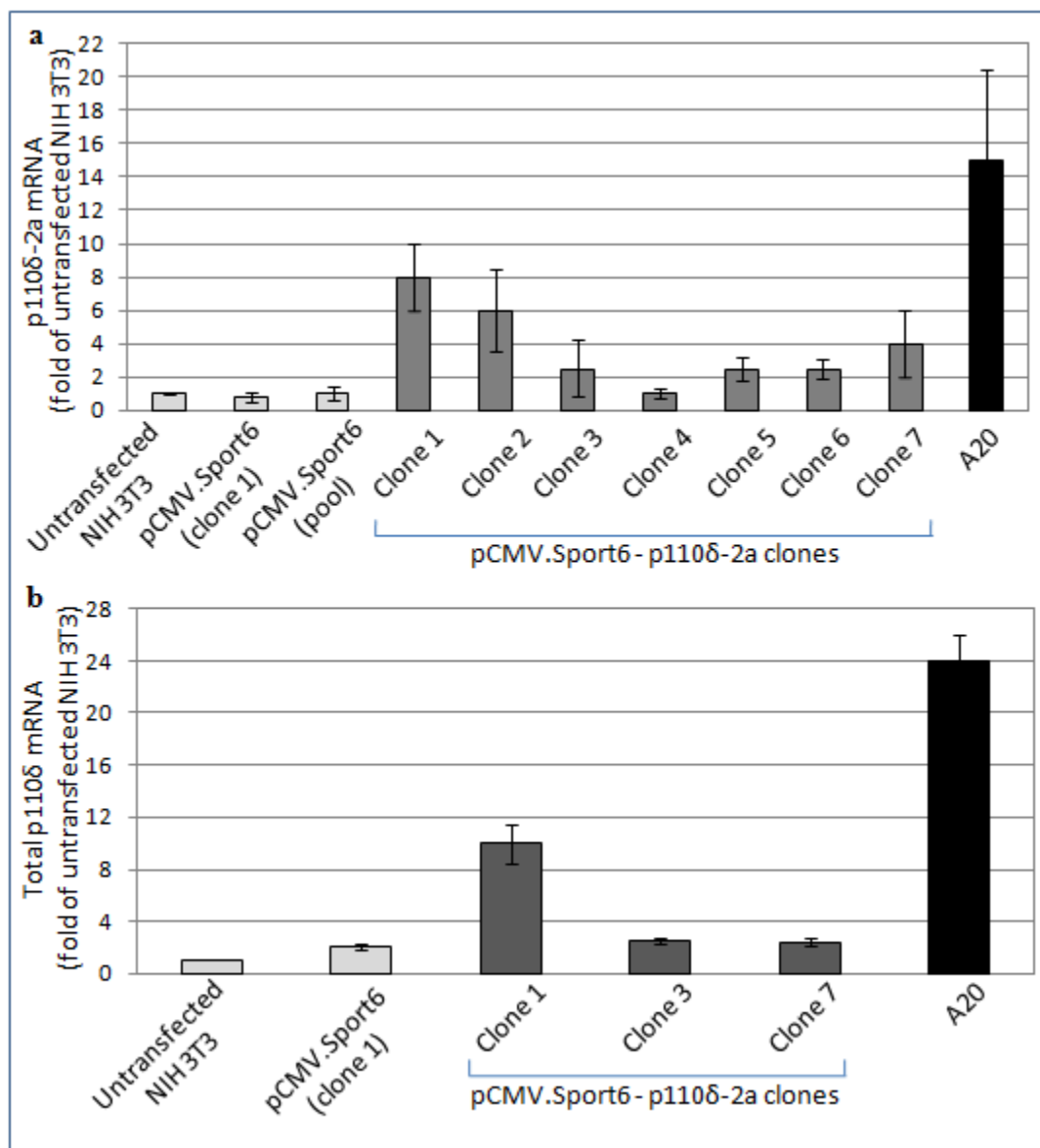
Figure 4.6: Level of p110δ-2a mRNA and total p110δ mRNA in NIH 3T3 clones transfected with p110δ-2a. (a) Relative amounts of p110δ-2a mRNA in transfected clones compared to untransfected NIH 3T3 cells. For pCMV.Sport6 vector control transfected cells, either a single colony that was expanded (clone 1) or colonies were pooled (pool). A20 mRNA was used as a positive control. **(b)** Relative amounts of total p110δ mRNA.

Next, total cell lysates were analysed for p110δ protein levels by western blot. There appeared to be no significant increase in p110δ expression in any of the transfectants (Figure 4.7). Thus, despite clones 1, 2 and 7 expressing increased levels of p110δ-2a mRNA, this did not lead to a concomitant increase in p110δ protein levels.
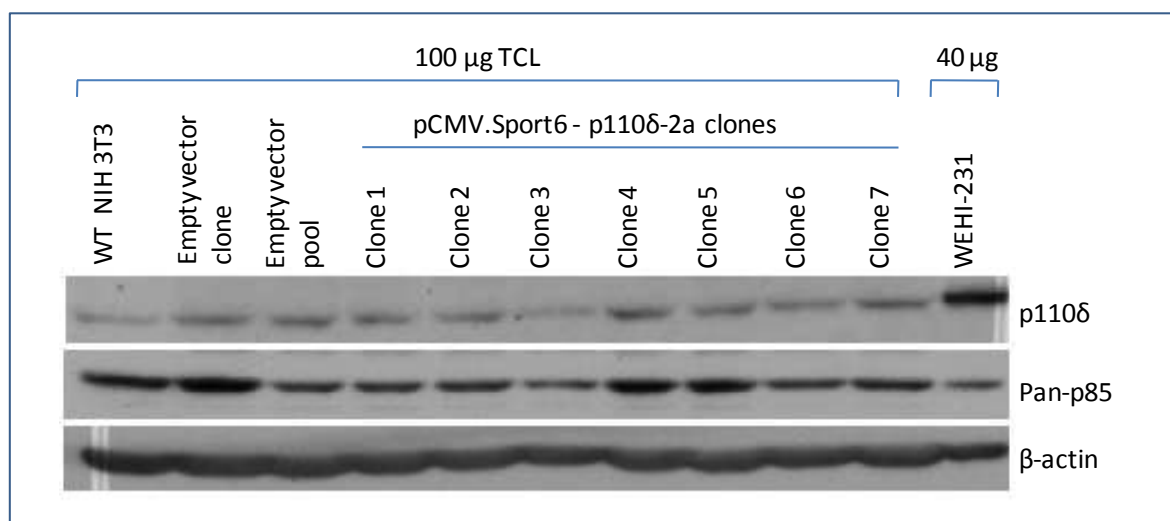
Figure 4.7: p110δ protein levels in NIH 3T3 p110δ-2a clones. Total cell lysate from the indicated cell lines were separated by SDS-PAGE and immunoblotted for p110δ and pan-p85. 100 μg of total cell lysate was loaded for the NIH 3T3 cells and p110δ-2a transfectants whereas 40 μg of WEHI-231 total cell lysate, used as a positive control, was loaded.

4.3.6 Proteasomal inhibition leads to p110δ protein expression in NIH 3T3 cells transfected with p110δ-2a cDNA

The data above indicate that stable overexpression of p110δ-2a mRNA is possible although this does not result in increased p110δ protein expression. This could be due to the failure of protein being translated from mRNA or the translated protein being subsequently degraded. Protein substrates can be marked for destruction by the covalent addition of a poly-ubiquitin tail, which is recognized by a proteasome complex that digests the protein. Cells from p110δ-2a clone 1 (the clone expressing the highest level of p110δ-2a mRNA) were treated with a tripeptide aldehyde proteasome inhibitor, N-Ac-Leu-Leu-norLeucinal (LLnL) for 24 and 48 h. Treatment of p110δ-2a clone 1 with LLnL for 24 h or 48 h resulted in a 2-fold and 3-fold increase in p110δ protein expression relative to the DMSO control, respectively. (Figure 4.8) The expression of cyclin D2, which was used as a positive control for proteasome inhibition, was increased in the control-transfected cells after 24 h or 48 h LLnL treatment, indicating successful proteasome inhibition. Cyclin D2 levels also increased after 24h LLnL treatment in p110δ-2a clone 1, however cyclin D2 expression surprisingly decreased upon 48 h of LLnL treatment. These data suggest that induced p110δ expression may have an effect on cyclin D2 expression. Treatment of control-transfected cells with LLnL for either 24 h or 48 h had no effect on p110δ protein expression, indicating that only exogenously expressed p110δ can be induced upon proteasome inhibition (Figure 4.8).

In general, these results indicate that the increase in p110δ mRNA expression in p110δ-2a clone 1 can indeed lead to an increase p110δ protein expression upon proteasome inhibition. This suggests that one reason for the failure of p110δ protein expression under normal cell culture conditions in cells expressing high p110δ mRNA, is due to p110δ protein instability and subsequent degradation.
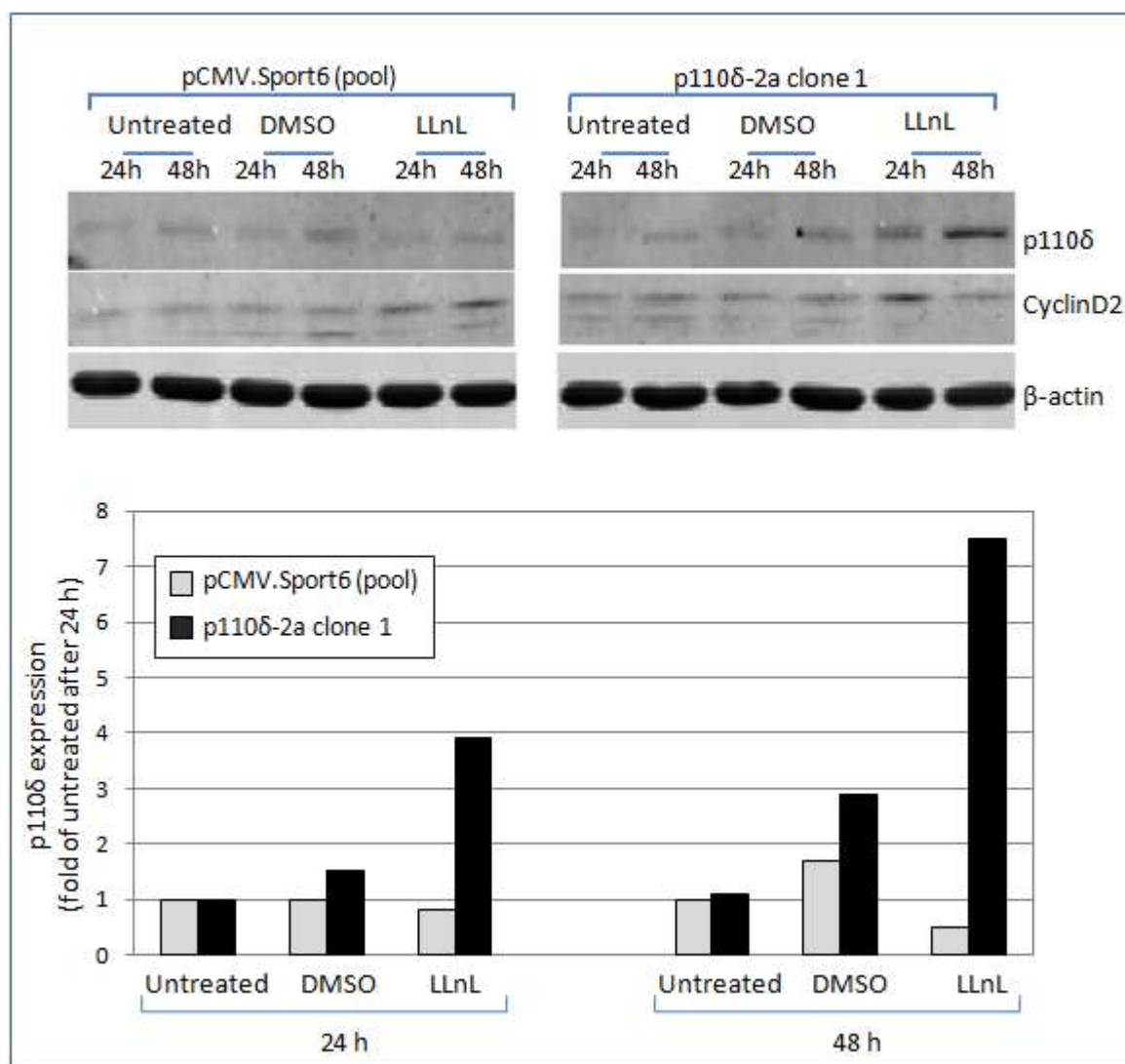
Figure 4.8: **Analysis of p110δ protein expression in p110δ-2a clone 1 upon proteasome inhibition.** Cells were treated with 50 μM LLnL or vehicle control (DMSO) for 24 h or 48 h, followed by separation of cell lysates by SDS PAGE and immunoblotting for p110δ and cyclin D2.

To find out how the 3-fold increase in p110δ protein levels after 48 h LLnL treatment compared to p110δ protein levels in a leukocyte cell line, the experiment was repeated with total cell lysate from the A20 leukocyte cell line separated by SDS PAGE alongside the other samples. After 24 h of LLnL treatment, a clear induction of p110δ expression was observed in p110δ-2a clone 1, which corresponded to approximately half of that expressed in A20 cells (Figure 4.9). It should be noted however, that since the loading control (β-

actin) was seen to decrease in p110δ-2a clone 1 after 24 h of LLnL treatment, p110δ expression has not been normalised to β-actin. Such normalisation would give an exceptionally high and misleading value for p110δ expression in p110δ-2a clone 1, which is likely to be a false readout since LLnL treatment did not reduce β-actin expression in untransfected and control transfected cells. This infers that the low β-actin expression in p110δ-2a clone 1 is likely to be an immunoblotting technical problem.
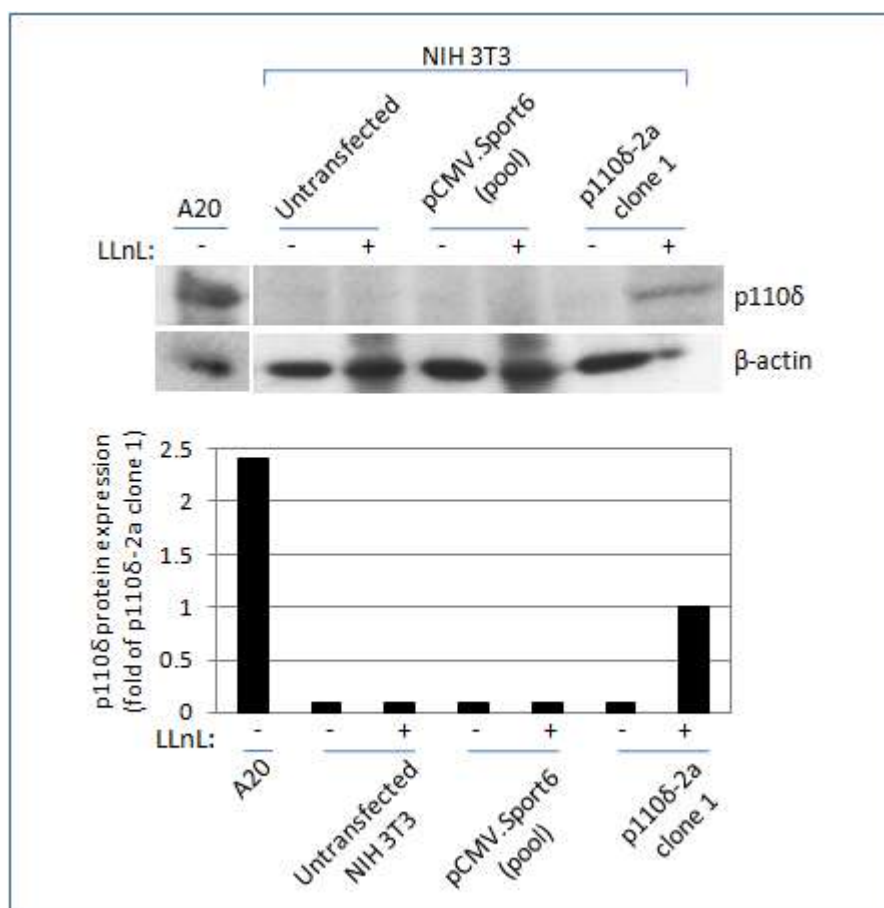
Figure 4.9: Analysis of p110δ protein expression in p110δ-2a clone 1 upon proteasome inhibition in comparison with p110δ expression in a leukocyte cell line. Cells were treated with 50 μM LLnL or vehicle control (DMSO) for 24 h, followed by separation of cell lysates by SDS PAGE and immunoblotting for p110δ. A20 total cell lysate from untreated cells was run on the same gel to compare p110δ expression.

4.3.7 Increased p110δ-2b mRNA in transfected clones does not correlate with increased p110δ protein expression

Exon -2b of p110δ mRNA has been found in all leukocyte cell lines screened so far and is absent or present in extremely low amounts in non-leukocyte cell lines (Kok, et al., in preparation). Although p110δ-2b mRNA was found to make up approximately only 10% of the total p110δ mRNA in the leukocyte cell line A20 (Figure 4.2), it is feasible that these low levels play a critical role in p110δ protein expression. p110δ-2b cDNA in

pcDNA3.1(+) under the control of a CMV promoter was transfected in NIH 3T3 cells (see section 2.12.1 for vector maps). pcDNA3.1(+) encodes a gene conferring neomycin-resistance, enabling transfected cells to be selected in neomycin, thus circumventing the need to cotransfect the cells with a separate vector conferring resistance neomycin (as was the case for transfection p110δ-2a cDNA). Neomycin-resistant transfectants were expanded and quantitative real time PCR was performed to assess p110δ-2b mRNA levels (Figure 4.10).
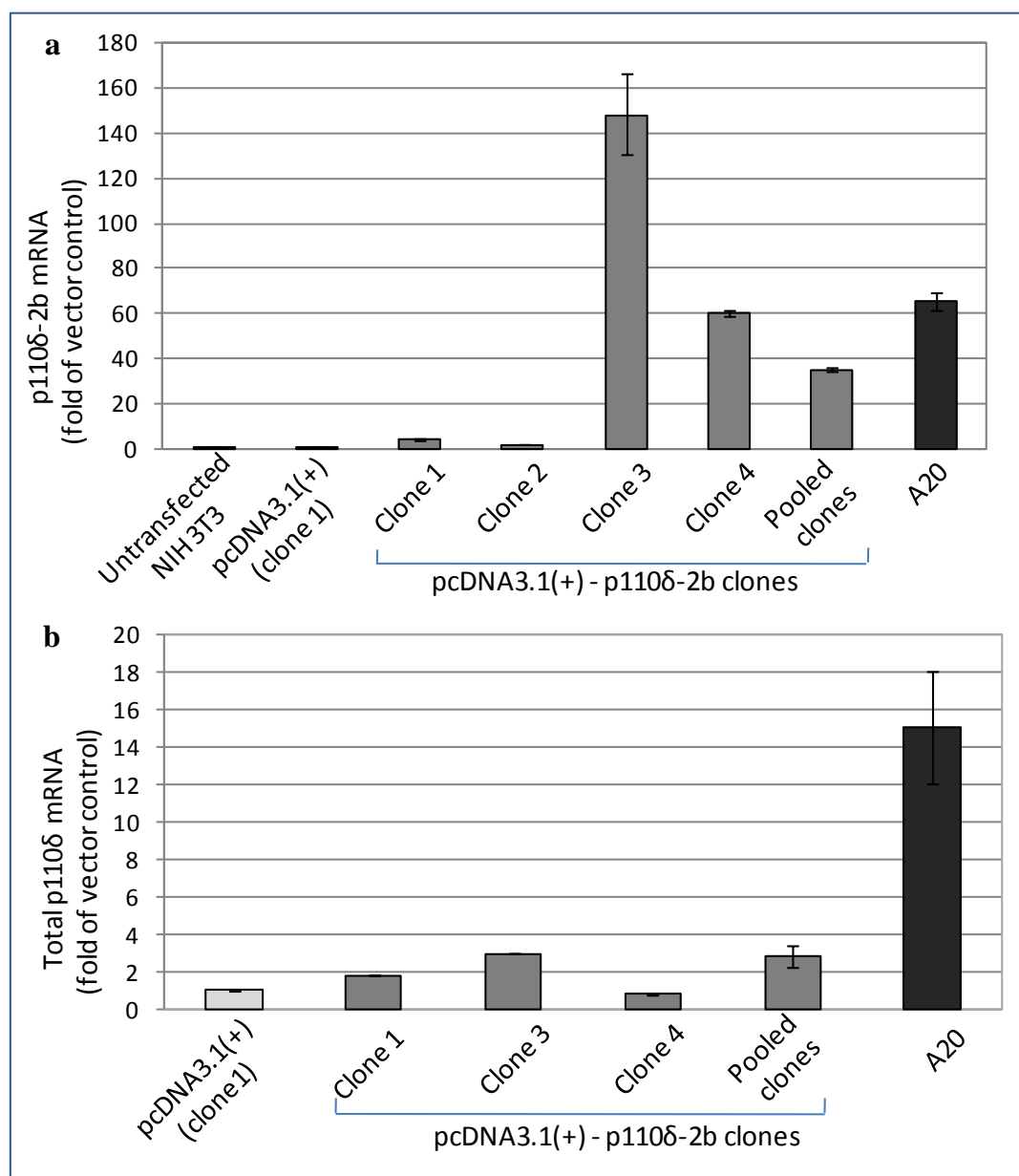
Figure 4.10: Levels of p110δ-2b mRNA and total p110δ mRNA in NIH 3T3 p110δ-2b clones. (a) Amounts of p110δ-2b mRNA in transfected clones relative to vector control transfected cells and compared to A20 cells. **(b)** Relative amounts of total p110δ mRNA p110δ-2b mRNA in transfected clones compared to vector control transfected cells and A20 cells.

Similarly, as was seen for the transfection with p110δ-2a cDNA, clones expressing varying levels of p110δ-2b mRNA were obtained (Figure 4.10a). Clone 3 expressed the highest levels of p110δ-2b mRNA, with a greater than 100-fold increase compared to the control transfected cells, correlating to approximately 2-fold more than the A20 leukocyte cell line (Figure 4.10a). However, and relevantly, this 100-fold increase in p110δ-2b mRNA in clone 3 was not reflected in a concomitant increase in the levels of *total* p110δ mRNA. Clone 3 had only a 3-fold increase in total p110δ mRNA compared to vector control transfected NIH 3T3 cells representing approximately 25% of that found in A20 cells (Figure 4.10b).

Taking into consideration that the total level of p110δ mRNA in NIH 3T3 cells represents only 5% of that in A20 cells (Figure 4.3a) and that in this pool of p110δ mRNA, p110δ-2b mRNA is likely to make up around 10%, (Figure 4.2) it is not surprising that although NIH 3T3 p110δ-2b clone 3 expresses 100-fold more p110δ-2b mRNA than vector control cells and 2-fold more than p110δ-2b mRNA in A20 cells, this only corresponds to around 20% of the *total* p110δ mRNA in A20 cells. This information is represented graphically and hopefully simplified in Figure 4.11.
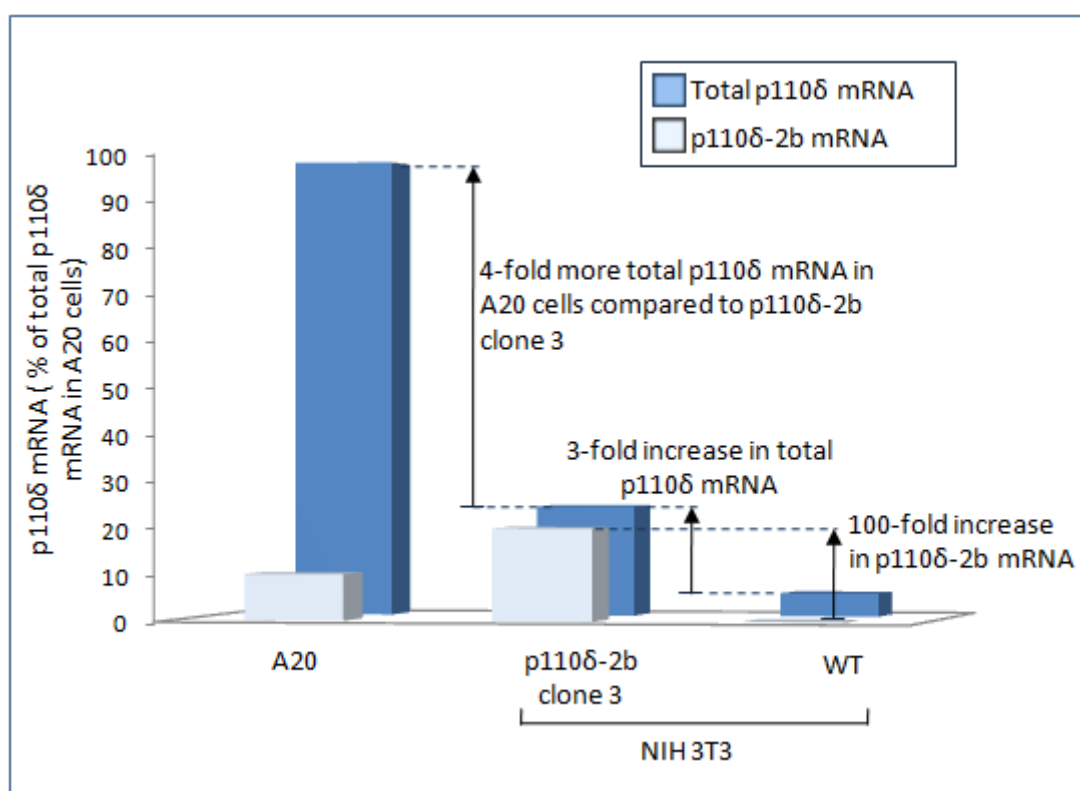
Figure 4.11: Diagram to illustrate the amount of p110δ-2b mRNA contributing to the total amount of p110δ mRNA in A20, NIH 3T3 cells transfected with p110δ-2b and WT NIH 3T3 cells.

To asses if the increase in p110δ mRNA in the p110δ-2b-transfected clones gave rise to an increase in p110δ protein, total cell lysates from clone 3, pooled p110δ-2b clones and control-transfected NIH 3T3 clones were immunoblotted for p110δ.   Neither clone 3 nor the pooled p110δ-2b clones expressed an increase in p110δ protein compared to the control transfectants (Figure 4.12). It is possible that the 3-fold increase in total p110δ mRNA in clone 3 is not sufficient to induce protein expression.
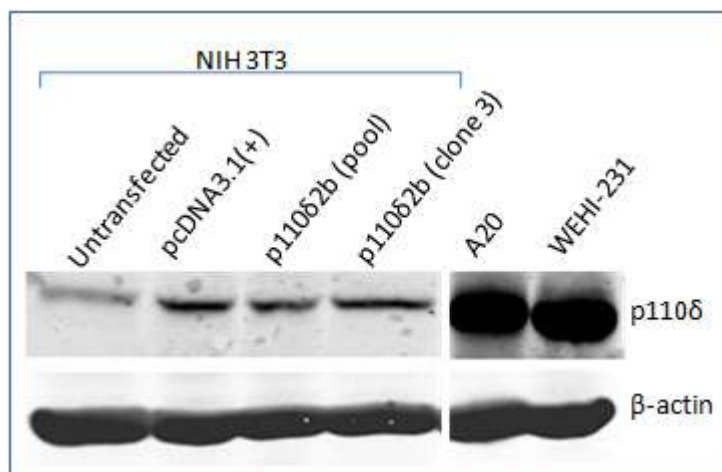
Figure 4.12: p110δ protein levels in NIH 3T3 p110δ-2b clones. Total cell lysate from untransfected, pcDNA3.1(+) control-transfected and p110δ-2b-transfected NIH 3T3 cells were separated by SDS-PAGE and immunoblotted for p110δ. A20 and WEHI-231 total cell lysate were ran on the same gel to use as a positive control for p110δ expression.

4.3.8 Stable coexpression of p85α and p110δ-2a cDNAs does not induce p110δ protein expression

Since p110 subunits of PI3K are more stable when in complex with the regulatory subunit (Yu *et al.*, 1998a), it was thought that cotransfection of a regulatory subunit with p110δ may promote stable p110δ overexpression. As there are three separate genes encoding regulatory subunits capable of binding p110δ, we first investigated if an increase in a specific PI3K regulatory subunit mRNA correlated with the high p110δ mRNA expression in leukocytes. This would give an indication of which p85 may be the most likely candidate to stabilise p110δ. Quantitative real time PCR was carried out on NIH 3T3, WEHI-231 and A20 cell lines to determine the mRNA levels of the different PI3K regulatory subunits compared to the p110 subunits (Figure 4.13).

These experiments revealed that there is approximately 1.6-fold more p85α mRNA expressed in WEHI-231 and A20 cells compared to NIH 3T3. Given that A20 and WEHI-231 cells expressed approximately 20-fold more p110δ mRNA than NIH 3T3 cells, this indicates p85α is unlikely be the stabilising regulatory subunit for p110δ. Assuming that

the level of mRNA directly correlates with protein expression, it seems unlikely that a 1.6-fold increase in p85α mRNA expression would be sufficient to stabilise a 20-fold increase in p110δ mRNA. p85β mRNA was the most highly expressed of all class IA regulatory subunits in all of the three cell lines. If p110δ was preferentially stabilised by p85β then one might expect that WEHI-231 and A20 cells to express more p85β mRNA than NIH 3T3 cells, however this was not the case. In fact, NIH 3T3 cells expressed approximately the same level of p85β mRNA as WEHI-231 cells. All three cell lines examined express very little p55γ, although NIH 3T3 cells expressed approximately 10 times more than WEHI-231 and A20 cells.
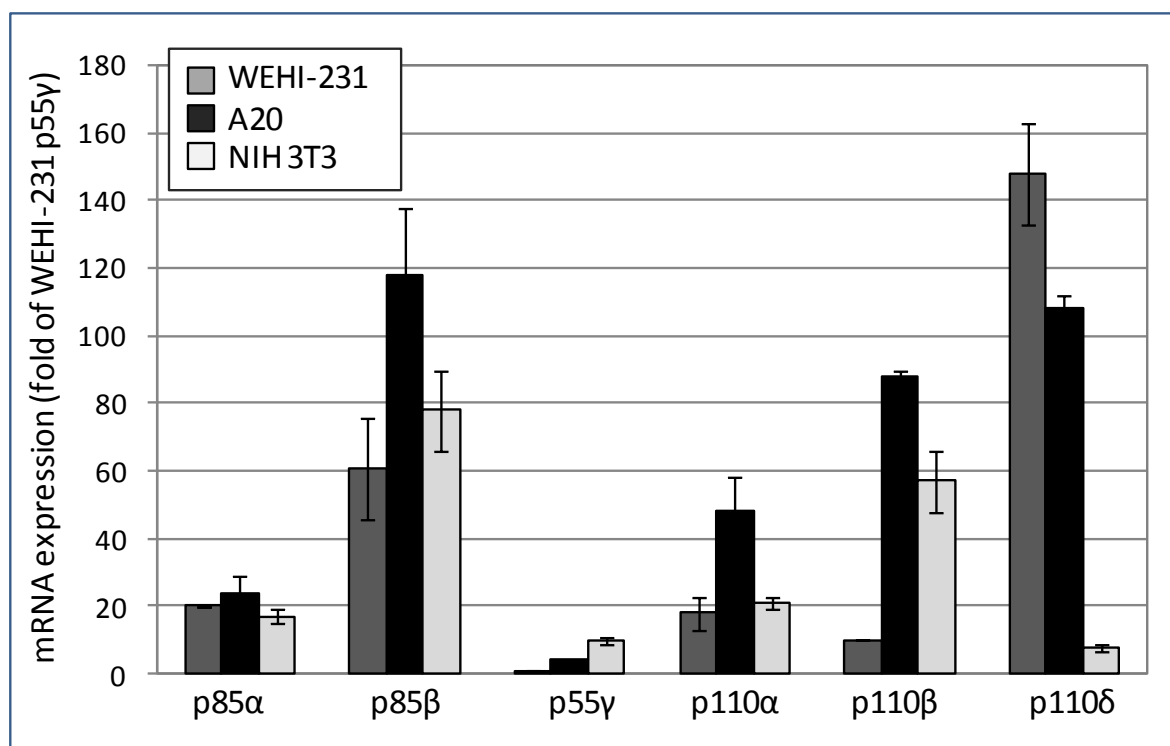
Figure 4.13: Quantitative real time PCR using primers specific for class IA PI3Ks on cDNA isolated from WEHI-231, A20 and NIH3T3 cells. Absolute quantification of class IA PI3K isoforms was achieved by comparing endogenous mRNA levels with known amounts of plasmid DNA containing cDNA for each class IA subunit. The values were standardized using GAPDH and expressed relative to the mRNA amount of the least expressed class IA PI3K subunit, which was p55γ in WEHI-231 cells.

This quantitative real time PCR data has been in used in combination with absolute protein quantification of p110 and p85 subunits from NIH 3T3 and WEHI-231 cells using mass spectrometry. A reasonably good correlation between mRNA and protein levels was found for each class IA PI3K isoform indicating that p110 and 85 protein expression is at least partly regulated at the transcriptional level (Geering, et al., 2007b).

Overall, these data did not give a clear indication of which specific p85 would be favoured to transfect p110δ-2a clone 1 in an attempt to stabilise and induce p110δ expression. Given that an *in vitro* translation of the vectors encoding p85α and p85β revealed that only the vector encoding p85α was functional (Figure 4.4) and taking into consideration the real time PCR results, it was decided to use p85α for cotransfection with p110δ.

Transfection of NIH 3T3 p110δ-2a clone 1 with expression vector for p85α

NIH 3T3 p110δ-2a clone 1, which expressed the highest amount of p110δ mRNA of all the NIH 3T3 clones transfected with p110δ expression plasmids (Figure 4.6), was selected for transfection with p85α. cDNA for murine p85α in pCMV.Sport6 vector was cotransfected with a vector conferring hygromycin-resistance (pBabe-Hygro) in p110δ-2a clone 1 cells. Individual hygromycin-resistant clones were selected and expanded. Total RNA was extracted from and reversed transcribed to cDNA for use in quantitative real time PCR using primers specific for p85α. Real time PCR showed that clones 4 and 5 transfected with p85α had the greatest increase in p85 mRNA expression (Figure 4.14). Total p85 and p110δ protein expression was therefore assessed in these clones (Figure 4.15).
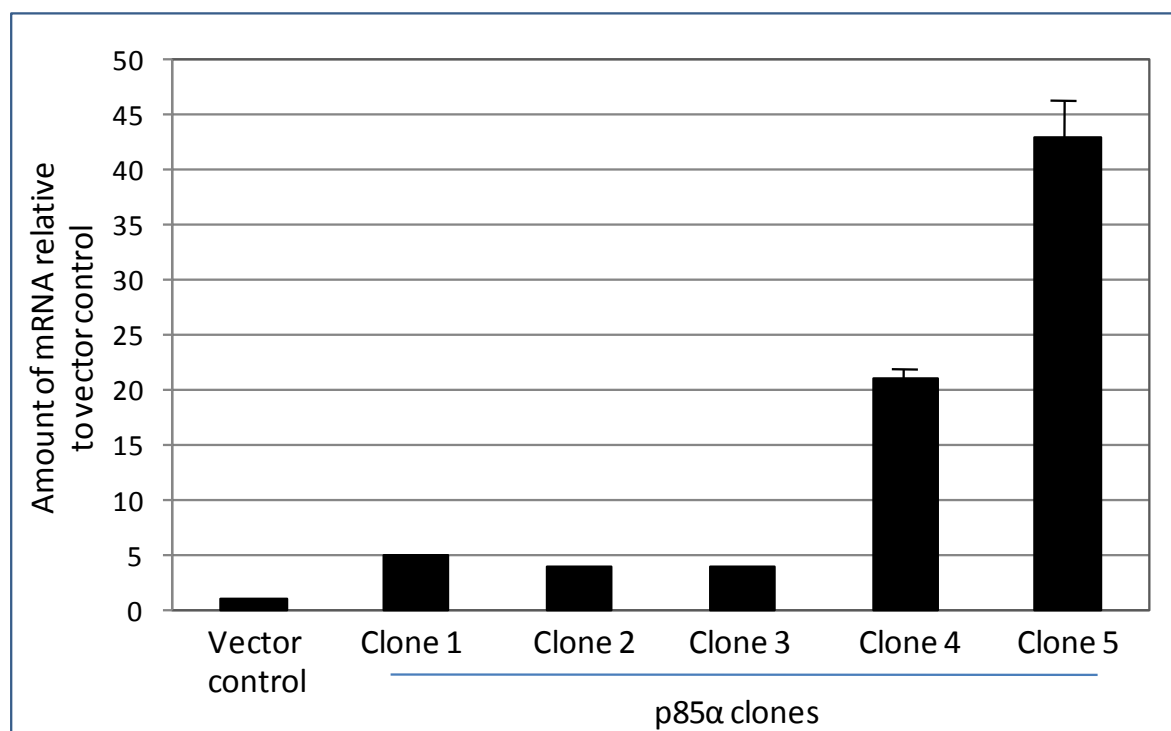
Figure 4.14: p85α mRNA expression in NIH 3T3 p110δ-2a clone 1 transfected with an expression vector for p85α. Quantitative real time PCR was carried out using primers specific for p85α from clones expanded from NIH 3T3 p110δ-2a clone 1 stably expressing p85α.

Although clones 4 and 5 showed increase p85α mRNA expression, western blot analysis revealed no change in p110δ or total p85 protein levels (Figure 4.15). Since stable overexpression of p85α protein was not achieved, it is not surprising that clones 4 and 5 have unaltered p110δ protein expression.
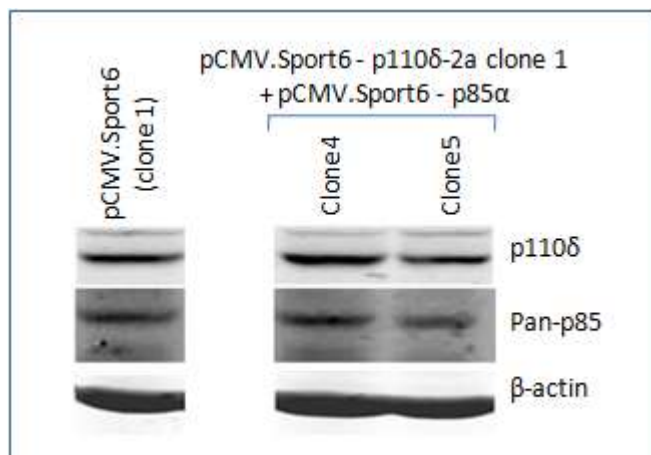
Figure 4.15: p110δ and p85 protein expression in NIH 3T3 p110δ-2a clone 1 transfected with an expression vector for p85α. Total cell lysate from clones expanded from pCMV.Sport6-transfected and p85α-transfected NIH 3T3 p110δ-2a clone 1 were separated by SDS-PAGE and immunoblotted for p110δ and pan-p85.

4.4 *Transient* transfection of expression vectors containing full length p110δ cDNA in NIH 3T3 cells

4.4.1 Introduction

Results presented in the previous section have demonstrated that it not possible to generate a NIH 3T3 stable cell line expressing significantly increased levels of p110δ protein through transfection of full length p110δ cDNA containing either upstream exon -2a or exon -2b in pCMV.Sport6 or pcDNA3.1(+). This work did however reveal that a stable increase in p110δ mRNA could be achieved and that a moderate increase in p110δ protein expression could be accomplished in p110δ-2a transfectants by treating the cells with a proteasome inhibitor. This raised the possibility that p110δ exogenously expressed in NIH 3T3 is targeted for proteasomal degradation.

Although the generation a stable NIH 3T3 cell line expressing high levels of p110δ was the ultimate objective of this part of our work, transient transfection of p110δ-2a or p110δ-2b cDNA was also considered worthwhile. In a transient transfection, the DNA introduced into the cell is not integrated into the chromosomal DNA (as in stable transfections) but is present at higher copies in the nucleus, typically generating higher protein expression than in a stable transfection. This approach may permit a substantial increase in p110δ

expression, albeit transiently, thereby avoiding complete degradation by the proteasome. In this way, we can ascertain whether full length p110δ constructs can at least give rise to a temporary increase p110δ expression.

HEK293T cells are commonly used for transient transfections as they are highly transfectable and stably express polyoma large T antigen, which leads to amplification of genes in plasmids containing an SV40 origin of replication (Pear, *et al.*, 1993). For these reasons, these cells were used in transfection experiments as a control for transfection efficiency and protein expression.

4.4.2 Transient transfection of p110δ-2a cDNA and p110δ-2b cDNA results in increased p110δ mRNA expression in both NIH 3T3 and HEK293T cells

cDNAs for p110δ-2a or p110δ-2b were transfected into NIH 3T3 or HEK293T cells with or without a plasmid encoding p85α. The mRNA levels of p110δ and p85α were first determined in the transfectants. Total RNA was extracted and reverse transcribed to cDNA, followed by determination of p110δ cDNA levels by quantitative real time PCR. Primers specific for exon -2a, exon -2b or primers that bound in the coding region of p110δ were used to amplify p110δ-2a cDNA, p110δ-2b cDNA or total p110δ cDNA, respectively. The level of p85α mRNA was also determined using primers specific for p85α cDNA.

In comparison to untransfected cells, NIH 3T3 and HEK393T cells transiently transfected with p110δ constructs and/or a p85α expression plasmid expressed a substantial increase in p110δ and/or p85α mRNA, respectively (Figure 4.16). In both cell types, transfection of p110δ constructs resulted in a level of p110δ mRNA significantly higher than the endogenous level of p110δ mRNA found in the leukocyte cell line, A20. In NIH 3T3 cells, transfection of p110δ-2a cDNA gave rise to around 20,000-fold more p110δ-2a and total p110δ mRNA compared to the endogenous levels of p110δ mRNA in A20 cells (Figure 4.16a).

Surprisingly, cotransfection of p85α with p110δ-2a cDNA in NIH 3T3 cells resulted in reduced p110δ-2a mRNA expression compared to transfection of p110δ-2a alone. Nonetheless, p110δ-2a mRNA expression in NIH 3T3 cells coexpressing p110δ-2a and p85α expression plasmids was still 3000-fold more than endogenous p110δ-2a mRNA in A20 cells. Moreover, total p110δ mRNA expression in NIH 3T3 cells coexpressing p110δ-2a and p85α was 400-fold more than endogenous total p110δ mRNA in A20 cells. In comparison to stable expression of p110δ-2a in NIH 3T3 cells (described in section 4.3.5),

which resulted in a 10-fold increase in p110δ mRNA compared to untransfected cells, corresponding to around half of that found in A20 cells, a 400-fold increase in total p110δ mRNA is a vast amplification in p110δ mRNA expression.
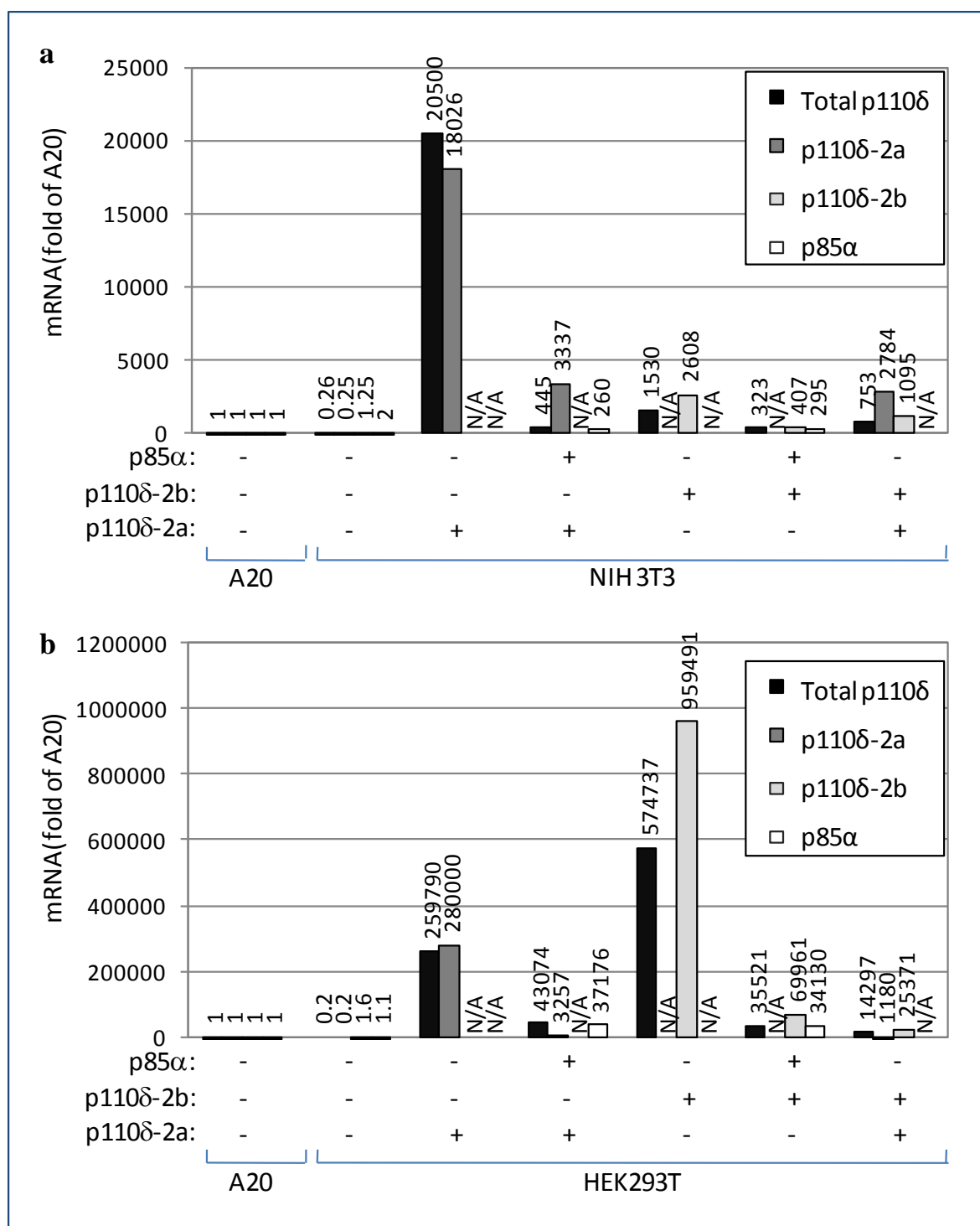
Figure 4.16: Levels of p110δ and p85α mRNA in NIH 3T3 and HEK293T transient transfectants. Relative amounts of total p110δ, p110δ-2a, p110δ-2b and p85α mRNA in transiently transfected **a)** NIH 3T3 cells and **b)** HEK293T cells relative to untransfected A20 cells. Cells were transfected with a total of 10 μg of the indicated cDNAs. Fold-increase values of mRNA with respect to A20 cells are given. N/A indicates the mRNA levels were not measured.

Transfection of p110δ-2b cDNA in NIH 3T3 cells gave rise to 1500-fold more total p110δ mRNA and 2500-fold more p110δ-2b mRNA compared to the endogenous levels of p110δ mRNA in A20 cells. Similar to cotransfection of p85α with p110δ-2a cDNA, cotransfection of p85α with p110δ-2b cDNA resulted in a decrease in total p110δ and p110δ-2b mRNA expression compared to transfection of p110δ-2b alone. Despite this decrease, total p110δ and p110δ-2b mRNA levels in NIH 3T3 cells cotransfected with p85α and p110δ-2b cDNA were around 400-fold more than the endogenous levels of p110δ mRNA in A20 cells.

Cotransfection of p110δ-2a cDNA with p110δ-2b cDNA in NIH 3T3 cells resulted in a decrease in p110δ-2a and p110δ-2b mRNA expression compared to transfection of each p110δ cDNA alone, although this still corresponded to 2700-fold (for p110δ-2a) and 1000-fold (for p110δ-2b) more than the endogenous levels of p110δ mRNA in A20 cells (Figure 4.16a).

Compared to transfections in NIH 3T3 cells, transfection of either p110δ-2a or p110δ-2b cDNAs in HEK293T cells, gave rise to an even higher increase in p110δ mRNA expression relative to the endogenous levels of p110δ mRNA in A20 cells (Figure 4.2.16b). Transfection of p110δ-2a cDNA in HEK293T cells resulted in around 280,000-fold more p110δ-2a mRNA and 260,000-fold more total p110δ mRNA compared to untransfected A20 cells. Transfection of p110δ-2b resulted in 600,000-fold more total p110δ mRNA and 960,000-fold more p110δ-2b mRNA relative to the endogenous p110δ levels in A20 cells. Since the vector backbone of p110δ-2b is pcDNA3.1(+), which contains an SV40 origin of replication, whereas the vector backbone of p110δ-2a (pCMV.Sport.6) does not contain an SV40 origin of replication, it was expected that HEK293T cells would amplify p110δ-2b mRNA expression to a greater extent than p110δ-2a mRNA.

In agreement with the data on cotransfecting p85α with p110δ cDNA in NIH 3T3 cells, cotransfection of p85α with p110δ-2a or p110δ-2b in HEK293T cells reduced total p110δ and p110δ-2a or p110δ-2b mRNA expression compared to transfection of the p110δ constructs alone (Figure 4.16b). These data highlight that transient transfection of cDNAs results in substantially more mRNA expression compared to stable transfections and that HEK293T cells are capable of producing excessive levels of exogenous mRNA compared to NIH 3T3 cells.

4.4.3 Transient transfection of p110δ-2a cDNA but not p110δ-2b cDNA results in increased p110δ protein expression in both NIH 3T3 and HEK293T cells

To assess whether the increased p110δ and p85α mRNA expression gave rise to increased p110δ and p85 protein levels, total cell lysates were extracted from transfectants and protein levels assessed by western blot (Figure 4.17).
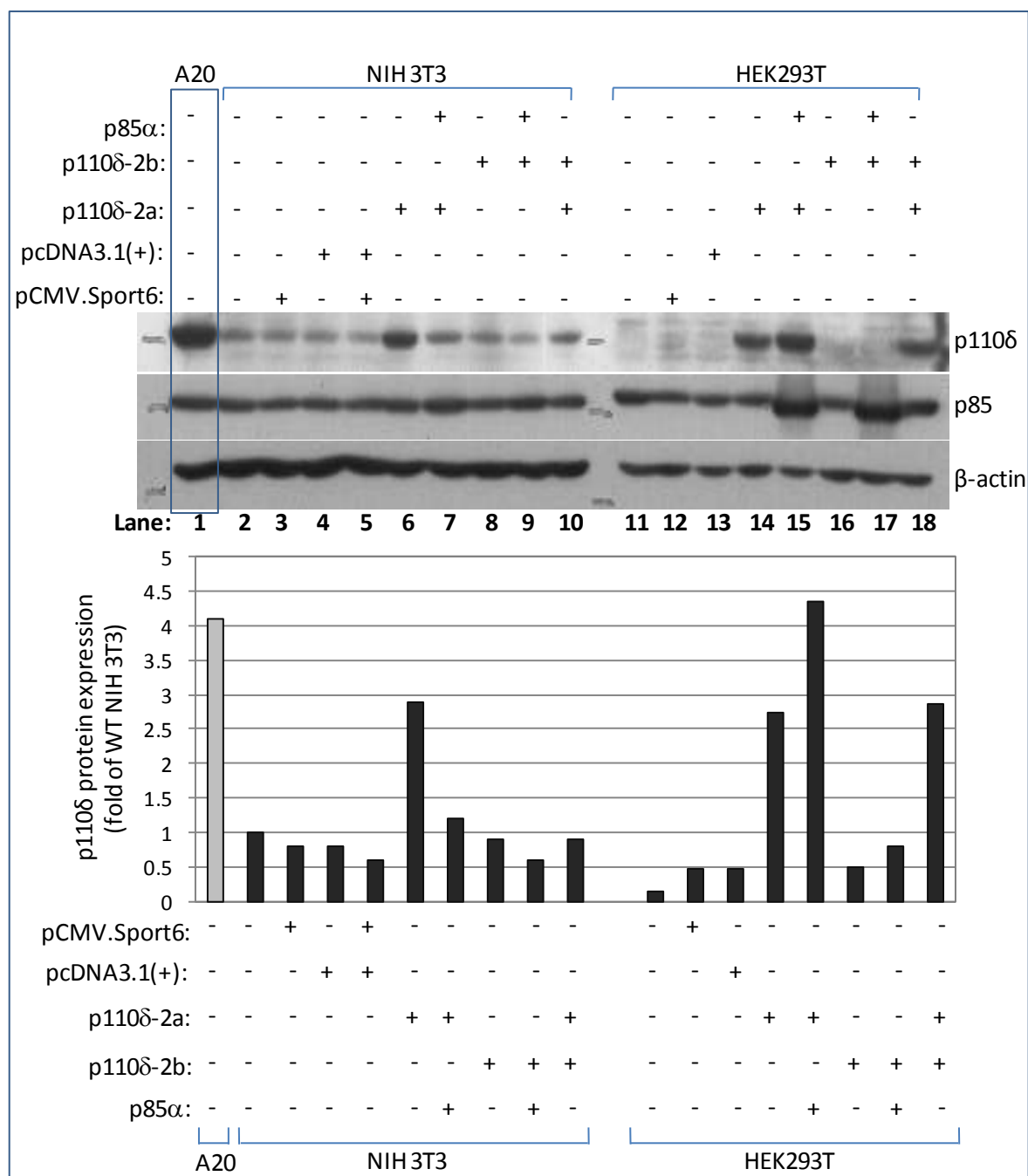
Figure 4.17: Analysis of p110δ and p85 protein expression in NIH 3T3 and HEK293T cells transiently transfected with p110δ-2a, p110δ-2b and p85α. Cells were transfected with a total of 10 μg of the indicated cDNAs. Cell lysates were separated by SDS PAGE and immunoblotted for p110δ and pan p85. A20 total cell lysate from untreated cells was run on the same gel to compare p110δ expression.

Transfection of p110δ-2a cDNA alone, in both NIH 3T3 and HEK293T cells gave rise to around a 3-fold increase in p110δ protein expression (lanes 6 and 14, respectively) compared to p110δ expression in untransfected cells (lanes 2 and 11).

In NIH 3T3 cells, cotransfection of p85α cDNA with p110δ-2a cDNA reduced p110δ protein expression (lane 7), whereas in HEK293T cells cotransfection of p85α cDNA with p110δ-2a cDNA further enhanced p110δ expression (lane 15). Interestingly, transfection of p85α cDNA only increased the total p85 protein expression in HEK293T cells (lanes 15 and 17) and not in NIH 3T3 cells (lanes 7 and 9). Since transfection of p85α cDNA in NIH 3T3 cells does not give rise to increased p85 protein expression, it is reasonable that the expression of p110δ is not enhanced.

Transfection of p110δ-2b cDNA (alone or cotransfected with p85α cDNA) did not result in increased p110δ expression in either NIH 3T3 or HEK293T cells (lanes 8 and 9 in NIH 3T3 cells and lanes 16 and 17 in HEK293T cells). This was a surprising result considering the substantial increase in total p110δ mRNA in HEK293T cells transfected with p110δ-2b cDNA.

4.4.4 Proteasome inhibition or varying cDNA concentrations does not substantially increase p110δ protein expression in HEK293T cells transiently transfected with a p110δ-2b expression plasmid

Transfection of 10 μg p110δ-2b cDNA did not result in increased p110δ expression in either NIH 3T3 or the more easily transfected cell line HEK293T. 10 μg of cDNA is a relatively high concentration of cDNA to be used in transfections, and it is possible that this concentration is inhibiting p110δ protein expression in p110δ-2b transfectants. Transfections of lower concentrations p110δ-2b cDNA in HEK293T cell were performed, to investigate whether a lower concentration of p110δ-2b cDNA could indeed induce p110δ protein expression. In parallel, the effect of proteasome inhibition on p110δ expression in HEK293T cells transiently transfected with p110δ-2b cDNA was also investigated.

There was little change in p110δ protein expression across all p110δ-2b cDNA concentrations transfected (Figure 4.18). The only induction of p110δ protein expression was observed upon cotransfection of 2 μg p110δ-2b cDNA with 1 μg p85α cDNA after treatment with a proteasome inhibitor (lane 11). The exogenously expressed murine p110δ protein is of a slightly higher molecular weight that the endogenous human p110δ in HEK293T cells, therefore induction of p110δ-2b protein expression appeared as a doublet.

These results indicate that some of the exogenously expressed p110δ-2b mRNA is translated into p110δ protein but the protein is subsequently targeted for proteasomal degradation.
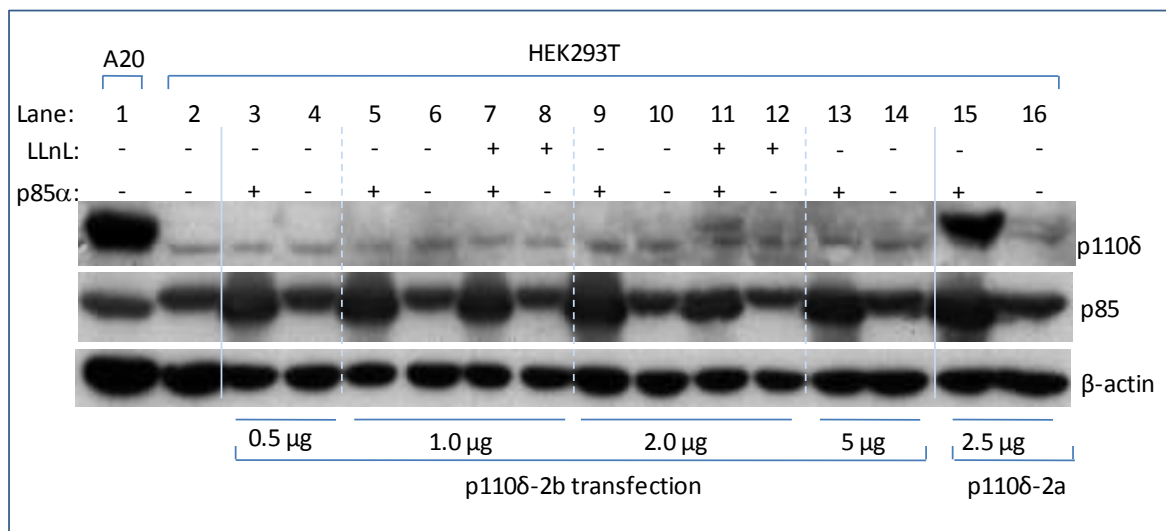
Figure 4.18: Analysis of p110δ expression in HEK293T cells transiently transfected with p110δ-2b cDNA. Cells were transfected with a total of 10 μg of the indicated cDNAs. Cells were treated with 50 μM LLnL for 48 h. Cell lysates were separated by SDS PAGE and immunoblotted for p110δ and pan p85. A20 total cell lysate from untreated cells was run on the same gel to compare p110δ expression.

Cotransfection of p110δ-2a cDNA with p85α cDNA, in the absence of proteasome inhibition, induced a substantially greater increase in p110δ proteins expression compared to any of the p110δ-2b cDNA transfections (lane 15), emphasizing that p110δ-2a mRNA is much more efficient in increasing p110δ protein expression compared to p110δ-2b mRNA.

4.4.5 Proteasome inhibition increases p110δ protein expression in NIH 3T3 cells transiently transfected with p110δ-2a cDNA but not p110δ-2b cDNA

To further investigate the induction of p110δ protein expression by proteasome inhibition, NIH 3T3 cells transiently transfected with p110δ-2a or p110δ-2b cDNA (+/- p85α cDNA) were treated with the proteasome inhibitor LLnL for 24 h or 48 h (Figure 4.19). In all conditions tested, transfection of p110δ-2b cDNA had no effect on the protein expression of p110δ (lanes 7-12) in comparison to untreated untransfected NIH 3T3 cells (lane 2). On the contrary, transfection of p110δ-2a cDNA resulted in increased p110δ protein expression compared to untransfected NIH 3T3 cells (lane 17 compared to lane 2), which was increased further upon 24 h of LLnL treatment (lane 14) and also 48 h of LLnL treatment (lane 13). This increase in p110δ expression was not associated with increased p85 expression. Cotransfection of p85α cDNA with p110δ-2a cDNA did not further increase p110δ expression upon LLnL treatment (lanes 15 and 16). Together these results further

corroborate the previous finding that p110δ-2a mRNA is much more efficient in increasing p110δ protein expression compared to p110δ-2b mRNA and that in NIH 3T3 cells transfection of p85 cDNA does not enhance p110δ expression.
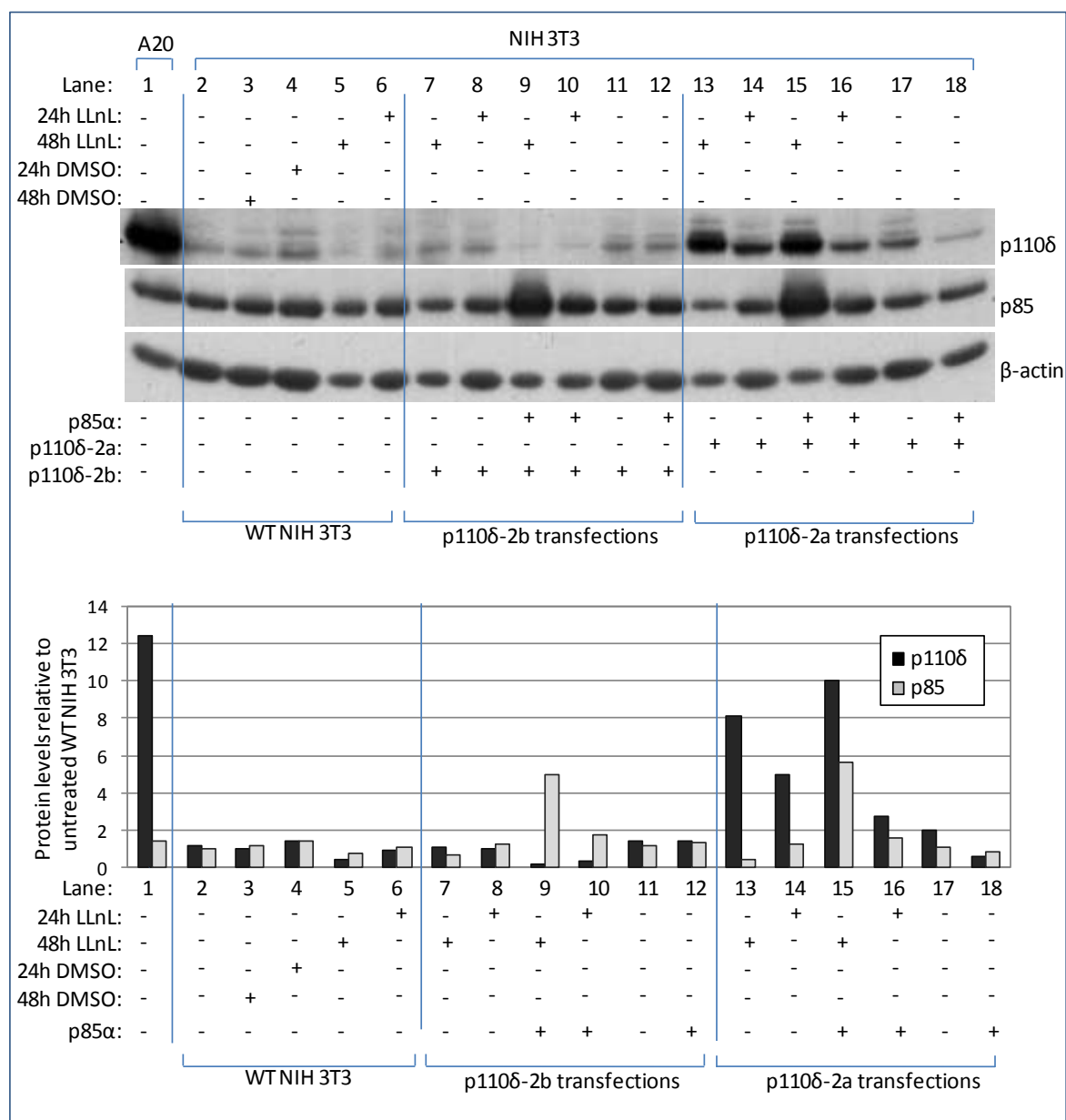
Figure 4.19: Analysis of p110δ and p85 expression in NIH 3T3 cells transiently transfected with cDNAs encoding p110δ-2a, p110δ-2b and p85α treated with or without a proteasome inhibitor. Cells were transfected with a total of 3 μg of the indicated cDNAs. Cells were treated with 50 μM LLnL or DMSO vehicle control for 24 h or 48 h. Cell lysates were separated by SDS PAGE and immunoblotted for p110δ and pan p85. A20 total cell lysate from untreated cells was run on the same gel to compare p110δ expression.

Interestingly, only after 48 h of LLnL treatment was increased p85 protein expression observed in NIH 3T3 cells in which p85α cDNA had been cotransfected with either p110δ-2a or p110δ-2b cDNA (lanes 9 and 15, respectively). No increase in p85 protein expression

was observed in untreated cells or cells treated for 24 h with LLnL in which p85α cDNA had been cotransfected with p110δ (lanes 10, 12, 16 and 18). This suggests that the exogenously expressed p85α is also targeted for proteasomal degradation in NIH 3T3 cells and despite low levels of p110δ protein expression, in the presence of a proteasome inhibitor high levels of exogenous p85α expression can be achieved (as shown in lane 9).

4.5 Discussion

4.5.1 Transfection of full length murine p110δ cDNA in NIH 3T3 cells does not result in stable constitutive p110δ overexpression

Multiple transcripts exist for p110δ with untranslated exons upstream of the first coding exon in both human and murine *PIK3CD*. During the course of my PhD work, the nature of these upstream exons has been investigated in an effort to elucidate their function. Although some progress has been made, the precise purpose of these 5' untranslated exons still remains unclear.

Previous attempts to stably overexpress p110δ in mammalian cells in the laboratory were unsuccessful. The identification of multiple p110δ transcripts, particularly highly expressed in leukocytes, raised the possibility that the untranslated upstream exons could be important in effective p110δ expression. It was hypothesized that transfection of full length p110δ cDNA, which incorporated the upstream exon -1 together with exon -2a (p110δ-2a) or exon -2b (p110δ-2b), may permit p110δ expression, for example through increasing p110δ mRNA stability. It is now known that the high expression of p110δ found in leukocyte cell lines does not result from increased p110δ mRNA stability, although the stability of each individual p110δ mRNA transcript has not been investigated (Kok, et al., in preparation).

Stable transfection of either p110δ-2a or p110δ-2b cDNA in the murine fibroblast cell line NIH 3T3 did not result in overexpression of p110δ protein despite an increase in p110δ mRNA expression in both cases. Transfection of p110δ-2a cDNA increased p110δ mRNA levels approximately 10-fold, however increased p110δ protein expression was only observed after treatment of cells with a proteasome inhibitor. This suggests that exogenously expressed p110δ is subsequently degraded by the proteasome. The stability of p110s is increased when they are part of a heterodimer with p85s (Yu, et al., 1998b). To assess if p110δ expression could be increased through such heterodimer formation, p85α cDNA was cotransfected with p110δ-2a cDNA. Despite an increase in p85α mRNA levels,

expression of total p85 protein was not increased in p85α stable transfectants and most likely as a result of this, transfection of p85α cDNA did not affect p110δ expression in p110δ-2a transfectants.

It is possible that the level of stably incorporated p110δ and p85α cDNA is not high enough to drive p110δ and p85α protein expression, respectively. At low levels of p110δ and p85 protein expression it is possible that that a third binding partner acting as a chaperone protein is necessary for efficient heterodimer formation, which would stabilise and protect p110 from degradation (Figure 4.20a). In the absence of a chaperone protein, which might not be expressed in cells that normally do not express high levels of p110δ, such as NIH 3T3 fibroblasts, p110δ and p85α monomers are targeted for proteasome degradation.
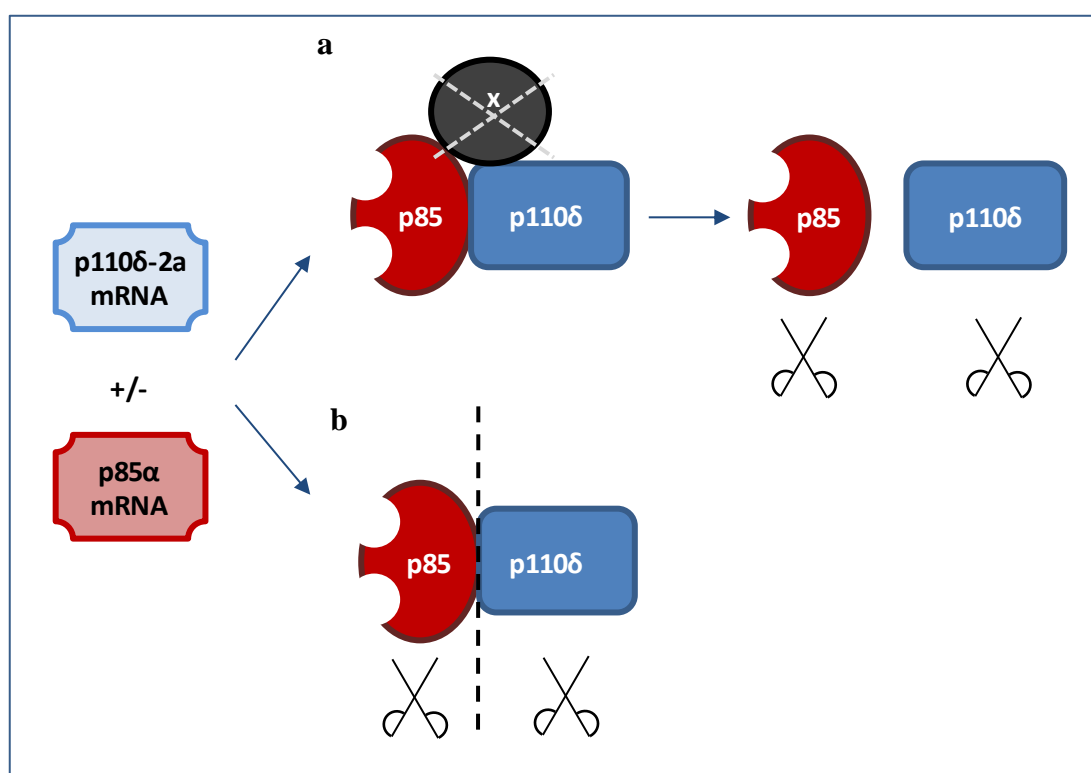
Figure 4.20: Hypothetical models to illustrate why increased p110δ and p85α mRNA expression is not associated with increased p110δ and p85α protein expression. (a) A third binding partner 'x' is required for the association of p110δ with p85 in NIH 3T3 cells, which may act to stabilise the heterodimer or offer a protective role to prevent p110 / p85 degradation. In the absence of chaperone protein 'x' p110δ and p85 monomers are degraded. **(b)** Transfected p85α and p110δ bind each other to form heterodimers, however the proteins are cleaved and are subsequently degraded by proteases present in NIH 3T3 cells.

Alternatively, transfected p85 and p110 proteins may form heterodimer complexes but complexes are also degraded by the proteasome (Figure 4.20b). It seems unlikely however that all exogenously expressed p110δ-p85α heterodimers, which form stable complexes, would be degraded.

Overall, we can conclude that the presence of the upstream exons -2a or -2b did not alter the expression level of p110δ protein, as compared to cDNAs which lacked these 5' untranslated exons.

4.5.2 Transient transfection of p110δ-2a cDNA but not p110δ-2b cDNA results in p110δ overexpression

As expected, in transient transfections of p110δ-2a or p110δ-2b, more substantial increases in p110δ mRNA expression were achieved in both NIH 3T3 cells and HEK293T cells compared to stable transfections. In particular, transfection of p110δ-2b cDNA in HEK293T cells resulted in massive increases of both p110δ-2b and total p110δ mRNA. This is due to the presence of an SV40 origin of replication in the p110δ-2b mammalian expression vector. In spite of this finding, only transfection of p110δ-2a cDNA and not p110δ-2b cDNA resulted in p110δ overexpression in HEK293T or NIH 3T3 cells. The data indicate that exon -2a is mediating a positive effect on p110δ expression which is not observed for exon -2b. Transfection of various concentrations of p110δ-2b cDNA and treatment of cells with a proteasome inhibitor only resulted in a marginal increase in p110δ protein expression in HEK293T cells only. Indeed, analysis of the contribution p110δ-2a and p110δ-2b transcripts make to the total amount of p110δ transcripts in the A20 leukocyte cell line, revealed that p110δ-2a contributes to 80% of the total p110δ mRNA, with p110δ-2b contributing to just 10%. It is possible that the high level of p110δ-2a mRNA expression in leukocytes is partly responsible for high p110δ protein expression. However, it is clear from the stable transfections of p110δ-2a that in non-leukocyte cell lines expression of p110δ-2a cDNA alone is not sufficient for constitutive p110δ overexpression.

In HEK293T p110δ-2a-transfectants, p110δ protein levels could be further increased upon transfection of p85α cDNA, whereas in NIH 3T3 p110δ-2a-transfectants, proteasome inhibition enhanced p110δ protein levels. This corroborated the findings from stable transfection of p110δ-2a cDNA, that exogenously expressed p110δ is also regulated at the protein level through stabilisation by p85 and proteasomal degradation, supporting the model proposed in Figure 4.20a. Indeed, the models proposed in Figure 4.20 for the failure of p110δ expression in stable p110δ-2a transfections of NIH 3T3 cells, could also explain the findings from transient transfection of p110δ-2a. In addition, the proposal that a high level of transfected p110δ and p85α cDNA is required to drive protein expression is

supported by the finding that in transient transfections, unlike stable transfections, a substantial increase in p110δ and/or p85 cDNA led to effective protein overexpression.

Interestingly, overexpression of p110δ protein in p110δ-2a transient transfectants, was not associated with an increase in endogenous levels of p85. There are at least three possible scenarios which can explain this phenomenon. The first is that exogenously expressed p110δ does not form heterodimers with p85 but exists as a monomer (Figure 4.21a). This possibility implies that p110δ expression does not absolutely require p85, but can exist at least transiently as a monomer, which does not discount the idea that binding of p85 would stabilise p110δ.
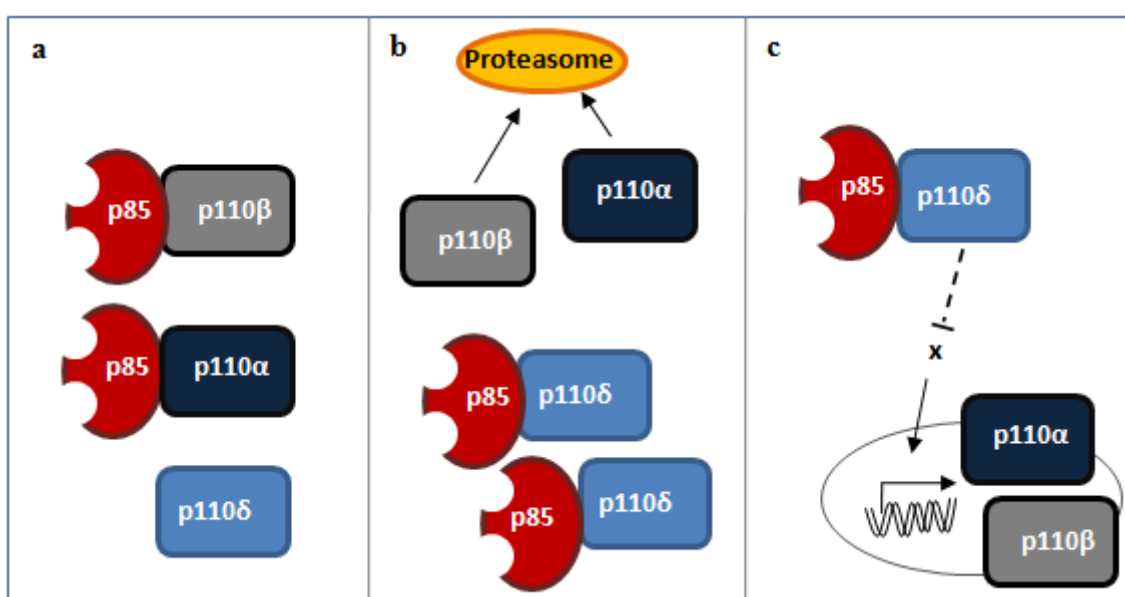
Figure 4.21: Hypothetical models showing why increased p110δ expression is not associated with increased p85 expression. (a) p110δ can transiently exist as a monomer giving rise to increased p110δ protein expression. **(b)** Exogenously expressed p110δ titrates endogenous expressed p110α and/or p110β from their regulatory subunit resulting in free p85 to which p110δ can bind. Monomeric p110α and p110β are subsequently degraded. **c)** Exogenously expressed p110δ downregulates p110α and/or p110β expression at the transcriptional level resulting in increased p85 to which p110δ binds.

The second possibility is that the exogenously expressed p110δ titrates endogenously expressed class IA p110s from their regulatory subunit, resulting in free p85 to bind p110δ (Figure 4.21b). Monomers of titrated p110 are likely to be subsequently degraded, resulting in downregulation of p110α and p110β protein expression. This possibility seems unlikely given that the binding of p110s to p85 has been shown to be extremely strong and can withstand high concentrations of urea, salt or detergent (Fry, et al., 1992). A third scenario is that expression of exogenous p110δ results in downregulation of other class IA p110s at the transcriptional level resulting in decreased endogenous p110 expression but

not p85 expression. Decreased protein expression of other class IA p110s would also result in increased free p85 that can bind and stabilise p110δ (Figure 4.21c). Transient overexpression of p110δ has indeed been found to result in downregulation of p110α and p110β in chicken embryo fibroblasts (Kang, et al., 2006) and taking into consideration results obtained through retroviral infection of 5'Myc-p110δ cDNA in NIH 3T3 cells (described in chapter 6), this possibility seems the most plausible.

4.5.3 Transient or stable transfection of p85α does not result in p85 overexpression NIH 3T3 cells

As mentioned in section 4.5.1, stable overexpression of p85α protein in NIH 3T3 cells was not possible despite an increase in p85α mRNA levels. Transient transfection of p85α cDNA in NIH 3T3 also failed to result in p85 overexpression. Increased p85 expression was only observed in NIH 3T3 cells transiently transfected with p85α cDNA after 48 h of proteasome inhibition. Interestingly, although the expression vector in which p85α was expressed did not contain an SV40 origin of replication, clear p85 overexpression was observed in HEK293T cells. HEK293T cells are more readily transfected than NIH 3T3 cells and indeed, quantitative real time PCR revealed that HEK293T cells expressed 37,000-fold more p85α mRNA relative to A20 cells, whereas NIH 3T3 expressed 260-fold more. It is possible that a certain threshold of mRNA expression first has to be reached in order for expression of exogenous p85 at such a level that it escapes complete proteasome degradation.

5 ANALYSIS OF THE PROMOTER ACTIVITY OF THE UPSTREAM UNTRANSLATED EXON -2A OF MURINE *PIK3CD*

5.1 Introduction

It has been well documented that p110δ is predominantly expressed in leukocytes, however the mechanism by which leukocyte-restricted p110δ expression is achieved it is not known. Before starting and throughout the course of my PhD work, members of the laboratory have investigated the regulation of p110δ gene expression, in an effort to gain some insight into the leukocyte-specific nature of p110δ expression (Kok, et al., in preparation; Verrall & Vanhaesebroeck, unpublished results). These investigations have, for the most part, led to negative data regarding the manner by which p110δ gene expression is regulated. In summary, p110δ expression does not appear to be regulated by acute stimulation in a variety of stimuli tested (TNFα, osmotic stress, UV radiation, proteasomal inhibition and aldosterone) in NIH 3T3 fibroblasts, or by DNA methylation and histone acetylation in the L929 fibrosarcoma cell line. In addition, high p110δ expression in leukocytes does not appear to be due to increased p110δ mRNA stability compared to non-leukocytes (Kok, et al., in preparation). However, these investigations have led to the identification of multiple p110δ transcripts, as previously described in section 4.2.1. The newly identified transcripts contain untranslated 5' upstream exons as far as 36 Kb from the ATG translational start site in murine exon 1 (Figure 4.1). Investigations into locating putative leukocyte-specific promoter regions upstream of the untranslated exons have been carried out to offer some mechanism for tissue-restricted p110δ gene expression.

5.2 *In silico* promoter analysis of the 5' UTR of *PIK3CD* genomic DNA

Although this work has been carried out by Dr. Elizabeth Verrall with the help of Klaartje Kok, it is important to summarise their findings to put the results I have obtained in this chapter into context. *In silico* analysis of the 5'UTR genomic sequence of murine *PIK3CD* identified regions of high homology with 8 other species, which is indicative of functionally conserved DNA sequences (Figure 5.1a). Some of these regions colocalized with CpG islands, which as discussed in section 1.9.3 are frequently found in promoter regions. DNA fragments upstream of exon 1 and the untranslated exons, in genomic regions of DNA indicated in Figure 5.1a, were cloned into a luciferase reporter vector and expressed in the mouse A20 leukocyte cell line and the NIH 3T3 fibroblast cell line in an effort to identify a leukocyte-specific *PIK3CD* promoter. The findings of the promoter activities of the different *PIK3CD* fragments are summarised below:

- **Transfection of 6 fragments ranging from 58 bp to 2 Kb upstream of exon -2b**
  → Low promoter activity was detected in both cell lines in transient transfections for all DNA fragments. In stable transfections, a modest increase in promoter activity was detected in NIH 3T3 cells, although not in A20 cells, with the 58 bp DNA fragment.

- **Transfection of 7 fragments ranging from 36 bp to 2 Kb upstream of exon -2a**
  → Transient and stable transfections resulted in similar low promoter activity detected in both NIH 3T3 and A20 cell lines for all DNA fragments.

- **Transfection of 7 fragments ranging from 185 bp to 2 Kb upstream of exon -1**
  → In transiently transfected cells the largest DNA fragment of 2 Kb gave rise to an unexpected significant increase in promoter activity in NIH 3T3 cells compared to A20 cells. In contrast, the smallest DNA fragment of 185 bp gave rise to a significant increase in promoter activity in A20 cells compared to NIH 3T3 cells. However, in both instances the promoter activity detected was relatively low compared to the positive promoter control (SV40).

- **Transfection of 9 fragments ranging from 56 bp to 2 Kb upstream of exon 1**
  → In transiently transfected cells high promoter activity was detected in both cell lines for most of the fragments, with no obvious difference between NIH 3T3 and A20 cells.

On the basis of these results, it was not possible to delineate specific sites in the genomic DNA which accounts for the tissue-specific regulation of *PIK3CD* (Verrall & Vanhaesebroeck, unpublished results).

5.2.1 Transcription factor binding cluster identified in mouse *PIK3CD* exon -2a

In silico analysis of TF binding sites within a 600 bp region flanking the 5' untranslated exons (500 bp upstream and 100 bp downstream) in murine *PIK3CD*, identified a cluster of TF binding sites within exon -2a (Figure 5.1b) (Kok, et al., in preparation). In comparison to the other upstream exons, the cluster of TF binding sites was tightly packed and correlated with a high TSS score. From the previously described *in silico* analysis of the 5'UTR of murine *PIK3CD*, it was observed that a region of high homology in the 9 species analysed in addition to a CpG island surrounds exon -2a. Collectively these data indicate a putative promoter region surrounding mouse exon -2a.
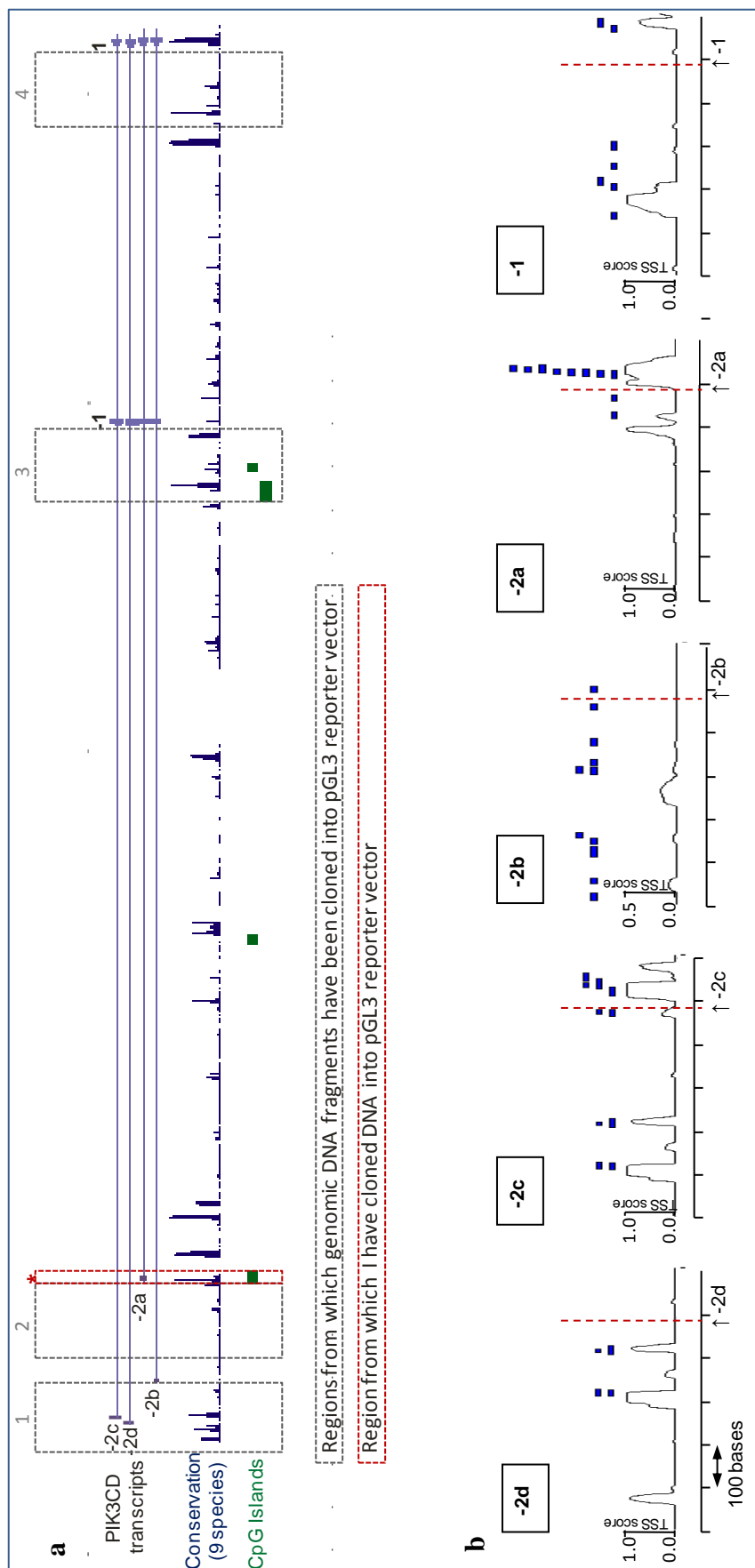
Figure 5.1: Promoter analysis of murine *PIK3CD* 5' UTR. (a) *In silico* analysis of genomic *PIK3CD* transcripts. The murine *PIK3CD* sequence was used as a reference sequence to determine regions of homology with genomic *PIK3CD* with 8 other species. Regions containing high CpG dinucleotides, CpG islands, are shown in green. Genomic regions of murine *PIK3CD* that have previously been analysed for promoter activity in leukocytes and non-leukocytes (Verrall, 2005) are indicated within the grey boxes, labelled 1–4. The region I have personally analysed for leukocyte-specific promoter activity is indicated within the red box. **(b)** Locations of TF binding sites, shown as blue boxes, located on the forward strand within a 600 bp region flanking the 5' untranslated exons (500 bp upstream and 100 bp downstream). The exon start site is indicated by a red dashed line. The degree of genomic conservation between 28 species is shown as calculated by the phastCons program which ranges from a minimum of 0.0 to a maximum of 1.00. Figure adapted from Kok, *et al* (In preparation).

The TFs that bind in the identified cluster in mouse exon -2a are shown in Table 5.1 with their DNA binding sequences illustrated in Figure 5.2. The region containing the TF binding cluster (TFB cluster), is highly conserved between species (Figure 5.2a), with at least 4 of the identified TFs being associated with leukocyte gene expression, namely ETSF, IRFF, NFAT and LEFF, which are discussed further in section 5.5.1. Collectively, these findings strongly supported the hypothesis that this TFB cluster may act as a tissue-specific promoter for *PIK3CD* gene expression. This region of DNA had not been analysed for promoter activity previously as it is contained within exon -2a itself, and only regions *upstream* of the untranslated exons were previously cloned into the luciferase reporter vector. It is unusual, but not unheard of, that promoter regions are contained within exons. Recent work from the ENCODE project (http://www.genome.gov/10005107 and http://genome.cse.ucsc.edu/ENCODE/) has revealed that proximal TF binding sites fall within 1 Kb of both sides, 5' and 3', on the TSS (Kok, et al., in preparation). Alignment of genomic *PIK3CD* DNA from human and mouse reveals that in actual fact, the TFB cluster is located 53 bp upstream of human exon -2a (Figure 5.2b), which fits in with the conventional idea of promoter location in relation the to the TSS.

TF Abbreviation	TF full name
IRFF	Interferon regulatory factor
FKHD	Forkhead
NFAT	Nuclear factor of activated T-cells
LEFF	Lymphoid enhancer factor-1 and T-cell factor
NKXH	NKX homeodomain factors
ETSF	ETS/Elk family [named after E26 (E twenty six) leukemogenic chicken virus]
RBPF	Mammalian transcription repressor RBP-Jkappa/CBF

Table 5.1: Transcription factor binding sites in mouse *PIK3CD* exon -2a.
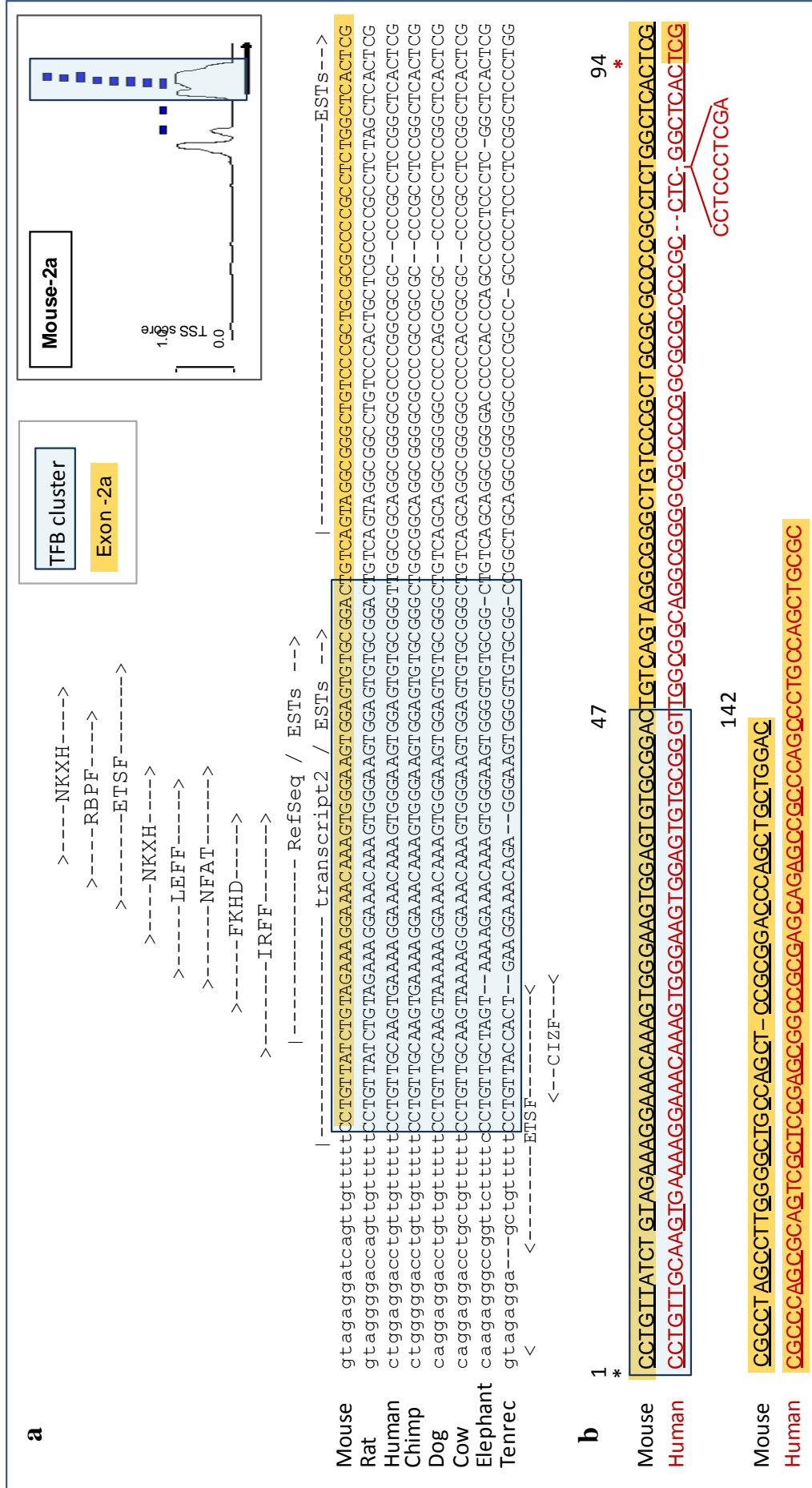
Figure 5.2: Inter species homology of TFB cluster located in mouse exon -2a. (a) Alignment of TFB cluster identified in mouse exon 2a with rat, human, chimp, dog, cow, elephant and tenrec genomic DNA. (b) Location of TFB cluster in relation to the TSS of exon -2a, indicated by a back asterisk in mouse and *PIK3CD* DNA and a red asterisk in human.

The location of the TFB cluster in relation the translational start site in *PIK3CD* in species other than human and mouse is illustrated in Figure 5.3. If the TFB cluster acts as a promoter for *PIK3CD* in these other species, it is likely that untranslated upstream exons also exist in these genomic sequences given that the TFB cluster lies up to 60 Kb upstream of the translational start site. The presence of upstream exons in *PIK3CD* species other than human and mouse has not yet been investigated, although the similar locations of the TFB cluster in human compared to chimp, and mouse compared to rat *PIK3CD*, in relation to the ATG start site, strongly supports their existence.

↑ = TFB cluster: CCTGTTATCTGTAGAAAGGAAACAAAGTGGGAAGTGGAGTGTGCGGAC

Distance of TFB cluster upstream of PIK3CD untranslated exons

	Exon 1	Exon -1	Exon -2a
Mouse	35 kb	24 kb	0 b
Human	60 kb	40 kb	53 b
Rat	34 kb	U	U
Chimp	60 kb	U	U
Cow	47 kb	U	U
Dog	40 kb	U	U

U = Unknown
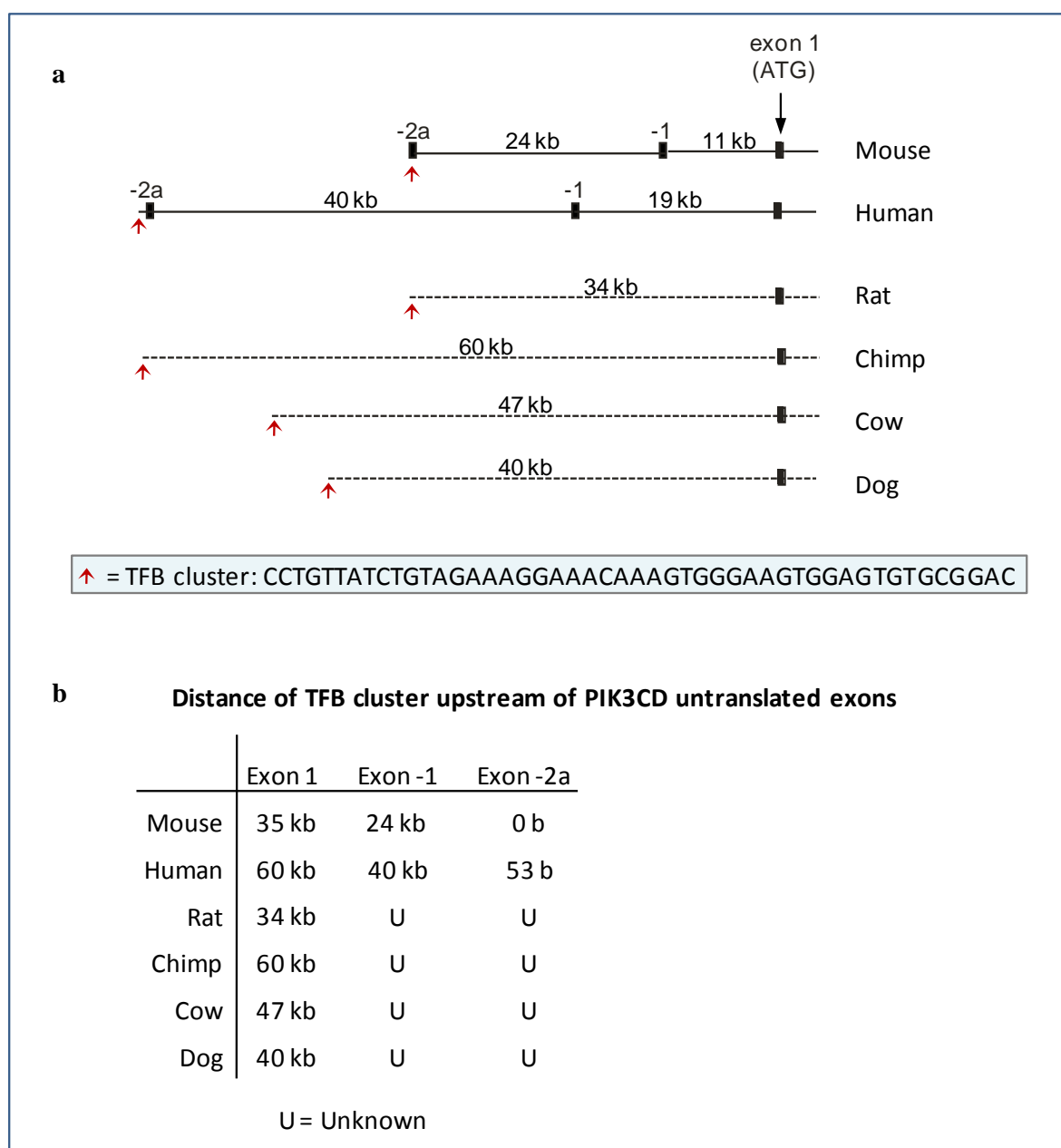
Figure 5.3: Location of TFB cluster relative to the translation start site of *PIK3CD* in six species. (a) Schematic to show the location of the TFB cluster in relation to the translational start site in mouse, human, rat, chimp, cow and dog *PIK3CD* genomic DNA and also in relation to exon -2a in mouse and human. **(b)** Table to show the distance between the TFB cluster and exon 1 and untranslated exons.

Two additional TF binding sites immediately upstream of the TFB cluster were also identified; MyoD, a member of a family of proteins known as myogenic regulatory factors that are involved in muscle differentiation, and SP1, a widely expressed activator of gene transcription in many cell types (Figure 5.4).

Considering the high conservation of the DNA sequence comprising the TFB cluster between species, the leukocyte-nature of certain TF binding sites located within the cluster, the high TSS score and the location of CpG islands in and surrounding the TFB cluster, the decision was taken to investigate the promoter activity of this region in leukocyte compared to non-leukocyte cells.
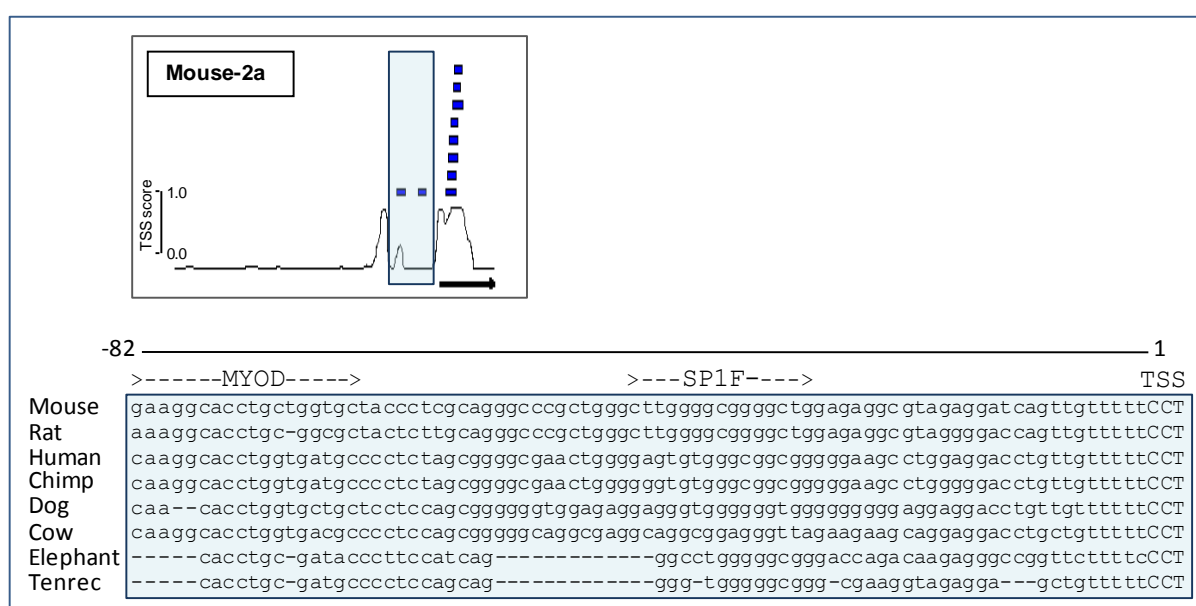
Figure 5.4: Interspecies homology of TF binding sites immediately upstream of the TFB cluster. Alignment of TFB cluster identified in mouse exon -2a with rat, human, chimp, dog, cow, elephant and tenrec genomic DNA identified two additional TF binding sites, MyoD and SP1F, 82 bp and 41 bp upstream of the TSS of mouse *PIK3CD* exon -2a, respectively.

5.3 Cloning of mouse *PIK3CD* exon -2a into a luciferase reporter vector

Using the mammalian expression vector containing the mouse p110δ-2a cDNA sequence (used for p110δ overexpression studies described in Chapter 4), exon -2a was amplified by PCR and cloned into the pGL3-Basic luciferase reporter vector (Figure 5.5 and described further in section 2.12.4). The pGL3-Basic vector, together with the other luciferase vectors used in the reporter assays, are described in section 2.12.3 and a vector map for pGL3-Basic is depicted in Figure 2.9.
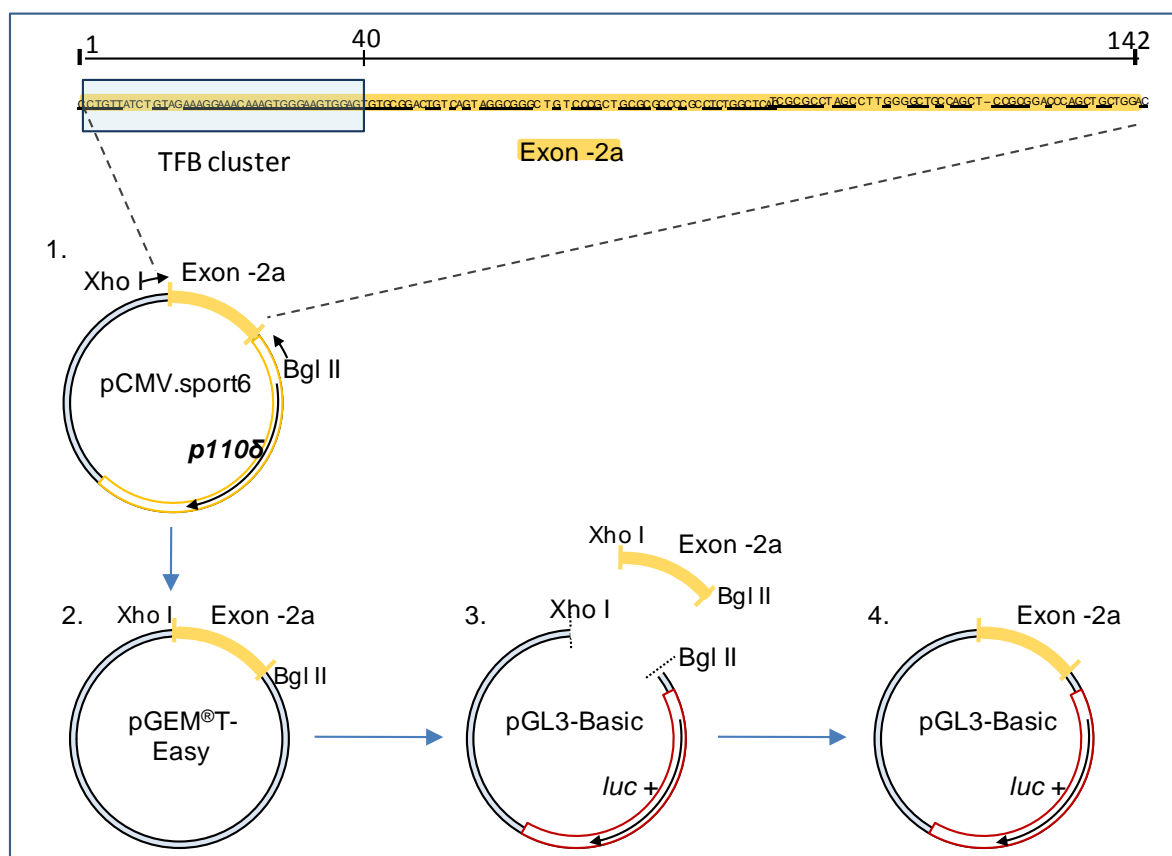
Figure 5.5: Cloning strategy used to obtain firefly *luciferase* in pGL3-Basic under the control of the putative mouse exon -2a *PIK3CD* promoter. (1) Mouse *PIK3CD* exon -2a was amplified from pCMV.sport6 mammalian expression vector containing p110δ-2a cDNA. PCR primers incorporated DNA sequences containing restriction enzyme digest sites for *Xho* I and *Bgl* II. (2) Amplified exon -2a was ligated into pGEM®T-Easy vector and used for transformation of competent cells. Transformation cultures were plated onto LB/ampicillin/IPTG/X-Gal plates and white colonies, containing ligation product, selected. (3) pGEM®T-Easy containing exon -2a and pGL3-Basic were digested with the restriction enzymes *Xho* I and *Bgl* II. (4) exon -2a was ligated into pGL3-Basic upstream of firefly *luciferase*.

5.4 Mouse *PIK3CD* exon -2a has enhanced promoter activity in leukocyte cell lines compared to non-leukocyte cell lines

Firefly *luciferase* under the control of the SV40 promoter (pGL3-Promoter, Figure 2.11), the putative exon -2a *PIK3CD* promoter (pGL3-Exon -2a, Figure 5.5) or the leukocyte-specific *Vav* promoter (pGL2-Vav, Figure 2.10) were transfected into the macrophage cell line, RAW 264.7 or the fibroblast cell line NIH 3T3. The pGL3-Basic vector which did not contain any promoter sequence upstream of firefly *luciferase* was used for transfections to assess the basal level of luminescence.

The luminescence detected, which acts as a readout for promoter activity, from cells transfected with pGL3-Exon -2a or pGL2-Vav has been expressed as a % of the

luminescence detected for pGL3-SV40. In all three transfections (pGL3-SV40, pGL2-Vav, pGL3-Exon -2a) the basal luminescence from pGL3-Basic has been subtracted (Figure 5.6).

In two independent experiments, in which transfection of each promoter construct was carried out in triplicate, exon-2a had increased promoter activity in RAW 264.7 cells compared to NIH 3T3 cells (Figure 5.6a). In RAW 264.7 cells, the promoter activity of exon -2a was around 75% of that observed for SV40, whereas in NIH 3T3 the promoter activity of exon -2a was around 15%. The leukocyte-specific *Vav* promoter produced 15% promoter activity in RAW 264.7 cells, whereas in NIH 3T3 cells no promoter activity was detected (Figure 5.6a). These results indicate that mouse exon -2a acts as a promoter in both cell types, however, promoter activity is enhanced in RAW 264.7 cells compared to NIH 3T3.
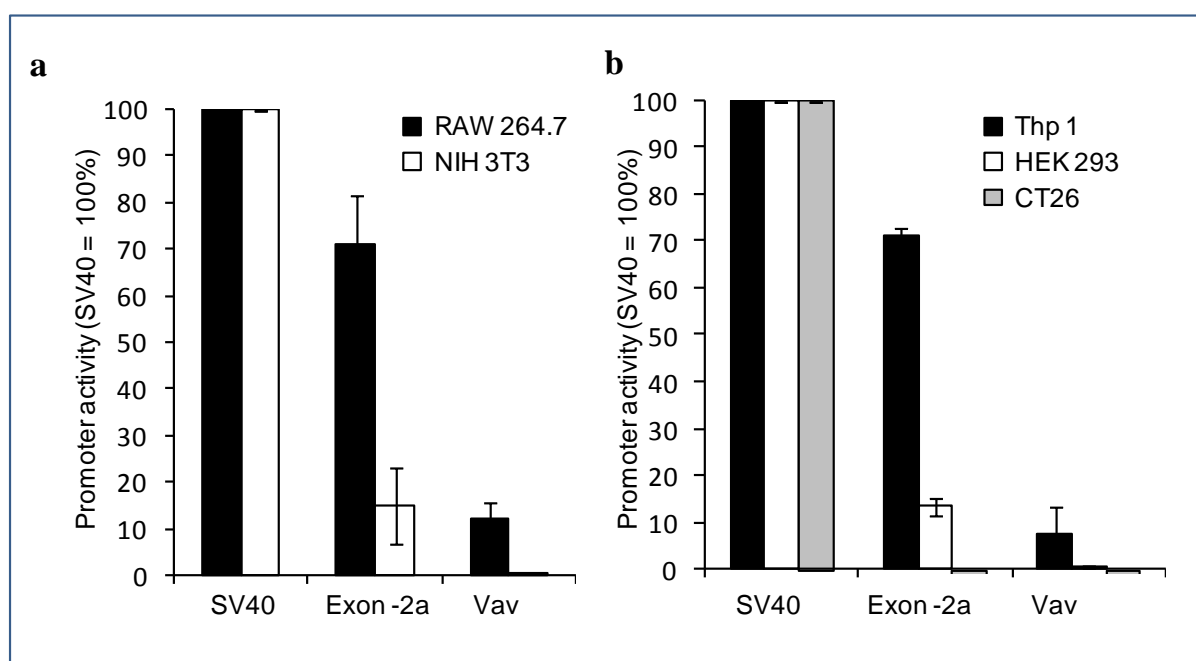
Figure 5.6: Promoter activity of mouse *PIK3CD* exon -2a in leukocyte *versus* non-leukocyte cell lines. The promoter activity of exon-2a and the *Vav* promoter is expressed as % of SV40 promoter activity after basal luminescence has been subtracted. Each transfection was carried out in triplicate with the error bars indicating the standard deviation between these triplicates. Leukocyte cell lines are indicated by black bars. **(a)** Promoter activity in RAW 264.7 and NIH 3T3 cells expressed as an average over two independent experiments. **(b)** Promoter activity in Thp1, HEK 293 and CT26 cells from a single experiment.

To analyse if exon -2a had increased promoter activity in an additional leukocyte cell line, the luciferase constructs were transfected in the monocytic cell line, Thp 1, and two non-leukocyte cell lines, HEK 293 (human embryonic kidney cells) and CT26 (a mouse carcinoma cell line) which both express low endogenous levels of p110δ. Similarly to exon

-2a promoter activity in RAW 264.7 cells, the promoter activity of exon -2a was around 75% of that observed for SV40 in Thp 1 cells (Figure 5.6b). Fittingly, the promoter activity of exon -2a was much lower in the non-leukocyte cell lines, around 15% in HEK 293 and undetectable in CT26 cells. Transfection of the leukocyte-specific *Vav* promoter resulted in 10% promoter activity in Thp 1 cells, whereas in HEK 293 and CT26 cells no promoter activity was detected (Figure 5.6b). Collectively, these data indicate that exon -2a, and most likely the TFB cluster identified within this region, may predominantly promote p110δ expression in leukocytes.

5.5 Discussion

5.5.1 Characterisation TFs identified in the putative *PIK3CD* promoter surrounding exon -2a

After a great deal of time invested in identifying a leukocyte-specific promoter for *PIK3CD* gene expression, the identification of a TFB cluster in mouse exon -2a as a putative *PIK3CD* promoter has offered some insight into the leukocyte-restricted expression of p110δ. Transfection of firefly *luciferase* under the control of the putative exon -2a *PIK3CD* promoter in leukocyte and non-leukocyte cell lines indicated that exon -2a has promoter activity in both cell types, with enhanced promoter activity in leukocyte cells. These results suggest that the TFB cluster contains TF binding sites for ubiquitously expressed TFs, which are able to drive *PIK3CD* gene expression in many cell types, in addition to TFs predominantly expressed in leukocytes, which enhances *PIK3CD* gene expression in this cell type only. Indeed, 4 of the 7 different TFs identified in the TFB cluster, namely ETSF, IRF, NFAT and LEFF, are associated with regulation of haematopoiesis and expression of leukocyte specific genes and are discussed in more detail below.

ETS family: Nearly 30 members of the ETS family have been identified, which are implicated in a wide range of physiological and pathological processes (Bartel*, et al.*, 2000). Although the precise role of ETS-family members has not yet been delineated, TFs of the ETS family have been shown to be important for diverse cellular functions such as haematopoiesis, haemostasis and lymphoid development, in addition to endothelial cell differentiation, angiogenesis, extraembryonic development and neurogenesis (Bartel, et al., 2000; Bassuk & Leiden, 1997; Dejana*, et al.*, 2007; Graves & Petersen, 1998; Orkin, 1998). Most ETS proteins activate gene transcription, although a few members exhibit transcriptional repression and some display both activating and repressing functions,

however all bind the same DNA consensus motif. The regulation of ETS function depends upon the expression profile, activity and interplay between ETS family members, other TFs and regulatory proteins within the cell. It is apparent from ETS gene-targeting studies that a number of ETS TFs (PU.1, ETS1, Spi-B, Fli1, and TEL1) play an important role in the regulation of haematopoiesis (Bories, *et al.*, 1995; Hart, *et al.*, 2000; Iwama, *et al.*, 1998; Muthusamy, *et al.*, 1995; Scott, *et al.*, 1997; Su, *et al.*, 1997; Wang, *et al.*, 1997). PU.1 is expressed specifically in haematopoietic tissues, with high levels of expression in monocytic, granulocytic, and B lymphoid lineages (Chen, *et al.*, 1995; Hromas, *et al.*, 1993). Mutation of the *PU.1* gene results in a block of the development of lymphoid and myeloid lineages in the fetal liver and yolk sac (Scott, et al., 1997; Scott, *et al.*, 1994). ETS1 is expressed predominantly in lymphoid cells in adult mice where it has been implicated in regulating transcription of lymphocyte-specific genes. In particular, ETS1 deficiency has dramatic, but different, effects on development and function of T- and B-lineage cells. Reduced numbers of ETS1-deficient splenic T cells are observed that are highly susceptible to cell death *in vitro*, whereas ETS1-deficient B cells are present in normal numbers but many show abnormal differentiation to IgM-secreting plasma cells (Bories, et al., 1995). Furthermore, ETS1-deficient murine T cells display a severe proliferative defect in response to multiple activational signals (Muthusamy, et al., 1995).

IRF family: There are 9 mammalian IRFs, which have been shown to be transcriptional mediators of many biological processes, such as the development of innate and adaptive immunity, cell growth, apoptosis and haematopoietic development (Takaoka, *et al.*, 2008). In particular, IRF TFs play a pivotal role in the induction of type I IFN signalling pathways providing a principal basis for host resistance against pathogens (Ozato, *et al.*, 2007). IRF family members are highly expressed, but not exclusively, in cells of the immune system and in addition to promoting IFN gene transcription, IRF family members stimulate expression of IFN responsive genes, proinflammatory cytokines, and expression of macrophage and B cell specific genes (Ozato, et al., 2007; Paun & Pitha, 2007).

NFAT family: Five different NFAT family proteins have been characterised, which are mainly found in T cells and other cells of the immune system, such as mast cells, NK cells and monocytes (Rao, 1994). NFAT was initially identified as an inducible factor that could bind to the promoter of IL-2 in activated T-cells (Shaw, *et al.*, 1988). Since this discovery, NFAT TFs have been shown to play a role in the regulation of various cytokines, including those involved in the regulation of haematopoietic cells such as granulocyte-macrophage colony stimulating factor, IL-4, IL-3, IL-13 and IL-5 (De Boer, *et al.*, 1999).

LEF family: Although there are only four members of the LEF/TCF family in vertebrates, extensive patterns of alternative splicing, alternative promoter usage and activities of repression, add to the complexity of LEF family TFs (Arce*, et al.*, 2006). LEF proteins frequently activate LEF target genes in association with the TF β-catenin (Behrens*, et al.*, 1996), although LEF activation of target genes can also be independent of β-catenin (Hsu*, et al.*, 1998). β-catenin is an important effector in the Wnt signalling pathway involved in various cellular processes such as cell differentiation and development. Wnt signals stabilise β-catenin in the cytosol and result in the accumulation and nuclear translocation of β-catenin (Eastman & Grosschedl, 1999). LEF-1/TCF proteins associated with β-catenin mediate a transcriptional response to Wnt signalling (Arce, et al., 2006).

LEF-1 was originally identified as a gene expressed specifically in pre-B and T lymphocytes, encoding a nuclear protein that binds to a functionally important site in the *TCRα* enhancer conferring maximal enhancer activity (Travis*, et al.*, 1991). This suggested that LEF-1 was a regulatory participant in lymphocyte gene expression and differentiation. Subsequently, LEFs have been linked to the regulation and expression of a number of lymphoid-specific genes. For example, the recombination-activating gene (*RAG*)-*1* and *RAG-2* are expressed specifically in immature B or T lineage cells undergoing *Ig* or *TCR* gene rearrangements. The failure of functional expression of *RAG* causes defect in the formation of functional antigen receptor of lymphocytes, and the block of lymphocyte development in mouse and human (Mombaerts*, et al.*, 1992; Shinkai*, et al.*, 1992). In immature B-cells, interaction of LEF-1 with β-catenin was found to be important for *RAG-2* expression, in concert with two additional TFs, implicating Wnt signalling and LEF-1 as important mediators in *RAG* transcription in B cells (Jin*, et al.*, 2002). The importance of LEF-1 expression in B cell maturation is also emphasized in LEF-1 deficient mice, which display defects of proliferation and survival of pro-B cells (Reya & Grosschedl, 1998). Regarding the regulation of T lymphocyte-specific genes during T lymphocyte development, additional binding sites for LEF-1 have been identified in transcriptional control regions of several T lymphocyte-specific genes, including those encoding adenosine deaminase (Brickner*, et al.*, 1995), CD4 (Sawada & Littman, 1991*)*, TCRβ, and TCRδ (Leiden & Thompson, 1994).

LEF-1 has also been identified as a decisive transcription factor in granulopoiesis, the haematopoiesis of granulocytes (neutrophils, eosinophils and basophils), controlling proliferation, proper lineage commitment, and granulocytic differentiation (Skokowa &

Welte, 2007). Indeed, myeloid progenitor cells of patients with severe congenital neutropenia (abnormally low number of neutrophil granulocytes) show a severe downregulation of LEF-1 and its target genes expression (Skokowa, *et al.*, 2006).

The leukocyte-specific nature of the TF binding sites identified in the TFB cluster identified in mouse exon -2a strongly supports the proposal that this region of DNA acts as leukocyte-specific promoter for *PIK3CD* gene expression. Moreover, the high conservation of the TFB cluster DNA sequence between species and its location within a CpG island further indicate this region as a gene promoter. It would be interesting to assess the importance of individual TF binding sites within the TFB cluster in driving leukocyte-specific gene expression, by mutational analysis. LEF-1 has been shown to have no transcriptional activation potential by itself, but act as an architectural protein in the assembly of multiprotein enhancer complexes (Giese, *et al.*, 1995). This opens up the possibility that a complex of TFs is required for the leukocyte-specific promoter activity.

Two other TF binding sites, MyoD and SP1, were identified immediately upstream of the TFB cluster in mouse exon -2a. SP1 is a widely expressed TF that was originally found to recognize and specifically bind to GC-rich sites within the SV40 promoter via three Cys_2His_2 zinc-finger motifs. Although widely expressed, SP1 is involved in regulated tissue-specific gene expression such as the differentiation of myeloid cells, and LPS-induced gene expression in macrophages and monocytes (Chanteux, *et al.*, 2007; Hirata, *et al.*, 2008; Liu, *et al.*, 2007; Resendes & Rosmarin, 2004). Characterisation of core promoters, which typically encompass the site of transcription initiation and extends approximately 35 nucleotides upstream or downstream, are commonly thought to contain TATA-like elements. For *PIK3CD* no TATA-like motifs were identified through *in silico* analysis. Interestingly, a genome-scale computational analysis has indicated that $\sim$ 76% of human core promoters lack TATA-like elements, have a high GC content, and are enriched in SP1-binding sites (Yang, *et al.*, 2007). Furthermore, in TATA-less promoters, SP1 binding has been found to have a pivotal role in initiating transcription (Chen, *et al.*, 1997; Colgan & Manley, 1995; Zenzie-Gregory, *et al.*, 1993; Zhang, *et al.*, 1994). Although the SP1 TF binding site was not included in the DNA region cloned into pGL3-basic for promoter analysis, it possible that it may enhance *PIK3D* gene expression. It would be interesting to investigate whether including the SP1 TF binding site would enhance promoter activity in an *in vitro* reporter assay, and whether this would augment the leukocyte-specific nature of the promoter.

5.5.2 *PIK3CD* core promoter elements

As mentioned in the introduction (section 1.9.3), the core promoter is the minimal stretch of DNA sequence that is sufficient to direct accurate initiation of transcription, which typically encompasses the TSS within the initiator (Inr) sequence and several other motifs including the TFIIB recognition element, a TATA box and downstream promoter element (DPE) (Figure 1.15). As previously stated, for *PIK3CD* no TATA-like motifs were identified through *in silico* analysis. DPE motifs commonly occur with TATA-less promoters located 28-32 bp downstream of the TSS. Downstream of the mouse exon -2a TSS, three possible DPE motifs exist (Figure 5.7), all of which have one nucleotide mismatch from one of the commonly occurring DPE sequence; AGT**C/T**G. 13 bps downstream of the human TSS for exon -2a, an exact match for the commonly found DPE sequence, AGTCG, is found. However further investigation would be required to assess whether these sequences are in fact important for transcription initiation, indeed in drosophila, DPE sequences are usually located precisely at 28-32 bp downstream of the TSS (Burke & Kadonaga, 1996), therefore in this respect the sequences identified do not fit the conventional characteristics of DPEs.

The initiator sequence typically encompasses the TSS with the consensus Py-Py(C)-A$_{+1}$-N-T/A-Py-Py, where A$_{+1}$ represents the common nucleotide at which transcription is initiated (Javahery, et al., 1994). However, the TSS may occur in the vicinity of Inr at not necessarily at A$_{+1}$ (Butler & Kadonaga, 2002). A possible Inr sequence (TC**A**GTTG) that differed only by the last nucleotide from the consensus, was found 5 bp upstream of the mouse exon -2a TSS (Figure 5.7). Interestingly, the adenine (**A**) nucleotide, which is the only specified nucleotide in the Inr consensus, within this putative Inr sequence, was not present in the human *PIK3CD* genomic sequence. This finding offers some explanation for the differing TSSs of mouse and human exon -2a. A putative Inr sequence, TC**A**CTCG, that contains the TSS of human exon -2a was found that also differs by the last nucleotide from the consensus Inr.
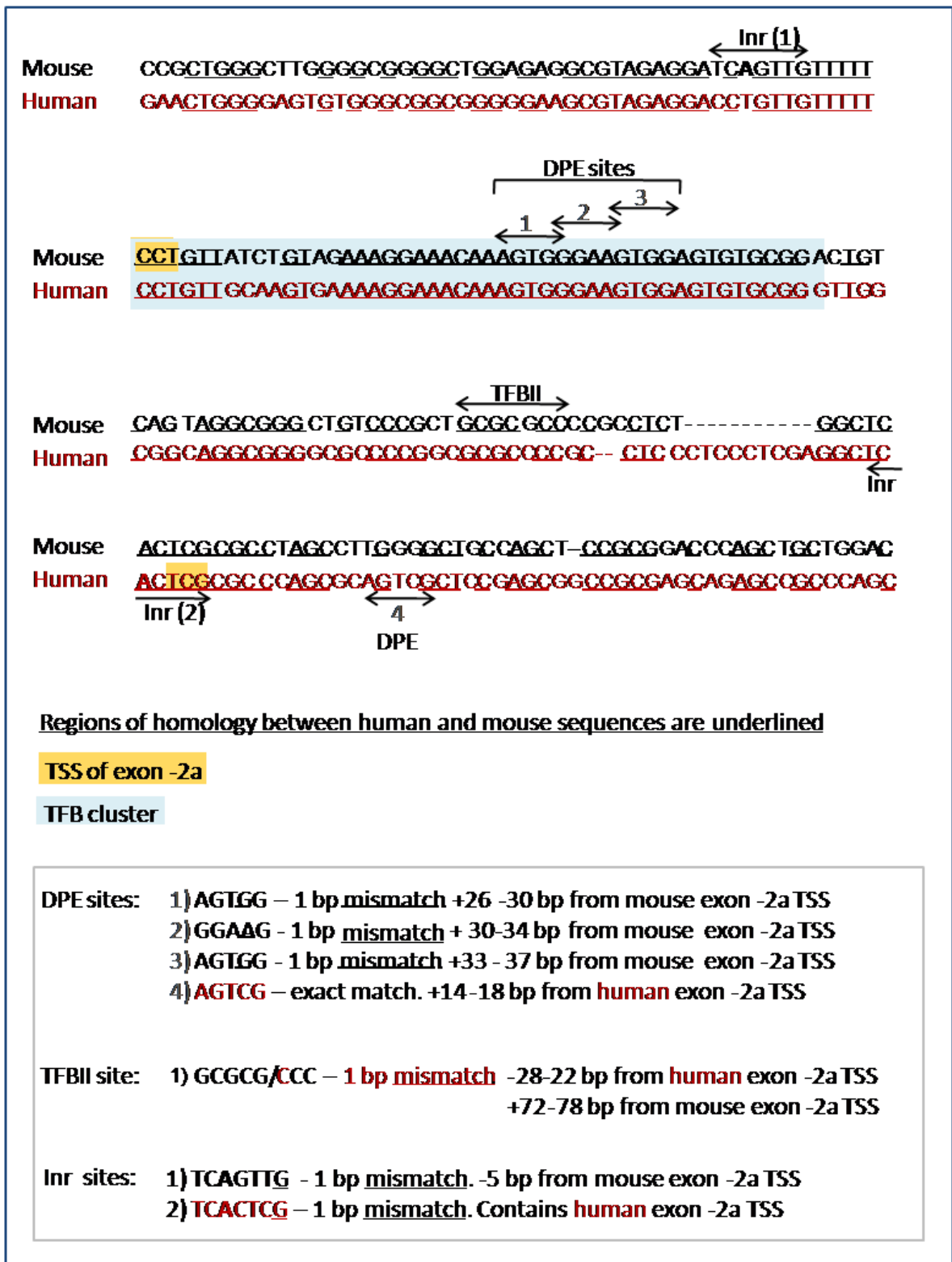
Figure 5.7: Location of putative core promoter elements for mouse and human *PIK3CD* transcripts containing exon -2a. The location of putative Inr, DPE and TFBII sites surrounding the TSS for mouse and human exon -2a.

The mechanism of transcriptional initiation from apparently TATA-less promoters is not firmly established, however it has been demonstrated that both TATA-containing and TATA-less promoters require the same basal transcription factors (Aso, *et al.*, 1994). A

possible TFIIB binding site was present on both mouse and human *PIK3CD* sequences, however given that it lies upstream of the putative Inr sequence and TSS of human exon -2a only, if this element is indeed functional, it is likely to only regulation transcription of human *PIK3CD* containing exon -2a and not mouse (Figure 5.7).

5.5.3 The TFB cluster in mouse exon -2a is the principal *PIK3CD* promoter region driving leukocyte-specific p110δ expression

Previous investigations have identified other DNA regions upstream of exon 1 and untranslated exons with relatively high promoter activity (Verrall & Vanhaesebroeck, unpublished results). A DNA fragment 185 bp upstream of the TSS in mouse exon -1 was found to be the most promising leukocyte-specific promoter. This region has TF binding sites for PU.1 (an ETS TF) and NFAT, described above, and for Oct1, a ubiquitously expressed TF that is important for B cell development (Brunner & Wirth, 2006; Pfisterer*, et al.*, 1994). In contrast, regions of genomic DNA upstream of exon 1 were found to have high promoter activity in both leukocytes and fibroblasts. It is possible that multiple promoters upstream or within untranslated exons exert leukocyte-restricted *PIK3CD* gene expression. However, *PIK3CD* transcripts containing exon -1 or exon -2a are the most abundantly expressed in a number of leukocyte cell lines tested and given that the level of *PIK3CD* transcripts containing exon -2a is almost equal to the level of *PIK3CD* transcripts containing translated exon 1 (Kok, et al., in preparation), this suggests that the majority of *PIK3CD* transcripts containing exon -1 also contain exon -2a. Corroborating these findings, quantitative real-time PCR results described in Chapter 4, demonstrated that mouse p110δ mRNA containing exon -2a contributed to ~80% of the total p110δ mRNA detected in the leukocyte cell line, A20 (Figure 4.2). These data indicate that the promoter region identified in mouse exon -2a is likely to be sufficient in mediating the majority of leukocyte-specific *PIK3CD* gene expression.

5.5.4 Possible regulation of p110δ expression by acute stimuli

The identification of leukocyte-associated TFs in the *PIK3CD* promoter raises the possibility that p110δ expression may be regulated by acute stimulation. Investigation into this area has previously been carried out, with the conclusion that p110δ is *not* regulated by acute stimulation. However, stimuli that regulate the expression and/or activation of the specific TFs identified in the TFB cluster, were not thoroughly investigated. Furthermore, it is conceivable that only certain cell types, which are capable of regulating the expression and/or activation of specific TFs that bind the TFB cluster are able to upregulate p110δ

expression. Indeed, preliminary experiments in primary endothelial cells and endothelial cell lines have shown upregulation of p110δ (and not p110α and p110β) in response to treatment with TNFα (Whitehead & Vanhaesebroeck, unpublished results). Indeed, TNFα and other pro-inflammatory stimuli have been shown to upregulate IRF in endothelial cells to regulate the transcription of inflammatory markers, such as selectins (Dagia, *et al.*, 2004; Neish, *et al.*, 1995). In addition, NFAT in endothelial cells has also been implicated in the upregulation of inflammatory cell adhesion molecules (Cockerill, *et al.*, 1995). It is tempting to speculate from these data that *PIK3CD* promoter activity is increased in endothelial cells through increased TF binding in the newly identified TFB cluster, in response to inflammatory stimuli, suggesting the role p110δ plays in inflammation is not limited to leukocytes.

5.5.5 Targeting the *PIK3CD* promoter in cancer

There are a number of instances where high expression levels of p110δ are observed in cells other than leukocytes, which are often associated with cancer, such as in breast tissue, melanoma and glioma (Sawyer, et al., 2003). No somatic mutations in *PIK3CD* have been reported, which suggests upregulation of p110δ expression occurs by some other mechanism. It is possible that upregulation or activation of leukocyte-associated TFs which bind in the newly identified TFB cluster, increases *PIK3CD* promoter activity resulting in high p110δ expression. To support this hypothesis, LEF/TCF interaction with β-catenin has been implicated in tumorigenesis, and in particular breast cancer progression (Ayyanan, *et al.*, 2006; Gebeshuber, *et al.*, 2007; Hatsell, *et al.*, 2003; Ravindranath, *et al.*, 2008). In addition, other leukocyte-associated TFs identified in the TFB cluster in mouse exon -2a, have also been implicated in breast cancer progression. For example, ETS-1 is overexpressed by invasive breast cancers and associated with poor prognosis (Span, *et al.*, 2002). Recent investigations have found ETS-1 to increase the invasive potential of mouse mammary tumour cells, through promoting hepatocyte growth factor activation and c-Met receptor overexpression (Furlan, *et al.*, 2008). ETS-2 mRNA has also found to be upregulated in breast tissue carcinomas compared to normal breast tissue (Buggy, *et al.*, 2006). The TF NFAT3 acts as a transcriptional coactivator of estrogen receptors (ERα and ERβ) and was found to enhance ER transcriptional activity in breast cancer cells and play an important role in regulation of breast cancer cell growth (Zhang, *et al.*, 2005). Recently, one study has implicated all 4 of the leukocyte-associated TFs identified in the TFB cluster in mouse exon -2a, in breast cancer progression. Using a computer program to analyse alterations in gene transcription of TFs in breast cancer from 6 of the largest microarray

cancer datasets, NFAT, IRF, ETS2 and LEF1 were in the 20 most frequently mapped TFs with differential activation (Teschendorff, *et al.*, 2007), although from this study it is not clear whether the alterations confer increased or decreased TF activation. From these observations, it is feasible that high p110δ expression observed in breast cancer tissue may result from increased *PIK3CD* promoter activity due to increased TF activation and DNA binding.

The results presented in this chapter shed some light onto the leukocyte-restricted expression of p110δ, however they can only lead to speculation regarding the nature of p110δ regulation in disease settings. Further investigations are needed to identify which TF binding sites are critical in driving *PIK3CD* gene expression. It would be interesting to analyse the promoter activity of mouse exon -2a in breast cancer cells and other non-leukocyte cells which express high levels of p110δ, to examine whether these cells, unlike other non-leukocyte cells tested, are able to utilize this promoter. Regulation of the promoter activity of *PIK3CD* may offer a novel therapeutic target for cases of aberrant p110δ expression.

6. STABLE RETROVIRAL INFECTION OF HUMAN ᴘ110δ cDNA IN THE NIH 3T3 CELL LINE

6.1 Introduction

Retroviral-mediated transfection has been employed in a number of studies investigating the effect of PI3K overexpression. For example, successful overexpression of p110α-3'CAAX and p110δ-3'CAAX in BMMCs has been achieved using the retroviral vectors pBabe or pMX-neo (Kinashi, et al., 1999; Kinashi, *et al.*, 2000). Furthermore, stable NIH 3T3 cell lines expressing a myristylated p110α were created using the retroviral mammalian expression vector pLNCX (Auger, et al., 2000). In an additional study, stable overexpression of myristylated p110α, p110β, p110γ and p110δ in Rat1 fibroblasts has also been achieved (Link, et al., 2005), using the retroviral vector pWZL-Blast, which is based on pBabe. It is interesting to note though that in each case of stable overexpression, the p110 subunit was modified by a membrane-localization signal.

Recently, untagged p110β, γ, δ isoforms were successfully overexpressed using the avian retroviral RCAS system in primary cultures of chicken embryo fibroblasts (Kang, et al., 2006). All 3 isoforms were found to induce the formation of transformed cell foci. Fusion of a myristylation signal to the N-terminus of p110 isoforms enhanced their oncogenic transforming ability, although p110δ and p110γ isoforms had potent transforming ability without the myristylation signal. Although overexpression of all three p110 isoforms was achieved leading to cell transformation, this did not lead to full immortalisation of the cells, which could only be maintained in culture for approximately 3-4 weeks (Vogt, P., Personal communication to Bart Vanhaesebroeck).

It is possible that the retroviral method of gene delivery into the cell induces higher gene expression than transfection of plasmid cDNA, therefore leading to effective protein expression. The human p110δ gene in a retroviral expression vector system was available to us (a gift from Tatsuo Kinashi (Kinashi, *et al.*, 2000)) for transfection of NIH 3T3 cells. This p110δ cDNA contained the coding region of p110δ (no 5' untranslated p110δ exons) with additional DNA sequences encoding an N-terminal Myc tag, which has the potential to stabilise p110 (Yu, *et al.*, 1998a), and a membrane-targeting CAAX sequence at the C-terminus.

6.2 Retroviral infection of 5'Myc-p110δ-3'CAAX and 5'Myc-p110α-3'CAAX in NIH 3T3 cells

6.2.1 p110δ can be stably overexpressed through retroviral infection of 5'Myc-p110δ-3'CAAX cDNA in NIH 3T3 cells

5'Myc-p110δ-3'CAAX was introduced into NIH 3T3 cells in a pMX-neo retroviral vector (see section 2.12.2 for vector maps) through retroviral infection. Infected cells were selected with neomycin and total cell lysate analysed for p110δ expression. A significant increase in p110δ expression was observed in transfected NIH 3T3 cells compared to WT NIH 3T3 cells, which corresponded to around half of that found in bone marrow-derived macrophages (Figure 6.1). This result indicates that despite the previous difficulties described in Chapter 4, stable overexpression of p110δ in NIH 3T3 cells is achievable, raising the question of whether this is as a result of the retroviral system used, the presence of a potentially stabilizing 5'Myc tag, the presence of the membrane targeting 3'CAAX motif, or a combination of all three.
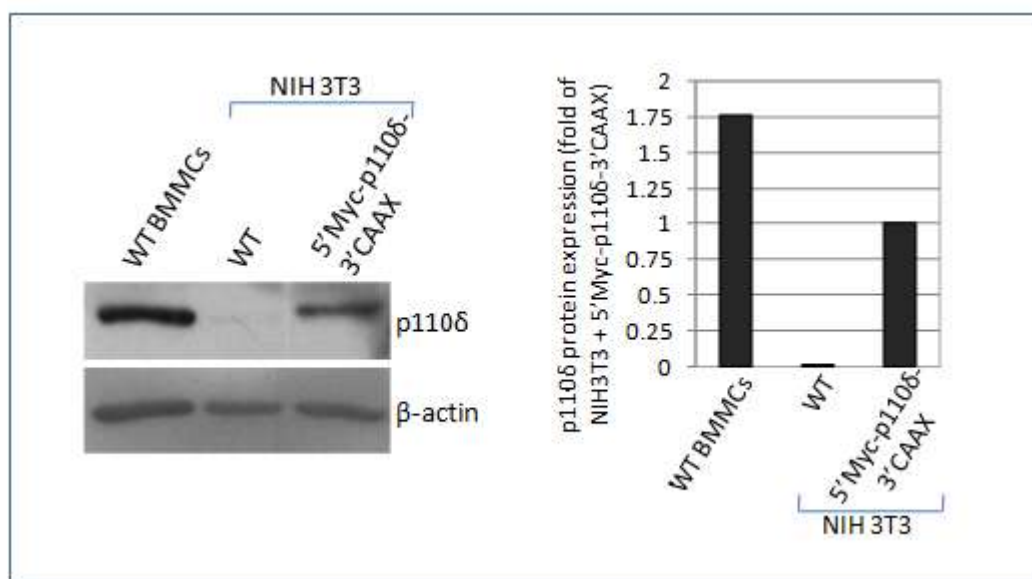
Figure 6.1: Stable expression of 5'Myc-p110δ-3'CAAX in NIH 3T3 cells by retroviral infection. 5'Myc-p110δ-3'CAAX in pMX-neo retroviral vector expressed in packaging cells was used for retroviral infection of NIH 3T3 cells. Stable transfectants were selected with neomycin and colonies pooled. Cell lysates were separated by SDS-PAGE and immunoblotted for p110δ. Total cell lysate from wild type bone marrow-derived mast cells (WT BMMCs) was run on the same gel to compare p110δ expression.

6.2.2 Stable overexpression of 5'Myc-p110δ-3'CAAX but not 5'Myc-p110α-3'CAAX results in high levels of constitutive phosphorylation of Akt

Packaging cells expressing 5'Myc-p110α-3'CAAX in pMX-neo retroviral vector were also accessible to us (a gift from Tatsuo Kinashi). To investigate whether this system could also give rise to p110α overexpression, NIH 3T3 cells were retrovirally infected with 5'Myc-

p110α-3'CAAX. In comparison to cells overexpressing 5'Myc-p110δ-3'CAAX, the exogenously expressed p110α was not as easily detected (although still detectable) in total cell lysates as the exogenously expressed p110δ (Figure 6.2a).
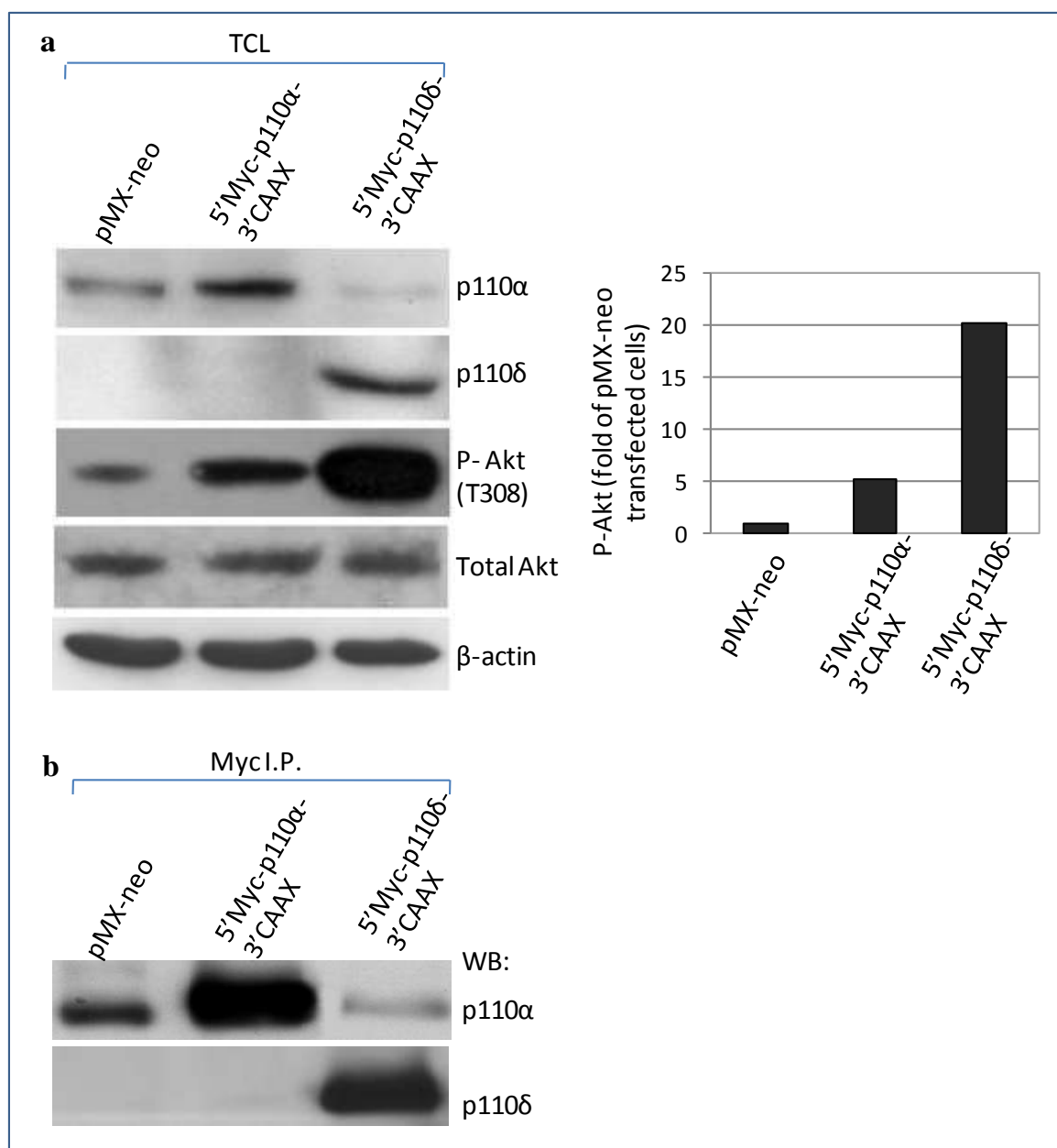
Figure 6.2: Stable expression of 5'Myc-p110δ-3'CAAX and 5'Myc-p110α-3'CAAX in NIH 3T3 cells by retroviral infection. 5'Myc-p110δ-3'CAAX and 5'Myc-p110α-3'CAAX in pMX-neo retroviral vector expressed in packaging cells were retrovirally infected into NIH 3T3 cells. Stable transfectants were selected with neomycin and colonies pooled. **(a)** Cell lysates were separated by SDS-PAGE and immunoblotted for p110α, p110δ and P-Akt. P-Akt levels are also represented graphically. **(b)** Cell lysates were subjected to an immunoprecipitation with an anti-Myc antibody and immunoblotted for p110α and p110δ.

Interestingly, NIH 3T3 cells stably overexpressing 5'Myc-p110δ-3'CAAX displayed considerably high basal levels of phosphorylated Akt compared to pMX-neo control

infected cells and 5'Myc-p110α-3'CAAX infected cells. NIH 3T3 cells overexpressing 5'Myc-p110δ-3'CAAX also appeared to express lower levels of p110α compared to pMX-neo control infected cells, an issue which is further discussed in section 7.2.1. An immunoprecipitation with an anti-Myc antibody clearly showed overexpression of 5'Myc-p110α or 5'Myc-p110δ where the corresponding constructs had been infected, compared to control infected cells (Figure 6.2b).

The activation of Akt in 5'Myc-p110α-3'CAAX or 5'Myc-p110δ-3'CAAX infected cells was further investigated under serum-starvation conditions and serum-stimulated conditions. Similarly to under basal growing conditions, NIH 3T3 cells overexpressing 5'Myc-p110δ-3'CAAX displayed the highest level of phosphorylated Akt under starvation conditions, which could be increased slightly further upon FBS stimulation (Figure 6.3).
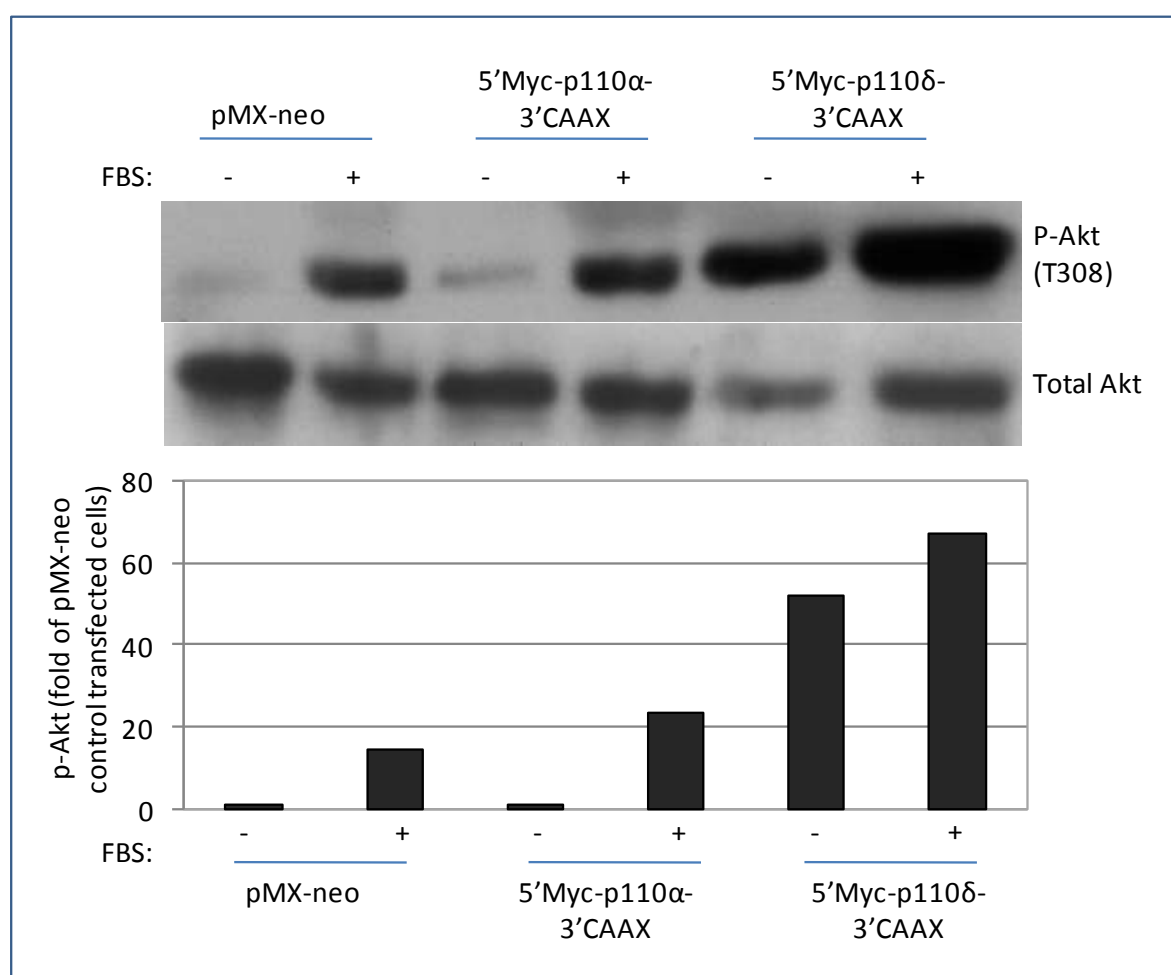
Figure 6.3: Akt phosphorylation in NIH 3T3 cells stably overexpressing of 5'Myc-p110δ-3'CAAX or 5'Myc-p110α-3'CAAX. NIH 3T3 cells stably infected with pMX-neo control vector, 5'Myc-p110α-3'CAAX or 5'Myc-p110δ-3'CAAX were starved of serum overnight. The following day, cells were stimulated with 10% FBS for 5 min. Cell lysates were separated by SDS-PAGE and immunoblotted for P-Akt.

NIH 3T3 cells overexpressing 5'Myc-p110α-3'CAAX displayed only a small increase in Akt phosphorylation under starvation and FBS stimulated conditions compared to pMX-neo control infected cells (Figure 6.3). These results indicate that expression 5'Myc-p110δ-3'CAAX in NIH 3T3 cells has a greater impact on Akt phosphorylation compared to 5'Myc-p110α-3'CAAX.

6.3 Cloning of 5'Myc-p110δ, p110δ-3'CAAX, and untagged p110δ into the pMX-neo retroviral vector

Retroviral infection of 5'Myc-p110δ-3'CAAX into NIH 3T3 cells gave rise to a substantial overexpression of p110δ. To assess the importance of the 5'Myc tag and the membrane-targeting 3'CAAX motif, untagged p110δ, 5'Myc-p110δ and p110δ-3'CAAX human cDNAs were cloned into the pMX-neo retroviral vector (Figure 6.4).
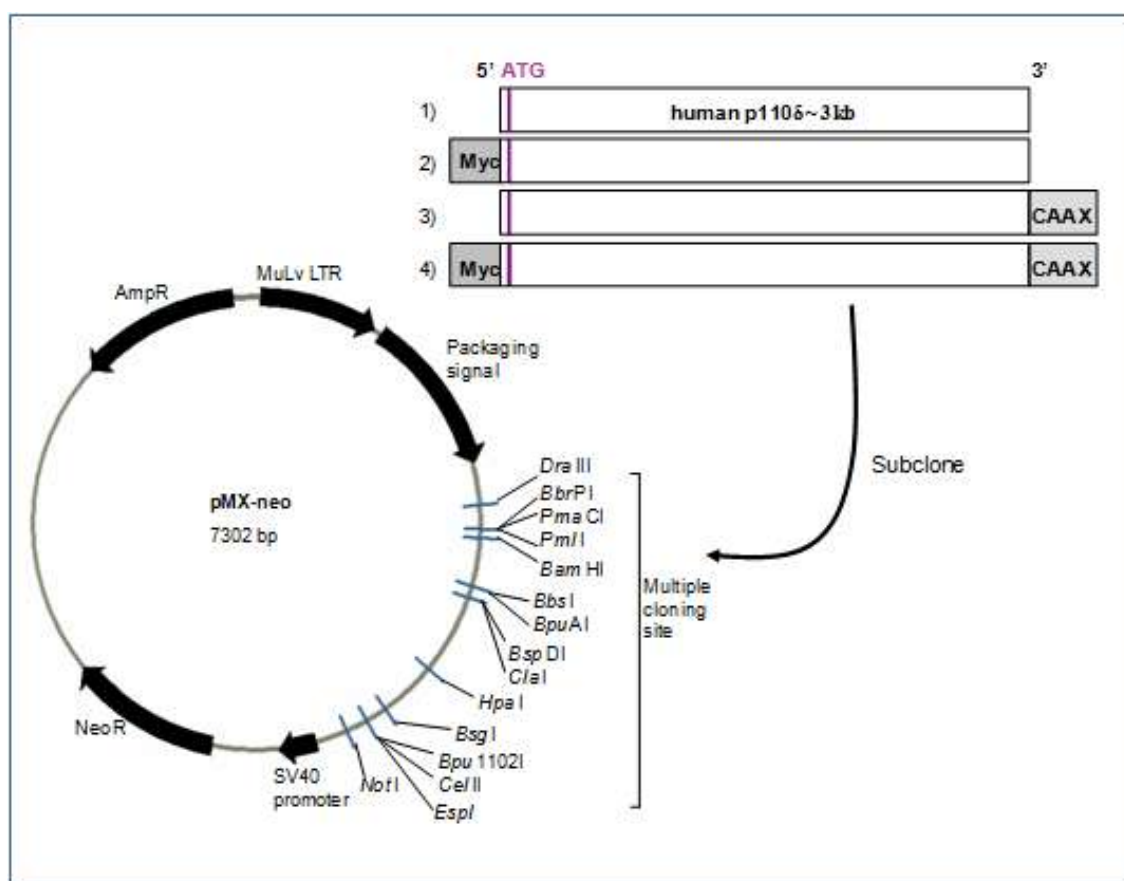
Figure 6.4: Schematic of cloning strategy to insert untagged p110δ, 5'Myc-p110δ and p110δ-3'CAAXcDNA into the pMX-neo retroviral vector. Construct number 4, 5'Myc-p110δ-3'CAAX, was available expressed in pMX-neo, therefore no further cloning was required for this construct. A more detailed description of the cloning strategy for the other p110δ constructs can be found in material methods, section 2.12.2.

6.3.1 Retroviral infection of untagged p110δ and p110δ-3'CAAX gives rise to Gag-p110δ fusion protein in GPE86 packaging cells and NIH 3T3 cells

Once the p110δ constructs had been successfully cloned into pMX-neo (cloning strategies can be found in section 2.12.2), a viral packaging cell line (GPE86) stably expressing each of the constructs was created, for future retroviral infection of NIH 3T3 cells. Total cell lysates were made from GPE86 cells stably expressing each p110δ construct to check p110δ protein expression (Figure 6.5a).
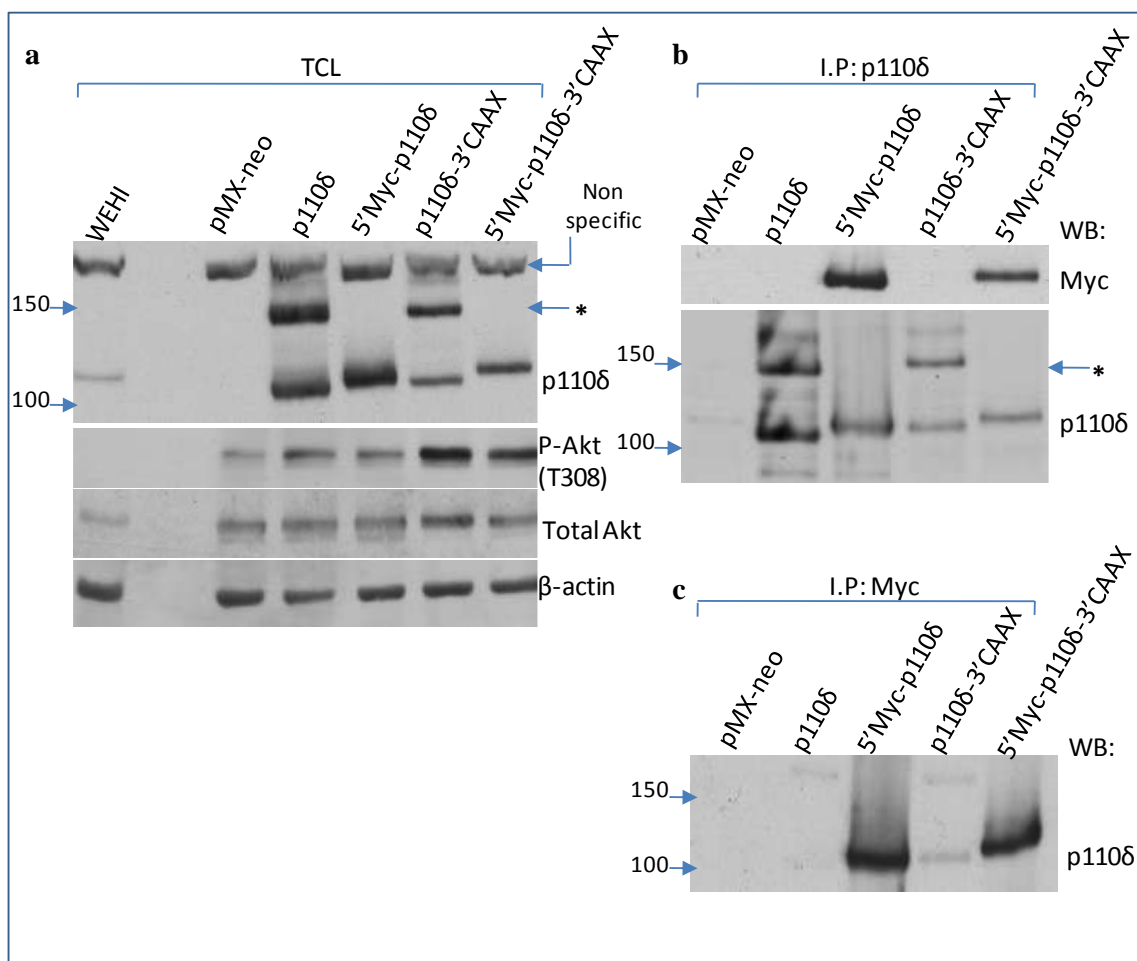
Figure 6.5: p110δ protein expression in the GPE86 packaging cell line stably expressing untagged p110δ, 5'Myc-p110δ, p110δ-3'CAAX and 5'Myc-p110δ-3'CAAX in the pMX-neo retroviral vector. (a) Cell lysates from GPE86 cells stably expressing the indicated p110δ constructs were separated by SDS PAGE and immunoblotted for p110δ and P-Akt. The asterisk indicates the higher molecular weight protein that immunoblots with the anti-p110δ antibody **(b)** Cell lysates were subjected to an immunoprecipitation with an anti-p110δ antibody and immunoblotted for Myc and p110δ. **(c)** Cell lysates were subjected to an immunoprecipitation with an anti-Myc antibody and immunoblotted for p110δ. The asterisk indicates the presence of the higher molecular weight proteins that are detected with the p110δ antibody.

Immunoblotting the total cell lysates for p110δ revealed substantial overexpression of p110δ for all of the p110δ constructs transfected compared to control transfected cells,

however it was also noticed that an additional band was present at around 130 kDa in GPE86 cells stably expressing untagged p110δ and p110δ-3'CAAX (i.e. in the absence of a 5'Myc-tag). This protein was also present in p110δ immunoprecipitates of GPE86 cells stably expressing untagged p110δ and p110δ-3'CAAX only (Figure 6.5b). Immunoprecipitation either with an antibody to p110δ or Myc confirmed the presence of the Myc tags in 5'Myc-p110δ and 5'Myc-p110δ-3'CAAX transfected GPE86 cells (Figure 6.5b, c).

Similar observations were made in NIH 3T3 cells retrovirally infected with the p110δ constructs. The appearance of a higher molecular weight band (~130 kDa) was detected after immunoblotting with an anti p110δ antibody in NIH 3T3 cells stably expressing untagged p110δ and p110δ-3'CAAX constructs only (marked with * in Figure 6.6). In fact, a second higher molecular weight protein (~120 kDa) could also be detected in NIH 3T3 cells infected with untagged p110δ and p110δ-3'CAAX constructs, (marked with ** in Figure 6.6), which was particularly apparent in cells expressing untagged p110δ. However, this band was much less prominent than the band observed at ~130 kDa.
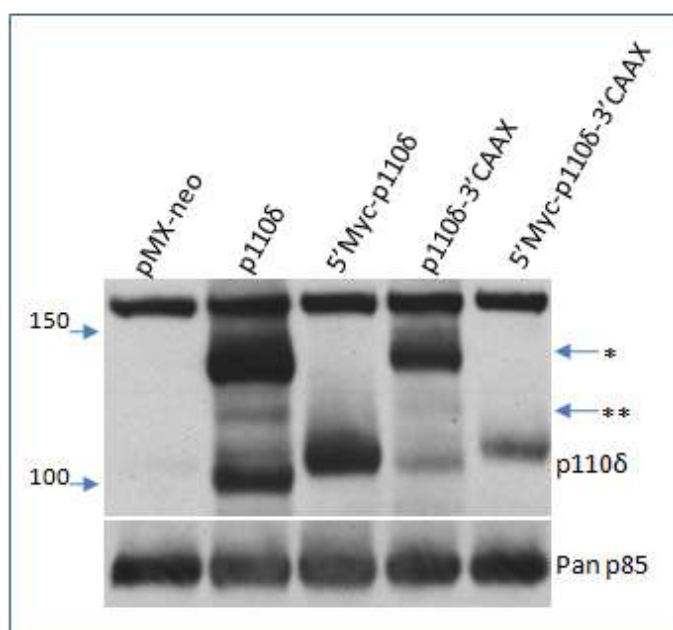
Figure 6.6: p110δ protein expression in NIH 3T3 cells stably infected with untagged p110δ, 5'Myc-p110δ, p110δ-3'CAAX and 5'Myc-p110δ-3'CAAX in the pMX-neo retroviral vector. Cell lysates from NIH 3T3 cells stably expressing the indicated p110δ constructs through retroviral infection were separated by SDS-PAGE and immunoblotted for p110δ and pan-p85. The asterisks indicate the higher molecular weight proteins revealed upon immunoblotting with the anti-p110δ antibody.

It was conceivable that the higher molecular weight protein that reacts with the p110δ antibody may have represented a modified p110δ protein, a modification that occurs at the

N-terminus of the protein that is prevented by the presence of a 5'Myc tag. To investigate the nature of the higher molecular weight protein and the possibility of a p110δ modification, the 130 kDa protein was isolated by SDS-PAGE and analysed by mass spectrometry.
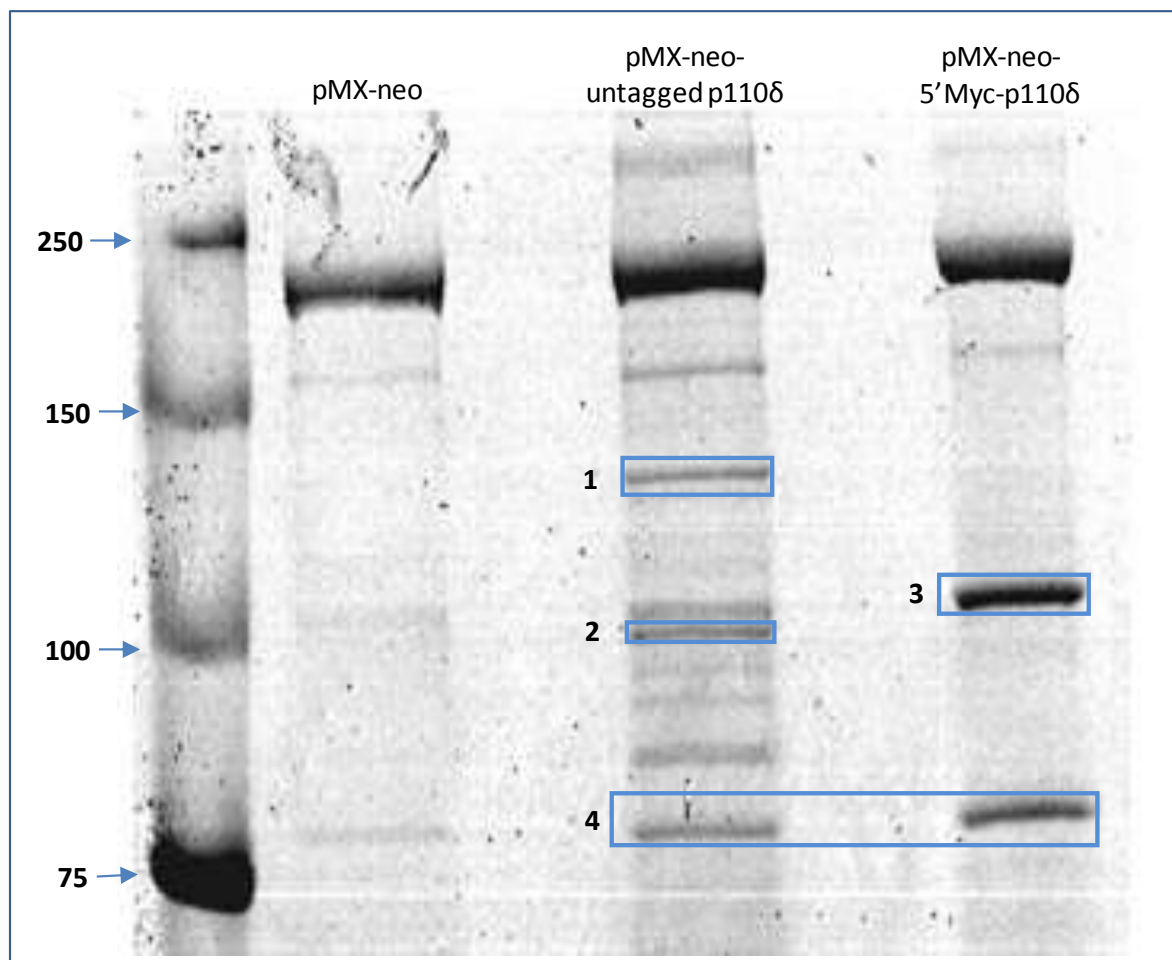
Figure 6.7: Coomassie-stained gel of p110δ immunoprecipitates of the indicated cell lines. Cell lysates from NIH 3T3 cells stably expressing pMX-neo, untagged-p110δ and 5'Myc-p110δ were subjected to immunoprecipitation using a p110δ antibody directed against the C-terminus, followed by separation by SDS-PAGE. Immunoprecipitates were visualized by colloidal Coomassie blue staining. The gel fragments indicated were excised and subjected to mass spectrometry analysis.

The four gel fragments indicated in Figure 6.7 were excised and subjected to mass spectrometry analysis. Fragment 1 represented the potential modified p110δ protein, however it was revealed that this fragment actually consisted of transfected human p110δ and a viral Gag protein. Closer inspection of the pMX-neo retroviral vector exposed a translational 'ATG' start site in the viral packaging sequence that was in frame with the translational start site of p110δ. This translational start site encodes 275 amino acids with a corresponding molecular weight of 30.7 kDa. The protein resulting from this translational start site is in fact a viral Gag-p110δ fusion protein. Where a 5'Myc-tag is present in the

p110δ insert, the 'ATG' in the viral packaging sequence is no longer in frame of the translational start site of p110δ, preventing the formation of a viral Gag-p110δ fusion protein. As expected, excised fragments 2 and 3 were found by mass spectrometry to be untagged human p110δ and Myc-tagged p110δ, respectively. Therefore, transfection of untagged p110δ in pMX-neo retroviral vector gives rise to two proteins; Gag-p110δ and untagged p110δ. As anticipated, the two fragments excised in box 4, consisted of a mixture of p85α and p85β.

6.4 Cloning of untagged and p110δ-3'CAAXinto pMXs-neo

An improved pMX-neo retroviral vector, called pMXs-neo, in which the ATG responsible for the translation of the viral Gag protein had been removed was provided for us by Tatsuo Kinashi (Kinashi, et al., 2000).
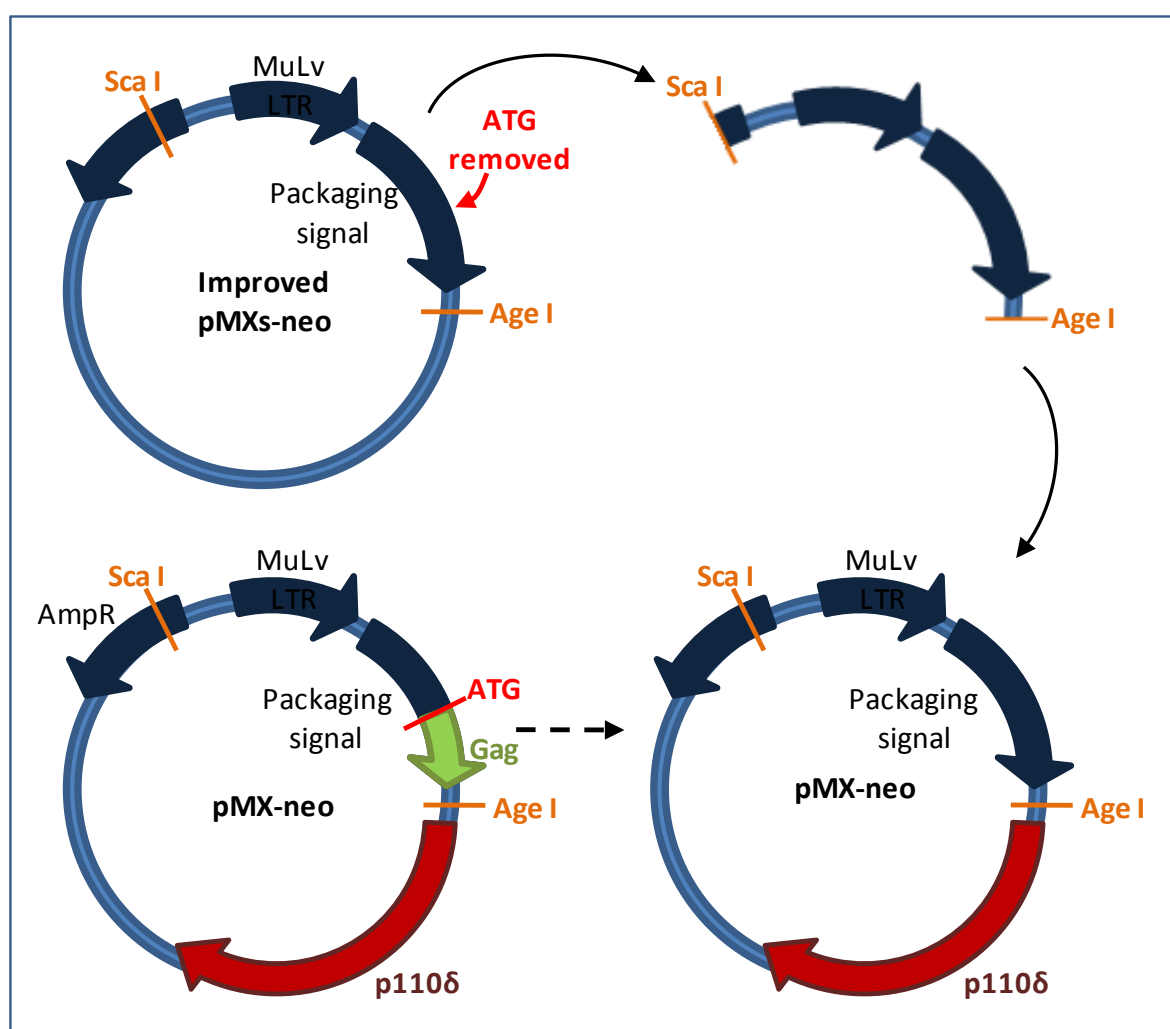
Figure 6.8: Schematic of cloning strategy to introduce the packaging sequence of pMXs-neo into pMX-neo-p110δ constructs. pMXs-neo and pMX-neo-p110δ constructs were digested with the restriction enzymes *Sca* I and *Age* I and the packaging signal sequence of pMXs-neo cloned into pMX-neo-p110δ constructs.

The group led by Tatsuo Kinashi had also experienced problems with the gene expression in pMX-neo retroviral vector leading to Gag-fusion proteins, which had led to the development of the improved pMXs-neo. It was assumed that expression of the p110δ constructs in this vector would prevent the formation of viral Gag-p110δ fusion proteins. The sequence for pMX-neo and pMXs-neo only differ in the viral packaging portion of the vector, therefore rather than cloning the p110δ constructs into the new pMXs-neo vector, the viral packaging sequence of pMX-neo was replaced with the new pMXs-neo sequence (Figure 6.8).

6.4.1 Overexpression of untagged and p110δ-3'CAAX in pMXs-neo in NIH 3T3 cells also gives rise to Gag-p110δ fusion protein expression

The new pMXs-neo-p110δ constructs were infected into NIH 3T3 cells. Once again, transfection of untagged or p110δ-3'CAAX resulted in the expression of a higher molecular weight protein that immunoblotted with p110δ (marked by ** in Figure 6.9). This protein had a molecular weight of around 120 kDa, as a opposed to the 130 kDa protein observed in the previous viral Gag-p110δ fusion protein product (marked by * in Figure 6.9). In fact, a protein of this molecular weight (~120 kDa) had also been detected in previous transfections of NIH 3T3 cells with untagged p110δ and p110δ-3'CAAX in pMX-neo (indicated by ** in Figure 6.6), although not expressed as strongly.

Analysis of the new pMXs-neo packaging sequence uncovered a second 'ATG' translational start site in frame with the translational start site of p110δ, which was downstream of the first detected viral Gag translational start site. This second translational start site encoded 110 amino acids with a corresponding molecular weight of 12.3 kDa, which is consistent with the second 120 kDa protein being another viral Gag-p110δ fusion protein. This finding was extremely disappointing especially as the formation of a second viral Gag-p110δ fusion protein could have been foreseen from previous NIH 3T3 p110δ-transfections and by paying closer attention to the pMXs-neo DNA sequence. In retrospect, more time should have been spent looking into the potential problems of using the seemingly improved retroviral vector.

The effect of this 12.3 kDa viral protein on p110δ function is unclear, and results obtained using cells overexpressing Gag-p110δ should be treated with caution. However, NIH 3T3 cells overexpressing 5'Myc-p110δ (which do not express a viral Gag-p110δ) and NIH 3T3 cells overexpressing untagged p110δ and p110δ-3'CAAX (both of which contain viral Gag-p110δ fusion proteins) all have barely detectable levels of p110α expression and high

basal levels of Akt phosphorylation (Figure 6.9), consistent with previous results illustrated in Figure 6.2. This suggests that the presence of a Gag-fusion protein is not involved with the apparent downregulation of p110α, but it is in fact as a result of overexpression of unmodified p110δ.
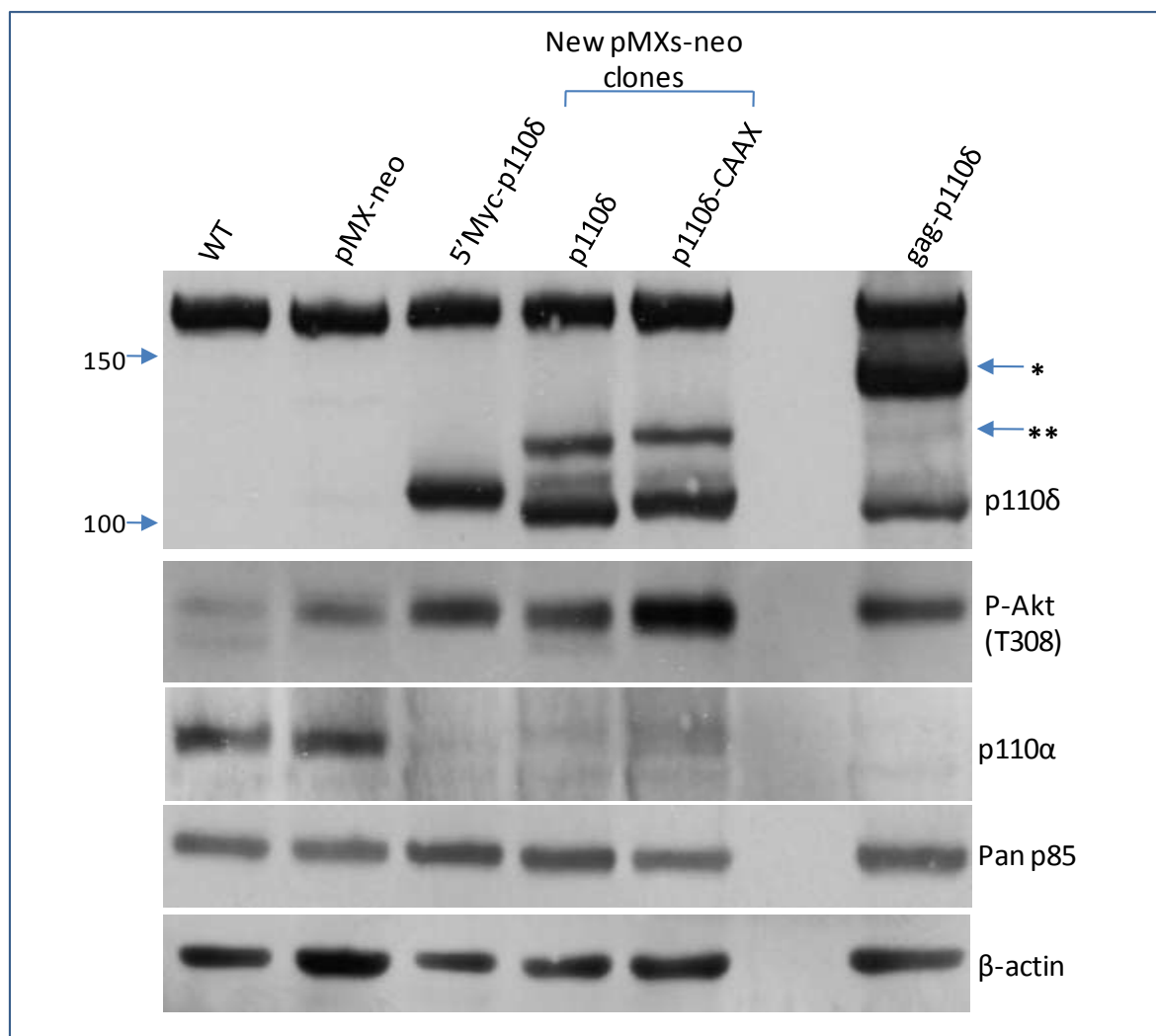
Figure 6.9: p110δ expression in NIH 3T3 cells stably infected with untagged p110δ and p110δ-3'CAAX expressed in pMXs-neo and 5'Myc-p110δ-3'CAAX expressed in the pMX-neo retroviral vector. Cell lysates from NIH 3T3 cells stably expressing the indicated p110δ constructs were separated by SDS-PAGE and immunoblotted for p110δ, P-Akt, p110α and pan-p85. Total cell lysate from NIH 3T3 cells expressing viral Gag-p110δ (Gag-p110δ) was included as a positive control for the presence of Gag-p110δ fusion protein. * indicates the first viral Gag-p110δ found and ** indicates the second lower molecular weight viral Gag-p110δ from the new pMXs-neo clones.

6.4.2 Overexpression of Gag-p110δ in NIH 3T3 cells has a different impact on cell morphology compared to overexpression of 5'Myc-p110δ or 5'Myc-p110δ-3'CAAX

As mentioned above, the effect of the 12.3 kDa viral protein has on p110δ function is not known and results obtained using cells overexpressing Gag-p110δ should be treated with caution. However, before the nature of the p110δ 'modification' was known, some studies

had already been carried out looking at the impact of p110δ overexpression on cell morphology.

The characterisation of NIH 3T3 cells overexpressing 5'Myc-p110δ is discussed in detail in the next chapter, but is summarised briefly here. In the presence of serum both 5'Myc-p110δ and 5'Myc-p110δ-3'CAAX overexpressing cells adhere over a greater surface area and display a more spread morphology compared to pMX-neo control infected cells (Figure 6.10). In contrast, NIH 3T3 cells expressing a Gag-p110δ fusion protein, either Gag-p110δ or Gag-p110δ-3'CAAX, do not have a spread morphology but more closely resemble pMX-neo control infected cells. In cells expressing p110δ with both an N-terminus Gag fusion and C-terminus membrane CAAX motif, increased focal contacts were observed (assessed by expression of phosphorylated FAK) which colocalized with F-actin puncta.

The difference between Gag-p110δ and 5'Myc-p110δ expressing NIH 3T3 cells becomes more apparent under serum-starvation conditions (Figure 6.11). Gag-p110δ expressing cells looked apoptotic with a rounded morphology. Gag-p110δ expressing cells were found in small clusters, which displayed high levels of phospho-FAK staining, with F-actin surrounding the nucleus only. In contrast, 5'Myc-p110δ expressing NIH 3T3 cells maintained a more spread morphology compared to pMX-neo control infected cells.
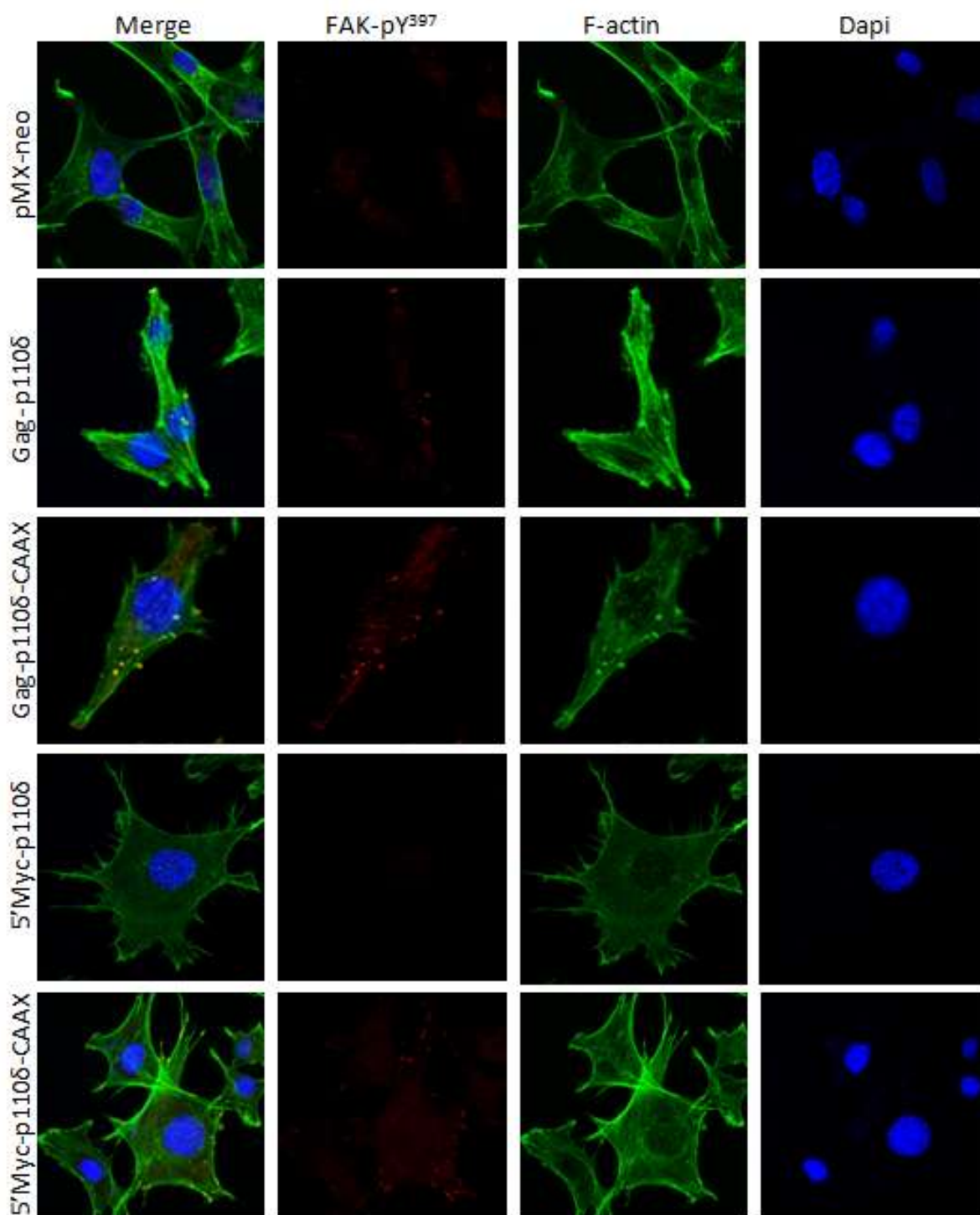
Figure 6.10: Cell cytoskeleton of Gag-p110δ and Gag-p110δ-3'CAAX overexpressing NIH 3T3 cells in normal growing conditions. Cells were seeded in media containing 10% FBS on glass coverslips in a 12-well plate and left to adhere overnight. The following day cells were fixed and stained for focal adhesions (phospho-FAK), F-actin (phalloidin), DNA (DAPI).
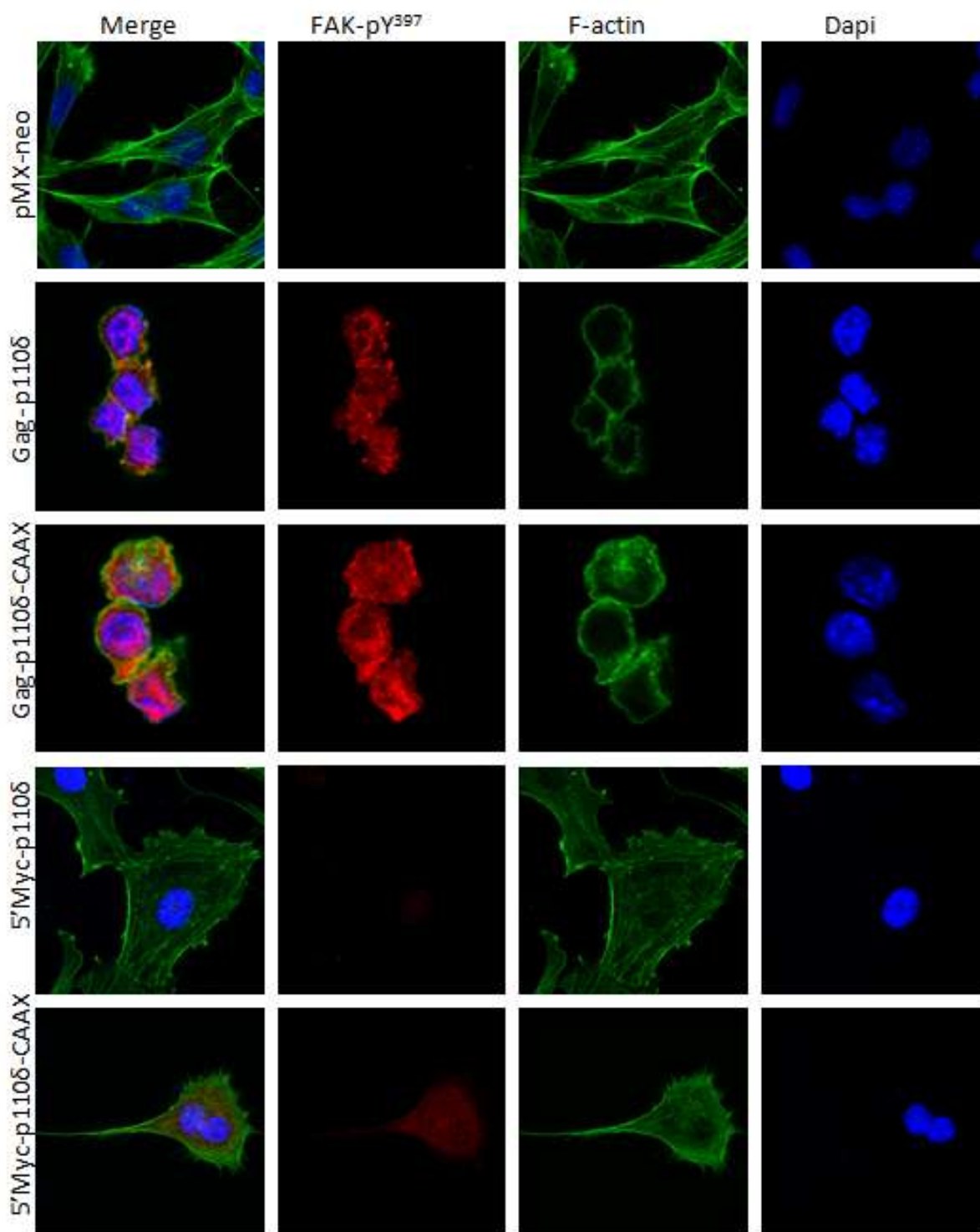
Figure 6.11: Cell cytoskeleton of Gag-p110δ and Gag-p110δ-3'CAAX overexpressing NIH 3T3 cells under serum-starvation conditions. Cells were seeded in media containing 10% FBS on glass coverslips in a 12-well plate and left to adhere for 6 h. After this time, media containing serum was replaced with starvation media (0% serum). The following day cells were fixed and stained for focal adhesions (phospho-FAK), F-actin (phalloidin), nuclear material (DAPI).

6.5 Discussion

6.5.1 Stable overexpression of p110δ in NIH 3T3 cells using pMX-neo retroviral vectors

Retroviral-mediated transfection has proved to be a highly successful way of stably overexpressing PI3K isoforms (Auger, et al., 2000; Kang, et al., 2006; Kinashi, et al., 1999; Kinashi, et al., 2000; Link, et al., 2005). In all but one of these studies, a membrane targeting motif has been employed to investigate overexpression of a constitutively active p110. Previous attempts to stably overexpress p110δ through transfection of full length p110δ cDNA in non-retroviral mammalian expression vectors were not hugely successful, as described in chapter 4. Using the retroviral expression vector, pMX-neo, the ability of the retroviral system to overexpress p110δ has been investigated.
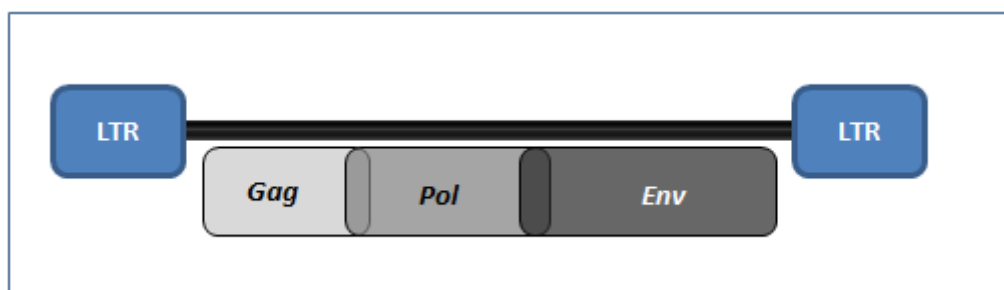
Figure 6.12: The Mo-MuLV genome

The pMX-neo retroviral vector contains the LTRs (long terminal repeats) of the Moloney murine leukaemia virus (Mo-MuLV). The Mo-MuLV has a very simple genome, which can be divided into three transcriptional units: *Gag, Pol* and *Env* (Figure 6.12). The LTR regions are found at either end of the gene and are important for initiating viral DNA synthesis and viral DNA integration into the host's genome (Barquinero*, et al.*, 2004). The *Gag* region encodes genes that comprise the capsid proteins which encapsulate the viral genetic material. In retroviral vectors, the viral genes located between the LTR regions are replaced with genes of interest. Transfection of retroviral vectors into packaging cell lines, which provide all the viral proteins (*Gag*, *Pol* and *Env* gene products) results in the production of mature viral particles containing the gene of interest, which can subsequently be infected into mammalian cells (Paar*, et al.*, 2007).

Retroviral vector-mediated gene transfer is advantageous over other mammalian expression vectors in that they have superior gene transfer efficiency and provide a high degree of stable integration of exogenous DNA into the host's genome. For the first time during the course of my PhD work, introduction of a p110δ cDNA gave rise to a substantial

constitutive overexpression of p110δ in NIH 3T3 cells. To ascertain whether stable p110δ overexpression was as result of the retroviral system used, the presence of a 5'Myc tag or a 3' membrane targeting CAAX motif, untagged p110δ, 5'Myc-p110δ and p110δ-3'CAAX were cloned into pMX-neo and also subsequently into the slightly modified pMXs-neo. Unfortunately, both retroviral vectors resulted in the production of p110δ-Gag fusion proteins when the p110δ cDNA used did not contain a 5'Myc tag. This was the result of viral Gag translational start sites being in frame with the translational start site of p110δ.

All retroviral vectors contain a packaging signal, which is a region adjacent to the 5'LTR which is involved in the packaging of viral genetic material into virions. The packaging signal for Mo-MuLV has been found to extend into the *Gag* region, indeed inclusion of a portion of the *Gag* region in different retroviral vectors has been found to increase the amount of vector RNA secreted by virus-producing cells (Bender*, et al.*, 1987). It is likely that the inclusion of a portion of the *Gag* sequence in the pMX-neo packaging signal was a feature intended to result in a high viral titer and enhanced viral infection of target cells. Irrefutably, expression of p110δ cDNA in pMX-neo resulted in considerable p110δ overexpression, however in the absence of a stop codon upstream of the translational start site of p110δ, a Gag-p110δ fusion protein was produced.

In hindsight, more careful inspection of the pMX-neo and pMXs-neo sequences and location of the p110δ cDNA inserts, could have avoided the time spent cloning p110δ constructs in pMXs-neo and analysing the nature of what was thought of as a potential p110δ modification.

6.5.2 Expression of viral Gag-cellular fusion proteins in mammalian cells

In the ASV16 oncovirus, which causes rapidly growing hemangiosarcomas in young chickens an induces oncogenic transformation in cultured chicken embryo fibroblasts (Chang*, et al.*, 1997), a defective retrovirus codes for a single protein consisting of viral Gag sequences fused to a cell-derived insert. The cellular sequence was found to contain most of the coding region for p110α. The newly identified oncogenic Gag-p110α fusion protein was termed P3K (Vogt*, et al.*, 2006). In addition to an N-terminal fusion with a partial Gag sequence, P3K also contains several point mutations (Chang, et al., 1997) and it was considered that the point mutations rather than Gag may confer P3K with its oncogenicity, which led to further investigations into the oncogenic potential of p110α (Aoki*, et al.*, 2001; Aoki*, et al.*, 2000; Kang*, et al.*, 2005).

Studies in which the wild-type cellular p110α sequence was cloned into the RCAS avian replication-competent retroviral expression vector and introduced into chicken embryo fibroblasts, did not induce generalize cell transformation but only the appearance of a few rare foci that emerged 2-3 weeks after incubation (Aoki, et al., 2000; Vogt, et al., 2006). Analysis of p110α in these foci showed that in every case the cellular sequences had become fused to partial Gag sequences, the length of the Gag sequences differing from focus to focus (Aoki, et al., 2000; Vogt, et al., 2006). In these transformation events, the oncogenicity of p110α derives from a peculiarity of the RCAS vector system which generates random fusions between Gag and the cellular insert in the course of RCAS viral replication (Vogt, et al., 2006). Using the RCAS avian replication-competent retroviral expression vector, the point mutations identified in p110α were found to not be essential for oncogenic transformation, but rather the N-terminal fusion of p110α to Gag (Aoki, et al., 2000).

Viral Gag proteins translocate to the plasma membrane and this seems to be the most likely function leading to activation of oncogenic p110α. Indeed, the addition of a myristylation signal to the N-terminus of cellular p110α or the addition of a farnesylation signal to the C-terminus, which both serve to target p110α to the plasma membrane, lead to increased oncogenicity (Aoki, et al., 2000). In oncogenic viral p110α, deletion of the p85-binding region and mutational inactivation of the Ras-binding domain do not abolish p110α oncogenicity, suggesting that membrane-bound p110α is constitutively active and is independent of p85 or Ras (Aoki, et al., 2000; Vogt, et al., 2006).

From the results presented in this chapter, the expression of Gag-p110δ in NIH 3T3 cells was found to have a severe impact of cell morphology under conditions of serum-starvation. It appears that this effect is not simply the result of plasma-membrane localization and constitutive activation of p110δ, given that expression of 5'Myc-p110δ with a membrane targeting 3'CAAX motif did not result in a similar phenotype. In fact, expression of 5'Myc-p110δ-3'CAAX resulted in higher levels of basal Akt phosphorylation compared to cells expressing Gag-p110δ, which had the same level of basal Akt phosphorylation as cell expressing the cytoplasmic 5'Myc-p110δ. This indicates that the 3'CAAX motif is more efficient at targeting p110δ to the plasma membrane than the presence of a 5'Gag sequence.

Surprisingly, in the absence of serum, the presence of Gag-p110δ in NIH 3T3 cells induced cell rounding, resembling an apoptotic phenotype, which is stark contrast the oncogenicity

observed for expression of Gag-p110α in chicken embryo fibroblasts. It is possible that this change in cell morphology is in fact indicative of cell transformation rather than cell death (Vogt, P., Personal communication). It would be interesting to carry out colony formation experiments with these cells in reduced serum concentrations, to assess their oncogenicity compared to WT and 5'Myc-p110δ-overexpressing NIH 3T3 cells.

In the presence of serum, Gag-p110δ expression does not have a huge impact on the overall cytoskeletal cell morphology of NIH 3T3 cells, although the expression of Gag-p110δ with a 3'CAAX motif did appear to result in increased focal adhesions associated with F-actin puncta, which possibly indicates increased invasive potential of these cells, although this would require further investigation.

My initial aim was to investigate the biological effects of p110δ overexpression in NIH 3T3 cells, and although the biological effects of N-terminus p110δ fusion to Gag appear to be interesting, this is unlikely to represent the true biological consequences of p110δ overexpression. If time was not a limiting factor, the effect of Gag-p110δ expression in NIH 3T3 cells could have been pursued, and cell growth, foci formation ability, cellular localization of Gag-p110δ and further investigation into the morphological consequences of Gag-p110δ expression considered. However, as the overexpression of 5'Myc-p110δ also resulted in phenotypically different cells compared to control infected cells, in the presence of serum and under serum-starvation conditions, the decision was taken to further characterise these cells, which is described in the subsequent chapter.

6.5.3 Overexpression of p110δ but not p110α results in constitutive Akt phosphorylation

The presence of a 5'Myc tag on the gene inserted into pMX-neo prevented the formation of a Gag-fusion protein. Some preliminary comparisons between NIH 3T3 cells overexpressing 5'Myc-3'CAAX versions of p110α and p110δ were carried out. Interestingly, overexpression of 5'Myc-p110δ-3'CAAX but not 5'Myc-p110α-3'CAAX resulted in significantly increased basal and FBS-stimulated Akt phosphorylation compared to control cells. This is a finding that has also been observed in other investigations looking into the effect of p110 overexpression. Stable overexpression of myristylated p110δ in rat fibroblasts triggers Akt phosphorylation much more efficiently than overexpression of myristylated p110α, p110β or p110γ, in both serum-starved or serum-stimulated conditions (Link, et al., 2005). Similarly, overexpression of wild-type p110δ in chicken embryo fibroblasts results in high basal levels of Akt phosphorylation under serum-

starvation conditions compared to overexpression of wild-type p110α, p110β or p110γ (Kang, et al., 2006).

The relative enzymatic activity of p110α is higher than that of the other p110 isoforms (Beeton, *et al.*, 2000; Meier, *et al.*, 2004), indicating that the low level of induced Akt activation in p110α transfectants is not due to the relatively low kinase activity of p110α. It is possible that differences in the expression level of the exogenous p110 proteins may account for differences of p110s to trigger Akt phosphorylation. Overexpression of p110α but not p110δ may be toxic, which results in cells expressing low levels of exogenous p110α that consequently fails to induce Akt activation (Kang, et al., 2006). Indeed, exogenously expressed p110δ was more easily detected in total cell lysates than p110α, although this may be due to differences in sensitivities of isoform detection by immunoblotting. Although the transfected p110α and p110δ both contain an N-terminal Myc tag, the antibody against Myc can only be used for immunoprecipitation of Myc and not for Myc detection in total cell lysate by immunoblotting.

It should be considered, however, that low level of p110α protein detection by immunoblotting could result from differential cellular localization of p110α compared to p110δ. Exogenously expressed p110α may predominantly localize in the membrane or nuclear cell fraction compared to p110δ. Subsequent cell lysis, using Triton X-100, may not result in full p110α expression in total cell lysate supernatant.

Another hypothesis to explain the ability of p110δ and not p110α to efficiently activate Akt, is that fibroblasts (which have been used in all the studies described) express low endogenous levels of p110δ compared to p110α and p110β, it has been proposed that the introduction of exogenous p110δ to these cells elicits the activity of downstream effectors more potently than p110α (Link, et al., 2005).

6.5.4 Membrane-targeting of p110δ is not required for stable p110δ overexpression

Although overexpression of different p110δ constructs in pMX-neo, aimed at investigating the necessity of a 5'Myc tag or 3'CAAX motif for successful stable overexpression, did not go entirely to plan, these investigations have revealed that the addition of a membrane targeting motif on p110δ is not essential for stable p110δ overexpression. In fact, retroviral infection of 5'Myc-p110δ in pMX-neo in NIH 3T3 cells resulted in levels of constitutive p110δ overexpression which were higher than that observed for retroviral infection of 5'Myc-p110δ-3'CAAX. Since 5'Myc-p110δ-3'CAAX is likely to be expressed at the

plasma membrane is probable that a portion of 5'Myc-p110δ-3'CAAX will be lost from the cytoplasmic fraction of the total cell lysate taken for SDS-PAGE. Nonetheless, retroviral infection of 5'Myc-p110δ resulted in a substantial stable overexpression of p110δ.

Expression of class IA p110 catalytic subunits is thought to be dependent on the availability of p85 regulatory subunits which stabilise p110s (Meier, et al., 2004; Ueki*, et al.*, 2002a; Yu, et al., 1998b). However, expression of 5'Myc-p110δ was achieved without coexpression of a regulatory subunit. Similarly, in other studies stable overexpression of p110s did not require exogenous p85 (Auger, et al., 2000; Kang, et al., 2006; Link, et al., 2005). It is possible that the 5'Myc tag may be acting to stabilise p110δ since for p110α the addition of a bulky N-terminal tag has been shown to supplant the requirement of p110α for p85 (Yu, et al., 1998b). Therefore, it is possible that overexpressed 5'Myc-p110δ may not be acting in the same way as overexpressed untagged p110δ might. The limitations of characterising NIH 3T3 cells overexpressing p110δ with an N-terminal Myc tag is further discussed in the following chapter.

7. CHARACTERISATION OF NIH 3T3 CELLS OVEREXPRESSING 5'Myc-p110δ

Although it was originally anticipated to characterise NIH 3T3 cells overexpressing an untagged p110δ cDNA, the problems encountered with regard to the generation of a viral Gag-p110δ fusion protein, severely limited the time available to generate new NIH 3T3 clones overexpressing untagged p110δ. Since the addition of a Myc tag at the N-terminus of p110δ prevented the formation of Gag-p110δ fusion protein, the decision was made to start characterising NIH 3T3 cells overexpressing 5'Myc-p110δ. Unlike the presence of a 3' Myc tag on p110 catalytic subunits, the presence of a 5'Myc tag does not alter the lipid substrate specificity of class I p110s (Bilancio & Vanhaesebroeck, unpublished results). However, the drawback of using a 5'Myc tag is that it has been shown to have a stabilizing effect on p110 subunits (Yu, et al., 1998b). In this respect, a 5'Myc tag may alter the dependency of p110δ on p85. The description of the phenotypes observed in 5'Myc-p110δ-overexpressing cells are described below and summarised in Table 8.1 on page 261.

7.1 Exogenously expressed 5'Myc-p110δ forms heterodimers with endogenous p85 in NIH 3T3 cells

The colloidal Coomassie staining of p110δ immunoprecipitates separated by SDS-PAGE, first shown in section 6.3.1 and again here (Figure 7.1), depicts p110δ immunoprecipitates from control infected, untagged p110δ (now known to be Gag-p110δ fusion protein) and 5-Myc-p110δ-overexpressing NIH 3T3 cells. This figure is included a second time to emphasize the p85-binding capacity of 5'-Myc-p110δ.
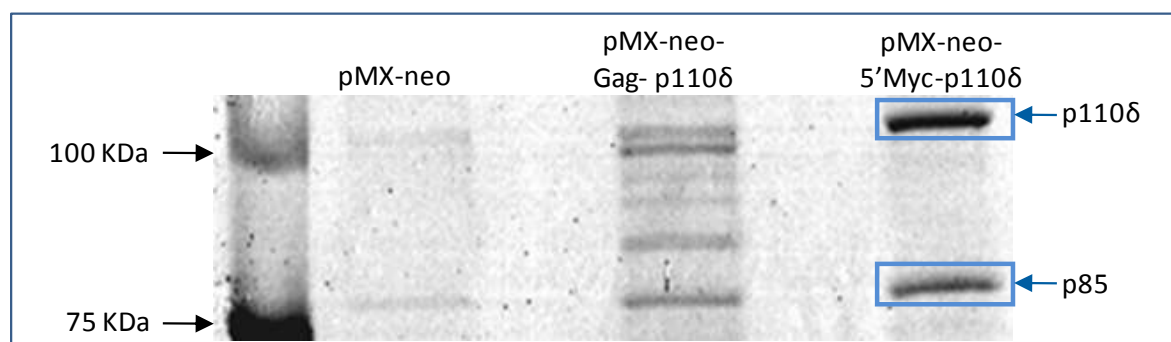
Figure 7.1: Coomassie staining of p110δ immunoprecipitates separated by SDS-PAGE. The bands indicated by arrows were excised and subjected to mass spectrometry analysis.

The fragments indicated were excised and subjected to mass spectrometry analysis. This identified p110δ and a mixture of p85α and p85β in each of the fragments, indicated in Figure 7.1. Although this result does not prove that the presence of the 5'Myc tag on p110δ does not alter the *level* of p85 binding, it does indeed show that 5'Myc-p110δ is still

capable of forming heterodimers with p85 regulatory subunits. This result indicates that the presence of a 5'Myc tag does not obliterate the need of p110δ to bind, and perhaps be stabilised by, p85.

7.2 NIH 3T3 cells stably overexpressing 5'Myc-p110δ have altered class IA p110 isoform expression and increased lipid kinase activity

7.2.1 Overexpression of 5'Myc-p110δ in NIH 3T3 cells results in reduced p110α and p110β isoform expression

It has been observed that reduced expression or overexpression of a particular PI3K isoform, either by PI3K overexpression or gene deletion, can result in deregulation of expression of the other PI3K isoforms (Fruman, et al., 2000; Kang, et al., 2006). Stable overexpression of 5'Myc-p110δ in NIH 3T3 cells resulted in severe attenuation of p110α expression and a lack of detectable p110β expression, whereas total p85 expression remains largely unaltered (Figure 7.2), which could be an indication that a limiting amout of p85 in cells plays a role in downregulation of p110α and p110β expression.
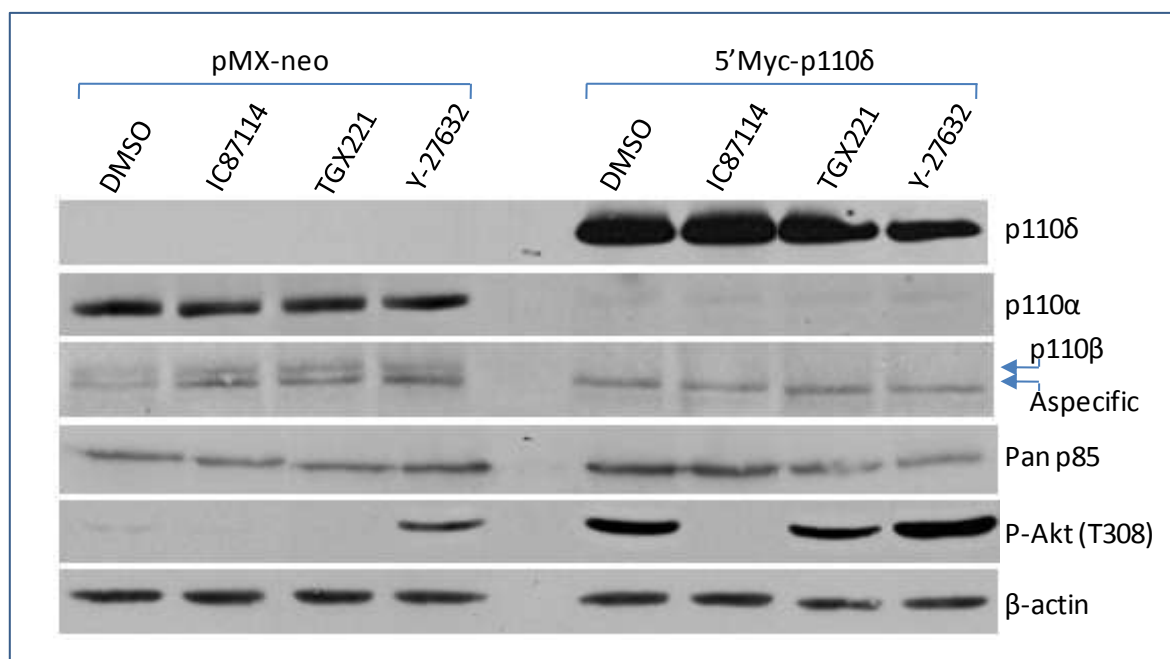
Figure 7.2: Class IA p110 isoform expression and Akt phosphorylation in NIH 3T3 cells stably expressing pMX-neo or 5'Myc-p110δ. Cells were treated with 5 μM IC87114 (p110δ-specific inhibitor), 50 nM TGX221 (p110β-specific inhibitor), 10 μM Y-27632 (ROCK inhibitor) or DMSO vehicle control for 1 h. Cell lysates were separated by SDS-PAGE and immunoblotted for p110δ, p110α, p110β, pan-85 and P-Akt.

The finding that p110δ overexpression results in reduced level of p110α expression had also been observed in NIH 3T3 cells infected with 5'Myc-p110δ-3'CAAX, described in the previous chapter (Figure 6.2). Inhibition of p110δ activity, using the p110δ-specific

inhibitor IC87114 did not alter p110α or p110β expression, indicating that the lipid kinase activity of p110δ is not critical for the impact on p110α and p110β expression.

7.2.2 Overexpression of 5'Myc-p110δ in NIH 3T3 results in constitutive phosphorylation of Akt

Consistent with observations made for NIH 3T3 cells stably expressing 5'Myc-p110δ-3'CAAX described in Chapter 6, 5'Myc-p110δ-overexpressing NIH 3T3 cells were found to have high constitutive Akt phosphorylation compared to pMX-neo control-infected cells, which had no detectable Akt phosphorylation under basal growing condition (Figure 7.2). Akt phosphorylation in 5'Myc-p110δ-overexpressing NIH 3T3 cells was reduced to non-detectable levels after treatment with the p110δ-specific inhibitor, IC87114. The p110β-specific inhibitor, TGX221, also had some minor effect on Akt phosphorylation levels. This is likely to be an off-target effect of p110δ inhibition, as p110β expression was not detected in 5'Myc-p110δ-overexpressing NIH 3T3 cells (see Table 2.1 for the IC_{50} values of PI3K isoform-selective inhibitors).

The ROCK inhibitor, Y-27632, induced Akt phosphorylation in pMX-neo control-infected cells and further increased Akt phosphorylation in 5'Myc-p110δ-overexpressing NIH 3T3 cells. ROCK is a downstream target of RhoA and it has been proposed that RhoA-induced ROCK activation in turn stimulates the phosphatase activity of PTEN, ultimately inhibiting PI3K activity (Li, et al., 2005; Papakonstanti, et al., 2007). If under normal growing conditions, there is a basal level of RhoA activity, inhibition of ROCK would suppress PTEN leading to increased PIP_3 levels and increased Akt activation. The results indicate that under basal growing conditions, in both pMX-neo and 5'Myc-p110δ-overexpressing NIH 3T3 cells, RhoA is indeed active to some degree and stimulating PTEN phosphatase activity. In an extension of this model, proposed by Papakonstanti *et al*, 2007, p110δ is shown to be a negative regulator of RhoA activity. However, it appears that in 5'Myc-p110δ-overexpressing NIH 3T3 cells, the high level of p110δ expression is not sufficient to inhibit RhoA activity under basal growing conditions, as if this was the case, the ROCK inhibitor would be expected to have no effect on Akt phosphorylation levels.

These data demonstrate that although the level of Akt phosphorylation is high in 5'Myc-p110δ-overexpressing NIH 3T3 cells, this does not represent the maximal level of Akt phosphorylation as it can be further increased.

7.3 NIH 3T3 cells stably overexpressing 5'Myc-p110δ exhibit differences in cell morphology and cell adhesion compared to pMX-neo control-infected cells

7.3.1 NIH 3T3 cells stably overexpressing 5'Myc-p110δ have an altered actin-based cytoskeleton structure, which is dependent on the presence of serum, compared to pMX-neo control-infected cells

NIH 3T3 cells stably overexpressing 5'Myc-p110δ were found to have a structurally different F-actin-based cytoskeleton compared to pMX-neo control cells in both normal growing conditions, i.e. in the presence of 10% serum, or under serum-starvation conditions (Figures 7.3, 7.4, 7.5). In the presence of serum, 5'Myc-p110δ-overexpressing cells appear to adhere to a greater surface area than control infected cells, with more actin stress fibres traversing the cytoplasm of the cell, often terminating with sites of focal contacts with the substrate (as assessed by P-paxillin staining) (Figures 7.3, 7.4). The difference in the cell adhesion area between NIH 3T3 cells stably expressing pMX-neo or 5'Myc-p110δ was extremely apparent. In some instances it was necessary to decrease the microscope objective to simply capture an image which contained a complete cell (Figure 7.3b). It should be emphasized, however, that although the majority of 5'Myc-p110δ-overexpressing cells had a greater adhesion surface area than pMX-neo-expressing cells, only a small minority of cells displayed a huge surface adhesion area, an example of which is shown in Figure 7.3b.

In pMX-neo control-expressing cells the majority of F-actin was tightly packed in bundles running along the cell periphery, indicated by strong phalloidin staining (Figure 7.4). In 5'Myc-p110δ-overexpressing cells, although there was also strong staining of F-actin at the cell periphery, in comparison to pMX-neo control-expressing cells this appeared reduced.

In general, 5'Myc-p110δ overexpressing cells appeared to have an increase number of focal adhesions compared to pMX-neo control infected cells, although this has not been numerically quantified. From staining with N-cadherin, there appeared to be no obvious difference in the ability of pMX-neo control or 5'Myc-p110δ overexpressing cells to form adherens junctions (Figure 7.3).
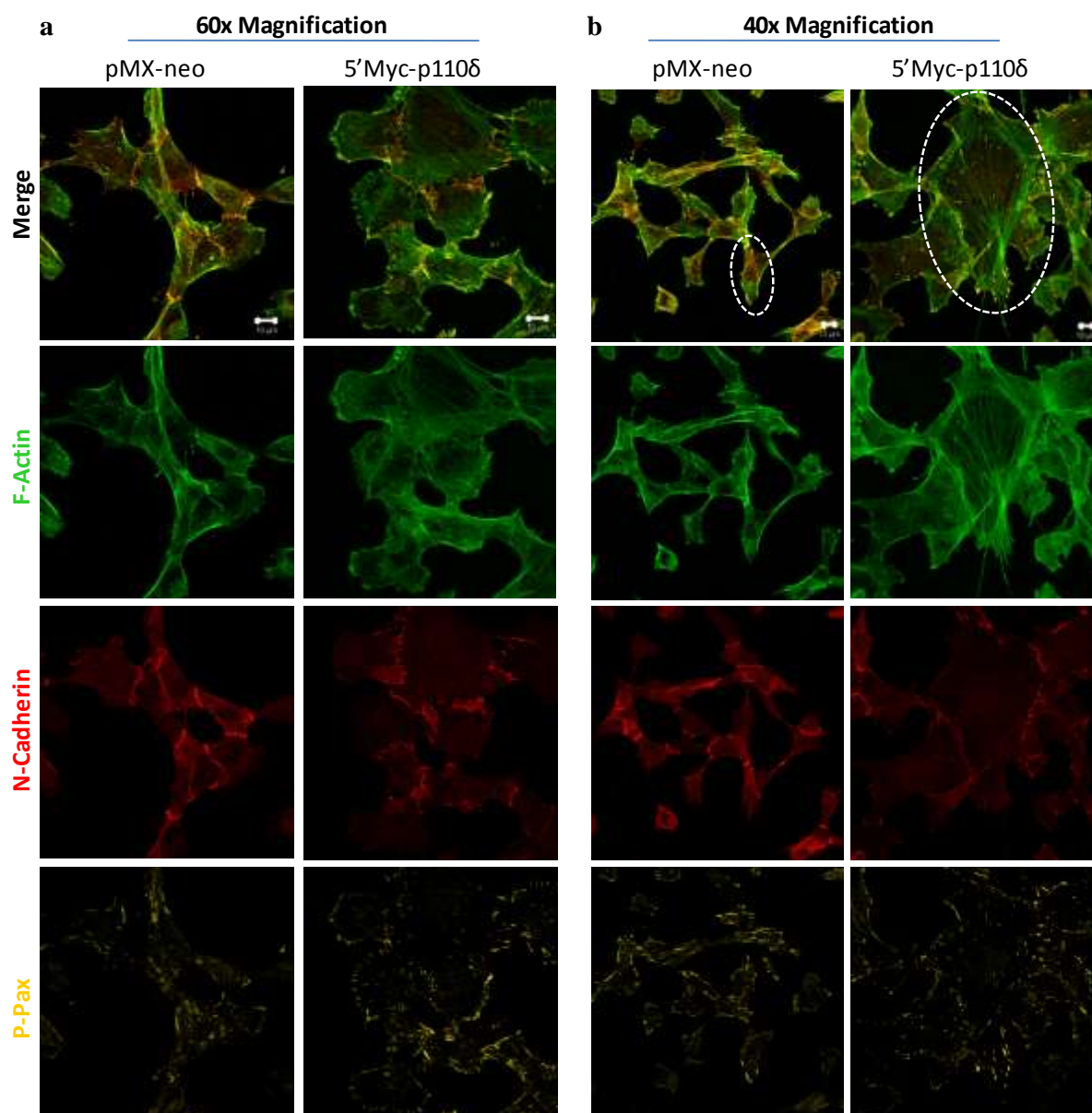
Figure 7.3: Cell cytoskeleton of NIH 3T3 cells stably expressing pMX-neo or 5'Myc-p110δ in normal growing conditions. Cells were seeded in media containing 10% FBS on glass coverslips in a 12-well plate. Cells were left to adhere overnight. The following day cells were fixed and stained for F-actin (phalloidin), adherens junctions (N-cadherin) and focal adhesions (P-paxillin). Images are shown for **(a)** 60x and **(b)** 40x magnifications. The white ellipses enclose a complete cell for pMX-neo control infected and 5'Myc-p110δ-overexpressing NIH 3T3 cells, highlighting an obvious difference in cell adhesion area observed. It should be noted that the 5'Myc-p110δ-overexpressing cell highlighted here was selected to show how large these cells can become, however this cell has an exceptionally large surface adhesion area and is not an accurate reresentative of 5'Myc-p110δ-overexpressing cells. Scale bar = 10 μM for both magnifications.
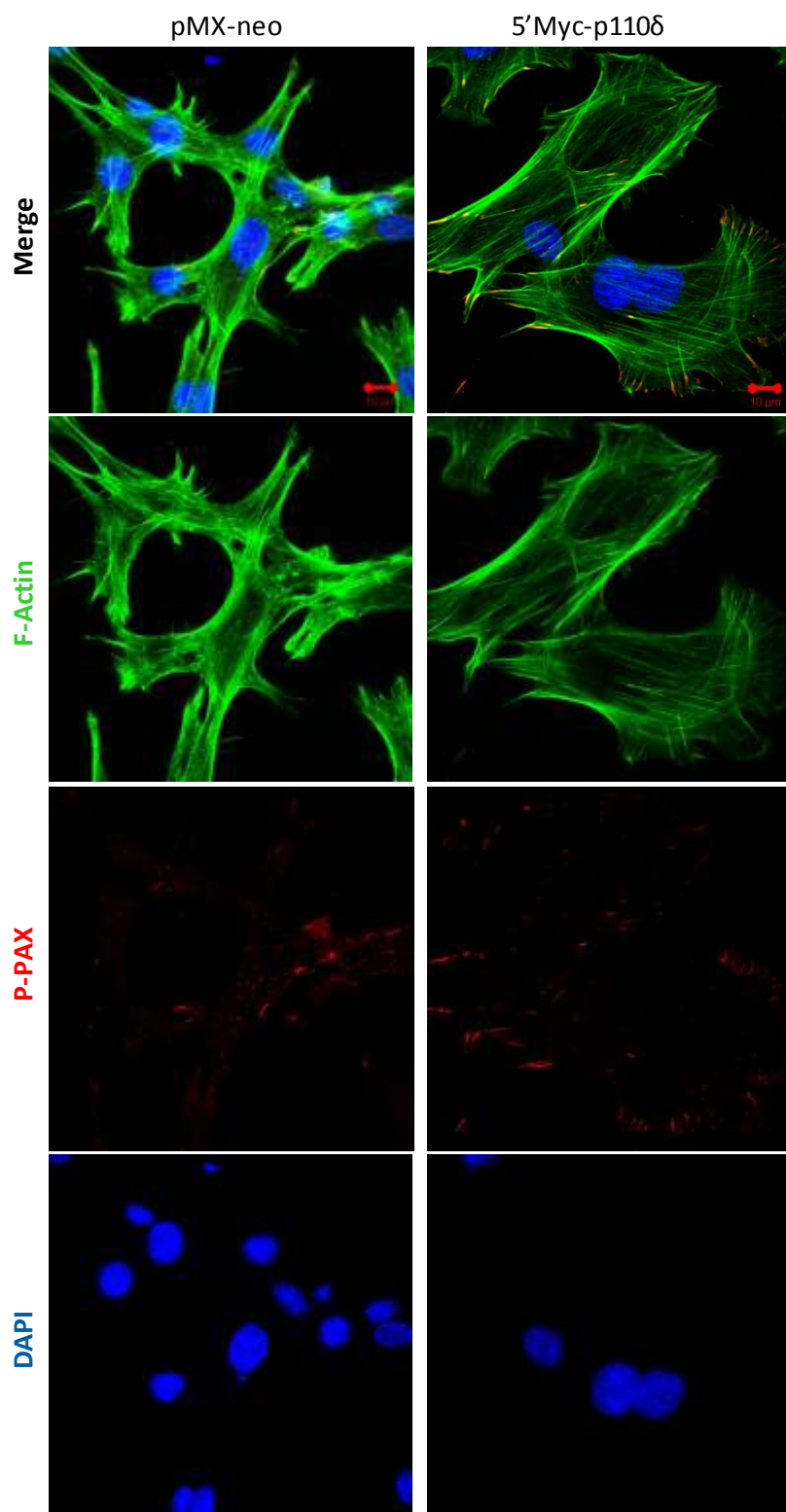
Figure 7.4: Cell cytoskeleton of NIH 3T3 cells stably expressing pMX-neo or 5'Myc-p110δ in normal growing conditions. Cells were seeded in media containing 10% FBS on glass coverslips in a 12-well plate. Cells were left to adhere overnight. The following day cells were fixed and stained for F-actin (phalloidin), DNA (DAPI) and focal adhesions (P-paxillin). Scale bar = 10 μM.

Upon overnight serum-starvation, 5'Myc-p110δ-overexpressing cells displayed striking differences in the actin-based cytoskeleton compared to normal growing conditions with 10% serum (Figure 7.5). Moreover, in the absence of serum, 5'Myc-p110δ-overexpressing cells also displayed a different morphology compared to pMX-neo-expressing cells (Figure 7.5).

Under starvation conditions, 5'Myc-p110δ-overexpressing cells did not contain actin stress fibres traversing the cell cytoplasm, which were observed in the presence of serum. In fact, in the absence of serum the overall staining of F-actin bundles appeared to decrease in 5'Myc-p110δ-overexpressing cells compared to pMX-neo-expressing cells and compared to 5'Myc-p110δ-overexpressing cells in 10% serum (Figure 7.5a). As previously observed in the presence of serum, pMX-neo-expressing cells expressed prominent bundles of F-actin along the cell periphery under serum-starvation conditions. In 5'Myc-p110δ-overexpressing cells, F-actin bundles were only observed running along the cell periphery, but in comparison to pMX-neo-expressing cells, F-actin staining appeared reduced (Figure 7.5a, b).

In terms of general cell morphology, 5'Myc-p110δ-overexpressing cells had a more flat and spread appearance compared to pMX-neo-expressing cells under starvation conditions. Myc-p110δ-overexpressing cells had a more spherical overall cell shape, which may be a consequence of the lack of F-actin stress fibres which determine the typical fibroblast cell morphology observed in pMX-neo-expressing NIH 3T3 cells (Figure 7.5a, b).

In some cells overexpressing 5'Myc-p110δ, punctate F-actin staining was observed (indicated by white arrowheads, Figure 7.5a), which were not linked to the cytoskeleton by F-actin fibres. F-actin puncta staining colocalized with P-paxillin staining, indicating that the F-actin puncta are associated with points of contact of the cell to the underlying substrate. This type of staining is typical for podosomes or invadopodia (Linder, 2007), suggesting that 5' Myc-p110δ-overexpressing cells may be more invasive, compared to pMX-neo-expressing cells (discussed in more detail in section 7.5.6).
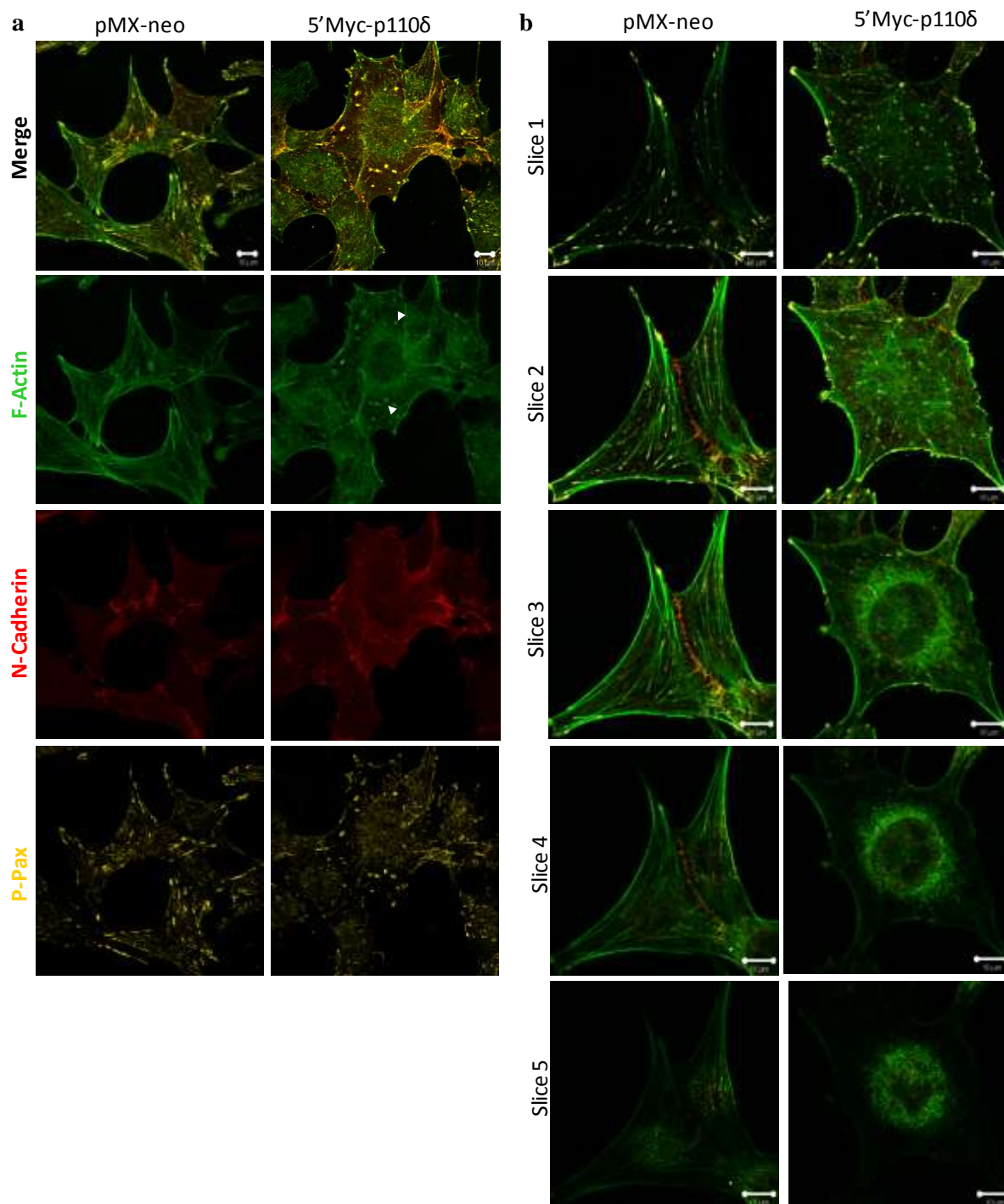
Figure 7.5: The cell cytoskeleton of NIH 3T3 cells stably expressing pMX-neo or 5'Myc-p110δ under serum-starvation conditions. (a) Cells were seeded in media containing 10% FBS on glass coverslips in a 12-well plate. Cells were left to adhere for 6 h before the media was replaced with media without FBS. The following day cells were fixed and stained for F-actin (phalloidin), adherens junctions (N-cadherin) and focal adhesions (P-paxillin). White arrowheads indicate punctate F-actin staining in 5'Myc-p110δ-overexpressing cells. Images are shown for 60 x magnifications. Scale bar = 10 μM. **(b)** Z-stack slices of pMX-neo control-infected and 5'Myc-p110δ-overexpressing NIH 3T3 cells under serum-starvation conditions. Z-stack slices taken at 0.5 micron intervals, starting at the cell substrate (slice 1) and proceeding up to the top of the cell (slice 5). Scale bar = 10 μM.

Cross section images of control and 5'Myc-p110δ-overexpressing cells taken at intervals of 0.5 microns (Z-stack slices) revealed further differences in the structure of the actin cytoskeleton (Figure 7.5b). In pMX-neo-expressing cells, actin stress fibres were observed to run along the cell periphery and across the cell cytoplasm in all of the Z-stack slices. In contrast, in 5'Myc-p110δ-overexpressing cells, long bundles of F-actin fibres were only observed at the cell periphery. Surrounding and appearing to cover the nucleus, short F-actin fibres were observed. In addition, the first Z-stack slice (the cross section of the cell taken at the level of cell contact with the underlying substrate) indicated that 5'Myc-p110δ-overexpressing cells have an increased number of cell contacts with the substrate as shown by P-paxillin staining.

7.3.2 The p110δ-specific inhibitor, IC87114, partially reverses the altered cytoskeletal phenotype observed in NIH 3T3 cells overexpressing 5'Myc-p110δ, but only under serum-starvation conditions

To investigate whether the cytoskeletal changes observed in 5'Myc-p110δ-overexpressing cells could be attributed to increased p110δ lipid kinase activity, cells were treated with the p110δ-specific inhibitor IC87114 either in the presence of serum or under starvation conditions. IC87114 treatment of NIH 3T3 cells stably expressing pMX-neo or 5'Myc-p110δ in the presence of serum induced a surprising result. For pMX-neo-expressing cells, inhibition of p110δ caused the cells to form distinct cell clusters (Figure 7.6). For 5'Myc-p110δ overexpressing cells, IC87114 treatment had a greater impact, causing the cells to form long 'string-like' clusters. This cluster formation could be mediated by longitudinal contraction of the cell, or by cell detachment from the substrate with cell-cell junctions remaining (indicated by N-cadherin staining of adherens junctions). It is remarkable that IC87114 treatment had an impact on pMX-neo-expressing cells, since these cells express particularly low levels of p110δ protein expression. These results are difficult to interpret, far from reversing the cytoskeletal phenotype observed in 5'Myc-p110δ overexpressing cells to that resembling pMX-neo-expressing cells, IC87114 treatment in the presence of serum actually exacerbates the difference between the cell lines.
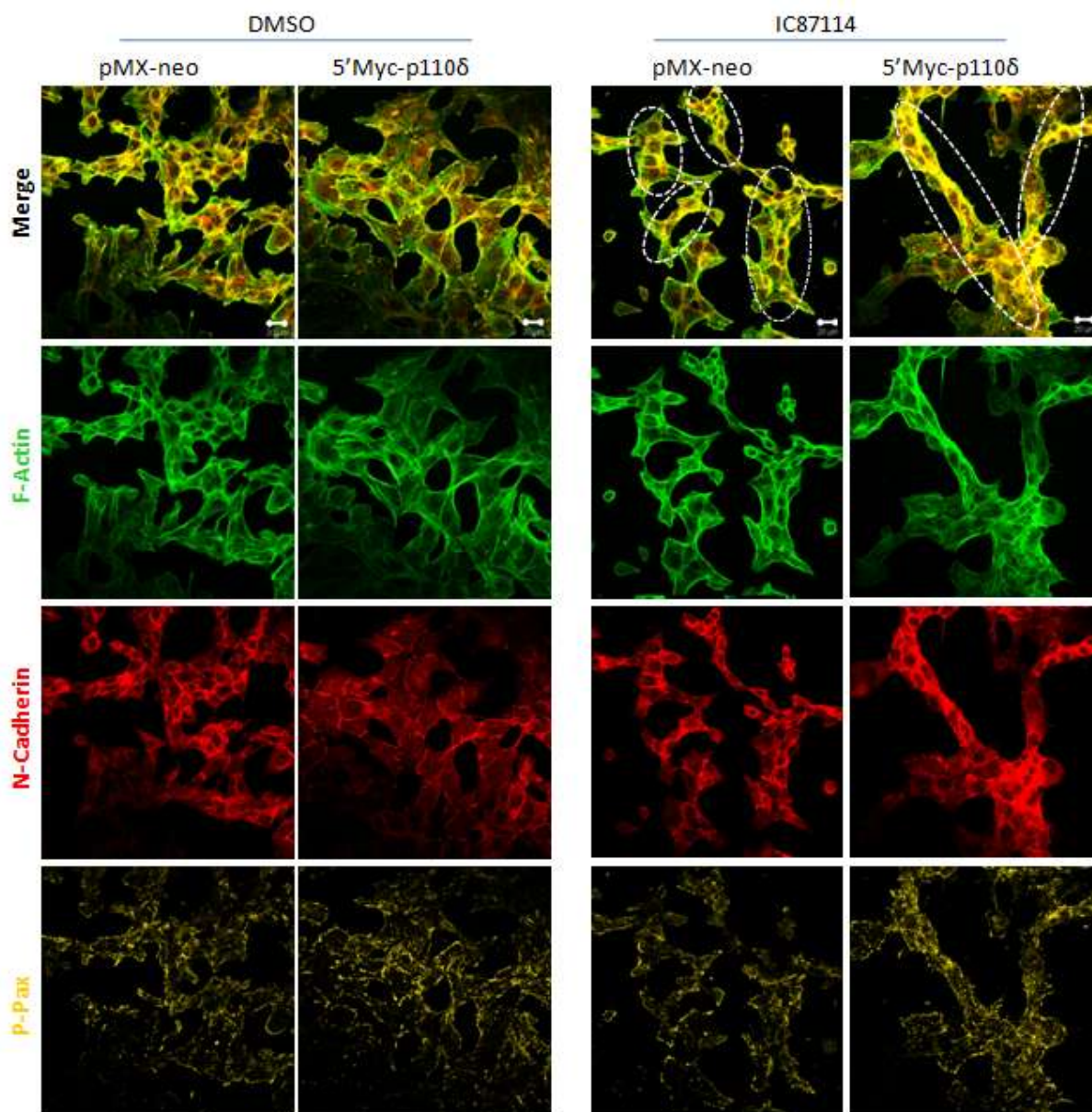
Figure 7.6: Effect of IC87114 on the cell cytoskeleton of NIH 3T3 cells stably expressing pMX-neo or 5'Myc-p110δ in 10% serum. Cells were seeded in media containing 10% FBS on glass coverslips in a 12-well plate. Cells were left to adhere overnight. The following day cells were treated with DMSO or 5 μM IC87114 for 1 h before fixation and staining for F-actin (phalloidin), adherens junctions (N-cadherin) and focal adhesions (P-paxillin). The white dashed elliptical lines enclose discrete cell clusters. Scale bar = 10 μM.

Surprisingly, under serum-starvation conditions, IC87114 did not induce cell clustering as observed in cell treatment in the presence of serum (Figure 7.7a). In fact, IC87114 treatment seemed to, at least to some extent, alter the overall cell morphology of 5'Myc-p110δ overexpressing cells so that it more closely resembled that of pMX-neo-expressing cells. More specifically, the overall cell adherence area of 5'Myc-p110δ overexpressing cells seemed to be reduced (Figure 7.7a) and on closer inspection, IC87114 treatment

induced the formation of F-actin stress fibres in 5'Myc-p110δ overexpressing cells to levels comparable with pMX-neo-expressing cells (Figure 7.7b).
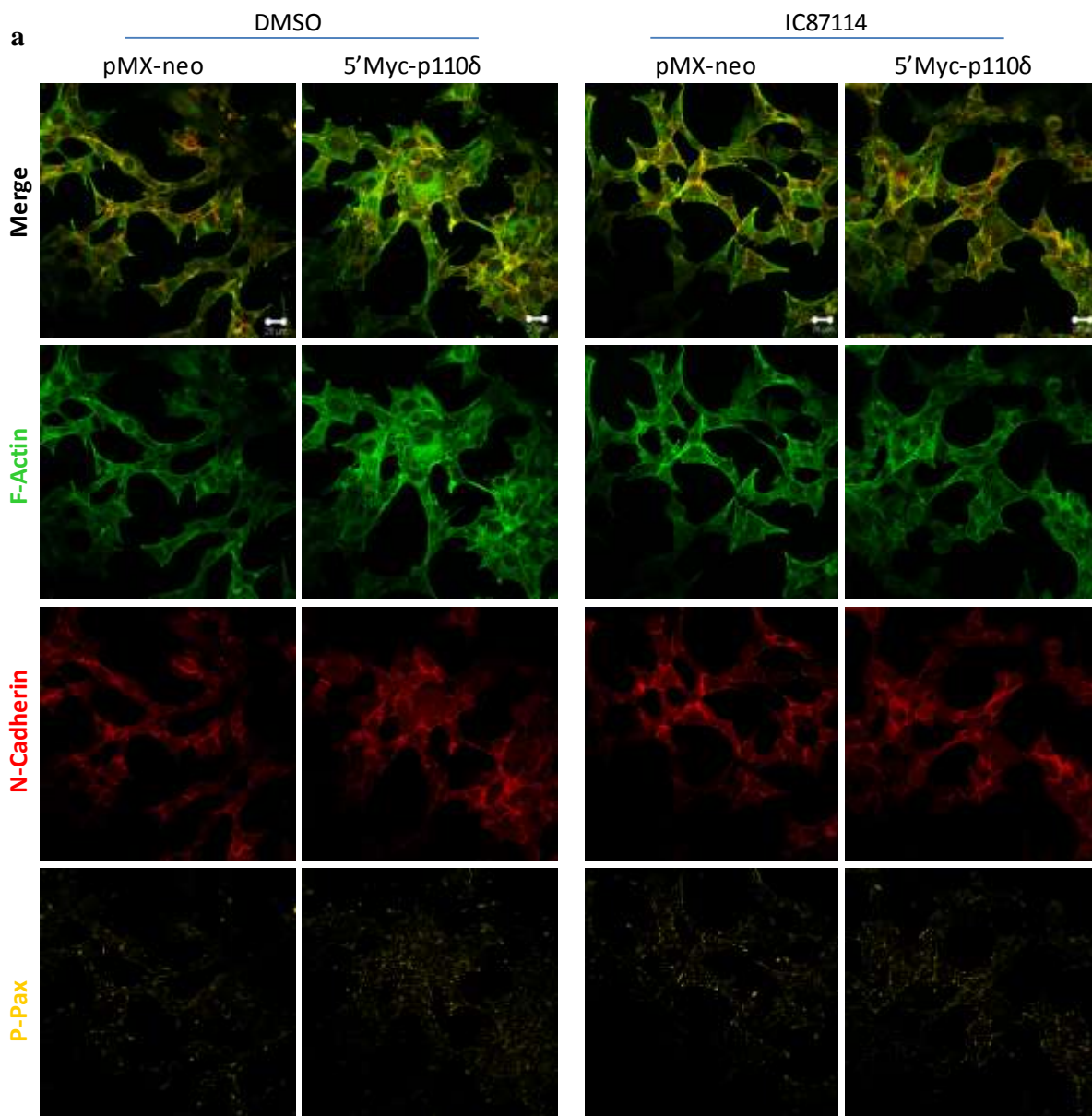
Figure 7.7: Effect of IC87114 on the cell cytoskeleton of NIH 3T3 cells stably expressing pMX-neo or 5'Myc-p110δ in the absence of serum. (a) *40x magnification:* Cells were seeded in media containing 10% FBS on glass coverslips in a 12-well plate and left to adhere for 6 h. After this time, media was replaced with media without serum and cells were left overnight. The following day cells were treated with DMSO or 5 µM IC87114 for 1 h before fixation and staining for F-actin (phalloidin), adherens junctions (N-cadherin) and focal adhesions (P-paxillin). Scale bar = 10 µM.

b
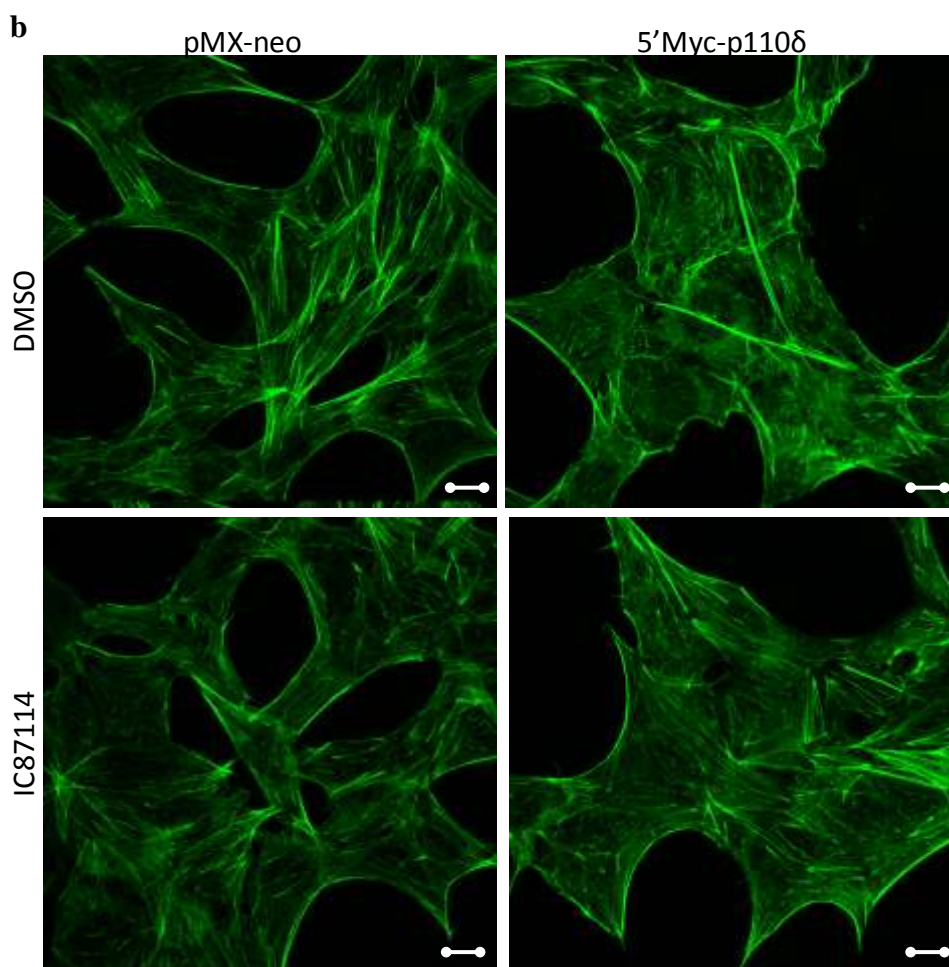
Figure 7.7: Effect of IC87114 on the cell cytoskeleton of NIH 3T3 cells stably expressing pMX-neo or 5'Myc-p110δ in the absence of serum. (b) *60x magnification:* NIH 3T3 cells stably expressing pMX-neo or 5'Myc-p110δ treated with IC87114 in the absence of serum. Confocal images of cells fixed and stained for F-actin (phalloidin). Scale bar = 10 μM.

To correlate the phenotype observed for IC87114 treatment of control infected cells and 5'Myc-p110δ-overexpressing with the level of Akt phosphorylation (indirectly assessing the lipid kinase activity of p110δ), cell lysates were taken after IC87114 treatment of cells in the presence of serum or under starvation conditions. 5'Myc-p110δ-overexpressing cells were found to have higher basal levels of phosphorylated Akt in both serum and starvation conditions compared to pMX-neo-expressing cells (Figure 7.8). Although in the absence of serum 5'Myc-p110δ-overexpressing cells only expressed low levels of phosphorylated Akt, in control infected cells phosphorylated Akt was undetectable. In the presence of serum the difference in Akt phosphorylation levels between the cell lines was more evident, with 5'Myc-p110δ-overexpressing cells expressing around 12-fold more phosphorylated Akt compared to pMX-neo-expressing cells (Figure 7.8).
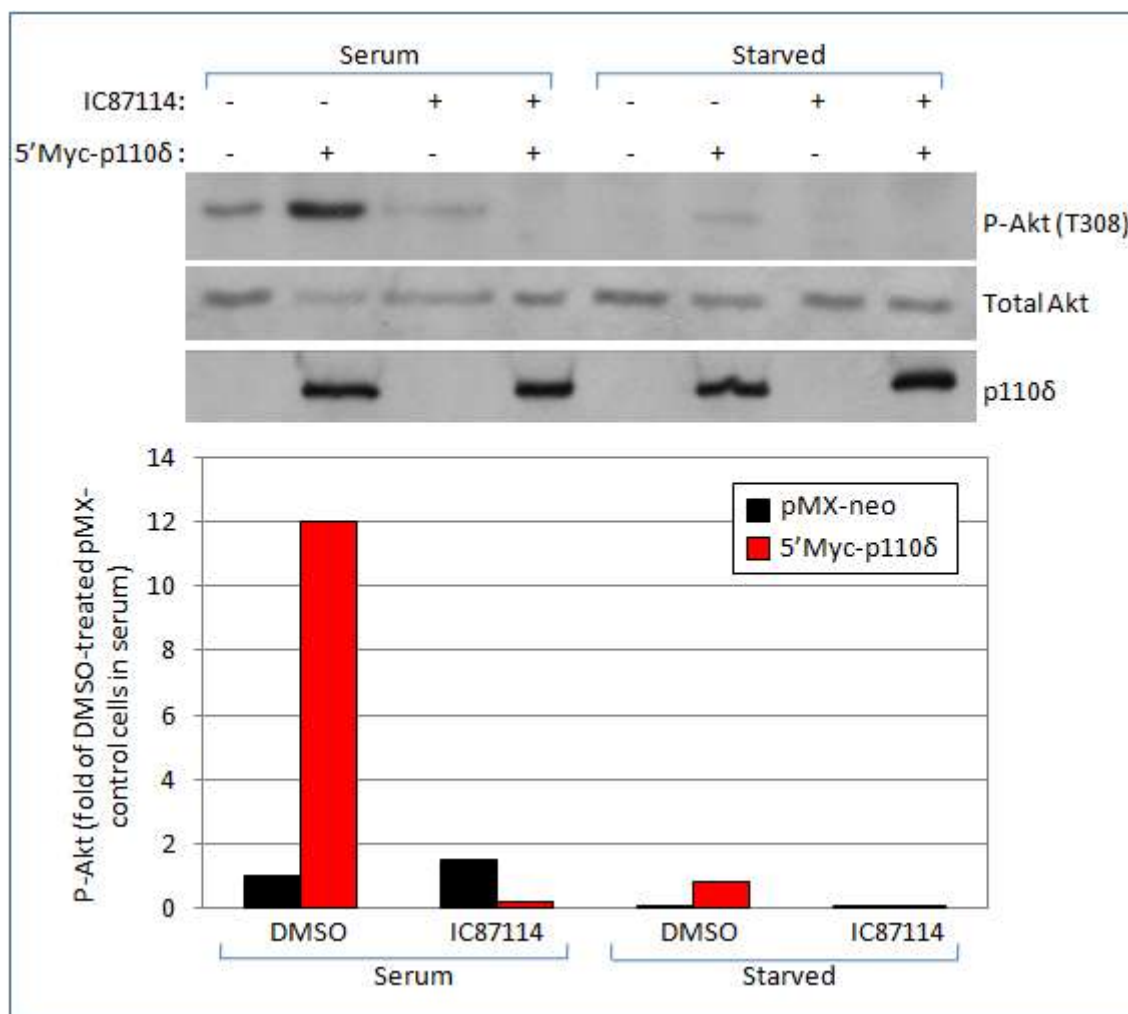
Figure 7.8: Levels of Akt phosphorylation in NIH 3T3 cells stably expressing pMX-neo or 5'Myc-p110δ. Cells were seeded in media containing 10% FBS and left to adhere for 6 h. After this time, media was replaced with media without serum for the samples indicated. The following day cells were treated with DMSO or 5 μM IC87114 for 1 h. Cell lysates were separated by SDS-PAGE and immunoblotting for P-Akt, total Akt and p110δ.

IC87114 treatment completely abrogated out all phosphorylation of Akt in 5'Myc-p110δ-overexpressing cells in both serum and starvation conditions, whereas IC87114 treatment of pMX-neo-expressing cells reduced but did not completely abrogate Akt phosphorylation in the presence of serum. This result corroborates the data indicating that p110δ has become the principle p110 isoform in 5'Myc-p110δ-overexpressing cells resulting from downregulation of p110α and p110β isoform expression (Figure 7.2), whereas in pMX-neo-expressing cells p110α and p110β expression remains high, allowing possibly some basal PI3K signalling.

Since IC87114 treatment completely abrogates, what was previously a high level of basal Akt phosphorylation, in 5'Myc-p110δ-overexpressing cells in serum, this could perhaps account for the dramatic change in cell morphology observed under these conditions.

Whereas in the absence of serum, the level of Akt phosphorylation in 5'Myc-p110δ-overexpressing cells is relatively low, indicating low basal p110δ activity, therefore inhibition of p110δ is likely to result in a more subtle change in cell morphology.

7.3.3 NIH 3T3 cells stably overexpressing 5'Myc-p110δ adhere to an increased surface area in normal culture conditions compared to control-infected cells

It was observed from the confocal images that 5'Myc-p110δ-overexpressing cells appear to spread out and adhere to a greater surface area compared to pMX-neo-expressing cells (Figure 7.3, 7.5). To formally prove this, using confocal images and the computer software *Image J* the cell area was calculated by manually drawing around individual cells and using *Image J* to calculate the enclosed area. Indeed, 5'Myc-p110δ-overexpressing cells were found to spread over a significantly increased surface area compared to pMX-neo-expressing cells in the presence or absence of serum (Figure 7.9a, b). There was a great deal of variability in cell area in 5'Myc-p110δ-overexpressing cells, which can be seen from the outlying values indicated in the box whisker plot. The high degree of heterogeneity in cell surface area may be as a result of pooling cells stably overexpressing 5'Myc-p110δ rather than expansion of a single clone, as individual cells amongst the independent transfectants are likely to express various levels of 5'Myc-p110δ overexpression.

7.3.4 IC87114 treatment in the absence of serum reduces cell adherence area of NIH 3T3 cells stably overexpressing 5'Myc-p110δ

To assess if IC87114 treatment of NIH 3T3 cells stably expressing 5'Myc-p110δ could reduce cell adherence area, confocal images and *Image J* were again used to calculate cell area. Since IC87114 treatment of cells in the presence of serum induced cell clustering (Figure 7.6), quantification of cell area of individual cells was not possible, therefore quantification of cell area was carried out on cells treated with IC87114 under starvation conditions. IC87114 treatment of NIH 3T3 cells stably expressing 5'Myc-p110δ under starvation conditions resulted in a reduction of cell adherence area to a level comparable with pMX-neo-expressing cells (Figure 7.9b). These data indicate that p110δ lipid kinase activity (at least under starvation conditions) mediates the increased cell adherence area observed in 5'Myc-p110δ-overexpressing NIH 3T3 cells.
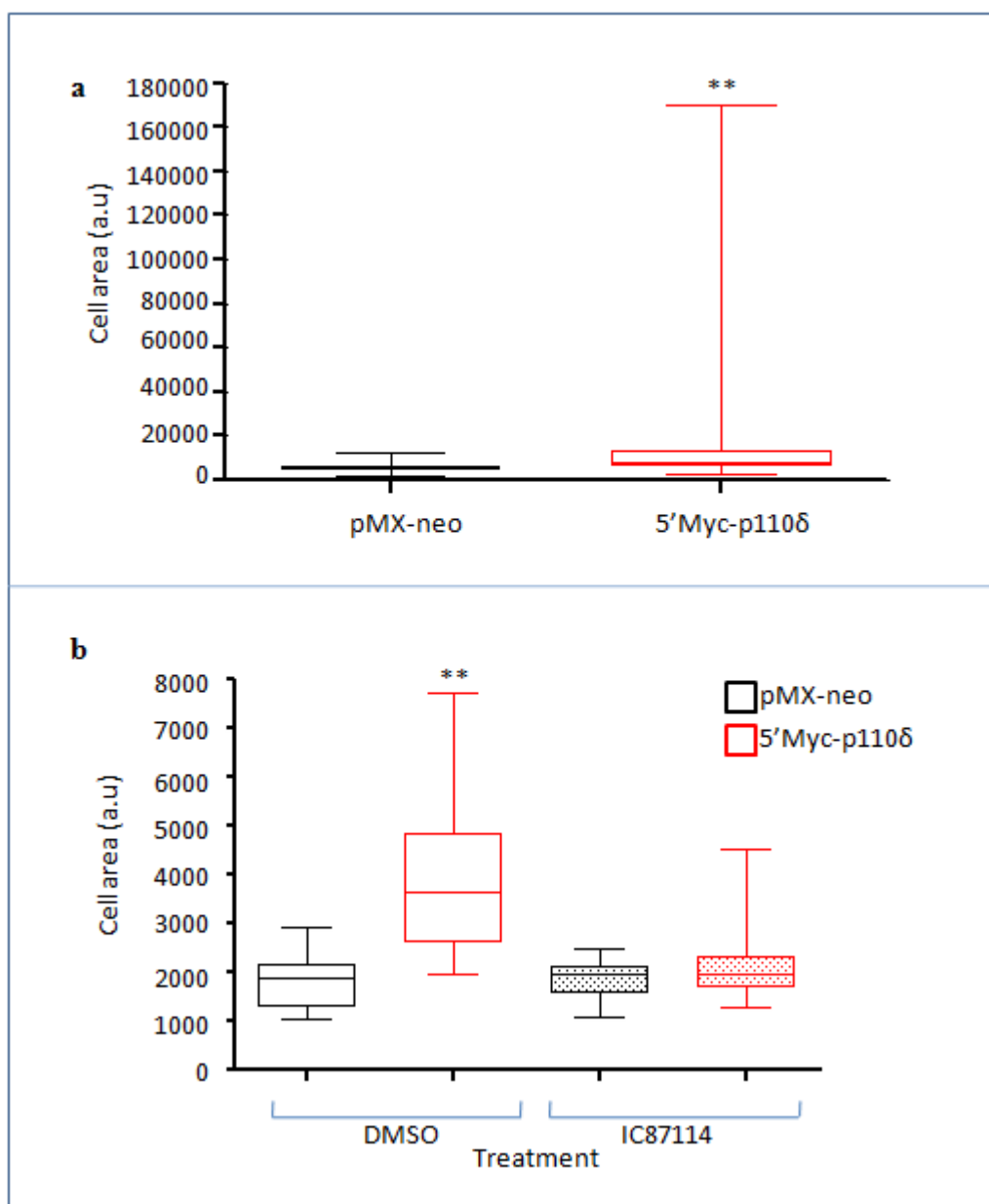
Figure 7.9: Cell area of NIH 3T3 cells stably expressing pMX-neo or 5'Myc-p110δ.
Cell area was calculated from confocal images of cells stained for F-actin using Image J
software. **(a)** *Cell area in the presence of serum:* Cells were seeded in media containing
10% FBS and left to adhere overnight. The following day cells were fixed and stained for
F-actin. **(b)** *Cell area under starvation conditions:* Cells were seeded in media containing
10% FBS and left to adhere for 6 h. After this time media was replaced with media
containing 0% FBS and cells were left overnight. The following day, cells were treated
with 5 μM IC87114 or DMSO vehicle control for 1 h after which cells were fixed and
stained for F-actin. Median, quartiles and highest lowest values are indicated on box
whisker plots. ** indicates $P < 0.01$ using the Mann-Whitney U-test, n > 75.

7.3.5 NIH 3T3 cells stably overexpressing 5'Myc-p110δ adhere and spread more quickly on a variety of substrates compared to pMX-neo-expressing cells

To investigate how 5'Myc-p110δ overexpression affects cell adhesion, cells were detached
and seeded onto glass coverslips. Fixing and staining of cells after 30 min or 1 h, revealed
that 5'Myc-p110δ-overexpressing cells display a different cell morphology at both time

points compared to pMX-neo-expressing cells (Figure 7.10). 30 min after seeding, pMX-neo-expressing cells exhibited multiple filopodia protrusions relatively evenly distributed around the cell periphery, whereas 5'Myc-p110δ-overexpressing cells appeared to form less overall filopodia protrusions, and the filopodia present were dispersed more irregularly around the cell periphery. Furthermore, 5'Myc-p110δ-overexpressing cells appeared to spread and adhere to larger surface area on the glass cover slip. 1 h after seeding the cells, there was no longer an obvious difference in cell adhesion area between the cell lines, however 5'Myc-p110δ-overexpressing cells displayed increased membrane ruffling compared to control infected cells and again displayed less filopodia protrusions but broader lamellipodia-like extensions.
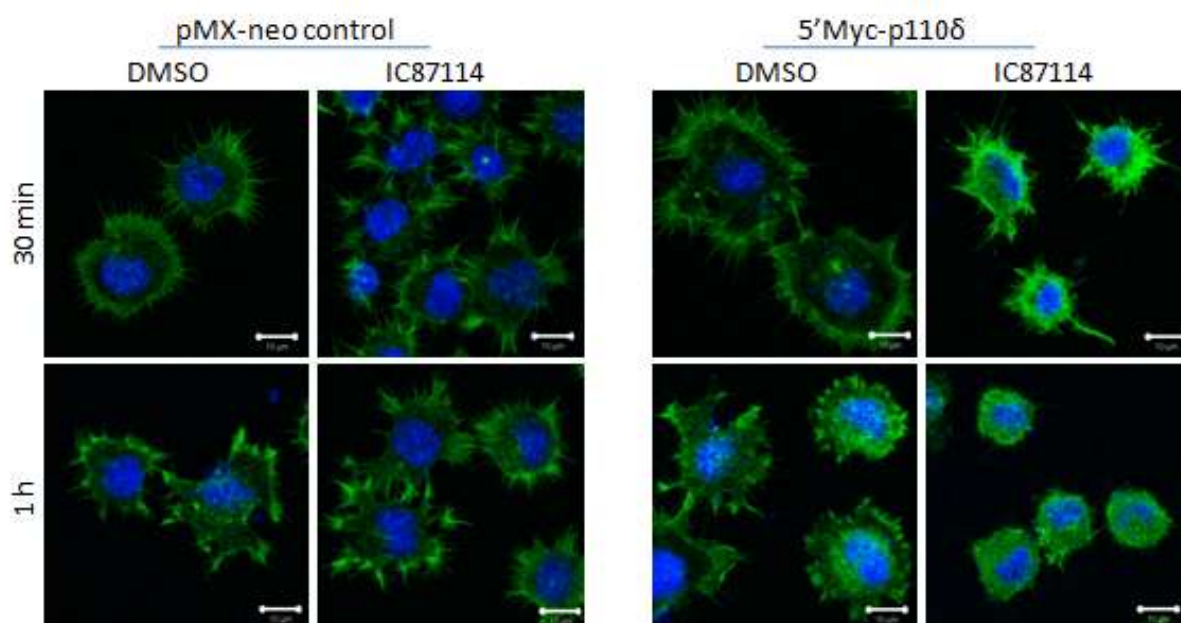
Figure 7.10: Cell adhesion of NIH 3T3 cells stably expressing pMX-neo or 5'Myc-p110δ onto glass coverslips. NIH 3T3 cells stably expressing either pMX-neo control vector or 5'Myc-p110δ were starved for 12 h, detached using trypsin and treated with either 5 μM IC87114 or vehicle control (DMSO). Cells were left to adhere onto glass coverslips in the absence of serum for the indicated times before fixation with 4% PFA. Permeabilised cells were stained with phalloidin (F-actin) and DAPI (DNA). Scale bar = 10 μM.

Treatment of cells with IC87114, reduced cell spreading of 5'Myc-p110δ-overexpressing cells at both 30 min and 1 h after seeding the cells, whereas in pMX-neo-expressing cells IC87114 treatment seemed to have little effect on cell spreading, although organisation of filopodia protrusions was affected (Figure 7.10). This suggests that in 5'Myc-p110δ-overexpressing cells, p110δ is playing an essential role in cell adherence and cell spreading, whereas in control infected cells p110δ appears to not have such an essential role although it does appear to be involved in organisation of filopodia extensions.

To investigate cell adherence on different substrates, glass coverslips were coated with either fibronectin or gelatin and cells, which had been starved of serum overnight, were left to adhere for 30 min, 2 h or 6 h in media without serum. At each time point, 5'Myc-p110δ-overexpressing cells appeared to spread over an increased surface area compared to pMX-neo-expressing cells (Figure 7.11). Quantification of cell area revealed a significant difference between 5'Myc-p110δ-overexpressing cells and pMX-neo-expressing cells at every time point and on both substrates (Figure 7.12).

30 min after seeding the cells, 5'Myc-p110δ-overexpressing cells displayed broad lamellipodia protrusions compared to the slender filopodia protrusion observed in pMX-neo-expressing cells on both fibronectin and gelatin. At 2 h and 6 h after seeding, 5'Myc-p110δ-overexpressing cells also displayed mutiple filopodia protrusions similar to pMX-neo-expressing cells. These data suggest that initiation of cell adherence and cell spreading is largely dependent on Rac activity in 5'Myc-p110δ-overexpressing cells indicated by the presence of lamellipodia (Kozma, et al., 1995; Ridley, et al., 1992). At later time points, Cdc42 appears to play a role in cell adhesion, indicated by the presence of filopodia. In contrast, in pMX-neo-expressing cells, initial cell spreading appears to be mediated largely by Cdc42 activity, indicated by the presence of multiple filopodia extensions at the early time point of cell-fixation (Kozma, et al., 1999).

Overall, the data indicate that p110δ plays a role in cell adhesion and spreading on a variety of substrates and is likely to mediate this function through activation of small Rho GTPases, specifically Rac.
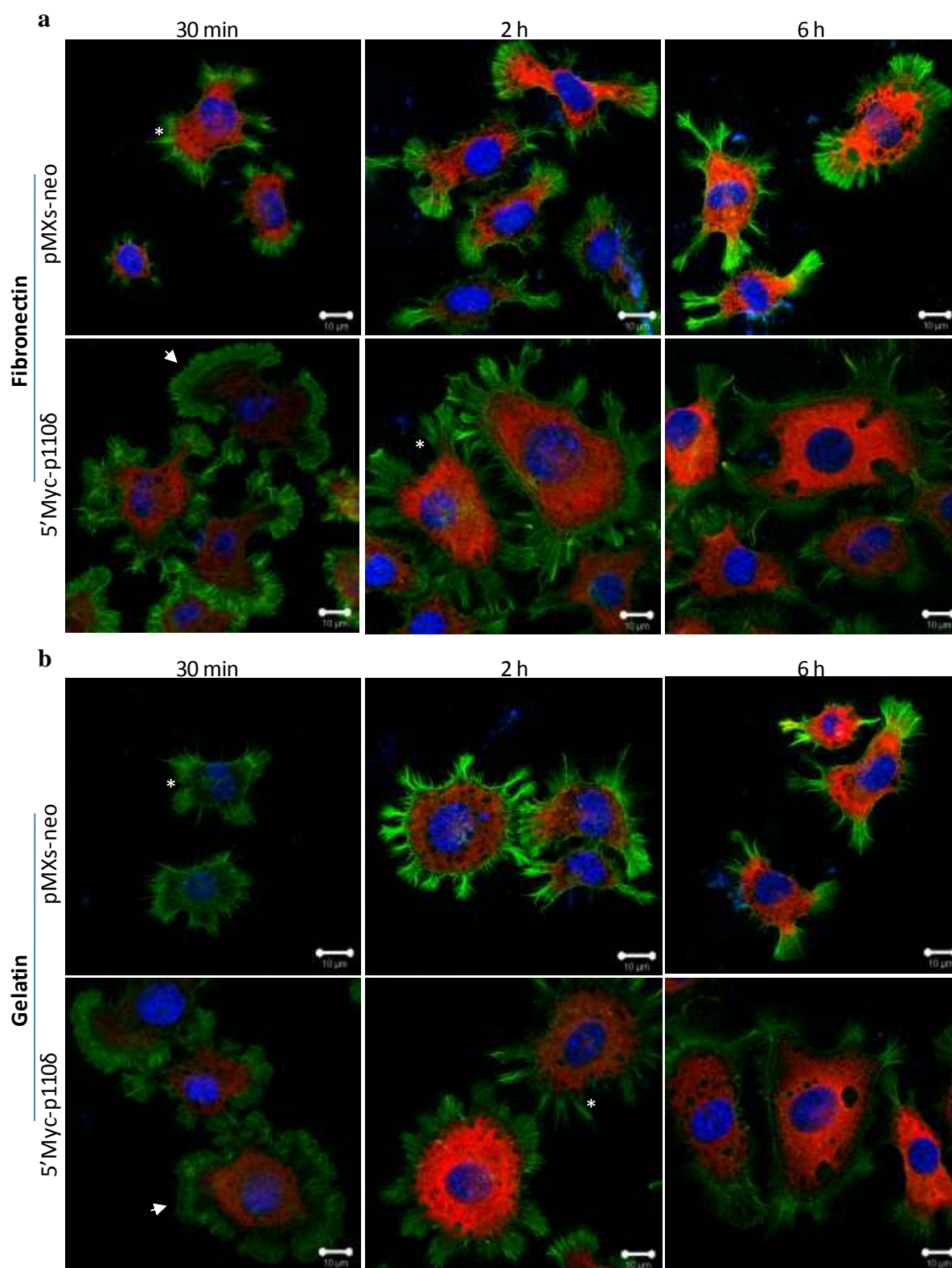
Figure 7.11: Cell adhesion and cell spreading of NIH 3T3 cells stably expressing pMX-neo or 5'Myc-p110δ on fibronectin- or gelatin-coated coverslips. NIH 3T3 cells stably expressing either pMX-neo control vector or 5'Myc-p110δ were starved for 12 h, detached using trypsin and seeded on **(a)** fibronectin- or **(b)** gelatin-coated coverslips in the absence of serum. After the indicated times, cells were fixed with 4% PFA. Permeabilised cells were stained with phalloidin (F-actin), DAPI (DNA) and vincullin. Arow heads indicate broad lamellipodia and asterisks indicate slender filopodia protrusions. Scale bar = 10 µM.
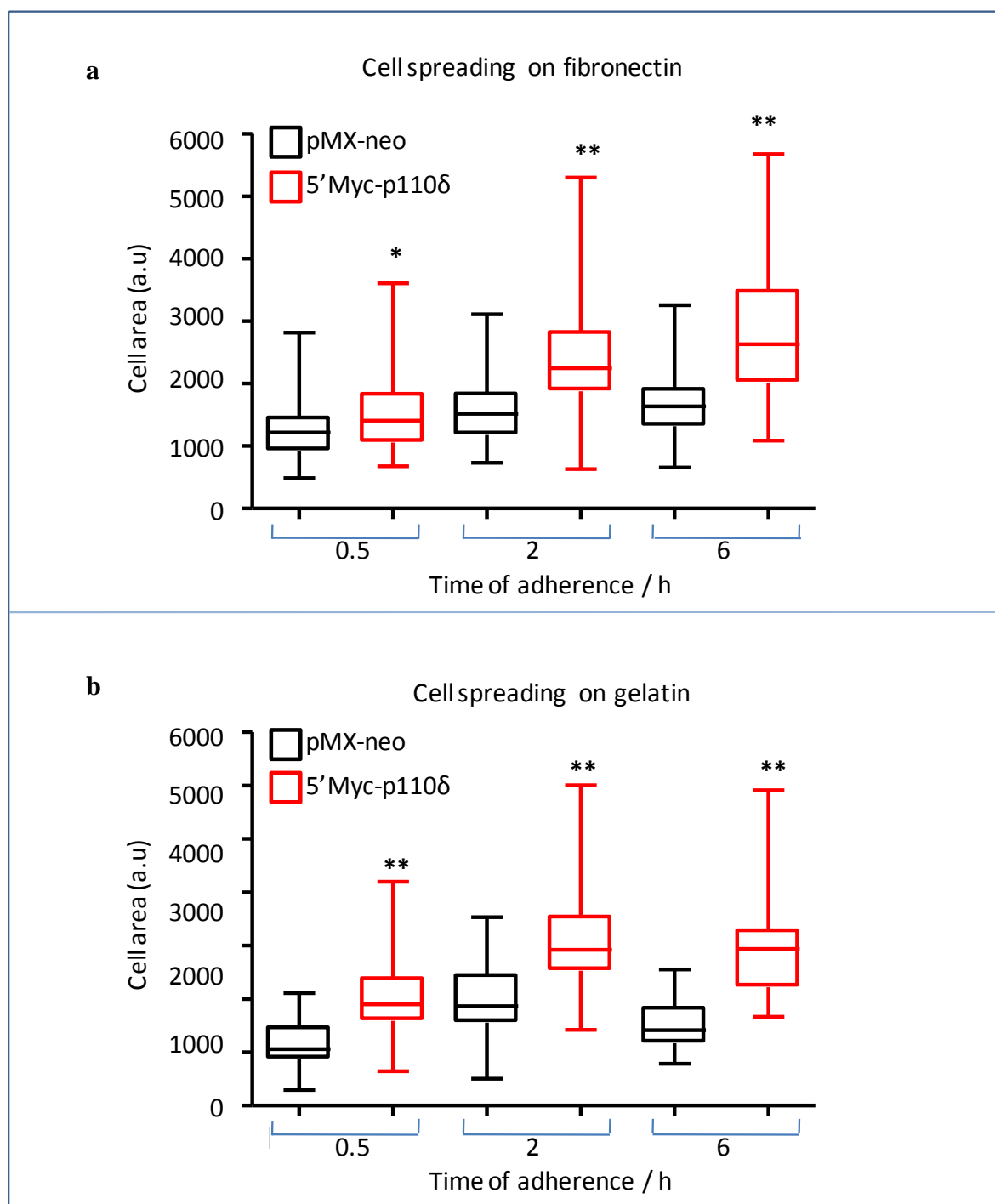
Figure 7.12: Quantification of cell spreading of NIH 3T3 cells stably expressing pMX-neo or 5'Myc-p110δ on fibronectin or gelatin-coated coverslips. Cell area was calculated from confocal images of cells adhering to **(a)** fibronectin- or **(b)** gelatin-coated coverslips, using *Image J* software. Median, quartiles and highest lowest values are indicated on box whisker plots. * indicates $P<0.1$ and ** indicates $P < 0.01$ using the Mann-Whitney *U*-test, $n > 75$.

7.3.6 p110δ may play a role in mediating cell-cell junction formation and in the formation of focal adhesions

Adherens junctions are calcium-dependent cell–cell contacts that link neighbouring cells through cadherin receptors. The formation of cell junctions requires regulation of the actin

cytoskeleton by Rho GTPases. In epithelial cells, Rac activation promotes E-cadherin-mediated cell-cell adhesion (Hordijk*, et al.*, 1997; Sander*, et al.*, 1998). In fibroblasts Rac activation has also been shown to induce an epithelial-like morphology through the formation of adherens junctions mediated by N- and P-cadherin (as these cells do not express E-cadherin) (Reynolds*, et al.*, 1996; Sander*, et al.*, 1999). In cells that had been starved overnight, N-cadherin was found to localize at points of cell-cell contact in both pMX-neo-expressing and 5'Myc-p110δ-overexpressing cells. A possible increased N-cadherin staining in 5'Myc-p110δ-overexpressing cells compared to pMX-neo-expressing cells was observed, although this was not an obvious difference and would be difficult to quantify (Figure 7.13). Upon PDGF stimulation, increased N-cadherin staining was observed for both pMX-neo-expressing and 5'Myc-p110δ-overexpressing cells, with no obvious difference between the cell lines, although some kind of quantification would need to be carried out to formally prove this (Figure 7.13). These results indicate that p110δ may possibly play a role in adherens junction formation under serum-starvation conditions, although this is not a major role. Likewise, overexpression of p110δ does not affect PDGF-induced N-cadherin expression and adherens junction formation.

PDGF stimulation induced focal adhesions in pMX-neo-expressing and 5'Myc-p110δ-overexpressing NIH 3T3 cells (Figure 7.13). As observed previously (Figures 7.4,7.5), 5'Myc-p110δ-overexpressing cells appeared to have an increased number of sites of focal contact with the underlying substrate than pMX-neo-expressing cells, in both starved and PDGF-stimulated conditions, suggesting p110δ has a role in mediating focal contacts.
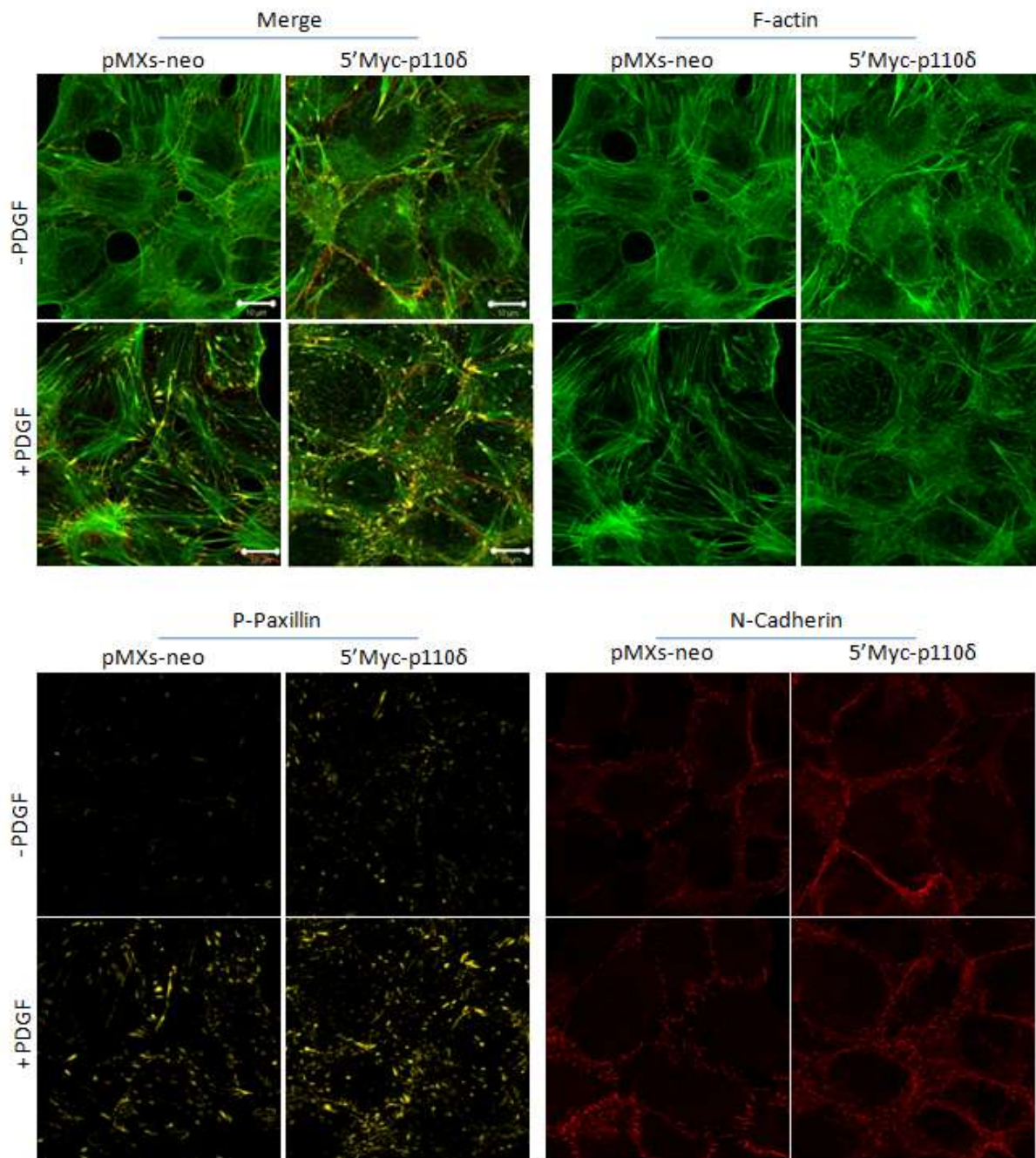
Figure 7.13: Cell-cell junction formation in NIH 3T3 cells stably expressing pMX-neo or 5'Myc-p110δ. NIH 3T3 cells stably expressing either pMX-neo or 5'Myc-p110δ were seeded on glass coverslips and starved for 12 h. Cells were stimulated with 50 ng/ml PDGF for 7 min before fixation with 4% PFA. Permeabilised cells were stained with phalloidin (F-actin) P-paxillin (focal adhesions) and N-cadherin (adherens junctions). Scale bar = 10 μM.

7.4 NIH 3T3 cells stably overexpressing 5'Myc-p110δ have altered Rho GTPase activity compared to control-infected cells

The data presented clearly show that 5'Myc-p110δ-overexpressing cells display an altered actin cytoskeleton and overall cell morphology compared to pMX-neo-expressing cells and this morphology differs depending on whether cells are in the presence of serum or under serum-starvation conditions. As central regulators of the cell cytoskeleton, the activities of the three best characterised Rho GTPases; RhoA, Rac1 and Cdc42, were investigated in these cells, by performing pull downs of the GTP-loaded Rho GTPase (Figure 7.14). The effect of p110δ inhibition, the effect of serum-starvation and the effect of acute serum-stimulation on Rho GTPase activity was analysed. The activity of RhoA, Rac1 and Cdc42 was determined. These results are described below and summarised in Table 8.1 on page 261.

7.4.1 p110δ appears to be both a positive and negative regulator of RhoA activity in the presence of serum in NIH 3T3 cells stably overexpressing 5'Myc-p110δ

The basal level of active RhoA in the presence of serum was found to be approximately 5-fold higher in 5'Myc-p110δ-overexpressing cells compared to pMX-neo-expressing cells (Figure 7.15a). This was an unexpected finding since p110δ has previously been found to be a negative regulator of RhoA activity in macrophages (Papakonstanti, et al., 2007), overexpression of p110δ was therefore expected to result in a decrease in basal RhoA activity. This result indicates that p110δ may be positively regulating basal RhoA activity in the presence of serum, in NIH 3T3 cells.

In agreement with previous findings, inhibition of p110δ activity (through IC87114 treatment) increased the level of GTP-loaded RhoA in 5'Myc-p110δ overexpressing cells by approximately 2-fold, indicating that p110δ is indeed having some role in negatively regulating RhoA activity. The tendency of 5'Myc-p110δ-overexpressing cells to have increased basal RhoA-GTP in serum compared to pMX-neo-expressing cells, which is further increased upon p110δ inhibition, was highly reproducible illustrated in two further independent experiments (Figures 7.16a, b).

Although pMX-neo-expressing NIH 3T3 express little endogenous p110δ, IC87114 treatment also increased RhoA activity by approximately 2-fold, suggesting that even low levels of p110δ expression is sufficient to negatively regulate basal RhoA activity (Figure 7.15a).

In the absence of serum, 5'Myc-p110δ overexpressing cells expressed higher basal RhoA activity compared to pMX-neo-expressing cells, although this increase is substantially less than the increase observed in the presence of serum (Figure 7.15a). This suggests, that under starvation conditions alternative signalling pathways are operating compared to in the presence of serum, in which p110δ does not exert such a marked positive effect on RhoA activation. This inference is corroborated by the finding that IC87114 treatment of both pMX-neo-expressing and 5'Myc-p110δ overexpressing cells under starvation conditions had only a slight increase on RhoA activity compared to the increase observed in the presence of serum.
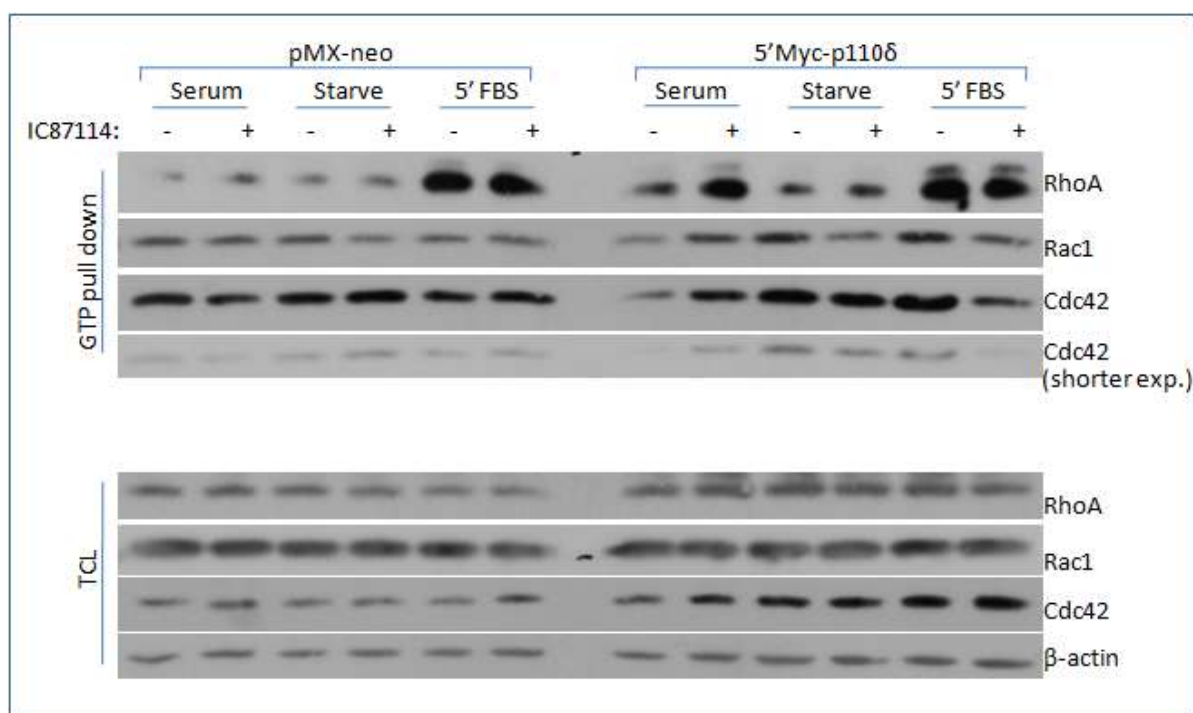
Figure 7.14: Effect of p110δ inhibition on Rho GTPase activity under basal growing, serum-starvation or serum-stimulated conditions in NIH 3T3 cells stably expressing pMX-neo or 5'Myc-p110δ. pMX-neo control infected or 5'Myc-p110δ-overexpressing cells were seeded either in media containing 10% serum or media without serum and left overnight. The following day cells were treated with 5 μM IC87114 or vehicle control for 1 h. Basal Rho GTPase activities were assessed under basal growing conditions (media containing 10% serum), serum-starvation conditions and serum-stimulated conditions. For cell stimulations, cells that had been starved overnight were stimulated for 5 min with 10% FBS. For each condition, equal volumes of cell lysates of pMX-neo control infected or 5'Myc-p110δ-overexpressing cells were subjected to a pull down assay with GST-RBD (RhoA-GTP) or GST-PBD (Rac1-GTP and Cdc42-GTP), followed by detection of precipitated Rho GTPases by western blot. Equal volumes of total cell lysates were resolved on a separate SDS-PAGE gel to blot for total levels of RhoA, Rac1 or Cdc42.
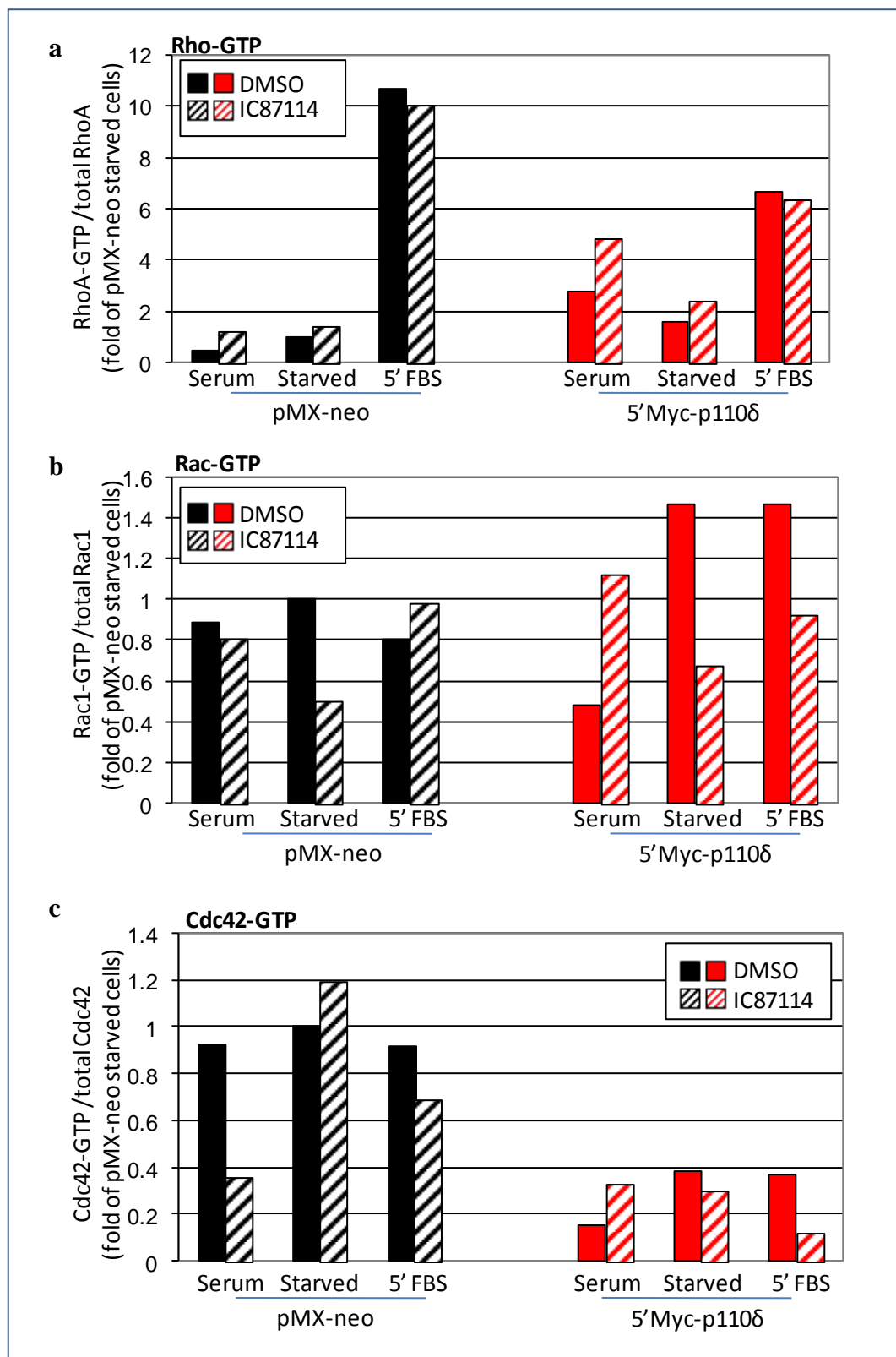
Figure 7.15: Quantification of RhoA, Rac1 and Cdc42 activity under basal growing, serum-starvation or stimulated conditions in NIH 3T3 cells stably expressing pMX-neo or 5'Myc-p110δ. Levels of GTP-bound **(a)** RhoA, **(b)** Rac1 or **(c)** Cdc42 were normalized against the total levels of each Rho GTPase and expressed as a fold-increase of pMX-neo control infected cells under serum-starvation conditions.
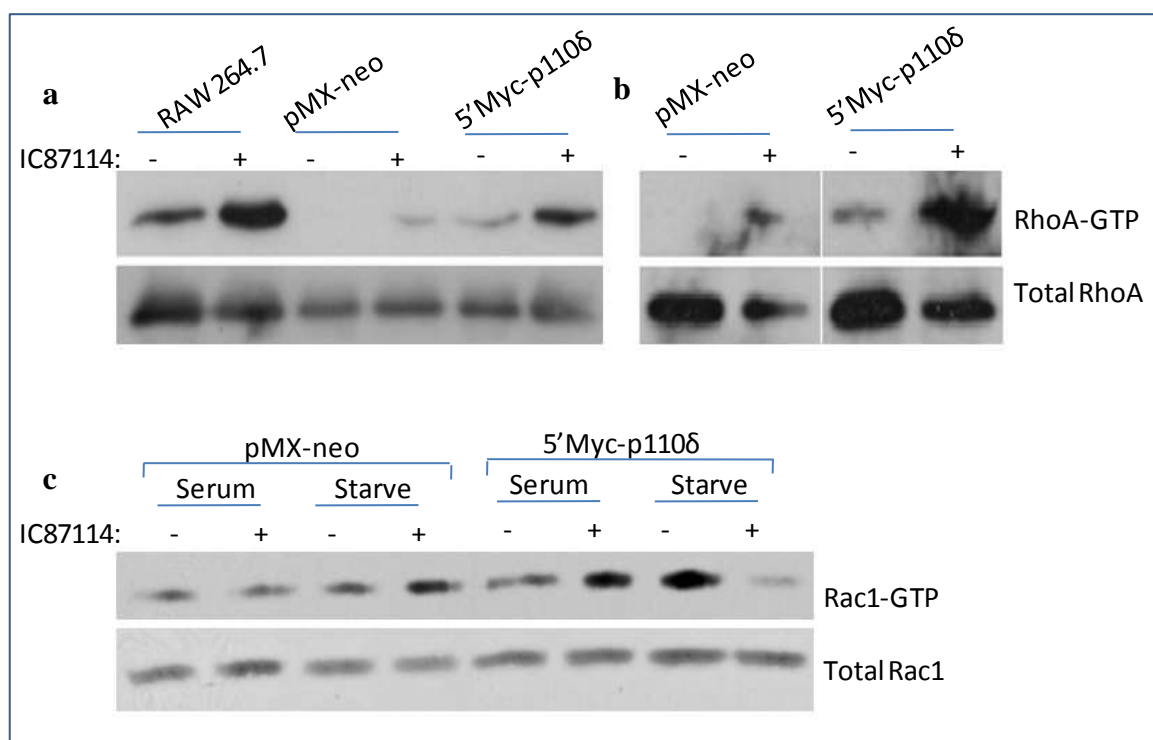
Figure 7.16: Effect of p110δ inhibition on Rho GTPase activity in the presence of serum or under serum-starvation conditions in pMX-neo control infected and 5'Myc-p110δ-overexpressing cells. (a) The RAW 264.7 macrophage cell line, pMX-neo control infected or 5'Myc-p110δ-overexpressing cells seeded in media containing 10% serum were treated with 5 μM IC87114 or vehicle control for 1 h. Equal volumes of cell lysates were subjected to a pull down assay with GST-RBD followed by detection of precipitated RhoA by western blot. Equal volumes of total cell lysates were resolved on a separate SDS-PAGE gel to blot for total levels of RhoA. (b) Repeat of experiment described in part a) without RAW 264.7 macrophage cell line as appositive control for RhoA activity. (c) pMX-neo control infected or 5'Myc-p110δ-overexpressing cells were seeded either in media containing 10% serum or media without serum and left overnight. The following day cells were treated with5 μM IC87114 or vehicle control for 1 h. Equal volumes of cell lysates were subjected to a pull down assay with GST-PBD followed by detection of precipitated Rac1 by western blot. Equal volumes of total cell lysates were resolved on a separate SDS-PAGE gel to blot for total levels of Rac1.

7.4.2 p110δ is not essential for acute serum-induced RhoA activation in NIH 3T3 cells

Interestingly, IC87114 treatment of both pMX-neo-expressing and 5'Myc-p110δ-overexpressing cells prior to serum-stimulation, did not enhance RhoA activity compared to DMSO-treated cells (Figure 7.15a). Serum stimulation induced a significant increase in RhoA activity in both pMX-neo-expressing and 5'Myc-p110δ-overexpressing cells compared to the level of GTP-bound RhoA under basal starvation conditions. In fact, serum-stimulation of pMX-neo-expressing cells resulted in higher RhoA-GTP levels than 5'Myc-p110δ overexpressing cells. These data demonstrate that RhoA activity can be rapidly and transiently increased upon addition of serum and that this response does not appear to be dependent upon p110δ lipid kinase activity.

7.4.3 p110δ appears to be a positive regulator of Rac1 under serum-starvation conditions in NIH 3T3 cells stably expressing pMX-neo or 5'Myc-p110δ

It has been shown that in some cellular contexts, Rac1 negatively regulates RhoA activity, given that low levels of Rac1 activity correlate with high levels of RhoA activity (Sander, et al., 1999). In contrast, it has been suggested that RhoA activity does not have an effect on Rac1 activity, suggesting unidirectional signalling from Rac to Rho (Sander, et al., 1999). Taking this into consideration, one would speculate that in 5'Myc-p110δ-overexpressing cells under starvation conditions, where RhoA activity is reduced in comparison to serum conditions, Rac1 activity would be higher than that observed in the presence of serum. Indeed, Rac1 activity was reduced in 5'Myc-p110δ-overexpressing cells in the presence of serum conditions compared to pMX-neo-expressing cells and this increased substantially in serum-starved in 5'Myc-p110δ-overexpressing cells (Figure 7.15b).

IC87114 treatment of 5'Myc-p110δ-overexpressing cells appeared to have opposing effects on Rac1 activity depending on whether cells were treated in the presence or absence of serum. In the presence of serum, IC87114 treatment induced a 2-fold increase in Rac1 activity, suggesting p110δ is negatively regulating Rac1. However, under serum-starvation conditions, IC87114 treatment reduced Rac1 activity, suggesting p110δ is positively regulating Rac1 under these conditions (Figure 7.15b). In pMX-neo-expressing cells, IC87114 treatment reduced Rac1 activity in both serum and starvation conditions, although the observed decrease in Rac1 activity was more apparent in the absence of serum.

The reproducibility of p110δ-dependent activity of Rac1 in 5'Myc-p110δ-overexpressing cells depending on the presence of serum is illustrated in a second independent experiment (Figure 7.16c). Overall these data suggest that in NIH 3T3 cells stably overexpressing 5'Myc-p110δ, p110δ may be positively regulating Rac1 activity under serum-starvation conditions, which opposes high levels of RhoA activity. In the presence of serum however, p110δ may be negatively regulating Rac1 activity, which allows for high RhoA activity induced by components of serum.

7.4.4 Acute stimulation with serum does not induce Rac1 activity in NIH 3T3 cells stably expressing pMX-neo or 5'Myc-p110δ

Unlike the induction of RhoA activity by serum, serum-stimulation of pMX-neo-expressing or 5'Myc-p110δ-overexpressing NIH 3T3 cells did not increase Rac1 activity. This

suggests that the components of serum that stimulate RhoA activity do not activate Rac1 and are unaffected by p110δ overexpression (Figure 7.15b). Interestingly, IC87114 treatment prior to serum stimulation reduced Rac1 activity in 5'Myc-p110δ-overexpressing cells, but had little effect on pMX-neo-expressing cells. This corroborates the finding that in 5'Myc-p110δ-overexpressing cells, p110δ is positively regulating Rac1 in the absence of serum (Figure 7.15b).

7.4.5 p110δ may positively regulate Cdc42 under serum-starvation conditions in NIH 3T3 cells stably overexpressing 5'Myc-p110δ

Activation of Cdc42 has been implicated in the downregulation of RhoA activity (Sander, et al., 1999). In general, Cdc42 activity under serum *versus* serum-starvation conditions followed a similar pattern to Rac1 activity. In 5'Myc-p110δ-overexpressing cells, Cdc42 activity was higher under serum-starvation conditions compared to in the presence of serum and this was not further increased upon serum-stimulation. IC87114 treatment increased Cdc42 activity in 5'Myc-p110δ-overexpressing cells in the presence of serum but reduced it slightly under serum-starvation conditions. The main difference between Cdc42 and Rac1 activation in 5'Myc-p110δ-overexpressing cells is that after quantification, overall Cdc42 activity appears to be lower in 5'Myc-p110δ-overexpressing cells compared to pMX-neo-expressing cells. This is largely due to the fact that the level of total Cdc42 is noticeably higher in 5'Myc-p110δ-overexpressing cells compared to pMX-neo-expressing cells.

7.4.6 Increased RhoA activity in NIH 3T3 cells expressing 5'Myc-p110δ does not appear to be due to decreased p190RhoGAP activity

NIH 3T3 cells-overexpressing 5'Myc-p110δ have been shown to have high levels of GTP-bound RhoA in normal growing conditions (in the presence of 10% serum). The activity of RhoA can be regulated by a number of GEFs and GAPs, such as p190RhoGAP. It was hypothesized that an increase in RhoA activity may result from a decrease in p190RhoGAP activity, which would inhibit RhoA inactivation by preventing hydrolysis of GTP to GDP. The activity of p190RhoGAP was examined by assessing the level of its phosphorylation on tyrosine residues, which has been shown to correlate with its activity (Zrihan-Licht, *et al.*, 2000). 5'Myc-p110δ-overexpressing cells growing in 10% serum were found to have a slight decrease in active p190RhoGAP (Figure 7.17).
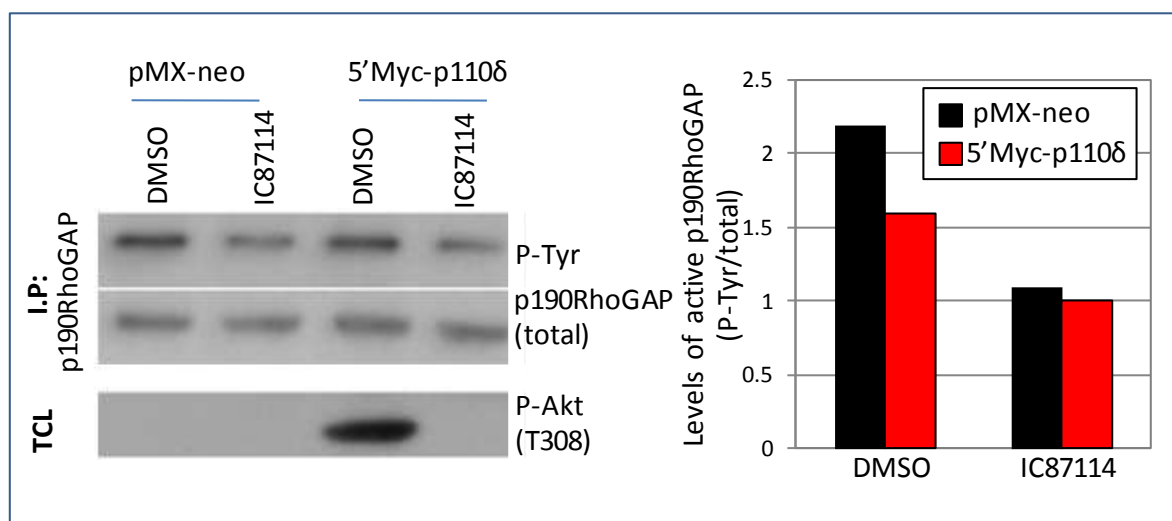
Figure 7.17: Effect of p110δ inhibition on p190RhoGAP activity in NIH 3T3 cells stably expressing pMX-neo or 5'Myc-p110δ. pMX-neo control infected and 5'Myc-p110δ-overexpressing cells were seeded in media containing 10% serum and left to adhere overnight. The following day cells were treated with 5 μM IC87114 or vehicle control for 1 h. Cell lysates were subjected to an immunoprecipitation with an anti p190RhoGAP antibody. Immunoprecipitates were separated by SDS-PAGE and immunoblotted for phospho-tyrosine or p190RhoGAP. Total cell lysates were resolved on a separate SDS-PAGE gel and immunoblotted for P-Akt.

Inhibition of p110δ with IC87114 further decreased p190RhoGAP activity, in both pMX-neo-expressing and 5'Myc-p110δ-overexpressing cells to the same extent (Figure 7.17). The finding that IC87114 reduces p190RhoGAP activity corroborates the finding that macrophages isolated from mice with homozygous gene inactivation of p110δ have reduced p190RhoGAP activity under basal and CSF-1-stimulated conditions (Papakonstanti, et al., 2007). However, it is surprising that IC87114 treatment of pMX-neo-expressing cells resulted in such a noticeable decrease in p190RhoGAP activity, since these cells express little endogenous p110δ. In spite of this, these results suggest that the increase in RhoA activity observed after treatment with IC87114 for both control and 5'Myc-p110δ-overexpressing cells in media containing serum is in part due to the decrease in p190RhoGAP activity. These results also imply that in 5'Myc-p110δ-overexpressing cells, p110δ does not regulate the basal activity of RhoA through p190RhoGAP alone.

7.4.7 Inhibition of Rho or Rac activity alters cell morphology in NIH 3T3 cells stably expressing pMX-neo or 5'Myc-p110δ

Cell adhesion and spreading: Increased RhoA activity is associated with a contractile phenotype. 5'Myc-p110δ-overexpressing cells were shown to have increased basal RhoA, particularly in the presence of serum, compared to pMX-neo-expressing cells and yet they also displayed an increased cell adherence area (Figure 7.9) and increased cell spreading in

adherence assays (Figures 7.10, 7.12). The increased cell spreading in the adhesion assays is most likely a result of increased Rac1 activity, rather than increased RhoA activity, given that they were carried out under serum-starvation conditions, which correlated with high Rac1-GTP levels (Figure 7.15b). To assess if RhoA activity was contributing to the increased cell spreading observed for 5'Myc-p110δ-overexpressing cells, a cell adherence assay under serum-starvation conditions on glass coverslips was carried out with or without the ROCK inhibitor, Y-27632.

Although increased cell spreading of 5'Myc-p110δ-overexpressing cells on glass coverslips is not as apparent as that observed on fibronectin or gelatin (Figure 7.12), the cells displayed increased membrane ruffling and less organized filopodia protrusions compared to control cells (Figure 7.18). As observed previously (Figure 7.10), treatment of cells with IC87114, reduced cell spreading of 5'Myc-p110δ-overexpressing cells and membrane ruffling at both 30 min and 1 h after seeding the cells. In pMX-neo-expressing cells, IC87114 treatment had little effect on cell spreading, implying that in 5'Myc-p110δ-overexpressing cells, p110δ is playing a more central role in the adhesion process. It appears that in 5'Myc-p110δ-overexpressing cells p110δ is not acting through RhoA to mediate cell adhesion since inhibition of ROCK does not result in the same phenotype observed after IC87114 treatment. Indeed, inhibition of ROCK results in a similar phenotype in pMX-neo-expressing and 5'Myc-p110δ-overexpressing cells, with both cell lines cells exhibiting numerous actin-rich cell processes typical of ROCK inhibition (Figure 7.18).
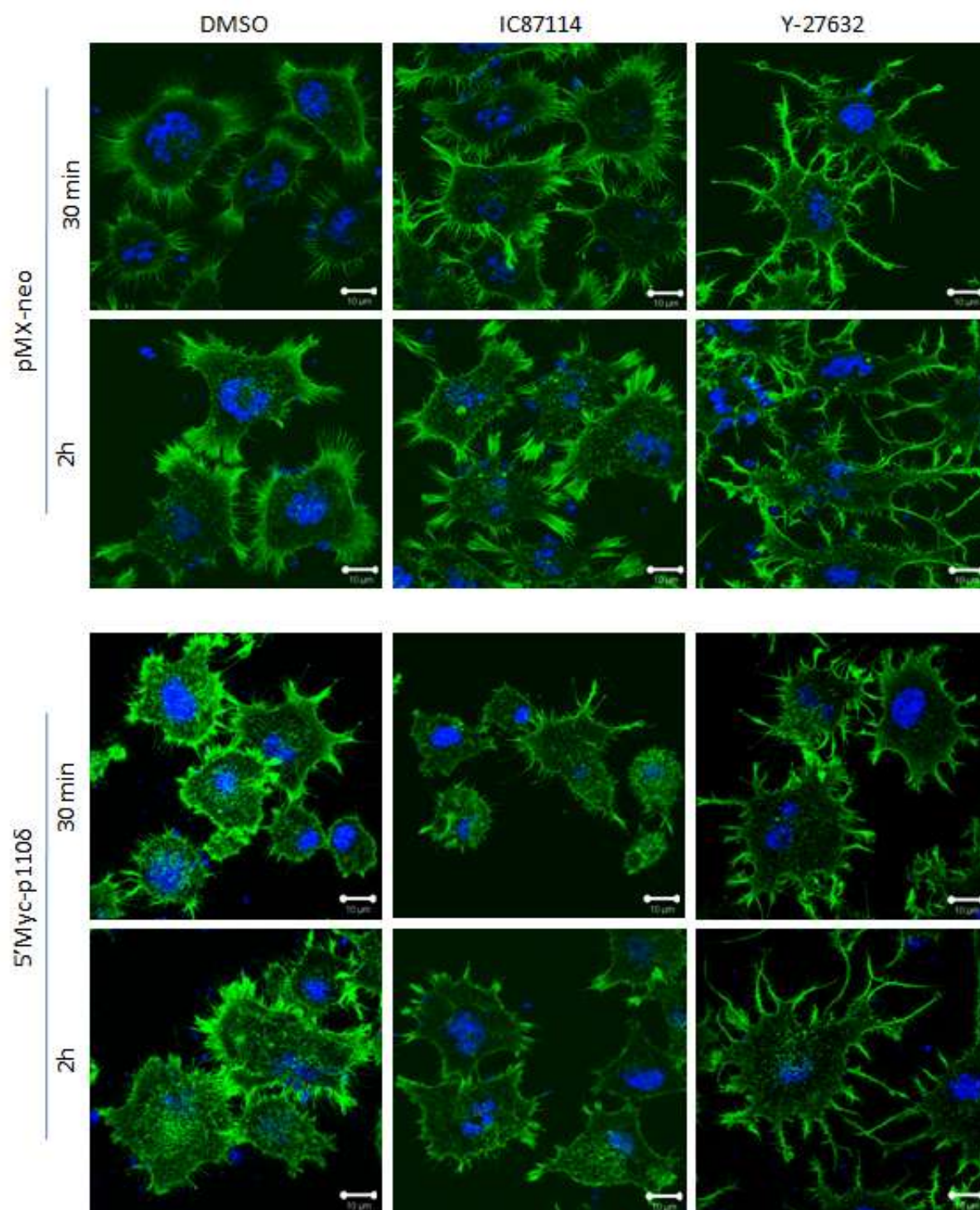
Figure 7.18: Effect of IC87114 and Y-27632 on cell adhesion of NIH 3T3 cells stably expressing pMX-neo or 5'Myc-p110δ on glass coverslips. NIH 3T3 cells stably expressing either pMX-neo control vector or 5'Myc-p110δ were starved for 12 h, detached using trypsin and treated with either 5 μM IC87114 or vehicle control (DMSO) or 10 μM Y-27632. Cells were left to adhere onto glass coverslips in the absence of serum for the indicated times before fixation with 4% PFA. Permeabilised cells were stained with phalloidin (F-actin) and DAPI (DNA). Scale bar = 10 μM.

Overall cell morphology on matrigel: To get an idea of the morphology of 5'Myc-p110δ-overexpressing cells on a three-dimensional matrix, images were taken of pMX-neo-expressing cells and 5'Myc-p110δ-overexpressing cells grown on matrigel 24 and 48 h after seeding.

After 24 h, numerous pMX-neo-expressing cells displayed a rounded morphology, whereas 5'Myc-p110δ-overexpressing cells had spread over the matrigel and displayed long membrane protrusions, indicating that 5'Myc-p110δ-overexpressing cells adhere and spread more quickly than pMX-neo-expressing cells (Figure 7.19a). Treatment of pMX-neo-expressing cells with the small molecule Rac1 inhibitor, NSC23766, which binds the surface groove of Rac1 known to be critical for GEF specification (Desire*, et al.*, 2005; Gao*, et al.*, 2004), resulted in an increase in the number of cells with a rounded morphology. In 5'Myc-p110δ-overexpressing cells, NSC23766 treatment appeared to prevent the formation of membrane protrusions and induced some cell rounding, although not to the same extent as pMX-neo-expressing cells (Figure 7.19a). As observed in the adhesion assay, Y-27632 treatment induced the formation of multiple long membrane protrusions in both pMX-neo-expressing cell and 5'Myc-p110δ-overexpressing cells.

After 48 h, pMX-neo-expressing cells had adhered and spread more over the matrigel compared to at 24 h. 5'Myc-p110δ-overexpressing cells had a similar morphology to that observed at 24 h (Figure 7.19b). Treatment of pMX-neo-expressing cells with NSC23766 resulted in increased cell rounding, as observed 24 h after treatment, and also induced a degree of cell clustering. Interestingly, 48 h after NSC23766 treatment of 5'Myc-p110δ-overexpressing cells, a striking change in cell morphology was observed. Cells formed long clusters, with an appearance not dissimilar from that observed for 5'Myc-p110δ-overexpressing cells treated with IC87114 in the presence of serum (Figure 7.6). As observed after 24 h of seeding the cells, Y-27632 treatment induced the formation of multiple long membrane protrusions in both pMX-neo-expressing cells and 5'Myc-p110δ-overexpressing cells at 48 h after seeding.

Collectively, these data indicate that 5'Myc-p110δ-overexpressing cells are able to adhere and spread to and form their overall final cell morphology on matrigel more quickly than pMX-neo-expressing cells. 5'Myc-p110δ-overexpressing cells display more membrane protrusions, possibly a tail retraction defect, that appears to mediated by Rac activity, indicated by a reduction of membrane protrusions after 24 h of Rac inhibition. However,

when cells are more confluent, after 48 h of seeding the cells, Rac inhibition induced 'string-like' cell clustering in 5'Myc-p110δ-overexpressing cells, which may be due to increased cell-cell contacts at this confluency. Given that Rac inhibition induces a more striking phenotype in 5'Myc-p110δ-overexpressing cells compared to pMX-neo-expressing cells, this suggests Rac activity has a more central role in this cell line.
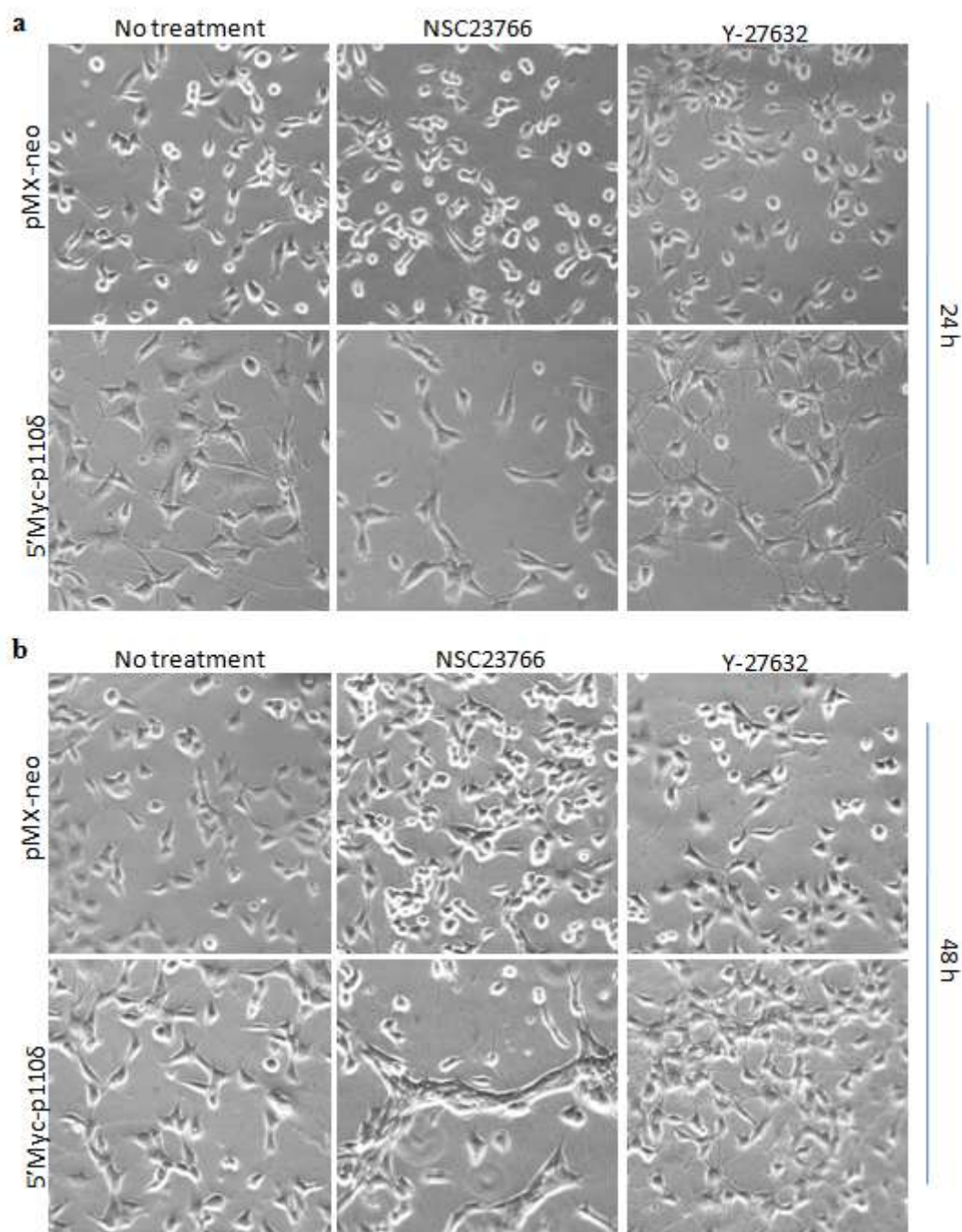
Figure 7.19: Morphology of NIH 3T3 cells stably expressing pMX-neo or 5'Myc-p110δ on matrigel. Cells were seeded in media containing 10% serum on matrigel. 20 μM NSC23766 or 10 μM of Y-27632 was added to the cell cuture media. Cell images were captured at **(a)** 24 h and **(b)** 48 h after seeding.

To assess the actin cytoskeleton of 5'Myc-p110δ-overexpressing cells on matrigel, pMX-neo-expressing cells and 5'Myc-p110δ-overexpressing cells seeded on matrigel were fixed and stained with Rhodamine-conjugated phalloidin. Compared to pMX-neo-expressing cells, 5'Myc-p110δ-overexpressing cells displayed multiple lamellipodia protrusions and had an overall more irregular cell morphology (Figure 7.20). This type of cell morphology is indicative of increased Rac activity, suggesting 5'Myc-p110δ-overexpressing cells have increased Rac activity compared to pMX-neo-expressing cells.
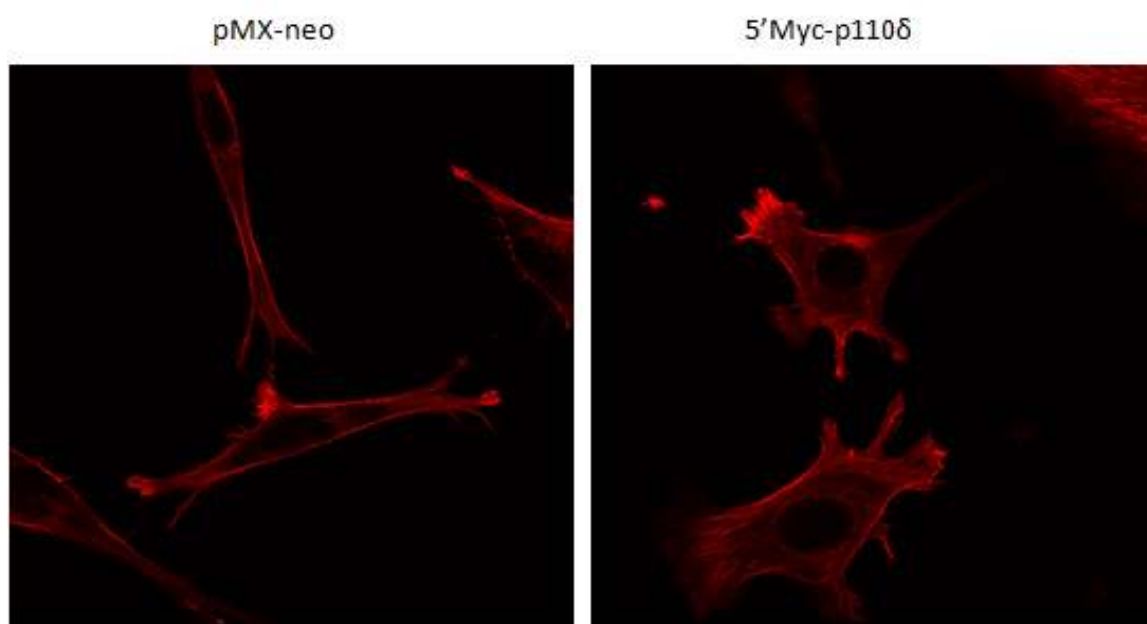
Figure 7.20: Actin cytoskeleton of NIH 3T3 cells stably expressing pMX-neo or 5'Myc-p110δ on matrigel. The indicated cell lines were seeded on matrigel in 10% serum. 48 h after seeding, cells were fixed and stained with Rhodamine-conjugated phalloidin.

7.5 Discussion

7.5.1 Overexpression of p110δ in NIH 3T3 cells downregulates p110α and p110β expression

A summary of the phenotypes observed in 5'Myc-p110δ-overexpressing cells, which are discussion in the following sections, can be found in Table 8.1 on page 261. Data presented in Chapter 6 indicated that overexpression of Gag-p110δ, Gag-p110δ-3'CAAX and 5'Myc-p110δ in NIH 3T3 cells resulted in reduction of p110α expression to a level undetectable by immunoblotting. Data presented in this chapter further corroborate the finding that in NIH 3T3 cells stably overexpressing p110δ, through transfection of 5'Myc-p110δ cDNA, endogenous p110α expression is severely attenuated and in addition, p110β expression appeared to be completely abrogated. These data indicate that the level of p110δ expression regulates the protein expression of the other class IA PI3K isoforms. NIH 3T3 cells have extremely low endogenous levels of p110γ protein expression,

therefore it is unlikely that downregulation of this isoform would have been detected in this cell line, although it was not investigated. It has been documented previously that overexpression one particular p110 isoform affects the expression levels of other isoforms that share the same regulatory subunit (Kang, et al., 2006). In chicken embryo fibroblasts, the endogenous levels of p110α are downregulated in cells overexpressing p110β or p110δ and overexpression of p110δ leads to reduced endogenous levels of p110α and p110β expression (Kang, et al., 2006).

There are also other examples in which high p110δ expression may be associated with low levels of p110α, p110β and/or p110γ expression. In four samples of primary human breast cancer tissue, which have high p110δ expression, three had low p110α expression and one sample had low expression of both p110α and p110β. In normal breast tissue, which is also found to express high levels of p110δ, p110α and p110β expression remained high (Sawyer, et al., 2003). Analysis of p110 expression in leukaemic blast cells from patients with acute myeloid leukaemia, has revealed that p110δ is detected at consistently high levels between all patients, whereas p110α, p110β and p110γ expression was highly variable (Sujobert, *et al.*, 2005). Interestingly, in this study the leukaemic blast cell sample which had the highest detectable level of p110δ expression had undetectable p110α and p110β expression and extremely low p110γ (Sujobert, et al., 2005). Similarly, in an independent investigation of PI3K isoform expression in leukaemic blast cells isolated from patients with acute myeloid leukaemia, p110δ expression was found to be consistently high in all samples in comparison to p110α, p110β and p110γ expression, which was highly variable between patient samples (Billottet, *et al.*, 2006). These data suggest that in some transformed cells, which endogenously express high levels of p110δ, a downregulation in p110α/p110β and/or p110γ expression can occur. In these cells p110δ has become the principle isoform in class I PI3K signalling. p110δ has been shown to control the directionality and, to a lesser extent, speed of migration in breast cancer cell lines (Sawyer, et al., 2003). It would have been interesting to investigate the invasive and migratory capacity of samples of breast cancer cells and leukaemic blast cells which appear to only express p110δ in comparison to cells in which expression all class I PI3K isoforms remains. It is possible that p110δ mediates the downregulation of other class I PI3K isoform in these cells to gain an invasive/migratory advantage. If this is the case, investigation into the mechanism by which downregulation of the other p110 isoforms occurs could offer novel therapeutic targets in breast cancer and acute myeloid leukaemia.

The level of p85 expression in in 5'Myc-p110δ-overexpressing cells appeared largely unaltered. There are strong indications that there is no excess monomeric p85 over p110 subunits (Geering, *et al.*, 2007b). A limiting amount of p85 in cells, which may preferentially bind the exogenous overexpressed p110δ subunits in 5'Myc-p110δ-overexpressing cells, may result in a downregulation of the other endogenous p110 subunits. Indeed, in other studies overexpression of p110 subunits has been achieved without cotransfecting cDNAs for p85 and the exogenously expressed p110 subunits have been found to bind endogenous p85 (Auger, et al., 2000, Kang, et al., 2006, Link, et al., 2005).

The NIH 3T3 cell line I have created, which stably overexpresses 5'Myc-p110δ, could be used to investigate the mechanism by which p110δ mediates downregulation of p110α and p110β. Downregulation may occur at the level of transcription, translation, or protein degradation. Analysis of the mRNA expression of p110α and p110β would help elucidate whether p110δ induces transcriptional repression of these isoforms, likewise treating cells with a proteasome inhibitor may determine whether p110δ mediates protein degradation of p110α and p110β. Acute inhibition of p110δ lipid kinase activity did not alter p110α and p110β protein expression in 5'Myc-p110δ-overexpressing NIH 3T3 cells (Figure 7.2), however, it would be interesting to treat cells with the p110δ inhibitor for a longer time period to assess whether long-term p110δ inhibition restores p110α and p110β expression. This would determine whether p110δ lipid kinase activity is essential for the downregulation of p110α and p110β. Another way to assess whether the lipid kinase activity of p110δ is required for the downregulation of p110α and p110β expression is to stably express a kinase-dead p110δ in NIH 3T3 cells and determine the level of p110α and p110β protein expression.

Although the observation that p110δ overexpression leads to attenuated p110α and p110β expression is interesting, the altered PI3K isoform expression in NIH 3T3 stably overexpressing 5'Myc-p110δ make it difficult to assign the phenotypes observed in these cells to p110δ overexpression or to p110α and/or p110β downregulation.

7.5.2 Serum-dependent activation of Rho GTPase signalling pathways

We observed a clear difference in the actin-cytoskeleton and overall cell morphology of 5'Myc-p110δ-overexpressing NIH 3T3 cells depending on whether cells were in 10% serum or whether cells had been starved of serum overnight. Given that cell morphology is highly dependent on the relative activities of Rho GTPases, this difference is likely to be a

direct reflection of the differential activities of RhoA and Rac1, described below, which result from both p110δ overexpression *and* p110β downregulation. The composition of serum is quite variable, containing numerous growth factors, such as IGF-1 and PDGF, and antibodies. However, an important active constituent of serum is lysophosphatidic acid (LPA) (Eichholtz*, et al.*, 1993). Given that p110β is activated downstream of LPA receptors (Guillermet-Guibert, et al., 2008, Yart, et al., 2002) the lack of p110β expression in 5'Myc-p110δ-overexpressing NIH 3T3 cells is more likely to affect cell morphology in the presence of serum. In the absence of serum, we may be more likely to observe the effect of p110δ overexpression on cell morphology rather than the effect of p110β downregulation. It should not be forgotten, however, that p110α was also downregulated in 5'Myc-p110δ-overexpressing NIH 3T3 cells, therefore it possible that the effect on cell morphology may be due to low levels of p110α expression in addition to high levels of p110δ expression.

Numerous studies have documented LPA-induced Rho GTPase signalling and LPA-induced p110β activation (Guillermet-Guibert, et al., 2008; Jalink*, et al.*, 1994; Kranenburg*, et al.*, 1999; Sugimoto*, et al.*, 2006; Tigyi & Miledi, 1992; Van Leeuwen*, et al.*, 2003; Yart, et al., 2002), and it is for these reasons that I have concentrated on possible differences downstream of LPA activation to explain the different phenotypes observed in pMX-neo-expressing and 5'Myc-p110δ-overexpressing in the presence or absence of serum. It is, however, important to emphasize that the phenotypes observed could be mediated by other constituents of serum.

LPA is a phospholipid that acts on its cognate GPCRs termed LPA_1, LPA_2, and LPA_3. LPA_1 is the most widely expressed and best characterised LPA receptor, whereas LPA_2, and LPA_3 have a more restricted distribution pattern (Moolenaar*, et al.*, 2004). LPA mediates a considerable array of cellular responses, all of which appear to be receptor-mediated. Not surprisingly for a platelet produced growth factor, LPA has all the hallmarks of a wound-healing agonist; stimulating the proliferation and migration of mesenchymal and epithelial cells, having vasoconstrictive actions, and enhancing the production of metalloproteases, which are all important events in tissue repair (Moolenaar, et al., 2004).

7.5.2.1 GPCR signalling

In common with other GPCRs, LPA receptors undergo rapid ligand-induced internalisation from the plasma membrane. LPA receptors can couple to at least three distinct G-protein families, namely $G\alpha_{q/11}$, $G_{i/0}$, and $G_{12/13}$ (Figure 7.21). G proteins are heterotrimeric proteins composed of α, β and γ subunits. They effectively function as dimers since

receptor signalling is mediated either by the Gα subunit or the stable Gβγ complex. Gα-GDP associates with Gβγ and with cytoplasmic portions of the typically seven-pass membrane receptor. Upon ligand activation, the receptor acts as a GEF stimulating the exchange of GDP for GTP on the α subunit. Gα-GTP dissociates from Gβγ and both entities can interact with effectors. Hydrolysis of GTP restores Gα-GDP, which then reassociates with Gβγ and the receptor to terminate signalling. Currently there are 20 known Gα, 6 Gβ, and 11 Gγ subunits. On the basis of sequence similarity, the Gα subunits have been divided into four families: G_s, $G_{i/o}$, $G_{q/11}$ and $G_{12/13}$, which define both receptor and effector coupling (Neves, et al., 2002).
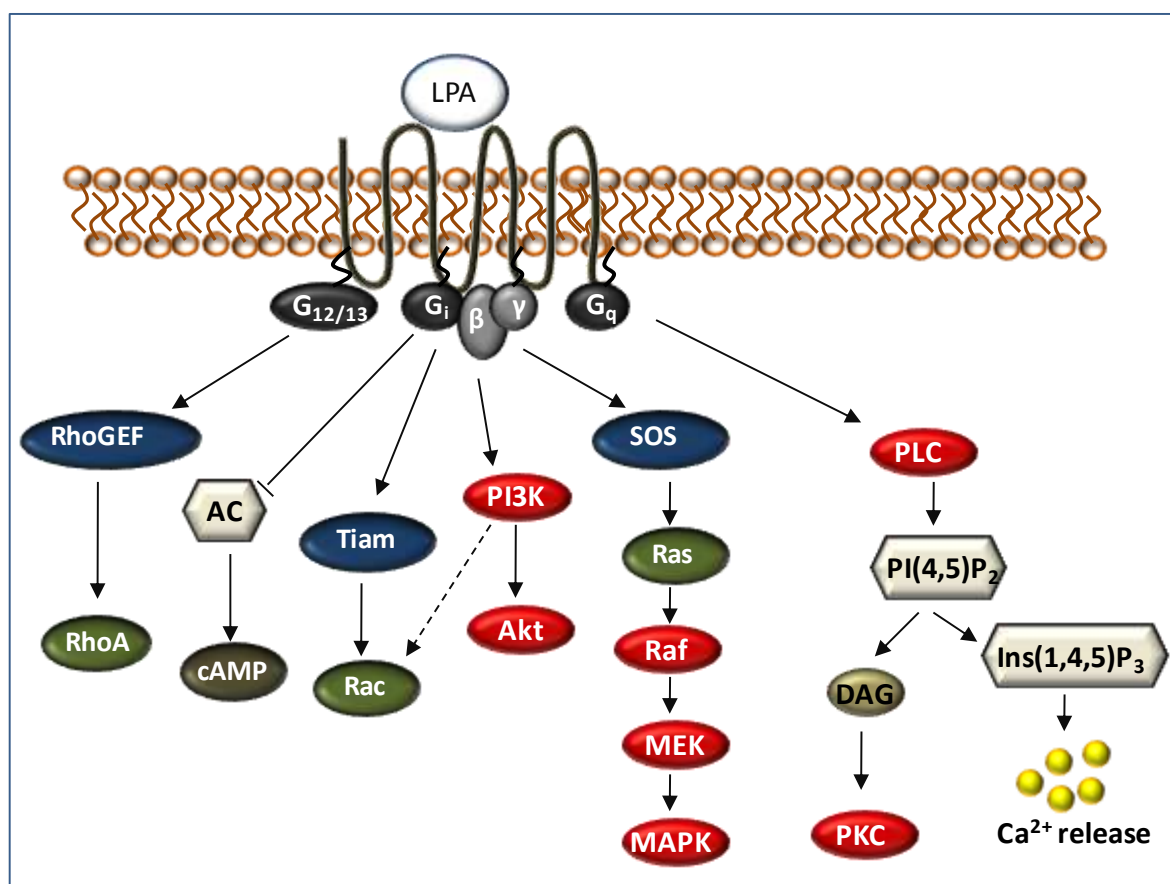
Figure 7.21: LPA-induced GPCR signalling. LPA receptors can couple to at least three distinct G-protein families, namely $G_{q/11}$, $G_{i/0}$, and $G_{12/13}$. The major signalling pathways activated downstream of these G-proteins are as follows: 1) $G\alpha_q$ activates phospholipase C (PLC) with subsequent PIP_2 hydrolysis and Ca^{2+} mobilisation from internal stores; 2) G_i mediates inhibition of adenylyl cyclase and activation of PI3K, which subsequently leads to activation of Rac; the corresponding βγ subunit to G_i is thought to couple to the Ras-MAPK signalling cascade; 3) $G_{12/13}$ has been implicated in activation of RhoA (Fukuhara, et al., 2000; Fukuhara, et al., 1999; Hart, et al., 1998; Kranenburg, et al., 1999).

$G\alpha_q$ and G_s pathways: $G\alpha_q$ activates phospholipases C (PLC) with subsequent PIP_2 hydrolysis and Ca^{2+} mobilisation from internal stores (Figure 7.21) (Fukuhara, *et al.*, 2000; Fukuhara, *et al.*, 1999; Hart, *et al.*, 1998; Kranenburg, *et al.*, 1999). The G_s pathway

involves the activation of the second messenger cAMP, which connects to multiple cellular pathways regulating a variety of downstream effectors such as ion channels, transcription factors, and metabolic enzymes (Neves, et al., 2002).

G_i Pathway: This pathway was originally identified by the ability of $G\alpha_i$ to inhibit adenylyl cyclase and is inhibited by pertussis toxin (PTX), which catalyzes adenosine diphosphate ribosylation of the $G\alpha$ subunit preventing it from interacting with the receptor. In this pathway, both $G\alpha$ and $G\beta\gamma$ subunits can communicate signals. $G\beta\gamma$ directly couples to at least four effector molecules, and indirectly to the small GTPase Ras, to activate MAPKs (Kranenburg & Moolenaar, 2001; Moolenaar, et al., 2004). The effectors directly regulated by $G\beta\gamma$ include PLC-β, K1 channels, adenylyl cyclase, and PI3K (Neves, et al., 2002).

G_{12} and G_{13} Pathways: Most of the experiments carried out to elucidate $G\alpha_{12}$ and $G\alpha_{13}$ protein signalling have been in infected cells. It is unclear which receptors endogenously couple through $G\alpha_{12}$ and $G\alpha_{13}$ pathways. Although $G\alpha_{12}$ and $G\alpha_{13}$ proteins share a high degree of sequence similarity, they have different signalling effectors. $G\alpha_{12}$ is thought to stimulate phospholipase D, c-Src, and PKC by as yet unidentified mechanisms, which in most cases results in activation of the MAPK family. $G\alpha_{12}$ can also been reported to directly interact with Ras-GAP and Btk (Neves, et al., 2002).

Two receptors that couple to $G\alpha_{13}$ in the native setting are the LPA receptor and the thromboxane A2 receptor. $G\alpha_{13}$ directly interacts with and activates the Rho-GEF, p115Rho-GEF, and thus activates Rho. $G\alpha_{13}$ may also engage the PI3K pathway to activate the protein kinase Akt and regulate NFκB, through the activation of PYK2 (Shi & Kehrl, 2001).

7.5.3 Regulation of RhoA activation by serum in 5'Myc-p110δ-overexpressing NIH 3T3 cells

LPA is well known for inducing a striking contractile response, mediated by RhoA activation, in non-muscle cells. This was first observed in neuronal cells, in which LPA induces rapid neurite retraction and cell rounding (Jalink, *et al.*, 1994; Tigyi & Miledi, 1992). The mechanism by which LPA activates RhoA is relatively well understood. RhoA activation proceeds via $G\alpha_{12/13}$ subunits, which bind directly to at least three Rho-specific GEFs promoting RhoA-GTP accumulation and activation of ROCK and serum response factor (SRF)-mediated gene transcription (Schmidt & Hall, 2002; Van Leeuwen, et al., 2003). There is also evidence to suggest LPA-mediated RhoA activation involves protein-

tyrosine kinase activity since pretreatment of cells with the tyrosine kinase inhibitors genistein or tyrphostin inhibits LPA-induced RhoA activation (Kranenburg, et al., 1999).

Following initial LPA-induced contractile events mediated by RhoA activation, the continuous presence of LPA promotes cell re-spreading, lamellipodia formation and cell migration, events mediated by Rac activation (Van Leeuwen, et al., 2003). Activation of RhoA by LPA is rapid but transient, with maximal RhoA activity typically detected within a few minutes in different cell types (Kranenburg, et al., 1999; Van Leeuwen, et al., 2003). In MEFs, RhoA activation is undetectable after 10 minutes of LPA stimulation (Van Leeuwen, et al., 2003), which suggests that after an initial induction of RhoA-GTP by LPA, prolonged LPA stimulation results in an eventual downregulation of RhoA-GTP.

As mentioned previously, RhoA activation leads to SRF-mediated gene transcription. It has been shown that $G\alpha_z$, a member of the $G\alpha_i$ subunit family, inhibits $G\alpha_{12/13}$, $G\alpha_q$ or Rho-GEF-induced SRE reporter activity, although it appears to have no effect on RhoA activation itself (Dutt, *et al.*, 2004).

In the presence of serum, NIH 3T3 cells stably expressing 5'Myc-p110δ had a substantially higher basal level of RhoA-GTP compared to pMX-neo-expressing cells (Figure 7.15a), although cells did not display the contractile phenotype associated with high RhoA activity (Figure 7.3). As previously mentioned, prolonged LPA stimulation causes cell respreading, therefore it is not unexpected that cells did not display a contractile phenotype under normal culturing conditions, however one might still expect 5'Myc-p110δ-overexpresing cells to have a more rounded cell morphology compared pMX-neo-expressing cells, rather than the more spread morphology actually observed. It would be interesting to investigate whether LPA is indeed the component of serum that mediates the high RhoA-GTP levels observed in cells stably expressing 5'Myc-p110δ. This could be investigated through incubating cells in serum-free media overnight, followed by prolonged stimulation with LPA. Alternatively, in principle, an LPA-neutralising antibody could be added to the serum to investigate the effect of blocking LPA signalling on RhoA-GTP levels in 5'Myc-p110δ-overexpresing cells. This approach of using neutralizing antibodies could also be used to assess the contributions of the serum constituents IGF-1 and PDGF on the activities of the small Rho GTPases and cell morphology.

In some cell types, LPA can activate the production of $PI(3,4)P_2$ and PIP_3 as strongly as growth factors. Indeed, PI3K activation by LPA is now regarded as an important aspect of

LPA signalling in different cellular systems (Fang, *et al.*, 2000; Roche, *et al.*, 1998). An increasing body of evidence has implicated p110β downstream of GPCRs, such as LPA receptors, from the finding that G protein βγ subunits dramatically increase the activation by phosphotyrosine motifs of p110β but not other class I PI3Ks (Maier, et al., 1999), to the finding that p110β is predominantly activated downstream of GPCRs rather than proteins tyrosine kinases in a panel of agonists tested (Guillermet-Guibert, et al., 2008). Upon LPA stimulation, Gab1 is phosphorylated by the transactivated EGF receptor, thereby possibly providing the phosphotyrosine motifs that are required for p110β activation (Laffargue, *et al.*, 1999).

Given that p110β expression in 5'Myc-p110δ-overexpresing cells was undetectable, it is likely that signalling pathways mediated by LPA-induced p110β activation are compromised in these cells. It is possible that after prolonged LPA stimulation, RhoA activity is downregulated by a Gα$_i$-pathway involving p110β in pMX-neo-expressing NIH 3T3 cells. Indeed, as mentioned previously Gα$_z$, (a member of the Gα$_i$ subunit family) inhibits Rho-GEF induced SRE reporter activity (Dutt, et al., 2004), therefore it is not inconceivable that RhoA is downregulation is mediated downstream of Gα$_i$. In 5'Myc-p110δ-overexpressing NIH 3T3 cells, this ability to down-regulate RhoA may be compromised by the lack of p110β expression, therefore high basal RhoA activity observed in these cells, in the presence of serum, is not as a direct result of p110δ overexpression but rather as a result of p110β downregulation (Figure 7.23).

One way in which the hypothesis that p110β is involved in regulating RhoA activity could be investigated is through examining the RhoA-GTP levels in MEFs isolated from mice homozygous for p110β gene inactivation. If the hypothesis is correct, one might expect to find increased basal RhoA activity in these cells compared to MEFs from WT mice. Other approaches include using siRNA to knock-down p110β expression or treating cells with p110β isoform-specific inhibitors. Given that in certain cellular responses the adaptor function of p110β rather than its lipid kinase activity has been found to be critical (Jia, *et al.*, 2008), a knock-down approach of p110β protein expression may be favourable.
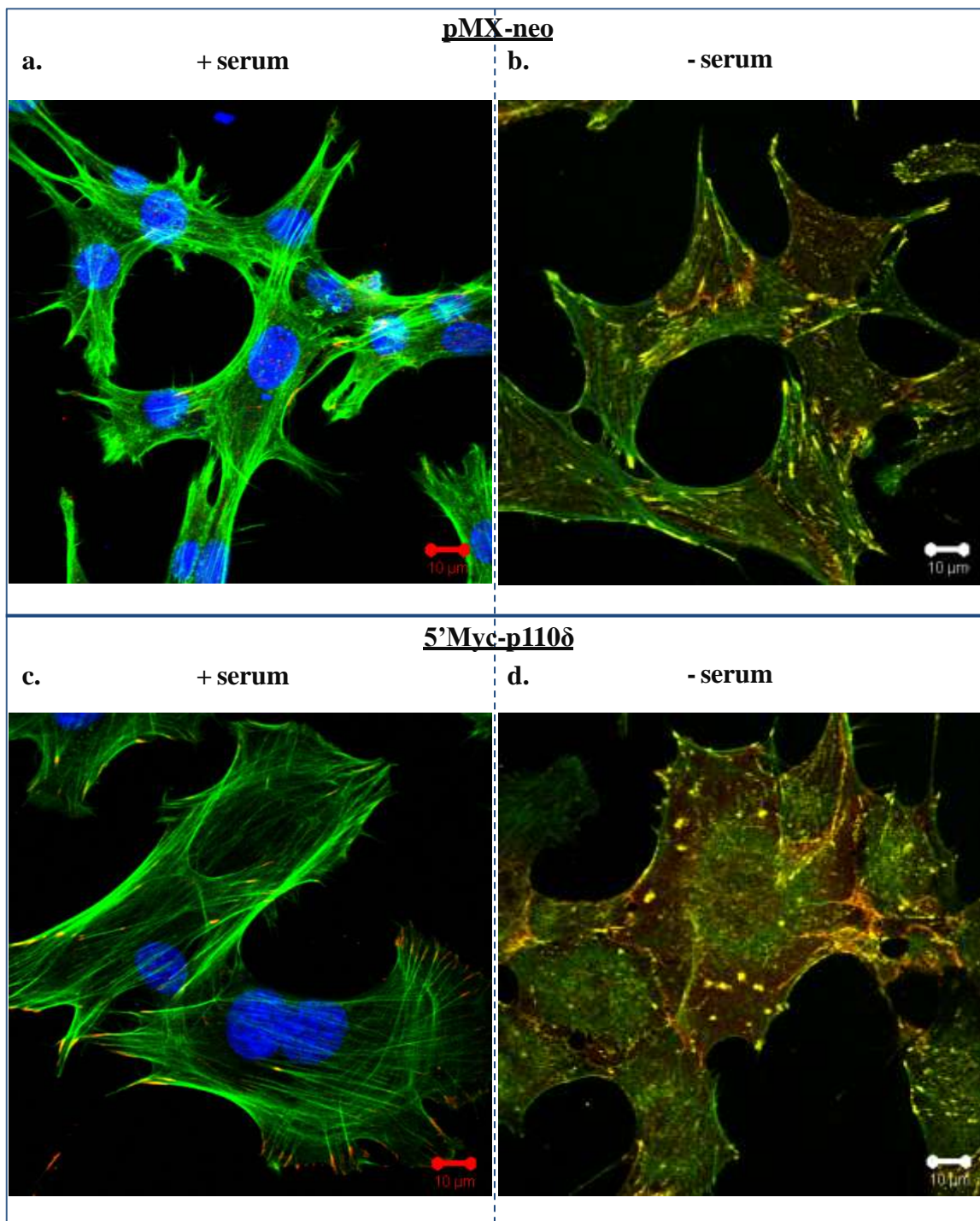
Figure 7.22: Representative confocal images of NIH 3T3 cells stably expressing pMX-neo or 5'Myc-p110δ in the presence or absence of serum of to support the hypothetical models propsed in Figure 7.23. Cells were seeded in media containing 10% FBS on glass coverslips. After 6 h, media was replaced with media without FBS for cells under serum-starvation conditions or left in media containing 10% FBS. Cells were fixed and stained after 24 h. **a)** and **c)** F-actin (green), DNA (DAPI) and P-paxillin (red); **b)** and **d)** F-actin (green), N-cadherin (red) and P-paxillin (yellow).
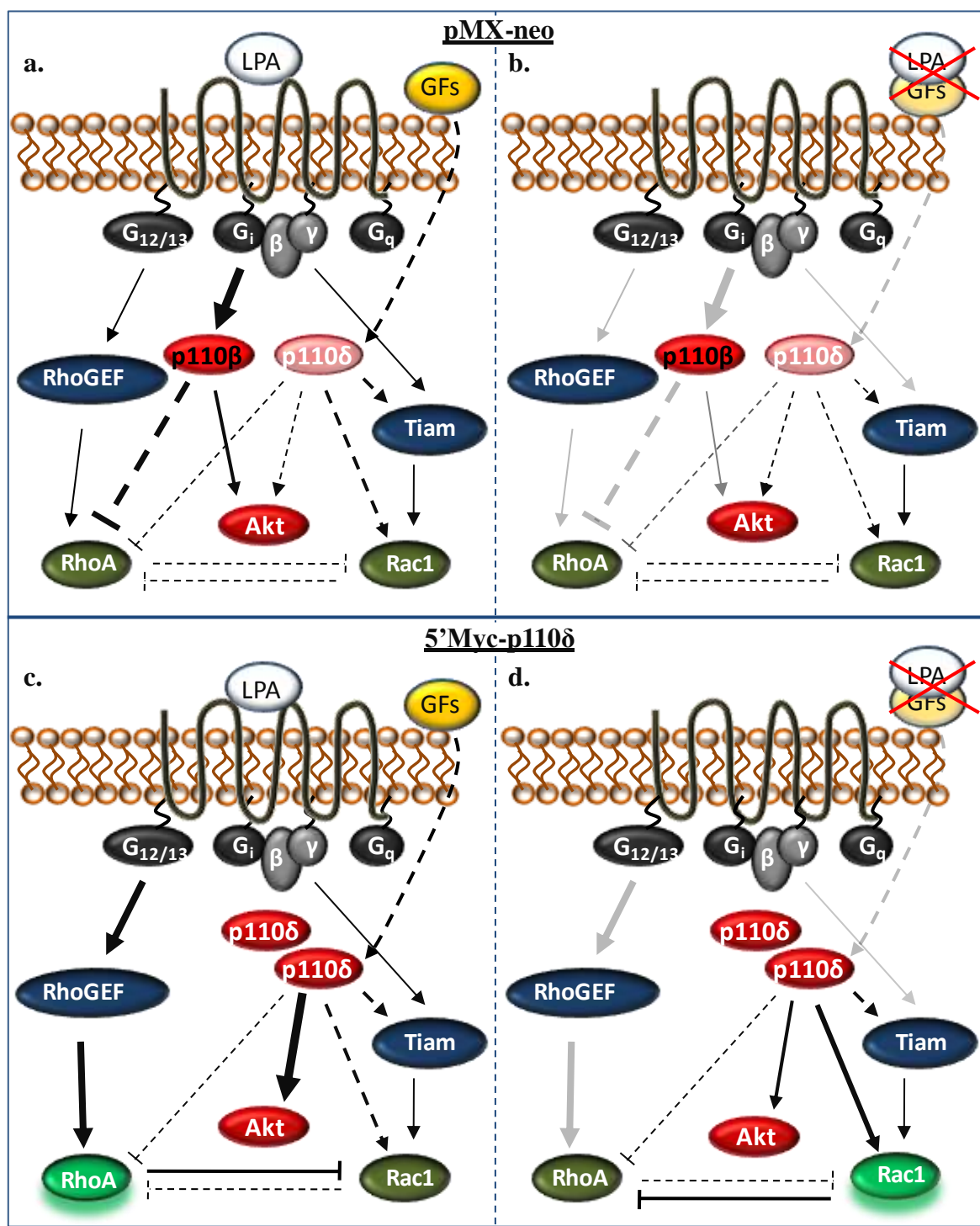
Figure 7.23: Hypothetical models for the activation of RhoA and Rac1 in the presence of serum and under serum-starvation conditions in NIH 3T3 cells stably expressing pMX-neo or 5'Myc-p110δ. *pMX-neo:* **(a)** Serum stimulation results in RhoA activation via $G_{12/13}$ pathways, however prolonged serum stimulation, specifically prolonged LPA stimulation, leads to RhoA downregulation, which is possibly mediated through p110β. Low endogenous levels of p110δ exert a mild negative effect of RhoA activity and a positive effect on Rac1 activity. **(b)** In the absence of serum neither $G_{12/13}$ nor p110β are activated consequently leading to low levels of RhoA activity. *5'Myc-p110δ:* **(c)** In the presence of serum RhoA activity is high through LPA-$G_{12/13}$ signalling through Rho-GEFs, which may inhibit Rac1 activity. The lack of p110β expression may prevent downregulation of RhoA activity after prolonged LPA stimulation. Growth factors and high p110δ expression lead to high levels of Akt phosphorylation. **(d)** In the absence of

serum and RhoA activity is attenuated through diminished $G_{12/13}$ signalling, exogenously expressed p110δ has some constitutive lipid kinase activity which activates Akt, Rac1 and exerts a mild negative effect on RhoA activity. Increased Rac1 activity is also likely to inhibit RhoA activity.

Although p110β may play a role in downregulating RhoA activity after prolonged serum-stimulation, it appears as though p110β is not involved in inhibiting the acute serum-induction of RhoA activity. The addition of serum induced a significant increase in RhoA activity in both pMX-neo-expressing and 5'Myc-p110δ-overexpresing cells (Figure 7.15a), which corroborates the finding that inhibition of p110β has no effect on acute CSF-1-induced RhoA activation in primary macrophages (Papakonstanti, et al., in preparation). Moreover, this result demonstrates that a high level of p110δ expression is not essential for the rapid induction of RhoA-GTP upon serum stimulation, given that serum-stimulation of pMX-neo-expressing cells resulted in a marginally higher level of RhoA-GTP compared to 5'Myc-p110δ-overexpressing cells and that IC87114 treatment did inhibit serum-induced RhoA-GTP in either cell line.

In both pMX-neo and 5'Myc-p110δ-overexpressing NIH 3T3 cells, IC87114 treatment resulted in an increase in RhoA-GTP, corroborating the finding that p110δ is negatively regulating RhoA activity (Papakonstanti, et al., 2007). These results demonstrate that a low endogenous level of p110δ is sufficient to mediate RhoA inhibition. In light of this, one would expect cells that have high expression of p110δ to have low RhoA activity, however as explained, 5'Myc-p110δ-overexpressing NIH 3T3 cells had higher levels of RhoA-GTP. These data indicates that expression of a solitary class I PI3K isoform, p110δ, is not sufficient to down-regulate RhoA activity and that other molecules, possibly p110β, are also required to attenuate RhoA-GTP levels.

7.5.4 Regulation of Rac activation by serum in 5'Myc-p110δ-overexpressing NIH 3T3 cells

In contrast to RhoA, little is known about how LPA receptors may modulate the activity of Rac and/or Cdc42. It has been shown that the LPA_1 receptor, in addition to transiently activating RhoA, mediates prolonged activation of Rac via a G_i-PI3K pathway that activates the Rac-GEF, Tiam1 (Figure 7.21) (Van Leeuwen, et al., 2003). To corroborate this, in neuroblastoma cells, LPA-induced activation of Rac is more robust and prolonged than LPA-induced activation of RhoA (Van Leeuwen, et al., 2003). This activation of Rac is inhibited by PTX and wortmannin, which supports the idea that Rac is activated via G_i-

mediated stimulation of PI3K activity. In chinese hamster ovary cells, LPA stimulates both Rac and Rho activity resulting in cell migration, indicating that both Rac and Rho can be activated at the same time (Sugimoto, *et al.*, 2006), whereas in the absence of G_i function, LPA induces inhibition, rather than stimulation of cellular Rac activity (Sugimoto, et al., 2006).

Although activated via distinct G-protein pathways (RhoA by $G\alpha_{12/13}$ and Rac by G_i), it is the balance between RhoA and Rac activation which determines cell morphology. Activated Rac has been shown to suppress RhoA activity and there is also evidence for the reverse being true (Sugimoto, et al., 2006; Yamaguchi, *et al.*, 2001).

In NIH 3T3 cells stably overexpressing 5'Myc-p110δ, Rac1 activity was reduced in the presence of serum compared to pMX-neo-expressing cells, whereas under serum-starvation conditions 5'Myc-p110δ-overexpressing cells had increased Rac1-GTP levels compared to pMX-neo-expressing cells (Figure 7.15b, Table 8.1). Although it is a common conception that Rac1 inhibition on RhoA activity is unidirectional, as mentioned above there is also evidence that RhoA also inhibits Rac1 activation (Sugimoto, et al., 2006; Yamaguchi, et al., 2001). High RhoA activity in 5'Myc-p110δ-overexpressing cells in the presence of serum may antagonize Rac1 activation. However, under serum-starvation conditions where RhoA activity is reduced, p110δ-induced Rac1 activation may be uninhibited (Figure 7.23).

7.5.5 p110δ may be a positive regulator of Rac1 activity and a negative regulator of RhoA activity in NIH 3T3 cells

These hypotheses put forward to explain the differential levels of RhoA and Rac1 activity in NIH 3T3 cells stably expressing pMX-neo or 5'Myc-p110δ, support the idea that p110δ positively regulates Rac1 activity and negatively regulates RhoA activity. It is only due to the altered expression of the other class IA PI3K isoforms, namely reduction of p110β expression, that results in decreased Rac1 activity and increased RhoA activity in p110δ-overexpressing cells in the presence of serum. To support this idea, under conditions of serum-starvation, IC87114 treatment induced a significant reduction in Rac1 activity in 5'Myc-p110δ-overexpressing cells, indicating that overexpression of p110δ in the absence of LPA and serum growth factors is sufficient to activate Rac1. In contrast, IC87114 treatment induced the greatest increase in RhoA activity in p110δ-overexpressing cells in the presence of serum, indicating that p110δ inhibition in addition to LPA and serum growth factors, is required for maximal RhoA activation.

7.5.6 Effect of p110δ overexpression in NIH 3T3 cells on the actin cytoskeleton and cell morphology

In the presence of serum, 5'Myc-p110δ-overexpressing cells had more actin stress fibres and sites of focal contact compared to pMX-neo-expressing cells, which correlated with the increased RhoA activity observed in these cells under these conditions (Table 8.1). Given that RhoA activity is involved in the assembly of focal adhesions (Hotchin & Hall, 1995; Ridley & Hall, 1992), this was an expected finding. In the absence of serum, 5'Myc-p110δ-overexpressing cells displayed a reduction in actin stress fibres compared to pMX-neo-expressing cells, which reflects the shift observed from RhoA activity to Rac1 activity in these cells. Interestingly, in the absence of serum 5'Myc-p110δ-overexpressing cells appeared to have more sites of focal contact compared to pMX-neo-expressing cells, indicating Rac1 activity may also be involved in focal adhesion formation. Indeed, Rac1 has been linked to the formation of actin stress fibres and focal adhesion assembly (Guo, *et al.*, 2006), therefore it is possible that the increase in focal adhesions in 5'Myc-p110δ-overexpressing cells is mediated through p110δ-induced Rac1 activation. It should also be considered that 5'Myc-p110δ-overexpressing cells have an increased number of focal complexes rather than focal adhesions. Focal complexes are the earliest forms of peripheral integrin-mediated contacts, which contain paxillin but do not contain the mature adhesion markers found in focal adhesions, such as zyxin (Zaidel-Bar, *et al.*, 2004). Focal complexes are an important in the formation of lamellipodia protrusion, a process regulated by Rac, therefore it is possible that 5'Myc-p110δ-overexpressing cells have an increased number of focal complexes mediated by p110δ-induced Rac1 activity. This could easily be investigated through immunofluorescence staining for the focal adhesion marker, zyxin.

In the absence of serum, F-actin puncta staining, which colocalized with P-paxillin was observed in 5'Myc-p110δ-overexpressing cells (Figure 7.5a). This type of staining resembles that observed for podosomes (Linder, 2007). Podosomes are dynamic adhesion sites enriched for filamentous actin, which were initially described in Src-transformed fibroblasts (David-Pfeuty & Singer, 1980). Podosomes mediate close contact with the underlying substratum and contain several proteins namely, integrin, paxillin, vinculin and talin. They are distinguishable from other adhesion foci by a dense actin core, organized as a column of small actin filaments surrounded by adhesion proteins (integrins) and scaffolding proteins such as cortactin (Destaing, *et al.*, 2003), PyK2 (Pfaff & Jurdic, 2001), WASP (Calle, *et al.*, 2004a) and gelsolin (Chellaiah, *et al.*, 2000). Podosomes are considered dynamic as they dissolve and reform in new locations, with a lifespan ranging

from 30 seconds to 12 min depending on cell type and the underlying substrate (Calle, et al., 2004a; Collin, *et al.*, 2006; Evans, *et al.*, 2003; Kanehisa, *et al.*, 1990). Although the precise role of podosomes remains to be elucidated, they are typically found in invasive cells and cells that cross tissue boundaries and they appear to be important for cell adhesion and substrate degradation (Burgstaller & Gimona, 2005; Lener, *et al.*, 2006). Given that podosomes are constantly generated in moving cells, it has been suggested that they possibly mediate effective progression of the leading edge during cell migration (Calle, *et al.*, 2006). Further investigations need to be carried out to assess whether the F-actin structures identified in 5'Myc-p110δ-overexpressing NIH 3T3 cells are indeed podosomes, such as staining for vinculin and cortactin. It is possible that the actin structures observed are in fact invadopodia, rather than podosomes, which like podosomes contain cortactin but unlike podosomes do not contain vinculin. Invadopodia are mostly formed as small clusters consisting of a few large actin-rich dots, rather than the more numerous evenly spaced podosomes, and form deeper root-like extensions into the matrix (Linder, 2007). Whereas podosomes are found in monocytic cells, endothelial cells and smooth muscle cells, invadopodia are frequently found in highly invasive carcinoma cells (Linder, 2007). However the distinction in fibroblasts is less clear cut, and podosome-type adhesions have been categorized both as podosomes or invadopodia. In either case, the presence of podosome-type adhesions in 5'Myc-p110δ-overexpressing NIH 3T3 cells suggests that these cells may be more invasive than pMX-neo-expressing cells, which would be an interesting avenue for further exploration.

One particularly interesting observation was the effect of IC87114 treatment on 5'Myc-p110δ and pMX-neo-expressing NIH 3T3 cells in the presence of serum. Under serum-starvation conditions, IC87114 treatment partially reversed the morphological phenotype of 5'Myc-p110δ-overexpresssing cells to one that more closely resembled pMX-expressing cells (Figure 7.7, 7.9). However, in the presence of serum, IC87114 treatment induced cell clustering, which was more apparent in 5'Myc-p110δ-overexpresssing cells (Figure 7.6). It is possible that these changes in cell morphology reflect an acute response to p110δ inhibition mediated by a component of serum. Indeed, many of the phenotypes observed for 5'Myc-p110δ-overexpressing cells alter between serum and serum-starvation conditions, an effect which has been partly attributed to the downregulation of p110β. Analysis of the levels of phosphorylated Akt revealed that 5'Myc-p110δ-overexpresssing cells had high levels of P-Akt in the presence of serum which is completely abrogated after 1 h of IC87114 treatment, whereas under serum-starvation conditions although the level of P-Akt is higher in 5'Myc-p110δ-overexpresssing cells compared to pMX-neo-expressing

cells, it is significantly lower than that observed in the presence of serum (Figure 7.8). These results indicate that the lipid kinase activity of p110δ is greater in the presence of serum, therefore it is possible that the difference in the effect of IC87114 treatment in the presence or absence of serum reflects the acute changes in PIP$_3$ production and subsequent activation of downstream effectors. It would be interesting to investigate the effect of p110δ inhibition over a longer time period to assess whether cells can adapt to low p110δ lipid kinase activity. Finally, the substantial increase in RhoA activity in cells after IC87114 treatment in the presence of serum (Figure 7.15) may induce a rapid lateral cell contraction, which results in the 'stringy' cell clustering of 5'Myc-p110δ-overexpressing cells. To further investigate this possibility, cells could be treated with a combination of IC87114 and the ROCK inhibitor Y-27632 to assess whether inhibition of the RhoA downstream effector prevents this type of cell clustering.

7.5.7 Future work

I have mentioned a number of possible future lines of investigation throughout this discussion, which are summarised below:

- Investigation into the mode of downregulation of p110α and p110β expression in 5'Myc-p110δ-overexpressing NIH 3T3 cells, such as analysis of p110α and p110β mRNA expression and proteasome inhibition to induced p110α and p110β expression.

- Determine whether LPA, or indeed other components of serum, such as growth specific growth factors, are responsible for the induction of different phenotypes observed for 5'Myc-p110δ-overexpressing cells in the presence or absence of serum.

- Investigation into the possible role of p110β in attenuating RhoA activity, through the use of p110β-specific inhibitors, use of MEFs isolated from mice homozygous for p110β gene-inactivation or use of p110β-targeted siRNA.

- Determine whether 5'Myc-p110δ-overexpressing cells express increased focal adhesions of focal complexes through staining for zyxin, to help elucidate whether these adhesions are a result of increase RhoA or Rac1 activity.

- Investigate the possible expression of podosomes/invadopodia in 5'Myc-p110δ-overexpressing cells express and assess whether this correlates with the invasive-potential of these cells.

- Examine the effect of p110δ inhibition on pMX-neo and 5'Myc-p110δ-overexpressing cells over a time period longer than 1 h and also the combination of p110δ and ROCK inhibition on cell morphology in the presence of serum.

There are other potentially interesting areas of investigation, which are discussed in more detail below.

7.5.7.1 Stable expression of untagged p110δ in NIH 3T3 cells

Although N-terminal Myc tags are commonly included on exogenously expressed proteins, the possibility that such a tag interferes with the function, localization and stability of the tagged protein should not be overlooked. Indeed, the addition of an N-terminal Myc tag on p110α enhances p110α protein stability (Yu, et al., 1998b). Ideally, it would have been more advisable to stably express untagged p110δ in NIH 3T3 cells, but due to unforeseen complications with the p110δ-containing retroviral vector (discussed in section 6.4) this was not possible. However, to gain a more reliable insight into the role of p110δ, future work should incorporate the characterisation of NIH 3T3 cells stably expressing untagged p110δ.

7.5.7.2 Investigation into possible downstream effectors of p110δ that may play a role in the altered actin cytoskeleton and cell morphology associated with NIH 3T3 cells overexpressing 5'Myc-p110δ

There are number of GEFs that specifically activate Rac, such as members of the Vav, Sos, Tiam, Swap-70 and P-Rex families (Hawkins, et al., 1995; Michiels, *et al.*, 1995). PIP_3 strongly activates the Rac-GEF activities of P-Rex1 and SWAP-70 *in vitro* (Shinohara, et al., 2002; Welch, et al., 2002) and weakly activates the Rac-GEF activities of Vav1, Sos1 and Tiam1 (Han, et al., 1998; Innocenti, et al., 2003), implicating PI3K as a regulator of Rac-GEFs. Indeed, in epithelial cells, Tiam1-mediated Rac activation is dependent on PI3K activity (Sander, et al., 1998). It would be of interest to explore the activity of some of these Rac-specific GEFs in NIH 3T3 cells overexpressing 5'Myc-p110δ. One particular Rac-GEF, β-Pix (p21-activated kinase [PAK]-interacting exchange factor), which has been shown to be activated downstream of PI3K (Park, *et al.*, 2004), makes an interesting candidate. Rac1 binds directly to the SH3 domain of β-Pix through the proline stretch in its carboxy-terminus (ten Klooster, *et al.*, 2006). In addition to a Rac-GEF, β-Pix also acts as a signalling organizer by binding to the Arf-GAP paxillin kinase linker (PKL) as well as the Rac effector Pak1 (Bagrodia, *et al.*, 1998; Manser, *et al.*, 1998) (Figure 7.24). It has been shown that the interaction of Rac1 with β-Pix mediates Rac1 targeting to membrane ruffles

and focal adhesions and Rac1-mediated cell spreading (ten Klooster, et al., 2006). The interaction of Rac1 with β-Pix is controlled by Pak1, which competes for binding with β-Pix. It would be interesting to assess the activity of β-Pix in NIH 3T3 cells stably overexpressing 5'Myc-p110δ, to determine whether p110δ-induced increased Rac1 activity is mediated through increased activation of β-Pix. Given that β-Pix is involved in the formation of focal adhesion complexes, increased β-Pix activity in NIH 3T3 cells stably overexpressing 5'Myc-p110δ would offer some explanation for the increased number of focal adhesion observed in these cells.
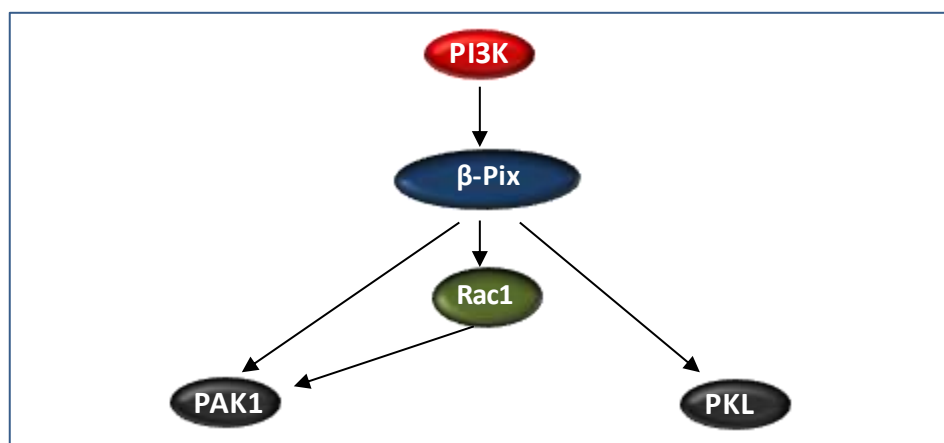
Figure 7.24: Activation of the Rac-GEF, β-Pix downstream of PI3K.

In addition to the apparent positive regulation p110δ appears to have on Rac1 in 5'Myc-p110δ-overexpressing cells, p110δ also seems to be negatively regulating RhoA activity. Downregulation of RhoA activity can be mediated through Rho-GAPs. There was no significant difference in the Rho-GAP activation of p190RhoGAP in 5'Myc-p110δ-overexpressing NIH 3T3 cells compared to pMX-neo-expressing cells as assessed by tyrosine-phosphorylation, implicating that either this method of assessing p190RhoGAP activation is not sufficient or that another Rho-GAP may be involved in RhoA-GTP hydrolysis. Inhibition of Rho-specific GEFs rather than activation of Rho-specific GAPs could also be involved in the inhibitory effect p110δ has on RhoA activity, which are areas that could be further explored.

There are many PIP_3 effectors which could be involved in the phenotype observed for 5'Myc-p110δ-overexpressing NIH 3T3 cells, one such effector is Pleckstrin-2 (PLEK2). The phenotypes observed in COS cells overexpressing PLEK2 (Hamaguchi, et al., 2007) closely resemble the phenotypes observed in NIH 3T3 cells stably overexpressing 5'Myc-p110δ. PLEK2 is a 353 amino acid protein identified through its similarity to PLEK1. Both PLEK1 and 2 contain two PH domains in their amino- and carboxy-termini (Hu, *et*

al., 1999). Unlike PLEK1, PLEK2 is a poor substrate for PKC, but is a PIP_3-binding protein, which is regulated by PI3K (Hamaguchi, *et al.*, 2007). Expression of PLEK2 in COS cells (which have low endogenous expression of PLEK2) induces increased cell spreading on fibronectin or collagen-coated plates with cells (the average footprint size of cells expressing PLEK2 40% greater than that of control cells) and cells also display increased membrane ruffles (Hamaguchi, et al., 2007). These phenotypes were abolished in cells expressing a PIP_3-binding mutant, indicating that production of PIP_3 is critical for PLEK2 activity. Furthermore, coexpression of RFP-RhoA, RFP-Cdc42 or RFP-Rac1 with GFP-PLEK2 revealed that RFP-Rac1 tightly colocalized with GFP-PLEK2, whereas RFP-RhoA or RFP-Cdc42 do not show colocalization with GFP-PLEK2 (Hamaguchi, et al., 2007). It would be interesting to investigate the role of PLEK2 in 5'Myc-p110δ-overexpressing NIH 3T3 cells and the possibility that increased PIP_3 production by p110δ mediates increased PLEK2 binding and induction of cell spreading.

There are a number of downstream effectors of Rho GTPases that are implicated in actin reorganization, but the two main effector proteins are Wiskott Aldrich syndrome protein (WASP) and a WASP-like Verprolin-homologous protein (WAVE) (Bishop & Hall, 2000). It is possible that WASP and/or WAVE may play a role in the increased lamellipodia formation during cell spreading and possible podosome formation in 5'Myc-p110δ-overexpressing cells. WASP expression is restricted to haematopoietic cells, but its homologue, N-WASP, is ubiquitously expresssed (Kolluri, *et al.*, 1996; Rohatgi, *et al.*, 1999). WASP directly binds the cytoskeletal organizer, actin-related protein (Arp) 2/3 complex (Machesky & Gould, 1999). The Arp2/3 complex functions to create a branching network of filamentous actin and is localized at sites of active actin polymerization such as lamellipodia and the base of filopodia (Burns, *et al.*, 2001; Mullins, *et al.*, 1998). WASP expression is also essential for podosome formation and is necessary for the recruitment of Arp2/3 complex to podosomes (Burns, et al., 2001; Calle, *et al.*, 2004b). *In vitro*, WASP binds specifically to the GTP-bound form of Cdc42 and to a lesser extent GTP-bound Rac (Aspenstrom, *et al.*, 1996; Kolluri, et al., 1996). Like WASP, WAVE also interacts with and activates the Arp2/3 complex (Machesky, *et al.*, 1999). WAVE precipitates with Rac and localizes to membrane ruffles, furthermore, an actin-binding domain mutant of WAVE inhibits Rac-induced ruffling, suggesting an *in vivo* link between WAVE and Rac (Miki, *et al.*, 1998). It would be interesting to investigate the expression and localization of WASP and WAVE in 5'Myc-p110δ-overexpressing cells.

7.5.7.3 Investigation into the motility and migratory capacity of NIH 3T3 cells expressing pMX-neo or 5'Myc-p110δ

Immunofluorescence staining of pMX-neo and 5'Myc-p110δ-expresspressing NIH 3T3 cells have revealed clear difference in the cell cytoskeleton, however there has not been any investigation into how these cells move. Given that organization of the cell cytoskeleton governs cell movement and that the different levels of Rho GTPase activity has a direct effect on cell migration (discussed in section 1.4.5), one might expect pMX-neo and 5'Myc-p110δ-expresspressing NIH 3T3 cells to have different motility and migratory capacities. It is possible that the increased Rac1 activity in 5'Myc-p110δ-expresspressing cells may results in an increased migratory capacity. Indeed, in a mouse tumour model increased Rac activation results in increased aggressiveness and infiltration of PI3K-induced lymphomas in both lymphoid and non-lymphoid organs (Strumane, *et al.*, 2008). However, since it is a coordinated activation of Rho GTPase that induces a migratory response, it is possible that a disruption of the balance between RhoA and Rac1 activity (as seen in 5'Myc-p110δ-expressing cells) may inhibit cell migration.

Further evidence indicating that 5'Myc-p110δ-expresspressing cells may have an increased migratory capacity over pMX-neo-expressing cells is that p110δ has be found to be important for the directionality and, to a lesser extent, speed of cell migration in breast cancer cell lines, whereas p110β was only required for speed of migration and p110α did not appear to play a role in either parameter (Sawyer, et al., 2003). Striking differences in cell migration of tumour cells has been found depending on whether the migration studies have been carried out on three-dimensional matrices or on two-dimensional tissue culture plates (Sahai & Marshall, 2003), therefore it will be important to carry out future migratory studies 5'Myc-p110δ-expressing cells on three-dimensional matrices in addition to two-dimensional studies.

7.5.7.4 Investigating the localization of p110δ, RhoA and Rac1 in NIH 3T3 cells expressing pMX-neo or 5'Myc-p110δ

Although the levels of active RhoA and Rac1 have been determined in NIH 3T3 cells expressing pMX-neo or 5'Myc-p110δ their cellular localization has not been investigated. It would be interesting to assess whether p110δ and RhoA and/or Rac1 colocalization occurs at the cell membrane, in the cytoplasm or possibly at podosomes. Furthermore, it would be interesting to assess whether the localization of RhoA and Rac1 differs in cells stably expressing 5'Myc-p110α or 5'Myc-p110β compared to cells stably expressing 5'Myc-p110δ. These investigations rely on antibodies that can be used for

immunofluorescence. Since the exogenously expressed p110δ contains an N-terminal Myc tag, the commonly used anti-Myc antibody in immunofluorescence could be used for the detection of Myc-tagged p110 subunits. It is possible to detect GTP-bound RhoA or Rac1/Cdc42 by immunofluorescence by incubating cells with a GST-tagged Rhotekin binding domain or GST-tagged Pak binding domain, respectively, followed by incubation with an anti-GST antibody that can subsequently be detected by a fluorescently-conjugated secondary antibody (Cascone, *et al.*, 2003). Therefore it would be feasible to carry out investigation into this area.

8 DISCUSSION

In this study, we have focused on furthering our understanding of the isoform-specific role of p110δ using various cell-based models and have addressed the following questions:

1) Is coupling of class IA PI3Ks to tyrosine kinase receptors altered in untranformed *versus* transformed cellular states?

2) Is the leukocyte-restricted p110δ gene expression mediated by a leukocyte-specific promoter?

3) What is the biological impact of p110δ overexpression in non-leukocyte mammalian cells?

These areas of investigation have not always been straightforward and it is clear that further work is needed to further expand our understanding of the isoform-specific role of p110δ. However, in some of these areas, significant advances have been made. The results presented in Chapters 3 to 7 are summarised and discussed below.

1) Is coupling of class IA PI3Ks to tyrosine kinase receptors altered in untransformed *versus* transformed cellular states?

In primary, untransformed cells, a single PI3K isoform often appears to mediate most PI3K activity downstream of a given receptor and inhibition of a single PI3K isoform downstream of a given tyrosine kinase receptor often results in a severe impact on the biological responses controlled by this tyrosine kinase receptor. For example, in primary leukocytes, p110δ is often the 'dominant' class IA isoform with p110δ inhibition having a major impact on specific tyrosine kinase receptor signalling, such as c-kit and CSF-1 (Ali, et al., 2004; Papakonstanti, et al., 2007; Papakonstanti, et al., in preparation). While my work was in progress, other scientists in the laboratory have documented that in primary macrophages, CSF-1 signalling is highly dependent on p110δ activity for the regulation of the activities of Akt, RhoA and PTEN, as well as proliferation and chemotaxis (Papakonstanti, et al., 2007; Papakonstanti, et al., in preparation). However in immortalized macrophage cell lines, the p110α isoform rather than p110δ takes up a more prominent role in CSF-1 receptor signalling, with more p110α becoming recruited to the CSF-1 receptor (Papakonstanti, et al., in preparation). It seems highly likely that coupling of class IA PI3Ks to tyrosine kinase receptors is altered in normal and transformed cellular states. I have investigated this question, focusing on the coupling of p110δ to the c-kit tyrosine kinase receptor, which is almost entirely dependent upon p110δ activity for c-kit signalling in primary BMMCs (Ali, et al., 2004).

Three approaches were taken to experimentally immortalise and transform primary BMMCs: 1) introduction of the HOX11 homeobox gene; 2) introduction of PMT; and 3) investigation into whether BMMCs with inactive p110δ [derived from our p110δ$^{D910A/D910A}$ mice (Okkenhaug, et al., 2002)] maintained in culture for more than 6 weeks undergo 'spontaneous transformation' in which another p110 isoform than p110δ might be able to signal downstream of c-kit to substitute for the kinase-dead p110δ, to restore c-kit signalling. This was based on some observations that p110δ$^{D910A/D910A}$ BMMCs maintained in culture for more than 6 weeks were often found to have increased p110α protein expression associated with increased p110α kinase activity compared to WT BMMCs, suggesting p110α may compensate for the kinase-dead p110δ (Ali & Vanhaesebroeck, unpublished results).

We found that introduction of HOX11 resulted in a less differentiated 'early progenitor-like' appearance of BMMCs, which had lost expression of c-kit and the other mast cell marker FcεRI. Given that these cells no longer expressed c-kit they could not be used to assess the coupling of p110δ to this receptor and this line of investigation was not further pursued.

We successfully introduced PMT in BMMCs by retroviral infection. PMT expression did not appear to fully transform cells, indicated by the continued dependency of PMT-expressing BMMCs on IL-3 for cell growth, albeit at a lower concentration than WT BMMCs. PMT-expressing BMMCs did not have increased levels of Akt phosphorylation, which is usually associated with PMT-induced cell transformation. Also, expression of PMT did not alter c-kit or FcεRI expression. c-kit appeared to remain functionally dependent on p110δ for SCF-induced signalling in PMT-expressing BMMCs, at a similar level to WT BMMCs. Most likely, this unaltered receptor coupling is related to the non 'fully' transformed state of the PMT-expressing cells.

SCF-induced Akt phosphorylation is almost completely abrogated in p110δ$^{D910A/D910A}$ BMMCs, emphasising the importance of p110δ in c-kit signalling (Ali, et al., 2004). However, we found that in p110δ$^{D910A/D910A}$ BMMCs maintained in culture for 12 weeks (long-term culture), SCF stimulation was capable of inducing substantial Akt phosphorylation, raising the possibility that these cells had undergone some alterations that permit c-kit signalling. After maintaining primary BMMCs in culture for longer than 6 weeks, we observed an upregulation of p110α expression in p110δ$^{D910A/D910A}$ BMMCs with a concomitant decrease in p110β and p110δ expression, whereas p110 isoform expression

remained largely unaltered in WT BMMCs. We found that in both long-term cultured WT *and* p110δ$^{D910A/D910A}$ BMMCs, p110δ *and* p110α were constitutively bound to c-kit with further recruitment of these isoforms to the receptor upon SCF stimulation. Constitutive p110 binding to c-kit may be related to an incomplete starvation of SCF before the receptor binding assays were performed (since BMMCs are cultured in media containing SCF). No such recruitment to c-kit was observed for p110β or p110γ, either constitutively or upon SCF stimulation. Given that p110β and p110γ are not recruited to c-kit upon SCF stimulation in either long-term cultured WT or p110δ$^{D910A/D910A}$ BMMCs, this makes p110α the most likely candidate to signal downstream of c-kit in long-term cultured p110δ$^{D910A/D910A}$ BMMCs.

Despite the binding of p110α to c-kit, WT BMMCs remained almost entirely dependent on p110δ for SCF-induced Akt phosphorylation. Thus if p110α is signalling downstream of c-kit in long-term cultured p110δ$^{D910A/D910A}$ BMMCs, the switch from p110δ to p110α signalling downstream of c-kit appears to have occured without altered p110 binding to c-kit. It is possible that in long-term cultured p110δ$^{D910A/D910A}$ BMMCs, p110α selectively recruits additional signalling proteins to the c-kit receptor complex, which does not occur in long-term cultured WT BMMCs, however this area would require further investigation (discussed in section 3.5.3). As mentioned in section 3.5.3, the time required and the cost of maintaining primary BMMCs in culture are factors that discourage further investigation into the 'spontaneous transformation' events that appear to occur in long-term cultured p110δ$^{D910A/D910A}$ BMMCs and this approach was no longer pursued.

Since the approaches taken transform WT BMMCs did not appear to result in full BMMC transformation, it has not been possible to address the question of whether p110δ would remain the principle PI3K isoform downstream of c-kit in transformed BMMCs, which is possibly an area for further investigation. Cell transformation can be achieved through overexpression of oncoproteins, such as SV40 large T antigen (Ali & DeCaprio, 2001), oncogenic p110α (Samuels & Velculescu, 2004), oncogenic Ras (Spandidos, *et al.*, 2002) or oncogenic c-kit (Nagata, et al., 1995). The human mastocytoma cell line, HMC-1, expresses an oncogenic c-kit receptor (mediated through two point mutations), which appears to be less dependent on p110δ (Billottet & Vanhaesebroeck, unpublished results). Since it is difficult to compare primary BMMC signalling with signalling in a mastocytoma cell line, it would be interesting to take primary BMMCs, transfect them with oncogenic c-kit, and assess the resulting dependency of c-kit on p110δ. This would allow a direct comparison between primary WT and oncogenic-c-kit-expressing BMMCs. However, it is

not clear whether introduction of oncogenic c-kit, or any of the other oncogenes mentioned, alone would result in transformation of primary BMMCs. Besides HMC-1, few other mast lines exist indicating that immortalization of primary BMMCs is not trivial. In addition, I have found that primary BMMCs are difficult to transfect, often resulting in a high proportion of cell death if using transfection reagents, or resulting in low transfection efficiency if retroviral infection has been employed, most likely due to the low proliferative rate of the cells. Therefore, future work in this area may prove to be relatively difficult. Future plans to assess the dependency of CSF-1 signalling in transformed primary macrophages, rather than immortalised cell lines, include using macrophages derived from Arf/p16-Ink4a null mice, which have previously been show to grow rapidly and continuously in culture whilst remaining CSF-1-dependent (Randle, et al., 2001). It could also be interesting to assess the dependency of c-kit on p110δ in BMMCs derived from these mice.

2) Is the leukocyte-restricted p110δ gene expression mediated by a leukocyte-specific promoter?

p110δ is produced from multiple transcripts with distinct upstream untranslated exons named, exon -1, -2a, -2b, -2c and -2d (exon 1 contains the ATG start codon). All of these are are more highly expressed in leukocytes compared to non-leukocytes. The most abundantly expressed p110δ transcript is p110δ-2a (containing exon -1 with exon -2a), followed by p110δ-2b (containing exon -1 with exon -2b) (Kok, et al., in preparation; Verrall & Vanhaesebroeck, unpublished results). Numerous regions of genomic DNA upstream of the 5' untranslated exons have been examined for promoter activity in leukocytes and non-leukocytes with little indication that any of these regions mediate leukocyte-restricted p110δ gene expression (Verrall & Vanhaesebroeck, unpublished results). However, bioinformatic approaches identified a 50 bp region of DNA _within_ mouse *PIK3CD* exon -2a (equivalent to a region immediately upstream of human *PIK3CD* exon -2a) which contains 7 different TF binding (TFB) sites. This TFB cluster contains binding sites for 4 TFs associated with regulation of haematopoiesis and expression of leukocyte specific genes, namely ETSF, IRF, NFAT and LEFF (discussed in depth in section 5.5.1) and is highly homologous across 8 species. In luciferase reporter studies, in which mouse exon -2a was cloned into the promoter-less vector pGL3-Basic, exon -2a possessed a significantly higher increase in promoter activity in the leukocyte cell lines compared to the non-leukocyte cell lines.

A TATA box, which is commonly found in gene promoters, was not identified upstream of the TFB cluster. TATA-less promoters commonly contain a binding site for the ubiquitously expressed TF, SP1 (Chen, et al., 1997). This was also the case for *PIK3CD* with an SP1 binding site located 40 bp upstream of the start of the TFB cluster. This SP1 binding site might be responsible for the 'basal' level of p110δ expression in most cell types. Although the SP1 binding site was not incorporated in the region of DNA cloned into pGL3-Basic, it is possible that this site may enhance the promoter activity of the TFB cluster and increase *PIK3CD* gene expression. Including the SP1 site with exon -2a in future luciferase reporter assays and subsequent mutational analysis of this site represents an area for further investigation. In addition, the relative importance of individual TF binding sites within the TFB cluster for *PIK3CD* gene expression was not investigated. It would be extremely interesting to determine which TF binding sites are critical for *PIK3CD* gene expression through mutational analysis of these sites for separate gene assays. IN addition, stable transfection of the reporter vectors containing the TFB cluster region, rather than the transient transfections that we carried out, could provide information regarding the epigenetic regulation of p110δ promoter activity.

The identification of a leukocyte-specific *PIK3CD* gene promoter could offer a new therapeutic target. In addition to leukocytes, a high level of p110δ expression is observed in other cell types often associated with cancer such as breast tumours, melanoma and glioma (Sawyer, et al., 2003). In breast cancer cell lines, p110δ has a pivotal role in cell migration, suggesting that high p110δ expression may confer breast cancer cells with an increased migratory capacity and possibly metastatic potential (Sawyer, et al., 2003). Interestingly, all of the leukocyte-associated TFs that bind in the TFB cluster (ETSF, IRF, NFAT and LEFF) have also been implicated in breast cancer tumorigenesis (discussed in section 5.4.4). It is possible that the high level of p110δ expression observed in breast cancer cells is mediated through increased activity of the newly identified *PIK3CD* gene promoter. Targeting TFs that bind in this TFB cluster, subsequently reducing p110δ expression, could therefore be of therapeutic benefit and represents an interesting area for future investigation. It would first be of interest to analyse the promoter activity of mouse exon -2a in breast cancer cell lines and other non-leukocyte cells which express high levels of p110δ, to examine whether these cells, unlike other non-leukocyte cells tested, are able to utilize this promoter.

3) What is the biological impact of p110δ overexpression in non-leukocyte mammalian cells?

It was hypothesised that transfection of full length p110δ cDNA (including the -2a or -2b exons) could result in more effective p110δ expression in cells, compared to previous failed attempts to overexpress p110δ in which only the coding region of p110δ cDNA was used (Verrall & Vanhaesebroeck, unpublished results). Upon stable transfection of such -2a or -2b exon-containing p110δ cDNAs in NIH 3T3 fibroblasts using plasmid-based transfection, we managed to increase p110δ _mRNA_ expression in both instances (up to 10-fold compared to vector control-infected cells), but this did not result in a parallel overexpression of p110δ _protein_. Pharmacological inhibition of the proteasome was found to lead to an increase in p110δ protein expression in p110δ-2a-transfectants, suggesting that exogenously expressed p110δ may be subsequently degraded by the proteasome. Coexpression of a p110-stabilising p85 subunit with p110δ-2a cDNA did not result in increased p110δ expression, however these data are difficult to interpret given that total p85 expression was also not increased in these cells.

In _transient_ transfections of p110δ-2a or p110δ-2b cDNAs in NIH 3T3 or HEK293T cells, a significant increase in the amount of p110δ mRNA expression (in the region of 100,000-fold compared to vector control-infected cells) was achieved for both p110δ cDNAs. However, only transfection of p110δ-2a cDNA and not p110δ-2b cDNA resulted in transient p110δ protein overexpression in HEK293T or NIH 3T3 cells. The importance of exon -2a in p110δ expression was further indicated by the finding that p110δ-2a makes up 80% of the total p110δ transcripts found in the A20 leukocyte cell line. Furthermore, promoter analysis of _PIK3CD_, discussed previously, identified a promoter region within exon -2a with enhanced leukocyte-specific promoter activity. Together these findings indicate that exon -2a plays a positive role in regulating p110δ expression, which may explain the effective transient p110δ overexpression observed through transfection of p110δ-2a and not p110δ-2b cDNA in NIH 3T3 and HEK293T cells.

Overall, plasmid-based transfection of full-length p110δ cDNA in NIH 3T3 did not result in stable p110δ overexpression. It is possible that the 10-fold increase in p110δ mRNA observed after stable transfection of p110δ cDNA gave rise to a low level of p110δ-overexpression, however this level of p110δ expression was not sufficient for efficient heterodimer formation and subsequent stabilization of p110δ, therefore exogenously expressed p110δ protein was degraded. Indeed, in transient transfections, in which

substantial p110δ overexpression was achieved, although not as high as p110δ expression observed in the A20 leukocyte cell line, p110δ mRNA was increased over 100,000-fold.

Retroviral-mediated transfection has been employed in a number of studies investigating the effect of PI3K overexpression (Auger, et al., 2000; Kang, et al., 2006; Kinashi, et al., 1999; Kinashi, et al., 2000; Link, et al., 2005). This method of gene delivery is advantageous over transfection of cDNAs in mammalian expression vectors as it results in superior gene transfer efficiency and a high degree of stable integration of exogenous DNA into the host's genome. Using the retroviral vector, pMX-neo (Kinashi, *et al.*, 2000), human p110δ cDNA containing a 5'Myc-tag and a 3' membrane-targeting CAAX motif was infected in NIH 3T3 cells, resulting in substantial stable overexpression of p110δ. Given that previous attempts to stably overexpression p110δ through transfection of p110δ-2a or p110δ-2b cDNA in pCMV.Sport6 or pcDNA3.1(+), respectively, had failed, this was a momentous result. It would have been interesting to compare the levels of p110δ mRNA in retrovirally-infected and p110δ cDNA-transfected cells, in order to assess whether the success of retroviral transduction in generating p110δ protein expression was due to enhanced mRNA production compared to plasmid-transfected cells.

Although the retroviral system resulted in substantial stable p110 overexpression, it was not without its setbacks. To determine whether stable p110δ overexpression was the result of the retroviral system used, the presence of a 5'Myc tag and/or the 3' membrane targeting CAAX motif, we cloned cDNAs for untagged p110δ, 5'Myc-p110δ or p110δ-3'CAAX into the pMX-neo vector and introduced these constructs into NIH 3T3 cells by retroviral infection. Unfortunately, transfection of pMX-neo containing untagged p110δ or p110δ-3'CAAX cDNA resulted, unexpectedly, in the production of Gag-p110δ fusion proteins. This was due to the presence of a translation start site of viral Gag, within the pMX-neo packaging signal, in frame with the translational start site of p110δ, which only occurred if a 5'Myc-tag upstream of p110δ was not present.

Overexpression of Gag fusion proteins has been employed to investigate a protein's function (Aoki, et al., 2000; Vogt, et al., 2006), however the precise function mediated by the Gag protein is unknown. Viral Gag translocates to the plasma membrane, therefore expression of Gag-p110δ is likely to result in localization of p110δ at the plasma membrane. From the results presented in Chapter 6, the expression of Gag-p110δ in NIH 3T3 cells is seen to have a severe impact of cell morphology but only under serum-starvation conditions. It appears that this effect is not simply the result of plasma-

membrane localization and constitutive activation of p110δ, given that expression of 5'Myc-p110δ with a membrane targeting 3'CAAX motif did not result in a similar phenotype. It is possible that this change in cell morphology, cell rounding, is in fact indicative of cell transformation as a result of the Gag sequence fused to p110δ (Vogt, P., Personal communication), although cell apoptosis is a more obvious conclusion. Gag proteins could also be made in NIH 3T3 cells stably expressing the control pMX-neo vector, which were observed to have a similar morphology to WT NIH 3T3 cells indicating that it is the fusion of Gag to p110δ which induces the change in morphology observed in Gag-p110δ-expressing cells. Further investigations into the oncogenicity of Gag-p110δ, such as performing colony formation assays on pMX-neo-expressing and Gag-p110δ-expressing cells could shed more light onto the impact Gag-p110δ expression on cell morphology, however the physiological relevance of these experiments is unclear.

p110 subunits are stabilised by heterodimer formation with PI3K regulatory subunits (Meier, et al., 2004; Ueki, *et al.*, 2002a; Yu, et al., 1998b). The addition of an N-terminal tag to p110α has been shown to supplant this requirement of p110α for p85 (Yu, et al., 1998b). It is therefore possible that the same is true for p110δ, given that we achieved stable overexpression of 5'Myc-tagged p110δ in NIH 3T3 cells without coexpression of regulatory subunits. Similarly, in other studies in which p110 isoforms have been overexpressed, transfection of exogenous p85 was not required (Auger, et al., 2000; Kang, et al., 2006; Link, et al., 2005). With respect to heterodimer formation with p85, overexpressed 5'Myc-p110δ may not act in the same way as overexpressed untagged p110δ. However, we found that 5'Myc-p110δ was still capable of forming heterodimers with p85 regulatory subunits, although it was not determined whether the 5'Myc-tag may affect the level of p85 binding. Despite the clear limitations of using an N-terminal Myc-tagged p110δ to be able to understand the impact of 'natural' untagged p110δ overexpression, our characterisation of 5'Myc-p110δ-overexpressing NIH 3T3 cells has led to some interesting observations, summarised in Table 8.1.

In NIH 3T3 cells stably expressing 5'Myc-p110δ, we found that endogenous levels of p110α and p110β expression was severely attenuated or undetectable, indicating that the level of p110δ expression regulates the protein expression of the other class I PI3K isoforms. In corroboration with this, overexpression of Gag-p110δ and Gag-p110δ-3'CAAX in NIH 3T3 cells also resulted in reduction of p110α expression to a level undetectable by immunoblotting.
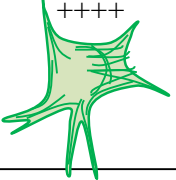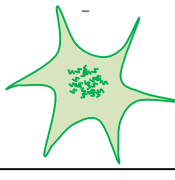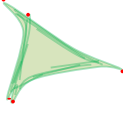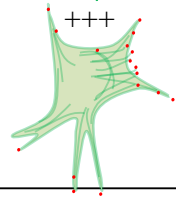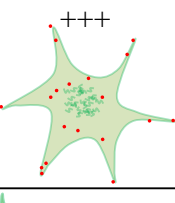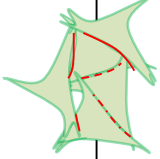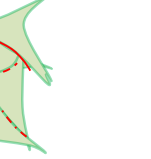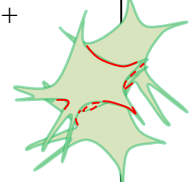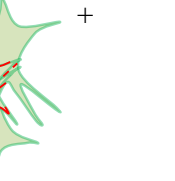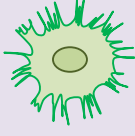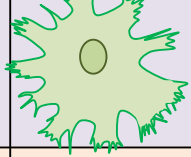
	pMX-neo		5'Myc-p110δ	
	10% serum	**Starved**	**10% serum**	**Starved**
p110δ	+	N/A	+++++	N/A
p110α	+++++	N/A	+	N/A
p110β	++++	N/A	-	N/A
p85	++++	N/A	+++++	N/A
p-Akt	+	-	++++++	+
Total Akt	+	+	+	+
RhoA-GTP	+	+	++++	++
Rac1-GTP	++	++	+	++++
Cdc42-GTP	++++	++++	+	++
p190RhoGAP (P-Tyr)	+	N/A	+	N/A
Stress fibres	+++	++	++++	-
Focal contacts (assessed by P-paxillin staining)	+	++	+++	+++
Adherens junctions (assessed by N-cadherin staining)	+	+	+	+
Cell surface area	+	+	+++++	+++++
Cell spreading Lamellipodia: Fillopodia: Area:	N/A N/A N/A	+ ++++ +	N/A N/A N/A	++++ ++ +++
Cell morphology on Matrigel 24 h after seeding:		N/A		N/A

Table 8.1: Summary of findings from NIH 3T3 cells stably overexpressing 5'Myc-p110δ. The relative level of expression of the indicated proteins or cytoskeletal entities between NIH 3T3 cells stably expressing pMX-neo or 5'Myc-p110δ. N/A indicates that this aspect has not been assessed.

Furthermore, in a study using chicken embryo fibroblasts, the endogenous levels of p110α are downregulated in cells overexpressing p110β or p110δ (Kang, et al., 2006). There are also indications that p110δ may regulate expression of other class I p110 isoform in tumourigenesis. High p110δ expression may be associated with low or undetectable p110α, p110β and/or p110γ expression in some primary human breast cancer tissue samples (Sawyer, et al., 2003) and in leukaemic blast cells from patients with acute myeloid leukaemia (Billottet, et al., 2006; Sujobert, et al., 2005). It is possible that in some transformed cells, which endogenously express high levels of p110δ, a downregulation of other class I p110 isoform expression occurs, which consequently results in p110δ being the principle class I isoform participating in PI3K signalling. The biological impact of these changes in p110 expression is unclear. Given that p110δ has been shown to control the directionality and, to a lesser extent, the speed of *in vitro* migration in breast cancer cell lines (Sawyer, et al., 2003), it is possible that an invasive/migratory advantage is gained in cells in which p110δ is the principle PI3K isoform.

Using the NIH 3T3 cells I have created, which stably overexpressing 5'Myc-p110δ, the mechanism by which p110δ mediates downregulation of p110α and p110β could be investigated. Analysis of the mRNA expression of p110α and p110β would help elucidate whether p110δ induces transcriptional repression of these isoforms, likewise treating cells with a proteasome inhibitor may determine whether p110δ mediates protein degradation of p110α and p110β. Acute inhibition of p110δ lipid kinase activity did not alter p110α and p110β protein expression in 5'Myc-p110δ-overexpressing NIH 3T3 cells, however it would be interesting to investigate whether chronic treatment with the p110δ inhibitor could restore p110α and p110β expression. Alternatively, stable expression of a kinase-dead p110δ would also help determine whether the lipid kinase activity of p110δ is required for downregulation of p110α and p110β expression.

The altered PI3K isoform expression in NIH 3T3 stably overexpressing 5'Myc-p110δ make it difficult to assign the phenotypes observed in these cells (Table 8.1) to p110δ overexpression or to p110α/p110β downregulation, or to both. A clear difference was observed in the cell morphology between pMX-neo-expressing and 5'Myc-p110δ-overexpressing NIH 3T3 cells. Immunofluorescence staining of the actin cytoskeleton revealed obvious differences in the number of actin stress fibres, the number of focal contacts, the rate of cell spreading and adherence and emphasized the difference in the overall cell shape between the two cell lines (summarised in Table 8.1). Moreover, these

differences were highly dependent on the presence of serum in the culture media. The activities of the small RhoGTPases, RhoA, Rac1 and Cdc42, are tightly linked with the actin cytoskeleton, therefore the differences observed in the actin cytoskeleton of pMX-neo-expressing and 5'Myc-p110δ-overexpressing NIH 3T3 cells are likely to reflect differential RhoGTPase activation, which may result from p110δ overexpression and/or p110α and p110β downregulation.

PI3K has been found to activate Rac1 (Hawkins, et al., 1995; Innocenti, et al., 2003; Kotani, et al., 1995) and more specifically p110δ has been found to negatively regulate RhoA activity (Papakonstanti, et al., 2007). In general, the results presented in Chapter 7 support the idea that p110δ is a positive regulator of Rac1 activity and a negative regulator of RhoA activity. However, the idea that p110δ positively regulate Rac1 and negatively regulates RhoA became more complicated when the activities of these Rho GTPases were assessed in cells under normal growing conditions (i.e. in the presence of serum). 5'Myc-p110δ-overexpressing cells displayed a significantly higher level of RhoA-GTP compared to pMX-neo cells in the presence of serum, which appears to contradict the idea that p110δ is a negative regulator of RhoA activity.

It is possible that p110β may be involved in the downregulation of RhoA activity after prolonged serum-stimulation, advocating LPA as the principal constituent of serum mediating this effect. LPA is one of the active constituents of serum that has been shown to stimulate both RhoA and p110β activation (Guillermet-Guibert, et al., 2008; Jalink, *et al.*, 1994; Kranenburg, *et al.*, 1999; Sugimoto, *et al.*, 2006; Tigyi & Miledi, 1992; Van Leeuwen, *et al.*, 2003; Yart, et al., 2002). Acute LPA stimulation induces cell contraction and rounding, mediated by RhoA activation (Kranenburg, et al., 1999; Van Leeuwen, et al., 2003), however activated RhoA is no longer detected after 10 minutes after LPA stimulation and cells begin to re-spread (Van Leeuwen, *et al.*, 2003), indicating that in the continuous presence of LPA RhoA activity is downregulated. Given that 5'Myc-p110δ-overexpressing cells displayed high levels of RhoA-GTP despite the documented inhibitory effect of p110δ on RhoA activity (Papakonstanti, et al., 2007) and given that they expressed undetectable levels of p110β, we hypothesize that p110β may play a role in the downregulation of RhoA-GTP in the continuous presence of serum, which is compromised in 5'Myc-p110δ-overexpressing cells. Therefore, high RhoA activity in 5'Myc-p110δ-overexpressing cells in the presence serum may not be a result of p110δ overexpression *per se*, but a result of p110β downregulation. Indeed, p110δ inhibition in 5'Myc-p110δ-

overexpressing cells in the presence of serum resulted in a significant increase in RhoA-GTP levels, indicating that p110δ is in fact negatively regulating RhoA activity under these conditions.

If the proposed model is correct, it is possible that the true effects of p110δ overexpression, as opposed to p110β downregulation, are observed in cells starved of serum. Indeed, in 5'Myc-p110δ-overexpressing cells starved of serum overnight, basal RhoA-GTP levels were reduced and basal Rac1-GTP levels were increased compared to that detected in the presence of serum. Moreover, the cell morphology observed in 5'Myc-p110δ-overexpressing cells under serum-starvation conditions correlated with high Rac1 activity. Under serum-starvation conditions 5'Myc-p110δ-overexpressing cells displayed a reduction in actin stress fibres and associated focal adhesions, they were more spread on the substratum, and they displayed increased lamellipodia and membrane ruffling (during cell adhesion) compared to pMX-neo-expressing cells, all features associated with increased Rac1 activity (summarsied in Table 8.1) (Nobes & Hall, 1995; Ridley, et al., 1992). Furthermore, p110δ inhibition in 5'Myc-p110δ-overexpressing cells substantially reversed some of these phenotypes, indicating that p110δ lipid kinase activity is needed for these responses.

It is clear that the effect of p110δ overexpression on the actin cytoskeleton and the activation of the small RhoGTPases in NIH 3T3 cells is complex and is further complicated by the downregulation of p110α and p110β expression. Although a hypothetical model has been proposed for the effect of prolonged exposure to serum on the phenotypes observed in 5'Myc-p110δ-overexpressing cells, this is purely speculative and the impact of growth factors, such as IGF-1 and PDGF, in addition to other constituents of serum, rather than LPA, may well be the causative agents for the phenotypes observed. Furthermore, the focus of this and the previous discussions in section 7.5, have been on p110β as a potential regulator of RhoA activity, however the impact of p110α downregulation in 5'Myc-p110δ-overexpressing cells should not be overlooked. Indeed, in endothelial cells, p110α has been shown to positively regulate RhoA activity (Graupera, et al., 2008). Further investigation is required to elucidate the regulatory roles of each PI3K isoform on RhoA/Rac1/ and Cdc42 activity in NIH 3T3 cells. One way in which this could be investigated, is through stable overexpression of 5'Myc-p110α or 5'Myc-p110β in NIH 3T3 cells, and compare the phenotypes observed with 5'Myc-p110δ-overexpressing NIH 3T3 cells. Ideally, characterisation of NIH 3T3 cells stably overexpressing *untagged* p110α/β/δ would be

carried out, to avoid any uncertainty regarding the biological function the 5'Myc-tag may be exerting.

There are numerous potentially interesting lines of investigation which could be carried out to further characterise NIH 3T3 cells overexpressing p110δ, which are discussed in more depth in section 7.5.7. However, one area of particular interest is investigation into the migratory capacity of these cells. There are indications that p110δ plays an important role in cell migration (Papakonstanti, et al., 2007; Sawyer, et al., 2003), therefore it would be interesting to investigate cell migration in cells in which p110δ has become the principle class I PI3K isoform. It is possible that p110δ-overexpressing cells have a migratory advantage over control cells, or conversely the disruption in p110 expression and Rho GTPase activation may have a negative effect on cell migration. Analysing tumour formation in nude mice after injection of 5'Myc-p110δ-overexpressing cells would help assess the tumorigenicity of these cells and may provide some insight the metastatic potential of solid tumours which express high levels of p110δ.

9 REFERENCES

Abe, K., 2008. Neural activity-dependent regulation of gene expression in developing and mature neurons. *Dev Growth Differ*, **50**(4), 261-71.

Ali, K., Bilancio, A., Thomas, M., Pearce, W., Gilfillan, A. M., Tkaczyk, C., Kuehn, N., Gray, A., Giddings, J., Peskett, E., Fox, R., Bruce, I., Walker, C., Sawyer, C., Okkenhaug, K., Finan, P. & Vanhaesebroeck, B., 2004. Essential role for the p110delta phosphoinositide 3-kinase in the allergic response. *Nature*, **431**(7011), 1007-11.

Ali, K., Camps, M., Pearce, W. P., Ji, H., Ruckle, T., Kuehn, N., Pasquali, C., Chabert, C., Rommel, C. & Vanhaesebroeck, B., 2008. Isoform-specific functions of phosphoinositide 3-kinases: p110 delta but not p110 gamma promotes optimal allergic responses in vivo. *J Immunol*, **180**(4), 2538-44.

Ali, K. & Vanhaesebroeck, B., unpublished results.

Ali, S. H. & DeCaprio, J. A., 2001. Cellular transformation by SV40 large T antigen: interaction with host proteins. *Semin Cancer Biol*, **11**(1), 15-23.

Allen, W. E., Zicha, D., Ridley, A. J. & Jones, G. E., 1998. A role for Cdc42 in macrophage chemotaxis. *J Cell Biol*, **141**(5), 1147-57.

Aoki, M., Blazek, E. & Vogt, P. K., 2001. A role of the kinase mTOR in cellular transformation induced by the oncoproteins P3k and Akt. *Proc Natl Acad Sci U S A*, **98**(1), 136-41.

Aoki, M., Schetter, C., Himly, M., Batista, O., Chang, H. W. & Vogt, P. K., 2000. The catalytic subunit of phosphoinositide 3-kinase: requirements for oncogenicity. *J Biol Chem*, **275**(9), 6267-75.

Arce, L., Yokoyama, N. N. & Waterman, M. L., 2006. Diversity of LEF/TCF action in development and disease. *Oncogene*, **25**(57), 7492-504.

Aso, T., Conaway, J. W. & Conaway, R. C., 1994. Role of core promoter structure in assembly of the RNA polymerase II preinitiation complex. A common pathway for formation of preinitiation intermediates at many TATA and TATA-less promoters. *J Biol Chem*, **269**(42), 26575-83.

Aspenstrom, P., Fransson, A. & Saras, J., 2004. Rho GTPases have diverse effects on the organization of the actin filament system. *Biochem J*, **377**(Pt 2), 327-37.

Aspenstrom, P., Lindberg, U. & Hall, A., 1996. Two GTPases, Cdc42 and Rac, bind directly to a protein implicated in the immunodeficiency disorder Wiskott-Aldrich syndrome. *Curr Biol*, **6**(1), 70-5.

Auger, K. R., Wang, J., Narsimhan, R. P., Holcombe, T. & Roberts, T. M., 2000. Constitutive cellular expression of PI 3-kinase is distinct from transient expression. *Biochem Biophys Res Commun*, **272**(3), 822-9.

Ayyanan, A., Civenni, G., Ciarloni, L., Morel, C., Mueller, N., Lefort, K., Mandinova, A., Raffoul, W., Fiche, M., Dotto, G. P. & Brisken, C., 2006. Increased Wnt signaling triggers oncogenic conversion of human breast epithelial cells by a Notch-dependent mechanism. *Proc Natl Acad Sci U S A*, **103**(10), 3799-804.

Bachman, K. E., Argani, P., Samuels, Y., Silliman, N., Ptak, J., Szabo, S., Konishi, H., Karakas, B., Blair, B. G., Lin, C., Peters, B. A., Velculescu, V. E. & Park, B. H., 2004. The PIK3CA gene is mutated with high frequency in human breast cancers. *Cancer Biol Ther*, **3**(8), 772-5.

Backer, J. M., 2008. The regulation and function of Class III PI3Ks: novel roles for Vps34. *Biochem J*, **410**(1), 1-17.

Bagrodia, S., Taylor, S. J., Jordon, K. A., Van Aelst, L. & Cerione, R. A., 1998. A novel regulator of p21-activated kinases. *J Biol Chem*, **273**(37), 23633-6.

Barbacid, M., 1987. ras genes. *Annu Rev Biochem*, **56**, 779-827.

Barber, M. A. & Welch, H. C., 2006. PI3K and RAC signalling in leukocyte and cancer cell migration. *Bull Cancer*, **93**(5), E44-52.

Barquinero, J., Eixarch, H. & Perez-Melgosa, M., 2004. Retroviral vectors: new applications for an old tool. *Gene Ther*, **11 Suppl 1**, S3-9.

Bartel, F. O., Higuchi, T. & Spyropoulos, D. D., 2000. Mouse models in the study of the Ets family of transcription factors. *Oncogene*, **19**(55), 6443-54.

Barthel, A., Okino, S. T., Liao, J., Nakatani, K., Li, J., Whitlock, J. P., Jr. & Roth, R. A., 1999. Regulation of GLUT1 gene transcription by the serine/threonine kinase Akt1. *J Biol Chem*, **274**(29), 20281-6.

Barton, C. A., Hacker, N. F., Clark, S. J. & O'Brien, P. M., 2008. DNA methylation changes in ovarian cancer: implications for early diagnosis, prognosis and treatment. *Gynecol Oncol*, **109**(1), 129-39.

Bassuk, A. G. & Leiden, J. M., 1997. The role of Ets transcription factors in the development and function of the mammalian immune system. *Adv Immunol*, **64**, 65-104.

Beeton, C. A., Chance, E. M., Foukas, L. C. & Shepherd, P. R., 2000. Comparison of the kinetic properties of the lipid- and protein-kinase activities of the p110alpha and p110beta catalytic subunits of class-Ia phosphoinositide 3-kinases. *Biochem J*, **350 Pt 2**, 353-9.

Beeton, C. A., Das, P., Waterfield, M. D. & Shepherd, P. R., 1999. The SH3 and BH domains of the p85alpha adapter subunit play a critical role in regulating class Ia phosphoinositide 3-kinase function. *Mol Cell Biol Res Commun*, **1**(2), 153-7.

Behrens, J., von Kries, J. P., Kuhl, M., Bruhn, L., Wedlich, D., Grosschedl, R. & Birchmeier, W., 1996. Functional interaction of beta-catenin with the transcription factor LEF-1. *Nature*, **382**(6592), 638-42.

Bender, M. A., Palmer, T. D., Gelinas, R. E. & Miller, A. D., 1987. Evidence that the packaging signal of Moloney murine leukaemia virus extends into the gag region. *J Virol*, **61**(5), 1639-46.

Bentley, D., 2002. The mRNA assembly line: transcription and processing machines in the same factory. *Curr Opin Cell Biol*, **14**(3), 336-42.

Berrie, C. P., 2001. Phosphoinositide 3-kinase inhibition in cancer treatment. *Expert Opin Investig Drugs*, **10**(6), 1085-98.

Bi, L., Okabe, I., Bernard, D. J. & Nussbaum, R. L., 2002. Early embryonic lethality in mice deficient in the p110beta catalytic subunit of PI 3-kinase. *Mamm Genome*, **13**(3), 169-72.

Bi, L., Okabe, I., Bernard, D. J., Wynshaw-Boris, A. & Nussbaum, R. L., 1999. Proliferative defect and embryonic lethality in mice homozygous for a deletion in the p110alpha subunit of phosphoinositide 3-kinase. *J Biol Chem*, **274**(16), 10963-8.

Bianco, R., Melisi, D., Ciardiello, F. & Tortora, G., 2006. Key cancer cell signal transduction pathways as therapeutic targets. *Eur J Cancer*, **42**(3), 290-4.

Bilancio, A. & Vanhaesebroeck, B., unpublished results.

Billottet, C., Grandage, V. L., Gale, R. E., Quattropani, A., Rommel, C., Vanhaesebroeck, B. & Khwaja, A., 2006. A selective inhibitor of the p110delta isoform of PI 3-kinase inhibits AML cell proliferation and survival and increases the cytotoxic effects of VP16. *Oncogene*, **25**(50), 6648-59.

Billottet, C. & Vanhaesebroeck, B., unpublished results.

Bishop, A. L. & Hall, A., 2000. Rho GTPases and their effector proteins. *Biochem J*, **348 Pt 2**, 241-55.

Blume-Jensen, P., Claesson-Welsh, L., Siegbahn, A., Zsebo, K. M., Westermark, B. & Heldin, C. H., 1991. Activation of the human c-kit product by ligand-induced dimerization mediates circular actin reorganization and chemotaxis. *Embo J*, **10**(13), 4121-8.

Boeger, H., Griesenbeck, J., Strattan, J. S. & Kornberg, R. D., 2003. Nucleosomes unfold completely at a transcriptionally active promoter. *Mol Cell*, **11**(6), 1587-98.

Bokoch, G. M., Vlahos, C. J., Wang, Y., Knaus, U. G. & Traynor-Kaplan, A. E., 1996. Rac GTPase interacts specifically with phosphatidylinositol 3-kinase. *Biochem J*, **315 (Pt 3**), 775-9.

Bories, J. C., Willerford, D. M., Grevin, D., Davidson, L., Camus, A., Martin, P., Stehelin, D. & Alt, F. W., 1995. Increased T-cell apoptosis and terminal B-cell differentiation induced by inactivation of the Ets-1 proto-oncogene. *Nature*, **377**(6550), 635-8.

Bos, J. L., 1989. ras oncogenes in human cancer: a review. *Cancer Res*, **49**(17), 4682-9.

Brachmann, S. M., Ueki, K., Engelman, J. A., Kahn, R. C. & Cantley, L. C., 2005. Phosphoinositide 3-kinase catalytic subunit deletion and regulatory subunit deletion have opposite effects on insulin sensitivity in mice. *Mol Cell Biol*, **25**(5), 1596-607.

Brennan, P., Babbage, J. W., Burgering, B. M., Groner, B., Reif, K. & Cantrell, D. A., 1997. Phosphatidylinositol 3-kinase couples the interleukin-2 receptor to the cell cycle regulator E2F. *Immunity*, **7**(5), 679-89.

Brickner, A. G., Gossage, D. L., Dusing, M. R. & Wiginton, D. A., 1995. Identification of a murine homolog of the human adenosine deaminase thymic enhancer. *Gene*, **167**(1-2), 261-6.

Broderick, D. K., Di, C., Parrett, T. J., Samuels, Y. R., Cummins, J. M., McLendon, R. E., Fults, D. W., Velculescu, V. E., Bigner, D. D. & Yan, H., 2004. Mutations of PIK3CA in anaplastic oligodendrogliomas, high-grade astrocytomas, and medulloblastomas. *Cancer Res*, **64**(15), 5048-50.

Brunner, C. & Wirth, T., 2006. Btk expression is controlled by Oct and BOB.1/OBF.1. *Nucleic Acids Res*, **34**(6), 1807-15.

Buggy, Y., Maguire, T. M., McDermott, E., Hill, A. D., O'Higgins, N. & Duffy, M. J., 2006. Ets2 transcription factor in normal and neoplastic human breast tissue. *Eur J Cancer*, **42**(4), 485-91.

Burbelo, P. D., Drechsel, D. & Hall, A., 1995. A conserved binding motif defines numerous candidate target proteins for both Cdc42 and Rac GTPases. *J Biol Chem*, **270**(49), 29071-4.

Burda, P., Padilla, S. M., Sarkar, S. & Emr, S. D., 2002. Retromer function in endosome-to-Golgi retrograde transport is regulated by the yeast Vps34 PtdIns 3-kinase. *J Cell Sci*, **115**(Pt 20), 3889-900.

Burgstaller, G. & Gimona, M., 2005. Podosome-mediated matrix resorption and cell motility in vascular smooth muscle cells. *Am J Physiol Heart Circ Physiol*, **288**(6), H3001-5.

Burke, T. W. & Kadonaga, J. T., 1996. Drosophila TFIID binds to a conserved downstream basal promoter element that is present in many TATA-box-deficient promoters. *Genes Dev*, **10**(6), 711-24.

Burns, S., Thrasher, A. J., Blundell, M. P., Machesky, L. & Jones, G. E., 2001. Configuration of human dendritic cell cytoskeleton by Rho GTPases, the WAS protein, and differentiation. *Blood*, **98**(4), 1142-9.

Butler, J. E. & Kadonaga, J. T., 2002. The RNA polymerase II core promoter: a key component in the regulation of gene expression. *Genes Dev*, **16**(20), 2583-92.

Cabezas, A., Pattni, K. & Stenmark, H., 2006. Cloning and subcellular localization of a human phosphatidylinositol 3-phosphate 5-kinase, PIKfyve/Fab1. *Gene*, **371**(1), 34-41.

Calle, Y., Carragher, N. O., Thrasher, A. J. & Jones, G. E., 2006. Inhibition of calpain stabilises podosomes and impairs dendritic cell motility. *J Cell Sci*, **119**(Pt 11), 2375-85.

Calle, Y., Chou, H. C., Thrasher, A. J. & Jones, G. E., 2004a. Wiskott-Aldrich syndrome protein and the cytoskeletal dynamics of dendritic cells. *J Pathol*, **204**(4), 460-9.

Calle, Y., Jones, G. E., Jagger, C., Fuller, K., Blundell, M. P., Chow, J., Chambers, T. & Thrasher, A. J., 2004b. WASp deficiency in mice results in failure to form osteoclast sealing zones and defects in bone resorption. *Blood*, **103**(9), 3552-61.

Campbell, I. G., Russell, S. E., Choong, D. Y., Montgomery, K. G., Ciavarella, M. L., Hooi, C. S., Cristiano, B. E., Pearson, R. B. & Phillips, W. A., 2004. Mutation of the PIK3CA gene in ovarian and breast cancer. *Cancer Res*, **64**(21), 7678-81.

Cascone, I., Giraudo, E., Caccavari, F., Napione, L., Bertotti, E., Collard, J. G., Serini, G. & Bussolino, F., 2003. Temporal and spatial modulation of Rho GTPases during in vitro formation of capillary vascular network. Adherens junctions and myosin light chain as targets of Rac1 and RhoA. *J Biol Chem*, **278**(50), 50702-13.

Chabot, B., Stephenson, D. A., Chapman, V. M., Besmer, P. & Bernstein, A., 1988. The proto-oncogene c-kit encoding a transmembrane tyrosine kinase receptor maps to the mouse W locus. *Nature*, **335**(6185), 88-9.

Chakravarthy, M. V., Abraha, T. W., Schwartz, R. J., Fiorotto, M. L. & Booth, F. W., 2000. Insulin-like growth factor-I extends in vitro replicative life span of skeletal muscle satellite cells by enhancing G1/S cell cycle progression via the activation of phosphatidylinositol 3'-kinase/Akt signaling pathway. *J Biol Chem*, **275**(46), 35942-52.

Chamberlain, M. D., Berry, T. R., Pastor, M. C. & Anderson, D. H., 2004. The p85alpha subunit of phosphatidylinositol 3'-kinase binds to and stimulates the GTPase activity of Rab proteins. *J Biol Chem*, **279**(47), 48607-14.

Chamberlain, M. D., Chan, T., Oberg, J. C., Hawrysh, A. D., James, K. M., Saxena, A., Xiang, J. & Anderson, D. H., 2008. Disrupted rabgap function of the p85 subunit of phosphatidylinositol 3'-kinase results in cell transformation. *J Biol Chem*.

Chan, W. Y., Kohsaka, S. & Rezaie, P., 2007. The origin and cell lineage of microglia: new concepts. *Brain Res Rev*, **53**(2), 344-54.

Chang, H. W., Aoki, M., Fruman, D., Auger, K. R., Bellacosa, A., Tsichlis, P. N., Cantley, L. C., Roberts, T. M. & Vogt, P. K., 1997. Transformation of chicken cells by the gene encoding the catalytic subunit of PI 3-kinase. *Science*, **276**(5320), 1848-50.

Chanteux, H., Guisset, A. C., Pilette, C. & Sibille, Y., 2007. LPS induces IL-10 production by human alveolar macrophages via MAPKinases- and Sp1-dependent mechanisms. *Respir Res*, **8**, 71.

Chantry, D., Vojtek, A., Kashishian, A., Holtzman, D. A., Wood, C., Gray, P. W., Cooper, J. A. & Hoekstra, M. F., 1997. p110delta, a novel phosphatidylinositol 3-kinase catalytic subunit that associates with p85 and is expressed predominantly in leukocytes. *J Biol Chem*, **272**(31), 19236-41.

Chaussade, C., Pirola, L., Bonnafous, S., Blondeau, F., Brenz-Verca, S., Tronchere, H., Portis, F., Rusconi, S., Payrastre, B., Laporte, J. & Van Obberghen, E., 2003. Expression of myotubularin by an adenoviral vector demonstrates its function as a phosphatidylinositol 3-phosphate [PtdIns(3)P] phosphatase in muscle cell lines: involvement of PtdIns(3)P in insulin-stimulated glucose transport. *Mol Endocrinol*, **17**(12), 2448-60.

Chellaiah, M., Kizer, N., Silva, M., Alvarez, U., Kwiatkowski, D. & Hruska, K. A., 2000. Gelsolin deficiency blocks podosome assembly and produces increased bone mass and strength. *J Cell Biol*, **148**(4), 665-78.

Chen, D., Mauvais-Jarvis, F., Bluher, M., Fisher, S. J., Jozsi, A., Goodyear, L. J., Ueki, K. & Kahn, C. R., 2004. p50alpha/p55alpha phosphoinositide 3-kinase knockout mice exhibit enhanced insulin sensitivity. *Mol Cell Biol*, **24**(1), 320-9.

Chen, H., Ray-Gallet, D., Zhang, P., Hetherington, C. J., Gonzalez, D. A., Zhang, D. E., Moreau-Gachelin, F. & Tenen, D. G., 1995. PU.1 (Spi-1) autoregulates its expression in myeloid cells. *Oncogene*, **11**(8), 1549-60.

Chen, J., Spector, M. S., Kunos, G. & Gao, B., 1997. Sp1-mediated transcriptional activation from the dominant promoter of the rat alpha1B adrenergic receptor gene in DDT1MF-2 cells. *J Biol Chem*, **272**(37), 23144-50.

Cherfils, J. & Chardin, P., 1999. GEFs: structural basis for their activation of small GTP-binding proteins. *Trends Biochem Sci*, **24**(8), 306-11.

Clayton, E., Bardi, G., Bell, S. E., Chantry, D., Downes, C. P., Gray, A., Humphries, L. A., Rawlings, D., Reynolds, H., Vigorito, E. & Turner, M., 2002. A crucial role for the p110delta subunit of phosphatidylinositol 3-kinase in B cell development and activation. *J Exp Med*, **196**(6), 753-63.

Cockerill, G. W., Bert, A. G., Ryan, G. R., Gamble, J. R., Vadas, M. A. & Cockerill, P. N., 1995. Regulation of granulocyte-macrophage colony-stimulating factor and E-selectin expression in endothelial cells by cyclosporin A and the T-cell transcription factor NFAT. *Blood*, **86**(7), 2689-98.

Colgan, J. & Manley, J. L., 1995. Cooperation between core promoter elements influences transcriptional activity in vivo. *Proc Natl Acad Sci U S A*, **92**(6), 1955-9.

Collin, O., Tracqui, P., Stephanou, A., Usson, Y., Clement-Lacroix, J. & Planus, E., 2006. Spatiotemporal dynamics of actin-rich adhesion microdomains: influence of substrate flexibility. *J Cell Sci*, **119**(Pt 9), 1914-25.

Conaway, R. C. & Conaway, J. W., 1997. General transcription factors for RNA polymerase II. *Prog Nucleic Acid Res Mol Biol*, **56**, 327-46.

Condliffe, A. M., Davidson, K., Anderson, K. E., Ellson, C. D., Crabbe, T., Okkenhaug, K., Vanhaesebroeck, B., Turner, M., Webb, L., Wymann, M. P., Hirsch, E., Ruckle, T., Camps, M., Rommel, C., Jackson, S. P., Chilvers, E. R., Stephens, L. R. & Hawkins, P. T., 2005. Sequential activation of class IB and class IA PI3K is important for the primed respiratory burst of human but not murine neutrophils. *Blood*, **106**(4), 1432-40.

Cornillet-Lefebvre, P., Cuccuini, W., Bardet, V., Tamburini, J., Gillot, L., Ifrah, N., Nguyen, P., Dreyfus, F., Mayeux, P., Lacombe, C. & Bouscary, D., 2006. Constitutive phosphoinositide 3-kinase activation in acute myeloid leukaemia is not due to p110delta mutations. *Leukaemia*, **20**(2), 374-6.

Cramer, P., Srebrow, A., Kadener, S., Werbajh, S., de la Mata, M., Melen, G., Nogues, G. & Kornblihtt, A. R., 2001. Coordination between transcription and pre-mRNA processing. *FEBS Lett*, **498**(2-3), 179-82.

Crofts, L. A., Hancock, M. S., Morrison, N. A. & Eisman, J. A., 1998. Multiple promoters direct the tissue-specific expression of novel N-terminal variant human vitamin D receptor gene transcripts. *Proc Natl Acad Sci U S A*, **95**(18), 10529-34.

Cully, M., You, H., Levine, A. J. & Mak, T. W., 2006. Beyond PTEN mutations: the PI3K pathway as an integrator of multiple inputs during tumorigenesis. *Nat Rev Cancer*, **6**(3), 184-92.

Czauderna, F., Fechtner, M., Aygun, H., Arnold, W., Klippel, A., Giese, K. & Kaufmann, J., 2003a. Functional studies of the PI(3)-kinase signalling pathway employing synthetic and expressed siRNA. *Nucleic Acids Res*, **31**(2), 670-82.

Czauderna, F., Santel, A., Hinz, M., Fechtner, M., Durieux, B., Fisch, G., Leenders, F., Arnold, W., Giese, K., Klippel, A. & Kaufmann, J., 2003b. Inducible shRNA expression for application in a prostate cancer mouse model. *Nucleic Acids Res*, **31**(21), e127.

Dagia, N. M., Harii, N., Meli, A. E., Sun, X., Lewis, C. J., Kohn, L. D. & Goetz, D. J., 2004. Phenyl methimazole inhibits TNF-alpha-induced VCAM-1 expression in an IFN regulatory factor-1-dependent manner and reduces monocytic cell adhesion to endothelial cells. *J Immunol*, **173**(3), 2041-9.

David-Pfeuty, T. & Singer, S. J., 1980. Altered distributions of the cytoskeletal proteins vinculin and alpha-actinin in cultured fibroblasts transformed by Rous sarcoma virus. *Proc Natl Acad Sci U S A*, **77**(11), 6687-91.

De Boer, M. L., Mordvinov, V. A., Thomas, M. A. & Sanderson, C. J., 1999. Role of nuclear factor of activated T cells (NFAT) in the expression of interleukin-5 and other cytokines involved in the regulation of hemopoetic cells. *Int J Biochem Cell Biol*, **31**(10), 1221-36.

Dejana, E., Taddei, A. & Randi, A. M., 2007. Foxs and Ets in the transcriptional regulation of endothelial cell differentiation and angiogenesis. *Biochim Biophys Acta*, **1775**(2), 298-312.

Denley, A., Kang, S., Karst, U. & Vogt, P. K., 2008. Oncogenic signaling of class I PI3K isoforms. *Oncogene*, **27**(18), 2561-74.

Desire, L., Bourdin, J., Loiseau, N., Peillon, H., Picard, V., De Oliveira, C., Bachelot, F., Leblond, B., Taverne, T., Beausoleil, E., Lacombe, S., Drouin, D. & Schweighoffer, F., 2005. RAC1 inhibition targets amyloid precursor protein processing by gamma-secretase and decreases Abeta production in vitro and in vivo. *J Biol Chem*, **280**(45), 37516-25.

Destaing, O., Saltel, F., Geminard, J. C., Jurdic, P. & Bard, F., 2003. Podosomes display actin turnover and dynamic self-organization in osteoclasts expressing actin-green fluorescent protein. *Mol Biol Cell*, **14**(2), 407-16.

Dunant, N. & Ballmer-Hofer, K., 1997. Signalling by Src family kinases: lessons learnt from DNA tumour viruses. *Cell Signal*, **9**(6), 385-93.

Dunham, I., Shimizu, N., Roe, B. A., Chissoe, S., Hunt, A. R., Collins, J. E., Bruskiewich, R., Beare, D. M., Clamp, M., Smink, L. J., Ainscough, R., Almeida, J. P., Babbage, A., Bagguley, C., Bailey, J., Barlow, K., Bates, K. N., Beasley, O., Bird, C. P., Blakey, S., Bridgeman, A. M., Buck, D., Burgess, J., Burrill, W. D., O'Brien, K. P. & et al., 1999. The DNA sequence of human chromosome 22. *Nature*, **402**(6761), 489-95.

Dutt, P., Jaffe, A. B., Merdek, K. D., Hall, A. & Toksoz, D., 2004. Galphaz inhibits serum response factor-dependent transcription by inhibiting Rho signaling. *Mol Pharmacol*, **66**(6), 1508-16.

Eastman, Q. & Grosschedl, R., 1999. Regulation of LEF-1/TCF transcription factors by Wnt and other signals. *Curr Opin Cell Biol*, **11**(2), 233-40.

Eichholtz, T., Jalink, K., Fahrenfort, I. & Moolenaar, W. H., 1993. The bioactive phospholipid lysophosphatidic acid is released from activated platelets. *Biochem J*, **291 (Pt 3)**, 677-80.

Elis, W., Triantafellow, E., Wolters, N. M., Sian, K. R., Caponigro, G., Borawski, J., Gaither, L. A., Murphy, L. O., Finan, P. M. & Mackeigan, J. P., 2008. Down-Regulation of Class II Phosphoinositide 3-Kinase {alpha} Expression below a Critical Threshold Induces Apoptotic Cell Death. *Mol Cancer Res*, **6**(4), 614-23.

Etienne-Manneville, S. & Hall, A., 2002. Rho GTPases in cell biology. *Nature*, **420**(6916), 629-35.

Evans, J. G., Correia, I., Krasavina, O., Watson, N. & Matsudaira, P., 2003. Macrophage podosomes assemble at the leading lamella by growth and fragmentation. *J Cell Biol*, **161**(4), 697-705.

Evans, R., Fairley, J. A. & Roberts, S. G., 2001. Activator-mediated disruption of sequence-specific DNA contacts by the general transcription factor TFIIB. *Genes Dev*, **15**(22), 2945-9.

Falasca, M., Hughes, W. E., Dominguez, V., Sala, G., Fostira, F., Fang, M. Q., Cazzolli, R., Shepherd, P. R., James, D. E. & Maffucci, T., 2007. The role of phosphoinositide 3-kinase C2alpha in insulin signaling. *J Biol Chem*, **282**(38), 28226-36.

Falasca, M. & Maffucci, T., 2007. Role of class II phosphoinositide 3-kinase in cell signalling. *Biochem Soc Trans*, **35**(Pt 2), 211-4.

Fan, Q. W., Knight, Z. A., Goldenberg, D. D., Yu, W., Mostov, K. E., Stokoe, D., Shokat, K. M. & Weiss, W. A., 2006. A dual PI3 kinase/mTOR inhibitor reveals emergent efficacy in glioma. *Cancer Cell*, **9**(5), 341-9.

Fang, X., Yu, S., LaPushin, R., Lu, Y., Furui, T., Penn, L. Z., Stokoe, D., Erickson, J. R., Bast, R. C., Jr. & Mills, G. B., 2000. Lysophosphatidic acid prevents apoptosis in fibroblasts via G(i)-protein-mediated activation of mitogen-activated protein kinase. *Biochem J*, **352 Pt 1**, 135-43.

Foster, F. M., Traer, C. J., Abraham, S. M. & Fry, M. J., 2003. The phosphoinositide (PI) 3-kinase family. *J Cell Sci*, **116**(Pt 15), 3037-40.

Foukas, L. & Vanhaesebroeck, B., unpublished results.

Foukas, L. C., Claret, M., Pearce, W., Okkenhaug, K., Meek, S., Peskett, E., Sancho, S., Smith, A. J., Withers, D. J. & Vanhaesebroeck, B., 2006. Critical role for the p110alpha phosphoinositide-3-OH kinase in growth and metabolic regulation. *Nature*, **441**(7091), 366-70.

Freeburn, R. W., Wright, K. L., Burgess, S. J., Astoul, E., Cantrell, D. A. & Ward, S. G., 2002. Evidence that SHIP-1 contributes to phosphatidylinositol 3,4,5-trisphosphate metabolism in T lymphocytes and can regulate novel phosphoinositide 3-kinase effectors. *J Immunol*, **169**(10), 5441-50.

Fruman, D. A., Mauvais-Jarvis, F., Pollard, D. A., Yballe, C. M., Brazil, D., Bronson, R. T., Kahn, C. R. & Cantley, L. C., 2000. Hypoglycaemia, liver necrosis and perinatal death in mice lacking all isoforms of phosphoinositide 3-kinase p85 alpha. *Nat Genet*, **26**(3), 379-82.

Fruman, D. A., Snapper, S. B., Yballe, C. M., Alt, F. W. & Cantley, L. C., 1999. Phosphoinositide 3-kinase knockout mice: role of p85alpha in B cell development and proliferation. *Biochem Soc Trans*, **27**(4), 624-9.

Fry, M. J., 1992. Defining a new GAP family. *Curr Biol*, **2**(2), 78-80.

Fry, M. J., Panayotou, G., Dhand, R., Ruiz-Larrea, F., Gout, I., Nguyen, O., Courtneidge, S. A. & Waterfield, M. D., 1992. Purification and characterization of a phosphatidylinositol 3-kinase complex from bovine brain by using phosphopeptide affinity columns. *Biochem J*, **288 (Pt 2)**, 383-93.

Fujita, H., Katoh, H., Hasegawa, H., Yasui, H., Aoki, J., Yamaguchi, Y. & Negishi, M., 2000. Molecular decipherment of Rho effector pathways regulating tight-junction permeability. *Biochem J*, **346 Pt 3**, 617-22.

Fukuhara, S., Chikumi, H. & Gutkind, J. S., 2000. Leukaemia-associated Rho guanine nucleotide exchange factor (LARG) links heterotrimeric G proteins of the G(12) family to Rho. *FEBS Lett*, **485**(2-3), 183-8.

Fukuhara, S., Murga, C., Zohar, M., Igishi, T. & Gutkind, J. S., 1999. A novel PDZ domain containing guanine nucleotide exchange factor links heterotrimeric G proteins to Rho. *J Biol Chem*, **274**(9), 5868-79.

Fukumoto, Y., Kaibuchi, K., Hori, Y., Fujioka, H., Araki, S., Ueda, T., Kikuchi, A. & Takai, Y., 1990. Molecular cloning and characterization of a novel type of regulatory protein (GDI) for the rho proteins, ras p21-like small GTP-binding proteins. *Oncogene*, **5**(9), 1321-8.

Fukuyama, T., Ogita, H., Kawakatsu, T., Inagaki, M. & Takai, Y., 2006. Activation of Rac by cadherin through the c-Src-Rap1-phosphatidylinositol 3-kinase-Vav2 pathway. *Oncogene*, **25**(1), 8-19.

Funamoto, S., Meili, R., Lee, S., Parry, L. & Firtel, R. A., 2002. Spatial and temporal regulation of 3-phosphoinositides by PI 3-kinase and PTEN mediates chemotaxis. *Cell*, **109**(5), 611-23.

Furitsu, T., Tsujimura, T., Tono, T., Ikeda, H., Kitayama, H., Koshimizu, U., Sugahara, H., Butterfield, J. H., Ashman, L. K., Kanayama, Y. & et al., 1993. Identification of mutations in the coding sequence of the proto-oncogene c-kit in a human mast cell leukaemia cell line causing ligand-independent activation of c-kit product. *J Clin Invest*, **92**(4), 1736-44.

Furlan, A., Vercamer, C., Desbiens, X. & Pourtier, A., 2008. Ets-1 triggers and orchestrates the malignant phenotype of mammary cancer cells within their matrix environment. *J Cell Physiol*, **215**(3), 782-93.

Futter, C. E., Collinson, L. M., Backer, J. M. & Hopkins, C. R., 2001. Human VPS34 is required for internal vesicle formation within multivesicular endosomes. *J Cell Biol*, **155**(7), 1251-64.

Gao, Y., Dickerson, J. B., Guo, F., Zheng, J. & Zheng, Y., 2004. Rational design and characterization of a Rac GTPase-specific small molecule inhibitor. *Proc Natl Acad Sci U S A*, **101**(20), 7618-23.

Gary, J. D., Wurmser, A. E., Bonangelino, C. J., Weisman, L. S. & Emr, S. D., 1998. Fab1p is essential for PtdIns(3)P 5-kinase activity and the maintenance of vacuolar size and membrane homeostasis. *J Cell Biol*, **143**(1), 65-79.

Gebeshuber, C. A., Sladecek, S. & Grunert, S., 2007. Beta-catenin/LEF-1 signalling in breast cancer--central players activated by a plethora of inputs. *Cells Tissues Organs*, **185**(1-3), 51-60.

Geering, B., Cutillas, P. R. & Vanhaesebroeck, B., 2007a. Regulation of class IA PI3Ks: is there a role for monomeric PI3K subunits? *Biochem Soc Trans*, **35**(Pt 2), 199-203.

Geering, B., Cutillas, P. R., Nock. G., Gharbi, S.I. & Vanhaesebroeck, B., 2007b. Class IA phosphoinositide 3-kinases are obligate p85-p110 heterodimers. *Proc Natl Acad Sci U S A*, **104**(19), 7809-14.

Giese, K., Kingsley, C., Kirshner, J. R. & Grosschedl, R., 1995. Assembly and function of a TCR alpha enhancer complex is dependent on LEF-1-induced DNA bending and multiple protein-protein interactions. *Genes Dev*, **9**(8), 995-1008.

Glotzer, M., 2001. Animal cell cytokinesis. *Annu Rev Cell Dev Biol*, **17**, 351-86.

Gottlieb, K. A. & Villarreal, L. P., 2001. Natural biology of polyomavirus middle T antigen. *Microbiol Mol Biol Rev*, **65**(2), 288-318 ; second and third pages, table of contents.

Graff, J. R., Konicek, B. W., McNulty, A. M., Wang, Z., Houck, K., Allen, S., Paul, J. D., Hbaiu, A., Goode, R. G., Sandusky, G. E., Vessella, R. L. & Neubauer, B. L., 2000. Increased AKT activity contributes to prostate cancer progression by dramatically accelerating prostate tumor growth and diminishing p27Kip1 expression. *J Biol Chem*, **275**(32), 24500-5.

Graupera, M., Guillermet-Guibert, J., Foukas, L. C., Phng, L. K., Cain, R. J., Salpekar, A., Pearce, W., Meek, S., Millan, J., Cutillas, P. R., Smith, A. J., Ridley, A. J., Ruhrberg, C., Gerhardt, H. & Vanhaesebroeck, B., 2008. Angiogenesis selectively requires the p110alpha isoform of PI3K to control endothelial cell migration. *Nature*.

Graves, B. J. & Petersen, J. M., 1998. Specificity within the ets family of transcription factors. *Adv Cancer Res*, **75**, 1-55.

Guillermet-Guibert, J., 2008. (Unpublished results). *Queen Mary's Institute for Cancer Research*.

Guillermet-Guibert, J., Bjorklof, K., Salpekar, A., Gonella, C., Ramadani, F., Bilancio, A., Meek, S., Smith, A. J., Okkenhaug, K. & Vanhaesebroeck, B., 2008. The p110beta isoform of phosphoinositide 3-kinase signals downstream of G protein-coupled receptors and is functionally redundant with p110gamma. *Proc Natl Acad Sci U S A*, **105**(24), 8292-7.

Guillermet-Guibert, J. & Vanhaesebroeck, B., unpublished results.

Guo, F., Debidda, M., Yang, L., Williams, D. A. & Zheng, Y., 2006. Genetic deletion of Rac1 GTPase reveals its critical role in actin stress fiber formation and focal adhesion complex assembly. *J Biol Chem*, **281**(27), 18652-9.

Gupta, S., Ramjaun, A. R., Haiko, P., Wang, Y., Warne, P. H., Nicke, B., Nye, E., Stamp, G., Alitalo, K. & Downward, J., 2007. Binding of ras to phosphoinositide 3-kinase p110alpha is required for ras-driven tumorigenesis in mice. *Cell*, **129**(5), 957-68.

Hall, A., 2005. Rho GTPases and the control of cell behaviour. *Biochem Soc Trans*, **33**(Pt 5), 891-5.

Hamaguchi, N., Ihara, S., Ohdaira, T., Nagano, H., Iwamatsu, A., Tachikawa, H. & Fukui, Y., 2007. Pleckstrin-2 selectively interacts with phosphatidylinositol 3-kinase lipid products and regulates actin organization and cell spreading. *Biochem Biophys Res Commun*, **361**(2), 270-5.

Han, J., Luby-Phelps, K., Das, B., Shu, X., Xia, Y., Mosteller, R. D., Krishna, U. M., Falck, J. R., White, M. A. & Broek, D., 1998. Role of substrates and products of PI 3-kinase in regulating activation of Rac-related guanosine triphosphatases by Vav. *Science*, **279**(5350), 558-60.

Harris, S. J., Parry, R. V., Westwick, J. & Ward, S. G., 2008. Phosphoinositide lipid phosphatases: natural regulators of phosphoinositide 3-kinase signaling in T lymphocytes. *J Biol Chem*, **283**(5), 2465-9.

Hart, A., Melet, F., Grossfeld, P., Chien, K., Jones, C., Tunnacliffe, A., Favier, R. & Bernstein, A., 2000. Fli-1 is required for murine vascular and megakaryocytic development and is hemizygously deleted in patients with thrombocytopenia. *Immunity*, **13**(2), 167-77.

Hart, M. J., Jiang, X., Kozasa, T., Roscoe, W., Singer, W. D., Gilman, A. G., Sternweis, P. C. & Bollag, G., 1998. Direct stimulation of the guanine nucleotide exchange activity of p115 RhoGEF by Galpha13. *Science*, **280**(5372), 2112-4.

Hatsell, S., Rowlands, T., Hiremath, M. & Cowin, P., 2003. Beta-catenin and Tcfs in mammary development and cancer. *J Mammary Gland Biol Neoplasia*, **8**(2), 145-58.

Hawkins, P. T., Anderson, K. E., Davidson, K. & Stephens, L. R., 2006. Signalling through Class I PI3Ks in mammalian cells. *Biochem Soc Trans*, **34**(Pt 5), 647-62.

Hawkins, P. T., Eguinoa, A., Qiu, R. G., Stokoe, D., Cooke, F. T., Walters, R., Wennstrom, S., Claesson-Welsh, L., Evans, T., Symons, M. & et al., 1995. PDGF stimulates an increase in GTP-Rac via activation of phosphoinositide 3-kinase. *Curr Biol*, **5**(4), 393-403.

Hawley, R. G., Fong, A. Z., Lu, M. & Hawley, T. S., 1994. The HOX11 homeobox-containing gene of human leukaemia immortalizes murine haematopoietic precursors. *Oncogene*, **9**(1), 1-12.

Hayakawa, M., Kaizawa, H., Kawaguchi, K., Ishikawa, N., Koizumi, T., Ohishi, T., Yamano, M., Okada, M., Ohta, M., Tsukamoto, S., Raynaud, F. I., Waterfield, M. D., Parker, P. & Workman, P., 2007a. Synthesis and biological evaluation of imidazo[1,2-a]pyridine derivatives as novel PI3 kinase p110alpha inhibitors. *Bioorg Med Chem*, **15**(1), 403-12.

Hayakawa, M., Kaizawa, H., Moritomo, H., Koizumi, T., Ohishi, T., Yamano, M., Okada, M., Ohta, M., Tsukamoto, S., Raynaud, F. I., Workman, P., Waterfield, M. D. & Parker, P., 2007b. Synthesis and biological evaluation of pyrido[3',2':4,5]furo[3,2-d]pyrimidine derivatives as novel PI3 kinase p110alpha inhibitors. *Bioorg Med Chem Lett*, **17**(9), 2438-42.

Hayakawa, M., Kawaguchi, K., Kaizawa, H., Koizumi, T., Ohishi, T., Yamano, M., Okada, M., Ohta, M., Tsukamoto, S., Raynaud, F. I., Parker, P., Workman, P. & Waterfield, M. D., 2007c. Synthesis and biological evaluation of sulfonylhydrazone-substituted

imidazo[1,2-a]pyridines as novel PI3 kinase p110alpha inhibitors. *Bioorg Med Chem*, **15**(17), 5837-44.

Heinrich, M. C., Blanke, C. D., Druker, B. J. & Corless, C. L., 2002. Inhibition of KIT tyrosine kinase activity: a novel molecular approach to the treatment of KIT-positive malignancies. *J Clin Oncol*, **20**(6), 1692-703.

Hiraoka, K., Kaibuchi, K., Ando, S., Musha, T., Takaishi, K., Mizuno, T., Asada, M., Menard, L., Tomhave, E., Didsbury, J. & et al., 1992. Both stimulatory and inhibitory GDP/GTP exchange proteins, smg GDS and rho GDI, are active on multiple small GTP-binding proteins. *Biochem Biophys Res Commun*, **182**(2), 921-30.

Hirata, Y., Masuda, Y., Kakutani, H., Higuchi, T., Takada, K., Ito, A., Nakagawa, Y. & Ishii, H., 2008. Sp1 is an essential transcription factor for LPS-induced tissue factor expression in THP-1 monocytic cells, and nobiletin represses the expression through inhibition of NF-kappaB, AP-1, and Sp1 activation. *Biochem Pharmacol*, **75**(7), 1504-14.

Hirsch, E., Katanaev, V. L., Garlanda, C., Azzolino, O., Pirola, L., Silengo, L., Sozzani, S., Mantovani, A., Altruda, F. & Wymann, M. P., 2000a. Central role for G protein-coupled phosphoinositide 3-kinase gamma in inflammation. *Science*, **287**(5455), 1049-53.

Hirsch, E., Lembo, G., Montrucchio, G., Rommel, C., Costa, C. & Barberis, L., 2006. Signaling through PI3Kgamma: a common platform for leukocyte, platelet and cardiovascular stress sensing. *Thromb Haemost*, **95**(1), 29-35.

Hirsch, E., Wymann, M. P., Patrucco, E., Tolosano, E., Bulgarelli-Leva, G., Marengo, S., Rocchi, M. & Altruda, F., 2000b. Analysis of the murine phosphoinositide 3-kinase gamma gene. *Gene*, **256**(1-2), 69-81.

Hochheimer, A. & Tjian, R., 2003. Diversified transcription initiation complexes expand promoter selectivity and tissue-specific gene expression. *Genes Dev*, **17**(11), 1309-20.

Hordijk, P. L., ten Klooster, J. P., van der Kammen, R. A., Michiels, F., Oomen, L. C. & Collard, J. G., 1997. Inhibition of invasion of epithelial cells by Tiam1-Rac signaling. *Science*, **278**(5342), 1464-6.

Hotchin, N. A. & Hall, A., 1995. The assembly of integrin adhesion complexes requires both extracellular matrix and intracellular rho/rac GTPases. *J Cell Biol*, **131**(6 Pt 2), 1857-65.

Hromas, R., Orazi, A., Neiman, R. S., Maki, R., Van Beveran, C., Moore, J. & Klemsz, M., 1993. Haematopoietic lineage- and stage-restricted expression of the ETS oncogene family member PU.1. *Blood*, **82**(10), 2998-3004.

Hsu, S. C., Galceran, J. & Grosschedl, R., 1998. Modulation of transcriptional regulation by LEF-1 in response to Wnt-1 signaling and association with beta-catenin. *Mol Cell Biol*, **18**(8), 4807-18.

Hu, M. H., Bauman, E. M., Roll, R. L., Yeilding, N. & Abrams, C. S., 1999. Pleckstrin 2, a widely expressed paralog of pleckstrin involved in actin rearrangement. *J Biol Chem*, **274**(31), 21515-8.

Hu, Q., Klippel, A., Muslin, A. J., Fantl, W. J. & Williams, L. T., 1995. Ras-dependent induction of cellular responses by constitutively active phosphatidylinositol-3 kinase. *Science*, **268**(5207), 100-2.

Huang, H. & Tindall, D. J., 2007. Dynamic FoxO transcription factors. *J Cell Sci*, **120**(Pt 15), 2479-87.

Hundley, T. R., Gilfillan, A. M., Tkaczyk, C., Andrade, M. V., Metcalfe, D. D. & Beaven, M. A., 2004. Kit and FcepsilonRI mediate unique and convergent signals for release of inflammatory mediators from human mast cells. *Blood*, **104**(8), 2410-7.

Iijima, M. & Devreotes, P., 2002. Tumor suppressor PTEN mediates sensing of chemoattractant gradients. *Cell*, **109**(5), 599-610.

Ikenoue, T., Kanai, F., Hikiba, Y., Obata, T., Tanaka, Y., Imamura, J., Ohta, M., Jazag, A., Guleng, B., Tateishi, K., Asaoka, Y., Matsumura, M., Kawabe, T. & Omata, M., 2005. Functional analysis of PIK3CA gene mutations in human colorectal cancer. *Cancer Res*, **65**(11), 4562-7.

Innocenti, M., Frittoli, E., Ponzanelli, I., Falck, J. R., Brachmann, S. M., Di Fiore, P. P. & Scita, G., 2003. Phosphoinositide 3-kinase activates Rac by entering in a complex with Eps8, Abi1, and Sos-1. *J Cell Biol*, **160**(1), 17-23.

Iwama, A., Zhang, P., Darlington, G. J., McKercher, S. R., Maki, R. & Tenen, D. G., 1998. Use of RDA analysis of knockout mice to identify myeloid genes regulated in vivo by PU.1 and C/EBPalpha. *Nucleic Acids Res*, **26**(12), 3034-43.

Jackson, S. P., Schoenwaelder, S. M., Goncalves, I., Nesbitt, W. S., Yap, C. L., Wright, C. E., Kenche, V., Anderson, K. E., Dopheide, S. M., Yuan, Y., Sturgeon, S. A., Prabaharan, H., Thompson, P. E., Smith, G. D., Shepherd, P. R., Daniele, N., Kulkarni, S., Abbott, B., Saylik, D., Jones, C., Lu, L., Giuliano, S., Hughan, S. C., Angus, J. A., Robertson, A. D. & Salem, H. H., 2005. PI 3-kinase p110beta: a new target for antithrombotic therapy. *Nat Med*, **11**(5), 507-14.

Jaffe, A. B. & Hall, A., 2005. Rho GTPases: biochemistry and biology. *Annu Rev Cell Dev Biol*, **21**, 247-69.

Jalink, K., van Corven, E. J., Hengeveld, T., Morii, N., Narumiya, S. & Moolenaar, W. H., 1994. Inhibition of lysophosphatidate- and thrombin-induced neurite retraction and neuronal cell rounding by ADP ribosylation of the small GTP-binding protein Rho. *J Cell Biol*, **126**(3), 801-10.

Javahery, R., Khachi, A., Lo, K., Zenzie-Gregory, B. & Smale, S. T., 1994. DNA sequence requirements for transcriptional initiator activity in mammalian cells. *Mol Cell Biol*, **14**(1), 116-27.

Jia, S., Liu, Z., Zhang, S., Liu, P., Zhang, L., Lee, S. H., Zhang, J., Signoretti, S., Loda, M., Roberts, T. M. & Zhao, J. J., 2008. Essential roles of PI(3)K-p110beta in cell growth, metabolism and tumorigenesis. *Nature*.

Jimenez, C., Jones, D. R., Rodriguez-Viciana, P., Gonzalez-Garcia, A., Leonardo, E., Wennstrom, S., von Kobbe, C., Toran, J. L., L, R. B., Calvo, V., Copin, S. G., Albar, J. P., Gaspar, M. L., Diez, E., Marcos, M. A., Downward, J., Martinez, A. C., Merida, I. & Carrera, A. C., 1998. Identification and characterization of a new oncogene derived from the regulatory subunit of phosphoinositide 3-kinase. *EMBO J*, **17**(3), 743-53.

Jin, Z. X., Kishi, H., Wei, X. C., Matsuda, T., Saito, S. & Muraguchi, A., 2002. Lymphoid enhancer-binding factor-1 binds and activates the recombination-activating gene-2 promoter together with c-Myb and Pax-5 in immature B cells. *J Immunol*, **169**(7), 3783-92.

Johnston, S. R., 2006. Targeting downstream effectors of epidermal growth factor receptor/HER2 in breast cancer with either farnesyltransferase inhibitors or mTOR antagonists. *Int J Gynecol Cancer*, **16 Suppl 2**, 543-8.

Jones, H. E., Goddard, L., Gee, J. M., Hiscox, S., Rubini, M., Barrow, D., Knowlden, J. M., Williams, S., Wakeling, A. E. & Nicholson, R. I., 2004. Insulin-like growth factor-I receptor signalling and acquired resistance to gefitinib (ZD1839; Iressa) in human breast and prostate cancer cells. *Endocr Relat Cancer*, **11**(4), 793-814.

Jones, P. A. & Baylin, S. B., 2002. The fundamental role of epigenetic events in cancer. *Nat Rev Genet*, **3**(6), 415-28.

Jones, P. A. & Gonzalgo, M. L., 1997. Altered DNA methylation and genome instability: a new pathway to cancer? *Proc Natl Acad Sci U S A*, **94**(6), 2103-5.

Jou, S. T., Carpino, N., Takahashi, Y., Piekorz, R., Chao, J. R., Carpino, N., Wang, D. & Ihle, J. N., 2002. Essential, nonredundant role for the phosphoinositide 3-kinase p110delta in signaling by the B-cell receptor complex. *Mol Cell Biol*, **22**(24), 8580-91.

Joyce, D., Bouzahzah, B., Fu, M., Albanese, C., D'Amico, M., Steer, J., Klein, J. U., Lee, R. J., Segall, J. E., Westwick, J. K., Der, C. J. & Pestell, R. G., 1999. Integration of Rac-dependent regulation of cyclin D1 transcription through a nuclear factor-kappaB-dependent pathway. *J Biol Chem*, **274**(36), 25245-9.

Kanehisa, J., Yamanaka, T., Doi, S., Turksen, K., Heersche, J. N., Aubin, J. E. & Takeuchi, H., 1990. A band of F-actin containing podosomes is involved in bone resorption by osteoclasts. *Bone*, **11**(4), 287-93.

Kang, S., Bader, A. G. & Vogt, P. K., 2005. Phosphatidylinositol 3-kinase mutations identified in human cancer are oncogenic. *Proc Natl Acad Sci U S A*, **102**(3), 802-7.

Kang, S., Denley, A., Vanhaesebroeck, B. & Vogt, P. K., 2006. Oncogenic transformation induced by the p110beta, -gamma, and -delta isoforms of class I phosphoinositide 3-kinase. *Proc Natl Acad Sci U S A*, **103**(5), 1289-94.

Karakas, B., Bachman, K. E. & Park, B. H., 2006. Mutation of the PIK3CA oncogene in human cancers. *Br J Cancer*, **94**(4), 455-9.

Katagiri, H., Asano, T., Inukai, K., Ogihara, T., Ishihara, H., Shibasaki, Y., Murata, T., Terasaki, J., Kikuchi, M., Yazaki, Y. & Oka, Y., 1997. Roles of PI 3-kinase and Ras on insulin-stimulated glucose transport in 3T3-L1 adipocytes. *Am J Physiol*, **272**(2 Pt 1), E326-31.

Katagiri, H., Asano, T., Ishihara, H., Inukai, K., Shibasaki, Y., Kikuchi, M., Yazaki, Y. & Oka, Y., 1996. Overexpression of catalytic subunit p110alpha of phosphatidylinositol 3-kinase increases glucose transport activity with translocation of glucose transporters in 3T3-L1 adipocytes. *J Biol Chem*, **271**(29), 16987-90.

Katzav, S., Martin-Zanca, D. & Barbacid, M., 1989. vav, a novel human oncogene derived from a locus ubiquitously expressed in haematopoietic cells. *EMBO J*, **8**(8), 2283-90.

Keaveney, M., Klug, J., Dawson, M. T., Nestor, P. V., Neilan, J. G., Forde, R. C. & Gannon, F., 1991. Evidence for a previously unidentified upstream exon in the human oestrogen receptor gene. *J Mol Endocrinol*, **6**(1), 111-5.

Keller, G., Kennedy, M., Papayannopoulou, T. & Wiles, M. V., 1993. Haematopoietic commitment during embryonic stem cell differentiation in culture. *Mol Cell Biol*, **13**(1), 473-86.

Khwaja, A., 1999. Akt is more than just a Bad kinase. *Nature*, **401**(6748), 33-4.

Kihara, A., Noda, T., Ishihara, N. & Ohsumi, Y., 2001. Two distinct Vps34 phosphatidylinositol 3-kinase complexes function in autophagy and carboxypeptidase Y sorting in Saccharomyces cerevisiae. *J Cell Biol*, **152**(3), 519-30.

Kim, Y. J., Bjorklund, S., Li, Y., Sayre, M. H. & Kornberg, R. D., 1994. A multiprotein mediator of transcriptional activation and its interaction with the C-terminal repeat domain of RNA polymerase II. *Cell*, **77**(4), 599-608.

Kinashi, T., Asaoka, T., Setoguchi, R. & Takatsu, K., 1999. Affinity modulation of very late antigen-5 through phosphatidylinositol 3-kinase in mast cells. *J Immunol*, **162**(5), 2850-7.

Kinashi, T., Katagiri, K., Watanabe, S., Vanhaesebroeck, B., Downward, J. & Takatsu, K., 2000. Distinct mechanisms of alpha 5beta 1 integrin activation by Ha-Ras and R-Ras. *J Biol Chem*, **275**(29), 22590-6.

Kitamura, Y., Go, S. & Hatanaka, K., 1978. Decrease of mast cells in W/Wv mice and their increase by bone marrow transplantation. *Blood*, **52**(2), 447-52.

Kjoller, L. & Hall, A., 1999. Signaling to Rho GTPases. *Exp Cell Res*, **253**(1), 166-79.

Klippel, A., Escobedo, M. A., Wachowicz, M. S., Apell, G., Brown, T. W., Giedlin, M. A., Kavanaugh, W. M. & Williams, L. T., 1998. Activation of phosphatidylinositol 3-kinase is sufficient for cell cycle entry and promotes cellular changes characteristic of oncogenic transformation. *Mol Cell Biol*, **18**(10), 5699-711.

Klippel, A., Reinhard, C., Kavanaugh, W. M., Apell, G., Escobedo, M. A. & Williams, L. T., 1996. Membrane localization of phosphatidylinositol 3-kinase is sufficient to activate multiple signal-transducing kinase pathways. *Mol Cell Biol*, **16**(8), 4117-27.

Knight, Z. A., Chiang, G. G., Alaimo, P. J., Kenski, D. M., Ho, C. B., Coan, K., Abraham, R. T. & Shokat, K. M., 2004. Isoform-specific phosphoinositide 3-kinase inhibitors from an arylmorpholine scaffold. *Bioorg Med Chem*, **12**(17), 4749-59.

Knight, Z. A., Gonzalez, B., Feldman, M. E., Zunder, E. R., Goldenberg, D. D., Williams, O., Loewith, R., Stokoe, D., Balla, A., Toth, B., Balla, T., Weiss, W. A., Williams, R. L. & Shokat, K. M., 2006. A pharmacological map of the PI3-K family defines a role for p110alpha in insulin signaling. *Cell*, **125**(4), 733-47.

Knobbe, C. B. & Reifenberger, G., 2003. Genetic alterations and aberrant expression of genes related to the phosphatidyl-inositol-3'-kinase/protein kinase B (Akt) signal transduction pathway in glioblastomas. *Brain Pathol*, **13**(4), 507-18.

Kok, K., Verrall, E. G., Nock, G. E., Mitchell, M. P., Hommes, D. W., Peppelenbosch, M. P. & Vanhaesebroeck, B., in preparation. Analysis of p110delta phosphoinositide 3-kinase gene expression.

Kolluri, R., Tolias, K. F., Carpenter, C. L., Rosen, F. S. & Kirchhausen, T., 1996. Direct interaction of the Wiskott-Aldrich syndrome protein with the GTPase Cdc42. *Proc Natl Acad Sci U S A*, **93**(11), 5615-8.

Kotani, K., Carozzi, A. J., Sakaue, H., Hara, K., Robinson, L. J., Clark, S. F., Yonezawa, K., James, D. E. & Kasuga, M., 1995. Requirement for phosphoinositide 3-kinase in insulin-stimulated GLUT4 translocation in 3T3-L1 adipocytes. *Biochem Biophys Res Commun*, **209**(1), 343-8.

Kozma, R., Ahmed, S., Best, A. & Lim, L., 1995. The Ras-related protein Cdc42Hs and bradykinin promote formation of peripheral actin microspikes and filopodia in Swiss 3T3 fibroblasts. *Mol Cell Biol*, **15**(4), 1942-52.

Kranenburg, O. & Moolenaar, W. H., 2001. Ras-MAP kinase signaling by lysophosphatidic acid and other G protein-coupled receptor agonists. *Oncogene*, **20**(13), 1540-6.

Kranenburg, O., Poland, M., van Horck, F. P., Drechsel, D., Hall, A. & Moolenaar, W. H., 1999. Activation of RhoA by lysophosphatidic acid and Galpha12/13 subunits in neuronal cells: induction of neurite retraction. *Mol Biol Cell*, **10**(6), 1851-7.

Krugmann, S., Cooper, M. A., Williams, D. H., Hawkins, P. T. & Stephens, L. R., 2002. Mechanism of the regulation of type IB phosphoinositide 3OH-kinase byG-protein betagamma subunits. *Biochem J*, **362**(Pt 3), 725-31.

Kuroda, S., Fukata, M., Nakagawa, M., Fujii, K., Nakamura, T., Ookubo, T., Izawa, I., Nagase, T., Nomura, N., Tani, H., Shoji, I., Matsuura, Y., Yonehara, S. & Kaibuchi, K., 1998. Role of IQGAP1, a target of the small GTPases Cdc42 and Rac1, in regulation of E-cadherin- mediated cell-cell adhesion. *Science*, **281**(5378), 832-5.

Kurosu, H., Maehama, T., Okada, T., Yamamoto, T., Hoshino, S., Fukui, Y., Ui, M., Hazeki, O. & Katada, T., 1997. Heterodimeric phosphoinositide 3-kinase consisting of p85 and p110beta is synergistically activated by the betagamma subunits of G proteins and phosphotyrosyl peptide. *J Biol Chem*, **272**(39), 24252-6.

Laffargue, M., Calvez, R., Finan, P., Trifilieff, A., Barbier, M., Altruda, F., Hirsch, E. & Wymann, M. P., 2002. Phosphoinositide 3-kinase gamma is an essential amplifier of mast cell function. *Immunity*, **16**(3), 441-51.

Laffargue, M., Raynal, P., Yart, A., Peres, C., Wetzker, R., Roche, S., Payrastre, B. & Chap, H., 1999. An epidermal growth factor receptor/Gab1 signaling pathway is

required for activation of phosphoinositide 3-kinase by lysophosphatidic acid. *J Biol Chem*, **274**(46), 32835-41.

Lafky, J. M., Wilken, J. A., Baron, A. T. & Maihle, N. J., 2008. Clinical implications of the ErbB/epidermal growth factor (EGF) receptor family and its ligands in ovarian cancer. *Biochim Biophys Acta*, **1785**(2), 232-65.

Lagrange, T., Kapanidis, A. N., Tang, H., Reinberg, D. & Ebright, R. H., 1998. New core promoter element in RNA polymerase II-dependent transcription: sequence-specific DNA binding by transcription factor IIB. *Genes Dev*, **12**(1), 34-44.

Lamarche, N. & Hall, A., 1994. GAPs for rho-related GTPases. *Trends Genet*, **10**(12), 436-40.

Lazar, M. A., 1993. Thyroid hormone receptors: multiple forms, multiple possibilities. *Endocr Rev*, **14**(2), 184-93.

Lee, K. S., Park, S. J., Kim, S. R., Min, K. H., Jin, S. M., Puri, K. D. & Lee, Y. C., 2006. Phosphoinositide 3-kinase-delta inhibitor reduces vascular permeability in a murine model of asthma. *J Allergy Clin Immunol*, **118**(2), 403-9.

Leiden, J. M. & Thompson, C. B., 1994. Transcriptional regulation of T-cell genes during T-cell development. *Curr Opin Immunol*, **6**(2), 231-7.

Lemmon, M. A. & Ferguson, K. M., 2000. Signal-dependent membrane targeting by pleckstrin homology (PH) domains. *Biochem J*, **350 Pt 1**, 1-18.

Lenardo, M. J. & Baltimore, D., 1989. NF-kappa B: a pleiotropic mediator of inducible and tissue-specific gene control. *Cell*, **58**(2), 227-9.

Lener, T., Burgstaller, G., Crimaldi, L., Lach, S. & Gimona, M., 2006. Matrix-degrading podosomes in smooth muscle cells. *Eur J Cell Biol*, **85**(3-4), 183-9.

Lennartsson, J., Jelacic, T., Linnekin, D. & Shivakrupa, R., 2005. Normal and oncogenic forms of the receptor tyrosine kinase kit. *Stem Cells*, **23**(1), 16-43.

Li, Z., Dong, X., Wang, Z., Liu, W., Deng, N., Ding, Y., Tang, L., Hla, T., Zeng, R., Li, L. & Wu, D., 2005. Regulation of PTEN by Rho small GTPases. *Nat Cell Biol*, **7**(4), 399-404.

Li, Z., Jiang, H., Xie, W., Zhang, Z., Smrcka, A. V. & Wu, D., 2000. Roles of PLC-beta2 and -beta3 and PI3Kgamma in chemoattractant-mediated signal transduction. *Science*, **287**(5455), 1046-9.

Linder, S., 2007. The matrix corroded: podosomes and invadopodia in extracellular matrix degradation. *Trends Cell Biol*, **17**(3), 107-17.

Lindmo, K. & Stenmark, H., 2006. Regulation of membrane traffic by phosphoinositide 3-kinases. *J Cell Sci*, **119**(Pt 4), 605-14.

Link, W., Rosado, A., Fominaya, J., Thomas, J. E. & Carnero, A., 2005. Membrane localization of all class I PI 3-kinase isoforms suppresses c-Myc-induced apoptosis in Rat1 fibroblasts via Akt. *J Cell Biochem*, **95**(5), 979-89.

Liston, D. R., Lau, A. O., Ortiz, D., Smale, S. T. & Johnson, P. J., 2001. Initiator recognition in a primitive eukaryote: IBP39, an initiator-binding protein from Trichomonas vaginalis. *Mol Cell Biol*, **21**(22), 7872-82.

Liu, Y. W., Chen, C. C., Wang, J. M., Chang, W. C., Huang, Y. C., Chung, S. Y., Chen, B. K. & Hung, J. J., 2007. Role of transcriptional factors Sp1, c-Rel, and c-Jun in LPS-induced C/EBPdelta gene expression of mouse macrophages. *Cell Mol Life Sci*, **64**(24), 3282-94.

Longley, B. J., Jr., Metcalfe, D. D., Tharp, M., Wang, X., Tyrrell, L., Lu, S. Z., Heitjan, D. & Ma, Y., 1999. Activating and dominant inactivating c-KIT catalytic domain mutations in distinct clinical forms of human mastocytosis. *Proc Natl Acad Sci U S A*, **96**(4), 1609-14.

Louis, D. N., 2006. Molecular pathology of malignant gliomas. *Annu Rev Pathol*, **1**, 97-117.

Lu, Y., Zi, X., Zhao, Y., Mascarenhas, D. & Pollak, M., 2001. Insulin-like growth factor-I receptor signaling and resistance to trastuzumab (Herceptin). *J Natl Cancer Inst*, **93**(24), 1852-7.

Luo, J., Field, S. J., Lee, J. Y., Engelman, J. A. & Cantley, L. C., 2005. The p85 regulatory subunit of phosphoinositide 3-kinase down-regulates IRS-1 signaling via the formation of a sequestration complex. *J Cell Biol*, **170**(3), 455-64.

Luo, J. L., Maeda, S., Hsu, L. C., Yagita, H. & Karin, M., 2004a. Inhibition of NF-kappaB in cancer cells converts inflammation- induced tumor growth mediated by TNFalpha to TRAIL-mediated tumor regression. *Cancer Cell*, **6**(3), 297-305.

Luo, J. M., Liu, Z. L., Hao, H. L., Wang, F. X., Dong, Z. R. & Ohno, R., 2004b. Mutation analysis of SHIP gene in acute leukaemia. *Zhongguo Shi Yan Xue Ye Xue Za Zhi*, **12**(4), 420-6.

Machesky, L. M. & Gould, K. L., 1999. The Arp2/3 complex: a multifunctional actin organizer. *Curr Opin Cell Biol*, **11**(1), 117-21.

Machesky, L. M., Mullins, R. D., Higgs, H. N., Kaiser, D. A., Blanchoin, L., May, R. C., Hall, M. E. & Pollard, T. D., 1999. Scar, a WASp-related protein, activates nucleation of actin filaments by the Arp2/3 complex. *Proc Natl Acad Sci U S A*, **96**(7), 3739-44.

Maffucci, T., Brancaccio, A., Piccolo, E., Stein, R. C. & Falasca, M., 2003. Insulin induces phosphatidylinositol-3-phosphate formation through TC10 activation. *EMBO J*, **22**(16), 4178-89.

Maffucci, T., Cooke, F. T., Foster, F. M., Traer, C. J., Fry, M. J. & Falasca, M., 2005. Class II phosphoinositide 3-kinase defines a novel signaling pathway in cell migration. *J Cell Biol*, **169**(5), 789-99.

Maier, U., Babich, A. & Nurnberg, B., 1999. Roles of non-catalytic subunits in gbetagamma-induced activation of class I phosphoinositide 3-kinase isoforms beta and gamma. *J Biol Chem*, **274**(41), 29311-7.

Malecova, B., Gross, P., Boyer-Guittaut, M., Yavuz, S. & Oelgeschlager, T., 2007. The initiator core promoter element antagonizes repression of TATA-directed transcription by negative cofactor NC2. *J Biol Chem*, **282**(34), 24767-76.

Malliri, A. & Collard, J. G., 2003. Role of Rho-family proteins in cell adhesion and cancer. *Curr Opin Cell Biol*, **15**(5), 583-9.

Manser, E., Loo, T. H., Koh, C. G., Zhao, Z. S., Chen, X. Q., Tan, L., Tan, I., Leung, T. & Lim, L., 1998. PAK kinases are directly coupled to the PIX family of nucleotide exchange factors. *Mol Cell*, **1**(2), 183-92.

Marcusohn, J., Isakoff, S. J., Rose, E., Symons, M. & Skolnik, E. Y., 1995. The GTP-binding protein Rac does not couple PI 3-kinase to insulin-stimulated glucose transport in adipocytes. *Curr Biol*, **5**(11), 1296-302.

Markovic, D. S., Glass, R., Synowitz, M., Rooijen, N. & Kettenmann, H., 2005. Microglia stimulate the invasiveness of glioma cells by increasing the activity of metalloprotease-2. *J Neuropathol Exp Neurol*, **64**(9), 754-62.

Mayo, L. D. & Donner, D. B., 2001. A phosphatidylinositol 3-kinase/Akt pathway promotes translocation of Mdm2 from the cytoplasm to the nucleus. *Proc Natl Acad Sci U S A*, **98**(20), 11598-603.

Mayr, B. & Montminy, M., 2001. Transcriptional regulation by the phosphorylation-dependent factor CREB. *Nat Rev Mol Cell Biol*, **2**(8), 599-609.

Medina-Tato, D. A., Ward, S. G. & Watson, M. L., 2007. Phosphoinositide 3-kinase signalling in lung disease: leucocytes and beyond. *Immunology*, **121**(4), 448-61.

Meier, T. I., Cook, J. A., Thomas, J. E., Radding, J. A., Horn, C., Lingaraj, T. & Smith, M. C., 2004. Cloning, expression, purification, and characterization of the human Class Ia phosphoinositide 3-kinase isoforms. *Protein Expr Purif*, **35**(2), 218-24.

Meili, R., Cron, P., Hemmings, B. A. & Ballmer-Hofer, K., 1998. Protein kinase B/Akt is activated by polyomavirus middle-T antigen via a phosphatidylinositol 3-kinase-dependent mechanism. *Oncogene*, **16**(7), 903-7.

Metcalfe, D. D., Baram, D. & Mekori, Y. A., 1997. Mast cells. *Physiol Rev*, **77**(4), 1033-79.

Michiels, F., Habets, G. G., Stam, J. C., van der Kammen, R. A. & Collard, J. G., 1995. A role for Rac in Tiam1-induced membrane ruffling and invasion. *Nature*, **375**(6529), 338-40.

Miki, H., Suetsugu, S. & Takenawa, T., 1998. WAVE, a novel WASP-family protein involved in actin reorganization induced by Rac. *EMBO J*, **17**(23), 6932-41.

Miled, N., Yan, Y., Hon, W. C., Perisic, O., Zvelebil, M., Inbar, Y., Schneidman-Duhovny, D., Wolfson, H. J., Backer, J. M. & Williams, R. L., 2007. Mechanism of two classes of cancer mutations in the phosphoinositide 3-kinase catalytic subunit. *Science*, **317**(5835), 239-42.

Minden, A., Lin, A., Claret, F. X., Abo, A. & Karin, M., 1995. Selective activation of the JNK signaling cascade and c-Jun transcriptional activity by the small GTPases Rac and Cdc42Hs. *Cell*, **81**(7), 1147-57.

Miralles, F., Posern, G., Zaromytidou, A. I. & Treisman, R., 2003. Actin dynamics control SRF activity by regulation of its coactivator MAL. *Cell*, **113**(3), 329-42.

Miranda, T. B. & Jones, P. A., 2007. DNA methylation: the nuts and bolts of repression. *J Cell Physiol*, **213**(2), 384-90.

Missy, K., Van Poucke, V., Raynal, P., Viala, C., Mauco, G., Plantavid, M., Chap, H. & Payrastre, B., 1998. Lipid products of phosphoinositide 3-kinase interact with Rac1 GTPase and stimulate GDP dissociation. *J Biol Chem*, **273**(46), 30279-86.

Miyake, K., Ogawa, W., Matsumoto, M., Nakamura, T., Sakaue, H. & Kasuga, M., 2002. Hyperinsulinemia, glucose intolerance, and dyslipidemia induced by acute inhibition of phosphoinositide 3-kinase signaling in the liver. *J Clin Invest*, **110**(10), 1483-91.

Mizoguchi, M., Nutt, C. L., Mohapatra, G. & Louis, D. N., 2004. Genetic alterations of phosphoinositide 3-kinase subunit genes in human glioblastomas. *Brain Pathol*, **14**(4), 372-7.

Mombaerts, P., Iacomini, J., Johnson, R. S., Herrup, K., Tonegawa, S. & Papaioannou, V. E., 1992. RAG-1-deficient mice have no mature B and T lymphocytes. *Cell*, **68**(5), 869-77.

Moolenaar, W. H., van Meeteren, L. A. & Giepmans, B. N., 2004. The ins and outs of lysophosphatidic acid signaling. *Bioessays*, **26**(8), 870-81.

Mullins, R. D., Heuser, J. A. & Pollard, T. D., 1998. The interaction of Arp2/3 complex with actin: nucleation, high affinity pointed end capping, and formation of branching networks of filaments. *Proc Natl Acad Sci U S A*, **95**(11), 6181-6.

Muraille, E., Pesesse, X., Kuntz, C. & Erneux, C., 1999. Distribution of the src-homology-2-domain-containing inositol 5-phosphatase SHIP-2 in both non-haemopoietic and haemopoietic cells and possible involvement of SHIP-2 in negative signalling of B-cells. *Biochem J*, **342 Pt 3**, 697-705.

Muthusamy, N., Barton, K. & Leiden, J. M., 1995. Defective activation and survival of T cells lacking the Ets-1 transcription factor. *Nature*, **377**(6550), 639-42.

Nagata, H., Worobec, A. S., Oh, C. K., Chowdhury, B. A., Tannenbaum, S., Suzuki, Y. & Metcalfe, D. D., 1995. Identification of a point mutation in the catalytic domain of the protooncogene c-kit in peripheral blood mononuclear cells of patients who have mastocytosis with an associated hematologic disorder. *Proc Natl Acad Sci U S A*, **92**(23), 10560-4.

Nan, X., Cross, S. & Bird, A., 1998a. Gene silencing by methyl-CpG-binding proteins. *Novartis Found Symp*, **214**, 6-16; discussion 16-21, 46-50.

Nan, X., Ng, H. H., Johnson, C. A., Laherty, C. D., Turner, B. M., Eisenman, R. N. & Bird, A., 1998b. Transcriptional repression by the methyl-CpG-binding protein MeCP2 involves a histone deacetylase complex. *Nature*, **393**(6683), 386-9.

Neish, A. S., Read, M. A., Thanos, D., Pine, R., Maniatis, T. & Collins, T., 1995. Endothelial interferon regulatory factor 1 cooperates with NF-kappa B as a transcriptional activator of vascular cell adhesion molecule 1. *Mol Cell Biol*, **15**(5), 2558-69.

Neves, S. R., Ram, P. T. & Iyengar, R., 2002. G protein pathways. *Science*, **296**(5573), 1636-9.

Nobes, C. D. & Hall, A., 1995. Rho, rac, and cdc42 GTPases regulate the assembly of multimolecular focal complexes associated with actin stress fibers, lamellipodia, and filopodia. *Cell*, **81**(1), 53-62.

Nobes, C. D. & Hall, A., 1999. Rho GTPases control polarity, protrusion, and adhesion during cell movement. *J Cell Biol*, **144**(6), 1235-44.

Ogilvy, S., Elefanty, A. G., Visvader, J., Bath, M. L., Harris, A. W. & Adams, J. M., 1998. Transcriptional regulation of vav, a gene expressed throughout the haematopoietic compartment. *Blood*, **91**(2), 419-30.

Okkenhaug, K., Bilancio, A., Farjot, G., Priddle, H., Sancho, S., Peskett, E., Pearce, W., Meek, S. E., Salpekar, A., Waterfield, M. D., Smith, A. J. & Vanhaesebroeck, B., 2002. Impaired B and T cell antigen receptor signaling in p110delta PI 3-kinase mutant mice. *Science*, **297**(5583), 1031-4.

Olson, M. F., Ashworth, A. & Hall, A., 1995. An essential role for Rho, Rac, and Cdc42 GTPases in cell cycle progression through G1. *Science*, **269**(5228), 1270-2.

Orkin, S. H., 1998. Embryonic stem cells and transgenic mice in the study of haematopoiesis. *Int J Dev Biol*, **42**(7), 927-34.

Owens, B. M., Zhu, Y. X., Suen, T. C., Wang, P. X., Greenblatt, J. F., Goss, P. E. & Hawley, R. G., 2003. Specific homeodomain-DNA interactions are required for HOX11-mediated transformation. *Blood*, **101**(12), 4966-74.

Ozato, K., Tailor, P. & Kubota, T., 2007. The interferon regulatory factor family in host defense: mechanism of action. *J Biol Chem*, **282**(28), 20065-9.

Ozes, O. N., Mayo, L. D., Gustin, J. A., Pfeffer, S. R., Pfeffer, L. M. & Donner, D. B., 1999. NF-kappaB activation by tumour necrosis factor requires the Akt serine-threonine kinase. *Nature*, **401**(6748), 82-5.

Paar, M., Schwab, S., Rosenfellner, D., Salmons, B., Gunzburg, W. H., Renner, M. & Portsmouth, D., 2007. Effects of viral strain, transgene position, and target cell type on replication kinetics, genomic stability, and transgene expression of replication-competent murine leukaemia virus-based vectors. *J Virol*, **81**(13), 6973-83.

Panaretou, C., Domin, J., Cockcroft, S. & Waterfield, M. D., 1997. Characterization of p150, an adaptor protein for the human phosphatidylinositol (PtdIns) 3-kinase. Substrate presentation by phosphatidylinositol transfer protein to the p150.Ptdins 3-kinase complex. *J Biol Chem*, **272**(4), 2477-85.

Pao, W. & Miller, V. A., 2005. Epidermal growth factor receptor mutations, small-molecule kinase inhibitors, and non-small-cell lung cancer: current knowledge and future directions. *J Clin Oncol*, **23**(11), 2556-68.

Papakonstanti, E., Bilancio, A., Shokat, K., Ridley, AJ. & Vanhaesebroeck, B., in preparation. Distinct roles of class IA PI 3-kinase isoforms in primary and immortalised macrophages.

Papakonstanti, E. A., Ridley, A. J. & Vanhaesebroeck, B., 2007. The p110delta isoform of PI 3-kinase negatively controls RhoA and PTEN. *EMBO J*, **26**(13), 3050-61.

Park, H. S., Lee, S. H., Park, D., Lee, J. S., Ryu, S. H., Lee, W. J., Rhee, S. G. & Bae, Y. S., 2004. Sequential activation of phosphatidylinositol 3-kinase, beta Pix, Rac1, and

Nox1 in growth factor-induced production of H2O2. *Mol Cell Biol*, **24**(10), 4384-94.

Patel, S., Lochhead, P. A., Rena, G., Fumagalli, S., Pende, M., Kozma, S. C., Thomas, G. & Sutherland, C., 2002. Insulin regulation of insulin-like growth factor-binding protein-1 gene expression is dependent on the mammalian target of rapamycin, but independent of ribosomal S6 kinase activity. *J Biol Chem*, **277**(12), 9889-95.

Paun, A. & Pitha, P. M., 2007. The IRF family, revisited. *Biochimie*, **89**(6-7), 744-53.

Pear, W. S., Nolan, G. P., Scott, M. L. & Baltimore, D., 1993. Production of high-titer helper-free retroviruses by transient transfection. *Proc Natl Acad Sci U S A*, **90**(18), 8392-6.

Penuel, E. & Martin, G. S., 1999. Transformation by v-Src: Ras-MAPK and PI3K-mTOR mediate parallel pathways. *Mol Biol Cell*, **10**(6), 1693-703.

Perkins, A. C. & Cory, S., 1993. Conditional immortalization of mouse myelomonocytic, megakaryocytic and mast cell progenitors by the Hox-2.4 homeobox gene. *Embo J*, **12**(10), 3835-46.

Perona, R., Montaner, S., Saniger, L., Sanchez-Perez, I., Bravo, R. & Lacal, J. C., 1997. Activation of the nuclear factor-kappaB by Rho, CDC42, and Rac-1 proteins. *Genes Dev*, **11**(4), 463-75.

Pfaff, M. & Jurdic, P., 2001. Podosomes in osteoclast-like cells: structural analysis and cooperative roles of paxillin, proline-rich tyrosine kinase 2 (Pyk2) and integrin alphaVbeta3. *J Cell Sci*, **114**(Pt 15), 2775-86.

Pfisterer, P., Annweiler, A., Ullmer, C., Corcoran, L. M. & Wirth, T., 1994. Differential transactivation potential of Oct1 and Oct2 is determined by additional B cell-specific activities. *EMBO J*, **13**(7), 1654-63.

Phillips, W. A., Russell, S. E., Ciavarella, M. L., Choong, D. Y., Montgomery, K. G., Smith, K., Pearson, R. B., Thomas, R. J. & Campbell, I. G., 2006. Mutation analysis of PIK3CA and PIK3CB in esophageal cancer and Barrett's esophagus. *Int J Cancer*, **118**(10), 2644-6.

Philp, A. J., Campbell, I. G., Leet, C., Vincan, E., Rockman, S. P., Whitehead, R. H., Thomas, R. J. & Phillips, W. A., 2001. The phosphatidylinositol 3'-kinase p85alpha gene is an oncogene in human ovarian and colon tumors. *Cancer Res*, **61**(20), 7426-9.

Pikarsky, E., Porat, R. M., Stein, I., Abramovitch, R., Amit, S., Kasem, S., Gutkovich-Pyest, E., Urieli-Shoval, S., Galun, E. & Ben-Neriah, Y., 2004. NF-kappaB functions as a tumour promoter in inflammation-associated cancer. *Nature*, **431**(7007), 461-6.

Puls, A., Eliopoulos, A. G., Nobes, C. D., Bridges, T., Young, L. S. & Hall, A., 1999. Activation of the small GTPase Cdc42 by the inflammatory cytokines TNF(alpha) and IL-1, and by the Epstein-Barr virus transforming protein LMP1. *J Cell Sci*, **112 (Pt 17)**, 2983-92.

Puri, K. D., Doggett, T. A., Douangpanya, J., Hou, Y., Tino, W. T., Wilson, T., Graf, T., Clayton, E., Turner, M., Hayflick, J. S. & Diacovo, T. G., 2004. Mechanisms and implications of phosphoinositide 3-kinase delta in promoting neutrophil trafficking into inflamed tissue. *Blood*, **103**(9), 3448-56.

Puxeddu, I., Piliponsky, A. M., Bachelet, I. & Levi-Schaffer, F., 2003. Mast cells in allergy and beyond. *Int J Biochem Cell Biol*, **35**(12), 1601-7.

Quon, M. J., Chen, H., Ing, B. L., Liu, M. L., Zarnowski, M. J., Yonezawa, K., Kasuga, M., Cushman, S. W. & Taylor, S. I., 1995. Roles of 1-phosphatidylinositol 3-kinase and ras in regulating translocation of GLUT4 in transfected rat adipose cells. *Mol Cell Biol*, **15**(10), 5403-11.

Randle, D. H., Zindy, F., Sherr, C. J. & Roussel, M. F., 2001. Differential effects of p19(Arf) and p16(Ink4a) loss on senescence of murine bone marrow-derived preB cells and macrophages. *Proc Natl Acad Sci U S A*, **98**(17), 9654-9.

Rao, A., 1994. NF-ATp: a transcription factor required for the co-ordinate induction of several cytokine genes. *Immunol Today*, **15**(6), 274-81.

Ravindranath, A., O'Connell, A., Johnston, P. G. & El-Tanani, M. K., 2008. The role of LEF/TCF factors in neoplastic transformation. *Curr Mol Med*, **8**(1), 38-50.

Resendes, K. K. & Rosmarin, A. G., 2004. Sp1 control of gene expression in myeloid cells. *Crit Rev Eukaryot Gene Expr*, **14**(3), 171-81.

Reya, T. & Grosschedl, R., 1998. Transcriptional regulation of B-cell differentiation. *Curr Opin Immunol*, **10**(2), 158-65.

Reynolds, A. B., Daniel, J. M., Mo, Y. Y., Wu, J. & Zhang, Z., 1996. The novel catenin p120cas binds classical cadherins and induces an unusual morphological phenotype in NIH3T3 fibroblasts. *Exp Cell Res*, **225**(2), 328-37.

Ridley, A. J. & Hall, A., 1992. The small GTP-binding protein rho regulates the assembly of focal adhesions and actin stress fibers in response to growth factors. *Cell*, **70**(3), 389-99.

Ridley, A. J., Paterson, H. F., Johnston, C. L., Diekmann, D. & Hall, A., 1992. The small GTP-binding protein rac regulates growth factor-induced membrane ruffling. *Cell*, **70**(3), 401-10.

Ridley, A. J., Schwartz, M. A., Burridge, K., Firtel, R. A., Ginsberg, M. H., Borisy, G., Parsons, J. T. & Horwitz, A. R., 2003. Cell migration: integrating signals from front to back. *Science*, **302**(5651), 1704-9.

Riento, K. & Ridley, A. J., 2003. Rocks: multifunctional kinases in cell behaviour. *Nat Rev Mol Cell Biol*, **4**(6), 446-56.

Riz, I. & Hawley, R. G., 2005. G1/S transcriptional networks modulated by the HOX11/TLX1 oncogene of T-cell acute lymphoblastic leukaemia. *Oncogene*, **24**(36), 5561-75.

Roche, S., Downward, J., Raynal, P. & Courtneidge, S. A., 1998. A function for phosphatidylinositol 3-kinase beta (p85alpha-p110beta) in fibroblasts during mitogenesis: requirement for insulin- and lysophosphatidic acid-mediated signal transduction. *Mol Cell Biol*, **18**(12), 7119-29.

Rohatgi, R., Ma, L., Miki, H., Lopez, M., Kirchhausen, T., Takenawa, T. & Kirschner, M. W., 1999. The interaction between N-WASP and the Arp2/3 complex links Cdc42-dependent signals to actin assembly. *Cell*, **97**(2), 221-31.

Rohrschneider, L. R., Fuller, J. F., Wolf, I., Liu, Y. & Lucas, D. M., 2000. Structure, function, and biology of SHIP proteins. *Genes Dev*, **14**(5), 505-20.

Rommel, C., Camps, M. & Ji, H., 2007. PI3K delta and PI3K gamma: partners in crime in inflammation in rheumatoid arthritis and beyond? *Nat Rev Immunol*, **7**(3), 191-201.

Ronnstrand, L., 2004. Signal transduction via the stem cell factor receptor/c-Kit. *Cell Mol Life Sci*, **61**(19-20), 2535-48.

Rosenblatt, J., Cramer, L. P., Baum, B. & McGee, K. M., 2004. Myosin II-dependent cortical movement is required for centrosome separation and positioning during mitotic spindle assembly. *Cell*, **117**(3), 361-72.

Roskoski, R., Jr., 2005. Structure and regulation of Kit protein-tyrosine kinase--the stem cell factor receptor. *Biochem Biophys Res Commun*, **338**(3), 1307-15.

Sadhu, C., Masinovsky, B., Dick, K., Sowell, C. G. & Staunton, D. E., 2003. Essential role of phosphoinositide 3-kinase delta in neutrophil directional movement. *J Immunol*, **170**(5), 2647-54.

Sahai, E. & Marshall, C. J., 2002. ROCK and Dia have opposing effects on adherens junctions downstream of Rho. *Nat Cell Biol*, **4**(6), 408-15.

Sahai, E. & Marshall, C. J., 2003. Differing modes of tumour cell invasion have distinct requirements for Rho/ROCK signalling and extracellular proteolysis. *Nat Cell Biol*, **5**(8), 711-9.

Salomon, D. S., Brandt, R., Ciardiello, F. & Normanno, N., 1995. Epidermal growth factor-related peptides and their receptors in human malignancies. *Crit Rev Oncol Hematol*, **19**(3), 183-232.

Samuels, Y., Diaz, L. A., Jr., Schmidt-Kittler, O., Cummins, J. M., Delong, L., Cheong, I., Rago, C., Huso, D. L., Lengauer, C., Kinzler, K. W., Vogelstein, B. & Velculescu, V. E., 2005. Mutant PIK3CA promotes cell growth and invasion of human cancer cells. *Cancer Cell*, **7**(6), 561-73.

Samuels, Y. & Velculescu, V. E., 2004. Oncogenic mutations of PIK3CA in human cancers. *Cell Cycle*, **3**(10), 1221-4.

Samuels, Y., Wang, Z., Bardelli, A., Silliman, N., Ptak, J., Szabo, S., Yan, H., Gazdar, A., Powell, S. M., Riggins, G. J., Willson, J. K., Markowitz, S., Kinzler, K. W., Vogelstein, B. & Velculescu, V. E., 2004. High frequency of mutations of the PIK3CA gene in human cancers. *Science*, **304**(5670), 554.

Sander, E. E., ten Klooster, J. P., van Delft, S., van der Kammen, R. A. & Collard, J. G., 1999. Rac downregulates Rho activity: reciprocal balance between both GTPases determines cellular morphology and migratory behavior. *J Cell Biol*, **147**(5), 1009-22.

Sander, E. E., van Delft, S., ten Klooster, J. P., Reid, T., van der Kammen, R. A., Michiels, F. & Collard, J. G., 1998. Matrix-dependent Tiam1/Rac signaling in epithelial cells promotes either cell-cell adhesion or cell migration and is regulated by phosphatidylinositol 3-kinase. *J Cell Biol*, **143**(5), 1385-98.

Sarbassov, D. D., Guertin, D. A., Ali, S. M. & Sabatini, D. M., 2005. Phosphorylation and regulation of Akt/PKB by the rictor-mTOR complex. *Science*, **307**(5712), 1098-101.

Sasaki, T., Irie-Sasaki, J., Jones, R. G., Oliveira-dos-Santos, A. J., Stanford, W. L., Bolon, B., Wakeham, A., Itie, A., Bouchard, D., Kozieradzki, I., Joza, N., Mak, T. W., Ohashi, P. S., Suzuki, A. & Penninger, J. M., 2000. Function of PI3Kgamma in thymocyte development, T cell activation, and neutrophil migration. *Science*, **287**(5455), 1040-6.

Sawada, S. & Littman, D. R., 1991. Identification and characterization of a T-cell-specific enhancer adjacent to the murine CD4 gene. *Mol Cell Biol*, **11**(11), 5506-15.

Sawyer, C., Sturge, J., Bennett, D. C., O'Hare, M. J., Allen, W. E., Bain, J., Jones, G. E. & Vanhaesebroeck, B., 2003. Regulation of breast cancer cell chemotaxis by the phosphoinositide 3-kinase p110delta. *Cancer Res*, **63**(7), 1667-75.

Sbrissa, D., Ikonomov, O. C. & Shisheva, A., 1999. PIKfyve, a mammalian ortholog of yeast Fab1p lipid kinase, synthesizes 5-phosphoinositides. Effect of insulin. *J Biol Chem*, **274**(31), 21589-97.

Schmidt, A. & Hall, A., 2002. Guanine nucleotide exchange factors for Rho GTPases: turning on the switch. *Genes Dev*, **16**(13), 1587-609.

Scott, E. W., Fisher, R. C., Olson, M. C., Kehrli, E. W., Simon, M. C. & Singh, H., 1997. PU.1 functions in a cell-autonomous manner to control the differentiation of multipotential lymphoid-myeloid progenitors. *Immunity*, **6**(4), 437-47.

Scott, E. W., Simon, M. C., Anastasi, J. & Singh, H., 1994. Requirement of transcription factor PU.1 in the development of multiple haematopoietic lineages. *Science*, **265**(5178), 1573-7.

Serve, H., Yee, N. S., Stella, G., Sepp-Lorenzino, L., Tan, J. C. & Besmer, P., 1995. Differential roles of PI3-kinase and Kit tyrosine 821 in Kit receptor-mediated proliferation, survival and cell adhesion in mast cells. *Embo J*, **14**(3), 473-83.

Shaw, J. P., Utz, P. J., Durand, D. B., Toole, J. J., Emmel, E. A. & Crabtree, G. R., 1988. Identification of a putative regulator of early T cell activation genes. *Science*, **241**(4862), 202-5.

Shayesteh, L., Lu, Y., Kuo, W. L., Baldocchi, R., Godfrey, T., Collins, C., Pinkel, D., Powell, B., Mills, G. B. & Gray, J. W., 1999. PIK3CA is implicated as an oncogene in ovarian cancer. *Nat Genet*, **21**(1), 99-102.

Shepherd, P. R., 2005. Mechanisms regulating phosphoinositide 3-kinase signalling in insulin-sensitive tissues. *Acta Physiol Scand*, **183**(1), 3-12.

Shewan, A. M., Maddugoda, M., Kraemer, A., Stehbens, S. J., Verma, S., Kovacs, E. M. & Yap, A. S., 2005. Myosin 2 is a key Rho kinase target necessary for the local concentration of E-cadherin at cell-cell contacts. *Mol Biol Cell*, **16**(10), 4531-42.

Shi, C. S. & Kehrl, J. H., 2001. PYK2 links G(q)alpha and G(13)alpha signaling to NF-kappa B activation. *J Biol Chem*, **276**(34), 31845-50.

Shinkai, Y., Rathbun, G., Lam, K. P., Oltz, E. M., Stewart, V., Mendelsohn, M., Charron, J., Datta, M., Young, F., Stall, A. M. & et al., 1992. RAG-2-deficient mice lack mature lymphocytes owing to inability to initiate V(D)J rearrangement. *Cell*, **68**(5), 855-67.

Shinohara, M., Terada, Y., Iwamatsu, A., Shinohara, A., Mochizuki, N., Higuchi, M., Gotoh, Y., Ihara, S., Nagata, S., Itoh, H., Fukui, Y. & Jessberger, R., 2002. SWAP-70 is a guanine-nucleotide-exchange factor that mediates signalling of membrane ruffling. *Nature*, **416**(6882), 759-63.

Shivakrupa, R., Bernstein, A., Watring, N. & Linnekin, D., 2003. Phosphatidylinositol 3'-kinase is required for growth of mast cells expressing the kit catalytic domain mutant. *Cancer Res*, **63**(15), 4412-9.

Simpson, L. & Parsons, R., 2001. PTEN: Life as a Tumor Suppressor. *Experimental Cell Research*, **264**(1), 29-41.

Skokowa, J., Cario, G., Uenalan, M., Schambach, A., Germeshausen, M., Battmer, K., Zeidler, C., Lehmann, U., Eder, M., Baum, C., Grosschedl, R., Stanulla, M., Scherr, M. & Welte, K., 2006. LEF-1 is crucial for neutrophil granulocytopoiesis and its expression is severely reduced in congenital neutropenia. *Nat Med*, **12**(10), 1191-7.

Skokowa, J. & Welte, K., 2007. LEF-1 is a decisive transcription factor in neutrophil granulopoiesis. *Ann N Y Acad Sci*, **1106**, 143-51.

Sotsios, Y. & Ward, S. G., 2000. Phosphoinositide 3-kinase: a key biochemical signal for cell migration in response to chemokines. *Immunol Rev*, **177**, 217-35.

Span, P. N., Manders, P., Heuvel, J. J., Thomas, C. M., Bosch, R. R., Beex, L. V. & Sweep, C. G., 2002. Expression of the transcription factor Ets-1 is an independent prognostic marker for relapse-free survival in breast cancer. *Oncogene*, **21**(55), 8506-9.

Spandidos, D. A., Sourvinos, G., Tsatsanis, C. & Zafiropoulos, A., 2002. Normal ras genes: their onco-suppressor and pro-apoptotic functions (review). *Int J Oncol*, **21**(2), 237-41.

Stephens, L., Williams, R. & Hawkins, P., 2005. Phosphoinositide 3-kinases as drug targets in cancer. *Curr Opin Pharmacol*.

Stephens, L. R., Eguinoa, A., Erdjument-Bromage, H., Lui, M., Cooke, F., Coadwell, J., Smrcka, A. S., Thelen, M., Cadwallader, K., Tempst, P. & Hawkins, P. T., 1997. The G beta gamma sensitivity of a PI3K is dependent upon a tightly associated adaptor, p101. *Cell*, **89**(1), 105-14.

Stirzaker, C., Song, J. Z., Davidson, B. & Clark, S. J., 2004. Transcriptional gene silencing promotes DNA hypermethylation through a sequential change in chromatin modifications in cancer cells. *Cancer Res*, **64**(11), 3871-7.

Strahle, U., Schmidt, A., Kelsey, G., Stewart, A. F., Cole, T. J., Schmid, W. & Schutz, G., 1992. At least three promoters direct expression of the mouse glucocorticoid receptor gene. *Proc Natl Acad Sci U S A*, **89**(15), 6731-5.

Strumane, K., Song, J. Y., Baas, I. & Collard, J. G., 2008. Increased Rac activity is required for the progression of T-lymphomas induced by Pten-deficiency. *Leuk Res*, **32**(1), 113-20.

Su, G. H., Chen, H. M., Muthusamy, N., Garrett-Sinha, L. A., Baunoch, D., Tenen, D. G. & Simon, M. C., 1997. Defective B cell receptor-mediated responses in mice lacking the Ets protein, Spi-B. *EMBO J*, **16**(23), 7118-29.

Sugimoto, N., Takuwa, N., Yoshioka, K. & Takuwa, Y., 2006. Rho-dependent, Rho kinase-independent inhibitory regulation of Rac and cell migration by LPA1 receptor in Gi-inactivated CHO cells. *Exp Cell Res*, **312**(10), 1899-908.

Suire, S., Coadwell, J., Ferguson, G. J., Davidson, K., Hawkins, P. & Stephens, L., 2005. p84, a New G[beta][gamma]-Activated Regulatory Subunit of the Type IB Phosphoinositide 3-Kinase p110[gamma]. *Current Biology*, **15**(6), 566-570.

Sujobert, P., Bardet, V., Cornillet-Lefebvre, P., Hayflick, J. S., Prie, N., Verdier, F., Vanhaesebroeck, B., Muller, O., Pesce, F., Ifrah, N., Hunault-Berger, M., Berthou, C., Villemagne, B., Jourdan, E., Audhuy, B., Solary, E., Witz, B., Harousseau, J. L., Himberlin, C., Lamy, T., Lioure, B., Cahn, J. Y., Dreyfus, F., Mayeux, P., Lacombe, C. & Bouscary, D., 2005. Essential role for the p110delta isoform in phosphoinositide 3-kinase activation and cell proliferation in acute myeloid leukaemia. *Blood*, **106**(3), 1063-6.

Sulewska, A., Niklinska, W., Kozlowski, M., Minarowski, L., Naumnik, W., Niklinski, J., Dabrowska, K. & Chyczewski, L., 2007. DNA methylation in states of cell physiology and pathology. *Folia Histochem Cytobiol*, **45**(3), 149-58.

Suzuki, H., Terauchi, Y., Fujiwara, M., Aizawa, S., Yazaki, Y., Kadowaki, T. & Koyasu, S., 1999. Xid-like immunodeficiency in mice with disruption of the p85alpha subunit of phosphoinositide 3-kinase. *Science*, **283**(5400), 390-2.

Tak, P. P. & Firestein, G. S., 2001. NF-kappaB: a key role in inflammatory diseases. *J Clin Invest*, **107**(1), 7-11.

Takai, Y., Sasaki, T. & Matozaki, T., 2001. Small GTP-binding proteins. *Physiol Rev*, **81**(1), 153-208.

Takaoka, A., Tamura, T. & Taniguchi, T., 2008. Interferon regulatory factor family of transcription factors and regulation of oncogenesis. *Cancer Sci*, **99**(3), 467-78.

Tanti, J. F., Gremeaux, T., Grillo, S., Calleja, V., Klippel, A., Williams, L. T., Van Obberghen, E. & Le Marchand-Brustel, Y., 1996. Overexpression of a constitutively active form of phosphatidylinositol 3-kinase is sufficient to promote Glut 4 translocation in adipocytes. *J Biol Chem*, **271**(41), 25227-32.

ten Klooster, J. P., Jaffer, Z. M., Chernoff, J. & Hordijk, P. L., 2006. Targeting and activation of Rac1 are mediated by the exchange factor beta-Pix. *J Cell Biol*, **172**(5), 759-69.

Terauchi, Y., Tsuji, Y., Satoh, S., Minoura, H., Murakami, K., Okuno, A., Inukai, K., Asano, T., Kaburagi, Y., Ueki, K., Nakajima, H., Hanafusa, T., Matsuzawa, Y., Sekihara, H., Yin, Y., Barrett, J. C., Oda, H., Ishikawa, T., Akanuma, Y., Komuro, I., Suzuki, M., Yamamura, K., Kodama, T., Suzuki, H., Yamamura, K., Kodama, T., Suzuki, H., Koyasu, S., Aizawa, S., Tobe, K., Fukui, Y., Yazaki, Y. & Kadowaki, T., 1999. Increased insulin sensitivity and hypoglycaemia in mice lacking the p85 alpha subunit of phosphoinositide 3-kinase. *Nat Genet*, **21**(2), 230-5.

Tertian, G., Yung, Y. P., Guy-Grand, D. & Moore, M. A., 1981. Long-term in vitro culture of murine mast cells. I. Description of a growth factor-dependent culture technique. *J Immunol*, **127**(2), 788-94.

Teschendorff, A. E., Journee, M., Absil, P. A., Sepulchre, R. & Caldas, C., 2007. Elucidating the altered transcriptional programs in breast cancer using independent component analysis. *PLoS Comput Biol*, **3**(8), e161.

Tigyi, G. & Miledi, R., 1992. Lysophosphatidates bound to serum albumin activate membrane currents in Xenopus oocytes and neurite retraction in PC12 pheochromocytoma cells. *J Biol Chem*, **267**(30), 21360-7.

Tolias, K. F., Cantley, L. C. & Carpenter, C. L., 1995. Rho family GTPases bind to phosphoinositide kinases. *J Biol Chem*, **270**(30), 17656-9.

Travis, A., Amsterdam, A., Belanger, C. & Grosschedl, R., 1991. LEF-1, a gene encoding a lymphoid-specific protein with an HMG domain, regulates T-cell receptor alpha enhancer function [corrected]. *Genes Dev*, **5**(5), 880-94.

Ueki, K., Fruman, D. A., Brachmann, S. M., Tseng, Y. H., Cantley, L. C. & Kahn, C. R., 2002a. Molecular balance between the regulatory and catalytic subunits of phosphoinositide 3-kinase regulates cell signaling and survival. *Mol Cell Biol*, **22**(3), 965-77.

Ueki, K., Yballe, C. M., Brachmann, S. M., Vicent, D., Watt, J. M., Kahn, C. R. & Cantley, L. C., 2002b. Increased insulin sensitivity in mice lacking p85beta subunit of phosphoinositide 3-kinase. *Proc Natl Acad Sci U S A*, **99**(1), 419-24.

Van Aelst, L. & D'Souza-Schorey, C., 1997. Rho GTPases and signaling networks. *Genes Dev*, **11**(18), 2295-322.

Van Leeuwen, F. N., Olivo, C., Grivell, S., Giepmans, B. N., Collard, J. G. & Moolenaar, W. H., 2003. Rac activation by lysophosphatidic acid LPA1 receptors through the guanine nucleotide exchange factor Tiam1. *J Biol Chem*, **278**(1), 400-6.

Vanhaesebroeck, B. & Waterfield, M. D., 1999. Signaling by distinct classes of phosphoinositide 3-kinases. *Exp Cell Res*, **253**(1), 239-54.

Vanhaesebroeck, B., Welham, M. J., Kotani, K., Stein, R., Warne, P. H., Zvelebil, M. J., Higashi, K., Volinia, S., Downward, J. & Waterfield, M. D., 1997. p110delta , a novel phosphoinositide 3-kinase in leukocytes. *PNAS*, **94**(9), 4330-4335.

Vartiainen, M. K., Guettler, S., Larijani, B. & Treisman, R., 2007. Nuclear actin regulates dynamic subcellular localization and activity of the SRF cofactor MAL. *Science*, **316**(5832), 1749-52.

Vazdarjanova, A., McNaughton, B. L., Barnes, C. A., Worley, P. F. & Guzowski, J. F., 2002. Experience-dependent coincident expression of the effector immediate-early genes arc and Homer 1a in hippocampal and neocortical neuronal networks. *J Neurosci*, **22**(23), 10067-71.

Verrall, E. & Vanhaesebroeck, B., unpublished results.

Vieira, O. V., Botelho, R. J., Rameh, L., Brachmann, S. M., Matsuo, T., Davidson, H. W., Schreiber, A., Backer, J. M., Cantley, L. C. & Grinstein, S., 2001. Distinct roles of class I and class III phosphatidylinositol 3-kinases in phagosome formation and maturation. *J Cell Biol*, **155**(1), 19-25.

Vignali, M., Hassan, A. H., Neely, K. E. & Workman, J. L., 2000. ATP-dependent chromatin-remodeling complexes. *Mol Cell Biol*, **20**(6), 1899-910.

Vogt, P. K., Bader, A. G. & Kang, S., 2006. Phosphoinositide 3-kinase: from viral oncoprotein to drug target. *Virology*, **344**(1), 131-8.

Voigt, P., Brock, C., Nurnberg, B. & Schaefer, M., 2005. Assigning functional domains within the p101 regulatory subunit of phosphoinositide 3-kinase gamma. *J Biol Chem*, **280**(6), 5121-7.

Wang, L. C., Kuo, F., Fujiwara, Y., Gilliland, D. G., Golub, T. R. & Orkin, S. H., 1997. Yolk sac angiogenic defect and intra-embryonic apoptosis in mice lacking the Ets-related factor TEL. *EMBO J*, **16**(14), 4374-83.

Ward, S. G., 2004. Do phosphoinositide 3-kinases direct lymphocyte navigation? *Trends Immunol*, **25**(2), 67-74.

Warne, P. H., Viciana, P. R. & Downward, J., 1993. Direct interaction of Ras and the amino-terminal region of Raf-1 in vitro. *Nature*, **364**(6435), 352-5.

Weber, J. D., Hu, W., Jefcoat, S. C., Jr., Raben, D. M. & Baldassare, J. J., 1997. Ras-stimulated extracellular signal-related kinase 1 and RhoA activities coordinate platelet-derived growth factor-induced G1 progression through the independent regulation of cyclin D1 and p27. *J Biol Chem*, **272**(52), 32966-71.

Weiner, O. D., Neilsen, P. O., Prestwich, G. D., Kirschner, M. W., Cantley, L. C. & Bourne, H. R., 2002. A PtdInsP(3)- and Rho GTPase-mediated positive feedback loop regulates neutrophil polarity. *Nat Cell Biol*, **4**(7), 509-13.

Welch, H. C., Coadwell, W. J., Ellson, C. D., Ferguson, G. J., Andrews, S. R., Erdjument-Bromage, H., Tempst, P., Hawkins, P. T. & Stephens, L. R., 2002. P-Rex1, a PtdIns(3,4,5)P3- and Gbetagamma-regulated guanine-nucleotide exchange factor for Rac. *Cell*, **108**(6), 809-21.

Welch, H. C., Coadwell, W. J., Stephens, L. R. & Hawkins, P. T., 2003. Phosphoinositide 3-kinase-dependent activation of Rac. *FEBS Lett*, **546**(1), 93-7.

Welsh, C. F., Roovers, K., Villanueva, J., Liu, Y., Schwartz, M. A. & Assoian, R. K., 2001. Timing of cyclin D1 expression within G1 phase is controlled by Rho. *Nat Cell Biol*, **3**(11), 950-7.

Whitehead, M. & Vanhaesebroeck, B., unpublished results.

Wickens, M., Anderson, P. & Jackson, R. J., 1997. Life and death in the cytoplasm: messages from the 3' end. *Curr Opin Genet Dev*, **7**(2), 220-32.

Wildin, R. S., Wang, H. U., Forbush, K. A. & Perlmutter, R. M., 1995. Functional dissection of the murine lck distal promoter. *J Immunol*, **155**(3), 1286-95.

Wullschleger, S., Loewith, R. & Hall, M. N., 2006. TOR signaling in growth and metabolism. *Cell*, **124**(3), 471-84.

Xiao, C. & Ghosh, S., 2005. NF-kappaB, an evolutionarily conserved mediator of immune and inflammatory responses. *Adv Exp Med Biol*, **560**, 41-5.

Yamaguchi, Y., Katoh, H., Yasui, H., Mori, K. & Negishi, M., 2001. RhoA inhibits the nerve growth factor-induced Rac1 activation through Rho-associated kinase-dependent pathway. *J Biol Chem*, **276**(22), 18977-83.

Yamamoto, M., Marui, N., Sakai, T., Morii, N., Kozaki, S., Ikai, K., Imamura, S. & Narumiya, S., 1993. ADP-ribosylation of the rhoA gene product by botulinum C3 exoenzyme causes Swiss 3T3 cells to accumulate in the G1 phase of the cell cycle. *Oncogene*, **8**(6), 1449-55.

Yang, C., Bolotin, E., Jiang, T., Sladek, F. M. & Martinez, E., 2007. Prevalence of the initiator over the TATA box in human and yeast genes and identification of DNA motifs enriched in human TATA-less core promoters. *Gene*, **389**(1), 52-65.

Yang, N., Huang, J., Greshock, J., Liang, S., Barchetti, A., Hasegawa, K., Kim, S., Giannakakis, A., Li, C., O'Brien-Jenkins, A., Katsaros, D., Butzow, R., Coukos, G. & Zhang, L., 2008. Transcriptional regulation of PIK3CA oncogene by NF-kappaB in ovarian cancer microenvironment. *PLoS ONE*, **3**(3), e1758.

Yart, A., Roche, S., Wetzker, R., Laffargue, M., Tonks, N., Mayeux, P., Chap, H. & Raynal, P., 2002. A function for phosphoinositide 3-kinase beta lipid products in coupling beta gamma to Ras activation in response to lysophosphatidic acid. *J Biol Chem*, **277**(24), 21167-78.

Yu, J., Wjasow, C. & Backer, J. M., 1998a. Regulation of the p85/p110alpha phosphatidylinositol 3'-kinase. Distinct roles for the n-terminal and c-terminal SH2 domains. *J Biol Chem*, **273**(46), 30199-203.

Yu, J., Zhang, Y., McIlroy, J., Rordorf-Nikolic, T., Orr, G. A. & Backer, J. M., 1998b. Regulation of the p85/p110 phosphatidylinositol 3'-kinase: stabilization and inhibition of the p110alpha catalytic subunit by the p85 regulatory subunit. *Mol Cell Biol*, **18**(3), 1379-87.

Zaidel-Bar, R., Cohen, M., Addadi, L. & Geiger, B., 2004. Hierarchical assembly of cell-matrix adhesion complexes. *Biochem Soc Trans*, **32**(Pt3), 416-20.

Zennaro, M. C., Keightley, M. C., Kotelevtsev, Y., Conway, G. S., Soubrier, F. & Fuller, P. J., 1995. Human mineralocorticoid receptor genomic structure and identification of expressed isoforms. *J Biol Chem*, **270**(36), 21016-20.

Zenzie-Gregory, B., Khachi, A., Garraway, I. P. & Smale, S. T., 1993. Mechanism of initiator-mediated transcription: evidence for a functional interaction between the TATA-binding protein and DNA in the absence of a specific recognition sequence. *Mol Cell Biol*, **13**(7), 3841-9.

Zhang, D. E., Hetherington, C. J., Tan, S., Dziennis, S. E., Gonzalez, D. A., Chen, H. M. & Tenen, D. G., 1994. Sp1 is a critical factor for the monocytic specific expression of human CD14. *J Biol Chem*, **269**(15), 11425-34.

Zhang, H., Xie, X., Zhu, X., Zhu, J., Hao, C., Lu, Q., Ding, L., Liu, Y., Zhou, L., Huang, C., Wen, C. & Ye, Q., 2005. Stimulatory cross-talk between NFAT3 and estrogen receptor in breast cancer cells. *J Biol Chem*, **280**(52), 43188-97.

Zhang, L., Yang, N., Katsaros, D., Huang, W., Park, J. W., Fracchioli, S., Vezzani, C., Rigault de la Longrais, I. A., Yao, W., Rubin, S. C. & Coukos, G., 2003. The oncogene phosphatidylinositol 3'-kinase catalytic subunit alpha promotes angiogenesis via vascular endothelial growth factor in ovarian carcinoma. *Cancer Res*, **63**(14), 4225-31.

Zhang, S. J., Shi, J. Y., Zhu, Y. M., Shi, Z. Z., Yan, S., Gu, B. W., Bai, X. T., Shen, Z. X. & Li, J. Y., 2006. The investigation of mutation and single nucleotide polymorphism of receptor tyrosine kinases and downstream scaffold molecules in acute myeloid leukaemia. *Leuk Lymphoma*, **47**(12), 2610-6.

Zhao, L. & Vogt, P. K., 2008. Helical domain and kinase domain mutations in p110alpha of phosphatidylinositol 3-kinase induce gain of function by different mechanisms. *Proc Natl Acad Sci U S A*, **105**(7), 2652-7.

Zheng, Y., Bagrodia, S. & Cerione, R. A., 1994. Activation of phosphoinositide 3-kinase activity by Cdc42Hs binding to p85. *J Biol Chem*, **269**(29), 18727-30.

Zhou, B. P., Liao, Y., Xia, W., Spohn, B., Lee, M. H. & Hung, M. C., 2001. Cytoplasmic localization of p21Cip1/WAF1 by Akt-induced phosphorylation in HER-2/neu-overexpressing cells. *Nat Cell Biol*, **3**(3), 245-52.

Zhou, T. & Chiang, C. M., 2001. The intronless and TATA-less human TAF(II)55 gene contains a functional initiator and a downstream promoter element. *J Biol Chem*, **276**(27), 25503-11.

Zhu, Y., Qi, C., Korenberg, J. R., Chen, X. N., Noya, D., Rao, M. S. & Reddy, J. K., 1995. Structural organization of mouse peroxisome proliferator-activated receptor gamma (mPPAR gamma) gene: alternative promoter use and different splicing yield two mPPAR gamma isoforms. *Proc Natl Acad Sci U S A*, **92**(17), 7921-5.

Zrihan-Licht, S., Fu, Y., Settleman, J., Schinkmann, K., Shaw, L., Keydar, I., Avraham, S. & Avraham, H., 2000. RAFTK/Pyk2 tyrosine kinase mediates the association of p190 RhoGAP with RasGAP and is involved in breast cancer cell invasion. *Oncogene*, **19**(10), 1318-28.